STEREOSELECTIVITY, IN β-ELIMINATIONS, TOWARDS PROCHIRAL LEAVING GROUPS

A Thesis presented by

Andrew John Kerslake, B.Sc., A.R.C.S.,

in partial fulfilment of the requirements for

the degree of

DOCTOR OF PHILOSOPHY

of the

UNIVERSITY OF LONDON

Thorpe-Whiteley Laboratory,
Department of Chemistry,
Imperial College,
London, S.W.7.

August 1978

To my wife, Mena,
whose patience and care
are reflected in every page.

ACKNOWLEDGEMENT

Firstly, my thanks are due to Dr. Laurie Phillips of Imperial College and Dr. Clive B.C.Boyce of Shell Research for providing me with the opportunity of studying for this thesis and for their friendship and guidance throughout the last four years. Also to Professor Sir Derek H.R.Barton, for the privilege of working in the Organic Chemistry Department.

I would like to mention my colleagues in the Thorpe-Whiteley Laboratory who made my post-graduate years most enjoyable - Soss, Peter, Mansoor, Mehrey, Malcolm (and the HMC), John (and Twinings) and Steve - their friendship and help will never be forgotten.

I thank Mrs. J.Lee (IC) and Dr. I.Howell (Shell) for the many excellent mass spectra they recorded for me, and Dr. S.J.Roberts and Mr. J.C.Burgess for their assistance when the HA100 or XL100 refused to cooperate. To both of the latter and to the members of ICCC Program Advisory also go my thanks for the many hours spent in discussing computing problems.

I would especially like to thank Drs. Roger H.Platt and Peter W.Vipond of Lever Brothers, who during the past, difficult, year have given me continued support and encouragement.

My wife, Mena's committal to helping with the typing, proof-reading, editing and correcting of this work has been total and without her support the task would not have been done - I cannot thank her enough.

Lastly, thanks are due to the Science Research Council and Shell Research Limited for the award of a CASE scholarship.

ABSTRACT

Three series of o & p substituted 2,2-dichloro-1-Y-phenylethanes (where Y = OH, F & Cl) have been prepared with a view to investigating the stereoselective control, by ortho ring substituents, of eliminations towards diastereotopic chlorine atoms; first observed in the 'abnormal' Michaelis-Becker reaction. When Y = OH, γ-eliminations produce α-chloroepoxides and when Y = F, β-eliminations produce fluorostyrenes. Eliminations were not performed on the Y = Cl series.

The work is split into three parts :

PART 1 deals with the necessary background and the preparation of the starting materials. General stereochemical concepts and the origins of the problem investigated are discussed. The main elimination mechanisms are outlined and the pertinent literature on stereoselective eliminations is reviewed. Conformational analysis by conventional nmr and by lanthanide induced shifts (LIS) is also reviewed.

PART 2 deals with the conformational analysis of the starting materials and the prediction of the elimination product isomer ratios. ABX spectral analyses were required as part of this work but standard texts were found to be confused. A detailed study of the ABX-system was therefore undertaken and is presented here.

The conformational data contained in the accurate ^{1}H, ^{19}F, and ^{13}C nmr spectra of the three series is discussed at length and indicates that the conformations adopted by the various derivatives are similar in all three series. The use of Karplus-type equations to calculate individual rotamer $^{3}J_{HF}$ & $^{3}J_{HH}$ couplings, in highly substituted species, is shown to be unfeasible by a re-examination of $^{3}J_{HF}$ couplings in a series of deoxyfluoro pyranoses. Values taken from these and other model systems are used to obtain accurate estimates of the individual rotamer $^{3}J_{HF}$ & $^{3}J_{HH}$ couplings in the Y = F series. These are then used, in a simple determinant method, to calculate the rotamer populations from the observed time-averaged couplings. From the qualified assumption that elimination should proceed to the product isomers in proportion to the rotamer populations, the expected elimination product isomer ratios for the Y = OH and F series, are predicted.

The development of a computer program, METFIND VII, for the rotational optimisation of molecules from their LIS data is discussed and two shift reagent studies on the Y = OH series, with $Eu(fod\text{-}d_9)_3$ and $Yb(fod\text{-}d_9)_3$, reported; the former being used to verify that conformational preferences, as monitored by coupling constants, remain unchanged on adding the LSR, the latter to optimise the molecular conformation. The LIS rotational optimisation results

generally support those obtained from the conventional nmr spectra.

PART 3 deals with the elimination reactions of the Y = OH and F series. The choice of base is discussed and the results of three sets of elimination reactions performed on each series presented. For both series several types of product were formed, with the major species usually from the desired reaction. The Y = F series underwent predominantly stereospecific elimination whilst the Y = OH series underwent both stereospecific and stereoselective eliminations, depending on the base employed; the latter approximately corresponding to the predicted product ratios. The factors controlling the mechanisms of both the main and side reactions are discussed. Under the conditions used, both series appeared to eliminate by an ElcB or ElcB-like mechanism.

CONTENTS

PAGE

PART 1 : INTRODUCTIONS, LITERATURE SURVEYS, PREPARATION OF STARTING MATERIALS

Chapter 1 STEREOSELECTIVITY IN ELIMINATION REACTIONS 16

1-1 Introduction - Prochirality, Enantiotopism and Diastereotopism 17

1-2 The E/Z Geometric Isomer Notation 21

1-3 Origins and Scope of the Problems Investigated 22

1-4 Elimination Reaction Mechanisms 33

1-4-1 The Main Mechanisms 33

1-4-1.1 The E2 Mechanism 33
1-4-1.2 The E1 Mechanism 33
1-4-1.3 The ElcB Mechanism 34
1-4-1.4 The Variable Transition State Theory 34

1-4-2 Stereochemistry 36

1-4-3 A Survey of the Pertinent Literature 38

1-4-3.1 Olefin Forming β-Eliminations 39
1-4-3.2 Epoxide Forming γ-Eliminations 40

1-5 Structure Determination in Solution 43

1-5-1 Conformational Dependence of Coupling Constants 44

1-5-2 Conformational Dependence of Chemical Shifts 48

1-6 Lanthanide Induced Shifts (LIS) 50

1-6-1 The Components of the Induced Shift 50

1-6-1.1 The Dipolar Interaction (Pseudo-Contact Shifts - PCS) 51
1-6-1.2 The Fermi-Contact Interaction (Contact Shifts - CS) 52
1-6-1.3 The Diamagnetic Interaction (Complex Formation Shifts - CFS) 54

1-6-2 Line Broadening 54

1-6-3 Properties of the Lanthanides - Choosing a Lanthanide Shift Reagent 55

1-6-4 Treatment of LIS data 58

1-6-4.1 Basic Assumptions 58
1-6-4.2 Basic Methods 59
1-6-4.3 Fit Factors and Significance Testing 60
1-6-4.4 Likely Sources of Error in calculating Metal Positions from LIS Data 61

1-6-5 Conformational Studies Using LIS 62

Chapter 1 Summary : 67

SCHEMES (1-31), EQNS (1-30), CCMPOUNDS (X-XXXIX), REFS (1-216)

CONTENTS continued

		PAGE
Chapter 2	PREPARATIVE CHEMISTRY LEADING TO THE THREE SERIES OF STARTING MATERIALS FOR ELIMINATION STUDIES	68
2-1	Introduction	69
2-2	Experimental	69
2-3	Preparation of the 2,2-Dichloroacetophenones (Type (III) Ketones)	70
2-3-1	Preparation of 2'-Bromoacetophenone	70
2-3-2	Methods Used in Preparing the 2,2-Dichloro-acetophenones	71
	METHOD 1 By Direct Chlorination	71
	METHOD 2 By Friedel-Crafts Acylation	72
	METHOD 3 By Direct Chlorination Under Mild Conditions	73
2-3-3	Physical Properties of the 2,2-Dichloroaceto-phenones	74
2-4	Preparation of the 2,2-Dichloro-1-phenyl ethanols (Type (IV) Alcohols)	75
2-4-1	General Sodium Borohydride Method	75
2-4-2	Physical Properties of the Type (IV) Alcohols	76
2-5	Preparation of the 2,2-Dichloro-1-fluoro-1-phenyl ethanes (Type (V) Fluorides)	78
2-5-1	Preparation of the Fluorinating Reagents and the Type (V) Fluorides	78
2-5-1.1	Problems Involved in the Preparation of Diethylamino-2-chloro-1,1,2-tri-fluoroethane (DACTE)	79
	PROCEDURE 1	81
2-5-1.2	Problems Involved in the Preparation of Diethylamino sulphur trifluoride (DAST)	82
	PROCEDURE 2	85
2-5-2	Physical Properties of the Type (V) Fluorides	86
2-6	Preparation of the 1,2,2-Trichloro-1-phenyl-ethanes (Type (VI) Chlorides)	89
2-6-1	General Phosphorus Pentachloride Method	89
2-6-2	Physical Properties of the Type (VI) Chlorides	89
2-7	Type (IV), (V) and (VI) Compounds Reported in the Literature	92
Chapter 2 Summary :		92

SCHEMES (32-42), COMPOUNDS (I-IX,XL-XLVIII), REFS (217-238)

CONTENTS continued PAGE

PART 2 : CONFORMATIONAL DETERMINATION OF THE STARTING MATERIALS 93

Chapter 3 BASIC SPECTRAL ANALYSIS 94

3-1 Obtaining the Spectral Parameters from an AB-System 95

3-2 Obtaining the Spectral Parameters from an ABX-System 96

3-2-1 Summary of Theory 96

3-2-2 Analysis of an ABX-System 99

3-2-2.1 Analysis (i) Assuming $D_+ \gg D_- \gg 0$ 100

3-2-2.2 Analysis (ii) Assuming $D_- \gg D_+ \gg 0$ 101

3-2-2.3 Analysis (iii) Assuming D_+ and D_- of Opposite Sign 102

3-2-3 The Origins of the ABX Spectral Lines 102

3-2-4 Line Assignment and Analysis of ABX Spectra 109

3-2-4.1 Line Assignment 109

3-2-4.2 Spectral Analysis of the ABX-Spin System 111

Chapter 3 Summary : 111

EQNS (31-65), REFS (239-245)

Chapter 4 CONFORMATIONAL ANALYSIS OF THE TYPE (IV), (V) AND (VI) COMPOUNDS FROM THEIR CONVENTIONAL ^{1}H, ^{13}C AND ^{19}F NMR SPECTRA 112

4-1 Experimental 113

4-1-1 Accuracy of Spectral Measurements 114

4-1-2 Naming Convention Used in NMR Assignments 114

4-2 Spectral Assignments 114

4-3 ABX Analysis of the ^{1}H and ^{19}F Spectra of the Type (V) Fluorides 115

4-4 Chemical Shift Data 119

4-4-1 ^{1}H Chemical Shifts 119

4-4-2 ^{19}F Chemical Shifts 122

4-4-3 ^{13}C Chemical Shifts 123

4-5 Coupling Constant Data 127

4-5-1 $^{3}J_{HH}$ Coupling Constants 128

4-5-2 $^{2}J_{HF}$ and $^{3}J_{HF}$ Couplings from the Type (V) Fluorides 128

4-5-3 $^{n}J_{CF}$ Couplings - Observed in the ^{13}C Spectra 129

CONTENTS continued PAGE

4-5-4 $^{n}J_{FF}$ Couplings in the Type (V) Fluorides 131

4-5-5 Verification of the ^{13}C Assignments of C-1 and C-2 in the Type (IV) Alcohols 131

4-5-6 Attempts at Obtaining $^{3}J_{H_BC_2}$, Couplings in the Type (IV) Alcohols 132

4-5-7 Temperature Effects in ^{1}H Spectra of the Type (IV) Alcohols 133

4-6 Parameters Governing Substituent Effects 135

4-7 Interpretation of the Chemical Shift Data 136

4-8 Interpretation of the Coupling Constant Data 149

4-8-1 Similarities Between the Type (IV), (V) and (VI) Coupling Constants 149

4-8-2 A Detailed Examination of the Three Bond Couplings 153

4-8-2.1 Trends Observed in the $^{3}J_{HH}$ and $^{3}J_{HF}$ Couplings 153

4-8-2.2 Empirical Approach to the Calculation of $^{3}J_{HH}$ and $^{3}J_{HF}$ 155

4-8-2.3 Calculation of Rotamer Populations in the Type (V) Fluorides 165

4-8-2.4 Trends Observed in the $^{3}J_{CF}$ Couplings 172

4-8-2.5 Empirical Approach to the Analysis of the $^{3}J_{CF}$ Couplings 172

4-8-3 Conformational Information Contained in the Long-Range Couplings 174

4-8-4 Conformational Information Contained in the Two Bond Couplings 176

4-8-4.1 The $^{2}J_{HF}$ Data 176

4-8-4.2 The $^{2}J_{CF}$ Data 177

4-8-4.3 The $^{2}J_{CH}$ Data 179

4-8-5 Conformational Information Contained in the One Bond Couplings 180

4-9 Summary of Conformational Observations 180

4-10 Prediction of Elimination Product Geometries from the Calculated Rotamer Preferences 182

Chapter 4 Summary : 183

EQNS (66-102), REFS (246-277)

CONTENTS continued PAGE

Chapter 5 METHODOLOGY / APPROACH TO CONFORMATIONAL ANALYSIS USING LANTHANIDE INDUCED SHIFTS 184

5-1 Basic Assumptions 185

5-2 Finding the "Best Metal Position" for a Rigid Substrate 186

5-2-1 Coordinate Systems 186

5-2-2 Data Required 187

5-2-3 Basic Calculations Performed 187

5-2-4 Tolerance Tests and Fitfactors 187

5-2-5 Metal Reflection Option 188

5-2-6 Methyl Group Rotation Option 189

5-2-7 METFIND Search Methods 189

5-3 Program Testing - Cholesterol 191

5-4 Approach to the Rotation Problem 193

5-4-1 Basic Concepts / Logistics of Rotational Optimisation 193

5-4-2 Requirements for Group Rotation 195

5-4-3 The Calculation of Rotated Coordinates 195

Chapter 5 Summary : 196

EQNS (103-106), REF (278)

Chapter 6 CONFORMATIONAL ANALYSIS OF THE TYPE (IV) ALCOHOLS FROM THEIR LANTHANIDE INDUCED SHIFTS 197

6-1 Experimental 198

6-2 Choice of LSR 199

6-3 Shifted Spectra of the Type (IV) Alcohols 199

6-3-1 Coupling Data from the Eu(fod-d_9)$_3$ Spectra 199

6-3-2 Shift Data from the Eu and Yb(fod-d_9)$_3$ Spectra 199

6-4 Substrate Coordinates 204

6-5 Approach to Rotational Optimisation (Rot/Opt) Using LIS and METFIND VII 205

6-5-1 Metal Search Based on Fixed Atoms 206

6-5-2 Rotational Optimisation 207

CONTENTS continued PAGE

6-5-3 Full MULTISCAN Search 211

6-6 Results of Rotational Optimisation Using the Eu- and Yb-LIS 211

6-6-1 Initial Maxima Found for the FIXED ATOMS 211

6-6-2 Results of the ROTATION MODE Runs 212

6-6-3 Results of the Full MULTISCAN Searches 219

6-7 Interpretation of the Yb-LIS Rot/Opt Results 219

Chapter 6 Summary : 225

REFS (279-280)

PART 3 : ELIMINATION REACTIONS / OVERVIEW 226

Chapter 7 ELIMINATION REACTIONS AND CONFORMATIONAL DETERMINATION OF THE PRODUCTS 227

7-1 Experimental 228

7-2 The Choice of Base 228

7-2-1 Trial Eliminations of HCl from the Type (IV) Alcohols 228

7-2-2 Trial Eliminations of HCl from the Type (V) Fluorides 231

7-3 Products of the Elimination Reactions of the Type (V) Fluorides 231

7-3-1 The Elimination Reactions 231

METHOD 1 (2.KOBu^t/THF) 231

METHOD 2 (2.LiOEt/EtOH) 231

METHOD 3 (3.LiOEt/EtOH) 232

7-3-2 GLC Analysis of the Type (V) Fluoride Elimination Products 232

7-3-3 GC/MS Identification of the Type (V) Fluoride Elimination Products 233

7-3-4 ^{1}H and ^{19}F NMR Spectra of the Type (V) Fluoride Elimination Products 235

7-3-5 ^{1}H and ^{19}F NMR Identification of the Geometry of the Type (VIII) Fluoro-Styrenes 239

7-3-6 Possible Elimination Mechanisms 241

7-4 Products of the Elimination Reactions of the Type (IV) Alcohols 245

CONTENTS continued PAGE

7-4-1 The Elimination Reactions 245

METHOD 1 ($2.KOBu^t/THF$) 245

METHOD 2 ($3.NaH/CCl_4$) 245

7-4-2 Identification of the Type (IV) Alcohol Elimination Products by METHOD 2 245

7-4-3 The Epoxide Product Isomer Ratios Produced by METHODS 1 and 2 249

7-4-4 Possible Elimination Mechanisms for Epoxide Formation 251

Chapter 7 Summary : 252

SCHEMES (43-54), COMPOUNDS (IL-LXIII), REFS (281-291)

Chapter 8 OVERVIEW 253

8-1 Stereoselectivity Towards Diastereotopic Leaving Groups - Was this Observed ? 254

8-2 Relationship of the Type (IV) and (V) Eliminations to the 'Abnormal' Michaelis-Becker Reaction 256

8-3 Success / Validity of the Approaches to Conformational Analysis Based on the Conventional NMR Spectra (Chapter 4) and the LIS Data (Chapters 5 & 6) 259

8-4 Areas for Further Work 262

Chapter 8 Summary : 262

SCHEME (45), COMPOUNDS (LXIV-LXIX)

APPENDICES 263

APPENDIX I : GRAPHICAL METHODS FOR SPECTRAL ANALYSIS 264

APPENDIX II : ABX ANALYSIS - CONDITIONS UNDER WHICH [14,15] > [10,11] 268

APPENDIX III : OPTIMISATION OF METAL REFLECTION 269

APPENDIX IV : METFIND VII (MET7IND) 270

IV-1 Input Data Decks 270

CONTENTS continued PAGE

IV-2 Card Formats and Brief Descriptions of the Various Parameters and Options 271

IV-3 Output 275

IV-4 Program Structure and Listing 281

APPENDIX V : MODEL FOR PLOTTING 3-D FITFACTOR CONTOURS 292

LITERATURE CITED 294

302

All SCHEMES, EQNS, COMPOUNDS and REFS are numbered sequentially throughout this work and as an aid to cross-reference are summarised after each Chapter in the Contents list.

As there are in excess of 250 FIGS. and TABLES these have not been indexed. Instead each FIG. or TABLE carries both the Chapter and SECTION number in which it occurs, as well as a sequential number, and may therefore be rapidly located via the Contents list.

Still round the corner there may wait
A new road or a secret gate,
And though we pass them by today,
Tomorrow we may come this way,
And take the hidden paths that run
Towards the Moon or to the Sun.

J.R.R.Tolkien

PART 1

INTRODUCTION, LITERATURE SURVEYS, PREPARATION OF STARTING MATERIALS.

CHAPTER 1

1 STEREOSELECTIVITY IN ELIMINATION REACTIONS

1-1 Introduction : Prochirality, Enantiotopism and Diastereotopism

The term "PROCHIRAL", although proposed by Hanson in 1966[1] (just two years after the general adoption of the term "CHIRAL" proposed by Cahn, Ingold and Prelog[2]), has not found wide usage and a definition is appropriate.

Of the six possible combinations of four groups arranged tetrahedrally about a central atom (see FIG.1-1.1), E and F stand out, as although they contain the same groups "ghij" they cannot be superimposed. This property of an asymmetric centre is termed "CHIRALITY" and the ENANTIOMERS E and F may be assigned an unambiguous configuration (R) or (S) by applying the sequence rules of Cahn, Ingold and Prelog.[2,3]

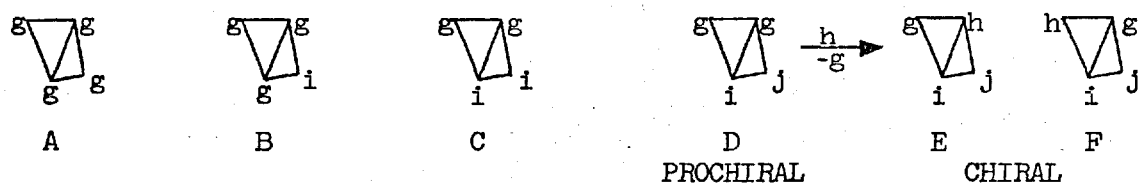


FIG.1-1.1 The Six Tetrahedral Arrangements

Hanson[1] pointed out that of the four remaining combinations D also has a special significance, because if either of the two "point ligands" "g" were replaced by an "h", a CHIRAL arrangement E or F would be produced. Point ligands have only two properties :

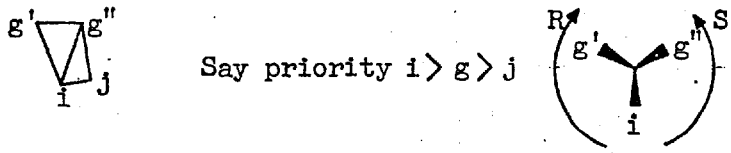
(1) Any two point ligands may be identical or non-identical.

(2) Any two point ligands cannot occupy the same point in space.

Definition[1]: If a chiral assembly is obtained when a point ligand in a finite non-chiral assembly of point ligands is replaced by a new point ligand, then the original assembly is PROCHIRAL (from PRO = before, CHIRAL).

C_{ggij} may be termed a PROCHIRAL CENTRE, just as C_{ghij} may be termed CHIRAL. The two ligands "gg" in a prochiral group are referred to as "paired". These may be assigned individual identifiers "pro-R" and "pro-S" by the following method :

Take one of the paired ligands and raise its sequence rule priority without affecting its priority relative to the unpaired ligands. Now arrange the modified (chiral) centre with the ligand of lowest priority away from the viewer (FIG.1-1.2) and assign its absolute configuration. If the modified

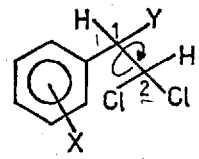


With g' elevated priority sequence is clockwise (R). With g" elevated priority sequence is anti-clockwise (S)

FIG.1-1.2 g' = pro-R; g" = pro-S

centre has R chirality then the elevated paired ligand is assigned as pro-R and the other as pro-S, and vice versa.

In the context of the title of this thesis, the expression "Prochiral Leaving Groups" refers to the two chlorine atoms on C-2 in compounds of the general structure :



Y = OH, F, Cl;

X = a range of ortho and para substituents.

FIG.1-1.3

As can be seen from FIG.1-1.3, C-2 is prochiral due to the two chlorine atoms, but the chlorines themselves cannot possess prochirality. It has been pointed out[4] that whereas R and CHIRAL refer to the same structural element in a molecule, pro-R and PROCHIRAL do not. For complete correctness, "Prochiral Leaving Groups" could be replaced by "Paired Leaving Groups on a Prochiral Centre", or alternatively "Diastereotopic Leaving Groups".*

Two identical groups attached to the same atom in a molecule may possess one of three stereoisomeric relationships, ie. they may be EQUIVALENT, ENANTIOTOPIC or DIASTEREOTOPIC. As the expanded definitions of these terms have been thoroughly examined in the definitive review of Mislow and Raban[5], only a brief description will be given here.

TABLE 1-1.1 The Principal Attributes of the Spatial Relationships Among Groups[5]

Type of Group	Symmetry Criterion	Substitution Criterion	Excluded Point Groups
EQUIVALENT	Interchangeable by C_n $(\infty > n > 1)$	No isomers are generated with achiral or chiral test groups	Conical (C_∞) and non-axial (C_1^v, C_s, C_i)
ENANTIOTOPIC	Interchangeable only by S_n	With achiral test groups enantiomers are generated. With chiral test groups diastereomers are generated	Linear ($C_{\infty v}$, $D_{\infty h}$) and chiral (C_n, D_n, T, O, I)
DIASTEREOTOPIC	Not interchangeable by any symmetry operation	With achiral or chiral test groups diastereomers are generated	Linear ($C_{\infty v}$, $D_{\infty h}$)

As, by definition, the unpaired ligands on a prochiral centre are non-identical, the paired ligands cannot be EQUIVALENT (see FIG.1-1.4).

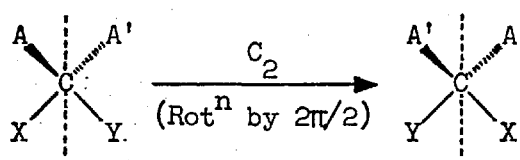


FIG.1-1.4 For A and A' to be equivalent, X must = Y. Equivalent groups are superimposable.

Paired ligands can meet the requirements for ENANTIOTOPISM (see FIG.1-1.5).

* Unfortunately, this common misapplication of the term "Prochiral"[10] was only appreciated after the thesis title was formally and irrevocably registered!

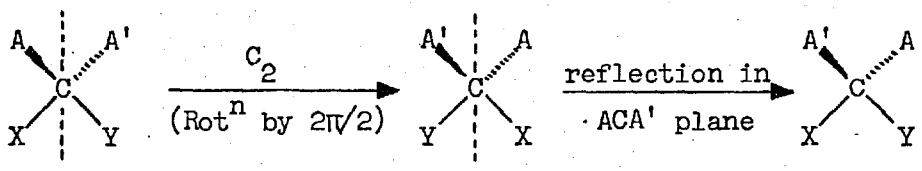


FIG.1-1.5 This rotation/reflection operation ($\sigma = S_1$), is the requirement for A and A' to be enantiotopic.

Enantiotopic groups are non-superimposable, but are normally "equivalent" being indistinguishable by nmr and by their reactivity towards achiral reagents.

When enantiotopic groups are reacted with chiral reagents, however, the transition states become diastereomeric; and as such states have different activation energies, the reactivity of the enantiotopic groups will become unequal and stereoselectivity* may be observed. Similarly, enantiotopic groups may become distinguishable by immersion in a non-racemic chiral solvent.

Frequently the distinctiveness of enantiotopic groups in chiral extramolecular environments is vanishingly small, but in some circumstances, especially in enzyme reactions, 100% selectivity (stereospecificity) of one enantiotopic group can occur with the formation of only one diastereotopic product.[6]

Naturally, paired ligands will meet the criteria for DIASTEREOTOPISM if one or both of the unpaired ligands is chiral (N.B. by definition the unpaired ligands are non-identical).

Diastereotopic groups are non-superimposable, and barring accidental equivalence (which occurs quite frequently in nmr), are non-equivalent. Such groups will therefore have different physical and chemical properties, even in achiral extramolecular environments, and a degree of intrinsic stereoselectivity is to be expected.

In the three series of compounds studied in the present work, the two chlorine atoms on C-2 are adjacent to a chiral centre (C-1) and are therefore diastereotopic (see FIG.1-1.3). Unfortunately, we are unable to directly observe their physical non-equivalence by nmr, but it should be borne in mind that this is present and cannot be removed by bond rotation!

For example, Pople[7] considered the phenomenon of the methylene group adjacent to a chiral centre (FIG.1-1.6). The three rotamers are physically distinct and in the frozen out spectrum,$ three AB quartets occur. Under rapid rotation, the environments of H_1 and H_2 cannot be averaged out, their

* Stereoselectivity may refer to (a) the discrimination between enantiotopic groups by a chiral reagent, or (b) the discrimination between diastereotopic groups by any reagent(5).

$ See footnote p.20.

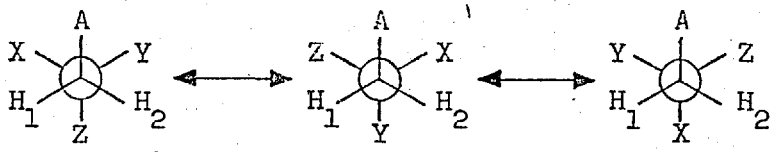


FIG.1-1.6

resultant time-averaged environments are still non-equivalent, and a single AB-quartet emerges. This chemical shift non-equivalence under conditions of rapid rotation has been termed "intrinsic anisochronism" ($\Delta\delta_i$) by Gutowsky.[8]

Dabrowski and Ejchart[9] have observed ^{1}H nmr non-equivalence in both methylene protons and isopropyl methyl groups, in compounds analogous to those examined here :

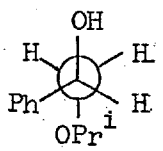
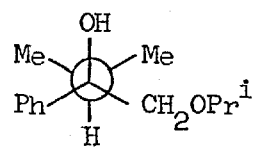


FIG.1-1.7

(Pr^i = iso-propyl)



$\Delta\delta_H$0.223ppm; J_{HH}gem9.42Hz.

$\Delta\delta_{Me}$0.141ppm; $\Delta J_{H\text{-}Me}$0.07Hz.

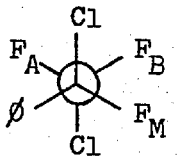
The literature contains several reviews on non-equivalence of diastereotopic groups.[5,10,11]

In the study of elimination reactions involving diastereotopic chlorine atoms (FIG.1-1.3) we observe a high degree of stereoselectivity, dependant on the nature of the aromatic ortho substituent X. It is our contention that the major cause of this stereoselectivity is not the chlorine atoms' intrinsic non-equivalence, but is the preferential population of certain rotamers in these molecules, prior to reaction. Such preferences have been reported by various authors studying diastereotopic non-equivalence.

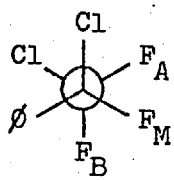
Norris and Binsch[12] have examined the ^{19}F nmr of a large number of penta-halo substituted phenyl ethanes at low and ambient temperatures (eg.FIG.1-1.8) The assigned shifts and couplings from the geminal fluorines in the "frozen-out" rotamers, weighted with the rotamer populations, were used to calculate the components of the time averaged geminal anisochronism ($\langle\Delta\rangle^{LT}$) and were found to be in good agreement with the anisochronism observed at ambient temperature (Δ_{AB}) (see TABLES 1-1.2 and 1-1.3).

Several interesting points arise from this data. The rotamer preferences are in accord with the expected steric repulsion of the bulky chlorine and phenyl groups. The intrinsic anisochronism term $\langle\Delta\rangle_i^{LT}$ dominates the observed anisochronism and is opposite in sign to the conformer population term $\langle\Delta\rangle_c^{LT}$. Rotamer (2) is an example of accidental equivalence of the geminal fluorines. This also occurs under rapid rotation, if $\langle\Delta\rangle_i$ and $\langle\Delta\rangle_c$ are equal

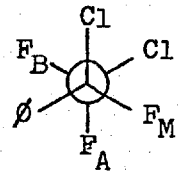
$ At low temperatures the rates of molecular rotation may be reduced sufficiently for individual rotamers to be observable on the nmr time scale. This is referred to as a "frozen out spectrum".



Rel.Pop^n. (1) 54.8%



(2) 8.5%



(3) 36.7%

FIG.1-1.8

TABLE 1-1.2 Low Temp. Spectrum (10%v/v in CF_2Cl_2) δppm @94.1MHz rel.int.$CFCl_3$

Rotamer	δ_A	δ_B	Δ_{AB}	J_{AB}	J_{AM}	J_{BM}	$\langle\Delta\rangle^{LT}$	$\langle\Delta\rangle^{LT}_i$	$\langle\Delta\rangle^{LT}_c$
1	-66.87	-66.46	-0.41	169.8	12.1	7.9			
2	-70.33	-70.33	0	A_2M	21.3	21.3	0.52	0.54	-0.02
3	-64.07	-66.09	2.20	174.5	2	11.9			

TABLE 1-1.3 Ambient Temp. Spectrum δppm @94.1MHz rel.int.$CFCl_3$

Solvent	Conc^n	δ_A	δ_B	Δ_{AB}	J_{AB}	J_{AM}	J_{BM}
CH_2=CHCl	10%	-65.970	-66.591	0.621	168.9	9.6	10.2
$CFCl_3$	0.4M	-66.177	-66.757	0.580	168.9	10.0	10.2

and opposite in sign.[12]

In an interesting re-examination of Intrinsic Asymmetry, Anderson,[13] instead of comparing diastereotopic groups, has examined individual groups in prochiral situations where no orientational preferences exist, (eg. comparing the low temp ^1H nmr shifts of geminal methyl groups in $Me_2XC.CYMe_2$). Differences of approximately 0.1ppm are claimed in $CHMe_2CClMe_2$.

From an examination of solvent effects on the J_{HF} and J_{FF} couplings of $CF_2BrCHFCl$, Soon Ng[14] concluded that the rotamer with hydrogen gauche to the geminal fluorines was the most populated. This is somewhat surprising on steric grounds (gauche Cl and Br) (see FIG.1-1.9). When Norris and Binsch[12] examined the frozen out spectrum of this compound they found the major rotamer (50%) to be the anti-periplanar form[15] (applying the sequence rules[2]) with the syn-clinal form, preferred by Soon-Ng, present in 42%.

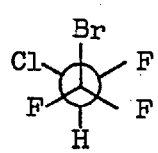
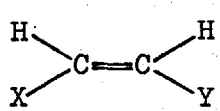


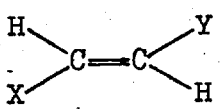
FIG.1-1.9

1-2. The E/Z Geometric Isomer Notation

The cis/trans isomer notation for distinguishing isomers of 1,2-disubstituted alkenes may be unambiguously applied by considering the spatial relationships of the two hydrogen atoms about the double bond (FIG.1-2.1).



CIS
(Latin - same)



TRANS
(Latin - opposite)

FIG.1-2.1

In the event of tri- or tetrasubstitution where no two groups are alike this simple nomenclature becomes ambiguous as deciding which group is cis or trans to which becomes purely arbitrary. Recently, the prefixes cis- and trans- to describe geometric isomerism have been replaced by the IUPAC descriptors E and Z.[16] The set of operating rules for this notation was suggested by Blackwood et al[17] :

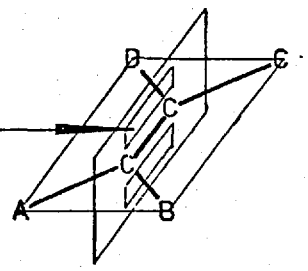


FIG.1-2.2

(1) Determine the relative priority of the groups A, B and C, D by applying the sequence rules of Cahn, Ingold and Prelog[2] (Normally the Atomic No. (Rule 2) of the directly attached atoms, or the size of the group when two alkyl groups are geminal, is sufficient).

(2) The configuration with the two groups of higher priority on the same side of the reference (π) plane is assigned as the Z-isomer (German ZUSAMMEN = same).

(3) The configuration with the two groups of higher priority on the opposite side of the reference plane is assigned as the E-isomer (German ENTGEGEN = opposite).

1-3 Origins and Scope of the Problems Investigated

This study was prompted by observations made by P.A.Worthington[18] whilst examining the course of the "Abnormal" Michaelis-Becker Reaction. In the "Normal" Michaelis-Becker Reaction,[19,20] (SCHEME 1), a dialkyl phosphonate is reacted with an alkyl' halide to form a dialkyl alkyl'phosphonate (X)*:

$$(RO)_2\overset{O}{\overset{\|}{P}}Na \quad + \quad R'X \longrightarrow \quad (RO)_2\overset{O}{\overset{\|}{P}}R' \quad + \quad NaX$$

(X)

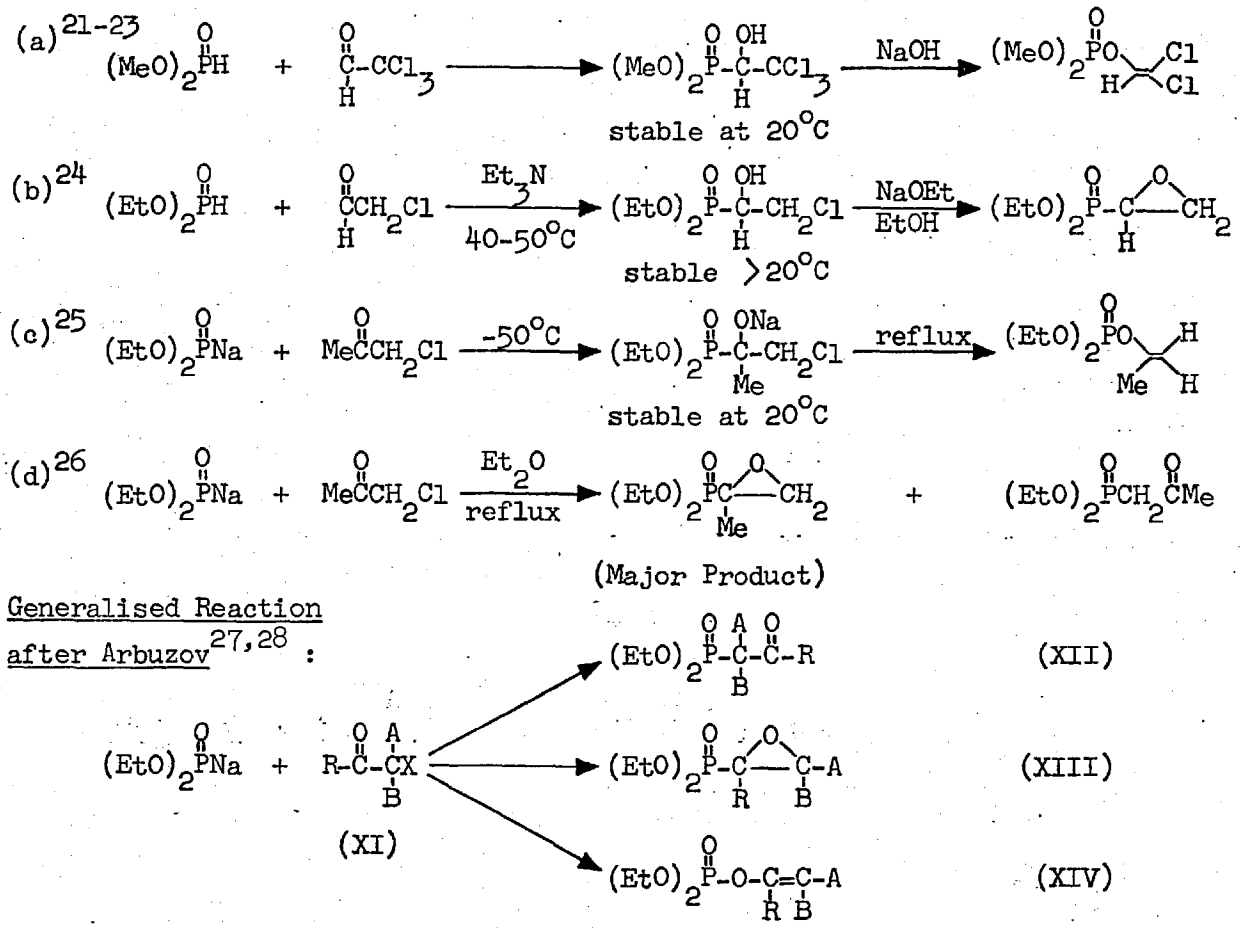
SCHEME 1 The Michaelis-Becker Reaction

When the alkyl halide is an α-halocarbonylcompound, however, the reaction can take several different courses (SCHEME 2).

Of the three main products, the ketophosphonates (XII) can be considered the 'normal product' by SCHEME 1. The 'abnormal products' are the epoxyphosphonates (XIII) and the vinyl phosphates (XIV).

The course of the reaction depends on the nature of R, A, B and X in (XI),[26-31] and the effect of variation of any of these groups on the product

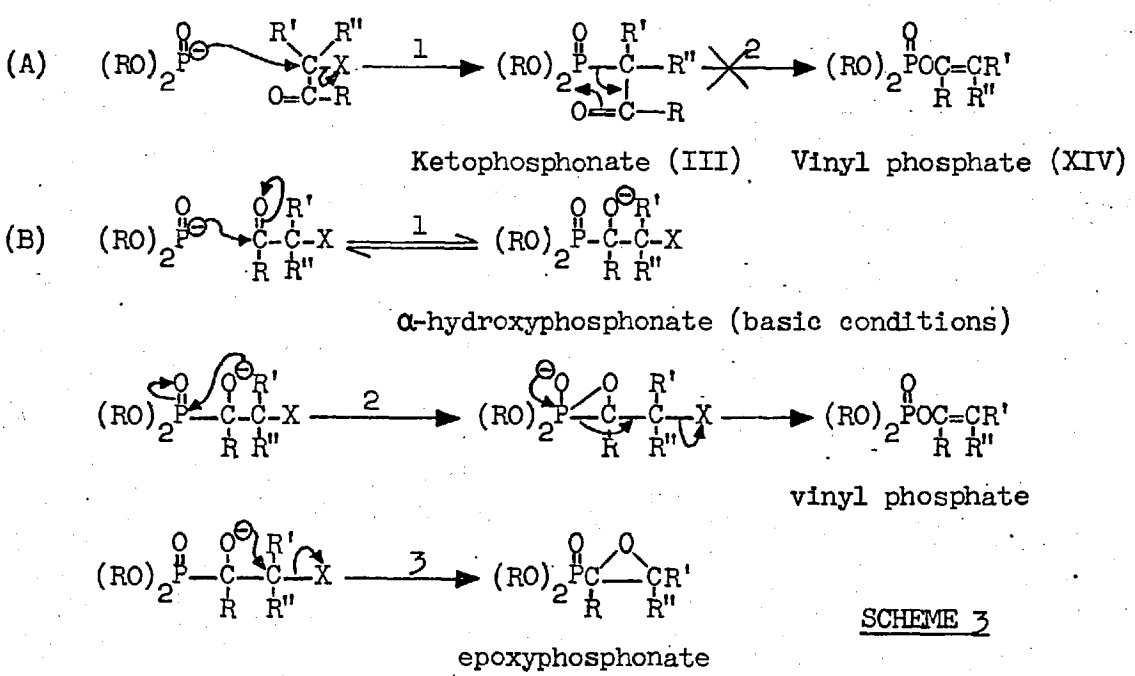
* Compounds (I) to (IX) have been reserved for the general series of compounds used in the experimental part of this work - see Chapter 2.



SCHEME 2 Products of the "Abnormal" Michaelis-Becker Reaction

ratios can now be fairly accurately predicted.

The nucleophilic species in both the normal and abnormal reactions is believed to be $(RO)_2P^{\ominus}=O$, because of the isolation of the α-hydroxyphosphonates[21,22](SCHEME 2(a-c)). The most likely mechanisms are shown in SCHEME 3 :

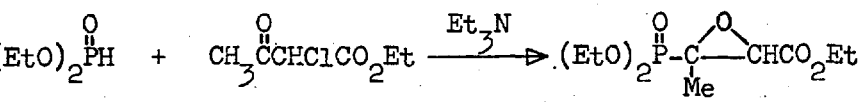


SCHEME 3

Step (A-1) is the most likely route to the normal Michaelis-Becker product, ie. attack on the α-carbon bearing the halogen. Step (A-2) via a Wittig type 4-centre rearrangement[32] to the vinyl phosphate proposed by Cramer[33] and Perkow[34] is unfeasible[35] as the ketophosphonate (XII) (R' = R'' = H; R = Ph) resisted all attempts to rearrange it to the isomeric vinyl phosphate (XIV).

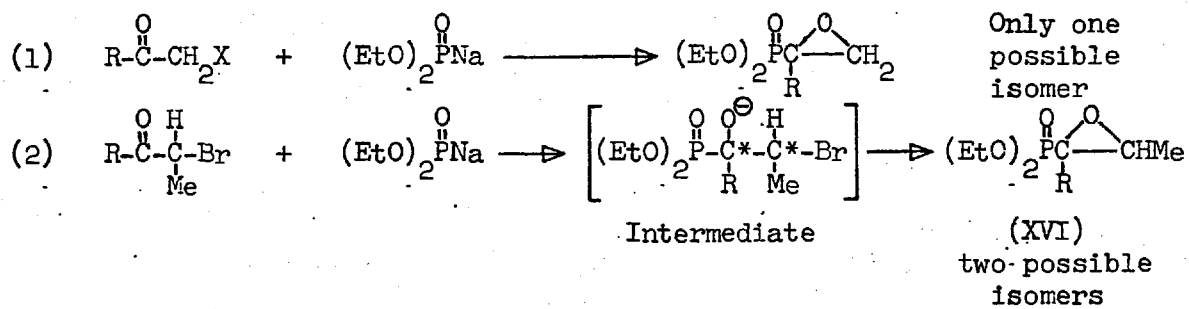
Step (B-1) with phosphorus attack on the carbonyl carbon and subsequent rearrangement to the vinyl phosphate (B-2), or elimination to epoxyphosphonate (B-3), was proposed by Bengledorf[36,37] and is supported by isolation of the α-hydroxyphosphonate intermediates[23-25] and their proven ability to rearrange to vinyl phosphates.[18,21-3,38] Preference for the two routes (B-2) or (B-3) depends on the relative electrophilic properties of the phosphorus and the α-carbon,[39] and the steric crowding of the α-carbon.[18] This leads to a delicate balance between the vinyl phosphate and epoxyphosphonate formation depending on the substituents on C-2.

Prior to Worthington's study,[18] the geometry of the products of the 'Abnormal' Michaelis-Becker Reaction was unreported apart from the observation by Pudovik[40] (SCHEME 4) that treatment of diethyl phosphonate with α-chloroethylacetoacetate in the presence of triethylamine gave one epoxide (XV) stereoselectively (Geometry undetermined but it was suggested that $^4J_{PH}$ might identify the E/Z isomer).



SCHEME 4 (XV)

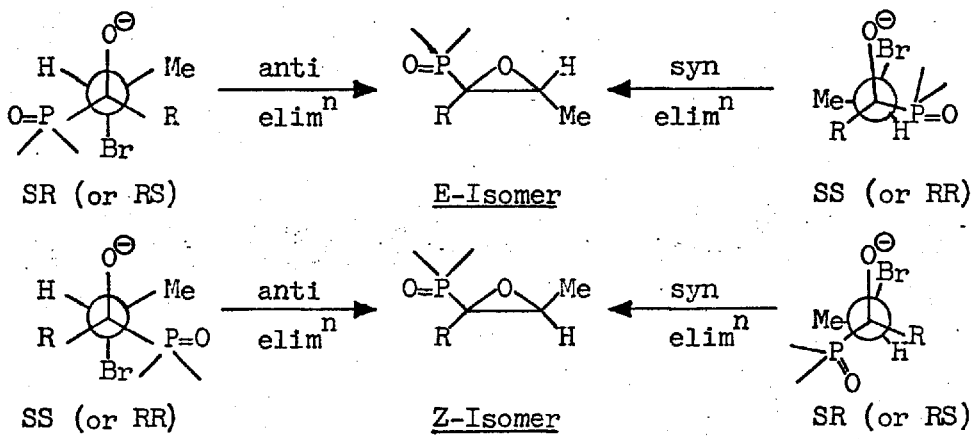
The epoxyphosphonate forming reaction (B-3) occurs less frequently than the vinyl phosphate forming reaction (B-2) and often produces only one isomer (eg. SCHEME 5.1).



SCHEME 5 (R = Me or Ø; X = Cl or Br) Geometry of (XVI) not disclosed in literature.[41]

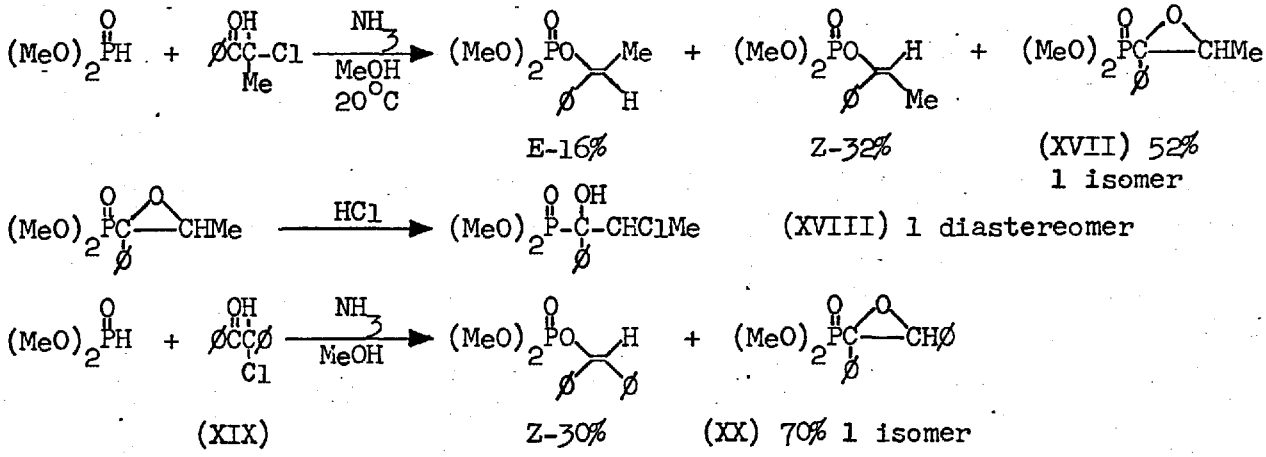
A study of the geometries of the reactions in SCHEMES 4 and 5.2 would be extremely interesting as the intermediates both contain two chiral centres (see SCHEME 5) and can exist as two diastereomeric pairs of enantiomers.

Elimination from enantiomers leads to the same products, but as there are two possible steric pathways (syn and anti - see SECTION 1-4.2) and two diastereomers of the intermediate, the reaction has four possible courses (SCHEME 6).* If both diastereomers of the intermediate are formed in equal amounts (formation of the intermediate is reversible,[18,37] so the lesser sterically favoured diastereomer may not be present) and both eliminate by the same route at similar rates, a 50 : 50 mixture of E/Z epoxides would result. But if one diastereomer preferentially eliminated by the syn-pathway and the other by the anti-pathway, or one eliminated at a much higher rate, a stereoselective elimination would occur and one isomer would predominate.



SCHEME 6

On reacting dimethyl phosphonate with 2-chloro propiophenone, Worthington[18] observed (from ^{1}H nmr) that only one isomer of the epoxyphosphonate (XVII) was formed (SCHEME 7). Subsequent isolation and treatment with



SCHEME 7

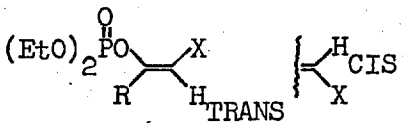
gaseous hydrogen chloride converted this to dimethyl 2-chloro-1-hydroxy-1-phenyl-propyl phosphonate (XVIII) (only one diastereomer by ^{1}H nmr). The

* An interesting discussion of this topic in terms of addition rather than elimination reactions is given in the introduction to S.I.Goldberg's "Asymmetric Selection via Eliminations," Selective Organic Transformations, 1, 363 (1970), (Ed. B.S.Thyagarajan)

geometry of the epoxide product was indeterminable in the absence of suitable models for the $^4J_{PH}$ coupling data. A similar reaction with 2-chlorobenzyl phenyl ketone (XIX) also produced only one isomer of the epoxide (XX).

The geometry of the vinyl phosphate-forming reaction was examined in considerable detail[18] to gain an understanding of the interactions controlling the E/Z isomer ratio. The results of these experiments are summarised in TABLES 1-3.1 to 1-3.4.

The E/Z isomers were assigned from the ^1H nmr. 1,2-Disubstituted ethylenes could be readily assigned from the coupling constants : $^3J_{HH}(trans) > {}^3J_{HH}(cis)$. It was hoped that the $^4J_{PH}$ would be similarly useful for the trisubstituted ethylenes, but the relative magnitude of the cis and trans J's varied with the substituent R (see FIG.1-3.1) making this technique unreliable. It was postulated[18] that when R = H, the (P-O-C=C) moiety is planar and there is little π-bond contribution to the $^4J_{PH}$ coupling path. With a bulky R group



For R = H $^4J_{PH}(CIS) < {}^4J_{PH}(TRANS)$

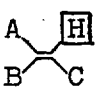
For R = ∅ $^4J_{PH}(CIS) > {}^4J_{PH}(TRANS)$

FIG.1-3.1

(Me or ∅) the system tends to be non-planar which introduces a negative π-bond contribution to the $^4J_{PH}$. As the two coupling constants are opposite in sign,[42] and $|^4J_{PH}(trans)|$ decreases and $|^4J_{PH}(cis)|$ increases on going from R = H to R = ∅, this phenomenon is readily explained if the trans J is positive and the cis J is negative, and both decrease as the (P-O-C=C) moiety becomes non-planar.

The ^1H chemical shifts were used as the main tool for assignment with $\delta_H(E) > \delta_H(Z)$. Application of the substituent shielding coefficients to the equation of Pascual et al,[43] below, was of but limited use as additivity only holds for small substituents :

$$\delta_H = 7.28 + \sigma CIS\ A + \sigma TRANS\ B + \sigma GEM\ C$$



Summary of Stereoselective Vinyl Phosphate Forming Reactions from RCO.CHXY

Basic Reaction :

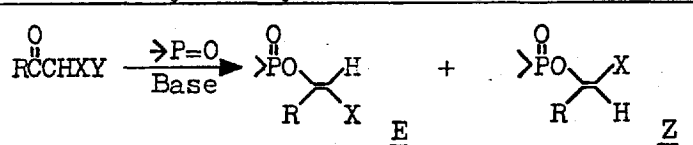


TABLE 1-3.1 Results of the Perkow Reaction

R	X Y	P	Base	Solvent	TEMP	%E	%Z
∅	Br	$(MeO)_3P$	/	MeCN	95°C	1	99
Me	Cl	$(MeO)_3P$	/	MeCN	115°C	92	8
∅ oH	Cl	$(MeO)_3P$	/	MeCN	20°C	40	60
∅ oF	Cl	$(MeO)_3P$	/	MeCN	20°C	12	88
∅ oCl	Cl	$(MeO)_3P$	/	MeCN	20°C	3	97

TABLE 1-3.2 Major Effects on Changing R, X, Y and Base/Solvent Conditions

R	X	Y	P	Base	Solvent	TEMP	%E	%Z
Me	Cl	Cl	$(MeO)_2PO.H$	NH_3 / Et_3N / NaH	MeOH / MeCN / THF	20°C	100	0
Ø	Cl	Cl	$(MeO)_2PO.H$	NH_3	MeOH	20°C	95	5
				Et_3N	MeCN	20°C	95	5
			$(MeO)_2PO.Na$	NH_3	MeOH	20°C	100	0
				Et_3N	MeCN	20°C	100	0
			$(MeO)_2PO.H$	NaH	THF	20°C	100	0
Ø	Br	Br	$(MeO)_2PO.H$	NaH	THF	20°C	0	100
Ø	Me	Cl	$(MeO)_2PO.H$	NH_3	MeOH	30°C	33	67
				Et_3N	MeCN	20°C	20	80
				NaH	THF	20°C	75	25
Ø	Ø	Cl	$(MeO)_2PO.H$	NH_3	MeOH	30°C	100	0

TABLE 1-3.3 Effects of Changing ortho and para Ring Substituents

R	X	Y	P	Base	Solvent	TEMP	%E	%Z
oH	Cl	Cl	$(MeO)_2PO.H$	Et_3N	MeCN	10°C	95	5
oF							60	40
oCl							17	83
Ø oBr							9	91
oMe							77	23
oOMe							5	95
oNO_2							37.5	62.5
pF	Cl	Cl	$(MeO)_2PO.H$	Et_3N	MeCN	10°C	95	5
pCl								
Ø pBr								
pOMe								
pNO_2								
o+pCl	Cl	Cl	$(MeO)_2PO.H$	Et_3N	MeCN	10°C	30	70
Ø o+pMe							83	17
2o+pF							83	17

Significant success in predicting ^1H chemical shifts was obtained through a 'model system' approach using observed substituent chemical shifts (SCS) in analogous compounds to those being studied. This had previously been suggested by Tobey[44] as the only reliable way of allowing for steric interactions between adjacent groups.

The most striking results of the vinyl-phosphate forming reactions are those in TABLE 1-3.3 where the variation of the o-substituent in 2,2-dichloro-

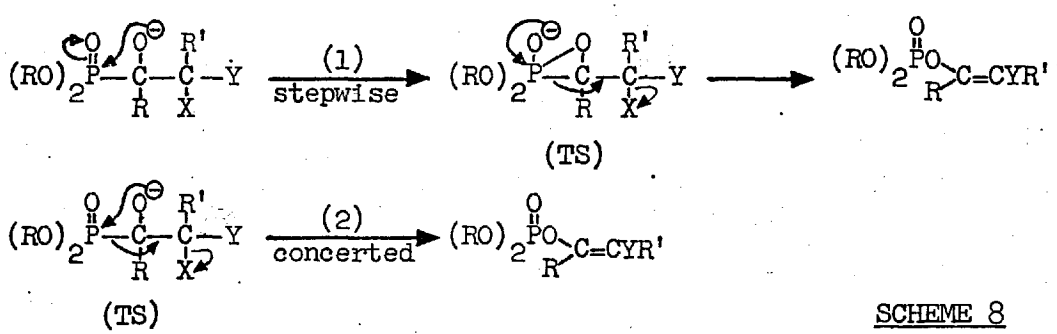
TABLE 1-3.4 Effects of Changing Phosphorus Reagent & Solvent/Base Conditions

R	X Y	P	Base	Solvent	TEMP	%E	%Z
oH						100	0
Ø oF	Cl	$(MeO)_2\overset{S}{\overset{\|}{P}}H$	Et_3N	MeCN	10°C	90	10
oCl						28	72
oCl			NaOMe	MeOH	20°C	40	60
Ø oCl	Cl	$(EtO)_2\overset{S}{\overset{\|}{P}}H$	NaH	THF	20°C	40	60
			NH_3	EtOH		50	50
oH			(1)NH_3	(1)MeOH	(1)20°C	95	5
Ø oF	Cl	$MeO(Me)\overset{O}{\overset{\|}{P}}H$				45	55
oCl			(2)Et_3N	(2)MeCN	(2)10°C	5	95
oH						77	23
Ø oF	Cl	$MeO(Me)\overset{O}{\overset{\|}{P}}H$	Et_3N	MeCN	10°C	35	65
oCl						5	95
Ø	Cl	$MeO(EtO)\overset{O}{\overset{\|}{P}}H$	NH_3	MeOH	20°C	85	15
Ø oCl	Cl	$MeO(Et)\overset{O}{\overset{\|}{P}}H$	NH_3	MeOH	20°C	0	100

The assignment of the E/Z isomers Presented in TABLES 1-3.1 to 1-3.4 was performed as noted in the text. The E/Z ratios were determined by averaging the integration from the ^1H nmr peaks and from the g.l.c. trace, which were always in close agreement.

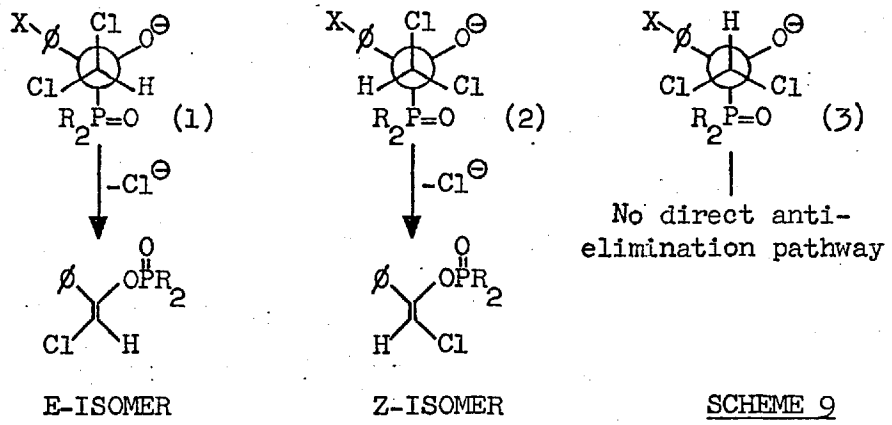
2'-substituted acetophenones has a marked effect on the E/Z isomer ratio.

The vinyl-phosphate forming reaction proceeds firstly to the α-hydroxy-phosphonate by an addition reaction (see step (B-1), SCHEME 3). The next, elimination step, may proceed by either a penta-covalent phosphorus species as an intermediate (PATHWAY 1), or as a concerted process (PATHWAY 2) SCHEME 8.



SCHEME 8

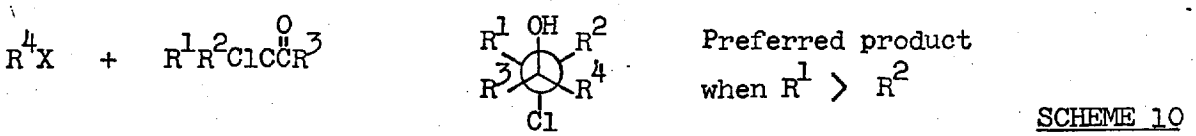
As kinetic studies were beyond the scope of the work, a mechanism could not be established. It was assumed that in either case the transition state (TS) for the elimination involved an anti-periplanar arrangement of the ($P-C_1$) and (C_2-X) bonds. Where X = Y = Cl, two such orientations could arise and the geometry of the final product was determined by the preferred conformations in the transition state (see SCHEME 9).



SCHEME 9

It was concluded[18] that a preponderance of E-isomer would occur where there is little interaction between the phenyl and dichloromethyl groups (ie. para X substituent). Under these conditions, Rotamer (1), with the negative oxygen moiety adjacent to the hydrogen atom on C-2, is preferred.

This situation is similar to that envisaged in Cram's rule for carbonyl addition reactions, which states that the preferred conformation is that in which the carbonyl group is flanked by the smallest group on the α-carbon.[45] Similarly, in additions of a nucleophilic reagent (R^4X) to α-chloro carbonyl compounds ($R^1R^2ClC.CO.R^3$) the major chlorohydrin product was predicted by Cornforth[46] to be that in which R^4 was anti to the larger group of R^1 and R^2 when the chlorine and hydroxy groups were also anti to each other (SCHEME 10).



SCHEME 10

An ortho substituent on the phenyl ring has a marked effect on the course of the elimination (see TABLE 1-3.3); (X = H,F,Me) gave predominantly the E-isomer, whilst (X = Cl,Br,OMe,NO_2) gave mainly the Z-isomer of the vinyl phosphate. The size of the ortho substituent could not be the only factor controlling the isomer ratio as the ortho methyl derivative (sterically similar to chlorine or bromine) gave 77% E-isomer. It was therefore proposed that the ortho substituents were interacting with the oxygen anion on the α-carbon in the reaction transition state.

An analagous system of several ortho substituted 4-fluoro-α,α-dimethyl benzyl alcohols had previously been studied in these laboratories.[47] Analysis of the ^{19}F chemical shift data indicated that ortho X = H,F,Me substituents

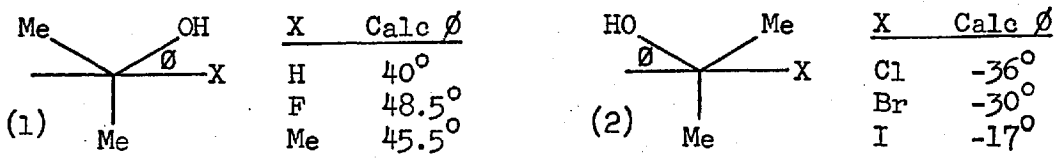


FIG.1-3.2

adopted conformation (1) (see FIG.1-3.2) whilst X = Cl,Br,I preferred (2).

If such alignment of the ring substituent and oxygen atom was present in the α-hydroxyphosphonate anion species then in the compounds with X = H,F,Me there would be little interaction between the ring substituent and the prochiral C-2 group. This would therefore adopt the preferred rotamer ((1) in FIG.1-3.3) as the major conformer, with a lesser amount of (2), and subsequent elimination would give the E-isomer as the major product.

With X = Cl,Br,OMe,NO_2 the ring substituent would lie away from the negative oxygen moiety and be well placed to interact with the two chlorines on C-2. This repulsive interaction would favour rotamer (2) over rotamer (1) and the Z-isomer should predominate :

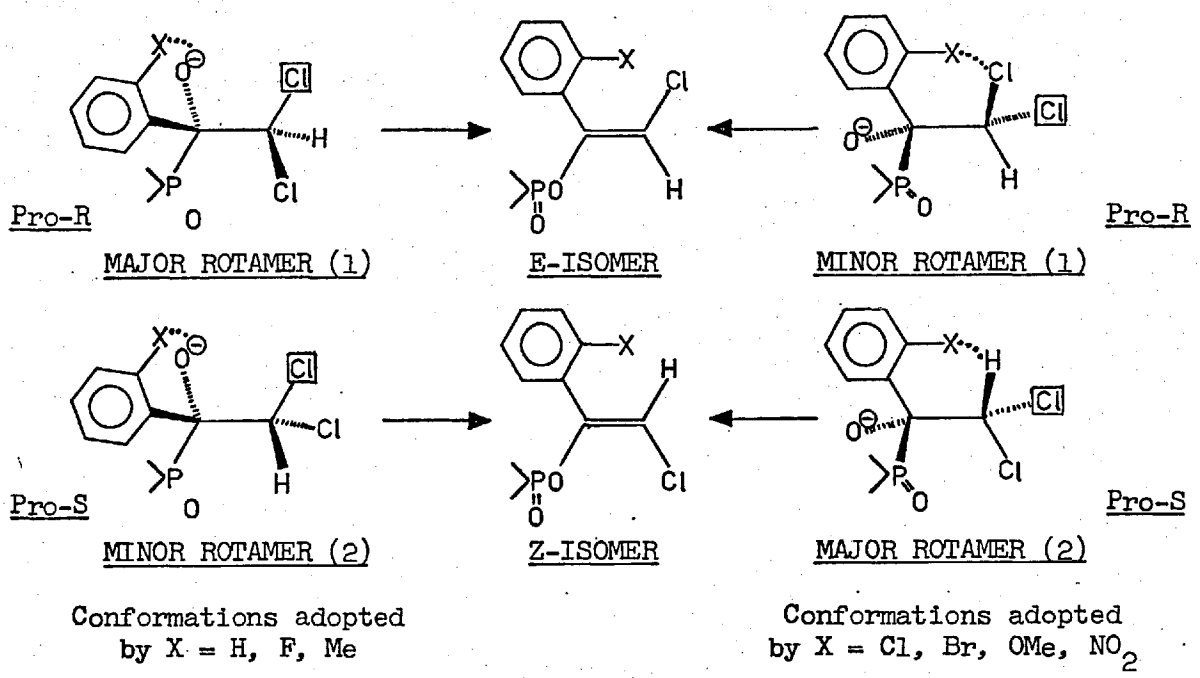
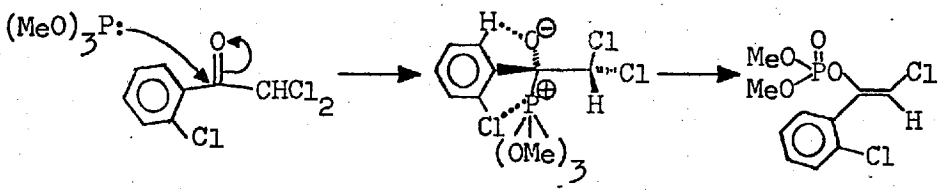


FIG.1-3.3 The descriptors Pro-R/S refer to the boxed chlorines. These are preferentially eliminated as they are anti-periplanar to the phosphoryl group.

Similar arguments explained the course of the reactions with the 2',4'-disubstituted (X = Cl,Me) and the 2',4',6'-trifluoro-acetophenones (the small size of the second ortho fluorine explained the lack of Z-isomer preference). It was suggested[18] that $^3J_{PH}$ coupling constants of the α-hydroxyphosphonate intermediates would have confirmed the proposed structuring of the transition state ($^3J_{PH}$ having a Karplus[48,49] relationship to the dihedral angle,[50] see SECTION 1-5-1), but these compounds were too reactive to isolate.

On changing the reactivity of the phosphorus reagent (see TABLE 1-3.5) the E:Z isomer ratio was still mainly determined by the ortho phenyl substituent. Trimethyl phosphite was slightly different as it carried out this reaction without added base (the Perkow Reaction), but otherwise appeared to conform to the structural habits of the dialkyl phosphonates and phosphinates

in the intermediate :



SCHEME 11 The Perkow Reaction

The varying ratios of the E:Z isomers produced with the five phosphonating reagents was linked to their reactivity. For the more reactive reagents, the transition state should resemble the preferred conformation in the acetophenone. Cram's rule[45] would apply, and the E-isomer would predominate. This represents kinetic control of the reaction.

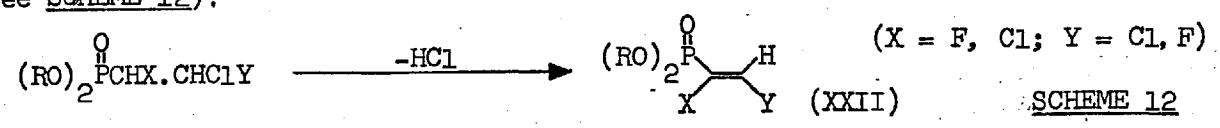
For a less reactive phosphorus reagent, the intermediate should be produced in equilibrium with the starting materials, giving ample time for the repulsive interactions between the ortho substituents and the chlorine atoms on C-2 of the intermediate to fully develop. This represents thermodynamic control and the Z-isomer would predominate.

TABLE 1-3.5 Effects of Modifying the Phosphorus Reagent on the E:Z Isomer Ratio

Increasing Reactivity (nucleophilicity)

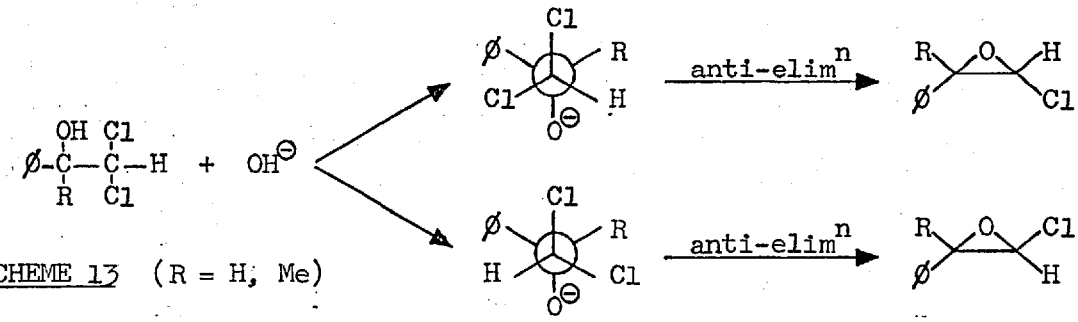
Deriv X	H		o-F		o-Cl	
P Reagent	%E	%Z	%E	%Z	%E	%Z
$(MeO)_3P$	40	60	12	88	3	97
$MeO(Me)P(=O)H$	77	23	35	65	5	95
$MeO(Me)P(=S)H$	95	5	44	56	5	95
$(MeO)_2P(=O)H$	95	5	60	40	17	83
$(MeO)_2P(=S)H$	100	/	90	10	40	60

The concept of elimination from the preferred rotamer controlling the geometry of the olefin product is supported by observations of the dehydrochlorination of 2-chloro alkyl phosphonates (XXI), the ground state conformations of which were determined by ^{1}H and ^{19}F nmr studies.[51] These eliminations occurred stereospecifically by both syn- and anti- routes probably via an ElcB mechanism, to form olefins in which X and Y are cis (XXII), an arrangement resembling that found in the ground state (see SCHEME 12).



SCHEME 12

The epoxide-forming reactions of Nouri-Bimorghi[52,53] were cited[18] as the only similar literature examples. In these elimination reactions both 2,2-dichloro-1-methyl-1-phenyl ethanol and 2,2-dichloro-1-phenyl ethanol formed just one epoxide (geometry unspecified) on treatment with potassium hydroxide (see SCHEME 13).



SCHEME 13 (R = H, Me)

Worthington suggested that if the proposed interactions between the ortho substituent and the dichloro methyl group in the α-hydroxyphosphonates were correct, then similar changes in the nature of the ortho substituent in the 2,2-dichloro-1-phenyl ethanols should bring about preferences for different isomers in the epoxide-forming eliminations.

This has been persued in the current work. These compounds have proved to be good models for the interactions suggested for the reactive intermediate in the "abnormal" Michaelis-Becker Reaction, as their preferred conformers may be examined whereas those of the α-hydroxyphosphonates could not. Their structures have been determined from the various coupling constants across the "free-rotation" bonds and from a study of the effects of adding Lanthanide Shift Reagents (LSR) to them in solution.

The directly analogous elimination reactions for the 2,2-dichloro-1-fluoro-1-phenylethanes have also been fully investigated. These were an obvious choice as inclusion of the fluorine atom greatly increases the nmr data, especially coupling constants, available in determining the geometries of both the starting materials and the elimination products.

A series of 1,2,2-trichloro-1-phenyl ethanes was also prepared with the intention of examining both their nmr properties and the products of elimination. Preliminary elimination reactions, however, showed significant reverse elimination of the C-1 chlorine. This, and the inherent difficulties in determining the geometry of the tri-substituted ethylene elimination products, heralded the abandonment of this set of reactions.

For comparative purposes it was desirable to have the same range of ortho and para derivatives in these series of compounds. A variety of electron withdrawing and donating groups were chosen in order to ascertain the electronic effects on preferred conformation. Availability of the starting materials and difficulties in synthesizing precursors led to a final total of fifteen compounds in each of the three series. These were (in Hammett Order) : ortho and para : OMe, Me, H, F, Cl, Br, CF_3, NO_2.

This number and range of compounds generated sufficient data for a realistic assessment of the properties of the three series.

1-4 Elimination Reaction Mechanisms

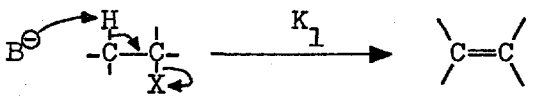
Kinetic studies were not carried out as part of this work, and as such no direct evaluation of the mechanisms of either the olefin-forming (β-) or epoxide-forming (γ-) eliminations could be undertaken. Analogy with the work of others, and scrutiny of the results does, however, make discussion of the mechanisms plausible. A resumé of the characteristics of the main mechanisms[54] will therefore be given as a background to this discussion.

1-4-1 The Main Mechanisms

The illustrations in this section will be confined to 1,2-(β-)eliminations, although much of the material also applies to 1,3-(γ-) and 1,4-(δ-)eliminations.

1-4-1.1 The E2 Mechanism ("Elimination, bimolecular")

This is the most common elimination mechanism and is typified by the base-induced loss of HX from a saturated hydrocarbon, to form an olefin (SCHEME 14). The accepted mechanism was proposed by Hanhart and Ingold in 1927.[55] The process is concerted and follows second order kinetics[56] (EQN.1).

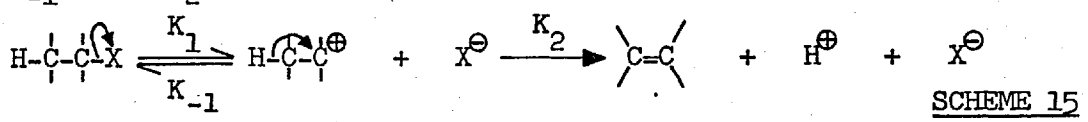


SCHEME 14

$$\text{Rate} = K_1[B^{\ominus}][RX] \qquad \text{EQN.1}$$

1-4-1.2 The E1 Mechanism ("Elimination, unimolecular")

This elimination occurs in the absence of base, as a reversible ionisation followed by the faster loss of a proton[57] (SCHEME 15). The overall rate of the reaction (EQN.3) may be deduced from the steady state approximation of the carbonium ion concentration (EQN.2). Normally the ionisation is irreversible ($K_{-1}[X^{\ominus}] \ll K_2$) and the rate reduces to first order (EQN.4) :



SCHEME 15

$$\frac{d[R^{\oplus}]}{dt} = 0 = K_1[RX] - K_{-1}[R^{\oplus}][X^{\ominus}] - K_2[R^{\oplus}] \qquad \text{EQN.2}$$

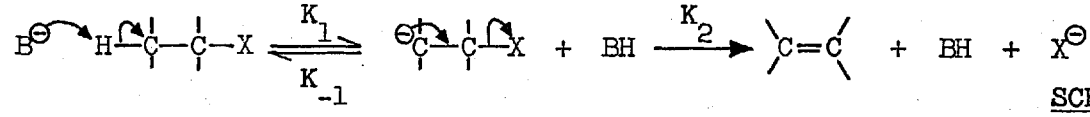
$$\text{Rate} = K_2[R^{\oplus}] = \frac{K_1K_2[RX]}{K_{-1}[X^{\ominus}] + K_2} \qquad \text{EQN.3}$$

$$\text{Rate} = K_1[RX] \qquad \text{EQN.4}$$

This mechanism need not be considered further, as apart from the small amount of auto-elimination observed in the 1,2,2-trichlorophenyl ethanes, all the eliminations performed in this study had to be induced by fairly strong bases.

1-4-1.3 The ElcB Mechanism ("Elim. unimolecular, from the conjugate base").

This is similar to the E2 mechanism, being promoted by a base-induced removal of the β-proton, but with the resulting carbanion stabilised and the leaving group departing in a separate step[58] (SCHEME 16).



SCHEME 16

By utilising the steady state approximation for the carbanion concentration the overall rate may be deduced in a similar manner to the E1 mechanism (EQN.5).

$$\text{Rate} = K_2[R^{\ominus}] = \frac{K_1K_2[RH][B^{\ominus}]}{K_{-1}[BH] + K_2} \qquad \text{EQN.5}$$

If the second step is much faster than the reversion to the starting material, the rate limiting step (r.l.s.) is the initial formation of the carbanion and the kinetics become second order and indistinguishable from E2 (EQN.1). Alternatively, if the rate of reversion to starting material dominates, the kinetics become more complex and in theory, distinguishable from E2 :

$$\text{Rate} = \frac{K_1K_2[RH][B^{\ominus}]}{K_{-1}[BH]} \qquad \text{EQN.6}$$

A third limiting case has been investigated by Bordwell[59] and Rappoport.[60] If the substrate is very acidic but the leaving group is poor, as excess of base will rapidly generate the carbanion which will then slowly undergo first order decomposition to products. Under these conditions the reaction will be first order in substrate but zero order in base (EQN.7).

$$\text{Rate} = K_2[RH] \qquad \text{EQN.7}$$

1-4-1.4 The Variable Transition State Theory

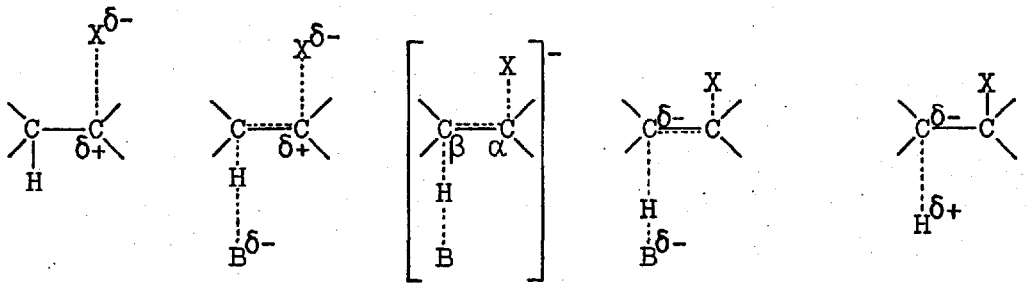
The idealised E2 mechanism involves the simultaneous formation of a base-hydrogen bond and a carbon-carbon π-bond, and the breaking of a hydrogen-carbon bond and a carbon-leaving group bond.

In the variable transition state theory the timings of these processes are expected to vary slightly under different circumstances, and hence in the transition state itself some processes may be more advanced than others.

Variation in the structure of the elimination transition state was cited by Cram et al[61] to explain observations of rate changes on modifying experimental parameters (leaving group, base, etc.). Similar theories by other authors were collated by Bunnett[62] who presented a comprehensive review of the theory and implications of the "variable transition state".

In the full realisation of this theory[63] the original concepts of three distinct elimination mechanisms become blended together in a "spectrum" of reactions; variations of the concerted E2 reaction forming the middle of this spectrum, with the stepwise E1 and E1cB mechanisms at the two extremes (see FIG.1-4.1). The prefix "Paene" (Latin = almost) was coined by Bunnett.

The transition state utilised in a particular reaction system may be predicted to some extent from the structure of the substrate. Thus introduction of an electron-withdrawing group at C_β should shift the transition state character to the right, whilst electron donors at C_α should give a leftward shift.[63] The central transition state should be stabilised by the same factors that stabilise the final product, and should have similar geometry.[61]



The Bunnett Variable E2H Transition State Spectrum FIG.1-4.1

It was further proposed[62] that the transition state in the central mechanism need not occur at 50% rupture of the C-H and C-X bonds and 50% formation of the C-C π-bond but could occur at any other point where these three processes were equally advanced. The ability of the transition state to be "Reactant-like" or "Product-like" completes the Bunnett elimination spectrum.

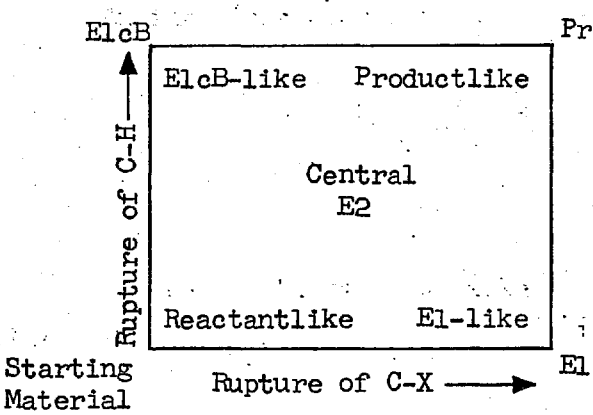
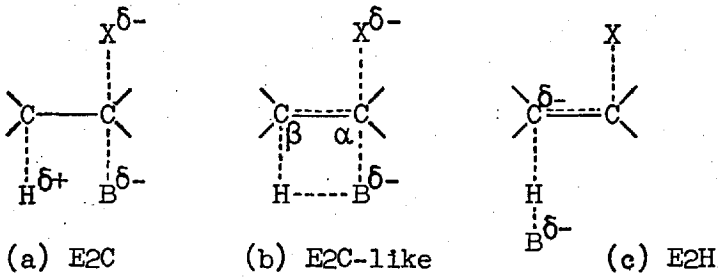


Fig 1-4.2 An ingenious schematic representation, developed by Závada et al,[64] illustrates all possible variations in elimination transition state structures with the exception of the syn- and anti- stereochemical types.

Observations that very weak bases which are good S_N2 nucleophiles, such as thiolate ions[65,66] and halide ions in acetone,[67] were some ten times more efficacious in inducing eliminations in tertiary-butyl chloride than ethoxide

ions in ethanol[65] (which is a factor of 10^{10} stronger as a base) lead to a search for a significantly different transition state for this type of system.

The common feature throughout the Bunnett spectrum[63] (FIG.1-4.1) is that the base attack is always at the β-proton. This system has therefore been labelled as E2H.[68] An alternative transition state spectrum was proposed by Winstein and Parker[69] to cater for the new circumstance. The initial suggestion[67] that the S_N2 and E2 reactions might proceed from a common intermediate, in which the nucleophile was bound to both the α-carbon and β-proton, was rejected[70] because the anti-stereochemistry of the elimination was retained even when the base and leaving group were identical. The so-called Winstein-ParkerE2C-E2H Transition State Spectrum[69] (FIG.1-4.3) favours base to α-carbon interactions for weaker bases and merges into the Bunnett Spectrum in the ElcB-like region as the base strength or substrate acidity increase.



(a) E2C (b) E2C-like (c) E2H

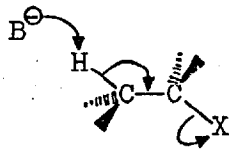
FIG.1-4.3 The Winstein-Parker E2C-E2H Transition State Spectrum

Numerous arguments have been presented for and against these two theories,[71] the deficiencies of which an intermediate spectrum by McLennan[68] has tried to circumnavigate. For our purposes an awareness of the continuum of mechanisms from E2 to ElcB should suffice.

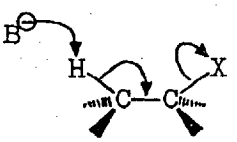
1-4-2 Stereochemistry

At one time it was thought that as the E2 mechanism is concerted, it should proceed stereospecifically via an anti-pathway; and since the carbanion intermediate in the ElcB mechanism is not configurationally stable, it should have no important stereochemical consequences. Both of these views, although largely true, have proven to be drastic over-simplifications.

As stated earlier, the idealised E2 reaction involves the synchronous making and breaking of four bonds, with two extreme geometries for the C_α-X and C_β-H bonds in the transition state of the process, ie. anti-periplanar or syn-periplanar[15] (see FIG.1-4.4). Planar alignment of the bonds involved is favoured on stereo-electronic grounds as this arrangement provides maximal orbital overlap for transfer of charge. As there is no readily available method of distinguishing between "periplanar" and "clinal" orientations in the transition state, it is normal practice to simply refer to anti- and syn-eliminations.



anti-periplanar



syn-periplanar

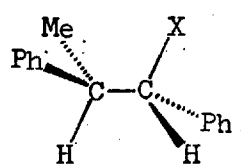
Preferred elimination transition states.

FIG.1-4.4

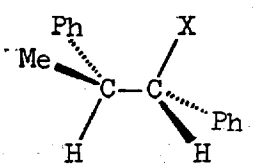
In the majority of elimination reactions the observed anti/syn preference is of the order of 1000.[72] Many factors have been invoked to explain this vast difference between arrangements which are quantum mechanically very similar.[54]

Electrostatic repulsion of the base and leaving group favours anti-elimination.[73] In the anti-orientation, electrons released from the C-H bond can displace the C-X bond by rear attack.[74,75] Steric repulsions in the staggered (anti-) configuration are likely to be at least 3Kcal/mole less than in the eclipsed (syn-) configuration. McLennan has pointed out that this factor alone makes the anti/syn ratio ~160.[76]

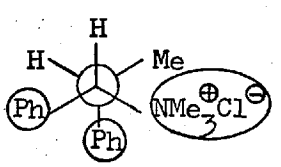
In the majority of cases where the syn- pathway dominates, elimination takes place across a bond which is rotationally constrained by the system, ie. within cyclic[77] or bicyclic[78] structures. Even in aliphatic cases of syn-elimination there is usually considerable steric congestion and the structure giving rise to the syn- pathway is closer to that of minimum energy than the anti- structure.[79] Cram et al[61] studied eliminations from a series of 1,2-diphenyl-1-X-propanes (X = Cl, Br, $NMe_3^{\oplus}$) with a range of solvent/base conditions. In every case the threo isomer (see FIG.1-4.5) gave the expected trans olefin and the erythro isomer, with the exception of X = $NMe_3^{\oplus}$, gave the cis olefin.



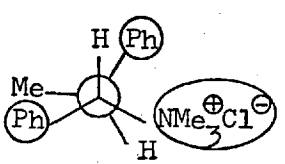
(a) THREO



(b) ERYTHRO



(c) ANTI-ROTAMER



(d) SYN-ROTAMER
Preferred as less steric conjestion

FIG.1-4.5

The preferred syn-elimination of the erythro isomer to the trans olefin when X = $NMe_3^{\oplus}$ may be rationalised by comparing steric congestion in the two rotamers (c) and (d) in FIG.1-4.5 (the bulkier groups are circled).

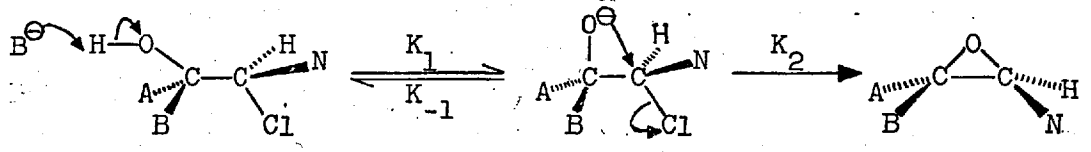
A recent quantum mechanical treatment by Charton has shown that steric considerations are probably more important than electronic factors in controlling the course of E2 eliminations from substrates with bulky β-alkyl groups.[80]

In the absence of recognisable extenuating circumstances the anti-rule for E2 eliminations from alicyclic reactants should apply.

If, in the ElcB reaction, the carbanion intermediate is fairly stable,

rotation of the C_α-C_β bond may be expected to occur before the second, elimination, step takes place. The stereochemical outcome will therefore be unpredictable. If on the other hand, the carbonium ion is fairly short lived, and external structural factors limit the rotation of the C_α group, some retention of configuration might be expected. Whether the mechanism is formally syn- or anti- would depend on the preferred structure of the starting material.[51]

The formation of epoxides (oxiranes) from the dehydrochlorination of chlorohydrins has been shown to proceed via a γ-ElcB mechanism,[81] with a formal anti-pathway leading to inversion at C_α (see SCHEME 17).[82,83]

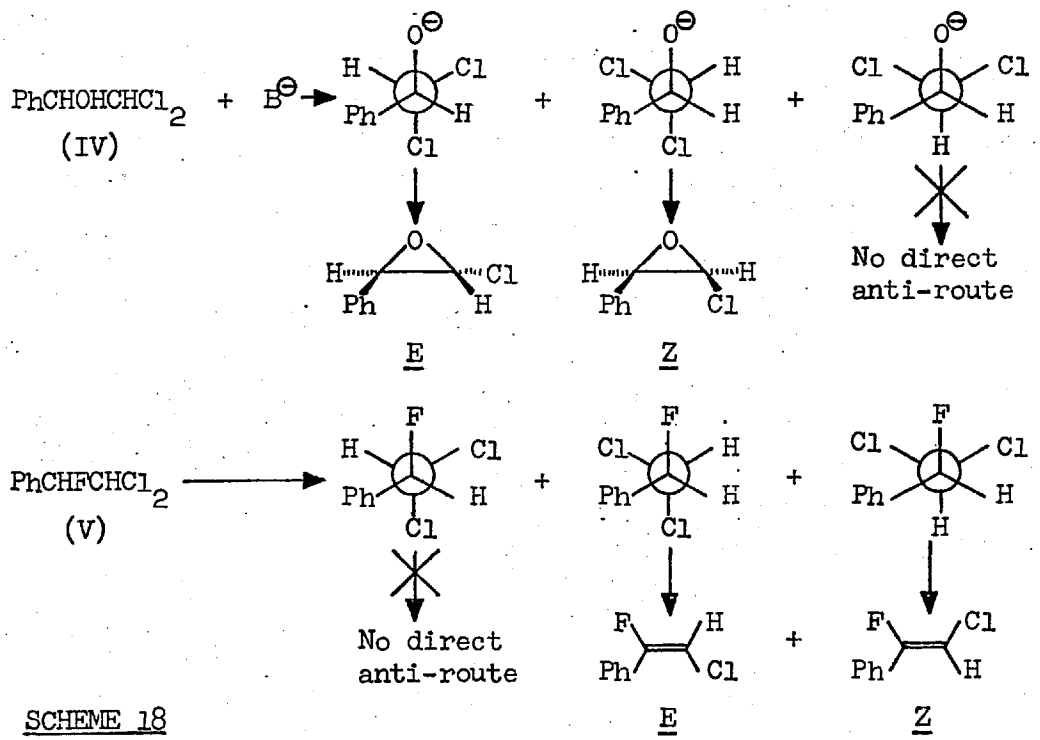


SCHEME 17

The rotation of the C_α group prior to the second step in order to attain the anti-configuration of the X-group would doubtless take place if this rotamer was not already significantly populated.

1-4-3 A Survey of the Pertinent Literature

In the current work, the results of two different sets of elimination reactions have been interpreted in the light of predicted rotamer preferences for the starting materials (see SCHEME 18). Both the olefin-forming



SCHEME 18

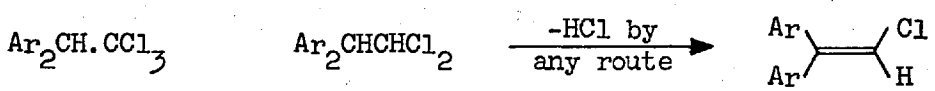
β-eliminations and epoxide-forming γ-eliminations have one proton available for abstraction by the base, while having a choice of two "identical" chlorine leaving groups. Even if the anti-mechanism operates exclusively, both series

can produce both the E and Z isomers by eliminating either of the diastereotopic chlorines.

As the reactions involved are dissimilar, the β-elimination may be E2 or ElcB whilst the γ-elimination is probably all ElcB; they will be dealt with separately.

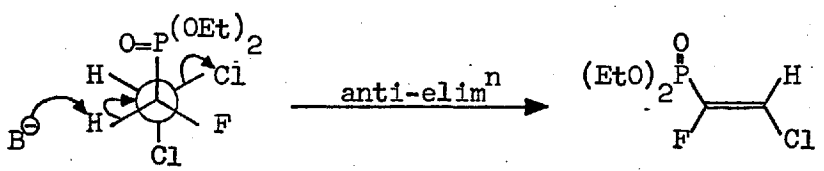
1-4-3.1 Olefin-forming β-Eliminations

It is common in the literature to find studies with a choice of β-protons for abstraction by the base (frequently on different carbons, leading to discussions of Hofmann[84,55]/Saytzeff[85] preferences)[54] but there are seldom cases with a choice of geminal leaving groups. In the cases of DDT (XXIII)[86] and DDD (XXIV)[87] studied by McLennan et al, both have choices of geminal leaving groups, but as the α-carbon is prochiral in both cases neither have interesting stereochemical consequences and no conclusions about the elimination pathway (syn/anti) can be drawn (SCHEME 19).



(XXIII) DDT (XXIV) DDD (Ar = pClC$_6$H$_4$-) SCHEME 19

The only literature example of a conventional β-elimination towards diastereotopic leaving groups, is that of Boyce et al.[51] Full nmr analysis of a series of 1,1,2,2-tetrasubstituted ethanes of which (XXV) is a member, showed that they exist predominantly in the single conformation in which the two hydrogens are gauche. Mild elimination (triethylamine in refluxing ether for seven days) proceeded stereospecifically by the anti-route to the E-vinyl phosphonate (XXVI) (SCHEME 20).

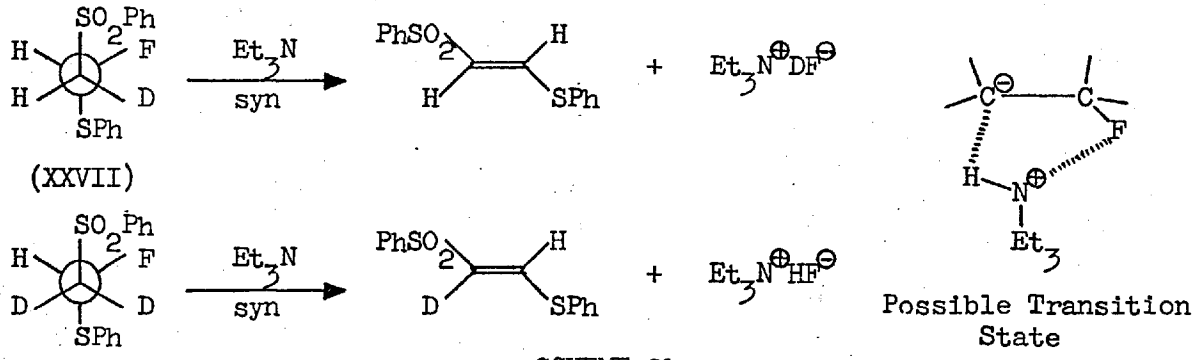


(XXV) (XXVI) SCHEME 20

Alunni and Baciocci have produced a series of papers in which they examined the cis/trans olefin ratios of compounds of the general type PhCH$_2$CHXMe, (X = Br, I, OTs).[88] They cite anti-stereochemistry with a predominance of the trans isomer (which has much less steric conjestion in the transition state than the cis isomer).

Most authors have interpreted their β-eliminations as concerted E2 or ElcB-like processes. The ElcB mechanism has found favour where α-electron withdrawing or resonating groups are present. DDT[86] has been shown to eliminate entirely by the ElcB mechanism whilst DDD[87] only uses this mechanism

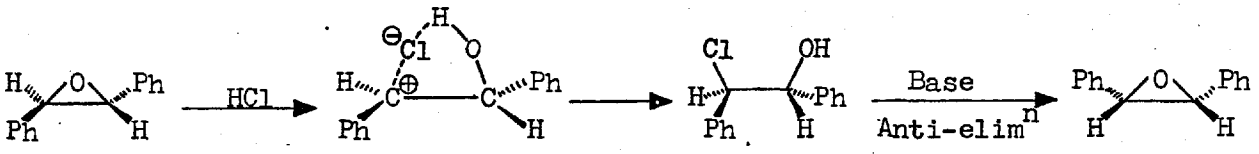
20-30% of the time. Rappoport[89] concluded that the base-promoted elimination of phenoxide from XCH_2CH_2OPh (X = electron-withdrawing group eg. NO_2, Ac, Bz) followed E1cB kinetics, whilst Fiandanese et al[90] interpreted the syn-stereospecific elimination of HF from the sulphonyl-activated fluoroethane (XXVII) as involving an E1cB mechanism with possible ion pairing (SCHEME 21).



SCHEME 21

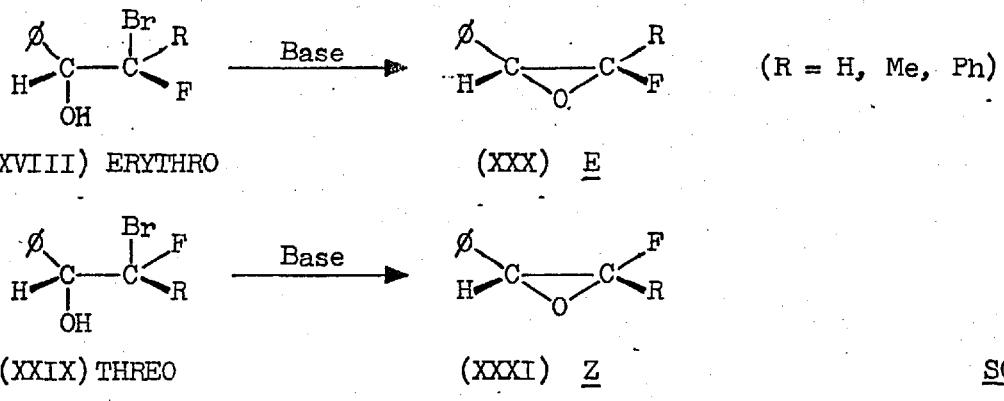
1-4-3.2 Epoxide Forming γ-Eliminations

The stereochemistry of epoxide synthesis was comprehensively reviewed by Berti[91] in 1974. He found that the majority of epoxides formed by 1,3-elimination reactions were derived from β-halohydrins (sometimes generated in situ), although other leaving groups such as tosylate, sulphonate and quaternary ammonium salts were also used. The mechanism of elimination was E1cB and the geometry of the products was consistent with an anti-periplanar arrangement of the hydroxy and leaving groups. An interesting demonstration of this is the ring opening of trans stilbene oxide, with hydrogen chloride in chloroform, which occurs by an ion-pairing mechanism (see SCHEME 22) to produce the threo-chlorohydrin exclusively. Subsequent recyclisation with base produces the cis-epoxide stereospecifically.[92]



SCHEME 22

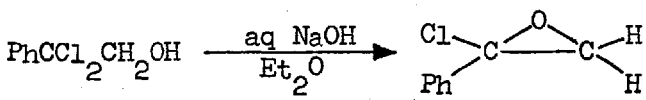
Elkik and Le Blanc[93] prepared several α-fluoro epoxides by elimination of HBr from mixtures of the diastereotopic alcohols (XXVIII) and (XXIX). They observed that the relative percentages of the E-(XXX) and Z-(XXXI) epoxides formed, corresponded to the ratio of the integrations of the ^{19}F signals of the erythro- (XXVIII) and threo- (XXIX) signals respectively. The sole participation of the anti-mechanism is apparent from this data (see SCHEME 23). A previous study by Atlanti and Leroy[94] on isomeric compounds had produced similar results.



SCHEME 23

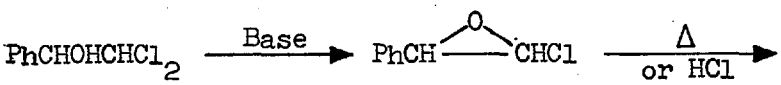
Unlike the β-eliminations, considerable work has been performed with γ-eliminations in which there are two geminal leaving groups. Even so, there has been relatively little investigation of the stereochemical consequences of this arrangement.

The bulk of these studies appear in the French literature, and are centered on the original and continuing work of Kirrmann, Duhamel and Nouri-Bimorghi,[95] who were the first group to successfully isolate and fully characterise α-chloro epoxides (SCHEME 24).



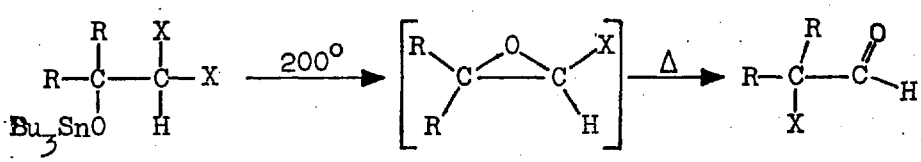
SCHEME 24

The main interest in these compounds was in their thermal and acid-induced rearrangements; so much so, that in subsequent papers,[96,97,98] where the preparation of the isomeric 2-chloro-1-phenyl ethylene oxide from 2,2-dichloro-1-phenyl ethanol was reported, on mention was made of its geometry :



SCHEME 25

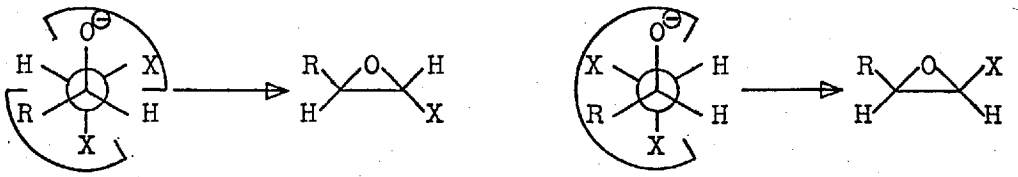
Delmond et al[99] have reported a series of studies involving the elimination of tributyl tin chloride from compounds analogous to those of Nouri-Bimorghi. Again the main interest was in the α-haloaldehyde product, although the symmetry of the starting materials excluded stereoisomers of the epoxide intermediate (SCHEME 26).



(R = H, Me; X = Cl, Br) SCHEME 26

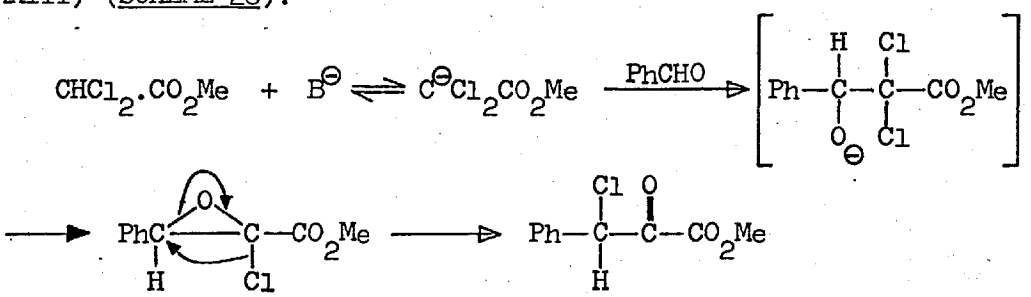
A geometry for the α-haloepoxides was first mentioned by the Duhamels. They prepared three α-haloepoxides[100,101] by elimination of HX from the corresponding alcohols ($RCHOHCHX_2$; R = ^{t}Bu, X = Cl, Br; R = $pNO_2\emptyset$, X = Br) and

showed from the $^{3}J_{HH}$ (all 1.0 - 1.5Hz) that the three products all had trans geometries. This indicates anti-elimination from the least-hindered rotamers :



(LEAST HINDRANCE) TRANS (MOST HINDRANCE) CIS SCHEME 27

Two years prior to Nouri-Bimorghi's isolation of the first α-chloro-epoxide, Martinov and Titov[102] had reported the preparation of the α-chloro-α-ester epoxide (XXXII) by the Darzens reaction[103] (see review ref. 91). From the data presented by the Russians, however, McDonald and Schwab[104] were able to show that they had in fact isolated the isomeric 1-chloro-1-phenyl-pyruvate (XXXIII) (SCHEME 28).



(XXXII) (XXXIII) SCHEME 28

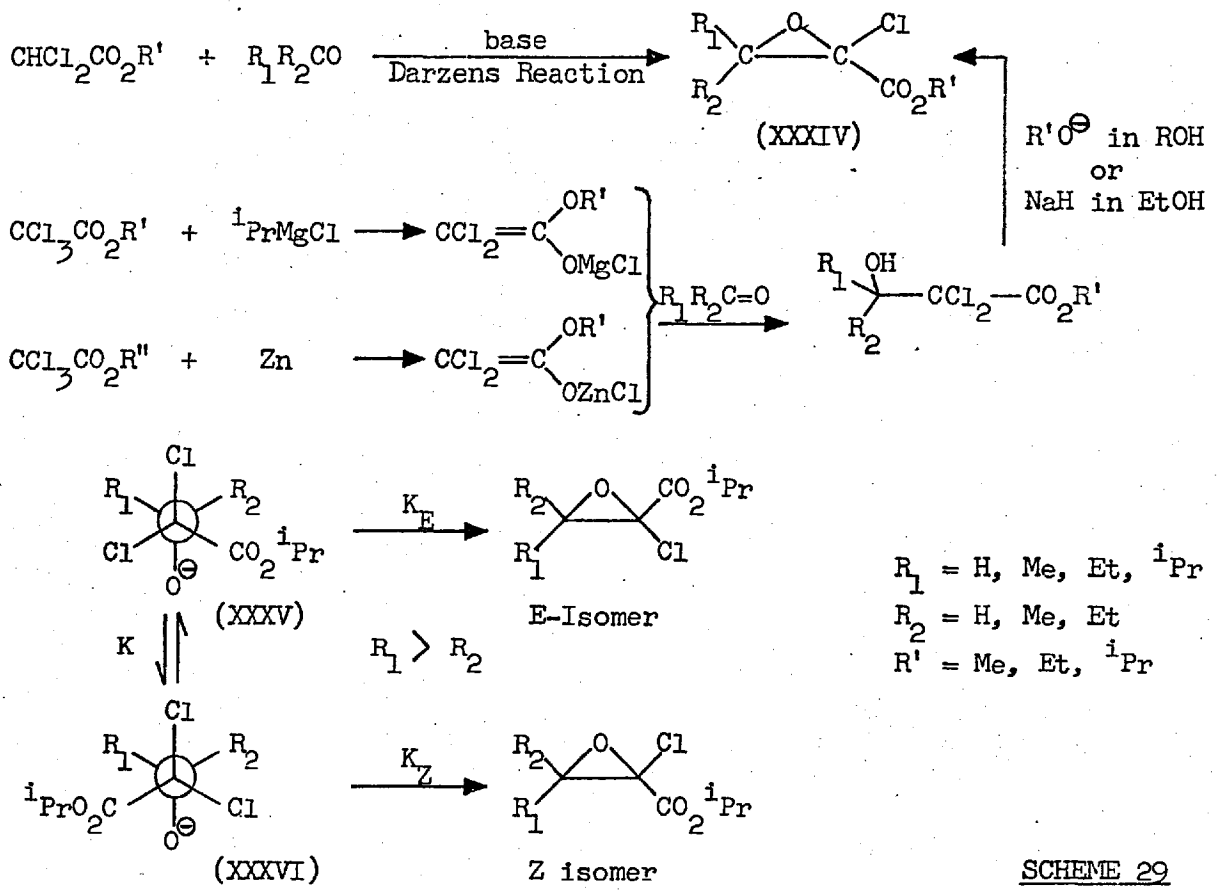
Compounds of this type were eventually prepared by Villieras et al,[105,106] using both the Darzens route, and a modification of the Nouri-Bimorghi route. The base for the latter route had to be similar to the group R' (SCHEME 29) in order to prevent transesterification. For one compound, sodium hydride in ether[105] was successfully used. The geometry of a series of epoxides (XXXIV) (R' = ^{i}Pr) produced by the Darzens reaction was determined by nmr. This indicated that the E:Z isomer ratio from this reaction was dependent on the relative size of R_1 and R_2 (see TABLE 1-4.1).

R_1	R_2	%E
Me	H	100
Et	H	100
^{i}Pr	H	100
^{i}Bu	H	100
Me	Me	(50)
Et	Me	75
^{i}Pr	Me	95

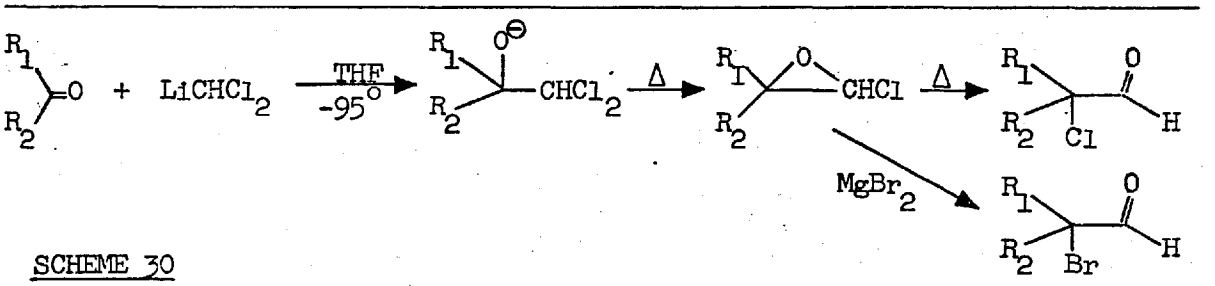
TABLE 1-4.1 Product Ratios of Darzens Reaction

The authors interpreted these results in terms of rapid interchange between the two rotamers (XXXV) and (XXXVI) with the ratio of elimination from the less hindered rotamer (XXXV) being faster than from the more hindered rotamer (XXXVI) ie $K > K_E > K_Z$.

Several more recent papers[107,108] have used the $LiCHCl_2$ modification of the Darzens reaction (SCHEME 30) as a route to forming α-haloaldehydes. The geometry of the α-haloepoxide intermediates received little attention as migration of the chlorine in the ring opening turns the α-carbon into an aldehyde.

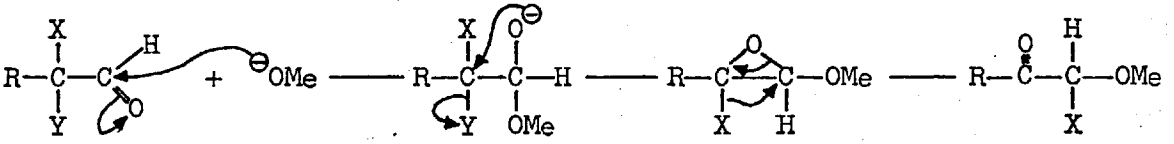


SCHEME 29



SCHEME 30

Finally Fougerousse and Riehl[109] have studied the addition/elimination reaction of methoxy ion to aldehydes of the general type (XXXVII). Unfortunately, all attempts to isolate the epoxide (XXXVIII) failed, as only the rearrangement product (XXXIX) is stable (SCHEME 31).



(XXXVII) (XXXVIII) (XXXIX)

Where (X = Y = Cl ; X = Y = Br ; R = pentyl, hexyl, phenyl) SCHEME 31

1-5 Structure Determination in Solution

In this work, we hope to prove that the results of the elimination of HCl from two series of similar compounds may be interpreted as arising from preferred conformations present in the ground state prior to reaction. An important part of this study, therefore, is to establish, by methods

independent of elimination results, that such preferences exist.

As the evidence presented in the previous section shows, the products of elimination reactions are expected to resemble the structures of the transition states. Similar criteria may be applied to other chemical processes, which make them an inappropriate tool for examining the ground state structures. We must turn, therefore, to physical techniques.

The obvious method of examining conformations in the solid state is X-ray crystallography, but the relevance of such observations to the structures pertaining in solution is arguable.

All of the three main spectroscopic techniques available to the organic chemist (UV, IR, NMR) may be performad in solution. Calculating rotamer preferences in complex molecules is, however, beyond the scope of standard low-resolution infrared spectroscopy. Also in this instance, electronic (UV/visible) spectroscopy would be of little help as alterations in the conformation of a side-chain, into which there is no conjugation, will have negligible influence on the $\pi \rightarrow \pi^*$ transitions in the phenyl ring. Furthermore any variations observed may be attributable to alterations in the excited (π^*) state and not in the ground state.

Fortunately there exist several well tried methods of studying conformation using various aspects of the nmr experiment. These fall into three fields :

(a) Coupling constants across the bonds in question (mainly ^3J constants).

(b) Chemical shifts of groups attached to the bonds and affected by their rotation.

(c) Lanthanide Induced Shifts (LIS).

Others have dealt comprehensively with these subjects in rigid, and to a lesser extent, in 'free' and 'hindered' rotation molecules. Here our interests lie in the latter case and so the discussion of these topics will be mainly in this area.

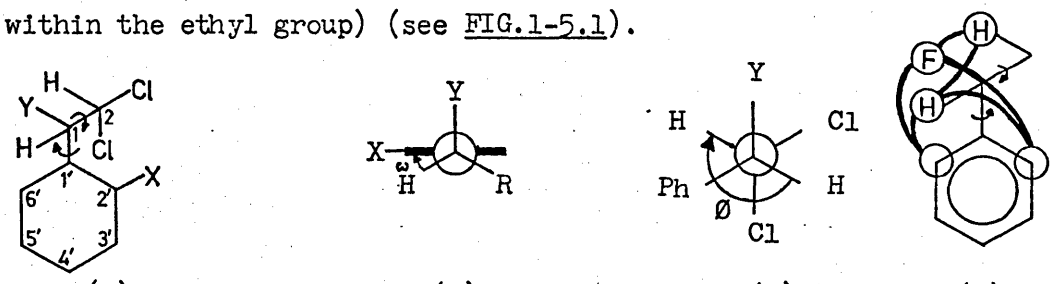
LIS is potentially the most powerful tool of the three in examining the overall conformation of a molecule, but the interpretation of LIS data is not completely straightforward and there may be considerable limitations in its sensitivity to moderately large rotational changes.

The structure determination of the elimination products (which have rigid side-chains) will be dealt with in Chapter 7.

1-5-1 Conformation Dependence of Coupling Constants

In the phenyl ethanes studied we are interested in rotational conformation about two bonds only, ie. the C-1'/C-1 bond (orientation of the side-chain to the plane of the phenyl ring) and the C-1/C-2 bond (orientation

within the ethyl group) (see FIG.1-5.1).



(a) (b) (c) (d)

Where Y = F, Cl, OH. Numbering convention | C-1'/C-1 Conformation | C-1/C-2 Conformation | Useful ^3J Couplings

FIG.1-5.1 The dihedral angles will be measured clockwise in the S enantiomer as shown above.

The main couplings useful in this context are those which depend on the dihedral angle determined by these bonds, ie. $^3J_{HH}$ and $^3J_{FH}$ for the latter and $^3J_{FC}$ and $^3J_{HC}$ for the former. The $^3J_{HH}$ couplings have obviously received most attention in the literature; the key work on quantifying their relationship to dihedral angle was first published by Karplus in 1959[48] (see EQNS.8 & 9). Later, whilst revising his original equations[49] (see EQN.10) Karplus pointed out that these simple relationships only hold under a small range of idealized conditions.

$$J = J^0\cos^2\phi - K \qquad (0^\circ < \phi < 90^\circ) \qquad \text{EQN.8}$$

$$J = J^{180}\cos^2\phi - K \qquad (90^\circ < \phi < 180^\circ) \qquad \text{EQN.9}$$

$$J = A + B\cos\phi + C\cos 2\phi \qquad \text{(for all ranges of } \phi) \qquad \text{EQN.10}$$

(Typical values of constants : $J^0 = 8.5$, $J^{180} = 9.5$, $K = 0.28$, $A = 4.42$, $B = -0.5$, $C = 4.5$). The earlier equations are easier to visualise and for most practical purposes produce identical results (see FIG.1-5.2).

"Perturbations" which can upset these relationships are associated with :

(a) adjacent electronegative substituents

(b) the orientation of the substituents

(c) the degree of hybridisation of the intermediate carbon atoms

(d) the relevant bond angles and bond lengths

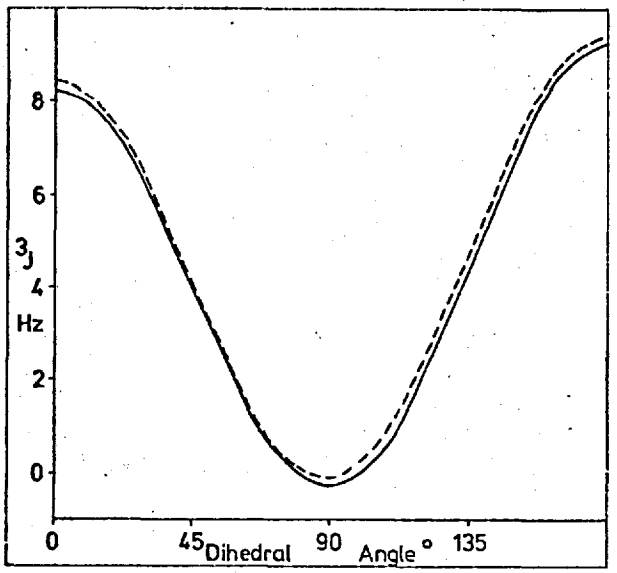
Perturbation (a) may be allowed for to some extent in free rotation systems, eg. mono-[110] or 1,1-disubstituted[111] ethanes, where there are no significant rotamer preferences :

in CH_3CH_2X $\quad ^3J_{HH} = 9.5 - 0.8E$ EQN.11*

in CH_3CHXY $\quad ^3J_{HH} = 18.0 - 0.8\Sigma E$ EQN.12

(Where E equals Huggins electronegativity)

* An alternative equation: $^3J_{HH} = 8.4 - 0.4E$ is given in the same reference[110] for the completely averaged coupling ie. $J_{HH} = 1/3(J_t + 2J_g)$.



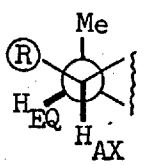
SOLID CURVE - EQNS. 8 and 9
BROKEN CURVE - EQN.10

FIG.1-5.2 Comparative plots of the Karplus Equations

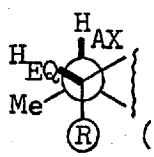
Additivity of electronegative effects of substituents breaks down for 1,2- or higher substitution, due to unequal rotamer populations and the varying orientations of the electronegative groups to the 'coupling path'. Evidence of substituent orientation dependence in vicinal couplings was presented by Bhacca and Williams[112] from $^3J_{ax,eq}$ and $^3J_{eq,ax}$ in sterols (see FIG.1-5.3).

Newman Projections along the C-2/C-3 bond of Ring A in a sterol.

(Ⓡ= OH, OAc)



(I) $^3J_{HH} = 5.5 \pm 1Hz$



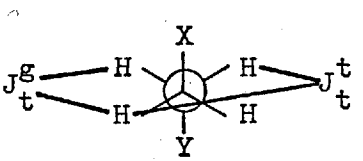
(II) $^3J_{HH} = 2.9 \pm 0.5Hz$

FIG.1-5.3

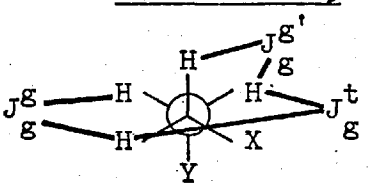
Their conclusion that Ⓡ exerts a greater electronegative effect when it is trans to the coupling path was supported by the work of Booth.[113] The effects of (c) and (d) are thoroughly examined by Jackman and Sternhell.[114]

A purely empirical approach to the variation of $^3J_{HH}$ in 1,2-disubstituted ethanes was adopted by Abraham and Gatti[115] who identified five different coupling arrangements (see FIG.1-5.4). Graphical solutions of the dependence of these couplings on the substituents X and Y led to EQNS.13-17. Phillips and Wray[116] later pointed out that EQNS.13 and 15 should produce the same results in mono-substituted ethanes but do in fact diverge as the electronegativity of the substituent increases. Using a modified graphical technique they reinterpreted the data of Abraham and Gatti to produce EQNS.18 and 19.

$^3J_{HH}$ in 1,2-disubstituted ethanes after Abraham and Gatti,[115]



Trans rotamer



Gauche rotamer

FIG.1-5.4 Superscripts denote the orientation of the coupled protons, subscripts denote the rotamer.

$$J^{g}_{t} = 1.35 + 0.63(E_X + E_Y) \qquad \text{EQN.13}$$

$$J^{t}_{t} = 18.07 - 0.88(E_X + E_Y) \qquad \text{EQN.14}$$

$$J^{g}_{g} = 8.94 - 0.94(E_X + E_Y) \qquad \text{EQN.15}$$

$$J^{g'}_{g} = 10.45 - 1.43(E_X + E_Y) \qquad \text{EQN.16}$$

$$J^{t}_{g} = 16.47 - 0.60(E_X + E_Y) \qquad \text{EQN.17}$$

$$J^{g}_{t} = 3.51 + (E_Y - 0.91)(0.367\,E_X - 0.402) \qquad \text{EQN.18}$$

$$J^{g}_{g} = 3.40 + (E_Y - 1.93)(2.950 - 1.003\,E_X) \qquad \text{EQN.19}$$

These equations are consistent with the earlier observations[112,113] that substituents exert a maximum effect when they are anti-periplanar to the coupled nuclei. As might be expected, on going from di- to tetra-substitution as in the compounds studied here, additivity of electronegative effects becomes both more complex and more uncertain. Reynolds & Wood[117-8] have studied several 1,2,2-trihalophenyl ethanes, predicting preferred rotamers in different solvents from Abraham's electrostatic theory of solvation[119] and M.O. calculations. Trends in the $^{3}J_{HH}$ couplings agreed with the calculated preference of the trans H-H orientation in basic H-bonding solvents, but specific work on quantifying electronegative effects on $^{3}J_{HH}$ was omitted.

$^{3}J_{HH}$ coupling across a saturated C-C bond operates almost entirely by the Fermi-contact mechanism. Even in olefins, the π-system is not involved in $^{3}J_{HH}$ coupling to any great extent.[120] With $^{3}J_{HC}$ and $^{3}J_{HF}$ the situation is not as simple.[120,121] In saturated systems these couplings may still obey the Karplus rule[122,123] as only σ-bonding electrons are used to transmit the coupling. In unsaturated systems, however, both σ- and π-bonds may be used and the simple Karplus relation can no longer be applied.

Wasylishen and Scheafer[122,124] found that the $^{3}J_{CH}$ coupling in propane obeyed the Karplus equation (EQN.10 : A = 4.26, B = -1.0, C = 3.56Hz) but the corresponding couplings in propene and toluene did not (see FIG.1-5.5). The weak dependence of the $^{3}J_{CH}$ in toluene on the dihedral angle was explained by considering the C-C linkage in the phenyl ring as a composite of the single and double bonds in propane and propene respectively.

Williamson et al[125] have shown that $^{3}J_{HF}$ behaves in a Karplus-like fashion with a general $\cos^{2}\phi$ dependence. Phillips and Wray[126] examined $^{3}J_{HF}$ couplings in a series of deoxyfluoro-D-glucopyranoses. As expected they observed the $^{3}J_{HF}$ trans $>$ $^{3}J_{HF}$ gauche and that directly attached electronegative substituents reduced these coupling constants in a stereospecific manner. They also observed the additional complication that these effects depend upon the carbon atom (ie. α- to H or F) to which the substituent is attached.

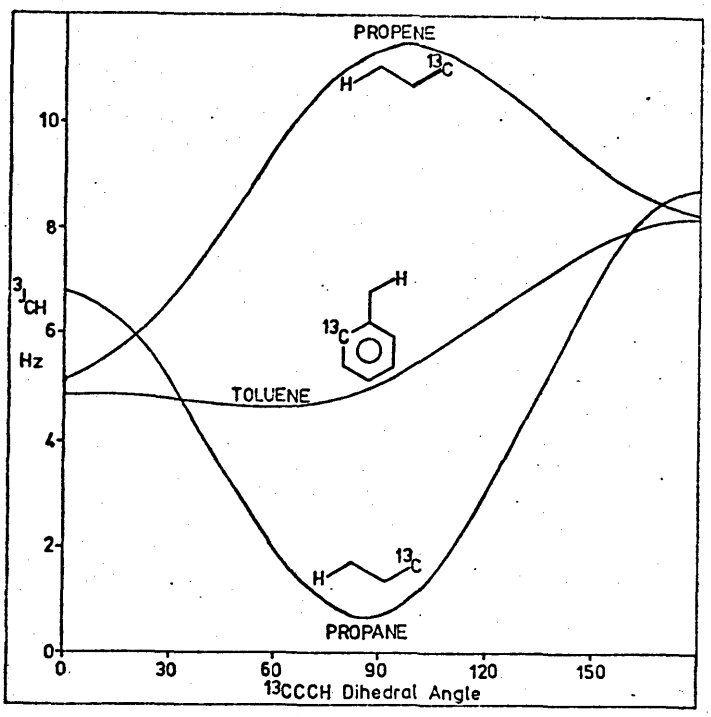


FIG.1-5.5 (Adapted from Refs. 122 and 124). The $^3J_{CH}$ coupling constants were all calculated using the FPT INDO method.

In three bond couplings involving a proton, transmission of the coupling is mainly via sigma bonding electrons. Unfortunately $^3J_{FC}$ couplings, even in saturated systems, use several competing mechanisms, including "through space," which makes their prediction/evaluation a hazardous procedure. A good example of the complications arising even in a fixed saturated system is that of a series of methyl-2,2-difluorobornanes studied by Grutzner et al,[127] which have been discussed in detail in Stother's book on ^{13}C nmr.[128] In FIG.1-5.6 a selection of these couplings are illustrated (by heavy bonds) for those cases where one fluorine shows markedly larger coupling than the other over 3 or 4 bonds. Illustrations 6 and 7 show results which are difficult to explain and which highlight the idiosyncrasies of the $^3J_{FC}$ coupling.

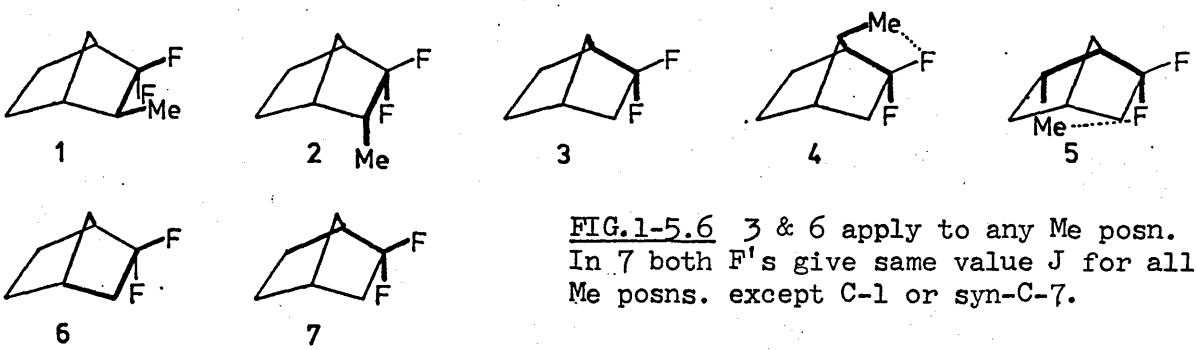


FIG.1-5.6 3 & 6 apply to any Me posn. In 7 both F's give same value J for all Me posns. except C-1 or syn-C-7.

1-5-2 Conformation Dependence of Chemical Shifts

In this rather broad subject, the circumstances involved and the interpretations used will vary considerably from one case to another. Each case,

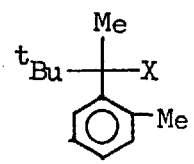
therefore, needs to be evaluated on its own merits by applying the criteria thought appropriate (for an example of ^{19}F conformational shift dependence[12] see FIG.1-1.8, TABLE 1-1.2).

Similar effects on chemical shifts in frozen-out rotamers are well documented for many systems. In our case, where there appears to be considerable rotational restriction at ambient temperatures, some benefit may be obtainable from a loose treatment of this kind which may at least indicate trends in the configurations adopted by the ethyl side-chain within a series of compounds.

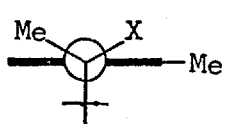
It may also be possible to obtain information on the C-1/C-1' bond orientation in the phenyl ethanes by analogy with the nmr data of phenyl vinyl phosphates.[18] Worthington found that the ^{1}H shifts of the C-2 proton in the Z-isomer of the 2'-substituted phenyl vinyl phosphates (SCHEME 9) did not produce a linear plot against the ^{1}H shift of the corresponding proton in the 2'-substituted styrenes, whereas similar plots for the E and Z 4'-substituted and E 2'-substituted isomers were linear. To explain this anomalous behaviour it was postulated that in certain cases the orientation of the side-chain brought the H-2 proton into the shielding cone of the benzene ring. Examination of Dreiding models of the phenyl ethanes studied shows that this interaction could easily occur for certain combinations of C-1/C-1' and C-1/C-2 rotamers (ie. the H-2 may penetrate the shielding cone which subtends an angle of $\sim 33^{\circ}$ to the centre of the plane of the benzene ring[129]).

The work of Phillips et al[47] on conformational preferences in ortho substituted para fluoroacetophenones, α-methyl styrenes and α,α-dimethyl benzyl alcohols (already cited) compared observed variations of the ^{19}F shift for various ortho substituents (ie. SCS - substituent chemical shifts) with the calculated π-electron densities at the para-carbon for a range of side-chain angles (using the CNDO/2 M.O. program) (see FIG.1-3.2). They were able to directly correlate the changes in the π-electron density at C-4 with the ^{19}F SCS by using a calculated proportionality constant of 661.5 ppm shift per unit electron density.

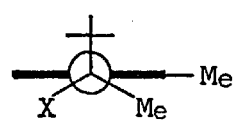
A recent study of a similar system (see FIG.1-5.7) by Anderson and Pearson[130] has used a combination of chemical shift information taken from ^{1}H dynamic nmr spectra, ^{13}C data and from shifts induced by the Lanthanide shift



(X = H, OH, OMe)



Major rotamer



Minor rotamer
(X = OH, OMe only)

FIG.1-5.7

reagent $Eu(fod)_3$. The overall evidence indicated only one major rotamer present at ambient temperatures in all three compounds, with the minor rotamer shown present when X = OH or OMe.

1-6 Lanthanide Induced Shifts (LIS)

In 1969 Hinckley[131] reported that bis pyridine tris β-diketone Europium (III) complexes induced large shifts in the ^1H nmr spectrum of cholesterol, without significant line broadening, and the field of "shift reagents" was born. The potential of shift reagents to simplify spectra was universally recognised and development of new shift reagents was rapid.[132,133] Early quantitative work on "LIS" which used an r^{-3} dependency for the induced shift (where r = the metal/proton distance) was shown to be invalid, as shifts of the wrong magnitude and sign were reported.[134] The necessity for an angular term in the shift equation was pointed out by Horrocks[135] and the simplified version of this, the already established McConnell-Robertson equation,[136] found wide acceptance[137] (see SECTION 1-6-4.1). This led to a flood of publications in which LIS data was used as a tool for studying molecular geometry as well as the "standard" uses for spectral assignment and simplification.

At its height (1972-74) the applications of LIS were the subject of several reviews[138-140] and have since been briefly reviewed annually in the Specialist Periodical Reports on NMR.[141] An excellent treatment of the applications of LIS in conformational analysis, by Hofer, appeared in 1976.[142] Very recently the whole field of Lanthanides, their electronic structure, complex formation, and interaction with organic molecules has been presented in the one review. This all encompassing introduction to the subject, by Mednejad,[143] was found extremely useful.

As part of the work undertaken in this project was the development of a computer program which optimises molecular conformation to achieve "best fit" of observed and calculated LIS data, it is necessary to review the relevant theoretical and practical aspects of analysing such data.

1-6-1 The Components of the Induced Shift

The formation of an adduct between a Lanthanide chelate and an organic substrate produces an internal anisotropic magnetic field around the substrate, which modifies its observed chemical shifts. If all these "induced shifts" were attributable to the same mechanism one would expect all the lanthanides to produce similar shift ratios with a given substrate. It was quickly noticed that this is not the case[133] as different lanthanides not only produce shifts of varying ratios but also of different signs. In fact the observed induced

shifts comprise three separate interactions[144-146] (see EQN.20), the degree of each present depending upon the particular lanthanide used, the nature of the binding site on the substrate, and the nucleus examined (eg. ^{1}H, ^{19}F, ^{13}C etc)

$$\Delta\delta_{observed} = \Delta\delta_{dipolar} + \Delta\delta_{contact} + \Delta\delta_{diamagnetic} \qquad \text{EQN.20}$$

Where $\Delta\delta_{observer}$ = the observed induced shift.
$\Delta\delta_{dipolar}$ = the through space or "pseudo-contact" interaction (PCS).
$\Delta\delta_{contact}$ = the through bond or "Fermi-contact" interaction (CS).
$\Delta\delta_{diamagnetic}$ = the directly bonded "complex-formation" interaction (CFS)

Frequently the pseudo-contact term dominates and it is now standard practice to ignore the CS and CFS terms under certain circumstances. In the treatment of LIS data undertaken in Chapter 6 this assumption is made and will therefore be justified in the following pages. The mathematical aspects of the CFS and CS terms need not be considered here as they play no important part in our results. They will only be mentioned qualitatively and for further details the reader should turn to the reviews already cited.[143,138-142]

1-6-1.1 The Dipolar Interaction (Pseudo-Contact Shift PCS)

This is a direct through-space interaction between the electron magnetic moment of the paramagnetic ion and the magnetic moment of the resonating nucleus. This averages to zero under conditions of rapid tumbling if the magnetic moment of the lanthanide ion is isotropic (as in La^{3+}, Gd^{3+} and Lu^{3+}, see SECTION 1-6.3). For an anisotropic lanthanide ion (ie. one in which the 4f orbitals are unsymmetrically filled) pseudo-contact shifts are produced. These are a function of the substrate geometry and the anisotropy of the molecular magnetic susceptibility tensor of the lanthanide complex and are given by the equation of Horrocks and Greenberg[147] :

$$\frac{\Delta H}{H}_{DIP} = -\frac{1}{3N}\left[x_Z - \tfrac{1}{2}(x_X + x_Y)\right]\left[\frac{3\cos^2\psi - 1}{r^3}\right] - \frac{1}{2N}\left[x_X - x_Y\right]\left[\frac{\sin^2\psi\cos 2\phi}{r^3}\right] \qquad \text{EQN.21}$$

Where x_X, x_Y, x_Z are the principal molecular susceptibilities
N is the Avogadro Number
r, ϕ, ψ are defined in FIG.1-6.1

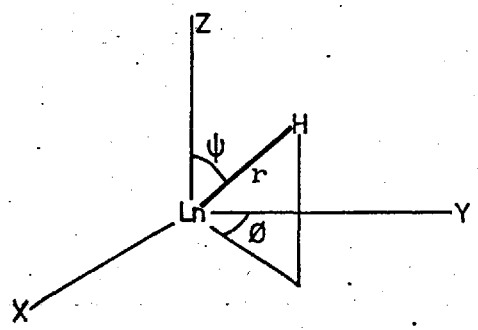


FIG.1-6.1 The definition of the polar coordinates r, ψ, ϕ in the system of the principal components of the magnetic susceptibility tensor.

When the magnetic moment of the complex has axial symmetry $x_X = x_Y$ and

EQN.21 simplifies to : $$\frac{\Delta H}{H}_{DIP} = -\frac{1}{3N}\left[x_Z - x_X\right]\left[\frac{3\cos^2\psi - 1}{r^3}\right] \qquad \text{EQN.22}$$

If the lanthanide is isotropic $x_X = x_Y = x_Z$ and $\Delta H_{DIP}/H$ averages to zero. The main assumption of virtually all computational approaches to "solving" the metal position relative to the substrate in a lanthanide-substrate adduct is that the complex formed has effective axial symmetry (this was not assumed by Cramer et al[148]). Under these conditions the simplified version of EQN.22, the McConnell-Robertson Equation (EQN.23) can be used :

$$\frac{\Delta H}{H}_{DIP} = K(3\cos^2\psi - 1)/r^3 \qquad \text{EQN.23}$$

The constant K is the same for all nuclei in a given complex and their relative shifts are given solely by the geometrical term.

The success of assuming axial symmetry in analysing LIS data is quite remarkable in the light of X-ray observations of lanthanide chelate-substrate complexes. For axial symmetry the complex should have at least a three fold symmetry axis passing through the lanthanide ion. This is definitely not the case in the solid state.[149-151] Horrocks[152] suggested that this apparent dichotomy could be rationalised if the lanthanide-substrate complex underwent a dynamic equilibrium between thirty or more geometrical isomers which were disposed such that the average orientation of the substrate lay in proximity to the lanthanide's maximum susceptibility axis. This model would justify assuming effective axial symmetry for the complex, and a "fixed" position of the metal relative to the substrate.

Not only does the assumption of effective axial symmetry seem fully justified by the success of its application, but the further assumption that this symmetry axis lies along the lanthanide-substrate "bond" has been profitably applied on many occasions. In several papers this orientation of the principal symmetry vector has been challenged but on optimisation has always been found to lie, within experimental error ($\approx 2^\circ$), along the metal-substrate vector.[153-159]

An interesting consequence of the McConnell-Robertson Equation (EQN.23) is that the value of $(3\cos^2\psi - 1)$ passes through zero when $\psi = 54^\circ 44'$ and the sign of the induced shift is inverted. This is the so-called "magic angle".

1-6-1-2 The Fermi-Contact Interaction (Contact Shift - CS)

This involves the direct delocalisation of unpaired 4f electrons of the lanthanide to the molecular orbitals of the substrate. The effect spreads over several bonds and the changes in the local electron densities induce contact shifts[160] which fall off rapidly with distance. As might be expected π-bonds

are better transmitters of this effect than σ-bonds.[161]

^{1}H nuclei, in contrast to ^{13}C and ^{15}N nuclei only suffer from CS to a very limited extent (CS ≪ 10% PCS for ^{1}H closest to binding site).[142] (relative CS 1.00 : 8.76 : 35.91).[138]

The degree of delocalisation is very dependent on the nature of the Ln (III)-substrate bond. As this bond becomes stronger (more covalent) the contact shift contribution increases.[162] As the higher lanthanides have smaller radii[163] (see SECTION 1-6.3) they are less able to form strong bonds. Variation of the lanthanide,[162,164-167] the β-diketone chelating group[168] and the substrate donor group[169] increase the contact shift :

Yb < Pr < Tm < Dy < Tb < Er < Ho < Nd < Eu

dpm < fmd < pfd < fod (the order of the chelate's Lewis acidity[170])

-OH < -COR ≃ $-CONR_2$ < $-NH_2$

Virtually all authors agree that Ytterbium based chelates are the ideal shift reagents for accurate LIS work[eg.162,165-167,169,171] as they produce shifts to lower field, (the alternative, Praseodymium, shifts to higher field) which have negligible CS contributions in all but the carbon α- to the binding site. In alcohols even the α-carbon has negligible contact shift (CS + CFS = 5%[167] in bicyclo heptanols - poss.4% CFS[169]). In fact several authors[166,167] have reported better fit of the calculated LIS data to the ^{13}C observed LIS than to the ^{1}H observed LIS.

Because of its spherical symmetry Gadolinium does not produce any PCS and has therefore been used by several authors[145,162] to study CS and CFS contributions; it has well established use as a "relaxation" or broadening agent (see SECTION 1-6.2).

Contact shifts may be expected to be larger in the α-nucleus transoid to the L-X bond (see FIG.1-6.2) than in the other α-nuclei.[158,172,173] This has been used to justify low CS in α-protons,[142] as relief of steric compression favours a cisoid relationship between the α-proton and the L-X bond.[195]

(L = lanthanide ion,
X = substrate donor)

%CS : $R_1 > R_2 \simeq R_3$

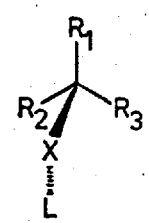


FIG.1-6.2

The interesting observation that contact shifts frequently alternate sign from the α- to the β-carbon has been made on several occasions.[165,171,174] In the case of $Eu(fod)_3$ with sterols[165] the α-carbon suffered a large downfield CS whilst the β-carbons suffered similar upfield CS's. Similar observations were made with the alcohols studied in this work (see Chapter 6).

1-6-1.3 The Diamagnetic Interaction (Complex Formation Shift - CFS)

This term is independent of the paramagnetism of the lanthanide and arises solely from perturbations of the substrate's electrons caused by the bonding to the shift reagent. Most authors have ignored CFS contributions in their calculations of induced shifts although its participation was questioned by Bleaney et al[175] in 1972.

As Lanthanum (La^{3+}) and Lutetium (Lu^{3+}) are diamagnetic (neither possess unpaired 4f electrons) and therefore do not produce PCS or CS shifts, their induced shifts, which are surprisingly similar for extreme lanthanides,[145,146] have been used to estimate the CFS contributions of other lanthanides.[169,176] this effect is normally only significant very close to the lanthanide binding site.[177] Chadwick and Williams[169] have estimated the CFS contribution to the $Yb(dpm)_3$ induced shifts of the α-carbon to be as high as 17% in ketones but only ~4% in alcohols. They suggested that the ability of the carbonyl group to donate electrons fron the oxygen atom, leads to efficient transmission of charge away from the α-carbon, and subsequent deshielding.

Most authors have concluded that CFS contributions to ^1H shifts may be disregarded in non-aromatic protons[142,169,177] but that it is worthwhile estimating it in other atoms α- to the binding site.[145,177] For most purposes the CFS and CS "contaminants" of lanthanide induced shifts are undesirable, and the technique of estimating both terms from the gadolinium induced shifts (which have no PCS contribution) has proven fairly popular.[145,162,175]

1-6-2 Line Broadening

As well as the included shifts already mentioned, the addition of a lanthanide chelate to an organic substrate in solution enhances the nuclear spin-spin relaxation rates which is observed as a broadening of the spectral lines. In molecules with little CS the line broadening may be interpreted solely from the metal-nucleus distance :

$$\text{Broadening } \left(\frac{1}{T_2}\right) \propto \frac{1}{r^6} \qquad \text{EQN.24}$$

This effect is very short-ranged and because there is no angular term is easy to calculate. It has found some use in configurational studies (invariably in conjenction with LIS data[155,178]) and is also a useful aid to line assignment. Gd(III) complexes are the ideal "relaxation reagents" as their induced shifts are usually small.

In many circumstances line broadening becomes a nuisance as essential information such as accurate shifts and coupling constants may be obscured.

1-6-3 Properties of the Lanthanides - Choosing a Lanthanide Shift Reagent

The Lanthanides or Rare Earths comprise 15 transition elements which form a subgroup within Group (III) of the Periodic Table. Through this series the 4f subshell is progressively though irregularly filled. Two electron configurations are found (see TABLE 1-6-1) :

$4f^{n-1}\ 5d^{1}\ 6s^{2}$ and $4f^{n}\ 5d^{0}\ 6s^{2}$

As the 4f electrons are well screened by the 5s and 5p subshells they play no part in bonding. Ln(III) is the most stable oxidation state and is formed by losing the $6s^2$ and a 4f (or $5d^1$ where present) electrons which results in a regular filling of the 4f subshell. The lanthanides are physically and chemically similar although the closed shell configurations in La^{3+} and Lu^{3+} make these diamagnetic whereas all other Ln^{3+} ions have unpaired 4f electrons and are paramagnetic.

The general decrease in ionic radii on going from La^{3+} to Lu^{3+} is known as the "Lanthanide Contraction"[179] and is caused by the shape of the 4f orbitals giving imperfect shielding between the 4f electrons. This leads to an increase in the effective nuclear charge causing contraction of the 4f subshell. Although the acidity of the Ln^{3+} ions increases along the series, a trend which would normally increase their binding strength, the reduction in available space for binding leads to steric hindrance. The strongest complexes with organic molecules are therefore found for Dy^{3+}, Tb^{3+} and Ho^{3+} which give the largest induced shifts,[133,145] but also have large CS contributions (see FIG.1-6.3).

The criteria applied in selecting a lanthanide shift reagent will depend on the specific purpose for which it is required. For the assignment of a ^{13}C (^{1}H noise decoupled) spectrum, a shift reagent with a large overall shifting ability eg. a Dy^{3+} or Tb^{3+} chelate would be ideal, as the amounts of CS or

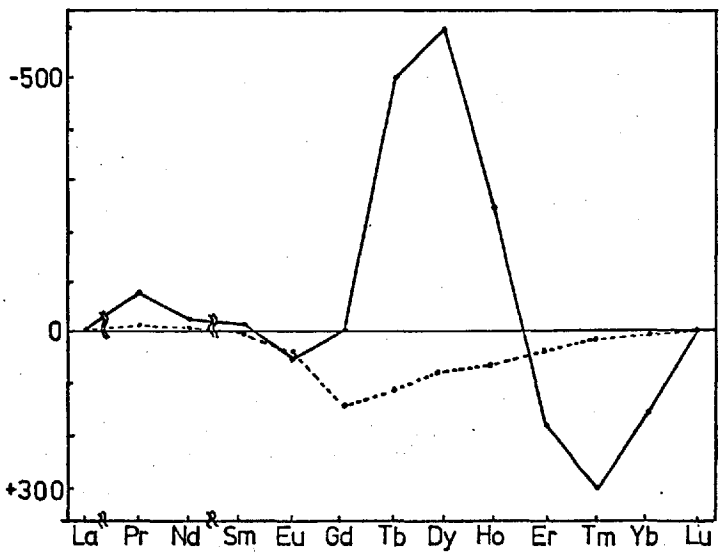


FIG.1-6.3

The PCS (Solid line) and CS (Broken line) for the α-carbon in n-octylamine

The shifts are in ppm (+ve to low field) for the $Ln(fod)_3$ chelates.[145]

TABLE 1-6.1 Properties of the Lanthanide (3+) Ions. (Compiled from refs : 143,145,151,163,180-183)

Element & Symbol		At No	Electron Configuration of Neutral Atoms			Config of Ln^{3+}		Ionic Radii Co-ord $N^{os} > 6$	Relationship between Colour & No. of Unpaired Electrons	Properties	$X=Ln(ch)_3$ Hydration Before & After Vacuum	Relative Shifts $\delta CS/\delta PCS$ α-C in n-octyl-amine	Relative Broadening	SEQ.
			4f	5d	6s	4f	5p							
Lanthanum	La	57	$4f^0$	$5d^1$	$6s^2$	$4f^0$	$5p^6$	1.061 12	colourless 0	DIAMAGNETIC CFS Only	$X_2.3H_2O$ $X_2.1H_2O$	CFS Only	/	/
Cerium	Ce	58	$4f^2$	$5d^0$	$6s^2$	$4f^1$	$5p^6$	1.034 /	colourless 1		"	/ /	/	/
Praseodymium	Pr	59	$4f^3$	$5d^0$	$6s^2$	$4f^2$	$5p^6$	1.013 8H 12	green 2	yellow on standing	"	-17 +0.15	0.005 B	4
Neodyium	Nd	60	$4f^4$	$5d^0$	$6s^2$	$4f^3$	$5p^6$	0.995 8H 12	reddish 3		"	-3 +0.70	/	8
Promethium	Pm	61	$4f^5$	$5d^0$	$6s^2$	$4f^4$	$5p^6$	0.979 /	pink/yellow 4	spontaneously decays ———				
Samarium	Sm	62	$4f^6$	$5d^0$	$6s^2$	$4f^5$	$5p^6$	0.964 8H 12	yellow 5		"	-0.5 /	0.02 B	/
Europium	Eu	63	$4f^7$	$5d^1$	$6s^2$	$4f^6$	$5p^6$	0.950 8H 12	pale pink 6	white on standing	"	+12 +0.80	0.003 B	9
Gadolinium	Gd	64	$4f^7$	$5d^1$	$6s^2$	$4f^7$	$5p^6$	0.938 8H 12	colourless 7	CS + CFS only	"	CFS +CS	/	/
Terbium	Tb	65	$4f^9$	$5d^0$	$6s^2$	$4f^8$	$5p^6$	0.923 7H	pale pink 6		$X.H_2O$ X^2	-27 -0.21	0.1 B	6
Dysprosium	Dy	66	$4f^{10}$	$5d^0$	$6s^2$	$4f^9$	$5p^6$	0.908 7H	yellow 5		"	-43 -0.13	/	3
Holmium	Ho	67	$4f^{11}$	$5d^0$	$6s^2$	$4f^{10}$	$5p^6$	0.894 7H	pink/yellow 4		"	-20 -0.19	0.002 B	5
Erbium	Er	68	$4f^{12}$	$5d^0$	$6s^2$	$4f^{11}$	$5p^6$	0.881 7H	reddish 3		"	+9 +0.25	/	7
Thulium	Tm	69	$4f^{13}$	$5d^0$	$6s^2$	$4f^{12}$	$5p^6$	0.869 7H	green 2		"	+20 +0.07	/	2
Ytterbium	Yb	70	$4f^{14}$	$5d^0$	$6s^2$	$4f^{13}$	$5p^6$	0.858 7H	colourless 1		"	+10 +0.05	0.02 B	1
Lutetium	Lu	71	$4f^{14}$	$5d^1$	$6s^2$	$4f^{14}$	$5p^6$	0.848 7H	colourless 0	DIAMAGNETIC CFS Only	"	CFS Only	/	/

SEQ. = The order of preference for LIS conformational analysis studies; H = co-ord. no. of the hydrate.

broadening present would not matter. For assignment of a spectrum with many fine couplings the best reagent would be a Eu^{3+} or Pr^{3+} chelate, for even though considerable CS would be present with Eu^{3+} both give very short spin lattice relaxation times ($\sim 10^{-12}$ secs) which result in narrow nmr lines and no loss of fine structure.[184] *

La^{3+}, Lu^{3+} and Gd^{3+} have found special uses for estimating CFS and CS contributions, whilst Gd^{3+} with its generally small overall shift (CFS and CS only) is extensively used as a broadening reagent.

For conformational analysis, shifts with the minimum of CFS and CS are essential and Yb^{3+} or Tm^{3+} chelates are ideal. The most commonly used reagents for this purpose are Yb^{3+} chelates, they do however produce significant line broadening and coupling information may be lost.[182] Birdsall et al[188] have shown that, in complex flexible molecules, consideration of the coupling information is as important as the LIS and broadening data when determining the overall conformation. Also comparison of couplings before and after adding a shift reagent is a good check that dramatic changes in conformation do not take place. This is most conveniently done with a Eu^{3+} chelate, although the shift data obtained is unreliable for conformational work.

Most authors have used a variety of LSR's in any one study to make allowance for CFS, CS and changes in conformation; so selection of appropriate reagents is very important.

As well as variation of the lanthanide there is also the choice of a variety of chelates.[143] In general chelates containing the polyfluorinated species (fod) (see FIG.1-6.4) have been found to be the most soluble in organic solvents, and due to the higher Lewis acidity of $Ln(fod)_3$ over other chelates, produce larger shifts.[170] As $Ln(fod)_3$ chelates are readily available and have the most favourable properties they were the automatic choice for this work. (N.B.to avoid confusion in ^1H spectra the two shift reagents used were both deuterated ie. $Eu(fod\text{-}d_9)_3$ and $Yb(fod\text{-}d_9)_3$).

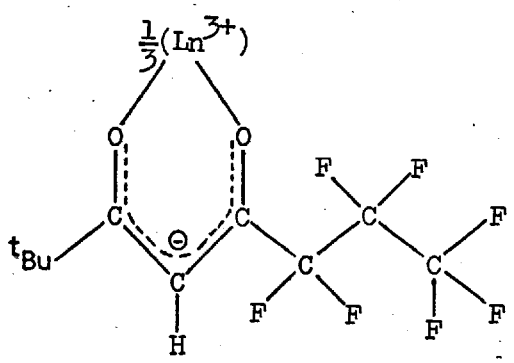


FIG.1-6.4

(fod) = 1,1,1,2,2,3,3-heptafluoro-7,7-dimethyloctane-4,6-dionate.

* Several aothors have reported varying amounts of "chemical exchange spin decoupling" when using shift reagents (185-187). This is observed as a decrease in coupling constants and in extreme cases couplings are completely removed.

1-6-4 Treatment of LIS Data

The use of LIS data in determining structural information in both rigid and flexible molecules has invariably involved some form of the McConnell-Robertson equation. A variety of assumptions and approximations are usually made and several different methods of obtaining the "metal position" are in general use. So much so that choosing and justifying a suitable method of handling LIS data becomes a difficult decision.

1-6-4.1 Basic Assumptions

That although the LSR-Substrate complex is in rapid equilibrium, the metal can be considered to occupy one fixed position relative to the substrate.

The more general aspects of this have already been mentioned[152] (see SECTION 1-6-1.1). Several authors have argued that the metal might occupy a pair of positions with a symmetrical substrate and have tried to allow for this by "reflecting" the metal test position in the plane of symmetry of the substrate.[142,155,159,169]

That the induced chemical shifts are proportional to $(3\cos^2\psi - 1)/r^3$ and that any shifts used in the calculation of the metal position are free from CS and CFS.

Some authors have either assumed that the LIS data used was free of CS and CFS and have accepted the consequences[137] or have deliberately omitted those shifts over which there was some doubt.[165] In the more precise work, various LSR's have been tested to find the best reagent[162,167] (usually a Yb^{3+} chelate) or allowances have been made for CS and CFS by using La^{3+}, Lu^{3+} and Gd^{3+} induced shifts.[145,169,188]

That the "Principal Symmetry Axis" of the metal complex lies along the metal-substrate donor atom vector.

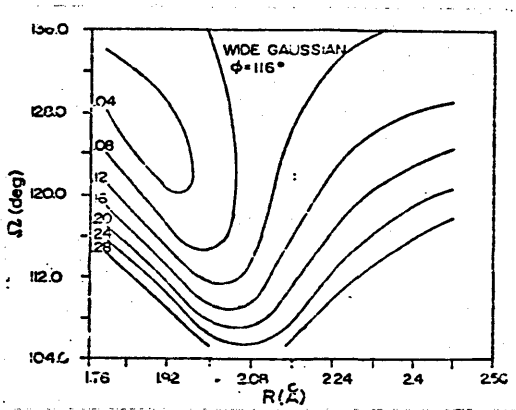
Most authors now accept this as a statement of fact. Optimisation of the direction of the metal's Principal Symmetry Axis has been performed on many systems by many different authors and all have found this assumption to be valid within experimental error.[153-159] Wing et al[157] did not even assume axial symmetry but found that the McConnell-Robertson equation was adequate.

That the geometry of the substrate does not change on binding to the LSR. This appears to be true in most examples in the literature, but should be checked in individual cases by monitoring coupling constants etc. before and after adding the LSR. For example, small conformational changes have been reported for hexanols on adding $Eu(dmp)_3$.[166]

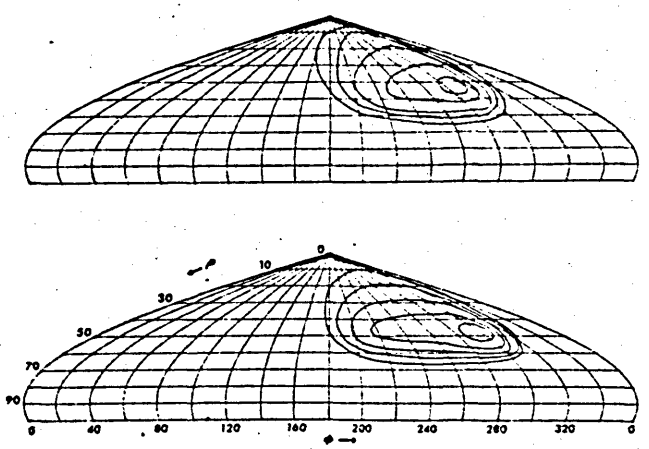
1-6-4.2 Basic Methods

There are several basic methods. All as their starting point assume that the coordinates of the substrate are obtained from standard geometries or specific X-ray data and that at least part of the molecule is rigid relative to the metal. It is also expected that the LIS data used will have been adjusted so that only PCS contributions are present.

The main method used involves "searching" a regular grid of possible metal positions (anything from 6 points on two vectors to 50,000 points at 0.1Å intervals throughout a hemisphere centered on the donor atom) to find the "best fit". At each search point the induced shifts of every atom are calculated from the McConnell-Robertson equation and the average error or "fit" of the calculated and observed data is determined. The main variation on this method, apart from the selection of the search points, is the formula used in determining the fit of the calculated data. Methods of error testing will be considered in the next subsection. This general method of multi-site searching has the advantage that "contour plots" of fit vs. metal position can be generated. For example, Armitage et al[189] have produced planar contours of normalised variance as a function of the lanthanide position (R,Ø,Ω), whilst Willcott et al[171,190] chose to display their polar coordinate contours using Sanson-Flamstead sinusoidal equal area projections :



Contours of normalised variance vs. lanthanide position for diacetone-glucose. One of a set of such maps by Armitage et al (189).



Contours of the agreement factor R at intervals of 0.12, with the outer contour @ R = 0.12. For each map the Ln-donor distance is constant (190).

FIG.1-6.5 Two Examples of Literature Representations of "Metal Search" Results

Most authors who have used this method, have defined their coordinate system with the donor atom at the origin and have located the metal search sites by polar coordinates. Some have chosen different origins (eg. Barry et al[155]) whilst one method[157] even places the lanthanide at the origin and recalculates

all of the substrate's coordinates for each search point!

Several alternative methods have been devised; for example ApSimon and Beierbeck[191] expanded the McConnell-Robertson equation into a Taylor series and used Newton's iterative method of linear least squares optimisation of the coordinates of the metal to obtain a rapid convergence onto the "best fit" metal position. Although they obtained similar results with borneol and isoborneol to previous literature work[137] there is always the disadvantage with this method that an overall picture of the "best fit" cannot be obtained and an initially poor guess might produce a false optimum position. This method was also used by Ammon et al.[156]

Rafalski et al[192] used the geometric term of the McConnell-Robertson equation to calculate the shifts for each proton in a variety of molecules. The constant K was found by a least squares fit of the observed and calculated shifts. The metal position was then varied over a regular grid and the error terms E and b (see EQNS.25 and 26) were plotted against metal-donor distance. The best fit was that position in which E and b were both at their lowest minimum.

$$S_i = K(3\cos^2\psi_i - 1)/r_i^3 + b \qquad \text{EQN.25}$$

$$E = (S_i(\text{obs}) - S_i(\text{calc}))^2 \qquad \text{EQN.26}$$

Hawkes et al,[153,158] in a similar approach, minimised the error function iteratively. In a study of LSR-substrate complex stoichiometry, by Johnston et al,[193] absolute rather than relative shifts were calculated. To reduce the coordinate variables, adamantane nitrile was chosen so that only the Ln-N distance had to be varied (see FIG.1-6.6). A computer non-linear regression method was used to isolate the Δ_1 (from LS) and Δ_2 (from LS_2) contributions to δ (see EQN.27) and to find the rate constants k_1 and k_2 (see EQN.28).

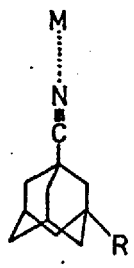


FIG.1-6.6

$$\delta = \delta_o + \frac{[LS]}{[S]}\Delta_1 + \frac{[LS_2]}{[S]}\Delta_2 \qquad \text{EQN.27}$$

$$L + S \underset{}{\overset{k_1}{\rightleftharpoons}} LS + S \underset{}{\overset{k_2}{\rightleftharpoons}} LS_2 \qquad \text{EQN.28}$$

1-6-4.3 Fit Factors and Significance Testing

The basic method method of comparing two sets of numbers is the root mean square of their difference (see EQN.29). This and the host of related tests which have been used to evaluate "goodness of fit" of LIS data have been reviewed by Hofer.[142] The Hamilton agreement factor R (see EQN.30), was

originally intended for use in a crystallographic context but since its introduction to LIS calculations in 1972[190] has found wide usage.

$$\text{Error} = \left[\frac{\Sigma_i(\Delta_i^{obs} - \Delta_i^{calc})^2}{n}\right]^{\frac{1}{2}} \quad (n = \text{total No. of observations}) \qquad \text{EQN.29}$$

$$R = \left[\frac{\Sigma_i w_i(\Delta_i^{obs} - \Delta_i^{calc})^2}{\Sigma_i w_i(\Delta_i^{obs})^2}\right]^{\frac{1}{2}} \qquad \text{EQN.30}$$

The R factor differs from most tests in that it has weighted factors w_i which are introduced to allow for those cases in which several equivalent atoms produce one shifted signal. As only one signal is observed it should not be treated preferentially to signals from single atoms and so the two or three calculated components of the signal are given weightings of 0.5 or 0.33 as appropriate so that each signal has a total weighting of 1.0.

The usefulness of the R factor becomes apparent if two minima are found in a grid search with agreement factors of R_1 and R_2 (R = 0 is a perfect fit whereas R < 0.04 corresponds to agreement within experimental error). Hamilton[194] has produced "Significance Tables" for R factor ratios (see TABLE 1-6.2) which may be used to express the "confidence level" at which one result may be rejected in favour of another. Defining the coordinates of the metal and scaling the calculated shifts involves four degrees of freedom. As the R factor ratio significance tables require one or more degrees of freedom at least 5 shifted centres are required. Say R_1 = 0.07, R_2 = 0.04 and there are 9 shifted centres; then R ratio = 1.75, degrees freedom = 5, so the R_1 minimum may be rejected at the 97.5% confidence level (from TABLE 1-6.2).

1-6-4.4 Likely Sources of Error in Calculating Metal Positions from LIS Data

The most likely errors are in the shift data itself, especially when shift reagents with high CS or CFS contributions are used. These can be minimised by careful choice of LSR and also where practical by ommitting data from the atoms nearest to the binding site.

Where shifts are very small (< 0.1ppm) errors of measurement alone may also be significant. The standard method of reducing this error is to use several additions of LSR and extrapolate the induced shift to a 0.5 : 1 or 1 : 1 ratio. Non-linearity of the plot of $\Delta\delta$ vs. moles LSR may be due to experimental error in weighing the necessary milligram quantities of LSR (ApSimon and Beierbeck[196] have considered this problem and have shown that this can be overcome) or to concentration effects of excess LSR.

Several authors have thought that the apparent insensitivity of the R

TABLE 1-6.2 R Factor Ratios Significance Table[194]

°Freedom	50%	75%	90%	95%	97.5%	99%	99.5%
1	1.414	2.613	6.392	12.746	25.471	63.665	100.000
2	1.155	1.512	2.294	3.203	4.500	7.089	10.012
3	1.093	1.294	1.687	2.092	2.610	3.517	4.418
4	1.066	1.205	1.462	1.711	2.014	2.510	2.972
5	1.051	1.157	1.346	1.524	1.732	2.062	2.357
6	1.042	1.127	1.276	1.413	1.571	1.814	2.026
7	1.035	1.107	1.230	1.341	1.467	1.658	1.822
8	1.031	1.092	1.197	1.290	1.395	1.552	1.684
9	1.027	1.081	1.172	1.252	1.342	1.474	1.585
10	1.024	1.072	1.153	1.223	1.301	1.416	1.511
11	1.022	1.065	1.137	1.200	1.269	1.370	1.453
12	1.020	1.059	1.125	1.181	1.243	1.333	1.407
13	1.018	1.054	1.114	1.166	1.222	1.303	1.369
14	1.017	1.050	1.105	1.153	1.204	1 278	1.338

factor to small changes in Ln-donor bond length* have meant that errors in the substrate coordinates were unimportant (eg. Willcott et al[190] and Williamson et al,[196] who both derived their coordinate measurements from applying rulers to Dreiding models!). Detailed studies of coordinate errors and their effects on LIS calculations have since been performed by Hinkley and Brumley,[197,198] who concluded that the expected coordinate errors of $\pm$ 0.1Å would make errors in calculating LIS greater than in measuring them; and although this would only lower the overall fit in rigid molecules, it may make it impossible to distinguish between closely related conformers. They suggested that using coordinate data from X-ray structures would minimise these errors and that suitable models should be chosen if necessary.

1-6-5 Conformational Studies Using LIS

Many LIS studies have been performed on rigid substrates of known geometry, using a variety of techniques for analysing the data. From this work several general observations can be made which provide a useful background for the more complex conformational studies.

(a) Most authors accept the McConnell-Robertson equation with the

* This phenomenon is well known (190,199,200) and has been the subject of several studies (169,201). Cramer et al (201) observed small changes in the R factor over the Eu-N bond range 2.15-3.15Å, for several nitrogen heterocycles which were almost insignificant when examined with Hamilton's confidence test (194). Similar observations lead Sneider and Weigand (167) to propose that variations in the fit of calculated LIS data of less than 3% were not significant.

metal's Principle Symmetry Axis lying along the Ln-donor bond.

(b) The donor atom is normally placed at the origin of the search co-ordinate system and search points are defined using polar coordinates.

(c) Hamilton's R factor is the most widely used error measurement for comparing the observed and calculated LIS. Fits better than R = 0.10 are acceptable though poor. The best fits reported have R factors of 0.02 to 0.015 (ie. less than 2% average error).

(d) Ln-donor bond lengths are usually in the range 2.5-3.5Å.

(e) Ln-bond angles depend on the nature of the donor group and usually fall in the range 110-180°, averaging ~130° for -OH and -C=O groups.

(f) Wherever possible the metal occupies the position with the least steric crowding.[167,195,202]

(g) In molecules with several potential binding sites, exclusive selectivity of the most favourable binding site has been observed[203,204] (ie. that with least crowding; not always the best donor[203]). Simultaneous bonding of the metal to two adjacent sites is well documented.[205-210] Two of these studies were on tetracycline[209,210] which has nine potential lanthanide binding sites, but at any one pH only offers one metal location. Celotti and Fazakerley[209] found three different sites populated at three different pH values, two of which had the metal "shared" between two donor groups.

Conformational work may be divided into two general areas :

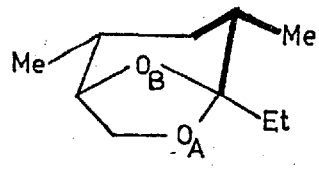
(1) The relatively simple task of deciding between a choice of isomers, eg. cis/trans, E/Z, endo/exo, axial/equatorial, etc.

(2) The more complicated task of selecting the preferred conformation in a molecule with a degree of flexibility, ie. a "free-rotation" bond or a distortable ring.

In many literature examples both of these problems are present in the same molecule and are tackled simultaneously.

Many claims have been made for the usefulness of lanthanide shift reagents, but that of Gore and Armitage,[199] that "Eu(fod)$_3$ could be mimicking some steric/electronic feature of the olfactory receptor sites of the European Elm Bark Beetle" was definitely a milestone. This conclusion was voiced after studying the shifted ^{1}H nmr of four diastereomers of multistriatin (a dioxabicyclo[3.2.1] octane), one of which was known to be the aggregating pheremone of the said insect. This molecule has two potential binding sites (see FIG.1-6.7) with one, O_B, more hindered than the other, but surprisingly favoured in the active α-isomer, drawn. In the three other structures, which had negligible biological activity, the lanthanide was found to favour O_A. The four isomers were identified from their shifted spectra.

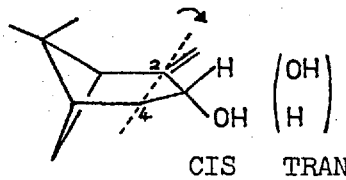
The four isomers were derived from the various combinations of axial and equatorial positions available to the two Me groups.



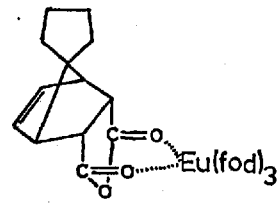
α-multistriatin

FIG.1-6.7

Hinkley and Brumley[197] were able to distinguish between cis and trans pinocarveol (see FIG.1-6.8) from their LIS but reported that their expected coordinate errors of $\pm 0.1\text{Å}$ made the determination of the degree of folding about the C-2/C-4 axis less certain.



Pinocarveol FIG.1-6.8



a bicyclo[2,2,1] octeneanhydride FIG.1-6.9

Craig et al[207] examined a series of endo- and exo- bicyclo octene anhydrides (see FIG.1-6.9). They found no difficulty in identifying the isomers and concluded that the Europium chelate was "shared" between the two keto-groups.

Several authors have studied simple rotating systems including the seemingly trivial problem of methyl group rotation, which has no effect on conformation but which can have marked effect on calculated LIS. In a comparative study of nmr and X-ray techniques the structure of 3,3-dimethylthietane-1-oxide.$Eu(dpm)_3$ was determined. The authors asserted that all reasonable methyl rotamer averaging should be done before the LIS assignment could be regarded as correct.[157] Lenkinski and Reuben[211] assessed various methods of averaging the rotation of the methyl and tertiary butyl group in pinacolone in conjunction with two proposed metal positions of different populations. Again they insisted that appropriate rotamer averaging was essential in calculating LIS.

Wherever possible LIS studies which have involved calculating preferred rotamers have been performed in systems which are partly rigid, so that the metal position can be fixed by using the "known" LIS data and then the "variable" LIS data can be adjusted (ie. the group rotated) to find the optimium position. Hofer[212] examined the orientation of an aryl methoxy group in three indanols(see FIG.1-6.10). Once the metal position was fixed the expected shifts of the methoxy groups could be calculated. Non-hindered methoxy groups were found to have two minima whilst hindered groups had one, always in the plane of the ring (preferred for oxygen orbital overlap with π-system). The results were in good agreement with observed shifts.

Montaudo et al[200,213] have reported several studies on a range of

Methoxy indanols - also had substitution at 1 and 3.

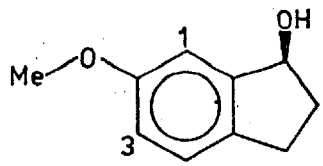
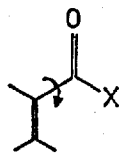
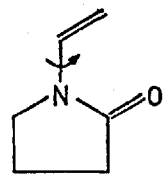


FIG.1-6.10

compounds which have two rigid parts connected by a rotatable bond (see FIG. 1-6.11). They found the best metal position from the "fixed" part of the molecule then added the data from the "rotating" part and optimised the rotamer from the overall fit of the calculated LIS. As all the systems studied were capable of conjugation they were able to ascertain which of the two "in plane" rotamers was preferred.



X = H -predonimantly trans
X = R & OR -cis/trans mixture
X = NR_2 -predominantly cis



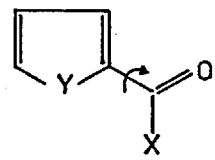


FIG.1-6.11

Armitage et al[189] considered the interesting problem of rotation in substrates which were rigid except for their point of attachment to the lanthanide (ie. via -OH and $-NH_2$ groups). They found that highly hindered molecules such as diacetone glucose (FIG.1-6.12) gave good calculated LIS fits for static complex models, but more compact substrates, such as aniline, required internal rotation to be taken into account before optimum fits could be found.

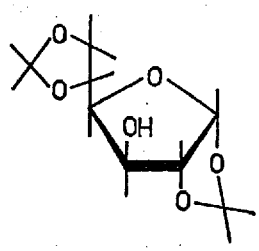


FIG.1-6.12 Diacetone glucose

Several studies which combine choice of isomer and selection of rotamer have been performed. Falk et al[214] determined the configuration of a 3,4-dimethylpyrromethanone using a combination of LIS data and Nuclear Overhauser measurements. Irradiation of the 4-Methyl group enhanced the olefinic proton by 30% (see FIG.1-6.13), hence indicating a Z-configuration. From LIS data with $Eu(dpm)_3$ the E-configuration could be rejected at the 99% confidence level. The final best fit for the Z-isomer was the twisted syn-configuration shown.

For the slightly more complex structure shown in FIG.1-6.14 Sullivan[215] found only poor correlation coefficient differences between the correct and incorrect assignments of the endo- and exo- diastereomers. He was unable to detect the effects of conformational changes of the non-rigid part of the molecule on the calculated LIS.

Studies of very complex systems, ie. those with three or more rotating bonds, several possible binding sites, or large difficult-to-assign structures, have met with varying success, and usually many different sources of data, not just LIS, have to be interpreted to produce sensible results.[188]

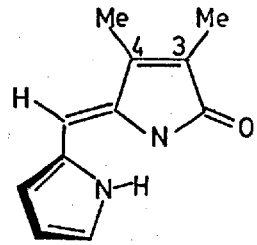


FIG.1-6.13 Twisted o.o.p. $\sim 40^{\circ}$

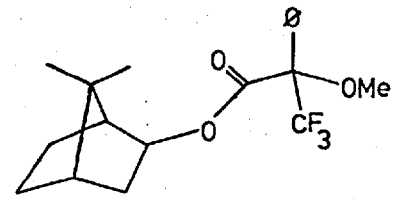


FIG.1-6.14

The earliest study on nucleotides was that of Barry et al[178] where the first problem tackled was how lanthanides bind to phosphate groups. Their conclusion, similar to that of later work by Lavallee and Zeltmann,[216] was that the metal lies in the plane of the phosphorus and two of the oxygens, with its Principal Symmetry Axis directed towards the phosphorus atom. The alternative metal position, ie. tetrahedrally disposed between the three available phosphate oxygens, produced no solutions to the LIS data.[178]

One of the weaknesses of Barry et al's work[178] on AMP and TMP was the scanty amount of ^{1}H LIS data used (5 shifts in both cases) considering that four free rotation bonds were being optimised. The later work of Angerman, Danyluk and Victor[208] on the antimalarial drug chloroquine (see FIG.1-6.15) was on a firmer footing with 14 ^{1}H shifts considered at two temperatures. Although this molecule has three potential binding sites, the ring nitrogen was found to be ten times better at complexing with the LSR than the side-chain amines. Firstly the LSR ($Pr(tmh)_3$) was fixed relative to the quinoline rings and then the side-chain was added stepwise, each group being rotated to the optimum position before adding the next. Both structures determined by this method varied considerably from the X-ray structure of diprotonated chloroquine. This is discussed in detail in the paper along with the methods of the nmr assignment and LIS analysis.

In a study which used both ^{1}H and ^{13}C LIS, Williamson et al[166] examined the conformations of all 18 possible C_6 alcohols. They assumed the Ln-O bond length was 3Å and the bond angle 130° and performed an initial crude screening of the large number of staggered conformations, by a manual search (ie. from a log-log plot of Ln-X distance vs. LIS they selected those conformers which gave a correlation coefficient of better than 0.5 to a line of slope -3). Having

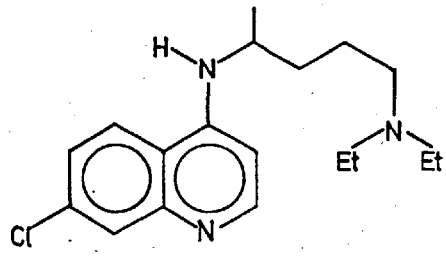
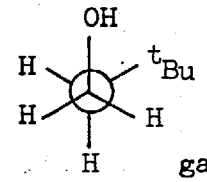
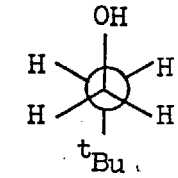


FIG.1-6.15 Chloroquine



gauche



trans

n-heptanol

Normally 25g : 75t
With LSR 10g : 90t

FIG.1-6.16

thus selected 6 or 7 trial conformers for each alcohol these were then subjected to a standard computer LIS calculating routine. Thus they were able to assign diastereotopic atoms with assurance, but warned that some LSR induced conformational changes occurred (see FIG.1-6.16).

A large number of studies of conformations in amides have appeared in the literature. As these have recently been reviewed by Mednejad[143] they will not be discussed here. The methods used are similar to those reported above and a typical example of a complex structure determination is that of N,N-di-isobutyl-1,1,1-trifluoro acetamide which has five rotatable bonds and was investigated by ^{1}H, ^{13}C and ^{19}F LIS.[143] Spectral analysis was very complex because the iso-butyl groups contain assymetric centres and the molecule therefore exists as a pair of diastereomers. A combination of double resonance experiments and computer analysis of the LIS data was necessary to assign the spectra; the conformational optimisation then followed using only the calculated LIS.

It is recognised that the examples in this section by no means exhaust the field and because of the need for brevity much interesting detail has had to be omitted. Once again the reader is referred to the article by Hofer,[142] which presents an overview of the rôle of LIS in conformational analysis, and to the references cited both here and by Hofer.

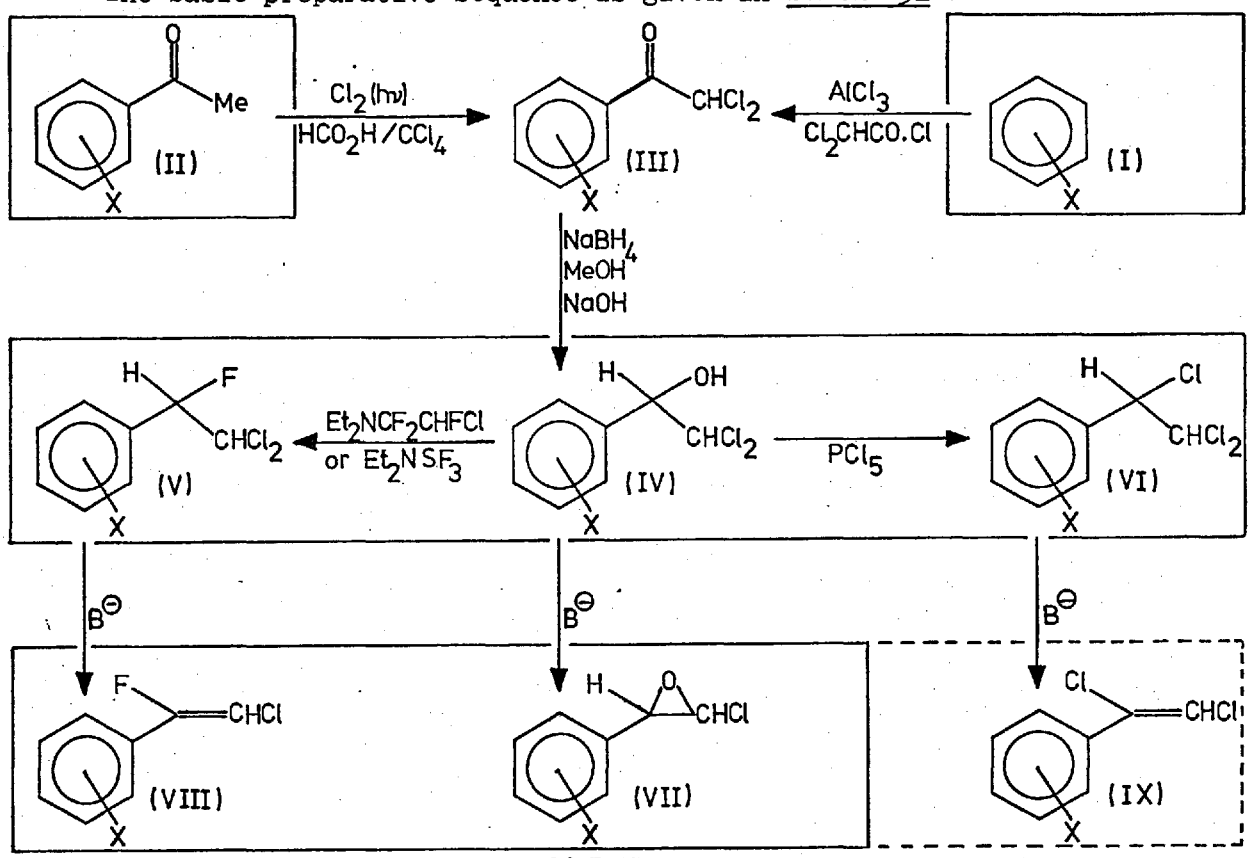
CHAPTER 2

2 PREPARATIVE CHEMISTRY LEADING TO THE THREE SERIES OF STARTING MATERIALS FOR ELIMINATION STUDIES

2-1 Introduction

The factors governing the choice of the starting materials have already been given.

The basic preparative sequence is given in SCHEME 32 :



SCHEME 32

Any compound may be identified by its series number (III), (IV), (V) etc. and its ring substituent.

eg : 2,2-dichloro-1-hydroxy-1-(4'-trifluoromethyl-phenyl) ethane could be referred to as the pCF_3 Type (IV) alcohol, or merely pCF_3(IV). This system of identification will be used where it aids the clarity of the text or where space (eg. within tables) demands.

As the preparative scheme overleaf shows the ability to make a particular Type (III) ketone is the linchpin of the synthetic approach as the steps from (III) to (IV), and (IV) to (V) and (VI), are fairly straightforward.

2-2 Experimental

Infrared spectra (IR) were recorded using either a Perkin Elmer 157 (Sodium Chloride Prism) Spectrophotometer or a Perkin Elmer 157G (Grating)

Spectrophotometer. Oils were recorded as thin films, solids as mulls in nujol.

Routine ^{1}H nmr spectra were recorded in either carbon tetrachloride or deuterio-chloroform solutions on one of four Varian Associates NMR spectrometers (depending on availability). Two 60MHz instruments, a T60 and latterly an EM-360A, were used (both without field/frequency locking facilities), and two 100MHz instruments, an HA 100 (somewhat modified) and an XL 100-12, both with field/frequency locks and homo-nuclear decoupling facilities. ^{19}F spectra were recorded on the XL 100-12 at 94.16MHz in $CDCl_3$ solution.

Gas liquid chromatography (glc) was carried out using a modified Perkin Elmer F11 gas chromatograph with a variety of 2m x 3mm OD columns and employing a flame ionisation detector. Approximate product ratios were determined manually.

Reactions were normally followed by thin layer chromatography (tlc) on home made plates (20 x 5cm and 7.6 x 2.5cm) using Merck silica gel F_{254}.

Column chromatography was carried out using Hopkins & Williams silica gel MFC (100-200 mesh) usually eluting with carbon tetrachloride/ethyl acetate mixtures.

Routine mass spectra (MS) were recorded on a V G Micromass 7070, whilst gas chromatography mass spectra (GC/MS) were recorded on either a Perkin Elmer MS 270 or an MS 30.

All boiling points were measured whilst distilling products under reduced pressure. (Distillations were stirred magnetically without air bleeds).

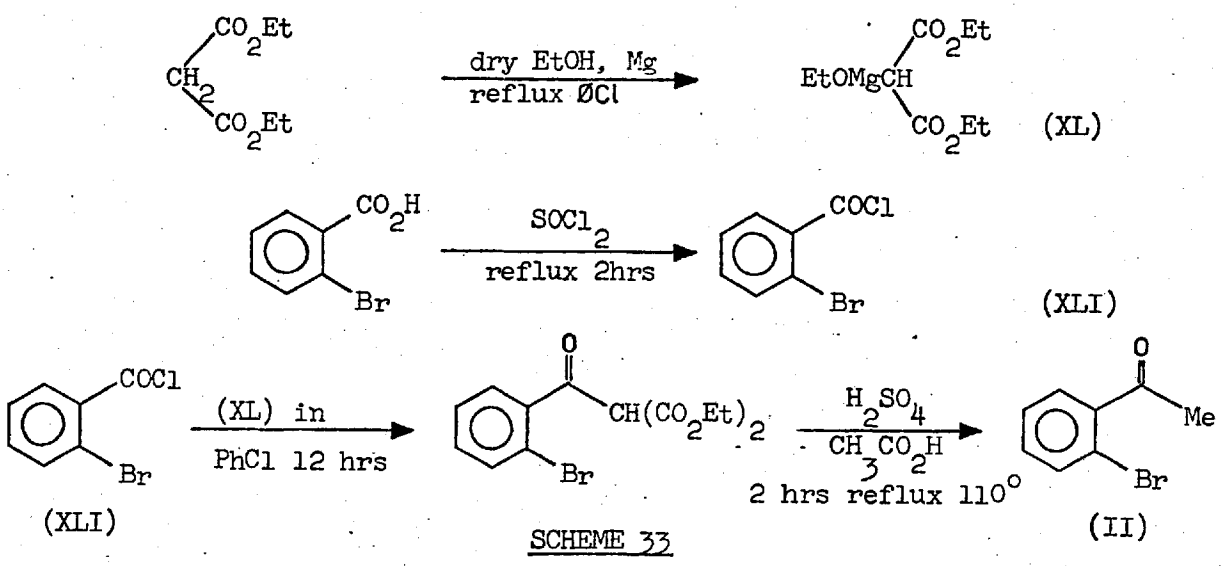
2-3 Preparation of the 2,2-Dichloroacetophenones (Type (III) Ketones)

The following acetophenones (compound (II) in SCHEME 32) were commercially available : X = H; ortho Cl, Me, OMe, NO_2, CF_3, NH_2;
para F, Cl, Br, OMe, NO_2, and CF_3.
Several other members of the series were available in this laboratory,[18] namely :
X = oF, pMe, and pNH_2.
Only the oBr acetophenone was unavailable.

2-3-1 Preparation of 2'-Bromoacetophenone[217]

This was prepared from 2'bromobenzoic acid as shown in SCHEME 33. 2'-Bromobenzoic acid (24.67g, 0.12M) was stirred with thionyl chloride (75ml, 124g, 1.10M) for twelve hours at 25°C, then refluxed for two hours. Excess thionyl chloride was removed at the pump. The product was distilled under reduced pressure to yield 2'-bromobenzoyl chloride (XI) (21.91g, 81.5%), B.P.117°C/ 10mm Hg (Lit.[217] 133-135/20mm Hg).

Dry ethanol (2.5ml, 0.04M) and dry carbon tetrachloride(0.5ml) were added



SCHEME 33

to magnesium turnings (3.95g, 0.16M) in a 500ml three necked flask equipped with a dropping funnel, condenser and dry nitrogen inlet. As soon as reaction started dry chlorobenzene (25ml) was added as solvent. Diethyl malonate (26g, 0.16M) in dry ethanol (10ml, 0.17M) was then added dropwise at 70°C. The mixture was then refluxed for one hour at 100°C and then cooled to room temperature. The resulting diethylethoxymagnesium malonate (XL) was then reacted in situ with the 2'-bromobenzoyl chloride (XLI) (21.91g, 0.1M) which was added dropwise in chlorobenzene (45ml) solution. The mixture was stirred at 25°C for twelve hours. 25% Sulphuric acid (25ml) was added and the organic layer was separated. This was concentrated in a rotorvapor at 100°C. Further 25% H_2SO_4 (25ml) and glacial acetic acid (25ml) were added and the mixture refluxed at 110°C for two hours. The product was worked up by ether/water extraction, neutralised with saturated sodium bicarbonate and then dried over anhydrous sodium sulphate to yield 2'-bromoacetophenone (18.6g, 93.5%), a colourless oil B.P.112°C/10mm Hg (Lit.[217] 133-5°C/20mm Hg), ^{1}H nmr δ 7.0-7.5(4H,m); 2.42(3H,s).

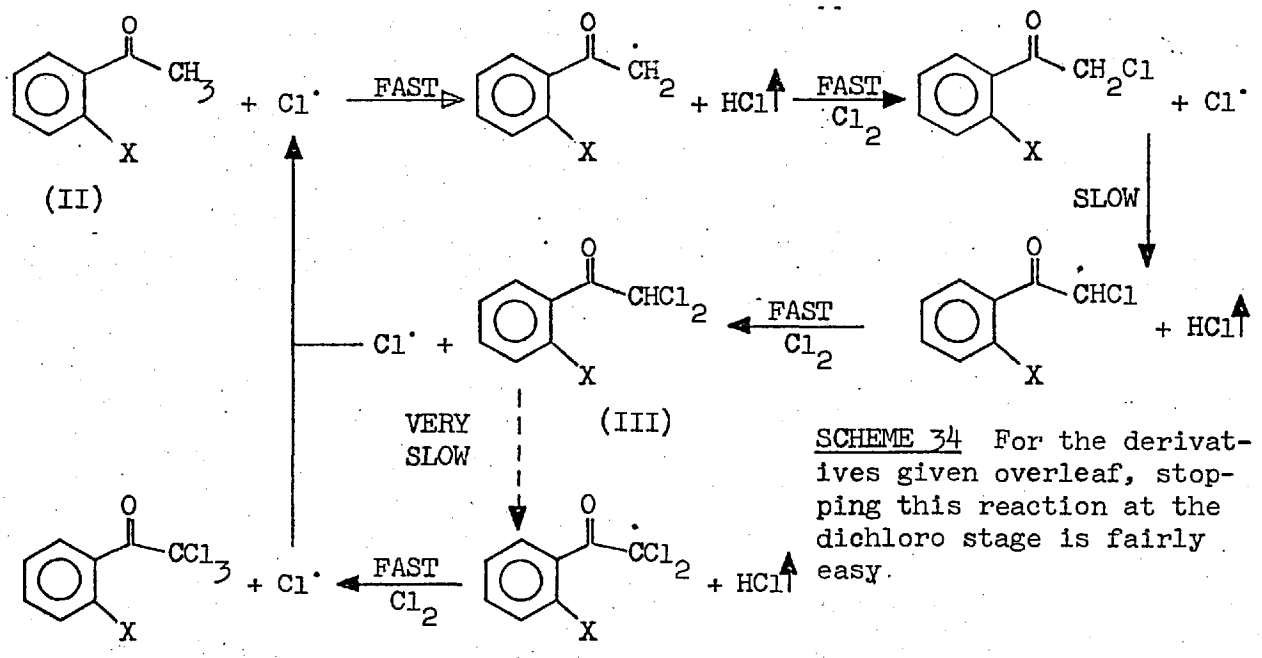
2-3-2 Methods Used in Preparing the 2,2-Dichloroacetophenones

Considerable difficulty was encountered in preparing some of the Type (III) dichloroketones, especially those containing methyl or methoxy ring substituents. Eventually three separate methods were adopted, which will be illustrated in turn with the substituents for which they were found best suited. All attempts at preparing the o and p amino derivatives failed and work on these substituents was eventually abandoned.

N.B. All handling of these chloro-ketones was done wearing gloves, in a fume cupboard, as they are powerful lachrymators and skin irritants.

METHOD 1 (Successfully used for X = H; oF, Cl, Br, NO_2, CF_3; pF, Cl, Br, NO_2 CF_3).

eg. Preparation of 2,2-dichloroacetophenone (H(III)) by Direct Chlorination



SCHEME 34 For the derivatives given overleaf, stopping this reaction at the dichloro stage is fairly easy.

Acetophenone (21.5g, 0.18M) was dissolved in 95% formic acid (75ml). The desired uptake of chlorine was calculated as 12.6g. The flask was tared and chlorine was slowly passed through the stirred mixture, whilst irradiating with a UV lamp for a total of 50 minutes. Periodically, small aliquots were extracted for micro-slide tlc (silica gel eluted with benzene) and the flask weighed. A typical tlc slide is shown in FIG.2-3.1, and the reaction was seen to proceed rapidly to the dichloroketone.

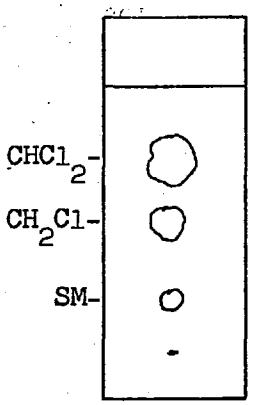


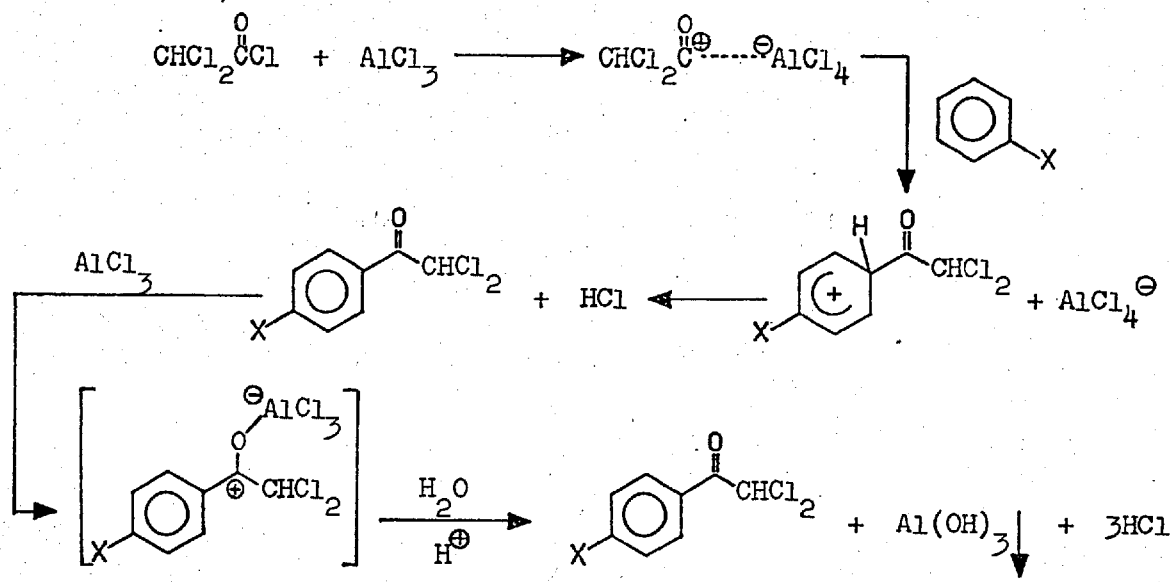
FIG.2-3.1

When the uptake of chlorine reached 13g, the supply was turned off and the flask stirred until tlc indicated that only the dichloroketone was present. Excess chlorine was removed by passing dry nitrogen through the mixture. The formic acid was evaporated off under reduced pressure on a rotorvapor. The product was ether extracted, neutralised with saturated sodium bicarbonate solution, dried over anhydrous sodium sulphate and then distilled under reduced pressure to yield 2,2-dichloroacetophenone as a colourless oil, B.P.83°C/0.4mm Hg (Yield 30.1g, 88%) ^{1}H nmr δ8.12-7.94(2H,m),8.68-8.31 (3H,m),6.66(1H,s).

METHOD 2 (Successfully used for X = H; pBr, Me, OMe)

eg. Preparation of 2,2-dichloro-4'-methyl acetophenone (pMe(III)) by Friedel Crafts Acylation (see SCHEME 35)

Dichloroacetyl chloride (29.6g, 0.2M) was added dropwise to a mechanically stirred suspension of finely powdered alumunium chloride (29.4g, 0.22M) in freshly distilled sodium-dried toluene (100ml), under dry nitrogen. Some



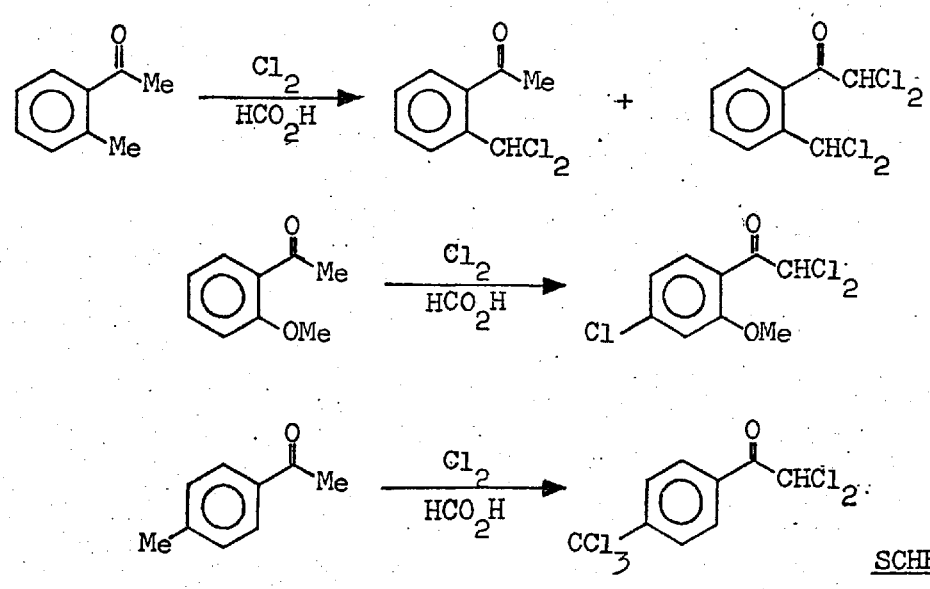
COMPLEX PRODUCT

SCHEME 35

cooling was necessary to control the reaction. When addition was complete the mixture was refluxed for one hour, then cooled to room temperature. Water (140ml) was added dropwise over 30 minutes to destroy any unreacted aluminuim chloride. Concentrated hydrochloric acid (15ml) was added to break up any remaining solid complexes. The organic layer was separated, ether/water extracted, neutralised with saturated sodium bicarbonate solution, and then dried over anhydrous sodium sulphate. 2,2-dichloro-4'-methyl acetophenone, a colourless oil, was purified by reduced pressure distillation. B.P.78°C/0.2mm Hg (Yield 23.16g,55%) ^{1}Hnmr δ 8.03-6.91(4H,m),6.12(1H,s),4.11(3H,s).

METHOD 3 (Successfully used for X = oMe, oOMe, pOMe)

When the ring substituent was methyl or methoxy, Method 1 led to the undesirable products shown in SCHEME 36.



SCHEME 36

The reaction scheme for Method 3 is similar to that for Method 1 (SCHEME 34) with conditions adjusted to favour chlorination of the acyl methyl group.

eg. Preparation of 2,2-dichloro-2'-methoxy-acetophenone (oOMe(III)) by Direct Chlorination under mild conditions

2'-methoxy acetophenone (20.4g, 0.136M) was dissolved in carbon tetrachloride (125ml) and deuteriochloroform (5ml). The flask was kept in semi-dark conditions at ~10°C. Chlorine gas was passed slowly for 30 seconds into the solution and the contents of the flask stirred until the yellow colouration had cleared, before passing chlorine for a further 30 seconds. After three of these additions a fine white precipitate started to form (the mono chloride). This was dissolved by adding 5ml aliquots of deuterio chloroform. After 7 additions a sample was withdrawn for ^{1}H nmr. Subsequent additions of chlorine were for 15 seconds only, with ^{1}H nmr at the completion of each stage. After the passage of chlorine for 315 seconds, ^{1}H nmr showed virtually 100% yield of the desired product. Any unreacted chlorine was blown off with dry nitrogen. The product was washed with saturated sodium bicarbonate and dried over anhydrous sodium sulphate to yield a colourless oil, 2,2-dichloro-2'-methoxyacetophenone, B.P.85°C/0.6mm Hg (29.4g, 98%yield) ^{1}H nmr δ8.03-6.91(4H,m);6.12(1H,s); 4.11(3H,s).

2-3-3 Physical Properties of the Type (III) Dichloroacetophenones

TABLE 2-3.1 Physical Properties of the Type (III) Dichloroacetophenones

DERIV X	M.W.	METHOD USED	B.P. °C/mm Hg	STATE	RECRYST SOLVENT	M.P.
H	189	1 & 2	83°/0.4	colourless oil		
o F	207	1	70°/0.1	colourless oil		
o Cl	223.5	1	74°/0.25	colourless oil		
o Br	268	1	94°/0.35	colourless oil		
o Me	203	3	85°/0.6	colourless oil		
o OMe	219	3	95°/0.5	colourless oil		
o NO_2	238	1		yellow oil	MeOH	84-85°
o CF_3	257	1	75°/0.3	colourless oil		
p F	207	1	71°/0.4	colourless oil		
p Cl	223.5	1		colourless cryst	MeOH	61-62°
p Br	268	1 & 2		colourless cryst	MeOH	62-63°
p Me	203	2	78°/0.2	colourless oil		
p OMe	219	2 & 3	146°/0.5	colourless oil		
p NO_2	238	1	119°/0.3	yellow oil since	cryst	
p CF_3	257	1	70°/0.2	colourless oil		

TABLE 2-3.2 ^{1}H NMR Data of the Type (III) Dichloroacetophenones*

DERIV X	AROMATIC PROTONS	SIDE-CHAIN ^{1}H	DERIV ^{1}H
H	8.68-8.31(3H,m), 8.12-7.94(2H,m)	6.66(1H,s)	
o F	7.90-6.90(4H,m)	6.63-6.60(1H,d, J=2.0Hz)	
o Cl	7.60-7.18(4H,m)	6.66(1H,s)	
o Br	7.70-7.20(4H,m)	6.60(1H,s)	
o Me	7.80-7.60(1H,m), 7.45-7.10(3H,m)	6.54(1H,s)	2.42(3H,s)
o OMe	8.03-6.91(4H,m)	6.12(1H,s)	4.11(3H,s)
o NO_2	8.36-8.10(1H,m), 7.90-7.35(3H,m)	6.32(1H,s)	
o CF_3	7.75-7.65(4H,broad s)	6.53(1H,s)	
p F	8.10-7.90(2H,dd,J=5.0/8.3Hz) 7.22-6.90(2H,t,J=8.3Hz)	6.37(1H,broad s)	
p Cl	8.02-7.80(2H,d,J=8.3Hz), 7.44-7.20(2H,d,J=8.3Hz)	6.42(1H,s)	
p Br	7.95-7.75(2H,d,J=8.3Hz), 7.62-7.40(2H,d,J=8.3Hz)	6.47(1H,s)	
p Me	7.97-7.74(2H,d,J=7.0Hz), 7.30-7.04(2H,d,J=7.0Hz)	6.48(1H,s)	2.36(3H,s)
p OMe	8.12-7.98(2H,d,J=9.0Hz), 7.04-6.68(2H,d,J=9.0Hz)	6.65(1H,s)	4.89(3H,s)
p NO_2	8.26-7.96(4H,m)	6.58(1H,s)	
p CF_3	8.18-8.07(2H,d,J=8.0Hz), 7.72-7.60(2H,d,J=8.0Hz)	6.45(1H,s)	

* All spectra were recprded in CCl_4 with internal TMS reference at 100 MHz

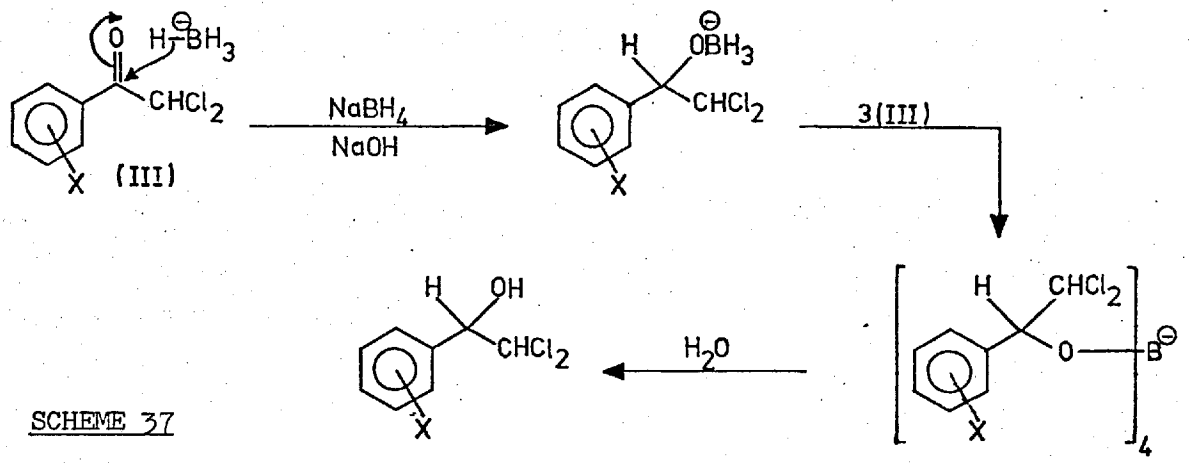
WARNING : All are pungent, very powerful lachrymators and irritants, immiscible with water and difficult to remove from the skin.

2-4 Preparation of the 2,2-Dichloro-1-phenyl ethanols (Type (IV) Alcohols)

The reduction of the Type (III) ketones to the Type (IV) alcohols was performed, in every instance, using the sodium borohydride method.[218] This was found to be quick, reliable and clean, unlike the similar lithium aluminium hydride method[52] which was found to be inconvenient and unreliable due to variations in the condition of the LAH itself.

2-4-1 General Sodium Borohydride Method (see SCHEME 37)

Sodium borohydride (2.0g,0.05M) (2-fold excess) in 0.2N aqueous sodium hydroxide (20ml) was added dropwise to the dichloroketone (III) (0.1M) in Analar methanol (100ml) at such a rate as to cause the methanol to gently reflux. Any borohydride clinging to the dropping funnel was washed into the reaction flask with water. The mixture was refluxed for 30 minutes before removing the methanol on a rotorvapor. The resulting white glutinous mixture was ether/water extracted, the organic layer being dried over anhydrous sodium



SCHEME 37

sulphate prior to removal of the ether and distillation. Yields were quantitative and the products very clean.

2-4-2 Physical Properties of the Type (IV) Alcohols

These are generally highly viscous oils, possessing a characteristic odour and mild irritant properties.

TABLE 2-4.1 Physical Properties of the Type (IV) Alcohols

DERIV X	M.W.	$n_D^{22.5}$	B.P. °C/mm Hg	STATE	RECRYST SOLVENT	M.P.
H	191	1.5590	77°/0.35	colourless oil	since	cryst.
o F	209	1.5382	73°/0.20	colourless oil	since	cryst.
o Cl	225.5	1.5702	78°/0.10	colourless oil		
o Br	270	1.5893	92°/0.30	colourless oil		
o Me	205	1.5581	93°/0.10	colourless oil		
o OMe	221	1.5590		colourless cryst	hexane	72-74°
o NO_2	240	1.5835	124°/0.30	yellow oil since	cryst	63-65°
o CF_3	259	1.4858	68°/0.05	colourless oil		
p F	209	1.5332	76°/0.25	pale yellow oil		
p Cl	225.5	1.5653	98°/0.225	pale yellow oil		
p Br	270	1.5942	103°/0.005	colourless oil		
p Me	205	1.5525	102°/0.25	colourless oil		
p OMe	221	1.5647	100°/0.25	pale yellow oil		
p NO_2	240	1.5888		yellow cryst	hexane	89-91°
p CF_3	259	1.4856	70°/0.20	colourless oil		

Detailed ^1H, ^{19}F and ^{13}C nmr spectra were recorded of the Type (IV), (V) and (VI) compounds and are fully discussed in Chapter 4.

In the mass spectra of the Type (IV) alcohols (see TABLE 2-4.2) a major species (underlined) present in all samples was the X-substituted hydroxy tropylium ion : (M = 106 + X).

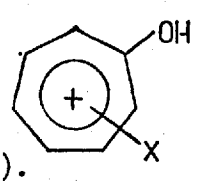


TABLE 2-4.2 Mass Spectral Data of the Type (IV) Alcohols

DERIV	M+	Sub^n Pattern	100%	2nd	3rd	4th	5th	6th
H	190(1)	2 Cl	107	79(57)	77(37)	51(17)	91(8)	108(8)
o F	208(1)	2 Cl	125	97(28)	77(22)	51(10)	126(8)	109(7)
o Cl	224(n)	3 Cl	141	77(73)	143(33)	51(17)	113(13)	50(11)
o Br	270(1)	2 Cl, 1 Br	77	185(90)	187(82)	125(32)	78(31)	51(30)
o Me	204(n)	2 Cl	121	93(44)	77(34)	91(34)	65(12)	39(11)
o OMe	220(5)	2 Cl	137	77(80)	125(79)	155(60)	107(60)	121(50)
o NO_2	235(n)	2 Cl	28	77(89)	125(75)	152(61)	121(50)	175(41)
o CF_3	*241(1)	2 Cl	155	127(73)	175(53)	156(13)	75(10)	77(9)
p F	208(n)	2 Cl	125	97(44)	77(34)	51(15)	109(14)	126(12)
p Cl	224(n)	3 Cl	141	77(67)	143(29)	113(14)	125(14)	51(14)
p Br	268(1)	2 Cl, 1 Br	185	187(95)	77(85)	78(40)	51(22)	50(20)
p Me	204(n)	2 Cl	121	93(36)	91(31)	77(30)	65(11)	122(9)
p OMe	220(2)	2 Cl	137	77(25)	109(17)	94(15)	121(11)	138(10)
p NO_3	235(1)	2 Cl	152	77(18)	78(16)	106(15)	51(13)	94(12)
p CF_3	*241(5)	2 Cl	175	127(72)	173(17)	176(13)	145(12)	147(9)

n = negligible % ; * indicated highest observed line not M+ but M-17

TABLE 2-4.3 Micro Analysis Data of the Type (IV) Alcohols

DERIV X	REQUIRED				FOUND			
	C	H	Cl	N,F,Br	C	H	Cl	N,F,Br
H	50.29	4.22	37.11		50.50	4.41	37.25	
o F	45.96	3.37	33.92	9.09(F)	46.17	3.40	34.06	9.22(F)
o Cl	42.61	3.31	47.16		42.70	3.15	46.63	
o Br	35.59	2.61	26.27	29.60(Br)	35.60	2.58	25.64	28.89(Br)*
o Me	52.71	4.92	34.57		52.60	4.87	33.87	
o OMe	48.89	4.56	32.07		48.66	4.35	32.80	
o NO_2	40.71	2.99	30.03	5.93(N)	41.81	3.40	28.98	5.46(N)
o CF_3	41.73	2.72	27.37	22.00(F)	41.73	2.70	25.30	22.26(F)
p F	45.96	3.37	33.92	9.09(F)	46.00	3.42	31.51	9.56(F)
p Cl	42.61	3.13	47.16		43.97	3.26	43.85	
p Br	35.59	2.61	26.27	29.60(Br)	36.55	2.93	27.71	31.08(Br)*
p Me	52.71	4.91	34.57		52.66	4.83	33.53	
p OMe	48.89	4.56	32.07		48.67	4.46	31.75	
p NO_2	40.71	2.99	30.03	5.93(N)	42.90	3.39	29.88	6.17(N)
p CF_3	41.73	2.72	27.37	22.00(F)	43.35	3.05	21.92	22.48(F)

* Cl and Br analysed for simultaneously.

TABLE 2-4.4 Infrared Data of the Type (IV) Alcohols.

DERIV X	Film Type	Peak 1	Peak 2	Peak 3	Peak 4	Peak 5	Peak 6	Peak 7	Peak 8	Peak 9	Peak 10	Peak 11	Peak 12
H	mull	3350 v	1490 m	1330 m	1190 s	1100 s	1070 s	1020 m	950 m	860 s	780 s	735 s	700 s
o F	liq	3450 s	1630 m	1580 m	1480 m	1450 s	1210 s	1070 s	1050 s	820 s	790 s	760 s	720 s
o Cl	liq	3350 s	1585 w	1565 w	1460 m	1430 s	1180 m	1085 s	1045 s	1030 s	840 m	760 s	715 m
o Br	mull	3250 s	1585 w	1560 w	1320 m	1200 s	1120 s	1090 s	1020 m	840 m	770 s	750 s	710 s
o Me	liq	3350 s	2900 m	1600 w	1480 m	1450 m	1200 m	1110 m	1040 s	780 s	740 s		
o OMe	mull	3250 v	1600 s	1580 m	1480 v	1280 s	1230 v	1080 s	1020 s	960 m	800 s	760 s	730 s
o NO_2	mull	3450 m	1600 m	1560 m	1500 v	1330 v	1220 s	1170 s	1090 v	860 s	805 s	770 s	740 s
o CF_3	liq	3350 s	2850 w	1600 w	1580 w	1450 m	1300 v	1160 v	1110 v	1040 s	790 s	770 s	740 s
p F	liq	3350 v	1600 s	1510 s	1220 v	1150 m	1050 m	840 s	800 s	790 m	745 m		
p Cl	liq	3350 v	1590 m	1490 s	1400 m	1190 m	1090 v	1010 s	830 m	790 s	770 s		
p Br	liq	3350 v	1580 m	1480 s	1390 m	1180 m	1070 s	1010 s	820 m	790 s	760 s		
p Me	liq	3400 v	2450 m	1605 w	1510 m	1190 s	1085 s	1040 s	820 s	800 s	740 s		
p OMe	liq	3400 s	2850 m	1610 s	1510 s	1300 m	1250 v	1170 s	1030 v	830 s	790 s	720 m	
p NO_2	mull	3450 m	1600 m	1520 v	1340 v	1180 m	1080 s	830 m	770 s	740 s	700 s		
p CF_3	liq	3350 s	1620 m	1410 m	1320 v	1160 v	1120 v	1060 s	1020 s	840 s	790 s	750 m	730 s

The major peaks are listed in descending order of their wavenumber (cm^{-1}).
Relative intensities : v = very strong; s = strong; m = medium; w = weak.

2-5 Preparation of the 2,2-dichloro-1-fluoro-1-phenyl-ethanes (Type (V) Fluorides)

The preparation of these compounds by the direct fluorination of the Type (IV) alcohols posed several practical problems, not the least of which was the preparation and handling of the fluorinating reagents. Reaction of the alcohol to give the fluoride was normally instantaneous and quantitative.

2-5-1 Preparation of the Fluorinating Reagents and the Type (V) Fluorides

Two reagents were used, diethylamino-2-chloro-1,1,2-trifluoro ethane (DACTE),[119-222] (XII) and diethylamino sulphur trifluoride (DAST) (XV);[223] both successfully, although both had their own disadvantages.

Two special sets of apparatus were designed for these reactions, The first (FIG.2-5.1) was rather makeshift, consisting of a variety of parts both readily available and specially made, and had to be dissembled during the preparation of the fluorinating reagent. The second, purpose built, (FIG.2-5.2), incorporated modifications which overcame most of these problems.

Both reagents were prepared in both sets of apparatus, but here the preparation of (DACTE) will be described using the first apparatus, and (DAST) using the second. All fluorinations were done in a specially prepared fume-cupboard, observing all the precautions necessary in the handling of such dangerous materials.

2-5-1.1 Problems Involved in the Preparation of Diethylamino-2-chloro-1,1,2-trifluoro ethane (DACTE).

The basic method of preparation was simply to bubble the gas, chlorotrifluoroethylene, through diethylamine for several hours and then distill off the product of the addition reaction :

$$Et_2NH + CF_2{=}CFCl \longrightarrow Et_2NCF_2CHFCl$$

SCHEME 38 (XL)

The main problems encountered were :

i) Increasing the reaction yield to more than 20%

ii) Wasting the minimum amount of chlorotrifluoroethylene

iii) Keeping the reagent under dry nitrogen at all times

iv) Handling an extremely dangerous fluorinating reagent which gives off HF fumes immediately on contact with air.

The basic apparatus for preparing the reagent is shown in FIG.2-5.1(a). After the apparatus had been flushed with dry nitrogen, the gas was passed through the anti-suck-back flask, through the reaction flask and condensed at the dry-ice cold finger. Any uncondensed gas or pressure fluctuation was released through a valve containing diethylamine.

Several factors need to be considered in attempting to increase the reaction yield :

(1) CF_2CFCl condenses at $-27^{\circ}C$.

(2) Et_2NH freezes at $-48^{\circ}C$.

(3) Rate of reaction decreases with decreasing temperature.

(4) Gas-liquid reactions are likely to be very inefficient compared to liquid-liquid reactions.

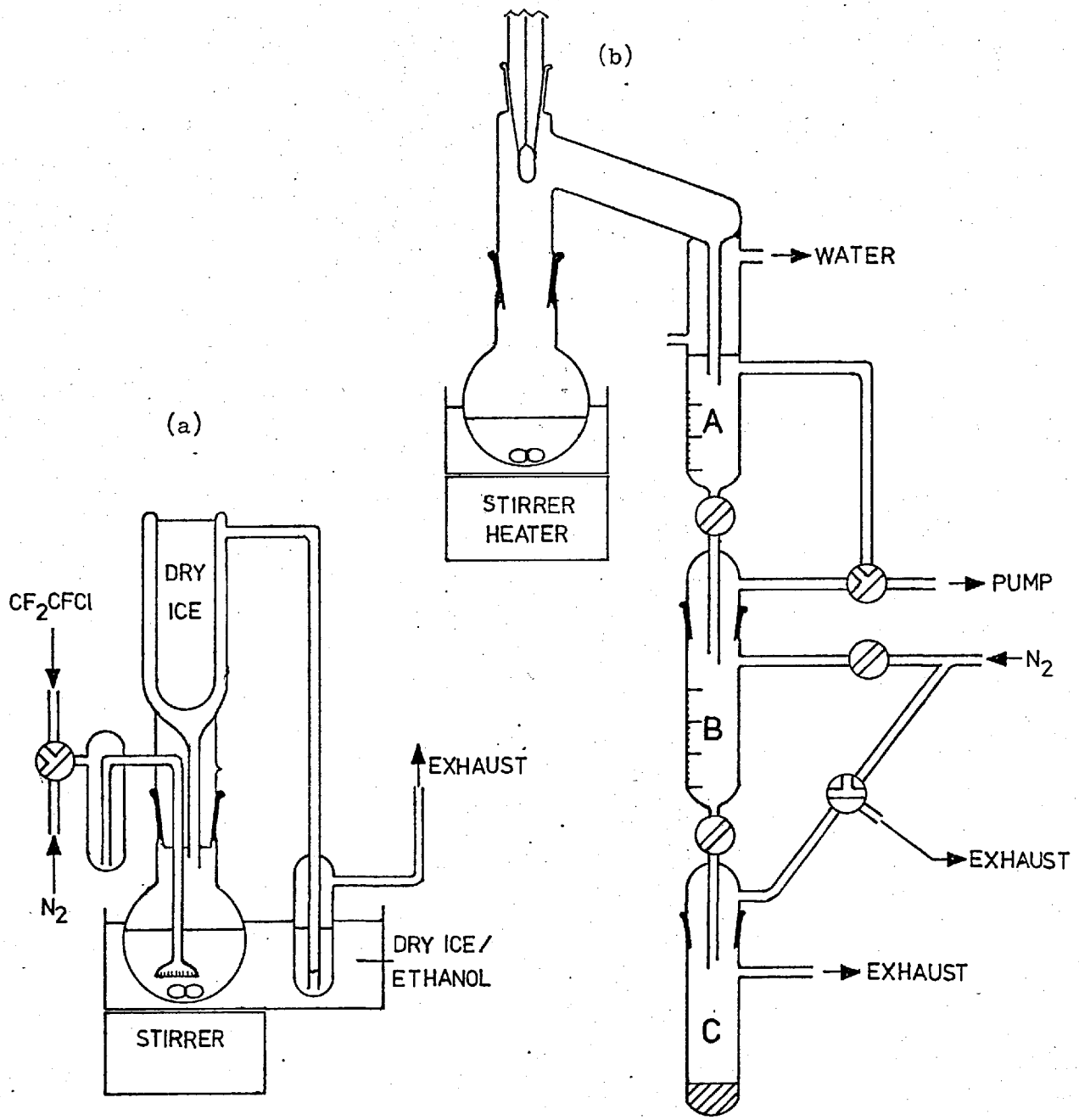
Assuming that the dry ice condenser (at $-78^{\circ}C$) condenses all of the chlorotrifluoroethylene it receives (a reasonable assumption) there are two basic, extreme methods for the preparation.

(A) Keep the reaction flask between 0° and $25^{\circ}C$. Pass the gas slowly and allow the condensate running back from the cold finger to react with the diethylamine. Continue for up to ten hours before flushing the unreacted gas and distilling off the product.

(B) Cool the flask to $-30^{\circ}C$. Pass the gas quickly until a slight excess has condensed. Stop the gas flow. Warm the flask (to $-10^{\circ}C$ if this is possible) and keep pouring dry ice into the condenser so as to contain the chlorotrifluoroethylene. Continue for as long as possible (usually 3 to 4 hrs) before flushing unreacted gas and distilling off the product.

Both of the above methods, and a variety of intermediates, were used with

FIG.2-5.1 Apparatus Used in the Preparation/Distillation/Reaction of DACTE



varying degrees of success. Method (B) generally seemed the more effective although average yields were only ~20%. (Yields of 44% & 61% have been reported).[219,220]

Early attempts at conventional reduced pressure distillation of the product produced a reagent which, although it fumed violently in air, was unreactive towards alcohols. On distillation the reagent was collected in a flask (which was later fitted with a suba-seal) under dry nitrogen, and was dispensed with a syringe. As this proved unsuccessful it was decided to react the reagent with the alcohols before it could deteriorate. To do this a distillation apparatus involving a "vacuum lock" was designed (FIG.2-5.1(b)). This will be described below.

PROCEDURE 1 Preparation of Diethylamino-2-chloro-1,1,2-trifluoroethane (DACTE)

Diethylamine (36.5g, 0.6M) (freshly distilled from anhydrous sodium carbonate) was placed in the flask (FIG.2-5.1(a)), with a further small quantity in the release valve, and cooled to -35°C in an ethanol/dry ice bath. The condenser was cooled to -78°C and the gaseous chlorotrifluoroethylene was slowly bubbled through the diethylamine until sufficient (56g, 0.5M) had condensed. The ethanol/dry ice bath was allowed to warm to -5°C (over 1hr) and the mixture was kept gently refluxing for 4hrs. (This required continual topping up of the ethanol/dry ice condenser. It was necessary to gently warm the lower bath to maintain it at -5°C as the refluxing gas withdrew heat from it at a significant rate).

The upper condenser was then allowed to warm up gradually so that any unreacted chlorotrifluoroethylene could be vented from the system. The flask was warmed to room temperature and flushed with a slow stream of dry nitrogen.

The distillation part of the apparatus (FIG.2-5.1(b)) was thoroughly flushed with dry nitrogen, and with the aid of several well placed jets of dry nitrogen, was attached to the reaction flask without exposing the reagent to the air.

The apparatus was connected to a rotary pump via a mercury manometer, a nitrogen trap and two air bleeds. The pressure was very slowly reduced until the unreacted diethylamine boiled off (25°/250mm Hg). This was condensed at the liquid nitrogen trap. The water condenser was connected, the flask heated, and the pressure further reduced until the reagent began to distill over (B.P.50-55°/20mm Hg; Lit: B.P.32-33°/6mm Hg[220]). This was collected in Vessel A which was always maintained at the distillation pressure. Vessel B was normally kept flushed with nitrogen but could readily be pumped down to the same pressure as A.

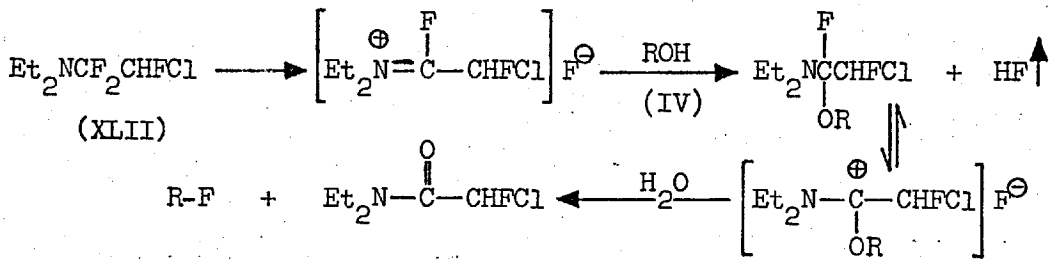
In this condition distillate could be run from A into B without stopping the distillation. Vessels A and B would then be isolated, distillation continuing in A whilst B was let up to room pressure under nitrogen. Vessel B was graduated so that aliquots of the fluorinating agent could be run directly onto the alcohol samples in the exchangeable reaction vessels C. Using this method as many as twelve samples have been fluorinated in quick succession.

The alcohols, if liquids, were reacted neat; if solids, dissolved in the minimum amount of analar dichloromethane. To each 0.5g of alcohol (MW 200-270) was added 1.5ml of (DACTE) (MW 189.5). More accurate measurements were not attempted as this allowance was considered generous and was always sufficient.

The reaction vessels C were B19 jointed side-arm test tubes. With this arrangement, dry nitrogen could be flushed over the reaction, and the copious

white fumes of HF liberated could be vented to the fume-cupboard flue.

Reactions were instantaneous and were characterised by the bright red colouration of the complex (XLII),[222] which was later broken up by the addition of water.



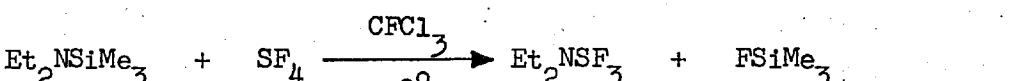
SCHEME 39

After shaking for a short period, the reaction products were treated with water, dissolved in dichloromethane and transferred to a separating funnel. The organic layer was repeatedly washed with water and then neutralised with saturated sodium bicarbonate solution. After drying over anhydrous sodium sulphate, the mixture was passed down a short Florosil column to remove the 1-chloro-1-fluoro-N,N-diethyl acetamide (XLIV) giving the Type (V) fluoride in good yield and in most cases, high purity. Trace impurities of the by-product (XLIV) in the final fluoride product were instantly characterisable by both ^{1}H and ^{19}F nmr, and were removed by repeat chromatography of the product. ((XLIV) ^{1}H nmr -CHFCl δ6.28(1H,d,J_{HF}=50.6Hz); ^{19}F nmr O/S 36190-36250 (Relative to $CDCl_3$ lock) ie. 142.8 $\pm$ 0.3ppm to highfield of $CFCl_3$ (J_{HF} 50.5 $\pm$ 0.6Hz) shift dependent on solution concentration).

This method was used successfully with the following Type (IV) alcohols : (X = H; oF, Cl, Br, Me, OMe; pF, Cl). It failed to incorporate fluorine in both o and pNO_2(IV), and was not tried with the remaining derivatives.

2-5-1.2 Problems Involved in the Preparation of Diethylamino Sulphur Trifluoride (DAST)

The basic method of preparation is similar to that of the (DACTE) in that it involves reaction of a gas with liquids at low temperatures, and purifying the reagent by distillation:[223]



SCHEME 40

The problems associated with this preparation are similar to those of the (DACTE) preparation. An additional problem was the volatility of the sulphur tetrafluoride and the fluorotrimethyl silane both of which tended to bump rather than distill. A very long distillation was therefore required,

during which the sulphur tetrafluoride (B.P.-40°C), fluorotrimethyl silane (B.P.17°C), and the trichlorofluoromethane (B.P.25°C), had to be removed before the DAST (B.P.56°/12mm Hg) could be isolated.

The apparatus used for this preparation is illustrated in FIG.2-5.2. It combines all the functions of the two sets of apparati FIGS.2-5.1(a) & (b) in one piece of glassware and therefore made the handling of the fluorinating reagents more efficient and safe.

The apparatus was thoroughly baked dry before use. On assembly it was kept flushed with dry nitrogen. A wide temperature range silicon grease was used on all joints except the B19 cone which took the exchangeable fluorination reaction vessels C. This was fitted with a ptfe sleeve to avoid joint seizure. The only two taps that the DAST reagent came into contact with were greaseless ptfe barrel "ROTAFLO" stopcocks (3) and (4).

Vessel A (a B29 test-tube, nominal capacity 60ml calibrated in 1ml divisions was equipped with a small ptfe coated magnetic follower. The main reasons for using a test tube as a reaction vessel were :

i) It could be calibrated

ii) It could be completely immersed in a dewar containing an ethanol/dry ice bath. This improved the efficiency of condensing the SF_4 gas and also reduced the amount of topping up necessary in the dry ice bath.

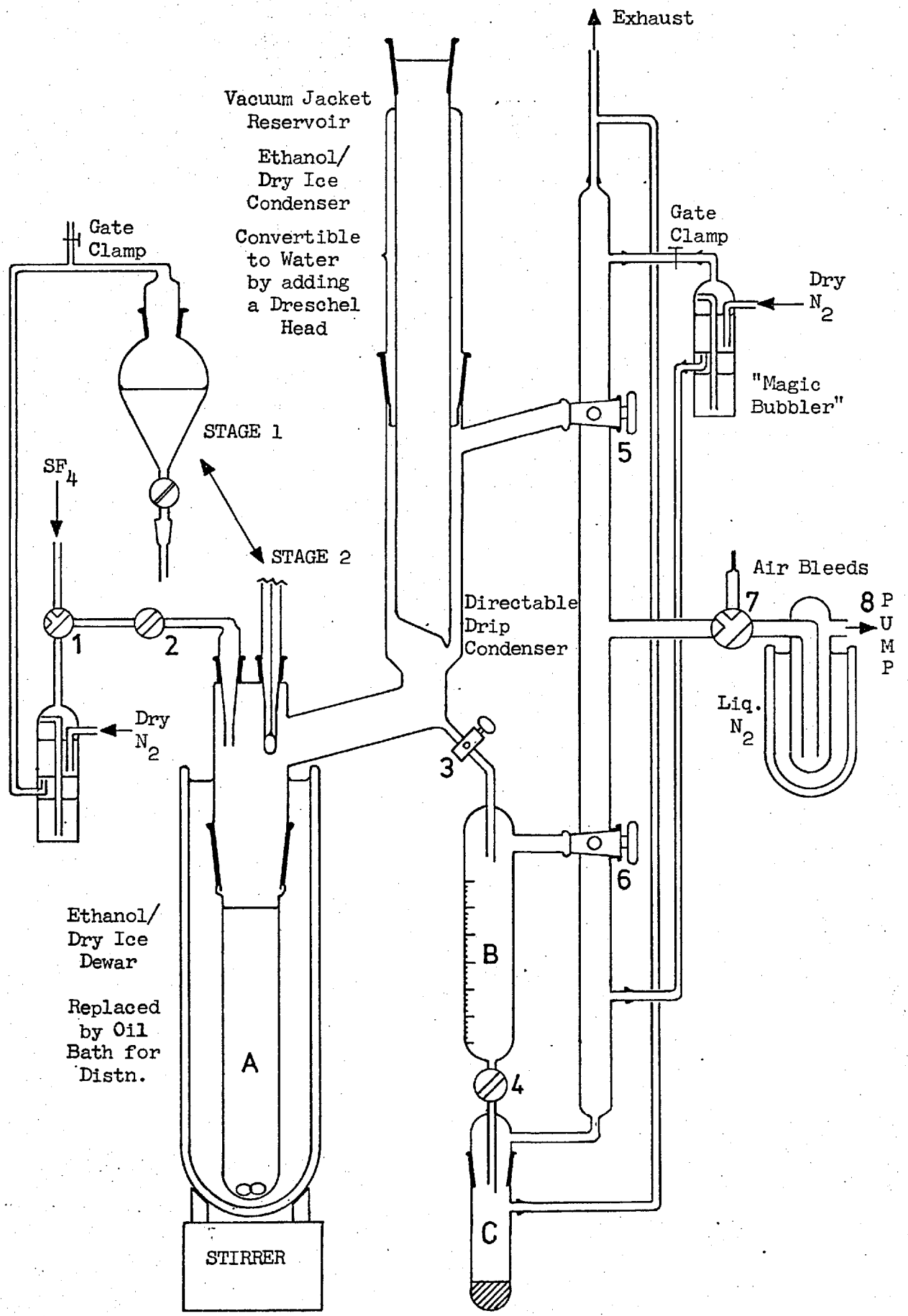
iii) If the mixture bumped during distillation it was easier to contain. Note that the joint in the reaction vessel A was well below the surface of the ethanol bath. This gave no problems with leakage. Also, stirring of the reaction mixture was necessary because the liquid partitioned into two phases.

The upper ethanol/dry ice condenser was designed with an angled drip for distillation purposes and was fitted with a large vacuum jacketed reservoir to reduce the frequency of "topping up" with dry ice. The top of the condenser assembly carried a B24 joint. For dry ice use this took a powder funnel, but later when a conventional water condenser was required a dreschel head with a polythene extension tube was fitted, and the condenser flushed with water in a normal fashion.

All flexible tubing used to carry gases, waste and vacuum was polythene and was renewed after each use. The waste outlet was continually flushed with nitrogen. As before vessel B was graduated for metering the amount of DAST used in each fluorination.

Only one minor change of configuration was required during the course of the reaction: the interchange of a dropping funnel with the B10 distillation thermometer, which was accomplished by using a slight positive pressure of nitrogen within the apparatus and the dropping funnel (empty at this stage).

FIG.2-5.2 Apparatus Used in the Preparation/Distillation/Reaction of DAST



PROCEDURE 2 Preparation of Diethylamino Sulphur Trifluoride (DAST)

Vessel A and the condenser were cooled to -78°C. Tap 3 was closed and tap 5 was opened to the flue. The nitrogen supply to tap 1 was stopped and the "magic bubbler" (see FIG.2-5.2) was used to test the opening of the needle valve on the sulphur tetrafluoride cylinder. The needle valve was closed and the traces of SF_4 in the bubbler were flushed into the apparatus with dry nitrogen. Tap 1 was then adjusted to isolate the bubbler, and a slow stream of sulphur tetrafluoride was passed into the apparatus. Periodically the ethanol/dry ice dewar was lowered to check the level of condensate. By this method a total of 5.7ml (0.1M) of sulphur tetrafluoride was collected. The gas supply was stopped and the inlet line flushed with nitrogen before being closed at (2). Chlorotrifluoromethane (15ml) previously chilled to -60° was run dropwise onto the sulphur tetrafluoride. A chilled (-60°) solution of diethylaminotrimethyl silane (13.6g, 0.09M) in chlorotrifluoro methane (14ml) was then added, very slowly, to the stirred reaction mixture. Two layers formed, the upper being dark red in colour and comprising about 60% of the mixture.

The mixture was slowly warmed to -20°C and allowed to reflux for 3hrs. During this period the upper layer contracted until it comprised only 10% of the mixture. The condenser was allowed to warm up and any unreacted sulphur tetrafluoride was gradually released to the flue; the reaction flask was allowed to warm to room temperature.

The oil pump was started with both air bleeds fully open and (5) open to the flue. Tap (6) was adjusted so that vessel B was connected to the nitrogen inlet. Tap 5 was opened to the pump, and very slowly (to prevent bumping) the air bleed at (7) was closed. The liquid nitrogen trap was positioned and the air bleed at (8) finely adjusted until the fluorotrimethyl silane gently boiled off, (16°/755mm Hg). The pressure was further reduced to remove the chlorotrifluoro methane (B.P.20°/600mm Hg). This stage took several hours, both volatile compounds being condensed in the liquid nitrogen trap.

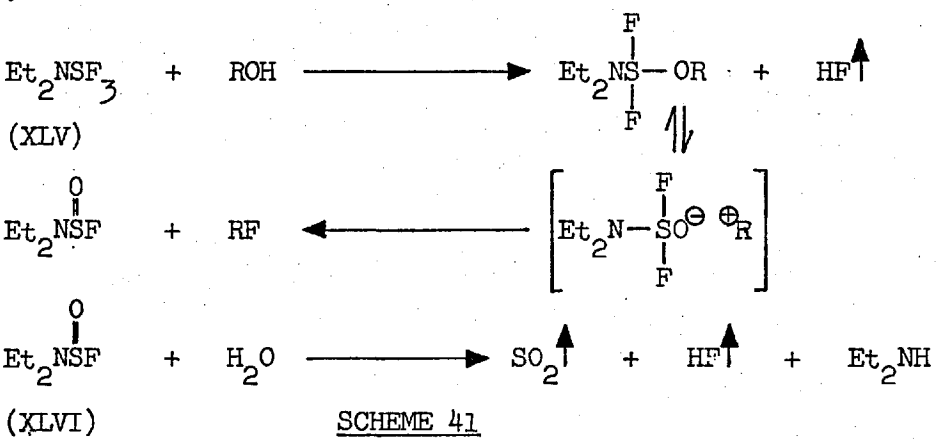
The water condenser was turned on, and vessel B was connected to the vacuum via tap 6. The pressure was further reduced and vessel A heated until the product diethylamino sulphur trifluoride (B.P.56°/12mm Hg) began to distill. Tap 3 at the reflux-ratio take-off was opened and the distillate run into vessel B. As before, vessel B could be isolated from the system and let up to room pressure for carrying out fluorinations.

A total of 13.5ml of DAST (a pale yellow liquid) was produced (100% theory yield = 14.5g, Lit. yield = 84%, density unknown ... probable yield ~80%), sufficient for nine successive fluorinations.

1.0g samples of the Type (IV) alcohols (MW 200-270) were dissolved in Analar dichloromethane (10ml) and cooled to -78°C. To each sample was added DAST (1.5ml, MW 161). The reactions were far less violent than the similar DACTE fluorinations. The treated samples (stoppered with a teat placed over the side-arm) were shaken, then warmed to room temperature and left overnight.

By this method all of the alcohols were successfully fluorinated with the exception of the oOMe derivative (which failed to incorporate fluorine three times. This was later fluorinated by the DACTE route).

The reactions were very clean as the only by-product (XLVI) decomposed on work-up :



SCHEME 41

2-5-2 Physical Properties of the Type (V) Fluorides

These compounds are readily soluble in a range of solvents, possess a characteristic odour and are mild irritants.

Notes on TABLE 2-5.1 (overleaf)

GLC conditions : 1µl injections; column : 2m x $\frac{1}{8}$"; 5% SP1000 on Chromosorb P (65-80 Mesh); @ 113°C (Range 5×10^2).

RT (retention time) normalised relative to H = 100. Actual retention time H = 8.65cm (from Et_2O) at chart speed 15"/hr = 13.5 mins. Impurity RT's normalised to individual derivative.

The figures in parentheses in the glc impurities are % relative to Type (V) Fluoride = 100%.

Both NO_2 derivatives were undetectable by flame ionisation,

TABLE 2-5.1 Physical Properties of the Type (V) Fluorides

DERIV X	MW	$n_D^{22.5}$	STATE	GLC Properties			
				Product RT	Impurities RT		
H	193	1.5375	colourless oil	100.0	47.4(1)	161.3(1)	
o F	211	1.5050	colourless oil	61.3	50.0(4)	11.3(0.5)	
o Cl	227.5	1.5394	colourless oil	167.6	50.7(2)	58.6(1)	39.3(0.5)
o Br	272	1.5585	colourless oil	287.9	53.8(8)		
o Me	207	1.5290	colourless oil	127.2			
o OMe	223	1.5324	colourless oil	342.2			
o NO_2	254	1.5460	yellow oil				
o CF_3	261	1.4674	colourless oil	41.0			
p F	211	1.5048	colourless oil	110.4	35.6(3)		
p Cl	227.5	1.5397	colourless oil	368.8	45.5(1)	30.4(1)	11.1(1)
p Br	272	1.5630	colourless oil	682.6	41.7(7)		
p Me	207	1.5260	colourless oil	157.3	73.5(1)	28.5(0.5)	
p OMe	223	1.5353	colourless oil	637.5			
p NO_2	254	1.5523	yellow oil				
p CF_3	261	1.4696	colourless oil	94.5	88.0(1)	47.8(1)	40.3(1)

TABLE 2-5.2 Mass Spectral Data of the Type (V) Fluorides.

DERIV X	M+	Sub^n Pattern	100%	2nd	3rd	4th	5th	6th
H	192(25)	2 Cl	109	110(27)	M+(25)	83(17)	157(16)	M+2(16)
o F	210(13)	2 Cl	127	128(16)	M+(13)	175(11)	M+2(8)	101(7)
o Cl	226(10)	3 Cl	143	145(48)	144(10)	M+(10)	M+2(9)	75(8)
o Br	*272(24)	2 Cl,1 Br	189	187(93)	108(36)	143(31)	M+2(24)	120(20)
o Me	206(14)	2 Cl	123	103(18)	124(17)	M+(14)	115(11)	77(10)
o OMe	222(16)	2 Cl	139	91(71)	109(24)	M+(16)	M+2(11)	140(9)
o NO_2	237(1)	2 Cl	154	109(82)	177(58)	123(46)	127(24)	51(23)
o CF_3	260(10)	2 Cl	177	127(51)	178(43)	168(18)	109(17)	151(17)
p F	210(4)	2 Cl	127	57(15)	107(15)	101(15)	75(14)	128(13)
p Cl	226(6)	3 Cl	143	145(40)	75(21)	107(20)	83(18)	50(18)
p Br	*272(13)	2 Cl,1 Br	187	189(98)	108(20)	M+2(13)	M+(8)	188(8)
p Me	206(5)	2 Cl	123	115(15)	83(12)	63(12)	103(11)	77(11)
p OMe	222(8)	2 Cl	139	96(22)	109(14)	63(13)	83(13)	85(9)
p NO_2	237(18)	2 Cl	154	95(25)	124(18)	M+(18)	155(14)	M+2(10)
p CF_3	260(6)	2 Cl	177	127(50)	178(17)	75(13)	169(10)	158(9)

* indicates M+2 line highest in molecular ion group

Again the major species present (100% line in every instance) was the X-substituted fluoro tropylium ion (M = 108 + X).

TABLE 2-5.3 Micro Analysis Data of the Type (V) Fluorides.

DERIV	REQUIRED					FOUND				
X	C	H	F	Cl	N,Br	C	H	F	Cl	N,Br
H	49.77	3.65	9.64	36.73		50.49	3.72	10.67	35.27	
o F	45.53	2.87	18.00	33.60		46.52	3.13	17.33	32.04	
o Cl	42.24	2.66	8.35	46.75		42.54	2.60	9.06	45.75	
o Br	35.33	2.22	6.99	26.07	29.38(Br)	36.77	2.30	7.42	25.03	28.20(Br)
o Me	52.20	4.38	9.17	34.24		41.27	3.07	8.89	28.51	
o OMe	48.46	4.07	8.52	31.79		48.45	4.32	8.68	31.62	
o NO_2	37.82	2.38	7.48	27.91	5.51(N)	36.68	2.08	8.50	25.96	4.54(N)
o CF_3	41.41	2.32	29.11	27.16		42.20	2.54	28.31	25.81	
p F	45.53	2.87	18.00	33.60		40.81	2.36	19.63	32.77	
p Cl	42.24	2.66	8.35	46.75		44.02	3.26	9.97	38.47	
p Br	35.33	2.22	6.99	26.07	29.38(Br)	36.40	2.47	7.19	23.81	26.84(Br)
p Me	52.20	4.38	9.17	34.24		52.63	4.42	9.32	33.63	
p OMe	48.46	4.07	8.52	31.79		46.76	4.14	9.59	31.87	
p NO_2	37.82	2.38	7.48	27.91	5.51(N)	40.79	2.66	8.23	24.08	5.84(N)
p CF_3	41.41	2.32	29.11	27.16		41.78	2.41	28.45	24.52	

* Cl and Br analysed for simultaneously. Due to instrumental problems the microanalysis of these samples was held up for 10 months during which time some decomposed.

TABLE 2-5.4 Infrared Data of the Type (V) Fluorides

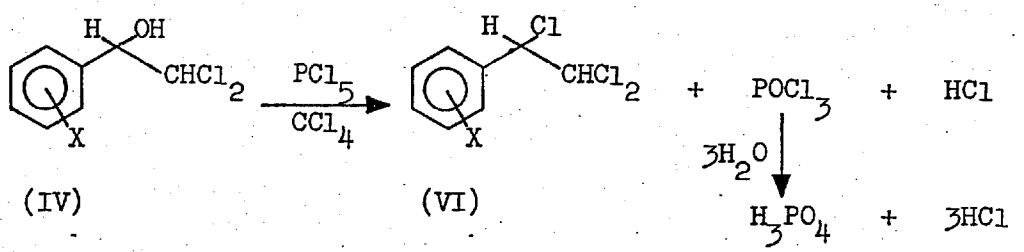
DERIV R	Peak 1	Peak 2	Peak 3	Peak 4	Peak 5	Peak 6	Peak 7	Peak 8	Peak 9	Peak 10	Peak 11	Peak 12	Peak 13	Peak 14	Peak 15
H	1485 w	1445 m	1210 m	1060 m	1025 m	1010 m	795 s	775 s	740 s	700 s					
o F	1615 m	1590 m	1490 s	1450 s	1225 s	1075 s	1020 s	825 s	800 s	765 s					
o Cl	1590 w	1570 w	1470 m	1440 m	1210 m	1130 m	1080 m	1050 m	960 m	800 s	780 v	760 s	720 m		
o Br	1590 m	1570 m	1470 s	1440 s	1275 m	1210 s	1125 s	1080 s	1020 s	960 s	830 m	800 s	780 s	760 v	720 s
o Me	1600 w	1480 m	1455 m	1210 m	1065 m	1005 m	805 m	790 s	765 m	745 s	720 m				
o OMe	2900 m	1600 s	1495 s	1460 s	1440 m	1285 s	1250 v	1075 s	1050 s	1015 s	960 m	800 s	765 s	730 s	
o NO_2	1603 w	1570 w	1530 v	1345 v	1305 m	1210 w	1090 m	1065 m	860 m	795 s	775 s	740 s	700 m		
o CF_3	1600 w	1580 w	1450 w	1310 v	1165 v	1120 v	1075 m	1060 m	1040 s	960 m	800 s	775 s	740 s		
p F	1605 s	1510 v	1225 v	1160 s	1070 m	1010 m	840 s	810 s	790 m	750 m					
p Cl	1590 m	1485 s	1400 m	1205 m	1090 s	1010 s	820 s	795 s	765 s	710 m					
p Br	1590 m	1480 m	1400 m	1205 m	1070 s	1010 s	820 m	795 s	765 s	705 m					
p Me	1605 m	1505 m	1200 m	1075 m	1020 m	1005 m	820 s	795 s	720 s	710 m					
p OMe	2900 m	1615 s	1585 m	1515 s	1460 m	1305 s	1250 v	1180 s	1065 m	1035 v	840 s	800 s	735 m		
p NO_2	1525 v	1340 s	1300 m	1090 m	1060 m	860 m	790 m	770 s	740 s	700 m					
p CF_3	1620 w	1415 m	1325 v	1170 s	1130 s	1070 s	1015 m	840 m	800 m	760 m					

All spectra were recorded on liquid films.
The major peaks are listed in descending order of their wavenumber (cm^{-1}).
The relative intensities are denoted by the abbreviations : v = very strong; s = strong; m = medium; w = weak.

2-6 Preparation of the 1,2,2-Trichlorophenyl Ethanes (Type (IV) Chlorides)

As with the preparation of the Type (IV) alcohols from the Type (III) ketones, this step was very straightforward and in most cases proceeded almost quantitatively and very cleanly.

2-6-1 General Phosphorus Pentachloride Chlorination Method



(IV) (VI)

SCHEME 42

The Type (IV) alcohol was dissolved in the minimum amount of analar carbon tetrachloride and two equivalents of finely powdered phosphorus pentachloride was added directly to the solution. The mixture was then refluxed, with stirring, for half an hour before cooling and carefully quenching with water. This converted the phosphoryl chloride and any unreacted phosphorus to orthophosphoric acid, which conveniently partitions into the aqueous layer. The organic layer was separated, washed with water and then saturated sodium bicarbonate solution, before drying over anhydrous sodium sulphate to yield the crude chloride (VI).

Pilot elimination reactions with the Type (VI) chlorides showed that "back elimination" of the α-chlorine readily took place. It was therefore decided not to continue with eliminations from this series. As these compounds were eventually prepared on a small (0.3g) scale, solely for comparative nmr studies, they were only purified, where necessary, by column chromatography.

2-6-2 Physical Properties of the Type (VI) Chlorides

As with the Type (V) fluorides these compounds are readily soluble in a range of solvents, possess a characteristic odour and are mild irritants.

Notes on TABLE 2-6.1 (overleaf)
GLC conditions : 4μl injection; column : 2m x $\frac{1}{8}$" 5% SP1000 on Chromosorb P (65-80) mesh (range 5 x 10^2).
All other notes as for TABLE 2-5.1 except H RT = 5.05 cm.

TABLE 2-6.1 Physical Properties of the Type (VI) Chlorides

DERIV X	MW	$n_D^{22.5}$	STATE	GLC Properties			
				Product RT	Impurities RT		
H	209.5	1.5605	colourless oil	100.0	17.8(1)	39.6(1)	
o F	227.5	1.5392	colourless oil	64.3	23.1(6)	49.2(3)	
o Cl	224.0	1.5706	colourless oil	155.4	22.3(17)	54.8(12)	
o Br	228.5	1.5888	colourless oil	257.4	22.6(7)	55.4(4)	13.0(0.5)
o Me	223.5	1.5600	colourless oil	108.9	16.3(3)		
o OMe	239.5	1.5520	colourless oil	271.3			
o NO_2	254.5	1.5802	yellow oil				
o CF_3	227.5	1.5020	colourless oil	41.6	19.1(15)		
p F	227.5	1.5379	colourless oil	114.8	18.1(2)	39.6(1)	
p Cl	244.0	1.5723	colourless oil	358.4	39.8(1)	17.1(1)	
p Br	288.5	1.5921	colourless oil	663.4	39.1(2)	16.7(1)	9.3(1)
p Me	223.5	1.5532	colourless oil	146.5	20.3(1)		
p OMe	239.5	1.5643	colourless oil	643.6	23.1(1)		
p NO_2	254.5	1.5830	yellow cryst				
p CF_3	277.5	1.4962	colourless oil	88.1	16.8(9)	7.9(5)	41.6(4)

TABLE 2-6.2 Mass Spectral Data of the Type (VI) Chlorides

DERIV X	M+	Sub^n Pattern	100%	2^{nd}	3^{rd}	4^{th}	5^{th}	6^{th}
H	208(12)	3 Cl	125	127(50)	51(17)	103(16)	77(13)	126(13)
o F	266(8)	3 Cl	145	145(47)	144(11)	121(10)	120(9)	191(8)
o Cl	*244(8)	4 Cl	159	161(60)	77(18)	137(18)	101(17)	136(16)
o Br	*288(13)	3 Cl,1 Br	205	203(85)	207(30)	136(23)	75(21)	101(17)
o Me	222(24)	3 Cl	139	141(80)	115(60)	103(33)	140(27)	222(24)
o OMe	238(7)	3 Cl	155	91(23)	125(16)	157(14)	89(9)	238(7)
o NO_2	253(n)	3 Cl	170	112(78)	28(65)	75(60)	51(58)	89(50)
o CF_3	276(5)	3 Cl	193	195(41)	151(26)	158(14)	194(12)	75(9)
p F	226(6)	3 Cl	143	145(42)	120(12)	121(11)	144(11)	101(9)
p Cl	*244(6)	4 Cl	159	161(64)	75(12)	101(11)	136(9)	137(9)
p Br	*288(10)	3 Cl,1 Br	205	203(75)	207(24)	136(14)	102(13)	188(10)
p Me	222(6)	3 Cl	139	141(28)	115(15)	103(8)	140(8)	117(6)
p OMe	238(6)	3 Cl	155	157(30)	168(14)	203(10)	89(9)	156(9)
p NO_2	253(7)	3 Cl	170	28(68)	172(33)	150(17)	136(17)	110(16)
p CF_3	276(4)	3 Cl	193	195(31)	151(10)	194(9)	171(7)	75(6)

* indicates M+2 line highest in molecular ion group.
Again the major species present (100% line in every instance) was the X-substituted chloro tropylium ion (M = 108 + X).

TABLE 2-6.3 Micro Analysis Data of the Type (VI) Chlorides

DERIV	CALCULATED			FOUND		
X	C	H	N	C	H	N
H	45.86	3.37		45.35	3.40	
o F	42.24	2.66		41.67	2.80	
o Cl	39.39	2.48		41.16	2.80	
o Br	33.32	2.10		34.78	2.32	
o Me	48.36	4.06		48.66	4.07	
o OMe	45.13	3.79		44.14	3.68	
o NO_2	37.76	2.38	5.50	40.27	2.72	5.42
o CF_3	38.95	2.18		40.44	2.45	
p F	42.24	2.66		44.38	2.97	
p Cl	39.39	2.48		41.38	2.86	
p Br	33.32	2.10		33.19	2.19	
p Me	48.36	4.06		49.49	4.04	
p OMe	45.13	3.79		45.70	3.95	
p NO_2	37.76	2.38	5.50	37.94	2.58	5.02
p CF_3	38.95	2.18		43.49	2.97	

All notes as for TABLE 2-5.3

TABLE 2-6.4 Infrared Data of the Type (VI) Chlorides

DERIV X	Peak 1	Peak 2	Peak 3	Peak 4	Peak 5	Peak 6	Peak 7	Peak 8	Peak 9	Peak 10	Peak 11	Peak 12	Peak 13
H	3000 m	1495 s	1400 s	1205 s	1190 m	1080 m	1010 m	810 s	745 s	720 v			
o F	2950 w	1620 m	1590 m	1490 v	1460 s	1240 s	1100 s	820 s	780 v	750 s	710 s		
o Cl	3000 m	1610 m	1595 m	1570 m	1470 s	1445 s	1275 m	1055 s	1040 s	920 m	820 s	760 s	740 s
o Br	3000 m	1615 m	1590 m	1575 m	1470 v	1440 v	1280 s	1190 s	1040 s	920 s	820 s	760 v	
o Me	2950 m	1600 w	1490 m	1460 m	1210 m	1180 m	810 s	760 s	740 s	705 s			
o OMe	2900 w	1600 m	1490 s	1465 s	1310 m	1250 v	1030 s	820 s	765 s	705 m			
o NO_2	3000 m	1610 m	1580 m	1530 v	1350 v	1190 m	1005 m	870 s	820 s	795 s	745 s		
o CF_3	2900 m	1610 m	1460 m	1310 v	1170 v	1125 v	1040 s	930 m	825 s	805 s	780 s	720 s	
p F	2900 w	1605 s	1515 s	1420 m	1230 v	1060 s	1020 m	850 s	810 s	740 s			
p Cl	2900 w	1600 m	1500 s	1410 m	1100 s	1020 s	860 m	840 s	780 s	740 s			
p Br	2900 w	1600 s	1490 s	1405 s	1080 s	1020 s	860 m	830 s	775 s	740 s			
p Me	2900 m	1610 m	1515 m	1205 m	1180 m	910 m	830 s	790 s	750 v	700 m			
p OMe	2900 m	1615 s	1510 s	1460 s	1310 s	1250 v	1180 s	1120 s	1040 v	840 s	800 s	750 v	
p NO_2	3000 m	1610 s	1530 s	1350 s	1215 m	1020 s	865 m	780 m	750 s	700 m			
p CF_3	2900 m	1620 m	1420 m	1325 s	1170 s	1130 s	1070 s	850 m	760 m	720 m			

All spectra were recorded on liquid films.
The major peaks are listed in descending order of their wavenumber (cm^{-1})
Relative intensities : v = very strong; s = strong; m = medium; w = weak.

2-7 Type (IV), (V) and (VI) Compounds Reported in The Literature

34 out of the 45 compounds in these series are unreported (formula index in Chemical Abstracts up to June 1977). Most of the reported compounds (see TABLE 2-7.1) were isolated in studies related to pesticides of the DDT (XXIII) and DDD (XXIV) type.

TABLE 2-7.1 Physical Properties of the Type (IV), (V) and (VI) Compounds Reported in the Literature.

DERIV	Series	Registry No.	Physical Properties	References
H	(IV)	2162-36-4	MP 54[52,224] 56[225,226]; n_D^{20} 1.5626 BP 93°/2mmHg[225] 121.5°/4mmHg[224] 170°/16mmHg[226]	52 224-7 238
o Cl		27683-60-9	BP 127°/4mmHg[230] n_D^{20} 1.5675	230-2,238
o Me		18067-50-0	BP 100-5°/4mmHg	225
p Cl		41521-04-4	BP 140-5°/2mmHg[228] 158°/4mmHg[229]	228-9,231,238
p Me		not reported	BP 132-4°/6mmHg	225
p OMe		58622-56-3	^{1}H nmr.δ 7.03(J=9),6.57(J=9), 5.78(J=5),4171(J=5).	233
p NO_2		not reported	MP 92°C (Recryst. Pet.Ether)	237
H	(V)	345-63-1	No details in paper.	234
H	(VI)	1674-29-9	BP 130°/17mmHg[226] 122°/10mmHg[235] n_D^{20} 1.5613[235]	117-8,226,235
p Cl		not reported	BP 99-101°/0.2mmHg ; n_D^{20} 1.5949 BP 150-2°/15mmHg ; n_D^{20} 1.5585	229 236
p Me		33236-97-4	^{1}H nmr ($CDCl_3$) ν_A 5.89, ν_B 5.09 J_{AB} 5.98 Hz.	117

PART 2

CONFORMATIONAL DETERMINATION OF THE STARTING MATERIALS

CHAPTER 3

3 BASIC SPECTRAL ANALYSIS

There are two basic nmr parameters, the chemical shift (δ), which depends on the applied field and is measured in ppm, and the coupling constant (J), which is independent of the applied field and is measured in Hz. The chemical shift parameter δ(delta) has its usual mathematical meaning - "difference"- and is used to indicate the frequency difference between a signal and a fixed reference point (eg. a TMS ^{1}H or ^{13}C resonance). In this section the additional term ν(nu) will be used for an absolute chemical shift (as in ν_A) and δ will retain its "difference" connotation (as in δ_{AB}).

The purpose of spectral analysis is to obtain these parameters from the spectrum for every resonating nucleus. This is a simple task in 1st order spectra as internuclear perturbations (spin-spin couplings) can occur without spectral distortions, ie. the mid-point of a doublet corresponds to the uncoupled resonance frequency of a nucleus. The basic condition for two nuclei A and X to engage in first order coupling is for $\delta_{AB} \geqslant 10.J_{AB}$. If this condition does not hold the spectrum will become 2nd order, distortions of the doublets will occur (an AB-system) and their simple analysis will become increasingly more inaccurate.

3-1 Obtaining the Spectral Parameters from an AB-System

AB-systems may be readily identified by their characteristic "quartet" appearance (see FIG.3-1.1). The system is absolutely defined by three parameters ν_A, ν_B and J_{AB} although only two parameters δ_{AB} (from $\nu_A - \nu_B$) and J_{AB} are necessary to define its appearance. Only two parameters, J_{AB} and ν_{AB} (the mid-point of the quartet), may be measured directly from the spectrum (see FIG.3-1.1); δ_{AB}, ν_A and ν_B require calculations. The whole system is defined by three equations (EQNS.31-33)[239] which also apply to the "apparent AB-quartets" of the ABX-spin system (see SECTION 3-2).

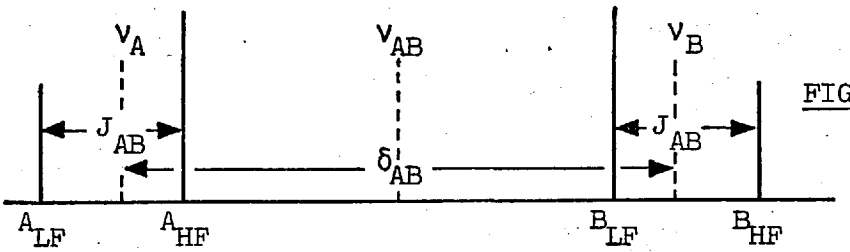


FIG.3-1.1

$$J_{AB} = A_{LF} - A_{HF} = B_{LF} - B_{HF} \qquad \text{EQN.31}$$

$$\delta_{AB} = \nu_A - \nu_B = \sqrt{(A_{LF} - B_{HF})(A_{HF} - B_{LF})} \qquad \text{EQN.32}$$

$$[A_{LF}]/[A_{HF}] = [B_{HF}]/[B_{LF}] = (A_{HF} - B_{LF})/(A_{LF} - B_{HF}) \qquad \text{EQN.33}$$

(Where LF = low field, HF = high field, and [ ] denotes intensity)

As δ_{AB} decreases, the distortions of the intensities of the two pairs of spectral lines increase, so that ν_A and ν_B remain approximately at the "centre of gravity" (ie. the average position of the peaks weighted by their intensities) of the lines from A and B. It should be emphasised that this commonly used analogy is only an approximation (see APPENDIX I).

In all cases where chemical shifts (ν_A and ν_B) were obtained from AB-systems, 2nd order analysis was performed graphically using EQN.32 in conjunction with EQN.34 (see APPENDIX I).

$$\nu_{AB} = \tfrac{1}{2}(\nu_A + \nu_B) = \tfrac{1}{4}(A_{LF} + A_{HF} + B_{LF} + B_{HF}) \qquad \text{EQN.34}$$

3-2 Obtaining the Spectral Parameters from an ABX-System

Obtaining spectral parameters from simple 1st order systems such as the two-spin AX and three-spin AMX-systems is trivial as both couplings and shifts may be read directly from the spectrum. As we have seen, analysis of the 2nd order AB-system remains straightforward but calculation is required to obtain the shifts. On proceeding to the three-spin partially 2nd order ABX-system many more complications arise; but, unlike the fully 2nd order ABC-system, analysis may still be accomplished by hand. In this work, the side-chains of the Type (V) fluorides provided classic examples of ABX-systems, ie. H_A, H_B, F_X (see FIG.3-2.1).

A detailed study of ABX spectral analysis was undertaken after attempts at working through the standard methods of analysis in the text book by Pople et al[239] and the article by Banwell[240] both produced contradictory results.[241]

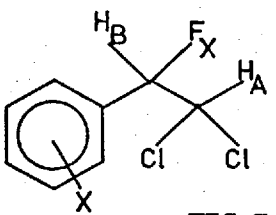


FIG.3-2.1

3-2-1 Summary of Theory

The quantum mechanical calculation of the transition frequencies and intensities which make up an nmr spectrum is based on evaluating the transition probabilities between nuclear spin energy levels. In a 1st order three spin system, AMX, the energy levels are the eigen values of a Hamiltonian operator with 8 "basic product spin functions" (bpsf's), simply obtained by taking all possible product combinations of the α and β nuclear spin wavefunctions of each nucleus (see TABLE 3-2.1).

In the partially 2nd order ABX-system mixing occurs between those bpsf's in which the A and B nuclei both change spins. This generates the new eigenfunctions 3', 4', 5' and 6' which reduce to 3, 4, 5 and 6 in the AMX limit. TABLE 3-2.1 lists the total spin (F_z) for each ABX stationary state wavefunction, together with explicit expressions for the corresponding energy levels in terms of experimental parameters (for definition of the additional

terms N, L, D and ϕ see EQNS.35-42).

TABLE 3-2.1 AMX Basic Product Spin Functions and ABX Stationary State Wavefunctions and Energies (Taken from Ref.239)

AMX-SYSTEM				F_z	ABX-SYSTEM		
STATE	BASIC PRODUCT SPIN FUNCTION A	M	X	($\sum m_z$)	STATE	STATIONARY STATE WAVEFUNCTION ABX	STATIONARY STATE ENERGY
1	α	α	α	$+\frac{3}{2}$	1	$\alpha\alpha\alpha$	$\frac{1}{2}(\nu_A+\nu_B+\nu_X) + \frac{1}{4}(J_{AB}+J_{AX}+J_{BX})$
2	α	α	β		2	$\alpha\alpha\beta$	$\frac{1}{2}(\nu_A+\nu_B-\nu_X) + \frac{1}{4}(J_{AB}-J_{AX}-J_{BX})$
3	α	β	α	$+\frac{1}{2}$	3'	$\cos\phi_+(\alpha\beta\alpha) + \sin\phi_+(\beta\alpha\alpha)$	$\frac{1}{2}\nu_X - \frac{1}{4}J_{AB} + D_+$
4	β	α	α		4'	$-\sin\phi_+(\alpha\beta\alpha) + \cos\phi_+(\beta\alpha\alpha)$	$\frac{1}{2}\nu_X - \frac{1}{4}J_{AB} + D_+$
5	α	β	β		5'	$\cos\phi_-(\alpha\beta\beta) + \sin\phi_-(\beta\alpha\beta)$	$-\frac{1}{2}\nu_X - \frac{1}{4}J_{AB} + D_-$
6	β	α	β	$-\frac{1}{2}$	6'	$-\sin\phi_-(\alpha\beta\beta) + \cos\phi_-(\beta\alpha\beta)$	$-\frac{1}{2}\nu_X - \frac{1}{4}J_{AB} - D_-$
7	β	β	α		7	$\beta\beta\alpha$	$\frac{1}{2}(\nu_X-\nu_A-\nu_B) + \frac{1}{4}(J_{AB}-J_{AX}-J_{BX})$
8	β	β	β	$-\frac{3}{2}$	8	$\beta\beta\beta$	$-\frac{1}{2}(\nu_A+\nu_B+\nu_X) + \frac{1}{4}(J_{AB}+J_{AX}+J_{BX})$

Basic Equations :

$$D_+\cos 2\phi_+ = \tfrac{1}{2}(\delta_{AB} + L) \qquad \text{EQN.35}$$

$$D_-\cos 2\phi_- = \tfrac{1}{2}(\delta_{AB} - L) \qquad \text{EQN.36}$$

$$D_+\sin 2\phi_+ = D_-\sin 2\phi_- = \tfrac{1}{2}J_{AB} \qquad \text{EQN.37}$$

$$D_\pm = \tfrac{1}{2}\left[(\delta_{AB} \pm L)^2 + J_{AB}^2\right]^{\frac{1}{2}} \qquad \text{EQN.38}$$

$$\nu_{AB} = \tfrac{1}{2}(\nu_A + \nu_B) \qquad \text{EQN.39}$$

$$\delta_{AB} = \nu_A - \nu_B \qquad \text{EQN.40}$$

$$N = \tfrac{1}{2}(J_{AX} + J_{BX}) \qquad \text{EQN.41}$$

$$L = \tfrac{1}{2}(J_{AX} - J_{BX}) \qquad \text{EQN.42}$$

N.B. D_+ and D_- were defined by Pople et al[239] as arbitrarily assigned interchangeable positive quantities. Banwell,[240] however, specified the relation : $D_+ \geqslant D_- \geqslant 0$

The fifteen transitions, allowed by the selection rule : $\Delta F_z = +1$, between the eight energy levels are given in TABLE 3-2.2. Three of these are

combination transitions in which nominally all nuclei change their spin simultaneously. In the AMX-system none of these lines are seen, but as two of the transitions (5'⟶4' & 6'⟶3') involve mixed states, they do appear in the ABX-system. (N.B. Transition 7⟶2 always has zero intensity except in ABC-systems).

TABLE 3-2.2 The 15 Allowed Transitions, and Their Origins, for an ABX-System

ΔF_z $+\frac{1}{2}\longrightarrow+\frac{3}{2}$	ORIGIN	ΔF_z $-\frac{1}{2}\longrightarrow+\frac{1}{2}$	ORIGIN	ΔF_z $-\frac{1}{2}\longrightarrow+\frac{1}{2}$	ORIGIN	ΔF_z $-\frac{1}{2}\longrightarrow+\frac{1}{2}$	ORIGIN	ΔF_z $-\frac{3}{2}\longrightarrow-\frac{1}{2}$	ORIGIN
2⟶1	X	5'⟶2	B	6'⟶2	A	7⟶2	COMB	8⟶5'	A
3'⟶1	B	5'⟶3'	X	6'⟶3'	COMB	7⟶3'	A	8⟶6'	B
4'⟶1	A	5'⟶4'	COMB	6'⟶4'	X	7⟶4'	B	8⟶7	X

The origins of these transitions (ie..the identity of the nucleus whose spin has changed) and the spin state(s) of the corresponding 1st order nuclei (ie. X for A or B, and A+B for X) are given in TABLE 3-2.3 together with the transition frequency (energy) and relative intensity (both of which were derived from the expressions in TABLE 3-2.1). Throughout this work we adopt the convention that B resonates to high field of A, ie. δ_{AB} is always +ve.

Several observations may be made from TABLE 3-2.3 :

1) The AB-region has eight lines and the X has six (although two of these are combination lines and may not be observed).

2) The AB-region consists of two apparent AB-quartets, namely lines 1-3-5-7 involving the parameters D_- and ϕ_-, and 2-4-6-8 involving D_+ and ϕ_+ (see EQNS.35-42), which have all the properties of normal AB-quartets with regard to line spacings and intensities (see SECTION 3-1).

3) The X-region is symmetrical about ν_X.

4) Many other relationships may be derived from the table - see EQNS.43-53.

Equations Derived from TABLE 3-2.3

$$|J_{AB}| = Sep^{n}_{8-6} = Sep^{n}_{7-5} = Sep^{n}_{4-2} = Sep^{n}_{3-1} \qquad \text{EQN.43}$$

$$Sep^{n}_{8-4} = 2D_+ \qquad \text{EQN.44} \; ; \quad Sep^{n}_{7-3} = 2D_- \qquad \text{EQN.45}$$

$$\text{Midpoint } \alpha\text{-quartet } (m_\alpha) - \text{Midpoint } \beta\text{-quartet } (m_\beta) = \tfrac{1}{2}|J_{AX}+J_{BX}| = N \qquad \text{EQN.46}$$

$$Sep^{n}_{12-9} = |J_{AX} + J_{BX}| = 2N \qquad \text{EQN.47}$$

$$Sep^{n}_{10-11} = 2(D_+ - D_-) \qquad \text{EQN.48} \; ; \quad Sep^{n}_{15-14} = 2(D_+ + D_-) \qquad \text{EQN.49}$$

$$Sep^{n}_{12-14} = Sep^{n}_{8-3} \qquad \text{EQN.50} \; ; \quad Sep^{n}_{15-12} = Sep^{n}_{5-2} \qquad \text{EQN.51}$$

TABLE 3-2.3 The Energies and Intensities of the 14 Observable ABX Transitions

TRANSITION		ORIGIN	ENERGY	RELATIVE INTENSITY
1	$8 \longrightarrow 6'$	B β	$\nu_{AB} - \frac{1}{2}(J_{AB} + N) - D_-$	$1 - \sin 2\phi_-$
2	$7 \longrightarrow 4'$	B α	$\nu_{AB} - \frac{1}{2}(J_{AB} - N) - D_+$	$1 - \sin 2\phi_+$
3	$5' \longrightarrow 2$	B β	$\nu_{AB} + \frac{1}{2}(J_{AB} - N) - D_-$	$1 + \sin 2\phi_-$
4	$3' \longrightarrow 1$	B α	$\nu_{AB} + \frac{1}{2}(J_{AB} + N) - D_+$	$1 + \sin 2\phi_+$
5	$8 \longrightarrow 5'$	A β	$\nu_{AB} - \frac{1}{2}(J_{AB} + N) + D_-$	$1 + \sin 2\phi_-$
6	$7 \longrightarrow 3'$	A α	$\nu_{AB} - \frac{1}{2}(J_{AB} - N) + D_+$	$1 + \sin 2\phi_+$
7	$6' \longrightarrow 2$	A β	$\nu_{AB} + \frac{1}{2}(J_{AB} - N) + D_-$	$1 - \sin 2\phi_-$
8	$4' \longrightarrow 1$	A α	$\nu_{AB} + \frac{1}{2}(J_{AB} + N) + D_+$	$1 - \sin 2\phi_+$
9	$8 \longrightarrow 7$	X $\beta\beta$	$\nu_X - N$	1
10	$5' \longrightarrow 3'$	X $\beta\alpha$	$\nu_X + (D_+ - D_-)$	$\cos^2(\phi_+ - \phi_-)$
11	$6' \longrightarrow 4'$	X $\alpha\beta$	$\nu_X - (D_+ - D_-)$	$\cos^2(\phi_+ - \phi_-)$
12	$2 \longrightarrow 1$	X $\alpha\alpha$	$\nu_X + N$	1
14	$5' \longrightarrow 4'$	Comb.(X)	$\nu_X - (D_+ + D_-)$	$\sin^2(\phi_+ - \phi_-)$
15	$6' \longrightarrow 3'$	Comb.(X)	$\nu_X + (D_+ + D_-)$	$\sin^2(\phi_+ - \phi_-)$

Equations Derived from TABLE 3-2.3 (ctd.)

$$Sep^{n}_{12\text{-}10} = Sep^{n}_{11\text{-}9} = Sep^{n}_{4\text{-}3} = Sep^{n}_{2\text{-}1} = J_{BX}(\pm J_{AB}) \qquad \text{EQN.52}$$

$$Sep^{n}_{12\text{-}11} = Sep^{n}_{10\text{-}9} = Sep^{n}_{8\text{-}7} = Sep^{n}_{6\text{-}5} = J_{AX}(\pm J_{AB}) \qquad \text{EQN.53}$$

3-2-2 Analysis of an ABX Spectrum

Let us adopt the analysis method given by Banwell[240] (essentially a step-wise treatment of the original text by Pople et al[239]) and apply it to the ABX spectrum of the side-chain of the o fluoro Type (V) fluoride (see FIG.3-2.2).

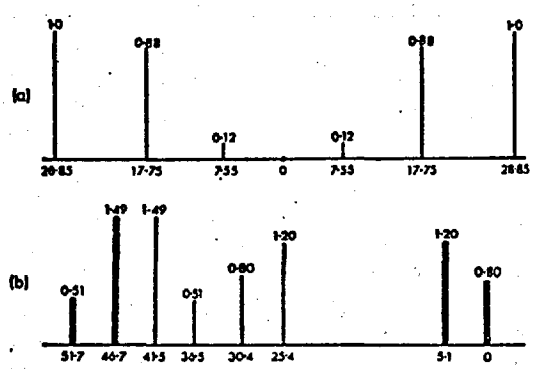


FIG.3-2.2 The ABX Spectrum of o F Type (V) Fluoride (line-form)
(a) The AB-region (^{1}H @ 100MHz)
(b) The X-region (^{19}F @ 94.1MHz)
The lower numbers are the shifts (in Hz), whilst the upper numbers are the intensities relative to lines 9 and 12 in the X-region.

Note that four lines in the AB-region are significantly broadened by long-range coupling.

The only equations used in both texts, were those defining D_+ and D_-, and those derived from TABLE 3-2.3, ie. EQNS.35-53. These are sufficient to obtain all the ABX spectral parameters excepting the sign of J_{AB}, which has no influence on the spectrum. Similarly, only the relative signs of J_{AX} and J_{BX} may be obtained.

3-2-2.1 Analysis (i) Assuming $D_+ \geqslant D_- \geqslant 0$

All six lines of the X-region are visible. Appling EQN.47, the separation of the strongest lines (9 and 12) gives : $|J_{AX} + J_{BX}| = 57.7$Hz.

Applying the D_+ rule (above) to EQNS.48 & 49, lines (14,15) must always lie outside lines $(\overline{10},11)$[240] giving the assignment for the X-region as : 12-15-10-11-14-9. The fact that the combination lines (14,15) are more intense than lines (10,11) in this assignment is surprising, but we shall proceed with the analysis.

From EQNS.48 & 49 : $2|D_+ - D_-| = 15.1$Hz ; $2(D_+ + D_-) = 35.5$Hz.
This leads to the solution $D_+ = 12.65$; $D_- = 5.1$Hz

In the AB-region the two quartets may be easily identified as they do not overlap, and application of EQNS.44 & 45 to determine Sep^n_{8-4} and Sep^n_{7-3} leads to the assignment : 7-5-3-1-8-6-4-2. $|J_{AB}|$ is immediatly seen to be 5.0Hz. From EQNS.46 & 47 the separation of the mid-points of the two quartets should equal $\frac{1}{2}\text{Sep}^n_{12-9}$, which it does. This assignment therefore passes all the checks given by Banwell.[240]

From EQN.37 : $\phi_+ = 5.7$ or 84.3° and $\phi_- = 14.67$ or 75.34°. Since in our assignment [14,15] > [10,11], $\cos^2(\phi_+ - \phi_-) < \sin^2(\phi_+ - \phi_-)$ (see TABLE 3-2.3). Therefore, either (a) $\phi_+ = 5.7$ and $\phi_- = 75.34$ or (b) $\phi_+ = 84.3$ and $\phi_- = 14.67^\circ$. These two results are of course equivalent with regard to the intensities of the X-region lines (due to the 'square term' masking the "trivial reversal of sign"[240]), but if both possibilities are utilised in EQNS.35 & 36 apparently different results emerge :

From EQN.35 : $\frac{1}{2}\delta_{AB} + \frac{1}{2}L$ = (a) 12.40 (b) -12.40
From EQN.36 : $\frac{1}{2}\delta_{AB} - \frac{1}{2}L$ = (a) -4.45 (b) 4.45
Adding EQNS.35 + 36 gives : δ_{AB} = (a) 7.95Hz (b) -7.95Hz
Subtracting EQNS.35 - 36 gives : $(J_{AX} - J_{BX})$ = (a) 33.7Hz (b) -33.7Hz

As $|J_{AX} + J_{BX}| = 57.7$, is numerically larger than $(J_{AX} - J_{BX})$ these functions must have the same sign. This leads to four possible solutions :
From (a) $\delta_{AB} = 7.95$ and (i) $J_{AX} = 45.7$; $J_{BX} = 12.0$Hz
or (ii) $J_{AX} = -12.0$; $J_{BX} = -45.7$Hz

From (b) $\delta_{AB} = -7.95$ and (iii) $J_{AB} = 12.0$; $J_{BX} = 45.7$Hz
or (iv) $J_{AX} = -45.7$; $J_{BX} = -12.7$Hz

Solutions (i) and (iii) are equivalent, as are (ii) and (iv), (A and B have merely interchanged in both cases), therefore (iii) and (iv) may be discarded. However, (i) and (ii) are not equivalent as the larger J resides on a different nucleus in each case. Choosing which solution is correct may be done from the AB-spectral region. From TABLE 3-2.3, lines (1-4) are derived from B and lines (5-8) from A. As $Sep^{n}_{3-1} > Sep^{n}_{7-5}$, the only acceptable solution is : $\delta_{AB} = 7.95$; $J_{AX} = 12.0$; $J_{BX} = 45.7$Hz.

The system is now fully analysed, but checking this by re-calculating the AB-region line positions and intensities according to TABLE 3-2.3 produces the bizarre spectrum shown in FIG.3-2.3. The calculated AB-region is in fact

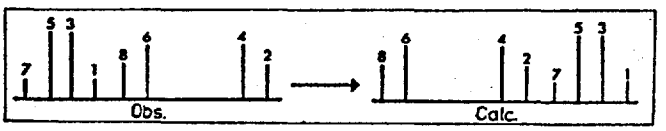


FIG.3-2.3

a mirror image of the original spectrum, but instead of the line assignment adopting the mirrored sequence, they have kept the original low to high field order with the 8-6-4-2 quartet now placed to low field of the 7-5-3-1 quartet.

Obviously something is amiss, and the problem may be traced to the statement that D_+ must be greater than D_-.[240]

3-2-2.2 Analysis (ii) Assuming $D_- \gg D_+ \gg 0$

Repeating the procedure used in analysis (i) leads to the assignments : 8-6-4-2-7-5-3-1 for the AB-region, and 12-15-10-11-14-9 for the X-region. This yields : $D_+ = 5.1$, $D_- = 12.65$, $J_{AB} = 5.0$ and (a) $\phi_+ = 75.34$ and $\phi_- = 5.7^\circ$ or (b) $\phi_+ = 14.67$ and $\phi_- = 84.3^\circ$.
Simultaneously solving EQNS.35 & 36 gives : δ_{AB} = (a) 7.95 (b) -7.95Hz
and $(J_{AX} - J_{BX})$ = (a) -33.7 (b) 33.7Hz

Again, this gives two non-equivalent solutions of which only : $J_{AX} = 12.0$; $J_{BX} = 45.7$Hz, fits the assigned line spacings.

The calculated spectrum now agrees in every detail with observed spectrum and in the absence of further information would be accepted as the correct analysis. In this case, however, four lines in the AB-region are broadened by long-range coupling into the aromatic ring. The broadened lines must be attributable to the same nucleus, but our assignment suggests that the low field pair are from A whilst the high field pair are from B!

This dichotomy arises from the statements[239,240] that D_+ and D_- are both positive. They may in fact have opposite signs and this alters the spectral assignment.

3-2-2.3 Analysis (iii) Assuming D_+ and D_- of Opposite Sign

A suitable assignment for the AB-region is 4-2-8-6-7-5-3-1 and for the X-region 12-11-15-14-10-9. Applying the usual relationships (as in analysis (i)) leads to the following parameters :

$D_+ = -5.1$; $D_- = 12.65$; $\phi_+ = 165.32^\circ$; $\phi_- = 5.7^\circ$

$\delta_{AB} = 7.95$; $J_{AB} = 5.0$; $J_{AX} = 12.0$; $J_{BX} = 45.7$Hz

The calculated spectrum now agrees exactly with experiment, and now the outermost pairs of lines in the AB-region originate from the same source, B. In addition lines (14,15) are of low intensity (as befits combination lines) unlike their counterparts in the earlier assignments. Note that lines (14, 15) lie within (10,11), contrary to statements elsewhere.[240]

This clearly is the correct solution, although it is identical to that obtained previously with both incorrect sets of assignments! Obviously a more systematic approach to this problem is necessary.

3-2-3 The Origins of the ABX Spectral Lines

It is valid to describe the AB-region of an ABX spectrum as resulting from the perturbation of a normal AB-quartet by the α and β spin states of X.[242] When J_{AX} and J_{BX} have the same sign (assumed to be positive for convenience), the interaction with X in the α spin state results in pairs of A_α and B_α lines to low field of their origins ν_A and ν_B. This is illustrated in FIG.3-2.4 :

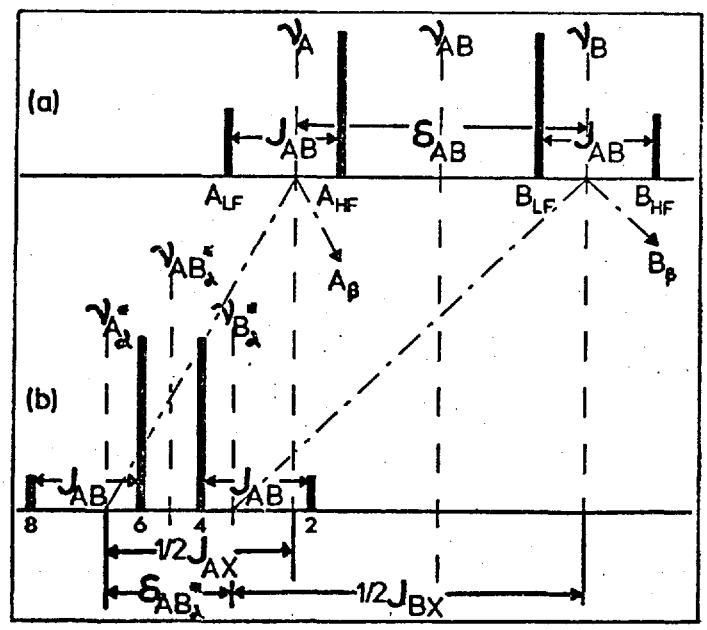


FIG.3-2.4

(a) The original AB-quartet in the absence of the X nucleus.

(b) The formation of the AB_α-quartet by perturbation from the α-spin state of X. The AB_β-quartet is formed in a similar manner.

The resulting AB-quartets, AB_α and AB_β obey the standard relationships (EQNS.31-34). If J_{AX} and J_{BX} have opposite signs (arbitrarily with J_{AX} negative) the α and β halves of the A spectrum change identity, ie. the A_α lines lie to highfield of the A_β lines, and the AB_α and AB_β-quartets are formed as

before, commonly with the AB -quartet within the AB -quartet.

Equations Derived from FIG.3-2.4[242] (N.B. * is used to denote "apparent")

$$\delta^*_{AB_\alpha} = \sqrt{(\mathrm{Sep}^{n}_{8-2})(\mathrm{Sep}^{n}_{6-4})} = \delta_{AB} + \tfrac{1}{2}(J_{AX}-J_{BX}) = \delta_{AB} + L \qquad \text{EQN.54}$$

$$\nu^*_{AB_\alpha} = \nu_{AB} + \tfrac{1}{4}(J_{AX}+J_{BX}) = \nu_{AB} + \tfrac{1}{2}N = m_\alpha \qquad \text{EQN.55}$$

$$\delta^*_{AB_\beta} = \sqrt{(\mathrm{Sep}^{n}_{7-1})(\mathrm{Sep}^{n}_{5-3})} = \delta_{AB} - \tfrac{1}{2}(J_{AX}-J_{BX}) = \delta_{AB} - L \qquad \text{EQN.56}$$

$$\nu^*_{AB_\beta} = \nu_{AB} - \tfrac{1}{4}(J_{AX}+J_{BX}) = \nu_{AB} - \tfrac{1}{2}N = m_\beta \qquad \text{EQN.57}$$

From EQNS.54 & 56 :

$$\delta^*_{AB_\alpha} - \delta^*_{AB_\beta} = 2L \qquad \text{EQN.58}$$

$$\delta^*_{AB_\alpha} + \delta^*_{AB_\beta} = 2\delta_{AB} \qquad \text{EQN.59}$$

From EQNS.55 & 57 :

$$\nu^*_{AB_\alpha} - \nu^*_{AB_\beta} = N \qquad \text{EQN.60}$$

$$\nu^*_{AB_\alpha} + \nu^*_{AB_\beta} = 2\nu_{AB} \qquad \text{EQN.61}$$

The formation of the AB-region from the original AB-quartet, for a range of values of δ_{AB} (decreased in steps of $\frac{1}{2}J_{AB}$, with J_{AB}, J_{AX} and J_{BX} held constant at 1, 3 and 5 respectively), is illustrated for J_{AX} and J_{BX} the same sign (FIG.3-2.5) and opposite signs (FIG.3-2.6). Note that both series of spectra suffer simplification of the AB-region by line overlap (cases (b), (d) and (f) in the former, and (h), (j) and (l) in the latter) and by a "collapsed quartet" when $\delta_{AB} = L$. For $\delta_{AB} > L$, in both series, D_+ and D_- are positive, ie. within both apparent quartets the lines originating from A are to low field of the lines from B, and the quartets may be termed "normal". For $\delta_{AB} < L$, in both series, D_+ and D_- have opposite signs, ie. one quartet is "inverted" with the lines from A to high field of the lines from B.

It is convenient to recognise four separate types of spectrum :

Type I : J_{AX} and J_{BX} same sign — I(a) D_+ and D_- same sign; I(b) D_+ and D_- opposite signs

Type II : J_{AX} and J_{BX} opposite signs — II(a) D_+ and D_- same sign; II(b) D_+ and D_- opposite signs

In the absence of the X-region, the (a) and (b) assignments of the two chosen quartets of any AB-region are indistinguishable. The spectrum "Type", for each assignment, may be determined as follows :

Type I Spectra have the A_α lines to low field of the A_β lines.

Type II Spectra have the converse (Arbitrarily fixing J_{BX} as +ve in both). Normally the "Type" of the spectrum (ie. I or II) is the same for both assignments, with the one exception that the alternative to a Type I(a) in which $\delta_{AB} > N$ is a Type II(b) in which $\delta_{AB} < N$.

The formation of the X-region spectrum from the original X-singlet may be explained in a similar manner to the formation of the AB-region, with the

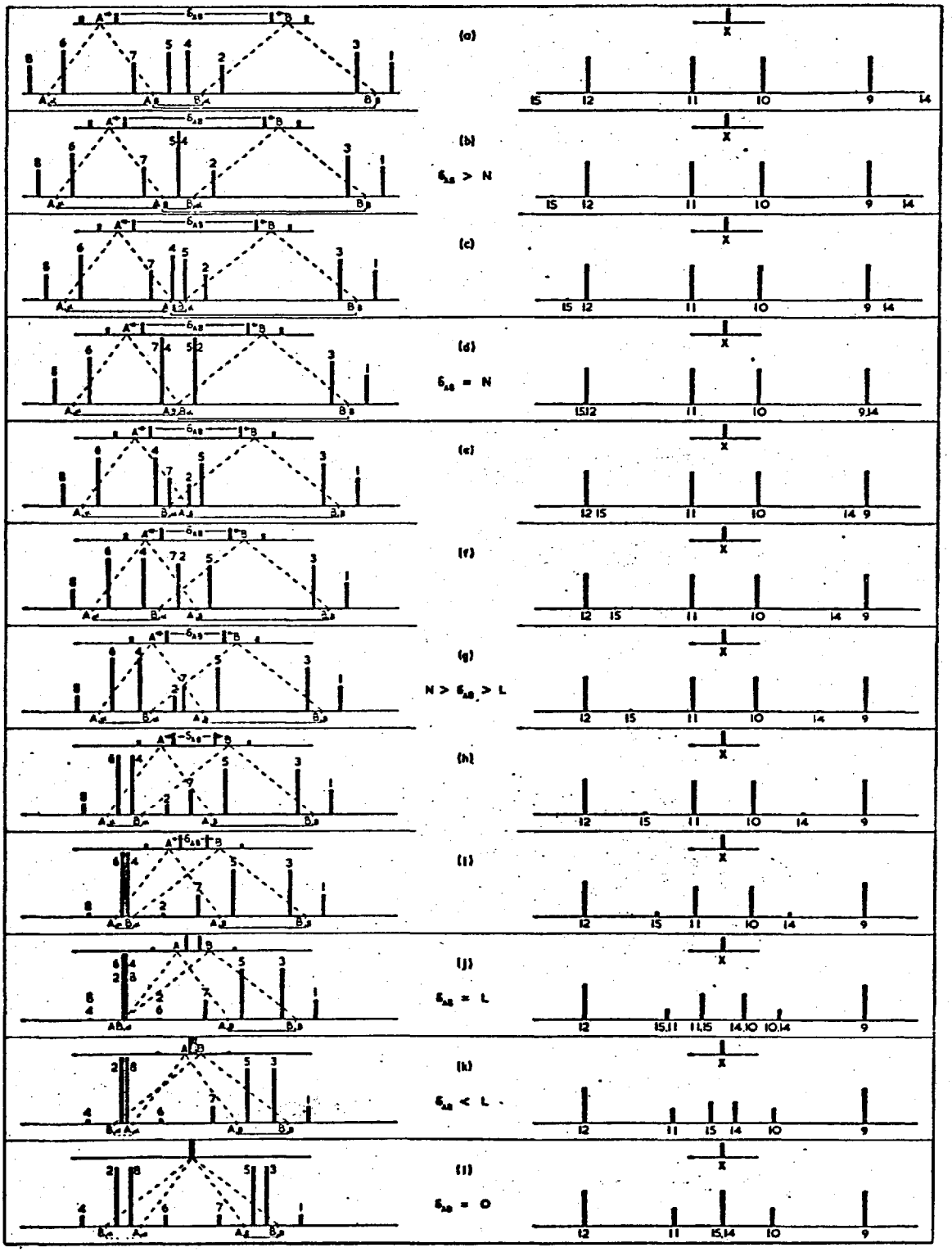


FIG.3-2.5 The Effect of Changing δ_{AB} on the Appearance of a Type I ABX Spectrum

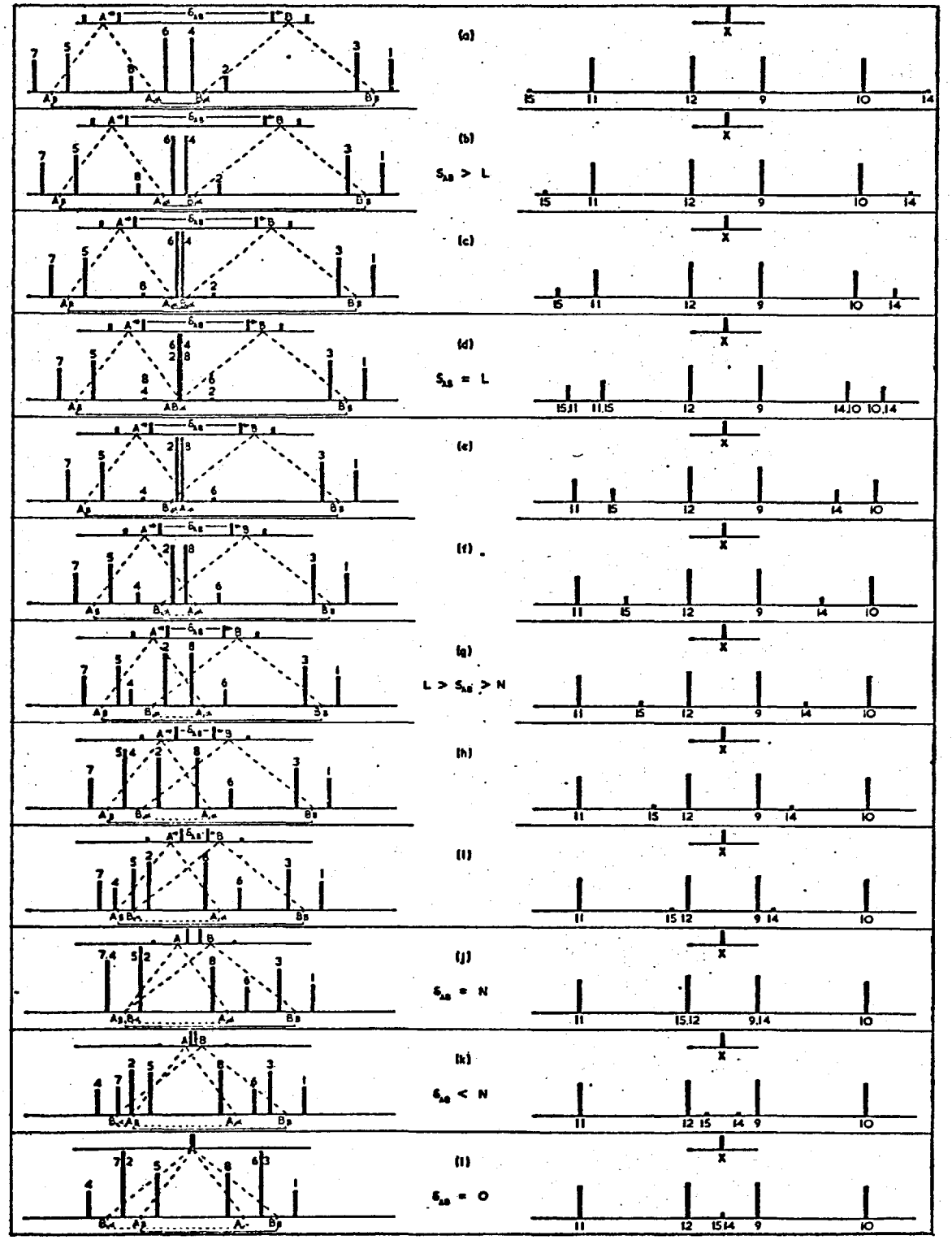


FIG.3-2.6 The Effect of Changing δ_{AB} on the Appearance of a Type II ABX Spectrum

added difficulty of the mixing of the A and B spins. With A and B in the same spin state their interaction with X produces an $\alpha\alpha$-line (12) and a $\beta\beta$-line (9), which always have unit intensity and whose shifts ($\pm N$) are independent of δ_{AB}.

The degree of mixing of the bpsf's 3 and 4 to give wave functions 3' and 4', and 5 and 6 to give 5' and 6' (see TABLE 3-2.3) in a system with fixed coupling constants, varies with δ_{AB}, as the mixing coefficients $\phi_{\pm}$ are dependent on δ_{AB} (see EQNS.35-37). Lines (10,11,14 and 15) are derived from transitions from states 5' and 6' to 3' and 4'. Consequently, changes in the positions and intensities of these lines (defined in terms of $D_{\pm}$ and $\phi_{\pm}$ respectively) on varying δ_{AB} are difficult to visualise. This is evidenced by the mis-interpretations of the X-region of ABX spectra in the literature, eg. in the analysis of 2,4-dichloro-6-fluorophenol,[239] the assignment of the spectrum is incorrect due to the wrongful definition of D_+ and D_- as positive. Surprisingly, correct analytical results are obtained (as in Analyses (i) and (ii) above) because the method used only relies on identifying lines 9 and 12 in the X-region, and then measuring the separations of the inner and outer pairs of lines (10,11 and 14,15) without needing to know which pair is which. This leads to the correct magnitudes for the D's, although not necessarily to the correct sign or assignment. The "flexibility of sign" possessed by EQNS.35-37 accounts for any earlier mistakes.

It is worthwhile examining the X-region in some detail, as this will clarify several problems that may arise in the process of line assignment and analysis.

The positions of lines (10,11) and (14,15) are dependent on $2D_+$ and $2D_-$. If these terms are plotted against δ_{AB} in a perfectly general ABX case, discontinuities occur when $\delta_{AB} = \pm L$ (see FIG.3-2.7). Although unexpected, reference to FIGS.3-2.5(i) to (k) will explain how Sep^{n}_{8-4} changes sign so rapidly as the AB_{α}-quartet inverts.

In FIG.3-2.8 the positions of lines (10,11,14 and 15) are plotted for a range of δ_{AB}. The "inner" and "outer" pairs of curves do not cross but are both asymptotic to the lines (Freq = $\pm L$) and (Freq = $\pm\delta_{AB}$), changing their identity where these lines intersect. Lines (10,11) are roughly parallel to (Freq = $\pm L$), whilst (14,15) parallel (Freq = $\pm\delta_{AB}$). Apart from a few exceptions[242-244] this change of identity when $\delta_{AB} = \pm L$ has been overlooked in the literature. For example, in the context of deceptive simplicity, the 1:2:1 X triplet is frequently incorrectly assigned as 12-(10,11)-9[240,242,245] when $\delta_{AB} = 0$, when it should be labelled as 12-(14,15)-9 (the former assignment is only correct if L is also exactly zero.

It should be noted that unlike lines (14,15) the ordering of (10,11) is dependent on the magnitudes of J_{AX} and J_{BX}, ie. 10 is to low field of 11 if

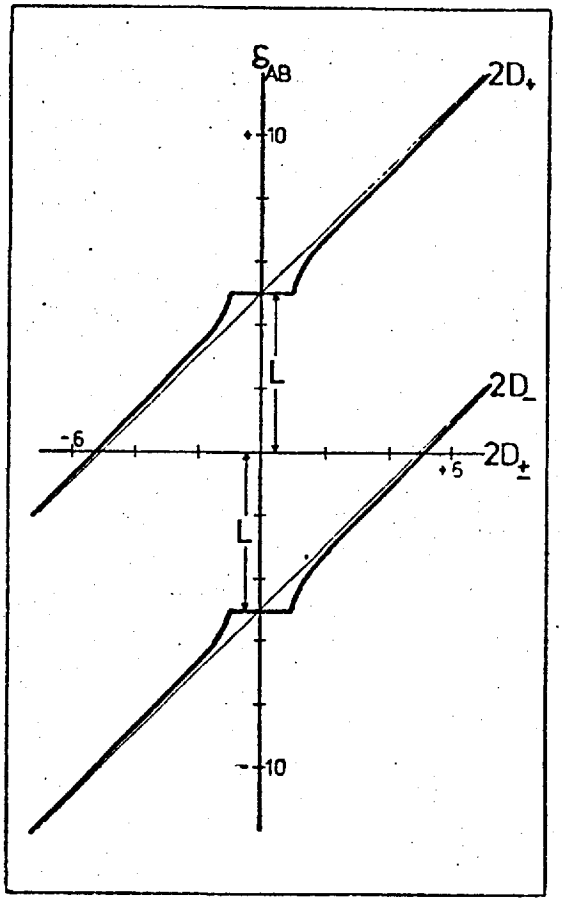


FIG.3-2.7 $L = 5.J_{AB}$; $J_{AX} < J_{BX}$

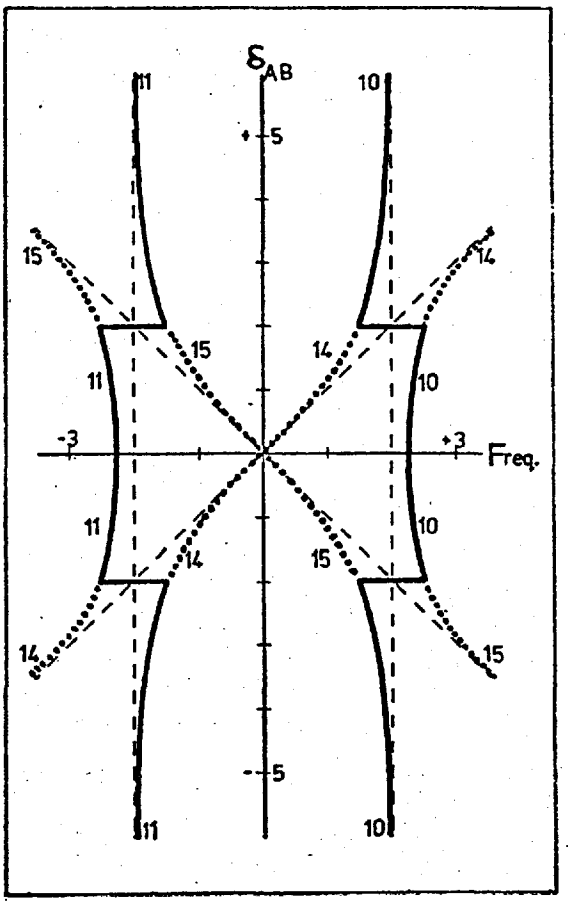


FIG.3-2.8 $L = 2.J_{AB}$. All axes in units of J_{AB}.

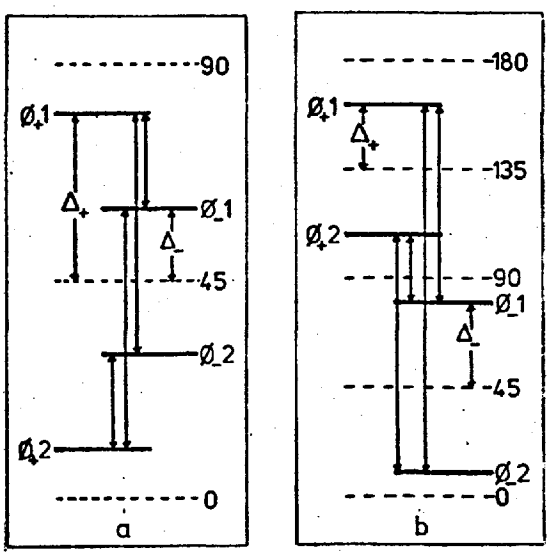


FIG.3-2.9 The choice of solutions for $(\phi_+ - \phi_-)$ and the definitions of Δ_+ and Δ_- :

(a) D_+ and D_- both positive, ie. Type I(a) or Type II(a)

(b) D_+ and D_- of opposite signs, ie. Type I(b) or Type II(b).

$$\Delta_\pm = \left|45 - \tfrac{1}{2}\sin^{-1}(J_{AB}/2D_\pm)\right| \qquad \text{EQN.62}$$

$J_{AX} > J_{BX}$, and vice versa.

From TABLE 3-2.3 [14,15] is given by $\sin^2(\phi_+ - \phi_-)$. Solving EQN.37 for ϕ_+ or ϕ_- (abbreviated $\phi_\pm$) will always give two values which will be symmetrically disposed about $\phi_\pm = 45^\circ$ if $D_\pm$ is positive or $\phi_\pm = 135^\circ$ if $D_\pm$ is negative (see FIGS.3-2.9(a) and (b) and EQN.62).

Therefore for any set of values of D_+, D_- and δ_{AB}, there will be two values of $(\phi_+ - \phi_-)$ and hence two values of [14,15]. In FIG.3-2.10 the

solutions for [14,15] are plotted over a range of δ_{AB} for the condition $L = J_{AB}$. Again note the discontinuity when $\delta_{AB} = L$. In FIG.3-2.11 the "acceptable" solutions for [14,15] (always the lower value), are plotted for several values of L. Obviously for $\delta_{AB} > L$ the solid curve in FIG.3-2.10 has the correct value for [14,15] (ie. given by $\sin^2|\Delta_+ - \Delta_-|$); for $\delta_{AB} < L$ it is not so apparent, but in our experience all solutions lie on the dotted rather than the solid curve (ie. $[14,15] = \sin^2|90 - (\Delta_+ - \Delta_-)|$). It may be easily proven that the range in which $[14,15] > 0.5$, is given by EQN.63. (see APPENDIX II):

$$\sin^2(\phi_+ - \phi_-) > 0.5 \quad \text{when:} \quad L > \delta_{AB} > \sqrt{(L^2 - J_{AB}^2)} \qquad \text{EQN.63}$$

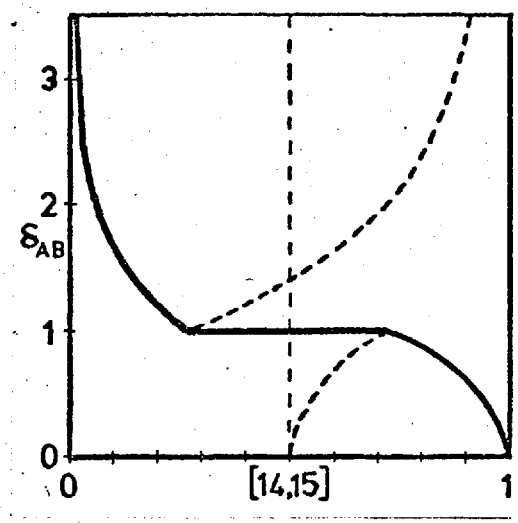


FIG.3-2.10

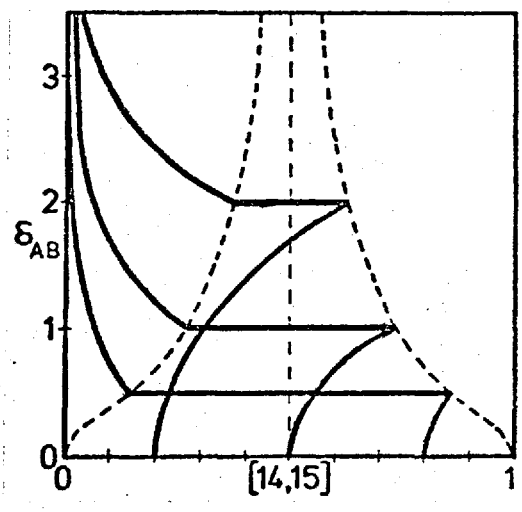


FIG.3-2.11

FIG.3-2.10 The solid lines represent solutions obtained from $\sin^2|\Delta_+ - \Delta_-|$ when $\delta_{AB} > L$ and $\sin^2(90 - |\Delta_+ - \Delta_-|)$ when $\delta_{AB} < L$; The broken lines are solutions of $\sin^2(\Delta_+ + \Delta_-)$ and $\sin^2|90 - (\Delta_+ + \Delta_-)|$.

FIG.3-2.11 The "acceptable" values of [14,15] for $L = \frac{1}{2}$, 1 and $2.J_{AB}$. The broken curves outline the "discontinuity envelope", the right hand curve also acts as the boundary for the maximum value of [14,15].

In FIG.3-2.11 the "inner" and "outer" pairs of lines (10,11) and (14, 15) interchange identity at the same point at which [14,15] undergoes its dramatic discontinuity. It is therefore more helpful to plot the variation in intensity of the "inner" and "outer" pairs of lines as δ_{AB} varies (see FIG.3-2.12). The smooth curves obtained when coupled with the smooth curves obtained in FIG.3-2.8, demonstrate how the change of identity of lines in the X-region is easily overlooked.

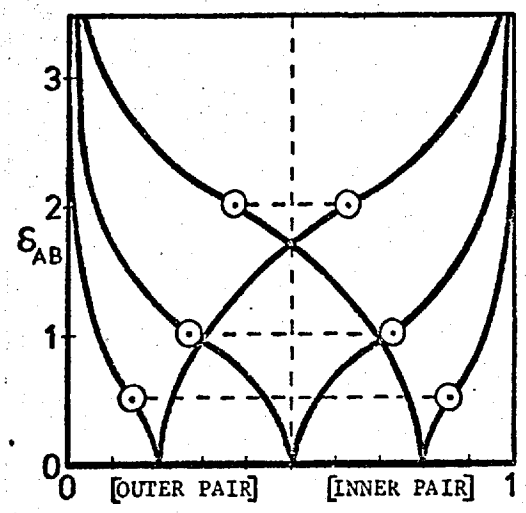


FIG.3-2.12 The intensities of the inner and outer pairs of X-region lines. The circles and broken lines indicate where the pairs interchange identity. The value of [outer] tends to zero as δ_{AB} increases.

3-2-4 Line Assignment and Analysis of ABX Spectra

This section is written in the form of a "working text" from which an inexperienced student should be able to assign and analyse virtually any ABX spectrum. FIGS.3-2.5 & 3-2.6 will be found particularly useful for identifying those conditions under which lines overlap and spectra simplify (ie. contain less than 14 lines).

3-2-4.1 Line Assignment

From the AB-region select two AB-quartets which comply with EQNS.31-33. Accurately measure the separation of the midpoints of the two earmarked quartets and check that this exactly equals half the separation of the two strongest lines in the X-region (see EQNS.46 and 47). (If the X-region only contains four approximately equally intense lines, this may correspond to the inner or outer pair of lines). If this test fails, the two AB-quartets have been chosen incorrectly and must be re-selected.

The quartets may now be assigned using the following rules :

(i) The AB_α-quartet has its midpoint to low field of the AB_β-quartet

(ii) The numbering of the lines is determined by their origin, ie :

lines originating	from	B	have	numbers		1-2-3-4
..	..	..	A	..	..	5-6-7-8
..	..	..	β	..	..	1-3-5-7
..	..	..	α	..	..	2-4-6-8

The lines always occur in pairs, separated by J_{AB}, so it follows that the numbering for each pair is : A_α = 8-6 ; A_β = 7-5 ; B_α = 4-2 ; B_β = 3-1. (With the larger number always to low field).

(iii) There are two possible assignments for any AB-region, only one of which

is correct. These assignments differ in one quartet only and for any spectrum this choice will only occur in the narrower quartet (ie. the quartet with the smaller δ^*_{AB} - see FIG.3-2.4).

The assignment of the broader quartet is therefore straightforward with the lines originating from B to high field of those from A.
ie. for the AB_α-quartet 8-6-4-2 ; for the AB_β-quartet 7-5-3-1

Of the two possible assignments for the narrower quartet, the "normal" assignment is given above, whilst the "inverted" assignment will be :

for the AB_α-quartet 4-2-8-6 ; for the AB_β-quartet 3-1-7-5

We now have the two possible assignments for the AB-region and will proceed to do likewise with the X-region.

The two most intense lines, used in the first test, may immediately be assigned as 12 and 9. The assignment of the pairs of lines (14,15) and (10, 11) may be rapidly carried out by using the relationships in EQNS.50-53, (NB. Use the sign convention that a measurement from low to high field is positive).

With both AB-quartets "normal", lines (14,15) should lie outside (10,11), and conversely for one AB-quartet "inverted". If J_{AX} and J_{BX} have the same sign (Type I system), (10,11) will be inside (9,12), ie. N > L. If J_{AX} and J_{BX} have opposite signs (Type II system) the converse is true, ie. N < L. Normally "inverting" one quartet will not change the general "Type" of the spectrum, but this may occur under certain circumstances (see SECTION 3-2.3).

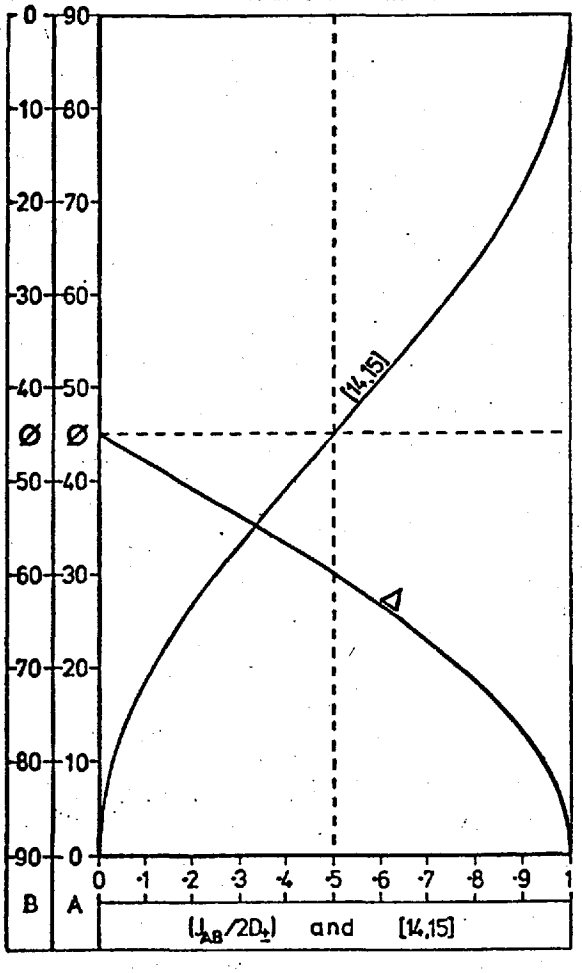


FIG.3-2.13 This is a "ready reckoner" for calculating [14,15] in any ABX spectrum (see text for instructions). The 'Δ' curve is simply a plot of $|45 - \frac{1}{2}\sin\emptyset|$, whilst the '[14,15]' curve is a plot of $\sin^2\emptyset$. A larger version of this figure will be found in APPENDIX I.

Having completed the two assignments, we must choose which is correct. This is simply done by determining the expected intensity of lines (14,15), for both assignments, and rejecting the one with the wrong

solution. It should be emphasised that it is perfectly in order for [14,15] (which, as combination lines, are expected to be weak) to be greater than [10,11]. A rapid method of calculating [14,15] is as follows :

(i) Calculate $|J_{AB}/2D_+|$ and $|J_{AB}/2D_-|$

(ii) Calculate Δ_+ and Δ_-, either using EQN.62, or the 'Δ' curve in FIG.3-2.13, reading $\Delta_\pm$ off on the ϕ(A) scale.

(iii) (a) For D_+ & D_- the same sign : calculate $|\Delta_+ - \Delta_-|$ and sight against the '[14,15]' curve, using the ϕ(A) scale; or use $\sin^2|\Delta_+ - \Delta_-|$.

(b) For D_+ & D_- opposite signs : calculate $(\Delta_+ + \Delta_-)$ and sight against the '[14,15]' curve, using the ϕ(B) scale; or use $\sin^2|90 - (\Delta_+ + \Delta_-)|$.

Only one assignment of the X-region will fit the predicted [14,15] and once this has been unambiguously obtained we can proceed with the analysis.

3-2-4.2 Spectral Analysis of the ABX Spin-System (The method used is essentially that of Abraham[242])

Having made the assignments, as above, only the AB-region is necessary for the subsequent analysis. $|J_{AB}|$ may be read directly from the spectrum (EQN. 43). The values of $\delta^*_{AB_\alpha}$, $\delta^*_{AB_\beta}$, $\nu^*_{AB_\alpha}$ and $\nu^*_{AB_\beta}$ may also be readily obtained (see FIG.3-2.4, EQNS.54-57 and APPENDIX I). It is important to note that when calculating δ^*_{AB} for an "inverted" quartet, the sign of the answer should be negative (ie. take the negative root of the product of two negative numbers). Application of EQNS.58-61 will give values for L, N, δ_{AB} and ν_{AB}, whilst EQNS. 64 & 65 give J_{AX} and J_{BX} (If careful attention is paid to the signs of L and N the relative values of J_{AX} and J_{BX} may be obtained unambiguously, without resorting to the selection procedure used in analyses (i) to (iii)).

From EQNS.41 & 42 $\quad J_{AX} = N + L$ EQN.64

$\quad J_{BX} = N - L$ EQN.65

D_+ and D_- will already be known from determining the correct assignment earlier. The acceptable combinations of values of ϕ_+ and ϕ_- for a Type I(a) or II(a) spectrum are given by :

$$\phi_+ = 45 - \Delta_+ \; ; \; \phi_- = 45 - \Delta_- \quad \text{Or} \quad \phi_+ = 45 + \Delta_+ \; ; \; \phi_- = 45 + \Delta_-$$

and for a Type I(b) or II(b) spectrum :

(i) $\phi_+ = 135 + \Delta_+ \; ; \; \phi_- = 45 - \Delta_- \quad \text{Or} \quad \phi_+ = 45 + \Delta_+ \; ; \; \phi_- = 135 - \Delta_-$

(ii) $\phi_+ = 135 - \Delta_+ \; ; \; \phi_- = 45 + \Delta_- \quad \text{Or} \quad \phi_+ = 45 - \Delta_+ \; ; \; \phi_- = 135 + \Delta_-$

It should be emphasised that it is always worthwhile to re-create the observed AB-region from the calculated parameters, as this is the most convincing method of verifying the analysis.

CHAPTER 4

4 CONFORMATIONAL ANALYSIS OF THE TYPE (IV), (V) AND (VI) COMPOUNDS FROM THEIR CONVENTIONAL ^{1}H, ^{13}C AND ^{19}F NMR SPECTRA

4-1 Experimental

All spectra were recorded on 0.5M solutions of the purified compounds in deuteriochloroform (MW in mg dissolved in 2ml $CDCl_3$) using a Varian Associates XL100-12WG spectrometer operating at 23.5 KGauss. Apart from the ^{1}H spectra of the Type (IV) alcohols, which were recorded in 5mm tubes, 10mm tubes were used throughout. All spectra were recorded with an internal deuterium frequency-field lock onto the deuteriochloroform signal.

^{1}H spectra were recorded at 100.1MHz in continuous wave (CW) mode for the Type (IV) and (V) series, and in Fourier transform (FT) mode, using a Varian 620L computer with 16K store, for the Type (V) and (VI) series. Where necessary, specific homonuclear and ^{19}F heteronuclear decoupling ($^{1}H[^{19}F]$) were performed. A little variable temperature work (ambient to -50°C) was performed on the Type (IV) alcohols to determine the temperature sensitivity of the ^{1}H chemical shifts, using 0.5M solutions made up in 1:1 $CDCl_3/CFCl_3$.

^{19}F spectra were recorded at 94.1MHz in the FT mode for the Type (IV) and (V) series only. Because of the need for accurate analysis of the ABX system of the Type (V) compounds, care was taken to ensure that the ^{1}H and ^{19}F spectra were recorded on the same solutions on the same day, to minimise concentration/temperature effects. All ^{19}F spectra were also recorded with ^{1}H noise decoupling ($^{19}F[^{1}H]$).

^{13}C spectra were recorded at 25.16MHz in the FT mode with broad band ^{1}H noise decoupling, ($^{13}C[^{1}H]$). ^{1}H "gated decoupled" ^{13}C spectra* ($^{13}C[GD-^{1}H]$), which give all the $^{n}J_{C-H}$ coupling information of a high resolution ^{13}C spectrum, but retain the signal/noise benefits of the Nuclear Overhauser enhancement (NOE), were recorded on the Type (IV) alcohols. These spectra were invaluble for assigning the side-chain ^{13}C resonances and also provided useful coupling information. Several attempts at observing $^{2\&3}J_{CH}$ couplings, by using specific narrow band ^{1}H decoupling (ie. irradiating the aromatic protons but not the side-chain protons) were unsuccessful. Previous work with single frequency ^{1}H decoupling[143] had been successful, but it was found impossible to irradiate a band 60Hz wide without giving off-resonance (partial decoupling) effects to ^{1}H signals 100-400 Hz from the edge of the band. This resulted in

*"Gated Decoupling" describes the following sequence of operations in an FT cycle: (1) Pulse delay with full noise decoupling; (2) Fire pulse; (3) Acquire free induction decay (FID). The noise decoupler is turned off during steps (2) and (3). Each cycle (1-3) may be repeated many thousand times before acquiring a ^{13}C (FID) suitable for Fourier Transformation.

residual couplings in the ^{13}C spectra.

Further details of spectral parameters will be given where appropriate.

4-1-1 Accuracy of Spectral Measurements

The manufacturer's specification for the 12" magnet XL100 Spectrometer, a signal resolution of at least 0.3Hz, was routinely obtainable.

All CW chemical shifts, shift differences and coupling constants were measured to the nearest 0.1Hz. Where two or more measurements were averaged, the result has been recorded to the nearest 0.05Hz.

In FT spectra the computer listings give shifts to the nearest 0.1Hz, but the digitisation rate (specified as Hz/point) was normally larger than this, ie :

^{1}H and ^{19}F spectra - max errors $\pm$ 0.2Hz (ie. $\sim$0.002ppm)

^{13}C spectra - max errors $\pm$ 0.5Hz or 0.63Hz (When X = F or OMe required sweep width of 2500Hz); (ie. $\sim$0.020ppm).

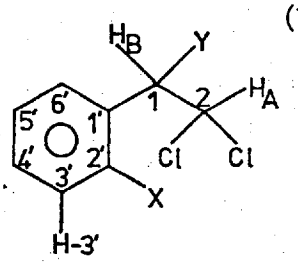
These errors are equivalent to the digitisation rate.

The likely errors in frequency between lines in different spectra should be better than $\pm$ 1.0Hz. In an exercise involving 11 samples, the absolute machine offset of the ^{1}H TMS resonance was determined by adding its offset from the edge of the FT spectral "window" to the spectral offset from the ^{2}D $CDCl_3$ lock signal. The average deviation of the 11 individual offsets from the overall mean (44811.6Hz) was $\pm$ 0.5Hz.

4-1-2 Naming Convention Used in NMR Assignments

The naming convention adopted is an extension of that used in Chapter 2, numbering ring substituents with a prime eg. X-n'. The α and β side-chain carbons are numbered 1 and 2 respectively whilst the protons are lettered A, B and C in low to high field order. Where necessary the side-chain fluorine will be numbered F_1 and the ring substituent fluorine F_2 (see FIG.4-1.1)

Type (IV) Y = OH_C
(V) Y = F_1
(VI) Y = Cl



When X is para, 5' and 6' degenerate to 3' and 2' respectively.

FIG.4-1.1

4-2 Spectral Assignment

^{1}H resonance assignments of the side-chain protons were straightforward and were aided, where necessary, by decoupling and deuterium exchange experiments. The assignment of the aromatic ^{1}H resonances was only attempted on the seven para substituted compound in each of the three series. The AA'BB'

spectra were treated as pseudo-AB spectra to obtain the relevant shifts, and no further analysis was attempted. Full AB or ABX analyses were performed on the side-chain protons in the Type (IV) and (VI) or Type (V) spectra.

^{19}F spectra provided no assignment problems. Where two fluorines were present their characteristic ^{1}H coupling patterns gave instant identification.

Assigning ^{13}C spectra was more difficult. Usually the ortho and para fluoro compounds in each series were assigned first, with the aid of the $^{n}J_{FC}$ couplings (which in fluorobenzene decrease regularly with distance, ie. C-1 -245.3; C-2 21.0; C-3 7.7; C-4 3.3Hz[246]) and subsequent assignments utilised readily available[128,246] benzene substituent chemical shifts (SCS). Once the Type (IV) alcohols had been assigned, the SCS data from this "model system" was used to assign the Type (V) and (VI) spectra. Assignments were checked by comparison with literature SCS data and in the case of the Type (IV) alcohols by $^{1}J_{CH}$ couplings from $^{13}C[GD-^{1}H]$ spectra, comparative NOE measurements, and analysis of LIS data.

4-3 ABX Analysis of the ^{1}H and ^{19}F Spectra of the Type (V) Fluorides

As this subject has already been treated in depth it is appropriate that this series of ABX analyses be listed in full. Although this is normally unnecessary, the fifteen analyses illustrate many of the points discussed in Chapter 3. TABLE 4-3.1 lists the shifts and heights of the 14 ABX lines and the 4 AB lines (from the $^{1}H[^{19}F]$ spectrum) for each derivative, together with the assignments allocated to the lines by the method given in SECTION 3-2-4.1. The relative shifts (offsets) of lines (i) to (vii) in the AB region are referred to line (viii) whose offset from TMS is given in Hz. Lines (I) to (IV) from the AB[X] spectrum are also referred to line (viii) for convenience. The X-region lines (i) to (vi) are referred to their overall mean, their absolute shifts being listed in SECTION 4-4-2. The height measurements (mm) are only consistent within individual spectral regions and are appended with the letter (b) where significant broadening (long range ^{1}H coupling) is present. The third row indicates the origin of the spectral lines (A or B) and its possible assignment(s). In each case the subscript indicates the incorrect assignment. The naming convention adopted for the side-chain protons is the same as that used in the Type (IV) and (VI) compounds (see FIG.3-2.1). On all but three occasions (X = oCl, oNO_2 and oCF_3) this labelling also agrees with the "nucleus B to highfield of nucleus A" convention. In these three cases, the structural assignments of A and B are retained in the analyses, so that J_{AX}, J_{BX}, δ_{AB}, ν_A and ν_B refer to the same coupled nuclei as in the remainder of the series. TABLE 4-3.2 shows the intermediate and final results of the analyses, using the method given in SECTIONS 3-2-4.1 & 3-2-4.2. The important coupling

TABLE 4-3.1 Relative Shifts, Intensities and Assignments of the ABX and AB[X] Decoupled Spectra of the Type (V) Fluorides

	AB-REGION								X-REGION						AB[X] from $^1H\{^{19}F\}$			
DERIV	(i)	(ii)	(iii)	(iv)	(v)	(vi)	(vii)	(viii)	(i)	(ii)	(iii)	(iv)	(v)	(vi)	(I)	(II)	(III)	(IV)
H	61.7 34 A 8_4	56.4 82 A 6_2	51.0 50 A 7	49.7 48b B 4_8	46.1 64 A 5	44.3 19b B 2_6	5.4 35b B 3	533.7 28b B 1	27.5 201 12	17.0 200 11_{15}			-17.2 193 10_{14}	-27.4 198 9	58.1 151 A	52.7 254 A	29.0 149b B	23.0 102b B
o F	50.5 36b B 4_8	45.4 122b B 2_6	41.3 148 A 8_4	36.2 41 A 6_2	30.2 66 A 7	25.1 104 A 5	5.1 87b B 3	565.2 59b B 1	28.4 179 12	17.2 159 11_{15}	7.8 37 15_{11}	-7.6 29 14_{10}	-17.2 159 10_{15}	-28.4 180 9	37.6 78 A	32.5 235 A	27.7 129b B	22.6 40b B
o Cl*	48.5 32b B 8	45.15 46b B 6	31.75 90 A 4	28.45 69 A 2	15.15 58 A 3_7	11.85 99 A 1_5	3.35 52b B 7_3	581.8 32b B 5_1	30.85 243 12	14.25 233 10_{15}	2.35 27 15_{10}	-2.45 26 14_{11}	-14.25 235 11_{14}	30.85 250 9	23.5 6 AB			
o Br	48.1 48b B 4_8	45.0 71b B 2_6	37.0 157 A 8_4	34.0 85 A 6_2	19.7 110 A 7	16.7 152 A 5	3.1 77b B 3	579.8 51b B 1	31.2 243 12	13.7 232 11_{15}	2.7 30 15_{11}	-2.7 29 14_{10}	-13.7 234 10_{14}	-31.1 246 9	29.2 70b Sh	26.7 161b AB		
o Me	52.9 40b B 4_8	46.5 112b B 2_6	40.8 168 A 8_4	34.4 56 A 6_2	32.2 97 A 7	25.9 140 A 5	6.3 88b B 3	557.1 50b B 1	27.45 202 12	19.05 170 11_{15}	8.05 37 15_{11}	-7.75 27 14_{10}	-18.95 169 10_{14}	-27.55 205 9	38.6 28 A	32.2 118 A	28.8 85b B	22.4 19b B
o OMe	49.6 30b B 4_8	46.0 134b B 2_6	45.3 279 A 8_4	41.9 40 A 6_2	28.5 165 A 7	25.1 200 A 5	3.4 63b B 3	573.2 49b B 1	31.45 212 12	14.95 167 11_{15}	10.55 56 15_{11}	-10.55 66 14_{10}	-14.75 162 10_{14}	-31.55 213 9	38.3 133 A	34.9 230 A	26.5 103b B	23.2 62b B
o NO_2*	56.8 43b B 8	54.8 48b B 6	21.5 105 A 4	19.5 98 A 2	11.1 37b B 7_3	9.1 57b B 5_1	2.0 120 A 3_7	611.7 85 A 1_5	32.5 139 12	13.1 135 10_{15}			-13.1 138 11_{14}	-32.6 138 9	33.7 122b B	31.7 150b B	12.0 236 A	10.1 208 A
o CF_3*	51.9 48b B 8	48.2 55b B 6	20.9 165 A 4	17.2 124 A 2	8.1 29b B 7_3	4.4 100b B 5_1	3.7 166 A 3_7	581.1 25 A 1_5	30.45 142 12	13.3 128 10_{15}			-13.25 132 11_{14}	-30.45 147 9	30.3 64b B	26.1 102b B	12.3 172 A	8.7 122 A
p F	60.7 98 A 8_4	55.3 281 A 6_2	50.9 215 A 7	49.7 151b B 4_8	45.5 222 A 5	44.4 61b B 2_6	5.3 101b B 3	533.5 79b B 1	26.95 151 12	17.15 139 11_{15}			-17.15 138 10_{14}	-26.95 148 9	55.6 176 A	50.2 273 A	27.6 125b B	22.2 95b B
p Cl	60.9 100 A 8_4	55.6 290 A 6_2	50.8 222 A 7	49.5 230b B 4_8	45.6 230 A 5	44.3 100b B 2_6	5.3 190b B 3	533.2 160b B 1	27.25 134 12	17.25 133 11_{15}			-17.25 147 10_{14}	-27.25 156 9	55.7 107 A	50.5 154 A	27.8 109b B	22.5 79b B
p Br	62.0 79 A 8_4	56.1 192 A 6_2	52.0 139 A 7	49.5 102b B 4_8	46.8 150 A 5	44.0 45b B 2_6	5.3 72b B 3	531.1 56b B 1	27.25 211 12	17.15 203 11_{15}			-17.15 202 10_{14}	-27.25 212 9	56.6 143 A	52.5 189 A	28.3 135b B	23.0 95b B
p Me	64.9 65 A 8_4	59.3 197 A 6_2	55.0 133 A 7	50.0 106b B 4_8	49.5 137 A 5	44.5 35b B 2_6	5.0 59b B 3	528.7 46b B 1	27.3 124 12	17.3 127 11_{15}			-17.3 119 10_{14}	127.3 127 9	60.5 67 A	54.8 89 A	29.0 57b B	23.5 39b B
p OMe	66.0 27 A 8_4	60.3 52 A 6_2	56.8 42 A 7	51.0 56 A 5	50.3 27b B 4_8	44.5 13b B 2_6	5.8 23b B 3	526.8 18b B 1	26.85 255 12	17.55 252 11_{15}			-17.55 252 10_{14}	-26.85 258 9	61.0 66 A	55.3 90 A	28.0 43b B	22.3 31b B
p NO_2	52.7 23 A 8_4	48.1 200 A 6_2	47.4 100b B 4_8	42.8 19b B 2_6	41.1 110 A 7	36.6 123 A 5	4.6 62b B 3	550.0 42b B 1	27.5 181 12	20.8 64 15_{11}	15.8 145 11_{15}	-15.8 124 10_{14}	-20.6 59 14_{10}	-27.5 187 9	46.9 106 A	42.3 158 A	27.6 119b B	23.0 67b B
p CF_3	56.0 34 A 8_4	51.0 183 A 6_2	49.0 67b B 4_8	45.2 90 A 7	44.2 17b B 2_6	40.2 130 A 5	5.0 43b B 3	542.6 34b B 1	27.35 172 12	16.65 169 11_{15}			-16.65 150 10_{14}	-27.35 183 9	50.7 110 A	46.0 164 A	27.9 91b B	23.0 58b B

and shift data produced in TABLE 4-3.2 appears elsewhere in this chapter in more convenient forms. Seven different line assignment patterns are found for the fifteen spectra (see TABLE 4-3.3), illustrating the pointlessness of producing line assignment aids - it is far quicker to perform this task empirically.

The characteristic broadening of the lines originating from H_B in the Type (V) ABX spectra is illustrated in FIG.4-3.1. Similar broadenings, due to weak long range couplings in the aromatic ring, ($^4J_{HH}$) were also observed throughout the Type (IV) and Type (V) AB-spectra.

* = Origin B to lowfield of Origin A (labels for A and B derived from structure not nmr).

TABLE 4-3.2 Intermediate and Final Results of the Type (V) ABX Analyses Using the Method in Sections 3-2-4.1 and 3-2-4.2

DERIV	ASSIGNMENT CHECK					SPECTRAL ANALYSIS				RESULTS						DATA FROM AB[X]		
	J_{AB}	$2D_+$	$J_{AB}/2D_+$	Δ_+	$[14,15]_1$	m_α	Σm	$\delta^*_{AB_\alpha}$	$\Sigma\delta$	J_{AX}	J_{BX}	ν_{AB}	δ_{AB}	ν_A	Abs ν_A	J_{AB}	ν_{AB}	δ_{AB}
	$J_{AX}+J_{BX}$	$2D_-$	$J_{AB}/2D_-$	Δ_-	$[14,15]_2$	m_β	Δm	$^*_{AB_\beta}$	$\Delta\delta$					ν_B	Abs ν_B			
H	5.40 54.90	12.05 46.15	0.448 0.117	31.6 41.4	0.030 0.040	53.02 25.77	78.80 27.25	10.797 45.827	56.62 -35.03	9.74	44.76	39.40	28.31	53.55 25.25	587.25 558.95	5.40	40.85	28.59
o F	5.10 56.80	9.20 25.10	0.554 0.203	28.1 39.0	0.150 0.035	43.35 15.10	58.45 28.25	-7.657 24.576	16.92 -32.23	12.14	44.36	29.23	8.46	33.45 25.00	598.65 590.20	5.10	30.10	8.91
o Cl*	3.30 61.70	16.73 11.83	0.197 0.279	39.1 36.8	0.060 0.005	38.46 7.59	46.05 30.87	16.391 -11.348	5.04 27.74	17.00	44.74	23.02	-2.52	21.76 24.28	603.55 606.10		23.50	
o Br	3.05 62.30	11.05 16.65	0.276 0.183	37.1 39.6	0.055 0.055	41.02 9.88	50.90 31.15	-10.621 16.368	5.75 -26.99	17.65	44.65	25.45	2.88	26.89 24.01	606.70 603.80		26.70	
o Me	6.35 55.00	12.10 25.90	0.525 0.245	29.2 37.9	0.150 0.025	43.65 16.10	59.75 27.55	-10.269 25.122	14.85 -35.39	9.85	45.25	29.88	7.43	33.59 26.16	590.70 583.25	6.40	30.50	7.42
o OMe	3.40 63.00	4.10 25.10	0.829 0.135	17.0 41.0	0.281 0.165	45.65 14.25	59.90 31.40	-2.291 24.869	22.58 -27.16	17.82	44.98	29.95	11.29	35.59 24.31	608.80 597.50	3.35	30.73	11.26
o NO_2*	2.00 65.10	35.30 9.00	0.056 0.222	42.3 38.5	0.005 0.025	38.15 5.55	43.70 32.60	35.243 8.877	44.12 26.37	19.42	45.78	21.85	-22.06	10.82 32.88	622.50 644.60	1.95	21.88	-21.56
o CF_3*	3.70 60.90	31.00 4.40	0.119 0.841	41.5 16.3	0.180 0.285	34.55 4.05	38.60 30.50	30.778 2.381	33.16 28.40	16.30	44.70	19.30	-16.58	11.01 27.59	592.10 608.70	3.70	19.35	-17.26
p F	5.40 53.90	10.95 45.55	0.493 0.119	30.1 41.5	0.040 0.100	52.52 25.42	77.94 27.10	9.554 45.235	54.79 -35.68	9.26	44.94	38.97	27.40	52.67 25.27	586.15 558.75	5.40	38.90	27.47
p Cl	5.25 54.50	11.35 45.55	0.463 0.115	31.1 41.6	0.035 0.085	52.57 25.42	78.00 27.15	10.063 45.246	53.31 -35.18	9.56	44.74	39.00	26.66	52.33 25.67	585.55 558.85	5.25	39.12	27.45
p Br	5.20 54.50	12.45 46.75	0.418 0.111	32.5 41.7	0.025 0.074	53.17 26.02	79.20 27.15	11.335 46.454	57.79 -35.12	9.59	44.71	39.60	28.90	54.05 25.15	585.15 556.25	5.20	40.35	28.94
p Me	5.50 54.60	14.85 49.50	0.370 0.111	34.1 41.7	0.018 0.060	54.67 27.50	82.17 27.17	13.774 49.193	62.97 -35.42	9.46	44.88	41.08	31.48	56.82 25.34	585.52 554.04	5.60	41.95	30.90
p OMe	5.70 53.70	15.80 51.00	0.361 0.112	34.3 41.7	0.018 0.060	55.25 28.40	83.65 26.85	14.140 50.669	64.81 -36.53	8.59	45.12	41.83	32.40	58.03 25.63	584.85 552.45	5.70	41.65	32.50
p NO_2	4.60 55.00	5.30 36.60	0.868 0.126	14.7 41.3	0.200 0.312	48.10 20.55	68.65 27.55	2.632 36.266	38.90 -33.63	10.73	44.37	34.33	19.45	44.05 24.60	594.05 574.60	4.60	34.95	18.74
p CF_3	5.00 54.70	6.90 40.20	0.725 0.124	21.7 41.4	0.115 0.205	50.05 22.60	72.65 27.45	4.858 39.888	44.75 -35.12	9.89	45.01	36.33	22.38	47.52 25.14	590.10 567.75	4.80	36.90	22.39

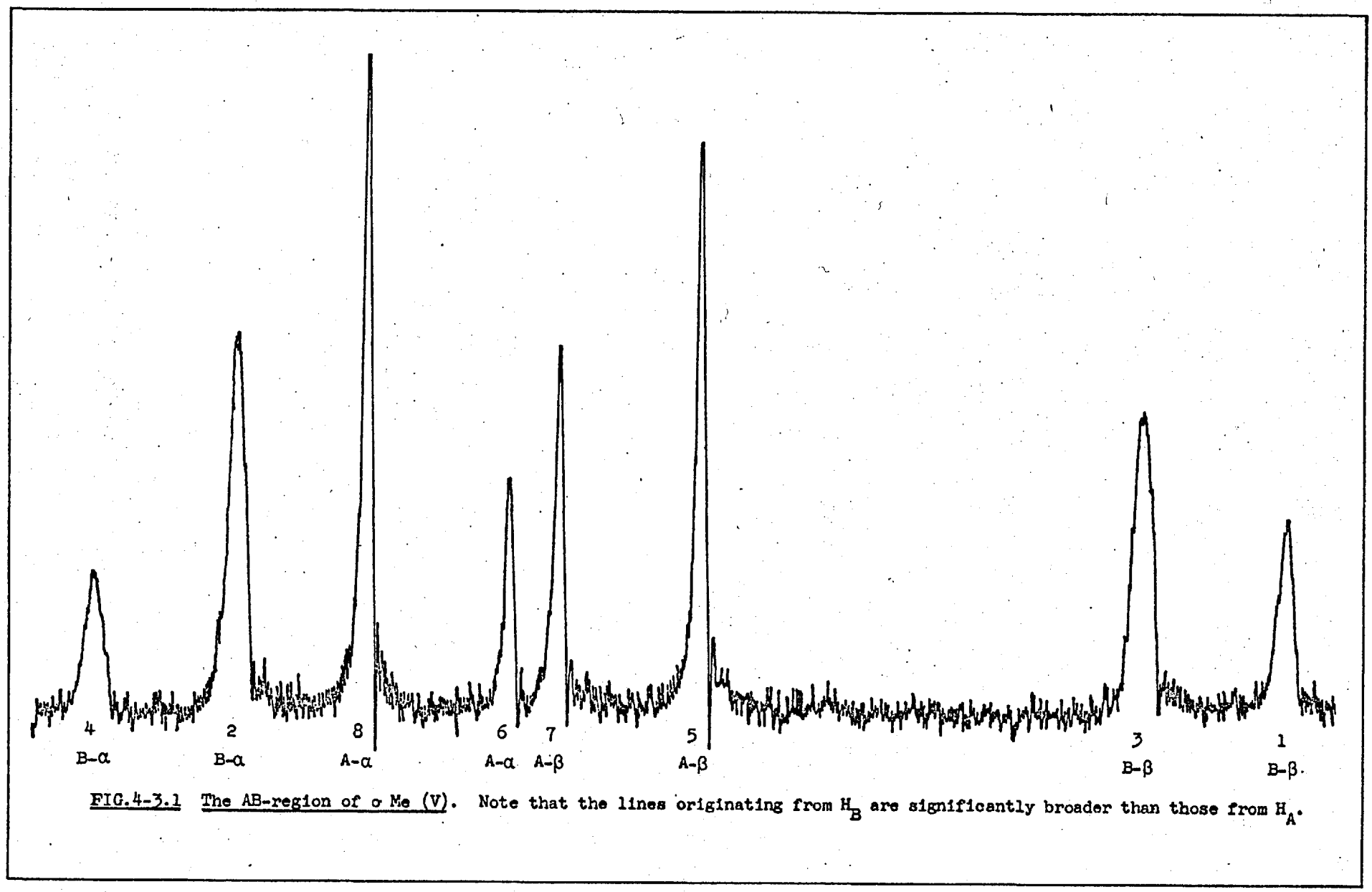


FIG.4-3.1 The AB-region of o Me (V). Note that the lines originating from H_B are significantly broader than those from H_A.

TABLE 4-3.3 ABX Line Assignments in the Type (V) Fluorides

DERIV	CORRECT ASSIGNMENT		ALTERNATIVE ASSIGNMENT	
	AB-REGION	X-REGION	AB-REGION	X-REGION
H, pF, pCl pBr, pMe	8-6-7-4-5-2-3-1	12-11-10-9	4-2-7-8-5-6-3-1	12-15-14-9
oF, oBr oMe, oOMe	4-2-8-6-7-5-3-1	12-11-15-14-10-9	8-6-4-2-7-5-3-1	12-15-11-10-14-9
oCl	8-6-4-2-3-1-7-5	12-10-15-14-11-9	8-6-4-2-7-5-3-1	12-15-10-11-14-9
oNO_2, oCF_3	8-6-4-2-7-5-3-1	12-10-11-9	8-6-4-2-3-1-7-5	12-15-14-9
pOMe	8-6-7-5-4-2-3-1	12-11-10-9	4-2-7-5-8-6-3-1	12-15-14-9
pNO_2	8-6-4-2-7-5-3-1	12-15-11-10-14-9	4-2-8-6-7-5-3-1	12-11-15-14-10-9
pCF_3	8-6-4-7-2-5-3-1	12-11-10-9	4-2-8-7-6-5-3-1	12-15-14-9

4-4 Chemical Shift Data

Analysis of the conformational data deducible from the various chemical shifts and coupling constants will be deferred to SECTIONS 4-7 & 4-8. It is hoped that the compact presentation of the raw data will make referencing more convenient.

4-4-1 ^1H Chemical Shifts

The chemical shifts of the sife-chain protons are listed in TABLE 4-4.1. The shifts of H_C, the hydroxy protons in the Type (IV) alcohols, are strongly

TABLE 4-4.1 Variations of the Chemical Shifts of H_A, H_B and H_C

DERIV	H_A			H_B			H_C	δ_{AB}		
X	(IV)	(V)	(VI)	(IV)	(V)	(VI)	(IV)	(IV)	(V)	(VI)
H	577.65	587.25	599.45	493.65	558.95	520.15	299.70	84.00	28.30	79.30
o F	593.95	598.65	606.85	531.85	590.20	552.80	303.95	62.10	8.45	54.00
o Cl	604.70	603.55	608.20	546.10	606.10	580.75	310.25	58.60	-2.55	27.45
o Br	607.50	606.70	607.75	544.20	603.80	580.40	322.00	63.30	2.90	27.35
o Me	580.85	590.70	602.45	520.00	583.25	547.05	295.40	60.85	7.45	55.40
o OMe	608.75	608.80	616.75	522.30	597.50	568.25	334.15	86.45	11.30	48.50
o NO_2	619.65	622.50	618.95	573.50	644.60	607.50	327.00	46.15	-22.10	11.45
o CF_3	589.40	592.10	602.25	545.75	608.70	563.05	312.10	43.65	-16.60	39.20
p F	573.75	586.15	595.35	493.95	558.75	518.15	302.00	79.80	27.40	72.20
p Cl	573.75	585.55	595.05	492.85	558.85	516.15	289.00	80.90	26.70	78.90
p Br	572.75	585.15	594.70	490.40	556.25	514.55	297.70	82.35	28.90	80.15
p Me	575.65	585.50	597.30	489.80	554.05	516.80	287.90	85.85	31.50	80.50
p OMe	573.45	584.85	595.50	448.15	552.45	515.80	297.10	85.30	32.40	79.70
p NO_2	583.05	594.05	601.35	512.75	574.60	529.00	328.00	70.30	19.45	72.35
p CF_3	578.35	590.10	599.55	502.10	567.75	525.15	305.30	76.25	22.35	75.40

TABLE 4-4.2 SCS of H_A, H_B and H_C in the Type (IV), (V) & (VI) Compounds (Hz)

DERIV	H_A			H_B			H_C	δ_{AB}		
X	(IV)	(V)	(VI)	(IV)	(V)	(VI)	(IV)	(IV)	(V)	(VI)
$H	577.65	587.25	599.45	463.65	558.95	520.15	299.70*	84.00	28.30	79.30
o F	16.30	11.40	7.35	38.20	31.25	32.65	4.25*	-21.90	-19.85	-25.30
o Cl	27.05	16.30	8.75	52.65	47.15	60.60	10.55*	-25.40	-30.85	-51.85
o Br	29.85	19.45	8.30	50.75	44.85	60.25	22.30	-20.70	-25.40	-51.95
o Me	3.20	3.45	3.00	26.25	24.30	26.90	-4.30*	-23.15	-20.85	-23.90
o OMe	31.10	21.55	17.30	28.85	38.55	48.10	34.45*	2.45	-17.00	-30.80
o NO_2	42.00	35.25	19.50	80.05	85.65	87.35	27.30	-37.85	-50.40	-67.85
o CF_3	11-75	4.85	2.80	52.10	49.75	42.90	12.40	-40.35	-44.90	-40.10
p F	-3.90	-1.10	-4.10	0.30	-0.20	-2.00	2.30	-4.20	-0.90	-2.10
p Cl	-3.90	-1.70	-4.40	-0.80	-0.10	-4.00	-10.70	-3.10	-1.60	-0.40
p Br	-4.90	-2.10	-4.75	-3.20	-2.70	-5.60	-2.00	-1.65	-0.60	0.85
p Me	-2.00	-1.75	-2.15	-3.85	-4.90	-3.35	-11.30	1.85	3.20	1.20
p OMe	-4.20	-2.40	-3.95	-5.50	-6.50	-4.35	-2.60*	1.30	4.10	0.40
p NO_2	5.40	6.80	1.90	19.10	15.65	8.85	28.30	-13.70	-8.85	-6.95
p CF_3	0.70	2.85	0.10	8.45	8.80	4.00	5.60	-7.75	-5.95	-3.90

$ All values are referred to those in the 'H' row, which are taken as zero.
* These protons showed couplings to H_B - normally only seen in very dry systems.

TABLE 4-4.3 Chemical Shifts and SCS of H-2' and H-3' in the para-Series

DERIV	H-2'			H-3'			$\delta_{2'-3'}$			
X	(IV)	(V)	(VI)	(IV)	(V)	(VI)	(IV)	(V)	(VI)	
H	737.00	742.00	742.70	737.00	742.00	742.70	0	0	0	
p F	738.05	742.95	745.20	704.80	712.05	707.20	35.25	30.90	38.00	
p Cl	734.10	738.70	737.70	734.10	738.70	737.70	0	0	0	
p Br	728.10	734.25	733.55	749.15	759.30	751.45	-21.05	-25.02	-17.90	
p Me	727.35	730.05	743.95	717.35	722.25	719.85	10.05	7.80	15.10	SHIFTS
p OMe	730.60	734.10	738.10	687.70	692.65	690.00	42.55	41.45	48.10	
p NO_2	763.60	763.10	769.65	821.20	826.10	823.95	-57.60	-63.00	-56.30	
p CF_3	755.10	756.80	763.10	763.10	768.50	763.10	-8.00	-11.70	0	
p F	1.05	0.95	2.50	-32.20	-29.95	-35.50		-2	-30	
p Cl	-2.90	-3.30	-5.00	-2.90	-3.30	-5.00		-6	-2	
p Br	-8.90	-7.75	-9.15	12.15	17.30	8.75	LIT.[114]	-13	+22	
p Me	-9.65	-11.95	-7-75	-19.65	-19.75	-22.85		-9	-17	SCS
p OMe	-6.40	-7.90	-4.60	-49.30	-49.35	-52.70	VALUES	-9	-43	
p NO_2	22.60	21.10	26.95	84.20	84.10	81.25		+17	+95	
p CF_3	18.10	14.80	20.40	26.10	26.50	20.40	(CCl_4)	+20	+80	
								H-2	H-3	

affected by traces of moisture and are not readily related to conformational properties of the molecules. Although these compounds were dried over anhydrous sodium sulphate during the ether extraction stage of preparation, and subsequently vacuum distilled and dessicated, this was probably insufficient to remove all traces of water. The ^1H SCS for H_A, H_B and H_C are given in TABLE 4-4.2.

TABLE 4-4.3 shows the chemical shifts of the H-2' and H-3' pairs of aromatic protons for the symmetrical (para) members of the series. These shifts were derived by the approximate analysis of the AA'BB'-system as an AB-system. A similar techneque could not be applied to the ortho compounds whose aromatic protons form ABCD-systems. In all three series, the unsubstituted derivative (X = H) gave ^1H spectra of the aromatic region which approximated to singlets. The offsets of these lines were used for calculating the SCS data.

The SCS data given in TABLES 4-4.2 and 4-4.3 illustrate the effects of changing the aromatic substituent (X) within the three series, while TABLES 4-4.4 and 4-4.5 illustrate the effects of changing the side-chain substituent (Y) on going from the Type (IV) alcohols to the Type (V) fluorides and Type (VI) chlorides. The average Y. SCS, with standard deviations are appended.

TABLE 4-4.4 SCS of H_A and H_B Between the Type (IV) and Type (V) or Type (VI) Compounds

DERIV	H_A		H_B	
X	(V)-(IV)	(VI)-(IV)	(V)-(IV)	(VI)-(IV)
H	9.60	21.80	65.30	26.50
o F	4.70	12.85	58.35	20.95
o Cl	-1.15	3.50	59.80	34.45
o Br	-0.80	0.25	59.40	36.00
o Me	9.85	21.60	63.35	27.15
o OMe	0.05	8.00	75.00	45.75
o NO_2	2.85	-0.70	70.90	33.80
o CF_3	2.70	12.85	62.95	17.30
p F	12.40	21.60	64.80	24.20
p Cl	11.80	21.30	66.00	23.30
p Br	12.40	21.95	65.80	24.10
p Me	9.85	21.65	64.25	27.00
p OMe	11.40	22.05	64.30	27.65
p NO_2	11.00	18.30	61.85	16.25
p CF_3	11.75	21.20	65.65	22.05
Average o Y.SCS	3.48 ± 4.06	10.02 ± 8.26	64.38 ± 5.49	30.24 ± 8.53
Average p Y.SCS	11.28 ± 0.98	21.23 ± 1.14	64.74 ± 1.26	23.88 ± 3.41

TABLE 4-4.5 SCS of H-2' and H-3' Between the Type (IV) and Type (V) or Type (VI) Compounds

DERIV	H-2'		H-3'	
X	(V)-(IV)	(VI)-(IV)	(V)-(IV)	(VI)-(IV)
H	5.00	5.70	5.00	5.70
p F	4.90	7.15	7.25	2.40
p Cl	4.60	3.60	4.60	3.60
p Br	6.15	5.45	10.25	2.30
p Me	2.10	7.60	4.90	2.50
p OMe	3.50	7.50	4.95	2.30
p NO_2	3.50	10.05	4.90	2.75
p CF_3	1.70	8.00	4.60	0.00
Average	3.93	6.88	5.81	2.69
p Y.SCS	± 1.42	± 1.82	± 1.86	± 1.48

TABLE 4-4.6 H-X Shifts and SCS Data

DERIV	SHIFTS			SCS (X)			SCS (Y)	
X	(IV)	(V)	(VI)	(IV)	(V)	(VI)	(V)-(IV)	(VI)-(IV)
o Me	235.0	241.9	240.0				6.9	5.0
p Me	232.0	236.8	236.6	-3.0	-5.1	-3.4	4.8	4.6
o OMe	380.5	385.2	387.1				4.7	6.6
p OMe	377.2	381.1	380.4	-3.3	-4.1	-6.7	3.9	3.2

4-4-2 ^{19}F Chemical Shifts

^{19}F chemical shifts were referred to the absolute machine offset from the ^{2}H ($CDCl_3$) lock signal, in preference to using an internal ^{19}F reference such as $CFCl_3$. This system was chosen because the accurate coupling measurements performed necessitated the use of narrow spectral widths (300Hz or less), and since the ^{19}F shifts observed ranged over 12700 Hz, with some lines 18000 Hz from the standard $CFCl_3$ resonance, incorporation of an internal reference was impossible. The original "machine offsets" have been set relative to $CFCl_3$ by subtracting the machine offset of a 10% $CFCl_3$ in $CDCl_3$ solution ($CFCl_3$ = 45956.1 Hz - the other observed shifts lay in the range 31500-44200 Hz, ie. to high field of $CFCl_3$). In TABLES 4-4.7 and 4-4.8 the shifts are expressed in ppm (1ppm = 94.1 Hz).

TABLE 4-4.7 ^{19}F Chemical Shifts and SCS for the Type (V) Side-Chain Fluorines

DERIV X	SIDE CHAIN F	
	SHIFT	SCS
H	-174.003	/
o F	-182.709	-8.706
o Cl	-190.713	-16.710
o Br	-189.630	-15.627
o Me	-172.845	+1.158
o OMe	-192.552	-18.549
o NO_2	-190.013	-16.010
o CF_3	-182.094	-8.091
p F	-172.143	+1.860
p Cl	-173.824	+0.179
p Br	-174.215	-0.212
p Me	-172.530	+1.473
p OMe	-169.729	+4.724
p NO_2	-176.633	-2.630
p CF_3	-175.986	-1.983

TABLE 4-4.8 ^{19}F Chemical Shifts and SCS for the -F and $-CF_3$ Aromatic Ring Substituents in the Type (IV) and (V) Series

DERIV X	Offset		SCS		
	(IV)	(V)	(IV)	(V)	(IV)-(V)
o F	-118.305	-117.496			+0.809
p F	-112.956	-111.412	5.349	6.084	+1.544
o CF_3	-58.024	-58.003			+0.021
p CF_3	-63.191	-63.342	-5.167	-5.339	-0.151

4-4-3 ^{13}C Chemical Shifts

For reasons similar to those discussed in SECTION 4-4-2 it was impractical to use an internal TMS ^{13}C reference. Instead, all ^{13}C spectra were initially referred to the centre line of the $CDCl_3$ triplet and subsequently set relative to TMS ($CDCl_3$ = 77.009 ppm from TMS). This enabled minimum spectral widths of 2000Hz or 2500Hz (where X = F or OMe) to be used throughout, giving digitisation rates of 0.5 or 0.63 Hz.

Because of the high degree of electronegative substitution in the ethyl group, the C-1 and C-2 shifts were within a few ppm of the $CDCl_3$ resonance in all three series.

The shifts in the following tables have all been derived from data to three decimal places. TABLES 4-4.9 to 4-4.11 list the observed ^{13}C chemical shifts of the three series of compounds. Where appropriate the ^{13}C shift of the ring substituent has been recorded.

TABLE 4-4.9 ^{13}C Chemical Shifts of the Type (IV) Alcohols (from TMS)

X	C-1'	C-2'	C-3'	C-4'	C-5'	C-6'	C-1	C-2	C-X
H	137.34	127.08	128.46	128.71	128.46	127.08	78.76	76.38	
o F	124.81	159.87	115.37	130.44	124.38	128.51	73.13	75.35	
o Cl	135.08	132.14	129.42	129.90	127.07	128.78	74.93	75.07	
o Br	136.69	122.21	132.70	130.24	127.63	129.14	76.95	75.13	
o Me	135.91	135.77	130.61	128.70	126.31	126.37	75.21	76.08	19.49
o OMe	125.73	156.11	110.40	129.71	120.81	128.53	75.31	75.43	55.41
o NO_2	132.94	147.81	124.71	129.61	133.63	130.13	73.60	75.61	
o CF_3	136.14	127.90	125.91	128.98	132.12	128.86	74.01	75.82	124.13
p F	133.12	128.96	115.42	162.98			78.15	76.28	
p Cl	135.74	128.53	128.64	134.86			78.09	77.09	
p Br	136.28	128.82	131.61	123.07			78.16	75.98	
p Me	134.49	127.00	129.16	138.86			78.70	76.49	21.09
p OMe	129.51	128.37	113.88	159.04			78.46	76.53	55.26
p NO_2	144.20	128.26	123.49	148.17			77.67	75.50	
p CF_3	141.14	127.62	125.39	*			78.13	75.89	123.89

TABLE 4-4.10 ^{13}C Chemical Shifts of the Type (V) Fluorides (from TMS)

X	C-1'	C-2'	C-3'	C-4'	C-5'	C-6'	C-1	C-2	C-X
H	133.92	127.01	128.48	129.83	128.48	127.01	94.99	72.00	
o F	121.87	159.84	115.62	131.58	124.46	128.64	90.00	71.06	
o Cl	132.33	131.84	129.62	130.80	127.17	128.58	91.88	70.87	
o Br	133.91	121.41	132.84	131.06	127.73	128.89	93.74	70.93	
o Me	132.78	136.04	130.82	129.69	126.31	126.84	92.39	71.98	19.35
o OMe	123.04	155.92	110.43	130.61	120.78	127.80	91.36	71.38	55.50
o NO_2	130.45	146.79	125.01	130.45	134.02	129.61	90.85	71.51	
o CF_3	*	*	126.23	129.96	132.25	128.80	91.09	71.66	123.99
p F	129.68	129.17	115.57	163.58			94.33	71.83	
p Cl	132.27	128.55	128.74	135.93			94.23	71.65	
p Br	132.67	128.77	131.66	124.15			94.12	71.53	
p Me	130.95	127.02	129.16	139.88			94.99	72.08	21.26
p OMe	125.89	128.60	113.89	160.71			94.86	72.15	55.24
p NO_2	140.09	128.21	123.48	148.78			93.46	71.01	
p CF_3	137.47	127.62	125.43	130.25			94.04	71.40	123.78

* Of the 330 carbon resonances present in these 45 compounds, only 4 could not be detected. These signals (C-4'pCF_3(IV), C-1' and C-2'oCF_3(V) and C-4' pCF_3(VI)) were all split into quartets (or double-quartets when Y = F), by coupling to the nearby -CF_3 groups and could not be distinguished from the spectral noise. Unobtainable data is indicated by * in the following tables.

TABLE 4-4.11 ^{13}C Chemical Shifts of the Type (VI) Chlorides (from TMS)

X	C-1'	C-2'	C-3'	C-4'	C-5'	C-6'	C-1	C-2	C-X
H	135.67	128.48	128.51	129.52	128.51	128.48	67.20	74.55	
o F	123.58	159.76	115.66	131.25	124.52	130.07	60.74	73.64	
o Cl	133.84	133.84	129.69	130.54	127.31	130.25	63.66	73.59	
o Br	135.45	123.41	132.97	130.78	127.92	130.43	66.05	73.66	
o Me	135.01	135.94	130.73	129.24	126.67	127.67	63.45	74.41	19.56
o OMe	124.54	156.24	110.79	130.56	120.83	129.74	63.17	73.96	55.68
o NO_2	130.54	148.40	124.76	130.35	133.43	131.66	61.78	73.96	
o CF_3	135.42	128.98	126.02	129.49	132.50	129.75	64.24	73.87	123.81
p F	131.29	130.49	115.51	163.23			66.17	74.48	
p Cl	133.88	129.96	128.71	135.61			66.12	74.25	
p Br	134.38	130.22	131.68	123.81			66.17	74.14	
p Me	132.75	128.32	129.19	139.58			67.14	74.67	21.19
p OMe	127.62	129.77	113.87	160.42			66.94	74.81	55.30
p NO_2	141.77	129.97	123.24	148.38			65.24	73.63	
p CF_3	139.16	129.19	125.49	*			65.95	73.98	123.76

TABLES 4-4.12 to 4-4.14 list the SCS within the three series. The C-X data is unchanged as there are no suitable references. The usual convention of +ve shifts to low field of the X = H shift are used throughout.

TABLE 4-4.12 ^{13}C SCS of the Type (IV) Alcohols (Relative to X = H)

X	C-1'	C-2'	C-3'	C-4'	C-5'	C-6'	C-1	C-2	C-X
H	137.34	127.08	128.46	128.71	128.46	127.08	78.76	76.38	
o F	-12.53	+32.78	-13.09	+1.46	-4.08	+1.43	-5.69	-1.04	
o Cl	-2.27	+5.06	+0.95	+0.92	-1.40	+1.69	-3.82	-1.31	
o Br	-0.69	-4.87	+4.24	+1.53	-0.83	+2.06	-1.81	-1.25	
o Me	-1.44	+8.69	+2.15	-0.28	-2.15	-0.71	-3.54	-0.30	19.49
o OMe	-11.62	+29.03	-18.06	+1.00	-7.65	+1.45	-3.45	-0.95	55.41
o NO_2	-4.41	+20.73	-3.75	+0.63	+5.17	+3.05	-5.15	-0.78	
o CF_3	-1.20	+0.81	-2.55	0.00	+3.66	+1.78	-4.75	-0.57	124.13
p F	-4.22	+1.88	-13.04	+34.00			-0.61	-0.11	
p Cl	-1.58	+1.45	+0.18	+5.89			-0.67	-0.29	
p Br	-1.07	+1.74	+3.14	-5.91			-0.61	-0.41	
p Me	-2.86	-0.08	+0.70	+9.89			-0.06	+0.10	21.09
p OMe	-7.84	+1.29	-14.58	+31.06			-0.30	+0.15	55.26
p NO_2	+6.86	+1.18	-4.98	+19.19			-1.09	-0.88	
p CF_3	+3.80	+0.54	-3.08	*			-0.63	-0.49	123.89

TABLE 4-4.13 ^{13}C SCS of the Type (V) Fluorides (Relative to X = H)

X	C-1'	C-2'	C-3'	C-4'	C-5'	C-6'	C-1	C-2	C-X
H	133.92	127.01	128.48	129.83	128.48	127.01	94.99	72.00	
o F	-12.05	+32.75	-12.85	+1.75	-4.02	+1.54	-5.00	-0.94	
o Cl	-1.59	+4.75	+1.14	+0.97	-1.31	+1.49	-3.11	-1.13	
o Br	0.00	-5.68	+4.36	+1.23	-0.75	+1.79	-1.25	-1.07	
o Me	-1.14	+8.95	+2.35	-0.15	-2.17	-0.26	-2.60	-0.02	19.35
o OMe	-10.87	+28.83	-18.05	+0.79	-7.70	+0.70	-3.63	-0.62	55.50
o NO_2	-3.46	+18.31	-3.47	+0.62	+5.55	+2.51	-4.14	-0.49	
o CF_3	*	*	-2.25	+0.13	+3.78	+1.71	+3.90	-0.34	123.99
p F	-4.24	+2.08	-12.91	+33.75			-0.66	-0.17	
p Cl	-1.69	+1.45	+0.26	+6.10			-0.76	-0.35	
p Br	-1.24	+1.68	+3.19	-5.68			-0.78	-0.47	
p Me	-2.97	-0.07	+0.70	+10.05			-0.01	+0.09	21.26
p OMe	-8.03	+1.50	-14.59	+30.88			-0.13	+0.15	55.25
p NO_2	+6.18	+1.12	-5.00	+18.97			-1.54	-0.99	
p CF_3	+3.56	+0.53	-3.04	+0.43			-0.95	-0.60	123.78

TABLE 4-4.14 ^{13}C SCS of the Type (VI) Chlorides (Relative to X = H)

X	C-1'	C-2'	C-3'	C-4'	C-5'	C-6'	C-1	C-2	C-X
H	135.67	128.48	128.51	129.52	128.51	128.48	67.20	74.55	
o F	-12.08	+31.30	-12.85	+1.73	-3.99	+1.60	-6.46	-0.91	
o Cl	-1.82	+5.37	+1.18	+1.02	-1.21	+1.77	-3.33	-0.97	
o Br	-0.21	-5.06	+4.46	+1.26	-0.59	+1.95	-1.14	-0.90	
o Me	-0.64	+7.46	+2.22	-0.28	-1.84	-0.81	-3.74	-0.14	19.56
o OMe	-11.42	+27.77	-17.73	+1.04	-7.68	+1.27	-4.02	-0.59	55.68
o NO_2	-5.12	+19.93	-3.76	+0.83	+4.91	+3.19	-5.42	-0.59	
o CF_3	-0.24	+0.51	-2.49	-0.03	+3.99	+1.28	-4.96	-0.68	123.81
p F	-4.38	+2.02	-13.00	+33.71			-1.02	-0.08	
p Cl	-1.79	+1.49	+0.20	+6.09			-1.07	-0.30	
p Br	-1.29	+1.75	+3.17	-5.72			-1.03	-0.41	
p Me	-2.91	-0.16	+0.68	+10.06			-0.05	+0.12	21.19
p OMe	-8.04	+1.29	-14.64	+30.90			-0.26	+0.26	55.30
p NO_2	+6.10	+1.50	-4.97	+18.86			-1.96	-0.92	
p CF_3	+3.50	+0.72	-3.02	*			-1.24	-0.57	123.76

TABLE 4-4.15 is analogous to TABLES 4-4.4 & 4-4.5 in that it presents the ^{13}C SCS due to changing the side-chain substituent (Y) on going from the Type (IV) alcohols to the Type (V) fluorides and Type (VI) chlorides. Again, average Y.SCS with their standard deviations are appended.

TABLE 4-4.15 ^{13}C SCS of the Type (V) and Type (VI) Series Relative to the Type (IV) Series

DERIV	C-1'		C-2'		C-3'		C-4'		C-5'		C-6'		C-1		C-2		C-X	
X	(V)Y	(VI)Y	(V)Y	(VI)Y	(V)Y	(VI)Y	(V)Y	(VI)Y	(V)Y	(VI)Y	(V)Y	(VI)Y	(V)Y	(VI)Y	(V)Y	(VI)Y	(V)Y	(VI)Y
H	-3.43	-1.68	+0.01	+1,39	+0.02	+0.05	+1.13	+0.82	+0.02	+0.05	+0.01	+1 39	+16.24	-11.56	-4.39	-1.83		
o F	-2.94	-1.23	-0.03	-0.09	+0.26	+0.30	+1.13	+0.81	+0.08	+0.14	+0.12	+1.56	+16.87	-12.39	-4.29	-1.71		
o Cl	-2.75	-1.24	-0.30	+1.70	+0.20	+0.28	+0.90	+0.64	+0.10	+0.24	-0.19	+1 47	+16 95	-11.27	-4.20	-1.49		
o Br	-2.78	-1 24	-0.80	+1.20	+0.14	+0.27	+0.83	+0.55	+0.10	+0.29	-0.25	+1.29	+16.79	-10.90	-4.21	-1.48		
o Me	-3.13	-0.89	+0.27	+0.17	+0.22	+0.12	+0.99	+0.54	0.00	+0.36	+0.47	+1.30	+17.19	-11.76	-4.11	-1.67	-0.15	+0.08
o OMe	-2.69	-1.19	-0.19	+0.13	+0.03	+0.39	+0.91	+0.85	-0.03	+0.02	-0.74	+1.21	+16.05	-12.14	-4 05	-1.48	+0.09	+0.27
o NO_2	-2.49	-2.40	-1.02	+0.59	+0.30	+0.04	+0.84	+0.74	+0.39	-0.21	-0.52	+1.53	+17.25	-11.83	-4.10	-1.65		
o CF_3	*	-0.72	*	+1.09	+0.32	+0.11	+0.98	+0.51	+0.13	+0.36	-0.06	+0.89	+17.08	-11.77	-4.16	-1.95	-0.41	-0.32
p F	-3.44	-1.84	+0.21	+1.53	+0.15	+0.09	+0.60	+0.25					+16.18	-11.97	-4.45	-1.80		
p Cl	-3.47	-1.87	+0.02	+1.43	+0.10	+0.07	+1.07	+0.74					+16.07	-11.97	-4 33	-1.84		
p Br	-3 61	-1.90	-0.05	+1.40	+0.06	+0.07	+1.08	+0.73					+16.05	-11.99	-4.45	-1.83		
p Me	-3.54	-1.74	+0.02	+1.32	-0.01	+0.03	+1.02	+0.72					+16.28	-11.56	-4.40	-1.82	+0.18	+0.10
p OMe	-3.62	-1.88	+0.23	+1.40	+0.01	-0.01	+0.67	+0.38					+16.40	-11.52	-4.36	-1.72	-0.01	+0.04
p NO_2	-4.11	-2.44	-0.05	+1.71	0.00	+0.05	+0.61	+0.21					+15.78	-12.44	-4.49	-1.88		
p CF_3	-3.67	-1.98	0.00	+1.57	+0.05	+0.10	*	*					+15.91	-12.18	-4.50	-1.91	-0.11	-0.13
Average	-2.89	-1.32	-0.29	-0.77	-0.91	+0.20	+0.96	+0.68	+0.10	+0.16	-0.15	+1.33	+16.80	-11.70	-4.19	-1.66		
o Y.SCS	±0.29	±0.48	±0.42	±0.62	±0.11	±0.12	±0.11	±0.13	±0.12	±0.19	±0.35	±0.21	±0.41	±0.44	±0.10	±0.16		
Average	-3.61	-1.92	+0.05	+1.47	+0.05	+0.06	+0.88	+0.55					+16.11	-11.90	-4.42	-1.83		
p Y.SCS	±0.21	±0.22	±0.10	±0.12	±0.05	±0.03	±0.22	±0.24					±0.19	±0.31	±0.05	±0.05		

4-5 Coupling Constant Data

As in the previous section, the data is presented by class of coupling rather than by type of compound, since this facilitates comparison between compounds. Again, conformational discussion will be avoided as the immediate aim is merely to present a large amount of data in a compact, logical fashion.

TABLE 4-5.1 $^3J_{HH}$ Couplings Between the Side-Chain Protons H_A, H_B and H_C

DERIV	J_{AB} Coupling Constant			J_{AB} X.SCC Rel to H			J_{AB} Y.SCC Rel (IV)		J_{BC}
X	(IV)	(V)	(VI)	(IV)	(V)	(VI)	(V)-(IV)	(VI)-(IV)	WHERE SEEN
H	5.35	5.40	5.90				+0.05	+0.55	3.95
o F	4.50	5.10	6.15	-0.85	-0.30	+0.25	+0.60	+1.65	4.50
o Cl	3.20	3.30	5.25	-2.15	-2.10	-0.65	+0.10	+2.05	4.30
o Br	3.00	3.05	5.05	-2.35	-2.35	-0.85	+0.05	+2.05	
o Me	6.00	6.35	7.40	+0.65	+0.95	+1.50	+0.35	+1.40	3.50
o OMe	4.10	3.40	5.50	-1.25	-2.00	-0.40	-0.70	+1.40	6.50
o NO_2	2.85	2.00	4.15	-2.50	-3.40	-1.75	-0.85	+1.40	
o CF_3	4.00	3.70	6.40	-1.35	-1.70	+0.50	-0.30	+2.40	
p F	5.50	5.40	5.50	+0.15	0.00	-0.40	-0.10	0.00	
p Cl	5.30	5.25	5.50	-0.05	-0.15	-0.40	-0.05	+0.20	
p Br	5.30	5.20	5.40	-0.05	-0.20	-0.50	-0.10	+0.10	
p Me	5.50	5.50	5.80	+0.15	+0.10	-0.10	0.00	+0.30	
p OMe	5.50	5.70	5.80	+0.15	+0.30	-0.10	+0.20	+0.30	3.50
p NO_2	4.90	4.60	5.25	-0.45	-0.80	-0.65	-0.30	+0.35	
p CF_3	5.15	5.00	5.50	-0.20	-0.40	-0.40	-0.15	+0.35	

4-5-1 $^{3}J_{HH}$ Coupling Constants

For the side-chain protons H_A, H_B (and H_C) the $^{3}J_{HH}$ couplings could be readily measured from the spectra to an accuracy of ±0.1Hz. These couplings and the equivalent of the SCS, the "substituent coupling constants" are given in TABLE 4-5.1. Similar information was also recorded for the aromatic protons H-2' and H-3' in the three sets of para derivatives (see TABLE 4-5.2) but because of the approximate nature of the AA'BB' analysis, the errors in measurement of the $^{3}J_{HH}$ couplings are probably larger eg. ±0.2Hz.

These coupling constants are only listed for completeness. J's marked "unknown" could not be determined because the aromatic proton signals had collapsed to broadened singlets.

TABLE 4-5.2 $^{3}J_{HH}$ Couplings Between H-2 and H-3 in the Para Derivatives of (IV), (V) and (VI)

DERIV X	$^{3}J_{HH}$ H-2' and H-3' (IV)	(V)	(VI)
F	8.6	8.8	8.6
Cl	unknown	unknown	unknown
Br	8.5	8.75	8.7
Me	8.5	8.6	8.55
OMe	8.85	8.7	8.7
NO_2	8.9	9.0	8.8
CF_3	8.5	8.6	unknown

4-5-2 $^{2}J_{HF}$ and $^{3}J_{HF}$ Couplings from the Type (V) Fluorides

These couplings were derived by the ABX analytical method detailed in SECTION 4-3 and are probably accurate to ±0.1Hz. In one case only (pF(V)),

TABLE 4-5.3 $^{n}J_{CF}$ Coupling Data for the ABX Analysis of the Type (V) Fluorides

DERIV X	$^{2}J_{HF} = J_{BX}$		$^{3}J_{HF} = J_{AX}$		$^{3}J_{HH} = J_{AB}$		$\Sigma(J_{AB} + J_{AX})$		Other $^{n}J_{HF}$
	J_{BX}	Rel to H	J_{AX}	Rel to H	J_{AB}	Rel to H	Σ	Rel to H	
H	44.75		9.75		5.40		15.15		
o F	44.35	-0.40	12.15	+2.40	5.10	-0.30	17.25	+2.10	
o Cl	44.75	0.00	17.00	+7.25	3.30	-2.10	20.30	+5.15	
o Br	44.65	-0.10	17.65	+7.90	3.05	-2.35	20.70	+5.55	
o Me	45.25	+0.50	9.85	+0.10	6.35	+0.95	16.20	+1.05	1.0 $^{5}J_{H_{Me}F}$
o OMe	45.00	+0.25	17.80	+8.05	3.40	-2.00	21.20	+6.05	
o NO_2	45.80	+1.05	19.40	+9.65	2.00	-3.40	21.40	+6.25	
o CF_3	44.70	-0.05	16.30	+6.55	3.70	-1.70	20.00	+4.85	
p F	44.95	+0.20	9.25	-0.50	5.40	0.00	14.65	-0.50	0.85 $^{4}J_{H_2',F_1}$
p Cl	44.75	0.00	9.55	-0.20	5.25	-0.15	14.80	-0.35	
p Br	44.70	-0.05	9.60	-0.15	5.20	-0.20	14.80	-0.35	
p Me	44.90	+0.15	9.45	-0.30	5.50	+0.10	14.95	-0.20	1.3 $^{7}J_{H_{Me}F}$
p OMe	45.10	+0.35	8.60	-1.15	5.70	+0.30	14.30	-0.85	
p NO_2	44.35	-0.40	10.75	+1.00	4.60	-0.80	15.35	+0.20	
p CF_3	45.00	+0.25	9.90	+0.15	5.00	-0.40	14.90	+0.25	

$^4J_{HF}$ couplings were observed between the two H-2' protons and the side-chain fluorine. As there was also a $^6J_{FF}$ coupling, the expected 4 line X region of the ABX system became a 24 line X region in an ABM_2XZ system. The two ^{19}F signals of the pF(V) fluoride are reproduced in FIG.4-5.1. N.B. Through space $^nJ_{HF}$'s of 0.3Hz were also observed in oF(VI)$\left[^5J_{H_AF}\right]$ and oCF_3(VI)$\left[^6J_{H_AF}\right]$.

4-5-3 $^nJ_{CF}$ Couplings - Observed in the ^{13}C Spectra

TABLE 4-5.4 $^nJ_{CF}$ Couplings Involving the -F and -CF_3 Ring Substituents

DERIV	C-1'			C-2'			C-3'		
X	(IV)	(V)	(VI)	(IV)	(V)	(VI)	(IV)	(V)	(VI)
o F	12.8	12.55	12.6	246.8	248.3	249.3	21.4	21.0	21.7
o CF_3	1.5	*	1.5	30.3	*	31.1	5.8	5.7	5.7
p F	2.4	3.2	3.5	8.1	8.45	8.5	21.8	21.9	22.2
p CF_3	1.5	1.5	~1.3	0	0	0	3.8	3.7	3.8
DERIV	C-4'			C-5'			C-6'		
X	(IV)	(V)	(VI)	(IV)	(V)	(VI)	(IV)	(V)	(VI)
o F	8.7	8.45	8.9	3.7	3.7	3.5	3.6	3.05	3.7
o CF_3	0	0	0	0.8	1.0	0.8	0	0	0
p F	247.6	249.6	249.5						
p CF_3	*	33.1	*						
DERIV	C-1			C-2			C-X		
X	(IV)	(V)	(VI)	(IV)	(V)	(VI)	(IV)	(V)	(VI)
o F	1.8	1.9	2.2	2.6	2.55	2.8			
o CF_3	2.2	2.5	2.5	1.6	1.7	0	274.0	273.5	274.0
p F	0	0	0	1.6	1.3	1.1			
p CF_3	0	0	0	0	0	0	272.2	272.5	273.5

Since these J's were measured from the ^{13}C spectra they are subject to an error of $\pm$0.5Hz. In practice, however, observed errors are normally $\pm$0.3Hz, as estimated from the $CDCl_3$ $^1J_{C^2H}$ couplings.

In the Type (V) series the side-chain fluorine showed coupling to all the carbons apart from those meta to the side-chain (ie. C-3' and C-5'). The only exception to this occurred in the oNO_2 derivative which possessed a $^4J_{CF}$ coupling to C-5' of 1.6Hz. The remaining couplings are listed in TABLE 4-5.5.

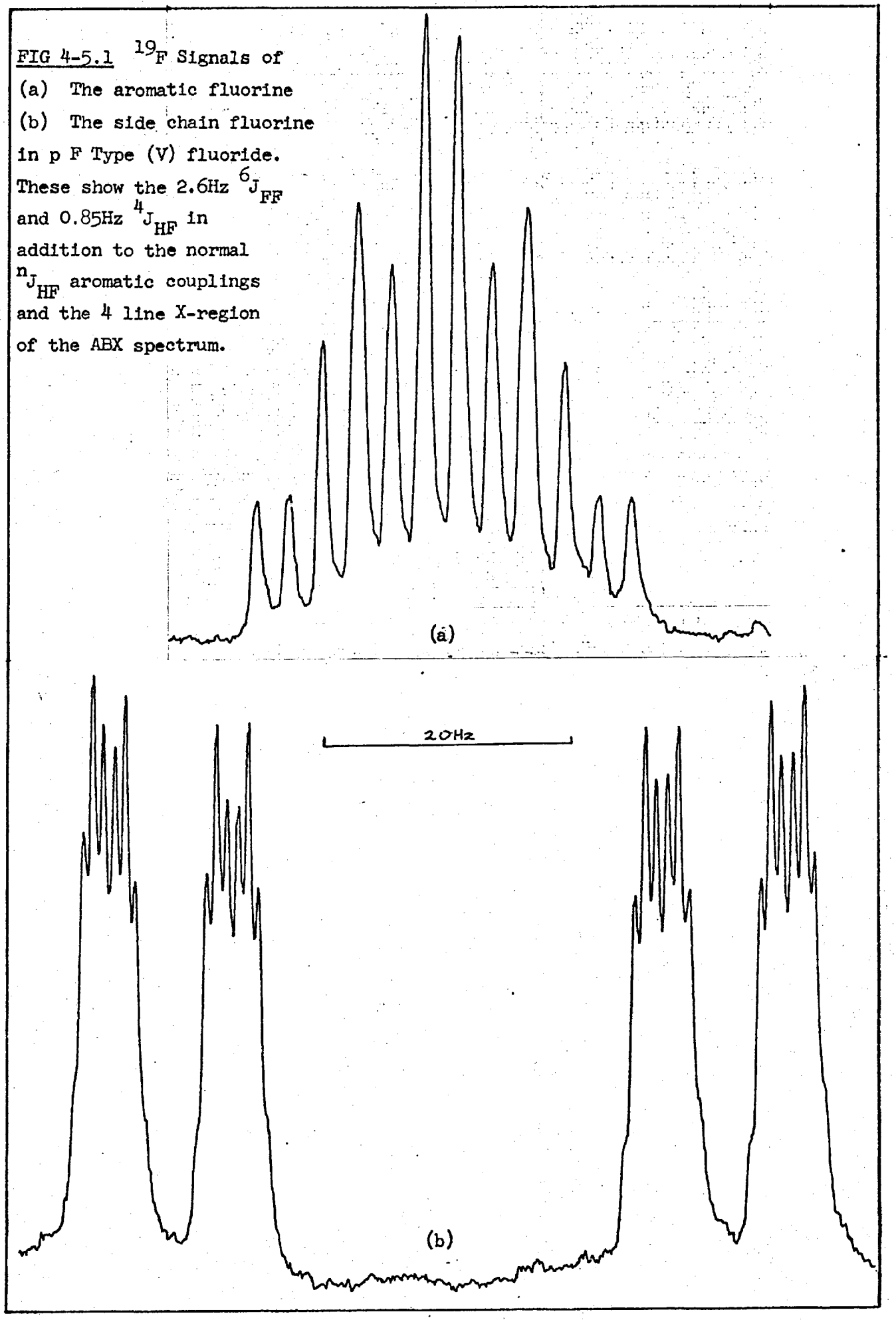


FIG 4-5.1 ^{19}F Signals of
(a) The aromatic fluorine
(b) The side chain fluorine
in p F Type (V) fluoride.
These show the 2.6Hz $^{6}J_{FF}$
and 0.85Hz $^{4}J_{HF}$ in
addition to the normal
$^{n}J_{HF}$ aromatic couplings
and the 4 line X-region
of the ABX spectrum.

TABLE 4-5.5 $^{n}J_{CF}$ Couplings Involving the Side Chain Fluorine in the Type (V) Fluorides.

DERIV	C-1'		C-2'		C-4'		C-6'		C-1		C-2	
X	J	ΔJ	J	ΔJ	J	ΔJ	J	ΔJ	J	ΔJ	J	ΔJ
H	20.7		6.6		1.8		6.6		186.8		32.5	
o F	21.95	1.25	5.6	-1.0	1.45	-0.35	6.95	+0.35	187.5	+0.7	30.05	-2.45
o Cl	22.3	1.6	5.7	-0.9	1.2	-0.6	9.0	+2.4	188.9	+2.1	26.7	-5.8
o Br	22.5	1.8	5.8	-0.8	1.0	-0.8	9.5	+2.9	189.5	+2.7	26.4	-6.1
o Me	19.5	-1.2	5.0	-1.6	2.0	+0.2	7.4	+0.8	185.5	-1.3	32.5	0
o OMe	21.2	0.5	5.5	-1.1	1.2	-0.6	9.4	+2.8	186.4	-0.4	26.5	-6.0
o NO_2	22.0	1.3	3.6	-3.0	0.9	-0.9	13.6	+7.0	189.8	+3.0	24.7	-7.8
o CF_3	*	/	*	/	1.8	0	9.1	+2.5	187.9	+1.1	27.6	-4.9
p F	21.2	0.5	6.65	+0.05	1.9	+0.1	6.65	+0.05	187.0	+0.2	33.1	+0.6
p Cl	21.3	0.6	6.8	+0.3	1.8	0	6.8	+0.2	187.5	+0.7	32.5	0
p Br	21.0	0.3	6.5	-0.1	2.0	+0.2	6.5	-0.1	187.5	+0.7	32.5	0
p Me	21.0	0.3	6.4	-0.2	1.5	-0.3	6.4	-0.2	186.4	-0.4	33.1	+0.6
p OMe	21.3	0.6	6.3	-0.3	1.0	-0.8	6.3	-0.3	186.0	-0.8	34.4	+1.9
p NO_2	21.0	0.3	7.2	+0.6	1.3	-0.5	7.2	+0.6	189.4	+2.6	31.5	-1.0
p CF_3	21.0	0.3	7.0	+0.4	2.0	+0.2	7.0	+0.4	188.4	+1.6	31.7	-0.8

4-5-4 $^{n}J_{FF}$ Couplings in the Type (V) Fluorides

TABLE 4-5.6 $^{n}J_{FF}$ Couplings in the Type (V) Fluorides

DERIV	oF	oCF_3	pF	pCF_3
$^{n}J_{FF}$	1.4	2.6	2.6	1.0
No.bonds	4	5	6	7

Although these couplings were taken from FT ^{19}F spectra, small spectral widths and therefore small digitisation rates were used. The errore should therefore be small eg. $\pm$0.1Hz.

The large $^{5}J_{FF}$ coupling in the oCF_3(V) fluoride is probably a good example of "through space" rather than "through bond" coupling.

4-5-5 Verification of the ^{13}C Assignments of C-1 and C-2 in the Type (IV) Alcohols

A preliminary analysis of the Eu(fod-d_9)$_3$ induced shifts of the Type (IV) alcohols indicated that the assignments of C-1 and C-2 in the oCl and oOMe derivatives might be incorrect (these signals are only separated by 0.139 and 0.124 ppm respectively). This was also suggested by the relative intensities of the signals compared to those in the other Type (IV) alcohols.

A check, using $^{13}C[^{1}H\text{-GD}]$ spectra (see SECTION 4-1) comfirmed the deductions made from the LIS data, as the $^{1}J_{CH}$ couplings were characteristic for the two carbons. The data is given in TABLE 4-5.7, using the correct assignments.

TABLE 4-5.7 Data Used for Verifying the ^{13}C Type (IV) Spectral Assignments

DERIV X	Data from 'Gated Dec.' Expt.				Ht Ratio C-1/C-2
	$^1J_{HC-1}$	$^1J_{HC-2}$	$^2J_{H_1C_2}$	Ht Ratio C-1/C-2	
H	147.9	179.2	3.45	0.56	1.32
o F	147.8	180.0	1.7	0.90	1.40
o Cl	150.8	179.2	2.7	0.68	1.13
o Br	150.4	178.1	b	0.68	1.47
o Me	148.0	178.3	3.8	0.83	1.27
o OMe	149.8	178.9	3.7	0.78	1.15
o NO_2	150.0	180.7	2.0	0.80	1.10
o CF_3	149.0	178.8	1.5	0.73	1.35
p F	148.6	178.0	b	1.05	1.76
p Cl	148.6	178.5	2.85	0.58	1.25
p Br	148.9	179.0	2.9	0.78	1.16
p Me	147.6	175.8	3.5	0.84	1.02
p OMe	148.3	175.9	3.45	1.00	1.33
p NO_2	149.6	178.5	b	0.57	0.94
p CF_3	148.6	178.3	2.05	0.60	1.57
Average	149.2	178.3			
Std.Dev	±1.6	±2.5			

Because of complex splitting patterns, the J's given in this table are likely to have errors of ±1.0Hz.

b - indicates unresolved coupling - only broadening observed.

4-5-6 Attempts at Obtaining $^3J_{H_BC_2}$ Couplings in the Type (IV) Alcohols

FIG.4-4.1 shows that determination of the $^3J_{H_BC_2}$ coupling should give some indication of the conformation about the C-1/C-1' bond. Unfortunately this information cannot be derived directly from the gated decoupled ^{13}C spectrum as the C-2' signal shows couplings to all the aromatic protons as well as the side-chain protons. Obviously what is required is a high resolution ^{13}C spectrum with selective decoupling of the aromatic protons.

Since some related work - ^{13}C assignment by single frequency ^1H decoupling of ^{13}C spectra - had been successfully performed by M. Mednejad[143] on the same instrument, it was thought that recording selective broad band ^1H decoupled ^{13}C would be straightforward. However this was not the case, for it was found impossible to irradiate the aromatic protons without giving off-resonance (partial decoupling) effects to the remainder of the $^nJ_{CH}$ couplings.

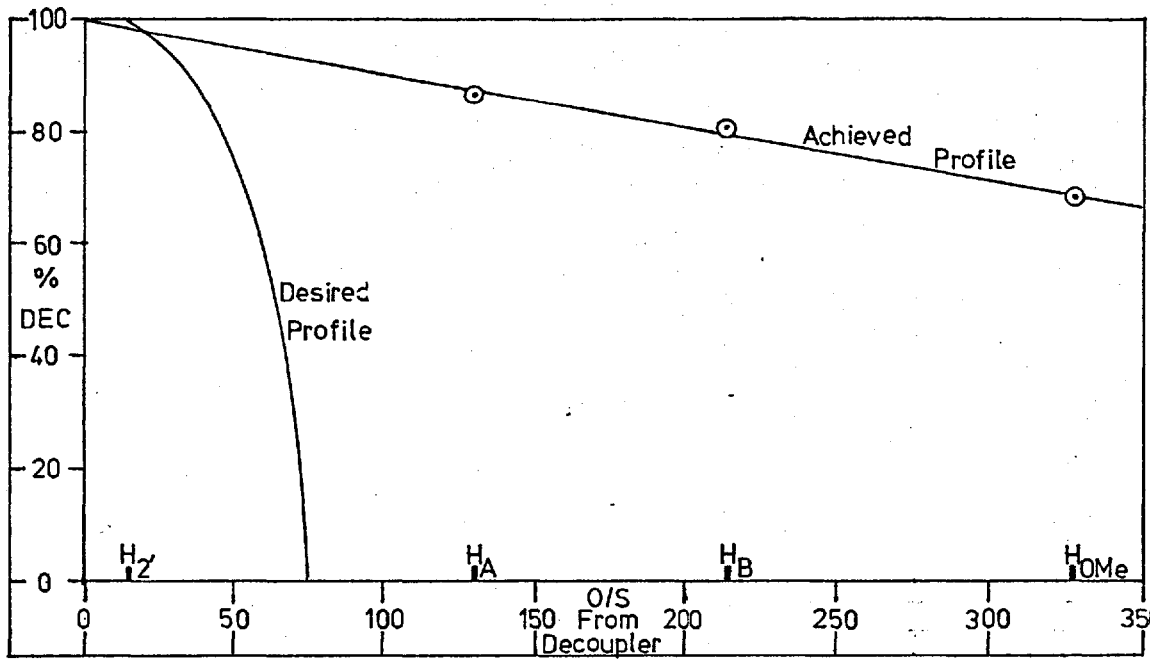
The pOMe Type (IV) alcohol was chosen as a model, because the C-2' and C-3' resonances were well separated. Spectral accumulation times were very long (24 hrs instead of 4 hrs) to compensate for the loss of NOE. In all the partially decoupled spectrum was attempted four times - initially with a 100Hz noise decoupled band at 10W power, and finally using single frequency decoupling

at 0.17W power. Even with this very weak localised decoupling, 70% decoupling efficiency was observed in $^{1}J_{CH}$ couplings whose protons lay 327Hz from the frequency being irradiated (see TABLE 4-5.8 and FIG.4-5.2).

Coupling	$^{1}J_{CH}$		% Decoupled	Distance ^{1}H from Dec.
	NORMAL	DEC		
C-2/H_A	148.5	19.8	86.7	130 Hz
C-1/H_B	176.5	34.9	80.2	216 Hz
C-X/H_{OMe}	144.1	46.4	67.8	327 Hz

TABLE 4-5.8 Extent of Decoupling 'Spillage' from Single Frequency Low Power Irradiation.

FIG.4-5.2 Desired vs. Achieved ^{1}H Decoupling Profile for Selective Decoupling



From FIG.4-5.2 it is obvious that even if better decoupling control could be achieved, there would undoubtedly be a degree of partial decoupling of the desired $^{3}J_{CH}$ couplings which would render them useless.

The successful use of single frequency decoupling in the earlier work[143] may be attributed to the criterion applied. In that exercise, "success" entailed the assignment of a ^{13}C signal by significantly diminishing its $^{1}J_{CH}$ coupling, the magnitude of the lesser affected coupling constants being unimportant, whereas in this study the magnitudes of the remaining couplings are critical.

4-5-7 Temperature Effects in ^{1}H Spectra of the Type (IV) Alcohols.

To facilitate the recording of low temperature (-50°C) spectra a 1:1 $CDCl_3/CFCl_3$ solvent mixture was used. The low temperature spectra showed that J_{AB} remained unchanged whilst significant chemical shift changes occured. Typical temperature induced shifts (for pMe(IV)) are shown in FIG.4-5.3 and

TABLE 4-5.9 Significance of ^{1}H Temperature Shifts.

H	Rate Hz/°C	Change in 5°C	% Error in LIS
H-2	0.13	0.65	1.25
H-3	0.04	0.20	1.30
H_A	0.25	1.25	2.00
H_B	0.34	1.70	1.65
H_C	3.40	17.00	4.25
OMe	0.01	0.05	0.50

summarised in TABLE 4-5.9. The major conclusion that may be drawn from this data is that the conformational preferences of the side-chain, as monitored by J_{AB}, appear to be insensitive to a lowering of the temperature by 75°C (ie. either a single conformation is significantly occupied at room temperature or no preferences exist over the temperature range studied).

A secondary motive in performing this experiment was that the spectrometer was overhauled between recording the spectra of the Type (IV) alcohols with and without shift reagent, and the changes in the magnet cooling system may have altered the ambient probe temperature by up to 5°C (although 1-2°C was more likely). The data in TABLE 4-5.9 clearly shows that any temperature induced errors in the LIS data would be very small (<2%). H_C was not used in the shift study, and a glance at its remarkable temperature dependence is sufficient to discount its SCS data as a source of conformational information.

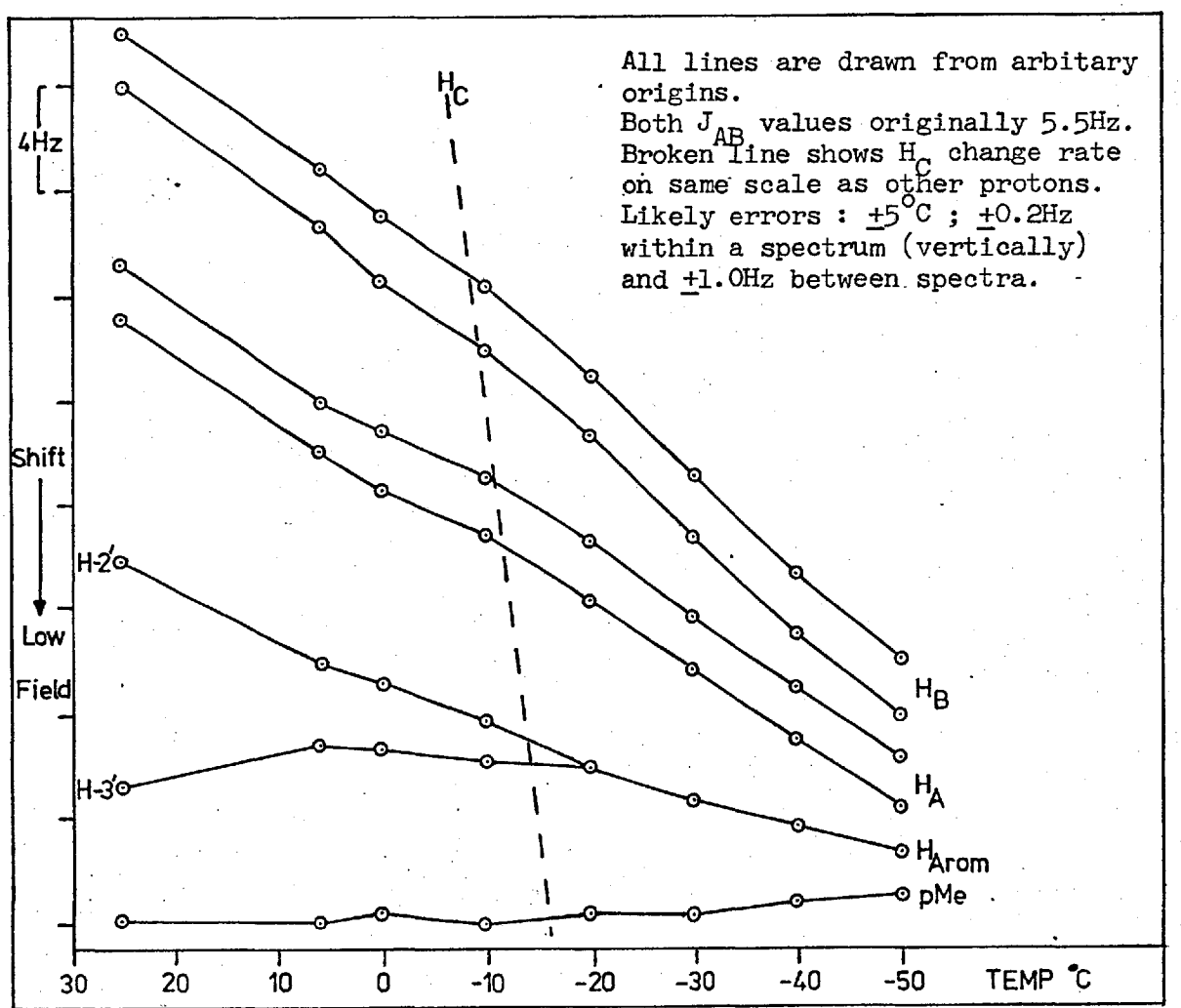


FIG.4-5.3 Variation of ^{1}H Shifts in pMe(IV) on Lowering the Temperature.

4-6 Parameters Governing Substituent Effects.

Several substituent properties, for example, steric size, electronegativity, ability to participate in resonance hibridization, etc., combine together to define the "substituent effects" observed in all aspects of organic chemistry.

TABLE 4-6.1 Parameters Governing Substituent Effects

SUB^{NT} X	σ_p ($\sigma_I + \sigma_R$)	σ_m (σ_I)	TAFT σ_I	TAFT σ_R	I & R EFFECTS	HUGGINS $E^{neg.}$ 1.14	ΔE^{neg} $E_X - E_H$
OMe	-0.268 ±0.02	0.115 ±0.02	0.23	-0.50	-I +R	3.50	1.3
Me	-0.170 ±0.02	-0.069 ±0.02	-0.05	-0.12	+I +R	2.50	0.3
H	0	0	0	0	/ /	2.20	0
F	0.062 ±0.02	0.337 ±0.02	0.50	-0.44	-I +R	3.95	1.75
Cl	0.227 ±0.02	0.373 ±0.02	0.47	-0.24	-I +R	3.20	1.0
Br	0.233 ±0.02	0.391 ±0.02	0.45	-0.22	-I +R	3.00	0.8
CF_3	0.54 ±0.10	0.43 ±0.10	0.42	0.12	-I -R	3.40	1.2
NO_2	0.778 ±0.02	0.710 ±0.02	0.63	0.15	-I -R	3.35	1.15
ø						3.0	0.8
OH						3.50	1.3

One of the more useful gauges of these effects, the Hammett Substituent Parameters (σ_m and σ_p),[248,249] are listed in TABLE 4-6.1. These parameters provide a measure of the total electronic influence of the various substituents, independent of any steric or conjugative effects, since they are derived from the linear free energy relationships between meta- and para- benzoic acid dissociation equilibrium constants :

$$\log K_X/K_H = \rho\sigma_X \qquad \text{EQN.66}$$

Where K_X is the dissociation equilibrium constant for the m- or p- substitituted benzoic acid; K_H is the dissociation equilibrium constant for the unsubstituted benzoic acid; ρ is defined as 1.00 for benzoic acid and may vary from -6 to +4 for other equilibria; σ_X is the Hammett Substituent parameter for the meta (σ_m) or para (σ_p) substituent.

σ_m is mainly a measure of polar (inductive) effects, and combines both inductive and resonance effects (these have been isolated by Taft[250] and are given in TABLE 4-6.1 as σ_I and σ_R). A large range of Hammett/Taft type parameters eg. σ_m, σ_p, σ_p^+, σ_p^-, σ^*, σ^o, σ_I, σ_R, σ', etc., have been generated in the literature (249) from substrates in which various other interactions, such as charge stabilisation by direct conjugation, can occur. Although correlation between some of these parameters and nmr chemical shifts are well

known (eg. 128,251) they will be used here only to establish general trends of similarities and differences. It is felt that more information than is available from these three series of compounds would be required to make any more constructive use of these parameters.

Huggin's Electronegativities (E_X - the list in TABLE 4-6.1 is from ref. 114) have also been correlated with certain ^{13}C chemical shifts,[252] but no such correlations were found in these series. Their relationships to coupling constants are, however, well established (see SECTION 1-5-1) and they will be used in this context later in this section.

4-7 Interpretation of the Chemical Shift Data

The first and obvious observations to make on the chemical shift data, are the similarities between the three series, especially between the para derivatives. In the ortho series differences are more apparent but in virtually every instance trends between the individual derivatives mirror those in the other series. This is illustrated for the ^1H data in FIGS.4-7.1 & 4-7.2 which essentially present the data given in TABLES 4-4.1 to 4-4.5. The scales of the plots should be noted as these vary considerably. Hence H_A, which is further away from the ring substituents than H_B, responds in a broadly similar manner to varying the ring substituent X, but at about half the scale (see FIG.4-7.1(a) & (b)).

The relative shifts of the Y SCS data (see FIG.4-7.1(c) & (d)) are, of course, dominated by the proximity of H_A and H_B to the side-chain substituent Y. The near linearity of the para Y SCS demonstrate that the "pure" through bond electronic effects of the X substituents are virtually independent of the nature of Y. The erratic nature of the variation in the ortho Y SCS, which should contain a similar, though probably stronger, electronic component to the corresponding para Y SCS (assuming a similar conformation), demonstrates the steric effects of the ortho substituent, which are not independent of Y, especially in the case of H_B which is adjacent to Y. Since the changes in the shifts of H_A and H_B on going from ortho to para X could arise from at least three interactions, their interpretation is not straightforward, ie :

1) Conformation changed; through bond electronic effect of X modified.

2) Conformation changed; local electronic effects (eg. of $CHCl_2$ on H_B) modified.

3) Direct through space shielding of the side-chain by X possible in ortho derivatives.

The para H-2' and H-3' data (shown in FIG.4-7.2) are dominated by the proximity of the protons to the substituent X. When the expanded scale of plots (c) and (d), and the likely error of $\pm$1.0Hz for the Y SCS, are taken

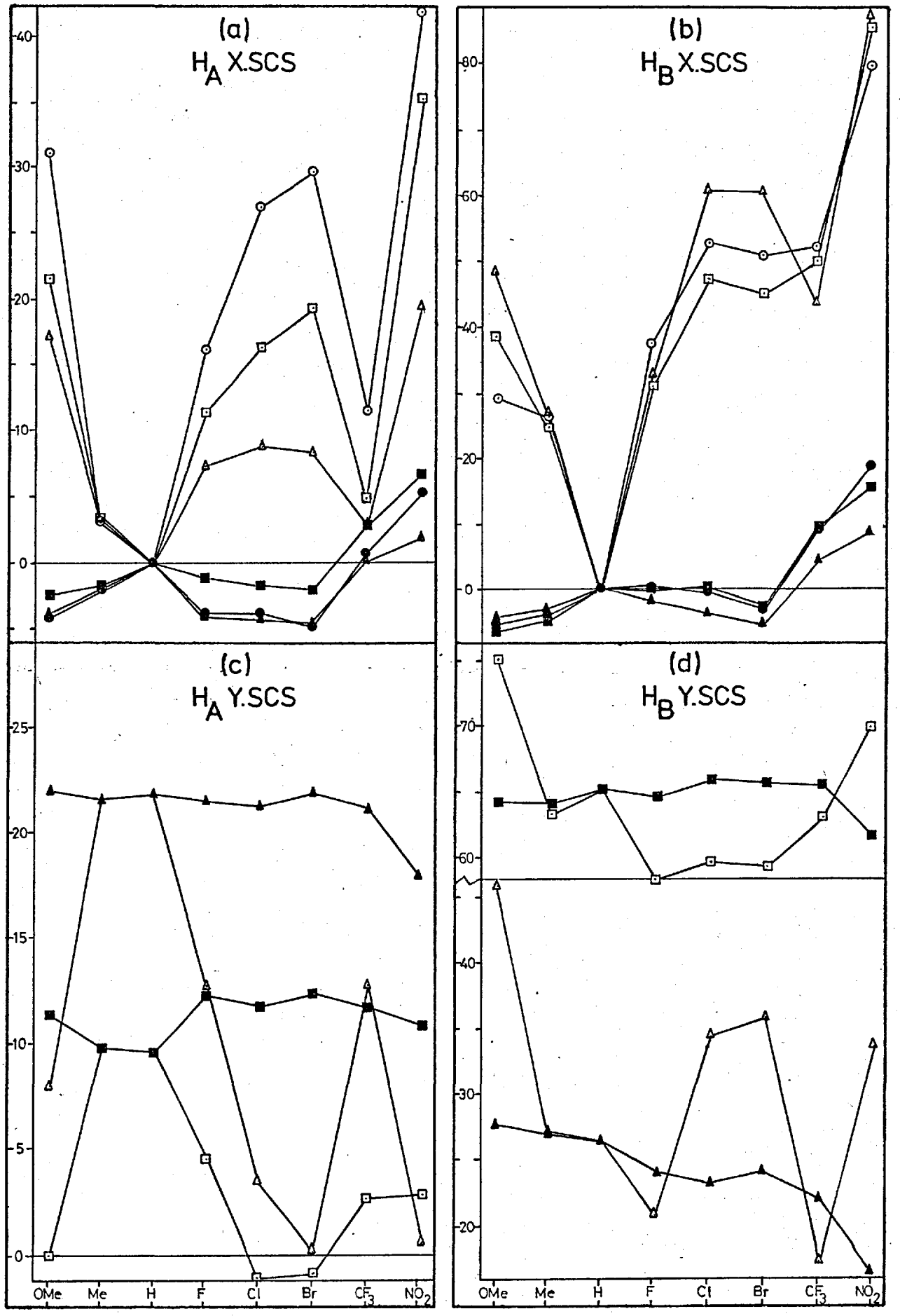


FIG.4-7.1 X & Y.SCS of H_A & H_B. Key: o/● = o/p(IV); □/■ = o/p(V); △/▲ = o/p(VI).

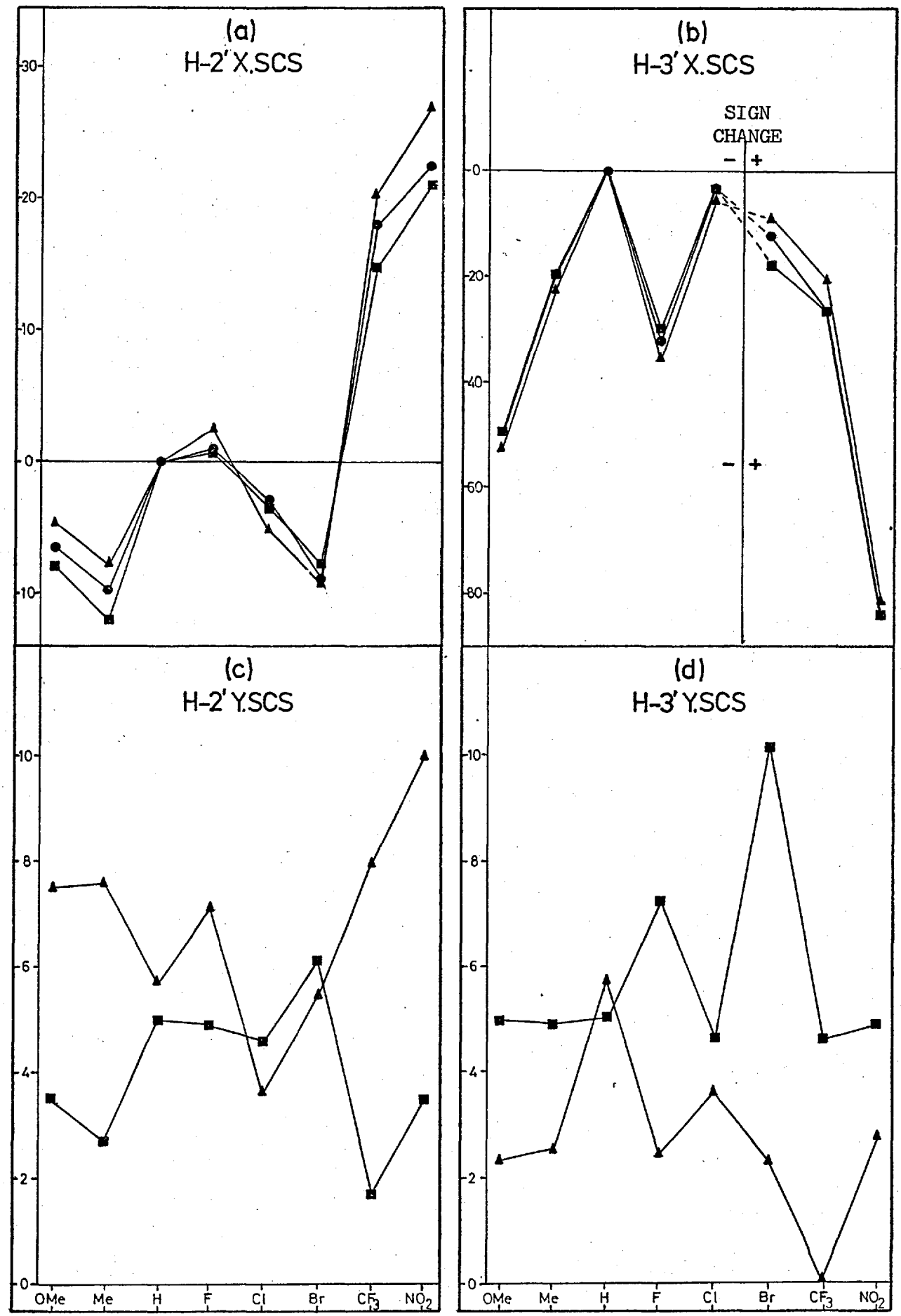


FIG.4-7.2 X & Y.SCS of H-2' & H-3'. Key as for FIG.4-7.1 (para data only)

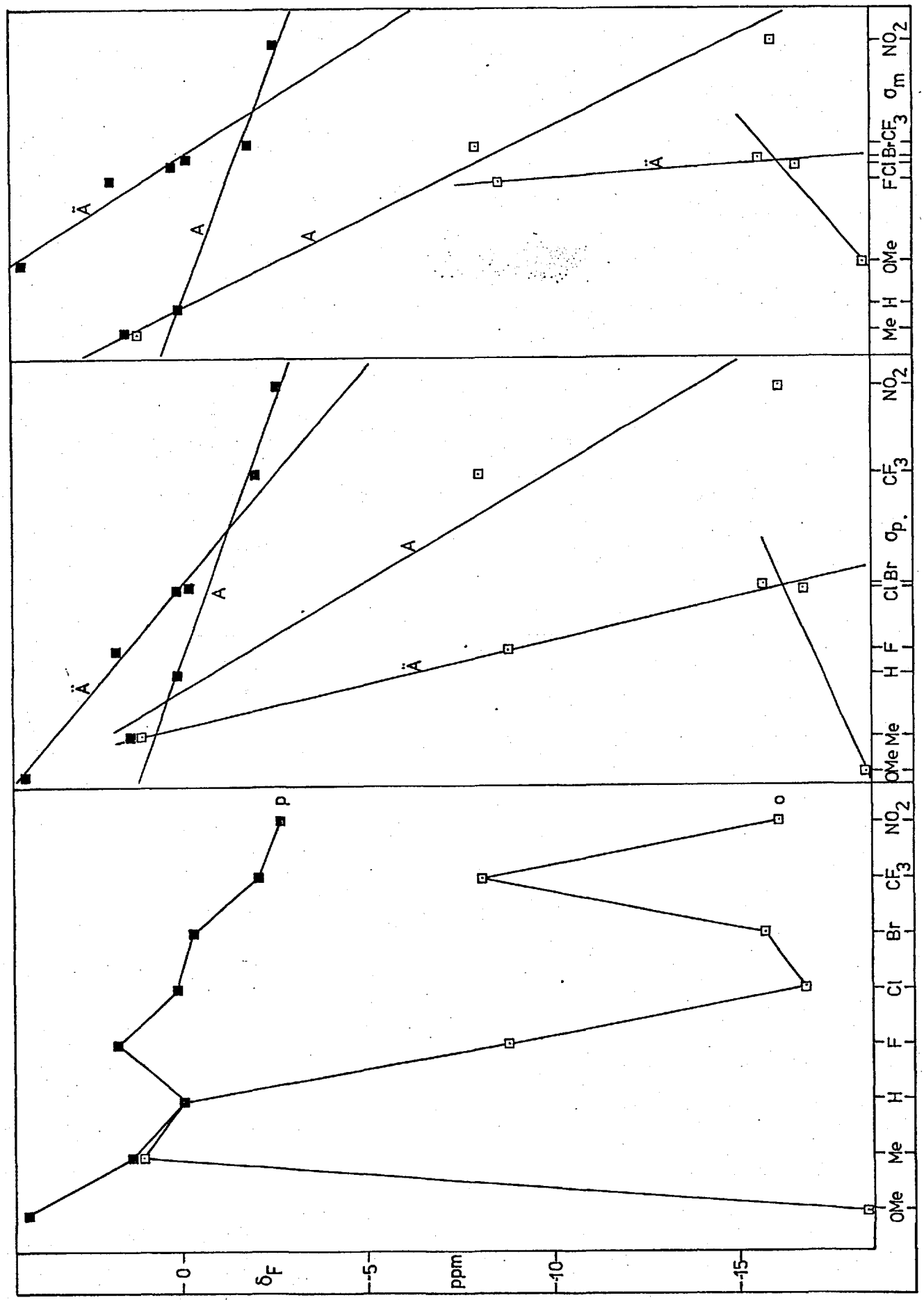


FIG.4-7.3 Type (V) Series Side-Chain ^{19}F SCS vs. Hammett σ_p and σ_m:

into account, the scatter of the Y SCS data is relatively small.

The side-chain ^{19}F SCS of the Type (V) compounds, and their relationship to Hammett's σ_p and σ_m are plotted in FIG.4-7.3. Again the changes in the para SCS are fairly small and "well behaved" when compared to the ortho SCS. The para data shows good correlation to σ_p and reasonable correlation to σ_m, provided the substituents are split into two groups.

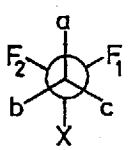
1) Those with lone-pair electrons eg. F, Cl, Br, OMe (also NR_2, OH, etc.), labelled A.[252]

2) Those without lone-pair electron eg. H, Me, CF_3, NO_2 (also CN, COMe etc.), labelled A.[252] (Although Me can behave as a "pseudo lone-pair donor" via hyperconjugation there is little evidence of this here).

This agrees with some of the findings of Inamoto et al[252] and is a recurrent trend throughout the ^{13}C SCS data. There is little correlation between the ortho SCS and either Hammett parameter (the F-Cl-Br apparent linearity is more a function of the closeness of the Hammett parameters than a property of the SCS data) apart from the A series with σ_m. This may, however, be purely coincidental since any changes in the side-chain conformation could have little effect on the ^{19}F chemical shift.

Phillips and Wray, as part of a series of papers on the structural dependence of the inductive effect, examined vicinal substituent effects on ^{19}F chemical shifts.[253,254] The difference in shielding between the two fluorines in the fixed conformation molecule $CF_2X.Cabc$ (see FIG.4-7.4) was considered[254] to be dependent only on the angular primary and secondary vicinal delocalisation interactions.[253]

FIG.4-7.4



Thus ΔF_1F_2 could be defined by EQN.67 :

$$\Delta F_1F_2 = E_FE_ck_{c1}(\cos180^\circ - \cos60^\circ) + E_FE_bk_{b1}(\cos60^\circ - \cos180^\circ) + E_FE_bk_{b2}(\cos180^\circ - \cos60^\circ) + E_FE_ck_{c2}(\cos60^\circ - \cos180^\circ) \quad \text{EQN.67}$$

$$= \tfrac{3}{2}E_F(E_B(K_{b1} - K_{b2}) + E_C(K_{c2} - K_{c1})) \quad \text{EQN.68}$$

If b and c are both halogens then $K_{b1} = K_{c1}$ and $K_{b2} = K_{c2}$, and EQN.68 reduces to : $\Delta F_1F_2 = \tfrac{3}{2}E_F(K_2 - K_1)(E_c - E_b)$ EQN.69

(N.B. the E_X values are the Huggins electronegativities of the substituents).

General values for the proportianality constants K_1 and K_2 could not be derived from the compounds studied, but literature data (255) indicated that ΔF_1F_2 was largely dependent on the value of ΔE_{bc}. (see TABLE 4-7.1 & FIG.4-7.5)

The ΔF_1F_2 value derived for compounds of the type $CF_2X.Cabc$ is directly

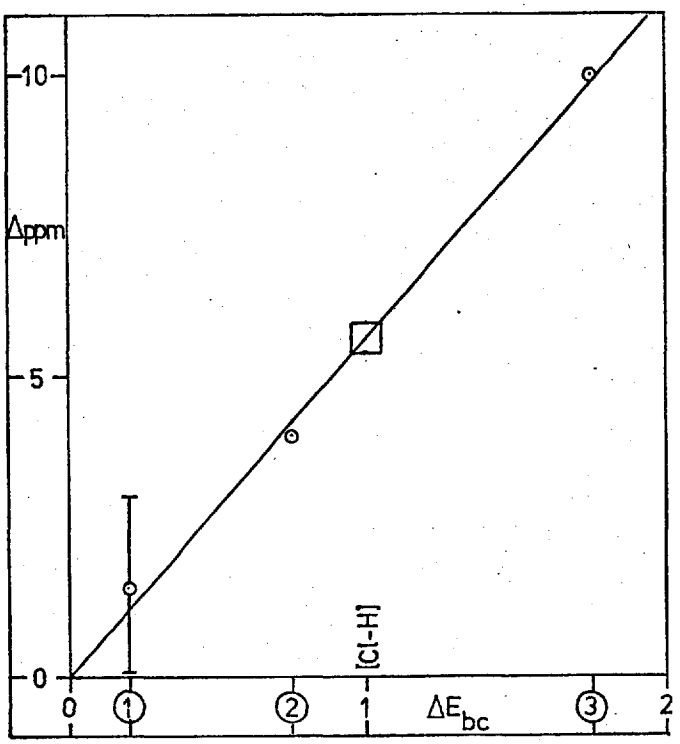


FIG.4-7.5 Relationship of ΔE_{bc} to ΔF_1F_2-

TABLE 4-7.1 Relationship of ΔE_{bc} to ΔF_1F_2-[254]

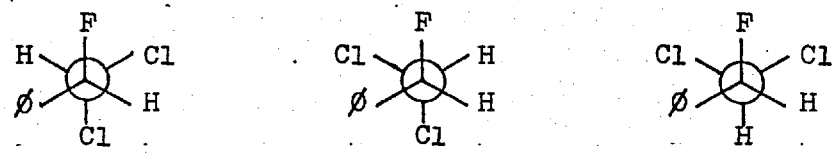
No.	Subnt. b	Subnt. c	ΔE_{bc} (Huggins)	ΔF_1F_2 ppm
①	Br	Cl	0.2	0-3
②	Cl	F	1.0	~4
③	H	F	1.75	~10

analogous to the change in shift of the Type (V) fluorine on changing the side-chain conformation. FIG.4-7.6 shows the vicinal inductive components of the ^{19}F chemical shifts of the three possible Type (V) rotamers. The components are equal in rotamers 1 and 2 (analogous to a = H; b = c = Cl in $CF_2X.Cabc$) which should therefore have very similar ^{19}F shifts. Rotamer 3 has different component shifts, (analogous to b = H, a = c = Cl in CF_2XCabc), and should therefore have a different ^{19}F shift. Since $\Delta E_{H-Cl} = 1.0$, by comparison to the data plotted in FIG.4-7.5, the expected ^{19}F shift difference between rotamer 3 and rotamers 1 or 2 is ~5.5ppm with rotamer 3 to higher field.

If modification of the C-1/C-2 conformation (through steric control by the ortho substituents) can induce ^{19}F shifts of 5-6 ppm, it is reasonable to expect that modification of the C-1/C-1' conformation can also induce ^{19}F shifts (ie: depending on whether the C-F bond is periplanar or orthogonal to the phenyl ring). In addition the ortho substituents are two bonds closer to the C-F moiety than the para substituents, and, as well as being able to influence the fluorine directly "through space", should have stronger "through bond" interactions. Considering the combined effects of these interactions, the differences in the ranges of the ortho (20ppm) and para (7ppm) ^{19}F shifts do not seem unreasonable. From FIG.4-7.3 the likelyhood of a high percentage rotamer 3 is : oOMe, Cl, Br, NO_2 > oF, CF_3 > oMe and para series.

To draw conclusions from the ^{13}C data, it is first necessary to sort it into some logical order. If the ring carbon SCS are plotted against X (as in FIG.4-7.1(a)), the shifts are seen to be dominated by the X substituent effects[128,247] with only slight effects from the Y side-chain substituent. The

FIG.4-7.6 Conformation Dependent Components of Vicinal Inductive Effects



	1	2	3
Rotamer :			
Gauche Component :	$\cos 60^\circ$(H+Cl)	$\cos 60^\circ$(H+Cl)	$\cos 60^\circ$(Cl+Cl)
Trans component :	$\cos 180^\circ$(Cl)	$\cos 180^\circ$(Cl)	$\cos 180^\circ$(H)

The same

Difference equivalent to FIG.4-7.4 (a = c = Cl, b = H)

TABLE 4-7.2 Carbons with Similar X SCS in the ortho and para Series.

X Substituent Effect	Carbon Atom	No Bonds from Y	Scatter in Y.SCS (V)-(IV)	Scatter in Y.SCS (VI)-(IV)	X.SCS Range ppm
ipso	o C-2'	3	0.49$	0.62$	40
	p C-4'	5	0.22$	0.24$	
o	o C-1'	2	0.29$	0.48$	23
	o C-3'	4	0.11	0.12	
	p C-3'	4	0.05	0.03	
m	o C-4'	5	0.11	0.13	4
	o C-6'	3	0.35*	0.20*	
	p C-2'	3	0.10	0.12	
p	o C-5'	4	0.12	0.19*	14
	p C-1'	2	0.21*	0.22*	
C (3 bonds)	o C-1	1	0.41*	0.44*	6.5
C (5 bonds)	p C-1	1	0.19*	0.31*	
C (4 bonds)	o C-2	2	0.10	0.16*	1.5
C (6 bonds)	p C-2	2	0.05	0.05	

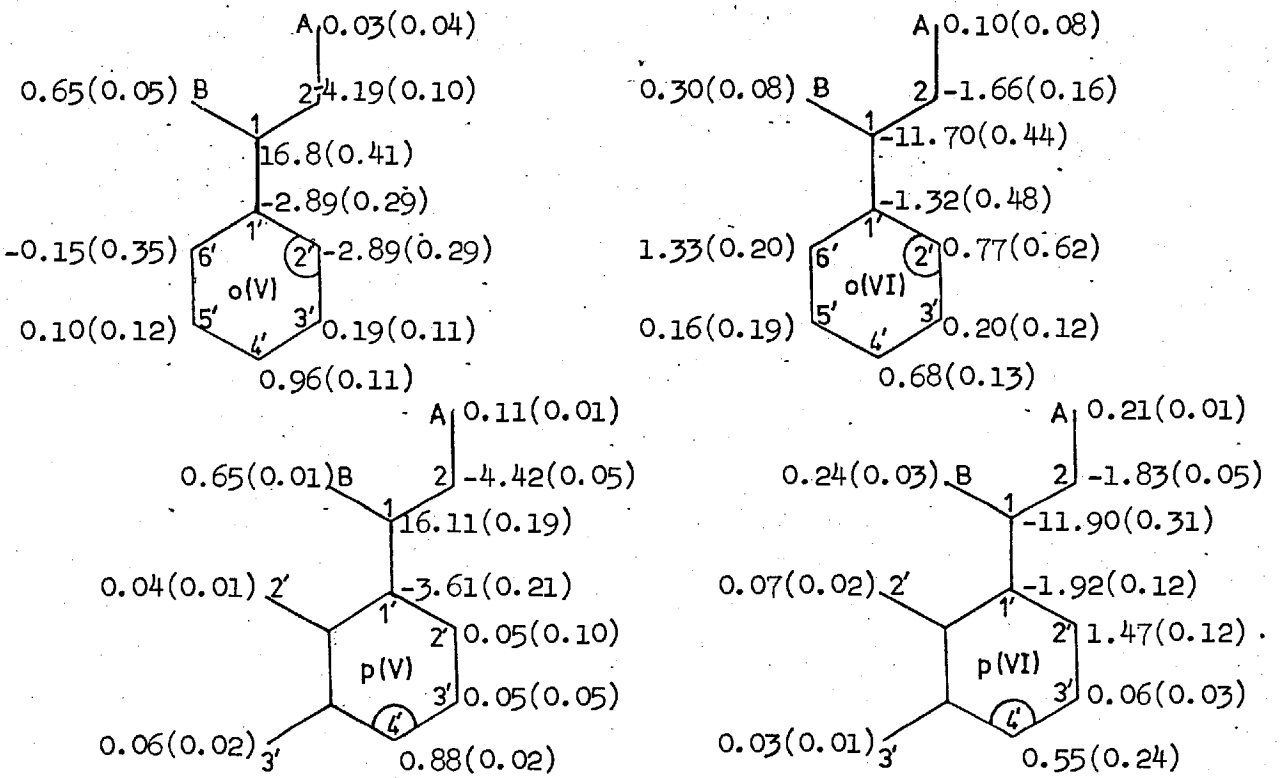
$ Y.SCS scatter, although large, is not unreasonable when compared to the range of the X.SCS

ring carbons therefore fall into the four groups listed in TABLE 4-7.2. If the X and Y effects were totally independent (ie. with the same conformations for all three Y substituents, and the two SCS were additive) then the ring carbon Y.SCS (see TABLE 4-4.15) would have very little scatter (eg. std.dev. 0.05ppm). Those carbons with rather more deviation in the Y.SCS than is reasonable from experimental error, are indicated by (*) in TABLE 4-7.2. The ^{13}C and ^{1}H Y.SCS are illustrated in FIG.4-7.7.

For the most part plots of the ring ^{13}C SCS merely follow the standard X.SCS profiles predicted in the literature,[128,247] and are therefore of little

FIG.4-7.7 ^{1}H and ^{13}C Y.SCS (From Mean Values of (V)X - (IV)X and (VI)X - (IV)X).

The ortho and para cases - standard deviation given in parenthesis.



help in determining the side-chain conformations. The only carbon shifts which might be of some help are those of C-1 and C-2 themselves, together with C-1' and C-X.

In TABLE 4-7.3 all the chemical shift data (^{13}C, ^{1}H and ^{19}F) available on the X substituent groups are summarised as the shifts incurred on changing from para X to ortho X. In the ^{13}C data, the average methyl group shift is quite large, whereas the methoxy and trifluoromethyl (with the exception of oCF_3 (IV)) groups barely shift at all. The obvious inference is that all the oMe derivatives and oCF_3(IV) prefer conformations in which they interact with the substituted ethyl side-chain, whilst all the oOMe derivatives and oCF_3(V) and (VI) favour the X and side-chain groups to be as far apart as possible. Unfortunately there is no supporting evidence for this in either the ^{1}H or ^{19}F data.

TABLE 4-7.3 ΔX Shifts (para - ortho)(ppm)

Nucleus	Deriv	(IV)	(V)	(VI)
^{13}C	Me	1.60	1.91	1.63
	OMe	-0.15	-0.26	-0.38
	CF_3	0.76	-0.21	-0.05
^{1}H	Me	-0.030	-0.051	-0.034
	OMe	-0.033	-0.041	-0.067
^{19}F	F	5.349	6.084	NO
	CF_3	-5.167	-5.339	DATA

The X and Y.SCS for C-1 and C-2 are plotted in FIG.4-7.8, and for C-1' in

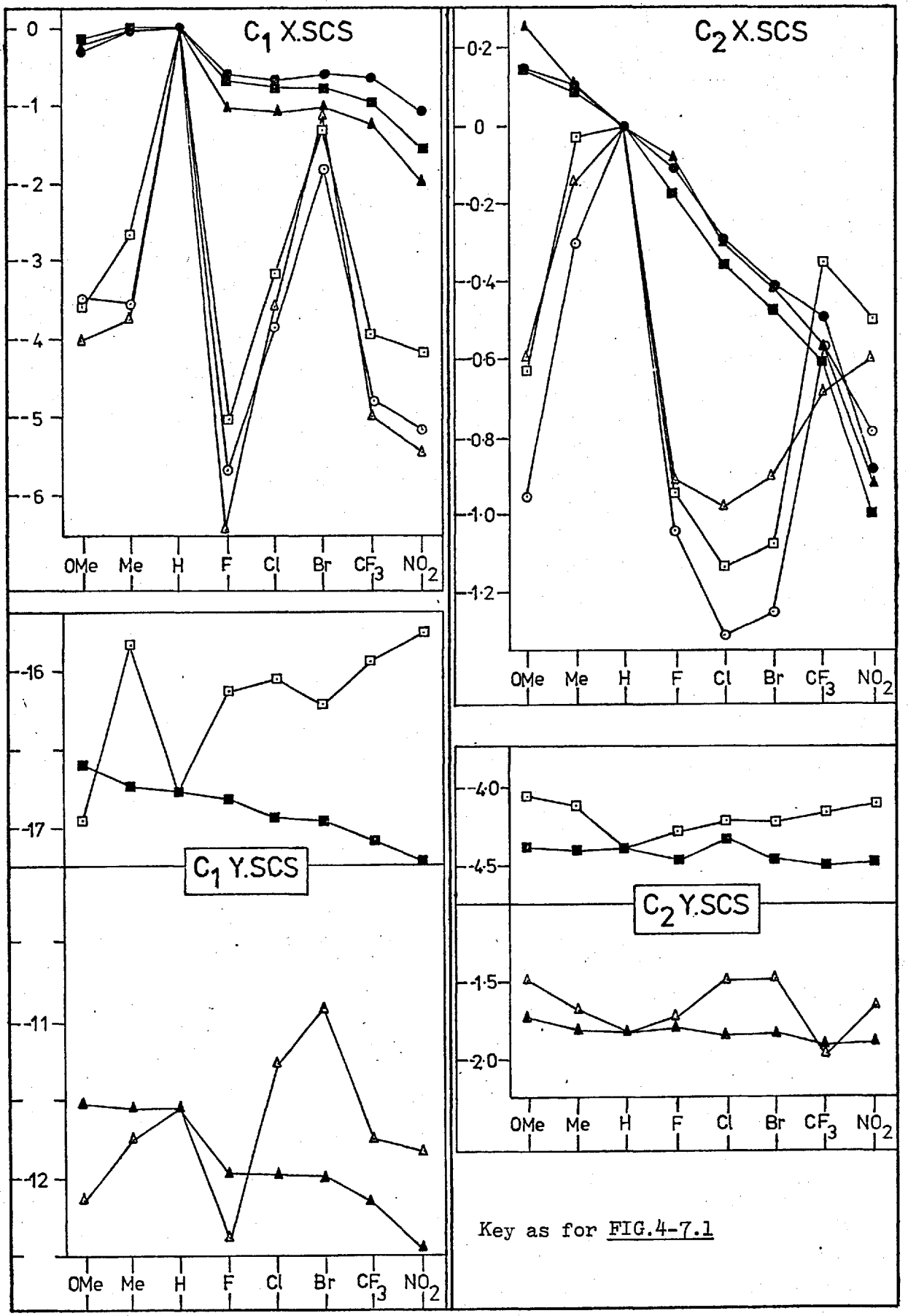


FIG.4-7.8 X and Y.SCS of the Side-Chain Carbons

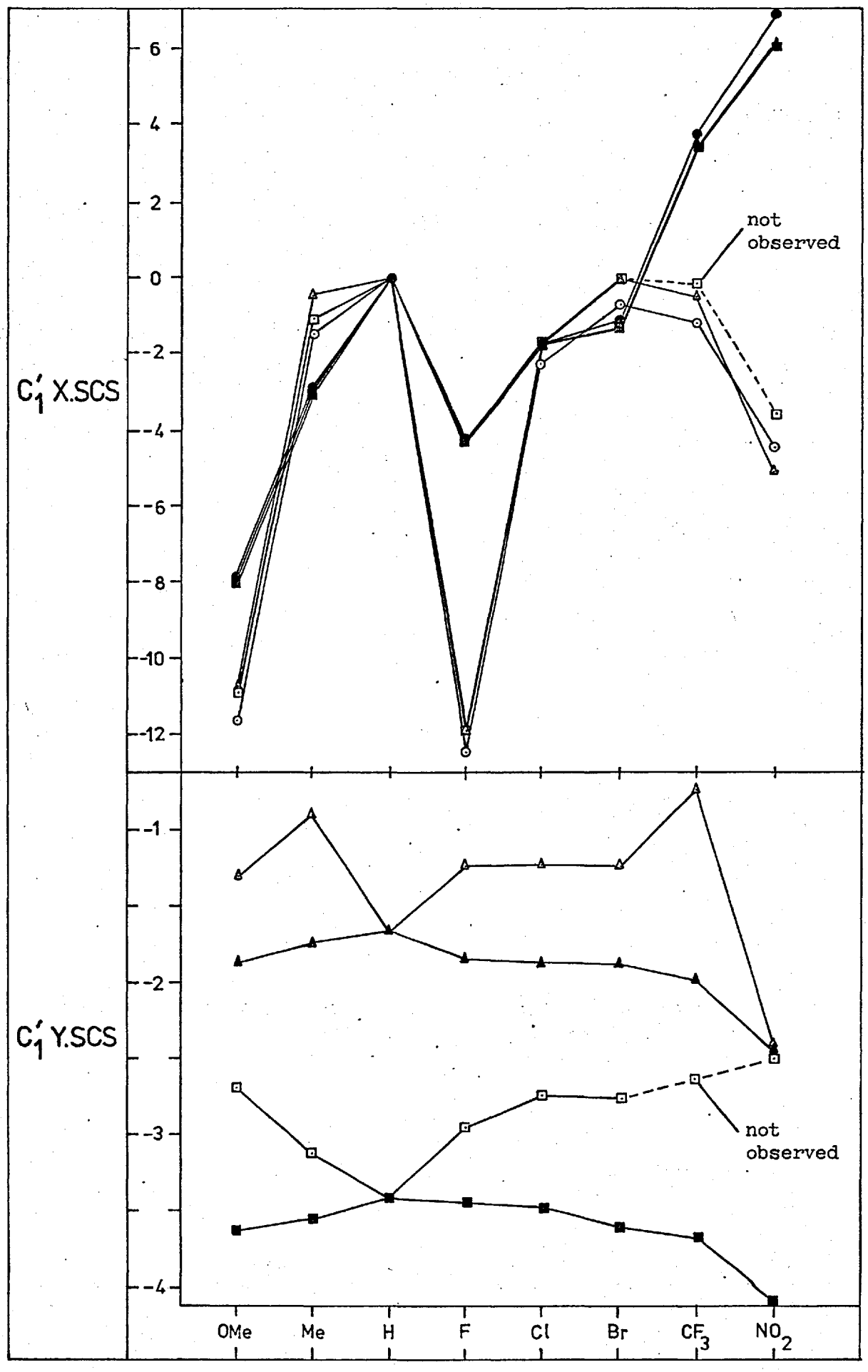


FIG.4-7.9 C-1' X and Y.SCS. Key as for FIG.4-7.1

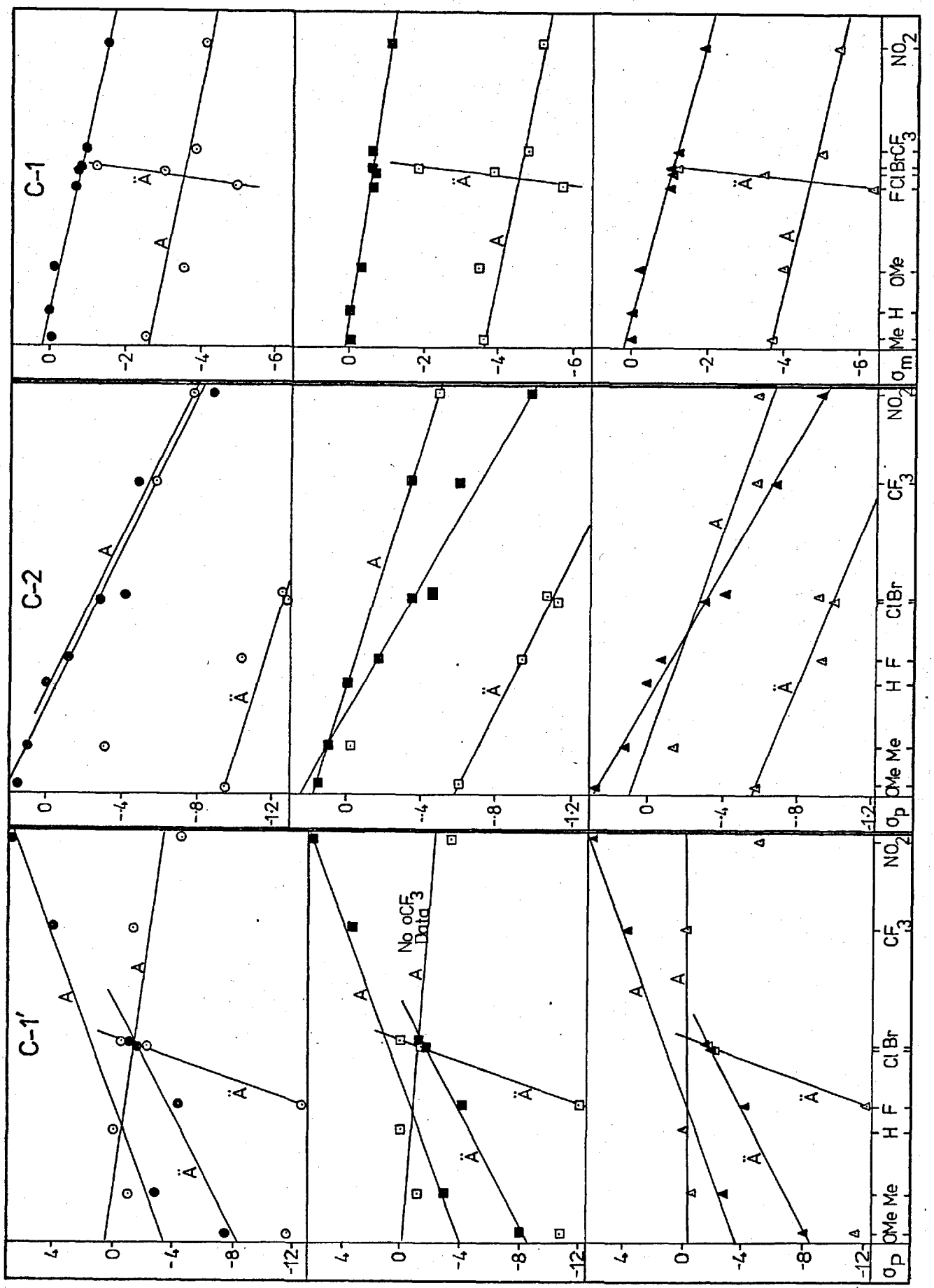


FIG.4-7.10 C-1' & C-2 X.SCS vs. Hammett σ_p. C-1 X.SCS vs. σ_m. Key as for FIG.4-7.1

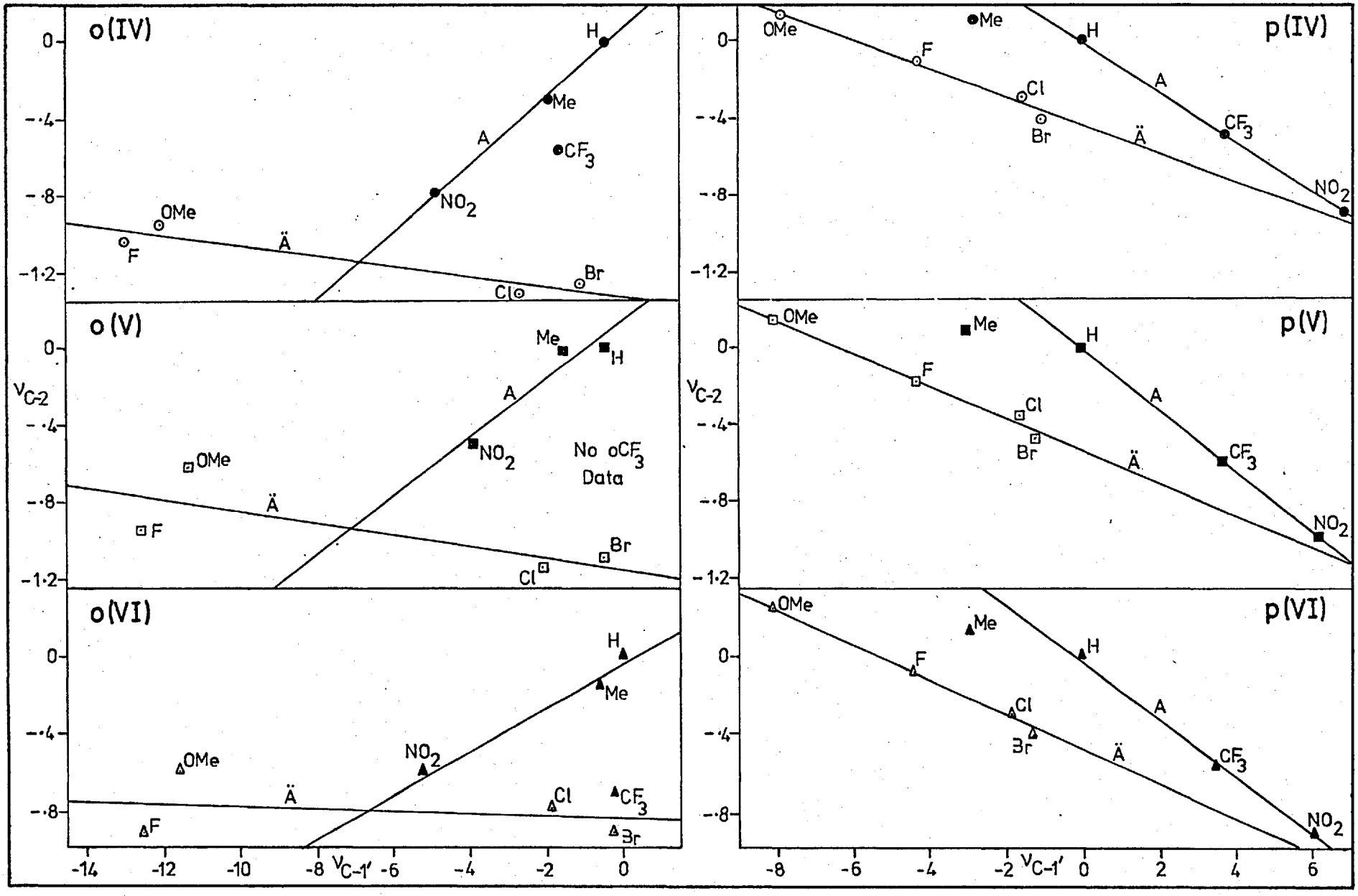


FIG.4-7.11 X.SCS C-2 vs. X.SCS C-1'

FIG.4-7.9. Again the trend for the para X.SCS to undergo regular variations is present whilst the oX.SCS are erratic. This is also in evidence in the Y. SCS for C-1, although for C-2 and C-1' both the ortho and para Y.SCS are fairly regular.* The carbon skeleton of the phenyl ethanes appears to behave as an alternate hydrocarbon, with pC-1' and pC-2 X.SCS correlating well with Hammett σ_p whilst pC-1 correlates with σ_m (see FIG 4-7.10). It is somewhat surprising that the two sp^3 side-chain carbons should fit into the alternate hydrocarbon scheme as this is a property usually associated with π-systems. The oC-1 and oC-2 X.SCS show a lesser degree of correlation with σ_m amd σ_p, with the A and Ä groups[252] falling on separate lines. Since Hammett parameters are not expected to correlate well with ortho substituent effects[248,249] (this is borne out in the oC-1' plot), the degree of correlation observed is quite surprising. Several groups (eg. oMe in the C-2 SCS, and H and oOMe in the C-1 SCS) consistently lie off the A or Ä lines indicating that steric as well as electronic factors contribute to the X.SCS.

FIG.4-7.11 illustrates the alternating nature of the ring substituent effects into the side-chain. ν_{C-1} shows little correlation to $\nu_{C-1'}$ or ν_{C-2} but ν_{C-2} is quite well correlated to $\nu_{C-1'}$ in both the ortho and para series. (a related effect is noticeable in the $^nJ_{CF}$ coupling data where both ortho and para fluorines show larger couplings to C-2 than to C-1 ! This effect is normally only seen when the side-chain is unsaturated, eg. in styrenes and stilbenes, where spin coupling is transmitted over long distances by resonance effects.[256,257] - see FIG.4-8.17).

Used by itself, the shift data is insufficient to deduce many specific details about molecular conformations; it does however provide several useful generalities :

1) Substituent effects are very similar within the three series - indicating similar overall properties.

2) The para series behave as predicted by Hammett parameters etc., and probably all have the side-chain in similar conformations or in "free rotation" with no conformational preferences.

3) The ortho series produce seemingly erratic shifts from the side-chain nuclei, which are paralleled in all three series. These indicate a considerable amount of steric control of the side-chain by the ortho ring substituents which is reasonably independent of Y, ie. possibly dominated by interactions between X and the $-CHCl_2$ group rather than between X and Y.

Further confirmatory details are undoubtedly contained in the shift data, which may only be unlocked by reference to the coupling information. Any such

* From the Y.SCS data the X = H derivative appears to fit well into the para series but poorly into the ortho series. Instances of this behaviour occur throughout the chemical shift data of all three nuclei.

points arising from the data presented here, or in SECTION 4-4 will be dealt with later in this chapter.

4-8 Interpretation of the Coupling Constant Data

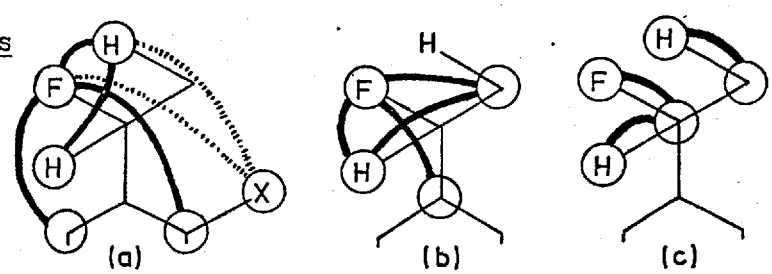
Before commencing detailed discussions on the various couplings measured, it is worthwhile briefly summarising which couplings are observable (or have been recorded) for each of the three series studied (see TABLE 4-8.1). The limited "common ground" between the three series, ie. $^{3}J_{AB}$ and $^{n}J_{CF}$ ($^{3}J_{2'3'}$ is neither accurate enough for detailed consideration nor very relevant to the molecular conformational analysis) must first be examined to establish their main similarities and/or differences. The wealth of data presented by the Type (V) fluorides and the Type (IV) alcohols may then hopefully be utilised in conjunction to interpret their conformational preferences. The coupling constants particularly useful in analysing the side-chain conformations are illustrated in FIG.4-8.1.

TABLE 4-8.1 A Summary of the Types of Coupling Data Recorded in Section 4-5

Coupling	Type (IV)	Type (V)	Type (VI)	All Series
$^{n}J_{HH}$	AB BC $H_{2'3'}$	AB $H_{2'3'}$	AB $H_{2'3'}$	* [*]
$^{n}J_{HF}$		AX BX F_1 long range	Ring F long range	
$^{n}J_{CF}$	Ring F/CF_3	Ring F/CF_3 Side-chain F	Ring F/CF_3	*
$^{n}J_{FF}$		Between ring F & side-chain F		
$^{n}J_{HC}$	Between H_A/H_B and C_1/C_2			

FIG.4-8.1 Useful Couplings

a) over 3 or more bonds
b) over 2 bonds
c) over 1 bond



4-8-1 Similarities Between the Type (IV), (V) and (VI) Coupling Constants

The $^{3}J_{HH}$ coupling constants listed in TABLE 4-5.1 are plotted in FIG.4-8.2. As with the chemical shift data (see FIG.4-7.1 (a & b)) the couplings in the

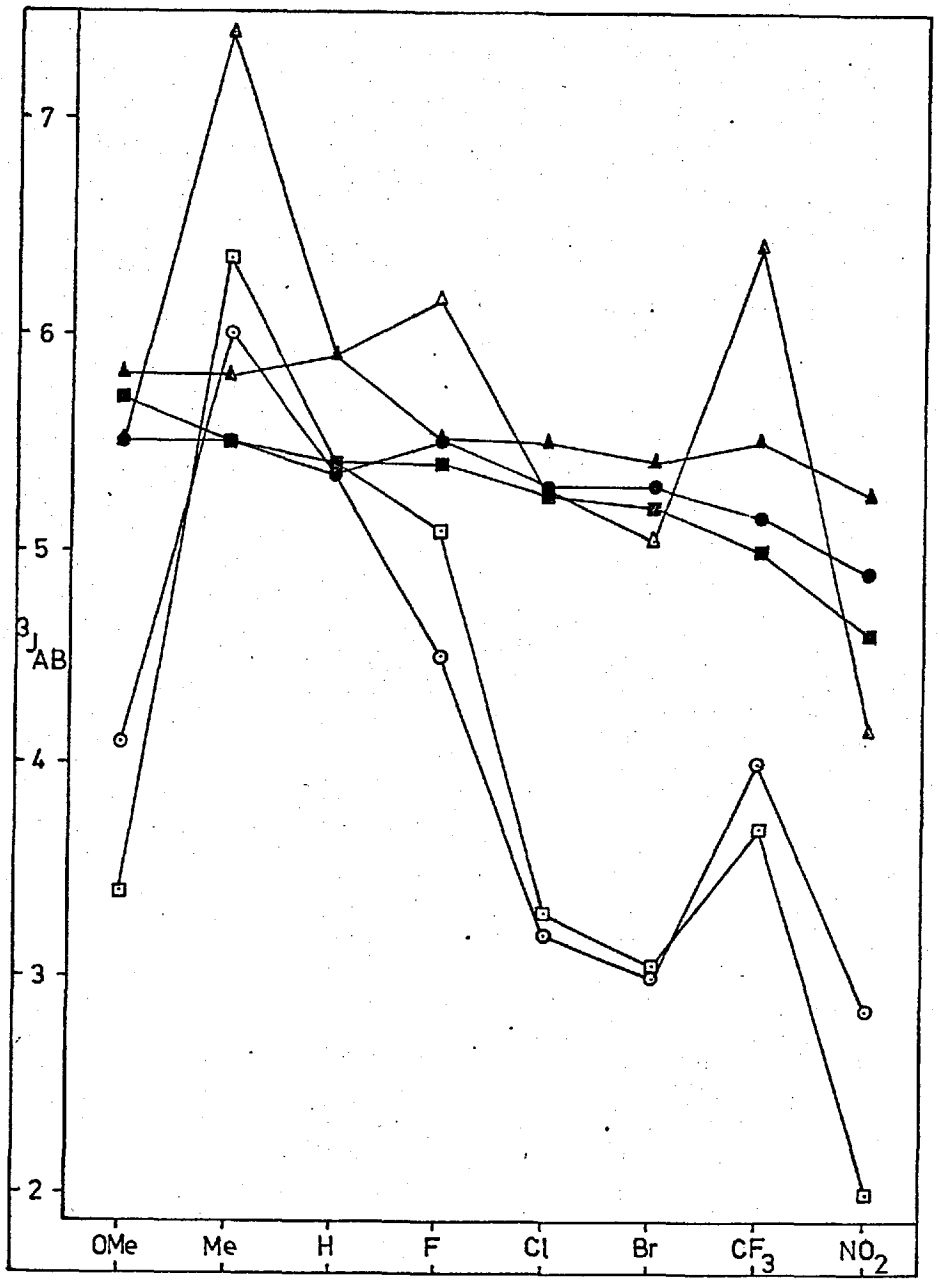


FIG.4-8.2 Variations in $^3J_{AB}$ Throughout the Type (IV), (V) and (VI) Series.

para derivatives show much less variation than those in the ortho derivatives. In all three series there is a small but fairly well defined trend for the para couplings to decrease along the Hammett σ_p series (from OMe to NO_2). This trend is also present in the ortho couplings with the notable exception of the oOMe derivatives and, to a lesser extent, the oCF_3 derivatives.

Although the couplings for the ortho (and to a lesser extent the para) Type (VI) chlorides are significantly larger than those for the corresponding Type (IV) or (V) compounds, the overall trends parallel each other fairly closely, indicating that this effect is probably mainly a consequence of the side-chain substituent (Y = Cl) contributing a smaller negative electronegative effect to the $^3J_{AB}$ than either the hydroxy- or fluoro- substituents (E_X : Cl = 3.2, OH = 3.5, E = 3.95). It is, however, unlikely to account for

all the observed differences, as the relative J's of the Type (IV) and (V) series are very similar even though the electronegativities are fairly dissimilar ($\Delta E_X = 0.45$).

Slight inconsistencies in the Type (VI) data relative to the Type (IV) or (V) series are not, fortunately, of major concern here as no elimination reactions were undertaken on this series. The very close parallel of the Type (IV) and (V) data is however crucial, for if the various coupling data collected from both series can be combined, then we have a very powerful tool for conformational analysis.

Turning to the $^{n}J_{CF_X}$ couplings (see TABLE 4-5.4) we find that all three series respond similarly with the scatter from the mean normally well within the expected $\pm$0.5Hz error. Only three couplings stand out, namely the o and pF(IV) $^{1}J_{CF}$ couplings to C-2' and C-4' respectively; and the oCF_3(VI) $^{5}J_{CF}$ coupling to C-2. It has already been mentioned that the oCF_3(VI) $^{3}J_{AB}$ coupling is slightly anomalous so it is probable that this compound adopts a different conformation to its Type (IV) and (V) analogues. This is, however, not thought to be the case in the o and pF Type (IV) alcohols.

It is well established that ^{19}F chemical shifts and $^{1}J_{CF}$ couplings are extremely sensitive to small changes in the electronic environment of the carbon atom.[128] Although this dependence is complex, Muller and Carr[258] noted that there is a linear relationship between ^{19}F shifts and $^{1}J_{CF}$ couplings within a family of compounds, such that the largest $^{1}J_{CF}$ values occur for the most deshielded fluorine. This has been shown to hold true in substituted fluorobenzenes by Weigert and Roberts[259] where the average slope of a plot of $^{1}J_{CF}$ vs. δ_F is -0.90 (extrapolated from Figure 7).[259] Not unexpectedly, the ortho substituent data shows considerable scatter in this plot. The gradient between the oF Type (IV) and oF Type (V) shifts and couplings is -0.55 whilst the pF gradient is -0.77 (both of these figures are subject to very large errors). The effects observed are therefore analogous to those reported in the substituted fluorobenzenes, ie. they merely reflect the different inductive effects of the side-chain Y substituents. Fluorine and chlorine can be considered fairly similar in this respect, ie. they are both strong σ-bond electron withdrawers with a weaker ability to donate electrons from the non-bonding p (or d) orbitals, whereas the oxygen of the hydroxy group is both a strong σ-bond withdrawer and a strong p electron donator. On balance, therefore, when Y = F or Cl, electrons will be withdrawn from the σ-bond framework thus deshielding the ring fluorine, whilst when Y = OH, the electron withdrawing/donating characteristics of the hydroxy group will tend to cancel.

On the basis of the rather limited comparative coupling data available, it is reasonable to conclude that the interactions observed in the Type (IV)

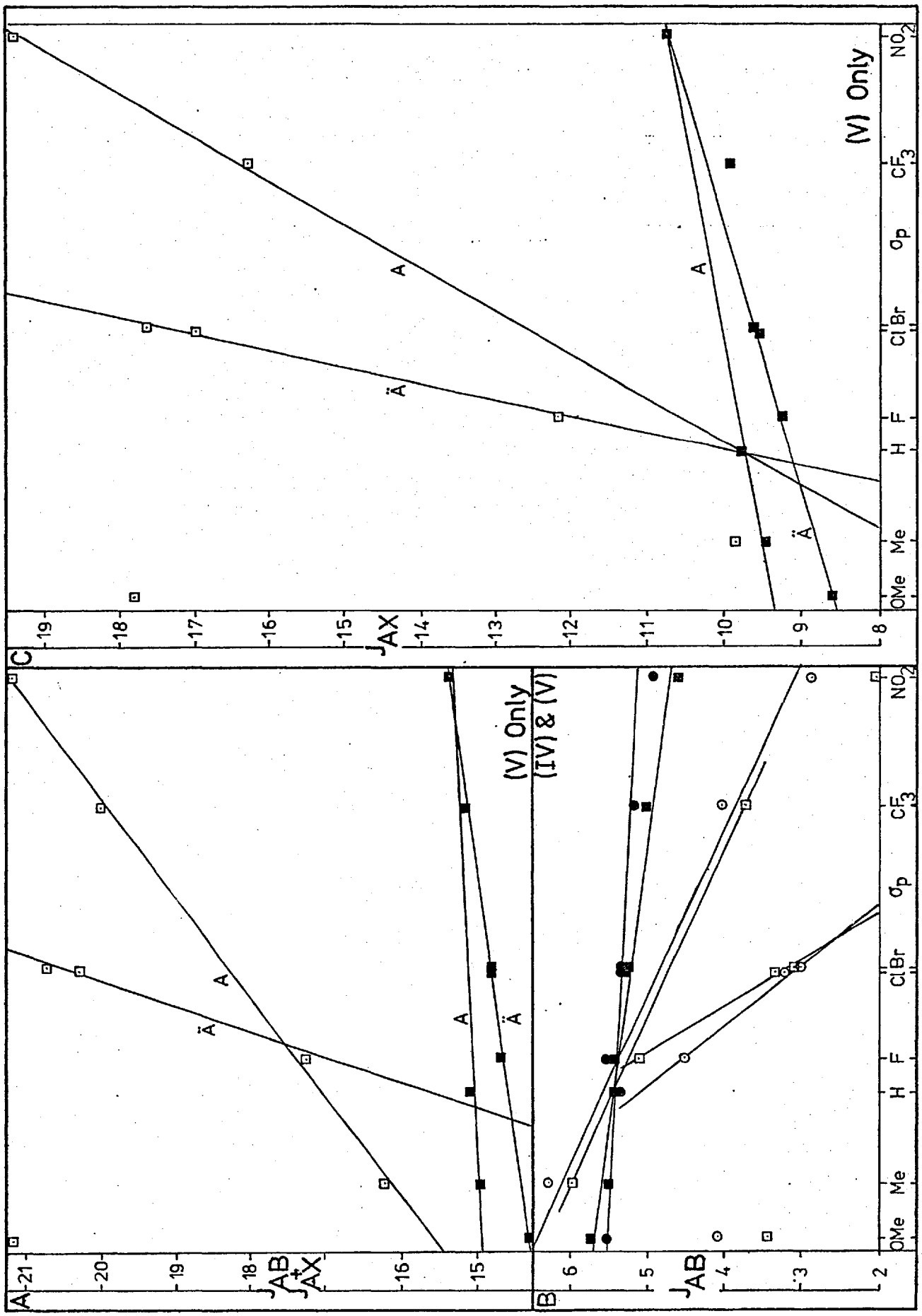


FIG.4-8.3 Side-Chain J_{HH} & J_{HF} vs. σ_p. (A) Type (V) $J_{AX} + J_{BX}$; (B) Type (IV) & (V) J_{AB}; (C) Type (V) J_{AX}.

and Type (V) series are very similar, indicating that the corresponding members of these series adopt similar side-chain conformations. There is some evidence that the Type (VI) chlorides behave slightly differently and this may be a consequence of the steric interactions present when Y = Cl.

4-8-2 A Detailed Examination of the Three Bond Coupling Data

4-8-2.1 Trends Observed in the $^3J_{HH}$ and $^3J_{HF}$ Couplings

The side-chain $^3J_{HH}$ and $^3J_{HF}$ couplings for the Type (IV) and Type (V) series are plotted in FIG.4-8.3 against σ_p. In the para couplings we observe the expected linearity with σ_p; $^3J_{HF}$ decreasing and $^3J_{HH}$ increasing as the electron donating ability of X increases. This reflects the opposite polarisation of the C-H and C-F bonds. Electron donation from the ring to C-1 reduces C-H ionic character but increases C-F ionic character thereby increasing the coupling transmitted in the C-H bond but decreasing the transmission in the C-F bond. These effects are very small (para $^3J_{HH}$ ranges over ~1Hz, para $^3J_{HF}$ over ~2Hz) indicating that similar conformational preferences persist throughout the para series. The average para couplings (including X = H) are $^3J_{HH}$(IV) = 5.32Hz; $^3J_{HH}$(V) = 5.26Hz; $^3J_{HF}$(V) = 9.61Hz and $^3J_{HH}$(VI) = 5.58Hz.

As with the chemical shifts (see FIGS.4-7.1 and 4-7.3), the ortho couplings appear to be very erratic. Some trends are present, eg. the A-line (NO_2-CF-H) and the Ä-line (Br-Cl-F-H) in the $^3J_{HF}$ data, but in all cases at least one member of the A- or Ä- group lies well off the line so the significance of these observations is debatable.

It is interesting to note that the H and pMe $^3J_{HF}$ couplings lie parallel to the "best fit" line of the remaining para derivatives (as in the chemical shift data - see FIG.4-7.3(b)) and that only poor correlation is available if an A line is considered. A similar effect has been observed in the chemical shift data of 4'-X substituted-4-fluoro-diphenyl acetylenes[256] and is currently under investigation.

In FIG.4-8.4 the $^3J_{HF}$ couplings are plotted against their corresponding ^{19}F shifts. The para data shows good correlation to a single straight line, and although more scattered, the ortho data follows a similar trend. This is analogous to the $^1J_{CF}$: δ_F relationship[258,259] mentioned earlier and demonstrates that both ^{19}F spectral parameters are highly dependent on the electronic character of the C-F bond.

From an inspection of FIG.4-8.4 the Type (V) fluoride appears to fall into three groups : (1) all the para derivatives and oMe; (2) oF & oCF_3; (3) oCl, Br, OMe, and NO_2, which are the same as the three groups observed in FIG.4-7.3. The temptation to assign characteristic structures (rotamers) to each of these groups will be resisted for the present, on the grounds of insufficient data.

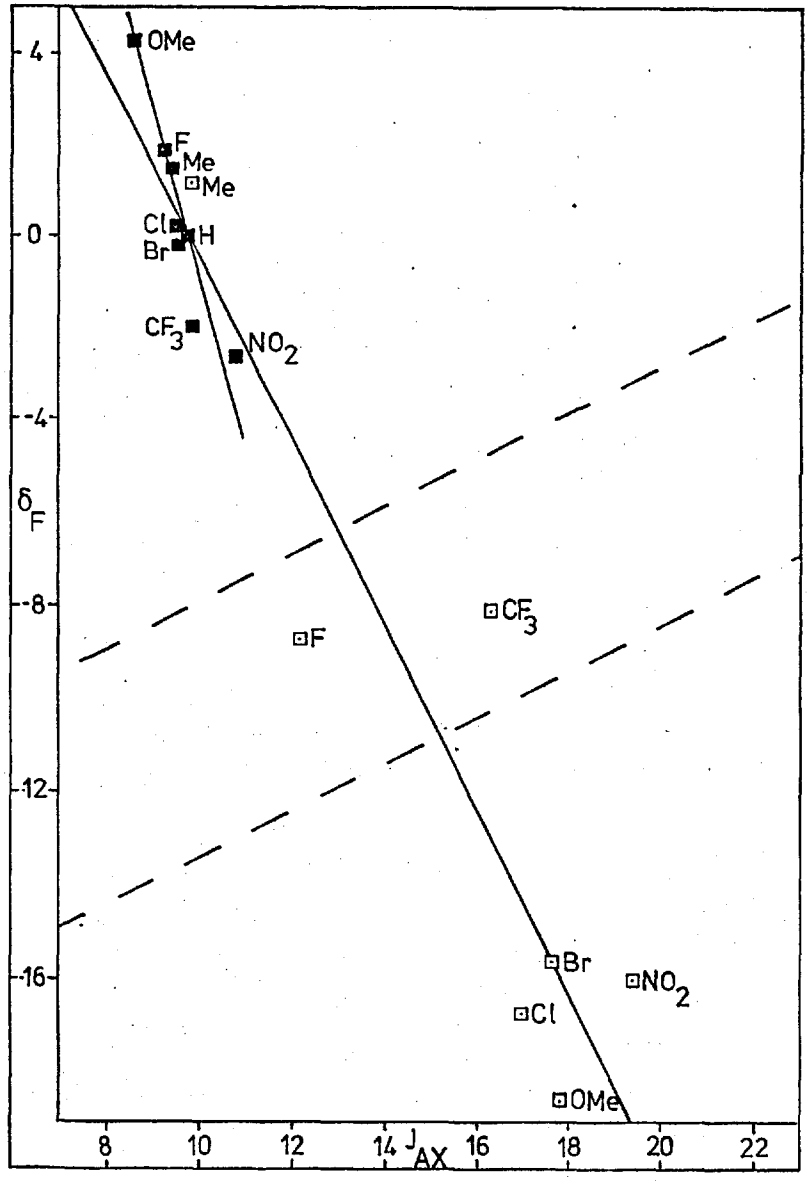


FIG.4-8.4 Type (V) δ_F vs. J_{AX}

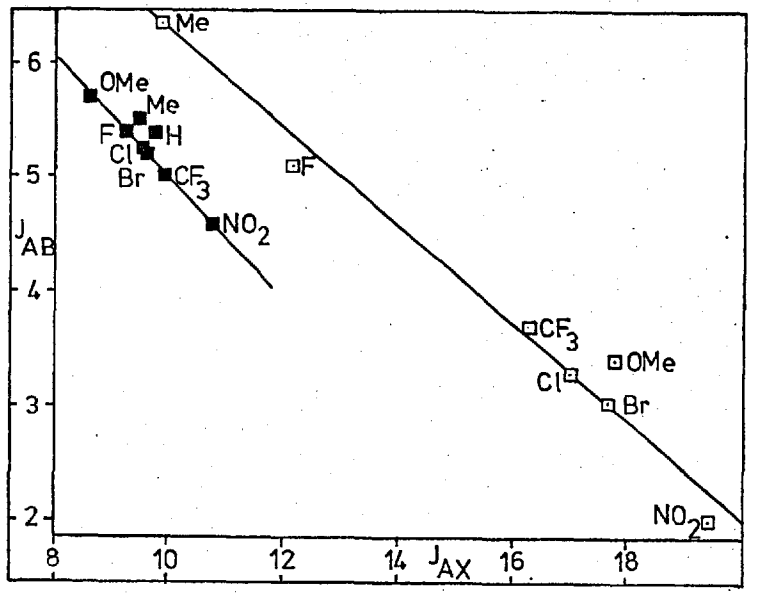


FIG.4-8.5 $^3J_{HH}$ vs. $^3J_{HF}$ for the Type (V) Fluorides

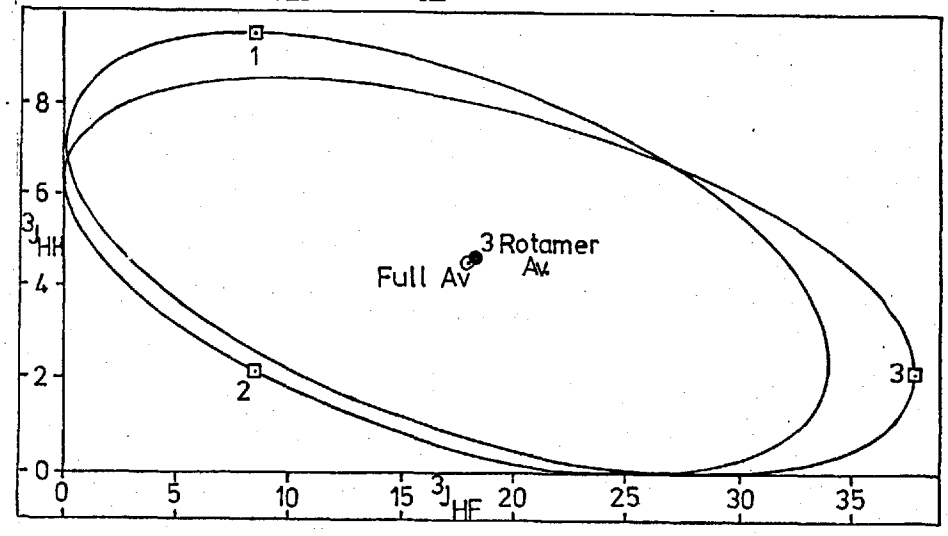


FIG.4-8.6 Synthesised $^3J_{HH}$ vs. $^3J_{HF}$ using $J = J^{0/180} \cos^2\phi$ where $J^0_{HH} = 8.5, JJ^{180}_{HH} = 9.5$Hz and $J^0_{HF} = 33.7$, $J^{180}_{HF} = 37.7$Hz.

In FIG.4-8.5 $^3J_{HH}$ is plotted against $^3J_{HF}$ for the Type (V) fluorides. Two straight line plots, one for each of the ortho and para series, emerge. Again the H and pMe derivatives lie parallel to the best fit para line, but even so the linearity of both series is good. This result was unexpected, for, if the angular dependence of the substituent electronegative effects is ignored, both J's are controlled by a $\cos^2\phi$ parameter[48] and since they are 120° out of phase some form of ellipsoid should be generated. This is illustrated in FIG.4-8.6 where the two synthesised coupling constants are plotted against each other over the full range of ϕ. Although an ellipsoidal relationship does exist between the individual values of $^3J_{HH}$ and $^3J_{HF}$, this is not produced when the observed couplings are plotted against each other because these J's are derived from weighted averages of all the molecular conformations adopted and not from a single rotamer. In the free rotation limit both J's will lie at the centre of the ellipsoid, (see FIG.4-8.6 - note that the "full" average J's are given by $(J^0 + J^{180})/4$ and the "three-rotamer" average J's (when $J^0 = 0.895J^{180}$) give a figure ~1.9% larger).

Interpretation of FIG.4-8.5 is therefore far from straightforward since each experimental point represents the weighted average of all the rotamers adopted. The plot is, however, useful for identifying groups which probably adopt similar conformations. Again three groups are apparent : (1) all the para derivatives and possibly oF and oMe; (2) oCl, Br, OMe, and CF_3; (3) oNO_2. Unfortunately the composition of these groups differs from the earlier groups seen in the plot of $^3J_{HF}$ vs. δ_F (see FIG.4-8.4).

In order to proceed further a closer look at the theoretical aspects of $^3J_{HH}$ and $^3J_{HF}$ couplings is necessary.

4-8-2.2 Empirical Approach to the Calculation of $^3J_{HH}$ and $^3J_{HF}$.

In SECTION 1-5.1 the dihedral angle dependence of $^3J_{HH}$ and $^3J_{HF}$ couplings was discussed in some detail. The straightforward Karplus relation (EQNS.8-10[48] breaks down in the presence of electronegative substituents but nevertheless remains a useful guide, even in systems with tetra-substitution (as in $^3J_{HH}$), as it defines the "maximum expected" coupling.

In the absence of electronegative effects $^3J_{HF}$ obeys the Karplus equation[125] :

$$J_{HF} = 31\cos^2\phi \qquad 0° < \phi < 90° \qquad \text{EQN.70}$$

$$J_{HF} = 44\cos^2\phi \qquad 90° < \phi < 180° \qquad \text{EQN.71}$$

EQN.71 was derived from the trans $^3J_{HF}$ coupling of 43.5Hz observed in the axial conformer of cyclohexyl fluoride at low temperature[260] and may represent a true "unperturbed" maximum for $^3J_{HF}$. EQN.70, however, is probably

an underestimate, as the 0° coupling on which it is based[125] (see FIG.4-8.7) is undoubtedly lowered by the electronegative effects of the two ester groups.

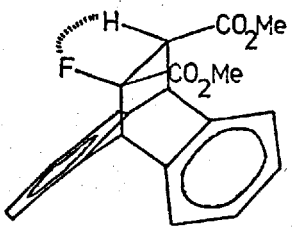


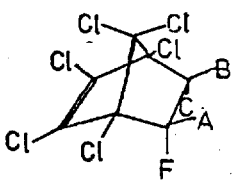
FIG.4-8.7 $^3J^0_{HF}$ = 30.8Hz

The linear decrease of averaged $^3J_{HH}$ with increasing electronegative substitution was mentioned in SECTION 1-5-1 (see EQN.12[111]). Following this work, Abraham and Cavalli[261] obtained a similar relation for $^3J_{HF}$:

$$^3J^{AV}_{HF} = 53.03 - 3.38\Sigma E \quad \text{(std.dev. 1.3Hz)} \qquad \text{EQN.72}$$

From this it appears that $^3J_{HF}$ couplings are ~4 times more sensitive to electronegative effects than $^3J_{HH}$.

In order to eliminate variations in bond and dihedral angles when studying vicinal couplings, Ihrig and Smith[262] examined couplings in the Diels-Alder adducts of hexachlorocyclopentadiene with various fluoroethylenes (see FIG.4-8.8).



Where ABC = H, AC = H, B = F.
AB = H, C = F; BC = H, A = F.
A = H, BC = F;

FIG.4-8.8

These systems are extremely rigid giving dihedral angles of 0° and 120° but with slightly distorted C-C-H bond angles of ~113°. The electronegative substituent effects were summarised by the equations :

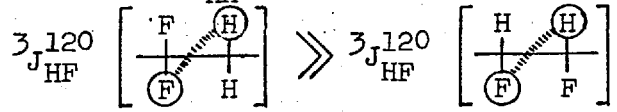
$$^3J^0_{HF} = 53.11 - 3.311\Sigma E \quad (\sigma = 2.44\text{Hz}) \qquad \text{EQN.73}$$

$$^3J^{120}_{HF} = 34.5 - 2.65\Sigma E \quad (\sigma = 1.83\text{Hz}) \qquad \text{EQN.74}$$

$$^3J^0_{HH} = 17.174 - 0.88\Sigma E \quad (\sigma = 0.355\text{Hz}) \qquad \text{EQN.75}$$

$$^3J^{120}_{HH} = 16.132 - 1.25\Sigma E \quad (\sigma = 0.419\text{Hz}) \qquad \text{EQN.76}$$

These indicate that for $^3J_{HF}$ the cis (0°) coupling, and for $^3J_{HH}$ the trans (120°) coupling, are slightly more sensitive to electronegative substitution (a factor which inhibits the derivation of a single equation that describes all rotamer/substituent effects on $^3J_{HF}$ or $^3J_{HH}$ couplings) and support the observation of Abraham and Cavalli[261] that $^3J_{HF}$ is considerably more sensitive to electronegative effects than $^3J_{HH}$. It was also noted that $^3J_{HF}$ was dependent on the siting of the substituents, eg. :



but this line was not persued.

By combining $^3J_{HF}$ data for ϕ = 60° and 180° (from unstrained systems) with ϕ = 0° and 120° data obtained from the [2.2.1] bicyclo heptenes (see FIG.4-4.8) (a risky practice as the bond angle sensitivity of $^3J_{HF}$ is well

established[125]), Ihrig and Smith also obtained a family of Karplus-type equations for different values of ΣE (ie. ΣE_X for the 4 substituents excluding the H and F nuclei) :

$$^3J_{HF} = A\cos^2\phi \quad 0 \leqslant \phi \leqslant 90 \qquad \underline{EQN.77}$$

$$^3J_{HF} = B\cos^2\phi \quad 90 \leqslant \phi \leqslant 180 \qquad \underline{EQN.78}$$

ΣE	A	B
9	24	52
11	15	32
13	8	16

The parameters A and B were found to obey the empirical relationships : $A = \frac{2 \times 10^4}{(\Sigma E)^3}$; $B \approx 2A$.

The linear dependence of $^3J_{HF}$ on substituent electronegativities (ie. $^3J_{HF} = A - B\Sigma E$), assumed by most authors was questioned by Hall and Jones.[263] They reasoned that if a substituent X reduced a coupling constant J from J_o to $(J_o - Y)$ then a second substituent X would not reduce J to $(J_o - 2Y)$ but rather should reduce it by the same fraction to $(J_o - Y)^2/J_o$.

ie. $dJ/dE = -kJ$ or $J = a.\exp(-kE)$ EQN.79

This argument is clearly more logical than the linear dependence of J on ΣE as the electron density along the coupling path cannot be limitless. This theory was tested on the $^3J_{HF}$ couplings observed in a series of fluoro-substituted acenapthenes (see FIG.4-8.9) where the dihedral angles are fixed at 0° and $\sim 100^\circ$. Both linear and exponential equations were calculated for the observed data (see EQNS.80-83), the exponential equations giving significantly better r.m.s. fits (N.B. ΣE only refers to the two non-participating substituents X and Y.

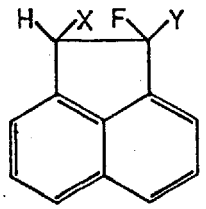


FIG.4-8.9

$$^3J^0_{HF} = 87.75 \exp(-0.2522\Sigma E) \text{ (Deviation } \pm 0.87) \qquad \underline{EQN.80}$$

$$^3J^{100}_{HF} = 985.68 \exp(-0.8749\Sigma E) \text{ (Deviation } \pm 0.18) \qquad \underline{EQN.81}$$

$$^3J^0_{HF} = 46.37 - 4.52\Sigma E \text{ (Deviation } \pm 1.32) \qquad \underline{EQN.82}$$

$$^3J^{100}_{HF} = 38.13 - 5.15\Sigma E \text{ (Deviation } \pm 3.35) \qquad \underline{EQN.83}$$

The various studies of three-bond couplings in rigid systems already discussed show that :

a) the unperturbed couplings possess a Karplus dependence on the dihedral angle ϕ.

b) as electronegative substitution increases the coupling decreases (possibly exponentially).

c) the rate of this decrease depends on the geometry of the rotamer (H-F dihedral angle ϕ).

d) the electronegative effect varies with the siting of the substituent.

Considerable attention has been paid to the $^nJ_{HF}$ couplings in fluorinated carbohydrates[126,264] as these provide "rigid" systems with the potential of a

large variety of substituent/geometrical arrangements. A closer inspection of the study by Phillips & Wray[126] (already cited - see SECTION 1-5-1), in which 10 deoxyfluoro-D-pyranoses giving rise to 4 trans and 14 gauche $^3J_{HF}$ couplings, were examined (see TABLE 4-8.2), is worthwhile here, as it illustrates the complex dependence of $^3J_{HF}$ couplings on both geometry and substitution patterns. In order to analyse substituent effects the "unperturbed" trans and gauche couplings were taken as 43.5[260] and 16.0Hz[261] respectively.

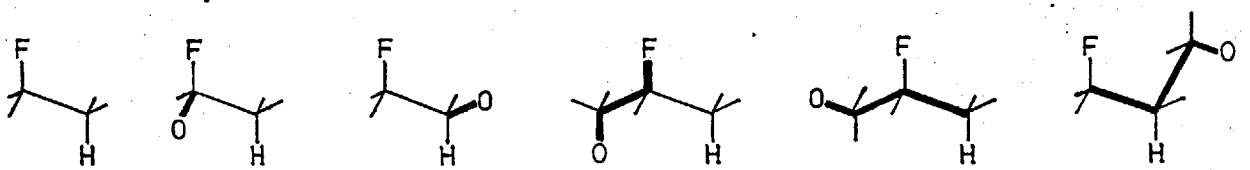
For the 4 trans $^3J_{HF}$ couplings, it was only noted that one oxygen on the "coupled fragment", ie. the $^{F}C-C_{H}$ bonds, reduced the coupling from its unperturbed value by ~10Hz (to 30/32Hz), whilst a second oxygen lowered the value still further (to 20/27.2Hz).[126] A closer inspection of the geometrical relationships of the various sugar oxygen functions to the coupled fragment identifies five possible electronegative interactions that might affect the observed couplings. These are indicated under each structure in TABLE 4-8.2 by a set of mnemonics and were selected by applying two criteria :

(1) Is the function directly attached to either carbon of the coupled fragment? This is a primary (1/2-bond) interaction and is denoted by the letters F or H to identify the carbon involved.

(2) Is the oxygen-carbon bond anti-periplanar to any of the bonds in the coupled fragment? This is a secondary (3-bond) interaction and is denoted by one of three symbols : F_S - anti-periplanar to the F-C bond;
S_H - anti-periplanar to the C-C bond from the H end;
S_F - anti-periplanar to the C-C bond from the F end.

If these interactions are assumed to be additive then the equations for the 4 trans coupled moieties may be solved simultaneously to produce the unique solutions illustrated in FIG.4-8.10. If these parameters are substituted back into equations of the type : $J = J_0 + \Sigma_1^n(\text{perturbation})$; the observed trans couplings are regenerated exactly.

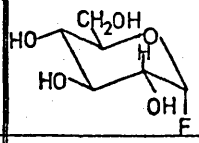
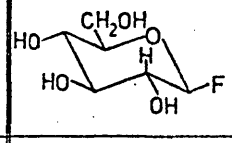
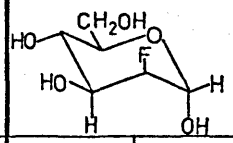
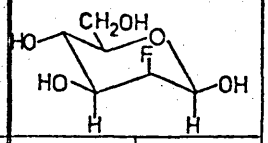
FIG.4-8.10 Perturbations to Trans $^3J_{HF}$ Couplings .

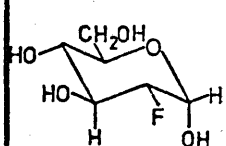
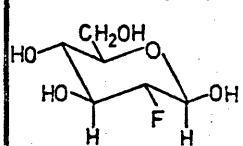
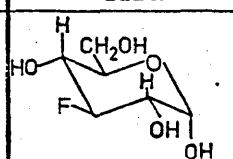
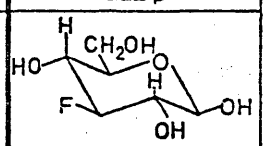


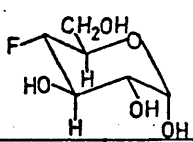
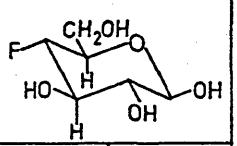
(43.5Hz) F -4.3Hz H -12Hz F_S -1.5Hz S_F +0.5Hz S_H 0 Hz

As trans $^3J_{HF}$ couplings in pyranoses involve di-axial groups, there is no possibility of planar W-type interactions. This simplification is not present in the 14 gauche couplings for which a total of 18 perturbations need to be considered (see TABLE 4-8.2). These were identified by extending the method already used to include W(4-bond) and 5-bond interactions. The criteria applied

TABLE 4-8.2 Stereospecific Electronegative Interactions in Deoxyfluoro-pyranoses

Name	Iα		Iβ		M-IIα		M-IIβ	
								
$^3J_{HF}$	t-H_2		g-H_2		g-H_1	t-H_3	t-H_1	t-H_3
Actual	27.2		12.0		7.5	30.0	20.0	32.0
Calc	(----)		(13.0)		(6.0)	(----)	(----)	(----)
Ring O	F		F		H	/	H	/
-OH_1	*		*		$H^e(F^a_S)$	F_S	H	S_F
-OH_2	H		H		*	*	*	*
-OH_3	S_H		$S^a_H(W_F)$		$S^a_F(W_H)$	H	S_F	H
-OH_4	/		$5_F O$		$5_H O$	S_H	/	S_H
-OH_6	/		/		/	/	/	/

Name	IIα		IIβ		IIIα		IIIβ	
								
$^3J_{HF}$	g-H_1	g-H_3	g-H_1	g-H_3	g-H_2	g-H_4	g-H_2	g-H_4
Actual	0.5	14.5	2.5	14.5	12.0	12.0	13.5	13.5
Calc	(2.0)	(15.5)	(2.0)	(15.5)	(11.5)	(11.5)	(13.5)	(11.5)
Ring O	$H^e(F^e_S)$	F^e_S	$H^a(F^e_S)$	F^e_S	/	/	/	/
-OH_1	H	/	H	S^e_F	H^a_S	/	$S^a_H(W_F)$	W_F
-OH_2	*	*	*	*	H	S^e_F	H	S^e_F
-OH_3	$S^e_F(W_H)$	H	S^e_F	H	*	*	*	*
-OH_4	$W_F(5_H)$	$S^a_H(W_F)$	W_F	$S^a_H(W_F)$	S^e_F	H	S^e_F	H
-OH_6	/	/	/	/	/	/	/	/

Name	IVα		IVβ	
				
$^3J_{HF}$	g-H_3	g-H_5	g-H_3	g-H_5
Actual	4.5	15.0	4.5	16.0
Calc	(4.5)	(15.5)	(4.5)	(15.5)
Ring O	F^e_S	$H^a(F^e_S)$	F^e_S	$H^a(F^e_S)$
-OH_1	/	/	$5_F O$	$5_F O_H$
-OH_2	$S^a_H(W_F)$	W_F	$S^a_H(W_F)$	W_F
-OH_3	H	S^e_F	H	S^e_F
-OH_4	*	*	*	*
-OH_6	T_F	$H_S S_H T_F$	T_F	$H_S S_H T_F$

KEY

Compound name :

α/β refers to C_1-X orientation

II etc. refer to position of F

M - indicates Mannose (all others are glucoses)

Couplings :

t = trans ; g = gauche ; all calc. and actual values taken from (126)

Interactions :

* = site of F ; / = no interaction

mnemonics are explained in text.

being similar to (2), ie :

(3) Is there a 4-bond 'trans-trans' planar path between the oxygen atom and either of the coupled nuclei? This is a tertiary (4-bond) interaction and is denoted by W_H or W_F. In cyclohexyl-type structures only di-equatorial groups can participate in W-interactions.

(4) Only one arrangement of groups (1-eq and 4-eq) in the D-pyranoses has the correct geometry for a 5-bond interactions between O and F (or H). Although the transmission of an electronegative effect has two potential routes, ie. via C_2-C_3 or C-C_5, only the latter is thought viable. This is supported by the observation of larger $^4J_{HH}$ couplings via oxygen-containing W-links, than via similar alkane arrangements.[126] Five bond interactions may be considered as two planar S-interactions (to the O-C_5 bond) with a dihedral angle of 60°. These are denoted by 5_H0 and 5_F0 in TABLE 4-8.2 with the additional parameter 5_F0_H indicating that two bonds of tne coupling path are involved in the 5-bond perturbation (see FIG.4-8.11).

The superscripts in the mnemonics indicate the orientation of the nucleus. TABLE 4-8.2 shows that some -OH functions give rise to several types of perturbation. These are listed in order of importance (primary > secondary, etc.). Two additional perturbations to coupled nuclei adjacent to the rotating C_6 fragment are included, namely T_F - a through-space interaction between $-OH_6$ and F_4, and $H_SS_HT_F$ - a multifunctional parameter for couplings between F_4 and H_5 (see FIG.4-8.11).

The evaluation of these parameters was performed in a similar manner to those of the trans couplings. Of the 18 perturbations considered (see FIG. 4-8.11) only 12 could be solved uniquely; these do,however, completely cover 12 of the 14 gauche couplings. The remaining 6 perturbations (marked * in FIG.4-8.11) each occurred only once; three in each of M-IIα(g-H_1) and IIα(g-H_1) and are therefore known only as two sets, ie :

$$H^e(F^e_S) + S^e_F(W_H) + W_F(5_H) = -11.5 \qquad \text{EQN.84}$$

$$H^e(F^a_S) + S^a_F(W_H) + 5_H0 = -4.5 \qquad \text{EQN.85}$$

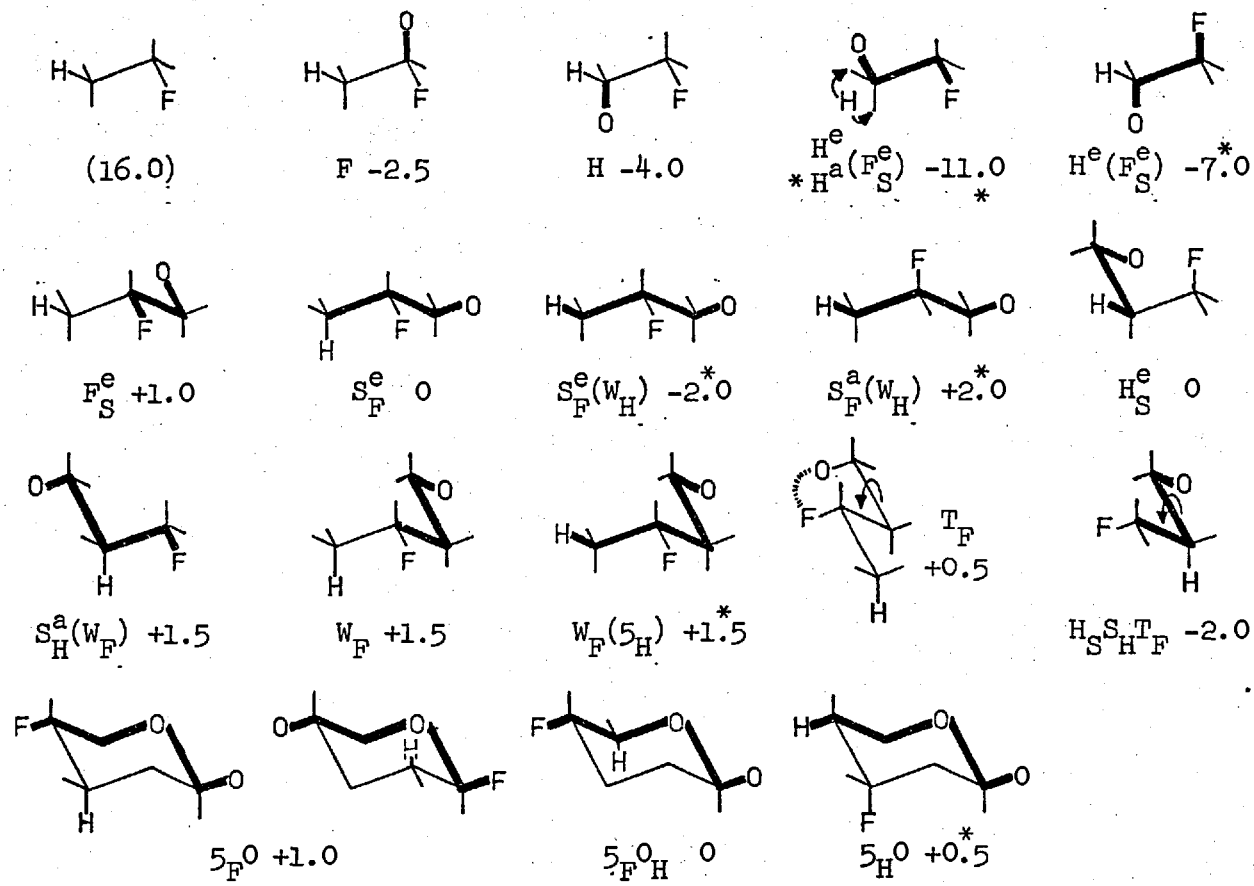
Tentative evaluation of these parameters has been performed by utilising several "justifiable" approximations, ie : $5_H0 \gg 1$; $W_F = W_F(5_H) = +1.5$; $H^e(F^e_S) = H^a(F^e_S) = -11$, etc.

In a similar, though far less extensive, examination of the gauche coupling data, Phillips and Wray[126] only identified five perturbations. These, using the mnemonics in FIG.4-8.11 were :

F or H = -2.5; any $H(F_S)$ = -7.0;

S^e_F or $S^e_F(W_H)$ = -2.0; $S^a_F(W_H)$ or $S^a_H(W_F)$ = +2.0.

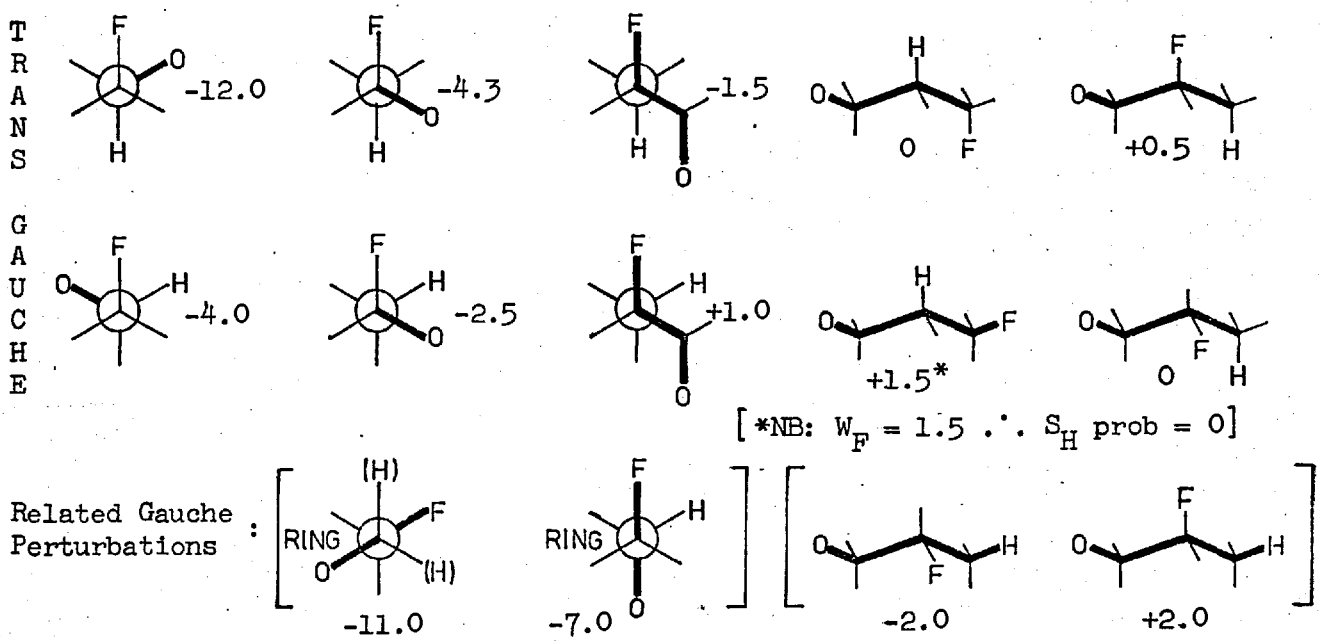
FIG.4-8.11 Perturbations to Gauche $^3J_{HF}$ Couplings



With this limited set of parameters the gauche couplings could be predicted with an average error of ±0.75Hz. With the full set of parameters given above, predicted and observed J's were identical in every case.

This illustrates the extreme sensitivity of $^3J_{HF}$ couplings to

FIG.4-8.12 Comparison of Perturbations Common to both Gauche and Trans $^3J_{HF}$.



substituent effects, even over 4 or 5 bonds. Comparison of the perturbations common to both the gauche and trans couplings (see FIG.4-8.12) gives an indication of the difficulties present in deriving equations of the form :

$$^3J_{HF} = J^0 f(\phi) + b\Sigma(E_X . f(\Psi)) + c \qquad \text{EQN.86}$$

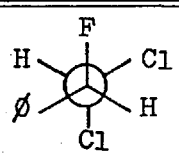
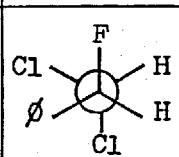
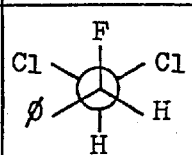
(where ϕ = the HF dihedral angle; Ψ = the XH or XF dihedral angles; and b and c are constants); which adequately define the dihedral angle and substituents/dihedral angle dependence of $^3J_{HF}$ in non-rigid systems. Such is the problem posed here for before the $^3J_{HF}$ and $^3J_{HH}$ coupling data of the Type (V) fluorides (which undoubtedly arises, not from single rotamers, but from population weighted rotamer averages) can be utilised to calculate preferred rotamer geometries we require some model on which to base accurate estimates of the individual rotamer couplings.

If the orientation dependence of the electronegative effects are taken into account it should be relatively easy to rank the three main rotamer couplings (even is their actual values are much harder to calculate). This is illustrated in TABLE 4-8.3 where EQN.86 has been applied with the following assumptions :

(1) both $f(\phi)$ and $f(\Psi)$ are $\cos^2$ functions, ie. gauche effects are $\frac{1}{4}$ the size of trans effects.

(2) the magnitudes of the electronegative effects are proportional to the "difference" Huggins electronegativity, ie. $E_X(X-H)$ - see TABLE 4-6.1.

TABLE 4-8.3 $^3J_{HH}$ and $^3J_{HF}$ - Prediction of the Relative Size of the Three Rotamer Couplings

ROTAMER NUMBER	CONFORMATION	$^3J_{HH}$ E_{neg} Contributions	$^3J_{HH}$ Expected Value	$^3J_{HF}$ E_{neg} Contributions	$^3J_{HF}$ Expected Value
1		HH trans Cl 0.5 F 0.25 ϕ 0.25	A - 1.15b + c	HH gauche 1 Cl 1.25 ϕ 0.25	0.25A' - 1.45b' + c'
2		HH gauche 1 Cl 1.25 F 0.25 ϕ 1.00	0.25A - 2.50b + c	HF gauche 2 Cl 1.25 ϕ 1.00	0.25A' - 2.05b' + c'
3		HH gauche 2 Cl 1.25 F 1.00 ϕ 0.25	0.25A - 3.20b + c	HF trans Cl 0.5 ϕ 0.25	A' - 0.70b' + c'

Even though A,A'b,b',c,&c' are unspecified in this approxixation the rank of the J's can readily be seen to be : J(trans) $\gg$ J(gauche 1) $>$ J(gauche 2).

From the figures overleaf, the time averaged couplings under free rotation are : 0.5A - 2.28b + c and 0.5A' - 1.40b' + c' ie. nearer J(gauche 1) than J(trans).

From purely steric considerations, the order of preference for the three rotamers (when the ring substituent is in the para position) would be :

Rotamer 1 $>$ Rotamer 3 $\gg$ Rotamer 2

this does not, however, take account of the more specific electronic repulsions present between the halogens in the Type (V) and (VI) series or between the hydroxy group and the two chlorine atoms in the Type (IV) alcohols. For example, the most stable rotamer in 1,1,2,2-tetrachloroethane has the hydrogens gaucne and not trans as might be expected.[265]

From a detailed examination of the temperature dependence (over the range 210-470°K) of the ^{1}H and ^{19}F spectra of a variety of polyhaloethanes, Gutowsky et al[265] were able to isolate the $^{3}J_{HH}$ and $^{3}J_{HF}$ couplings due to the individual rotamers. Although the values of these couplings are the main concern here, the analytical method used is of direct relevance to any further work on the compounds under study and will therefore be briefly summarised.

The observed couplings (or shifts) may be given by an equation of the type :

$$\langle J_{ij} \rangle = x_1 J_1^{ij} + x_2 J_2^{ij} + x_3 J_3^{ij} \qquad \text{EQN.87}$$

Where the indices refer to the rotamers and x denotes the mole fraction.

The population ratios $x_1 : x_2 : x_3$ are dependent on the relevant energies of the three rotamers. If we define $\Delta E_1 = E_1 - E_3$ and $\Delta E_2 = E_2 - E_3$ then :

$$x_1 : x_2 : x_3 \qquad \exp(-E_1/RT) : \exp(-E_2/RT) : 1 \qquad \text{EQN.88}$$

The averaged coupling is then given by EQN.89 :

$$\langle J_{ij} \rangle = \frac{[J_1^{ij}\exp(-\Delta E_1/RT) + J_2^{ij}\exp(-\Delta E_2/RT) + J_3^{ij}]}{[\exp(-\Delta E_1/RT) + \exp(-\Delta E_2/RT) + 1]} \qquad \text{EQN.89}$$

If the temperature dependence of $\langle J_{ij} \rangle$ results only from changes in the equilibrium proportions of the rotamers then it is possible, by a five parameter least squares type analysis, to calculate the individual couplings (or shifts) and ΔE's involved.

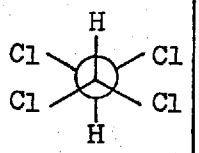
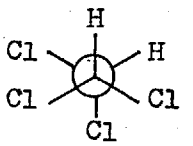
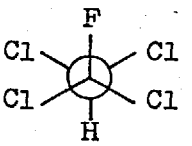
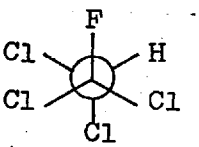
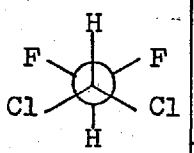
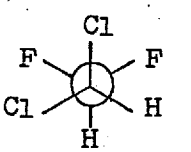
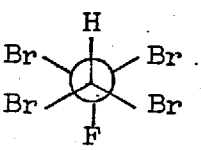
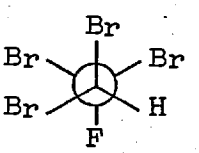
The couplings calculated for several halo-ethanes are given in TABLE 4-8.4 with particular attention paid to $CHFCl.CHCl_2$ in TABLE 4-8.5.

In TABLE 4-8.5, the assignments of the two $^{3}J_{HH}$ gauche couplings (marked '*') have been interchanged with those given by Gutowsky et al,[265] because :

(1) The assignment given[265] is much less likely than the one chosen above; ie. trans effects should be stronger than gauche effects.

(2) The method used derived the $^{3}J_{HH}$ and $^{3}J_{HF}$ couplings independently from

TABLE 4-8.4 $^3J_{HH}$ and $^3J_{HF}$ Couplings in Polyhaloethanes, from ref.265 unless otherwise stated.

trans $^3J_{HH}$		gauche $^3J_{HH}$	trans $^3J_{HF}$	gauche $^3J_{HF}$
	Average $^3J_{HH}$ 6.70 Obs: 3.10 (@ 22°C)			
16.35 ± 0.8		2.01 ± 0.08	17.9 ± 0.5[267] 18.20 ± 0.08	<2[267] 1.00 ± 0.02
	Average $^3J_{HH}$ 4.76 Obs: 7.75 (@ 22°C) $^3J_{HF}$ obs 7.75			
10.25 ± 0.4		2.01 ± 0.09	22.2[266]	1.15[266]

each other and the structures. The assignment of the couplings to the rotamers was then performed "by eye", using the calculated ΔE values (which in this case were very variable) as a guide. The authors stated that the $^3J_{HF}$ gauche couplings could be misassigned because of the poor ΔE agreement between the J_{HF} and J_{HH} analyses. From our experience it appears more likely that the $^3J_{HH}$ data is misassigned (see also SECTION 4-3-2.3).

Repeated attempts, both graphical and algebraic, at deriving single equations to describe the $^3J_{HF}$ couplings observed in the three cases shown in TABLES 4-8.4 and 4-8.5 and in the unperturbed case (J_t = 43.5, J_g = 16.0Hz), were unsuccessful. The approaches used were based on EQN.86 and its "improved" successors EQNS.90 and 91.

$$^3J_{HF}^{60} = J_g + F\Sigma(E_F f(\Psi)) + H\Sigma(E_H f(\Psi)) + f(G) \qquad \text{EQN.90}$$

$$^3J_{HF}^{180} = J_t + F\Sigma(E_F f(\Psi)) + H\Sigma(E_H f(\Psi)) + f(G) \qquad \text{EQN.91}$$

Where J_g, J_t, F and H are constant for all compounds.

E_F and E_H are the separated vicinal E_{neg} interactions to F and H respectively.

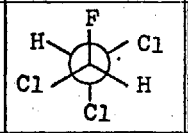
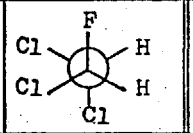
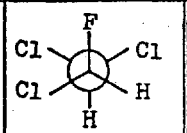
$f(\Psi)$ is a dihedral angle function such as $\cos^2\Psi$, $\cos\Psi$, $|\cos\Psi|$, etc.

$f(G)$ is a geminal geometric term, constant for all three rotamers of any compound.

The E_F and E_H terms were calculated with and without the electronegative interactions of the coupled nuclei themselves using Huggins and "difference" Huggins values.

Since a unique solution could not be found for these simple cases (three

TABLE 4-8.5 $^3J_{HH}$ and $^3J_{HF}$ Couplings in $CHFCl.CHCl_2$[265]

ROT No.	CONFORMATION	$^3J_{HH}$ E_{neg} CONTRIBUTIONS	OBSERVED $^3J_{HH}$ EXPECTED $^3J_{HH}$	$^3J_{HF}$ E_{neg} CONTRIBUTIONS	OBSERVED $^3J_{HF}$ EXPECTED $^3J_{HF}$	$^2J_{HF}$
1		HH trans	16.5 ± 0.3	HF gauche 1	13.2 ± 0.4	
		Cl 0.75 F 0.25	A - 1.19b + c	Cl 1.150	0.25A' - 1.50b' + c'	49.1 ± 0.2
2		HH gauche 1 Cl 2.25 F 0.25	1.63 ± 0.15* 0.25A - 2.69b + c	HF gauche 2 Cl 2.25	-2.8 ± 0.4 0.25A' - 2.25b' + c'	49.1 ± 0.2
3		HH gauche 2	-2.62 ± 0.65*	HF trans	37.3 ± 0.3	
		Cl 1.5 F 1.0	0.25A - 3.24b + c	Cl 0.75	A' - 0.75b' + c'	49.1 ± 0.2
EXPECTED TIME Av COUPLINGS			5.17 0.5A - 2.38b + c		15.9 0.5A' - 1.5b' + c'	49.1 ± 0.2
OBSERVED AT 22°C			3.64 ± 0.07 3.7[268]		9.07 ± 0.13 9.4[268]	49.1 ± 0.2

of the four compounds having only one gauche coupling) this approach was abandoned. Although unable to calculate "from scratch" values for $^3J_{HF}$ and $^3J_{HH}$ couplings in the Type (V) compounds, a clear route to their close estimation from the analysed model systems of Gutowsky et al[265] was still open. The constituent couplings of $CHCl_2.CHFCl$ are particularly helpful here, as, in terms of electronegativities, this model is almost identical to the Type (V) fluorides (see TABLES 4-8.3 & 4-8.5).

4-8-2.3 Calculation of Rotamer Populations in the Type (V) Fluorides.

If the constituent $^3J_{HH}$ and $^3J_{HF}$ couplings are known for each rotamer of a compound such as $CHFX.CHCl_2$ then the relative rotamer populations may be calculated from the observed population weighted values (ie. $\langle {}^3J_{HH} \rangle$ & $\langle {}^3J_{HF} \rangle$) by using the following equations :

$$\langle {}^3J_{HH} \rangle = x_1 {}^3J_1^{HH} + x_2 {}^3J_2^{HH} + x_3 {}^3J_3^{HH} \qquad \text{EQN.92}$$

$$\langle {}^3J_{HF} \rangle = x_1 {}^3J_1^{HF} + x_2 {}^3J_2^{HF} + x_3 {}^3J_3^{HF} \qquad \text{EQN.93}$$

$$1 = x_1 + x_2 + x_3 \qquad \text{EQN.94}$$

$$x_1 = \frac{\begin{vmatrix} \langle J_{HH} \rangle & J_2^{HH} & J_3^{HH} \\ \langle J_{HF} \rangle & J_2^{HF} & J_3^{HF} \\ 1 & 1 & 1 \end{vmatrix}}{\begin{vmatrix} J_1^{HH} & J_2^{HH} & J_3^{HH} \\ J_1^{HF} & J_2^{HF} & J_3^{HF} \\ 1 & 1 & 1 \end{vmatrix}} = x_2 = \frac{\begin{vmatrix} J_1^{HH} & \langle J_{HH} \rangle & J_3^{HH} \\ J_1^{HF} & \langle J_{HF} \rangle & J_3^{HF} \\ 1 & 1 & 1 \end{vmatrix}}{\begin{vmatrix} J_1^{HH} & J_2^{HH} & J_3^{HH} \\ J_1^{HF} & J_2^{HF} & J_3^{HF} \\ 1 & 1 & 1 \end{vmatrix}} = x_3 = \frac{\begin{vmatrix} J_1^{HH} & J_2^{HH} & \langle J_{HH} \rangle \\ J_1^{HF} & J_2^{HF} & \langle J_{HF} \rangle \\ 1 & 1 & 1 \end{vmatrix}}{\begin{vmatrix} J_1^{HH} & J_2^{HH} & J_3^{HH} \\ J_1^{HF} & J_2^{HF} & J_3^{HF} \\ 1 & 1 & 1 \end{vmatrix}} = 1 \qquad \text{EQN.95}$$

If the coupling constants for $CHFCl.CHCl_2$ in TABLE 4-8.5 are taken as being (a) correct and (b) approximately equal to the couplings in the Type (V) fluorides, the above determinant (EQN.95) can be expanded to EQNS.96-98 to directly calculate the rotamer populations in the Type (V) fluorides (see TABLE 4-8.6 and FIG.4-8.13.

$$x_1 = (53.463 - 40.1\langle J_{HH}\rangle - 4.25\langle J_{HF}\rangle)/-664.286 \qquad \text{EQN.96}$$

$$x_2 = (-650.034 + 24.1\langle J_{HH}\rangle + 19.12\langle J_{HF}\rangle)/-664.286 \qquad \text{EQN.97}$$

$$x_3 = (-67.716 + 16.0\langle J_{HH}\rangle - 14.87\, J_{HF})/-664.286 \qquad \text{EQN.98}$$

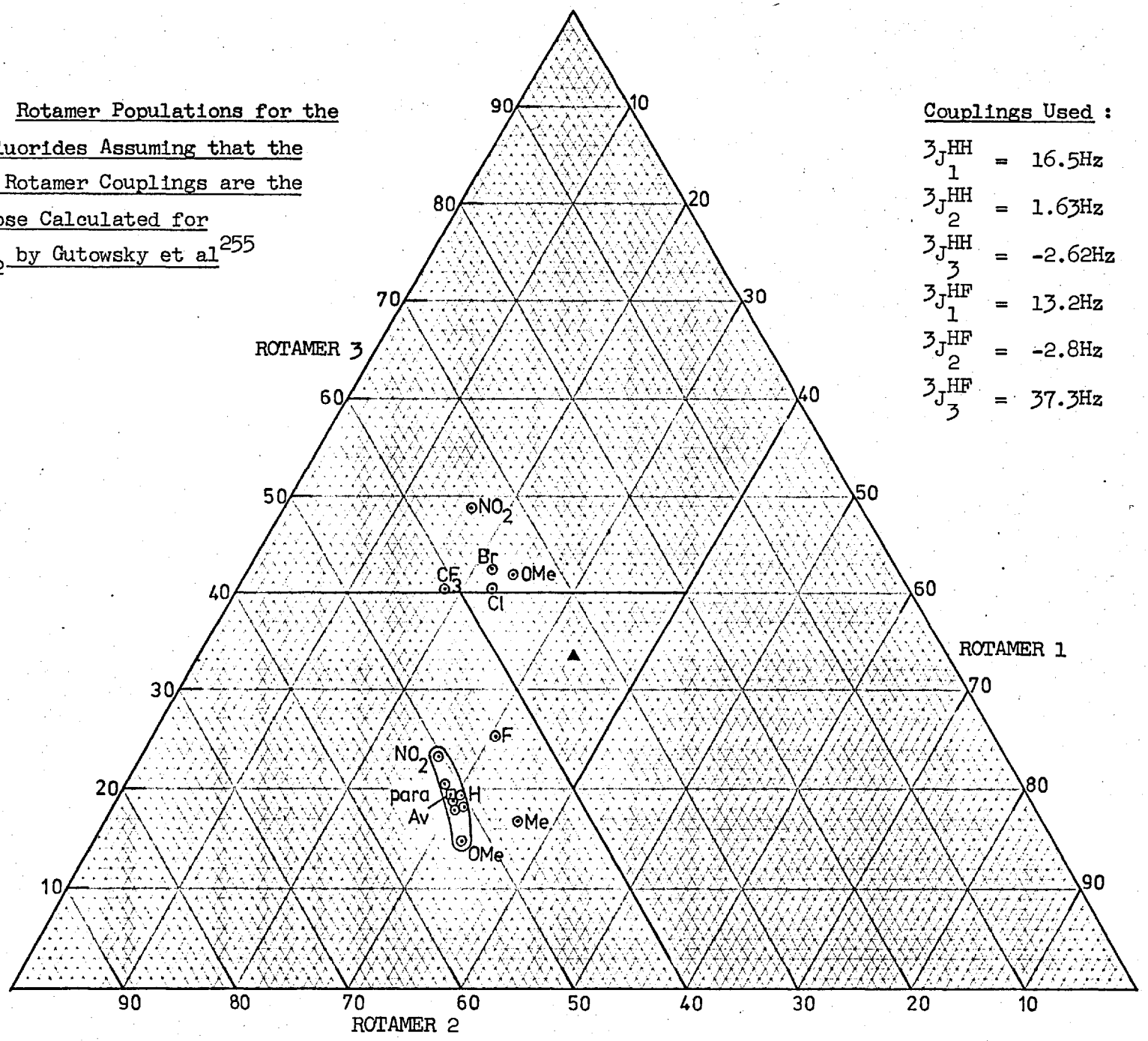
Unfortunately on inspection the calculated couplings for $CHFCl.CHCl_2$[265] are rather dubious. This is particularly noticeable in the two trans J's : $^3J_{HH} = 16.5$; $^3J_{HF} = 37.3$Hz. The former is 4Hz or so larger than the normally expected range of trans $^3J_{HH}$[114] whilst the latter is barely reduced at all from the unperturbed value of 43.5Hz.[260]

The problem undoubtedly lies in the difficulty of the analysis undertaken by Gutowsky et al.[265] Whereas all the compounds in TABLE 4-8.4 have two equivalent gauche rotamers and only require a three parameter analysis, $CHFCl.CHCl_2$ has three non-equivalent rotamers giving rise to five parameters. Errors in the analytical method are therefore more prominent in the latter case.

TABLE 4-8.6 First Approximation to the Rotamer Populations in the Type (V) Fluorides

Deriv X	$\langle^3J_{HH}\rangle$	$\langle^3J_{HF}\rangle$	x_1	x_2	x_3
H	5.40	9.75	30.79	50.20	19.01
o F	5.10	12.15	30.51	44.38	25.11
o Cl	3.30	17.00	22.75	36.95	40.30
o Br	3.05	17.65	21.66	35.99	42.36
o Me	6.35	9.85	36.65	46.47	16.95
o OMe	3.40	17.80	23.86	34.29	41.85
o NO_2	2.00	19.40	16.44	34.76	48.80
o CF_3	2.70	16.30	18.68	41.14	40.18
p F	5.40	9.25	30.47	51.64	17.89
p Cl	5.25	9.55	29.75	51.32	18.93
p Br	5.20	9.60	29.48	51.35	19.16
p Me	5.50	9.45	31.20	50.70	18.10
p OMe	5.70	8.60	31.86	52.42	15.72
p NO_2	4.60	10.75	26.60	50.22	23.18
p CF_3	5.00	9.90	28.47	51.22	20.31
Av.pX(inc H)	5.26	9.61	29.79	51.18	19.04

FIG.4-8.13 Rotamer Populations for the Type (V) Fluorides Assuming that the Individual Rotamer Couplings are the Same as Those Calculated for $CHFCl.CHCl_2$ by Gutowsky et al[255]



Couplings Used :

$^3J_1^{HH}$ = 16.5Hz

$^3J_2^{HH}$ = 1.63Hz

$^3J_3^{HH}$ = -2.62Hz

$^3J_1^{HF}$ = 13.2Hz

$^3J_2^{HF}$ = -2.8Hz

$^3J_3^{HF}$ = 37.3Hz

If the trans $^3J_{HF}$ couplings in $CFCl_2CHCl_2$ (18.2Hz) and $CFBr_2CHBr_2$ (22.2Hz) are taken as being correct then it is found that they are fairly accurately predicted by a modification of the method developed earlier for the deoxyfluoro pyranoses (see FIG.4-8.10). This merely involves scaling the perturbation to the electronegativity of the new substituent eg. perturbation 'F' when substituent = Cl is given by $-4.3(E_{Cl} - E_H)/(E_O - E_H) = -3.3$Hz. Thus the following trans $^3J_{HF}$ couplings may be calculated :
$CFCl_2CHCl_2$(18.4Hz); $CFBr_2CHBr_2$(23.4Hz); $CHFClCHCl_2$(21.7Hz); $CHF\emptyset CHCl_2$(22.4Hz).
If allowance is made for the apparent systematic error ie. $CFCl_2CHCl_2$ adjusted to 18.2Hz and $CFBr_2CHBr_2$ to 22.4Hz we obtain $CHFClCHCl_2$ (20.9Hz) and $CHF\emptyset CHCl_2$ (21.4Hz). Before adjustment there was excellent agreement between them and the values for the two symmetrical molecules as calculated by the method of Gutowsky et al.[265,266] This was clearly not the case for $CHFCl.CHCl_2$ indicating some fundamental error in the five parameter fitting routine used.[255] We will use the adjusted values as the "best estimate" of the trans $^3J_{HF}$ couplings.

A similar approach to the calculation of the gauche $^3J_{HF}$ couplings, using the "additive perturbation method", may be adopted.

From observation of the factors affecting both the gauche and trans $^3J_{HF}$ couplings (see FIGS.4-8.10 & 11 and the work of Abraham and Cavalli[261]) there is an obvious trend for perturbations which withdraw electrons from the C-H bond (ie. perturbations 'H' or '$F(H_S)$') to reduce the coupling significantly more than those affecting the C-F bond (ie. 'F' or '$H(F_S)$'). This is presumably because transmission of the coupling depends on the electron density throughout the "coupling path" and it is far easier to withdraw electrons from the C-H bond (hence reducing the transmission) than from the C-F bond. As stated in the previous sub-section it was found impossible to solve EQNS.90 & 91 for the $^3J_{HF}$ data considered, particularly for the gauche couplings in $CFBr_2CHBr_2$ (1.8Hz) and $CFCl_2CHCl_2$ (1Hz). Since the latter has the same basic substituents as $CHFClCHCl_2$ and $CHF\emptyset CHCl_2$ it is a better model than the former. Using the ratio C-H : C-F perturbations = 4 : 2.5, we obtain : 'H' = 4, 'F' = 2.5, '$H(F_S)$' = 5 and '$F(H_S)$' = 8. These give the following gauche couplings : $CFCl_2CHCl_2$ (1Hz), $CHFClCHCl_2$ (7.15,2.92Hz) and $CHF\emptyset CHCl_2$ (7.54,4.15Hz), which although approximate, are probably more realistic than those given by Gutowsky et al.[265]

The "best fit" $^3J_{HH}$ coupling constants for a number of 1,1,2-trihalophenylethanes and 1,1,2-trihalopropanes have been calculated by Reynolds and Wood[118] (see SECTION 1-5-1) to be 9.3, 2.6 and 1.8Hz. These were assigned to rotamers 1, 3 and 2[118] but as with $CHFClCHCl_2$ earlier (see FIG.4-8.5) the gauche assignments have been reversed here. In fact, if the original assignments are used with the oNO_2 Type (V) data, a negative population is found for

rotamer 1! The population calculated by Reynolds and Wood for 1,1,2-trichlorophenyl ethane (ie. the unsubstituted Type (VI) chloride) were 0.53, 0.34 & 0.13 for rotamers 1, 2 and 3 respectively. These give calculated $^3J_{HH}$ couplings of 5.88Hz by their assignment and 6.05Hz by the assignment used here. The latter compares favourably with the observed $^3J_{HH}$ of 5.98Hz.[118] The resequenced $^3J_{HH}$ values of Reynolds and Wood will be used for the Type (V) fluorides. The derived values for the various couplings in $CHF\emptyset CHCl_2$ are therefore :

TABLE 4-8.7 Best Estimates for the $^3J_{HH}$ and $^3J_{HF}$ Couplings in the Type (V) Fluorides

ROTAMER	1	2	3
$^3J_{HH}$	9.3	2.6	1.8
$^3J_{HF}$	7.54	4.15	21.4

If the calculated values of $^3J_{HH}$ and $^3J_{HF}$ for $CHF\emptyset CHCl_2$ are substituted in EQN.95 the following equations are obtained :

$$x_1 = (48.17 - 17.25\langle J_{HH}\rangle - 0.8\langle J_{HF}\rangle)/-118.287 \qquad \text{EQN.99}$$

$$x_2 = (-185.448 + 13.86\langle J_{HH}\rangle + 7.5\ J_{HF})/-118.287 \qquad \text{EQN.100}$$

$$x_3 = (18.991 + 3.39\langle J_{HH}\rangle - 6.7\langle J_{HF}\rangle)/-118.287 \qquad \text{EQN.101}$$

The calculated rotamer populations from the "raw" Type (V) coupling data are shown below :

TABLE 4-4.8 Rotamer Populations in Type (V) Fluorides using "Best Estimate" Coupling Data

Deriv X	$\langle^3J_{HH}\rangle$	$\langle^3J_{HF}\rangle$	x_1	x_2	x_3
H	5.40	9.75	44.62	31.69	23.69
o F	5.10	12.15	41.87	19.98	38.15
o Cl	3.30	17.00	18.90	10.32	70.78
o Br	3.05	17.65	15.69	9.13	75.18
o Me	6.35	9.85	58.54	19.92	21.54
o OMe	3.40	17.80	20.90	4.08	75.02
o NO_2	2.00	19.40	1.56	10.34	88.10
o CF_3	2.70	16.30	9.68	21.79	68.53
p F	5.40	9.25	44.28	34.86	20.86
p Cl	5.25	9.55	42.30	34.71	22.99
p Br	5.20	9.60	41.60	34.98	23.42
p Me	5.50	9.45	45.98	32.42	21.71
p OMe	5.70	8.60	48.22	35.46	16.32
p NO_2	4.60	10.75	33.63	34.72	31.65
p CF_3	5.00	9.90	38.89	35.42	25.69
Av.pX(inc.H)	5.26	9.61	42.48	34.21	23.30

Since the para substituents can have no steric influence on the rotamer preferences of the ethyl side-chain, their only mechanism of affecting the coupling constants is electronic. This may take two forms :

(a) The rotamer preferences are the same for all the para derivatives and the differences observed in the couplings merely reflect the electron donating/withdrawing abilities of the ring substituent.

(b) By donating/withdrawing varying levels of electron density from the side-chain the para substituents alter the relative energies of the three rotamers. This would lead to slight differences in the rotamer population from one substituent to another.

The latter case is allowed for in TABLE 4-8.8. If the approximation that the through bond electronic influence of the substituents is the same in both the ortho and para derivatives then the variations in the coupling constants not due to rotamer preferences in the ortho substituent may be allowed for, (see TABLE 4-8.9). In reality a mixture of these two interactions probably occurs.

Since the couplings observed when X = H (see FIG.4-8.5) lie off the straight line given by the remainder of the para derivatives, the deviation of the couplings for the individual substituents are referred to the overall average of the para couplings.

The rotamer population calculated in TABLES 4-8.8 & 4-8.9 can only be assumed to be rough guides to the structures pertaining in the chloroform solutions, because of the inaccuracies inherent in the various routes adopted

TABLE 4-8.9 Rotamer Populations in the Type (V) Fluorides using para-Adjusted ortho Coupling Data

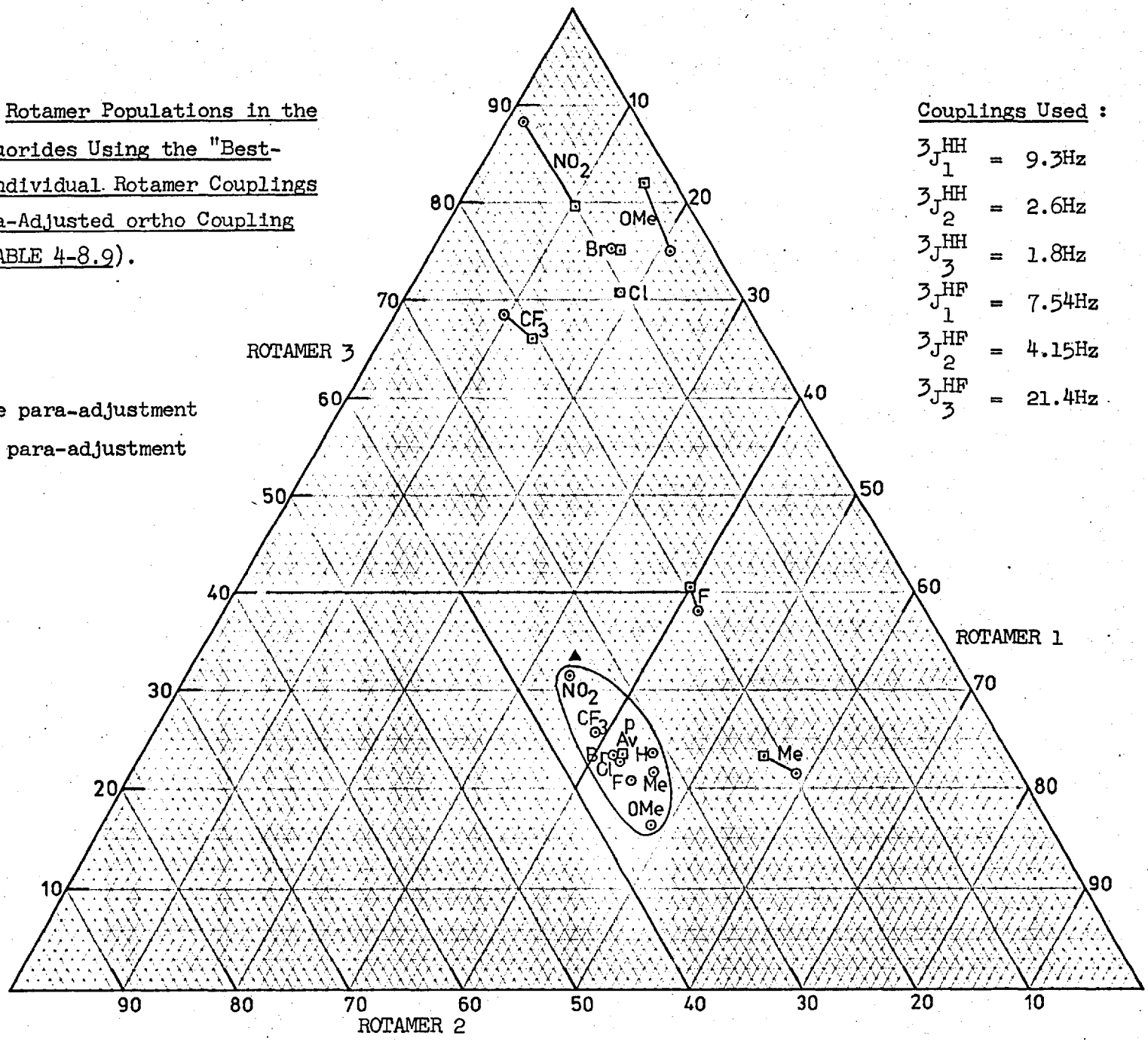
DERIV	$\langle {}^3J_{HH} \rangle$				$\langle {}^3J_{HF} \rangle$				Adjusted Rotamer Populations		
	para		ortho		para		ortho				
X	Obs J	ΔJ	Obs J	Adj J	Obs J	ΔJ	Obs J	Adj J	x_1	x_2	x_3
para Av	5.25				9.60				42.33	34.39	23.28
o F	5.40	+0.15	5.10	4.95	9.25	-0.35	12.15	12.50	39.92	19.52	40.56
o Cl	5.25	0	3.30	3.30	9.55	-0.05	17.00	16.95	18.87	10.64	70.50
o Br	5.20	-0.05	3.05	3.10	9.60	0	17.65	17.65	16.42	8.54	75.03
o Me	5.50	+0.25	6.35	6.10	9.45	-0.15	9.85	10.00	55.00	21.90	23.10
o OMe	5.70	+0.45	3.40	2.95	8.60	-1.00	17.80	18.80	15.01	3.01	81.98
o NO_2	4.60	-0.65	2.00	2.65	10.75	+1.15	19.40	18.25	10.27	10.01	79.72
o CF_3	5.00	-0.25	2.70	2.95	9.90	+0.30	16.30	16.00	13.12	20.76	66.12

to estimate the individual rotamer coupling constants. The rotamer distributions calculated in TABLES 4-8.8 and 4-8.9 are shown graphically in FIG.4-8.14.

FIG.4-8.14 Rotamer Populations in the Type (V) Fluorides Using the "Best-Estimate" Individual Rotamer Couplings and the para-Adjusted ortho Coupling Data (see TABLE 4-8.9).

⊙ = Before para-adjustment

⊡ = After para-adjustment



Couplings Used :

$^3J_1^{HH}$ = 9.3Hz

$^3J_2^{HH}$ = 2.6Hz

$^3J_3^{HH}$ = 1.8Hz

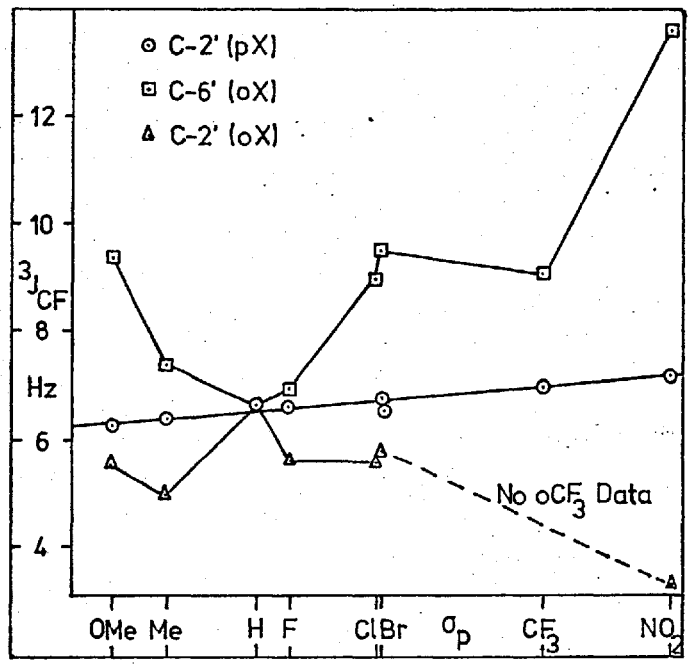
$^3J_1^{HF}$ = 7.54Hz

$^3J_2^{HF}$ = 4.15Hz

$^3J_3^{HF}$ = 21.4Hz

4-8-2.4 Trends Observed in the $^3J_{CF_1}$ Couplings

The relevant $^3J_{CF_1}$ couplings fron TABLE 4-5.5 are plotted in FIG.4-8.15 againt Hammett σ_p.



As expected the couplings for the para derivatives show a linear relationship to σ_p. This is not the case for the ortho derivatives and it is again tempting to assume that this is solely a conformational effect. Some of the idiosyncrasies of $^3J_{CF}$ couplings have already been mentioned (see SECTION 1-5-1), but a further examination of $^3J_{CF}$ couplings in models approximating to the system studied here is required.

FIG.4-8.15 $^3J_{CF_1}$ Couplings in the Type (V) Fluorides

4-8-2.5 Empirical Approach to the Analysis of $^3J_{CF}$ Couplings

Ortho-substituted trifluoromethyl benzene was used as a model for the measurement of substituent effects on $^3J_{CF}$ couplings. Although many $^1J_{CF}$ coupling studies have been reported there are still surprisingly few reports of $^nJ_{CF}$ couplings. In the absence of a suitable reference, therefore, the less satisfactory substituted fluoro benzenes have been used.

The $^2J_{CF}$ and $^3J_{CF}$ couplings for a range of ortho- and meta- substituted fluorobenzenes[269-272] are plotted in FIG.4-8.16. These clearly show that the magnitude of the couplings to symmetrically disposed nuclei have a high dependence on the nature of the substituents they carry. Further examples of this are seen in the work of Doddrell et al,[273,274] (see FIG.4-8.17).

With the exception of the ortho-fluoro trifluoromethylbenzene data,[272] which although incomplete indicates that the presence of the ortho-fluorine reduces the coupling to C-2 by ~1.3Hz, there is little available data for systems directly analogous to the Type (V) fluorides. The data presented does however establish the sensitivity of $^nJ_{CF}$ couplings to ring substituents and in the light of the insensitivity of $^3J_{CH}$ in toluene to dihedral angle[124] (see FIG.1-5.5) there is insufficient evidence to enable conformational data to be deduced from the $^3J_{CF}$ couplings with any confidence.

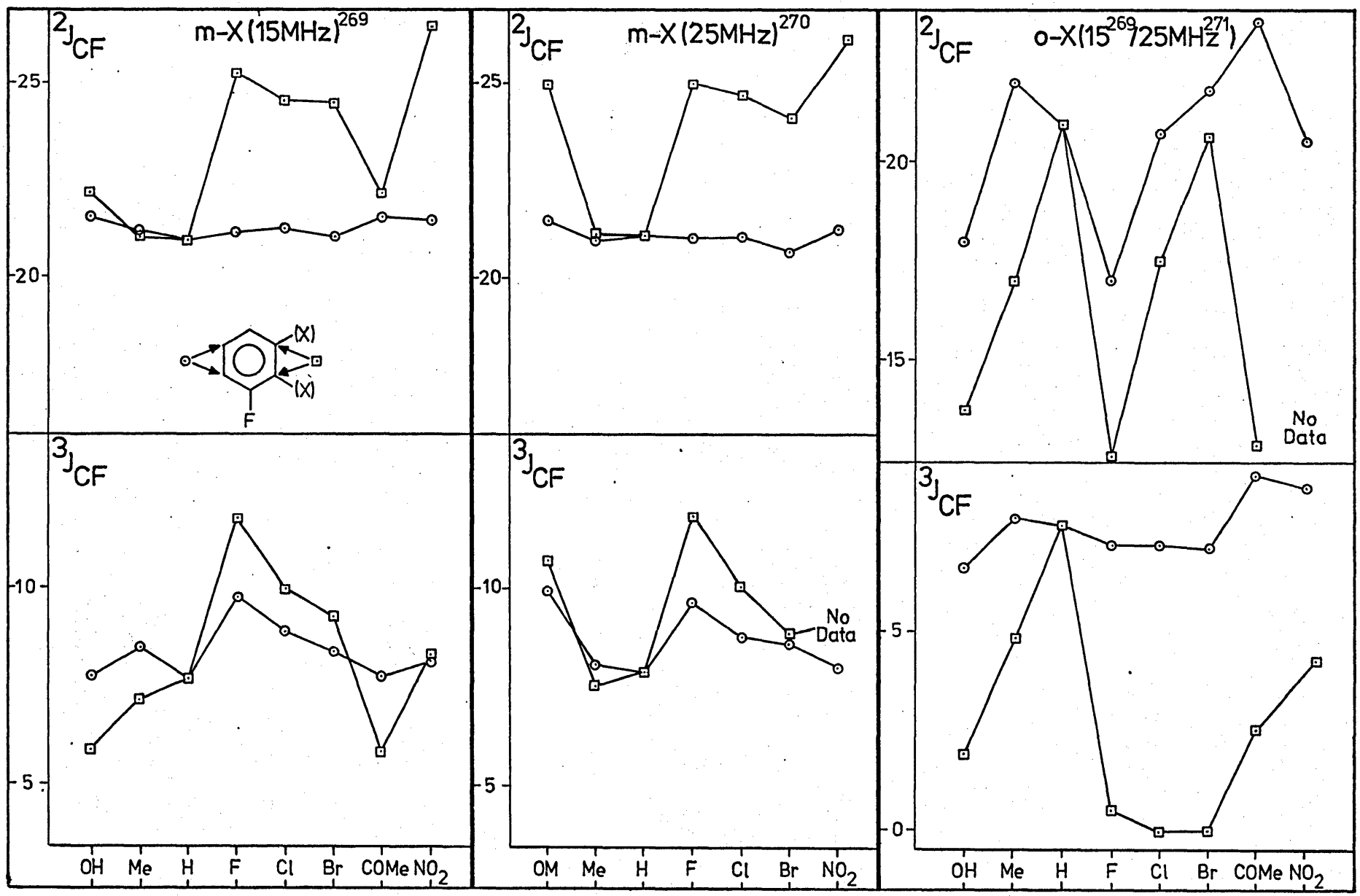


FIG.4-18 $^2J_{CF}$ and $^3J_{CF}$ in meta- and ortho-substituted Fluorobenzenes.[269-271]

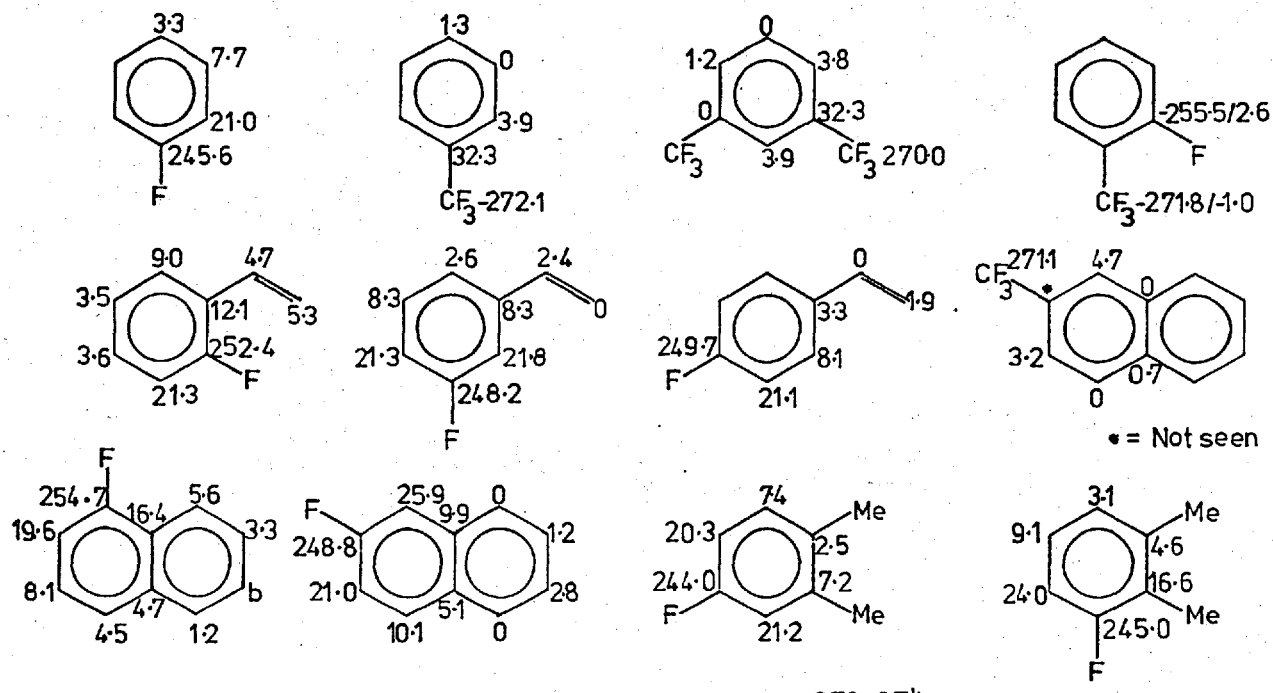


FIG.4-8.17 Substituent Effects on $^{n}J_{CF}$ Couplings[272-274]

4-8-3 Conformational Information Contained in the Long-Range Coupling Data

There are several sets of long range couplings between various nuclei :

The Type (V) fluorides have both $^{5}J_{HF}$ and $^{7}J_{HF}$ couplings to the ortho and para methyl substituents of 1.0 and 1.3Hz respectively. Since the longer range coupling is larger, the 1.0Hz coupling to the ortho methyl protons cannot be considered to be a through space interaction.

Conversely both the ortho fluoro and ortho trifluoromethyl groups in the Type (VI) chlorides show a 0.3Hz coupling ($^{5}J_{H_AF}$ and $^{6}J_{H_AF}$ respectively) to the side-chain proton H_A. These are almost definitely through space interactions indicating that these compounds have the side-chain predomonantly in rotamers 1 or 3 (see TABLE 4-8.3).

In rotamer 2 through space interactions between an ortho ring substituent and the side-chain H_A proton are impossible because of the trans arrangement of H_A and the phenyl ring. This is not so in either rotamers 1 or 3 (see FIG. 4-8.18). Since the relative populations of the oF(V) and oCF_3(V) are : 40 : 20 : 40 and 10 : 20 : 70 respectively (both spend 80% of the time in rotamers 1 or 3) then the oF(VI) and oCF_3(VI) data is not incompatible with the calculations performed on the Type (V) series (see SECTION 4-8-2.3).

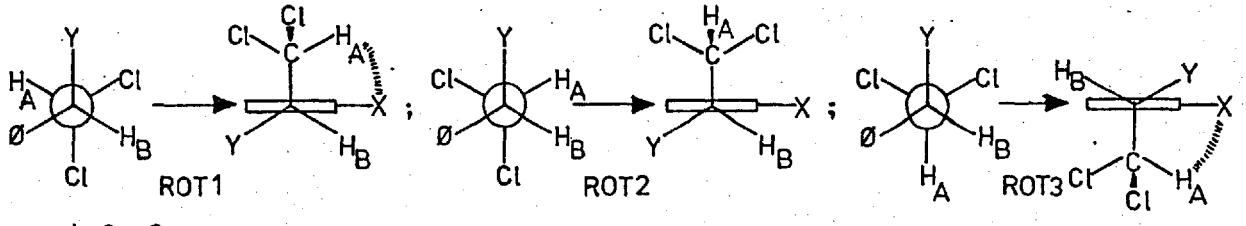


FIG.4-8.18 Through Space Coupling Interactions to H_A

Long range $^{n}J_{FF}$ couplings were observed in the four Type (V) fluorides with ring fluorine substituents. Of these the 2.6Hz coupling to the oCF_3 group ($^{5}J_{FF}$ - cf. $^{4}J_{FF}$ to oF of 1.4Hz) is probably a through-space interaction, which is most likely to occur in the conformation shown in FIG.4-8.19.

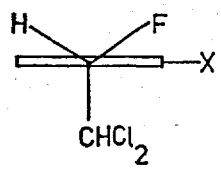


FIG.4-8.19

Among the remaining long range couplings are the $^{5}J_{F_1C_{4'}}$ couplings in the Type (V) fluorides. Not unexpectedly these are rather small (see FIG.4-8.20) and because of the high uncertainty (±0.5Hz) contain no useful conformational data.

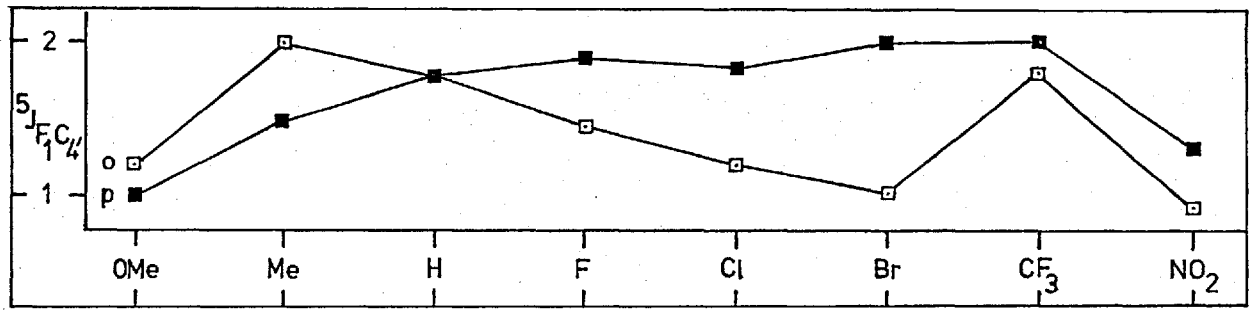


FIG.4-8.20 $^{5}J_{F_1C_{4'}}$ Couplings in the Type (V) Fluorides.

Similarly the $^{n}J_{CF_2}$ couplings in the Type (IV), (V) & (VI) series contain little data of use for conformational analysis. They are, however, of interest in themselves and are therefore illustrated in FIG.4-8.21. Note that the couplings to C-2 are stronger than those to C-1 in all the fluoro derivatives. Similar phenomena have been reported in fluoro-styrenes and napthenes[273,274] (see FIG.4-8.17) and in diphenyl acetylenes.[256]

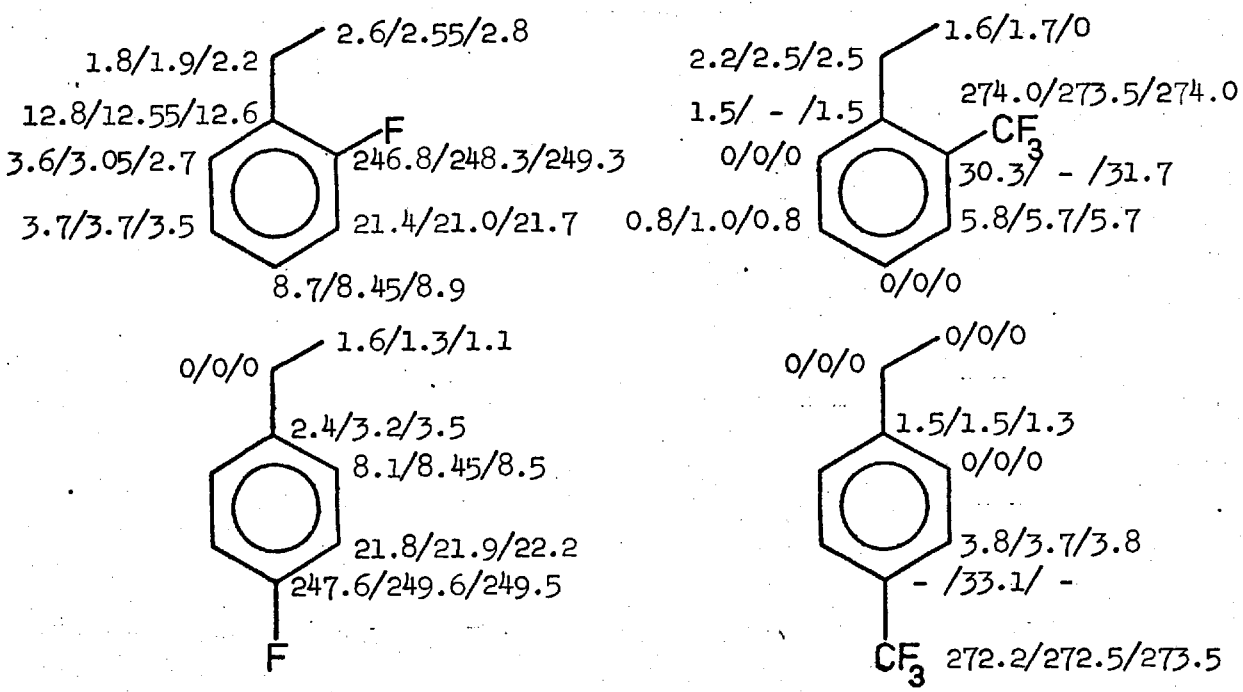


FIG.4-8.21 $^{n}J_{CF}$ Couplings in the Type (IV), (V) & (VI) Series Respectively.

4-8-4 Conformational Information Contained in the Two Bond Couplings.

4-8-4.1 The $^2J_{HF}$ Data.

The electronegative effects of both geminal[275] and vicinal substitution[276] on $^2J_{HF}$ couplings have been studied by Phillips et al. In the Type (V) series, the substituents on the H—C—F moiety were not changed directly, although the electronegativity of the phenyl ring substituent was, of course, modified. Assuming the electronegativities of the $-CHCl_2$ and phenyl groups to be 2.6 and 3.0 respectively, EQN.102, derived by Phillips et al,[275] gives the values of $^2J_{HF}$ in the Type (V) fluorides as 51Hz. This is rather high compared to the average observed value of 44.8Hz.

$$^2J_{HF} = 78.76 + 8.45(E_X E_Y) - 16.73(E_X + E_Y) \qquad (\sigma \pm 2.1\text{Hz}) \qquad \text{EQN.102}$$

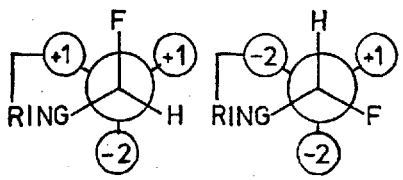
From an analysis of the $^2J_{HF}$ couplings found in several series of fluorocarbohydrates (including those examined in SECTION 4-8-2.2 - see TABLE 4-8.2[126]) Phillips & Wray[276] deduced a simple set of additive rules for the calculation of the effects of vicinal substituents. These assumed a chair conformation for the ring and were as follows :

Basic $^2J_{HF}$ = 50±1Hz (replacement of α-C by O = +1Hz, by S = -4Hz)

Substituent effects for X (= F, OH, OR) vicinal to H-F :

F axial	X axial	-2Hz	F equatorial	X axial	-2Hz
	X equatorial	+1Hz		X equatorial	+1Hz
	O or S in ring	+1Hz		O or S in ring	-2Hz

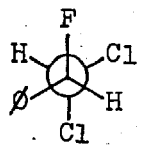
These effects are illustrated in FIG.4-8.22 :



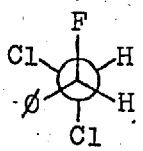
Changing X from eq to ax lowers $^2J_{HF}$ by -3Hz
Changing F from eq to ax has no effect unless X is a ring C (or S) in which case $^2J_{HF}$ is raised by +3Hz

FIG.4-8.22 Vicinal Substituent Effects on $^2J_{HF}$ (Overall accuracy ±1Hz).

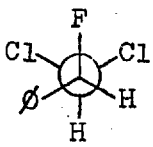
Application of these parameters to the three rotamers of the Type (V) fluorides is, unfortunately, complicated by the idiosyncrasy present in the magnitude of the effect when X is trans to H. In the absence of a ring system as a reference, these two situations cannot be resolved. Let us assume that any substituent trans to H reduces the $^2J_{HF}$ coupling by 2Hz. If an α-oxygen (E_O = 3.5) raises $^2J_{HF}$ by 1Hz and an α-sulphur (E_S = 2.5) lowers $^2J_{HF}$ by 4Hz then a reasonable estimate for the effect of an α-phenyl ring (E_ϕ = 3.0) would appear to be -2.5Hz. In FIG.4-8.23 the additive rules of Phillips & Wray,[276] with the assumptions made above, are applied to the three Type (V) fluoride rotamers :



I



II



III

Effects :	-2.5 -2 +1	-2.5 -2 -2	-2.5 -2 +1
$^2J_{HF}$	46.5Hz	43.5Hz	46.5Hz

FIG.4-8.23 Calculated $^2J_{HF}$ for the Type (V) Fluoride Rotamers

The coupling in rotamer 2 is thus 3Hz smaller than those in rotamers 1 and 3. In FIG.4-8.24 the three calculated $^2J_{HF}$ couplings have all been lowered by 1Hz, then used to calculate population weighted average couplings using the rotamer population calculated in TABLE 4-8.9. The fit of this calculated data to the observed data is mediocre, but if the assumptions/approximations made above and the small range of the data is taken into account this is not unreasonable.

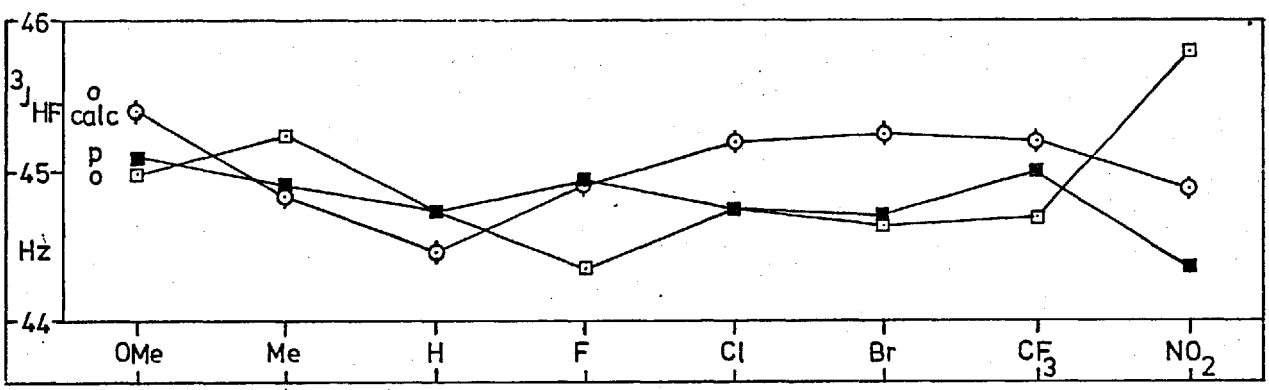


FIG.4-8.24 Observed vs. Calculated $^2J_{HF}$ Couplings

The evidence presented indicates that the $^2J_{HF}$ couplings are too insensitive to be of significant help in determining conformational preferences.

4-8-4.2 The $^2J_{CF}$ Data

The Type (V) fluorides possess $^2J_{CF}$ couplings from the side-chain fluorine to both C-2 and C-1'. These are illustrated in FIG.4-8.25 (a & b).

The para $^2J_{C_2F}$ coupling shows a Hammett σ_p relation to the ring substituent. The overall appearance of the $^2J_{C_2F}$ data is reminiscent of the $^3J_{HH}$ data (see FIG.4-8.2), and in FIG.4-8.25(c) the two are plotted against each other. There is extremely good linearity in the ortho data but not in the para. This is unusual as all previous relationships of this type have given better fits in the para data. There is no obvious explanation for this, but knowing that the $^3J_{HH}$ couplings are dependent on the C-1/C-2 rotamer populations (see SECTION 4-8-2.3) it is reasonable to expect the $^2J_{C_2F}$ couplings to be similarly

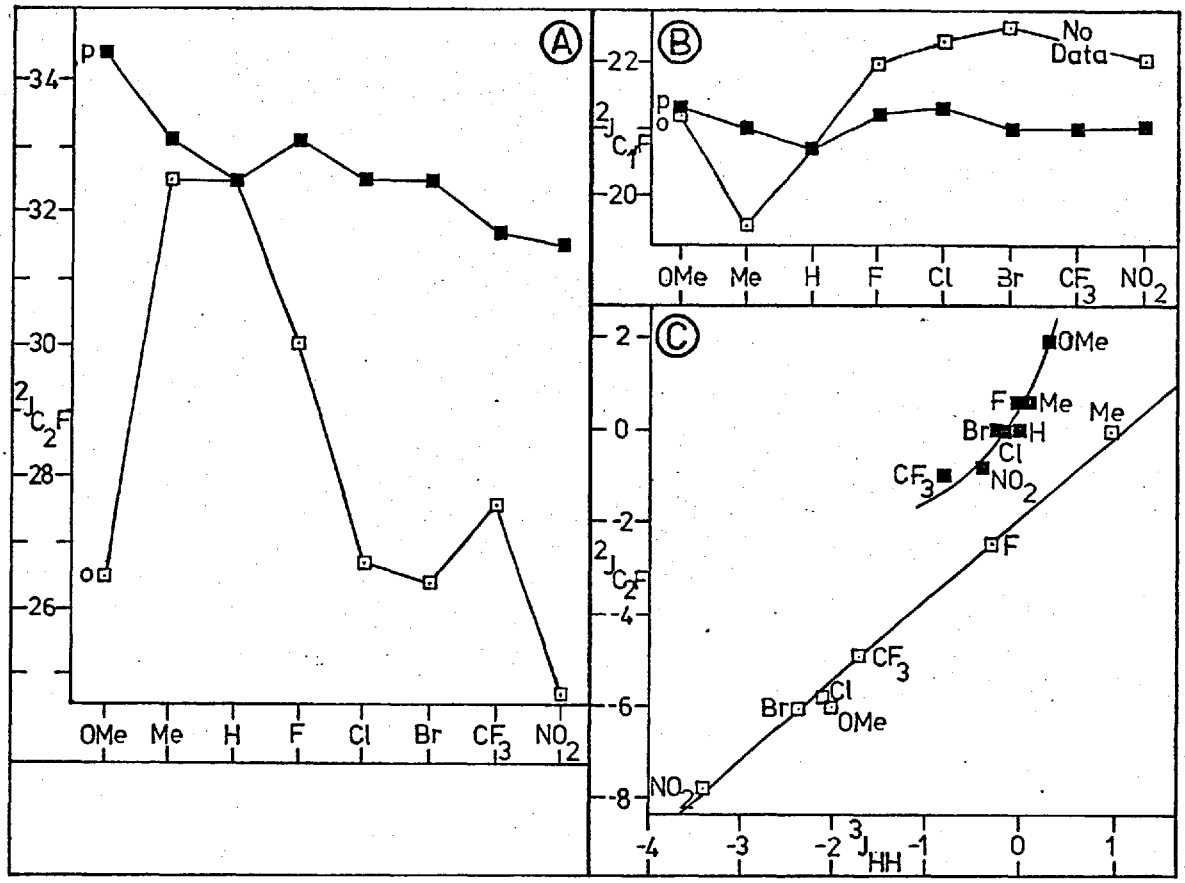


FIG.4-8.25 Two Bond F-C Couplings in the Type (V) Fluorides

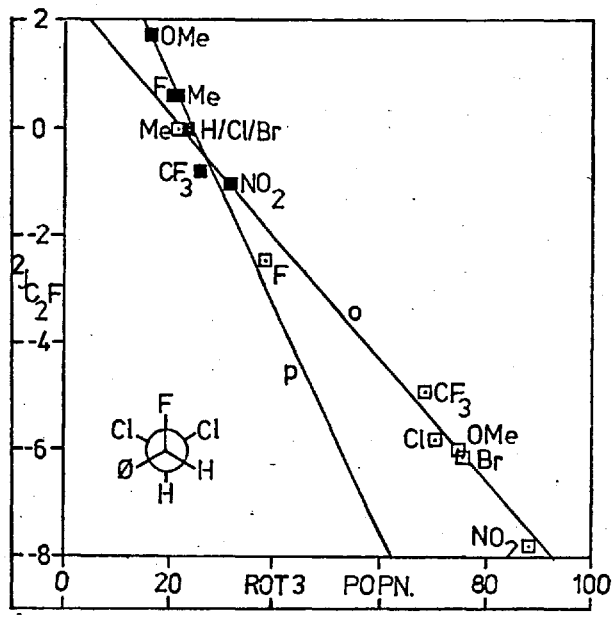


FIG.4-8.26 Relationships of $^2J_{C_2F}$ to Rotamer 3 Population

dependent. If the magngtudes of $^2J_{C_2F}$ are compared with the rotamer populations, from the "best estimate" $^3J_{HH}$ and $^3J_{HF}$ couplings (see TABLE 4-8.8), there is an obvious link to the relative population of rotamer 3, as shown in FIG.4-8.26.

The linearity of the plot is very good, indicating that $^2J_{C_2F}$ is highly dependent on the percentage of rotamer 3 present and fairly insensitive to the levels of rotamers 1 or 2.

The higher the level of rotamer 3 the lower the observed coupling. Extrapolation of the ortho line in FIG.4-8.26 gives the expected values of $^2J_{C_2F}$ in rotamer 3 to be (32.5 - 9.0Hz), and in rotamers 1 and 2 to be 35.3Hz. Unlike the $^2J_{HF}$ couplings, therefore, the $^2J_{C_2F}$ couplings are sensitive enough to be useful in conformational analysis.

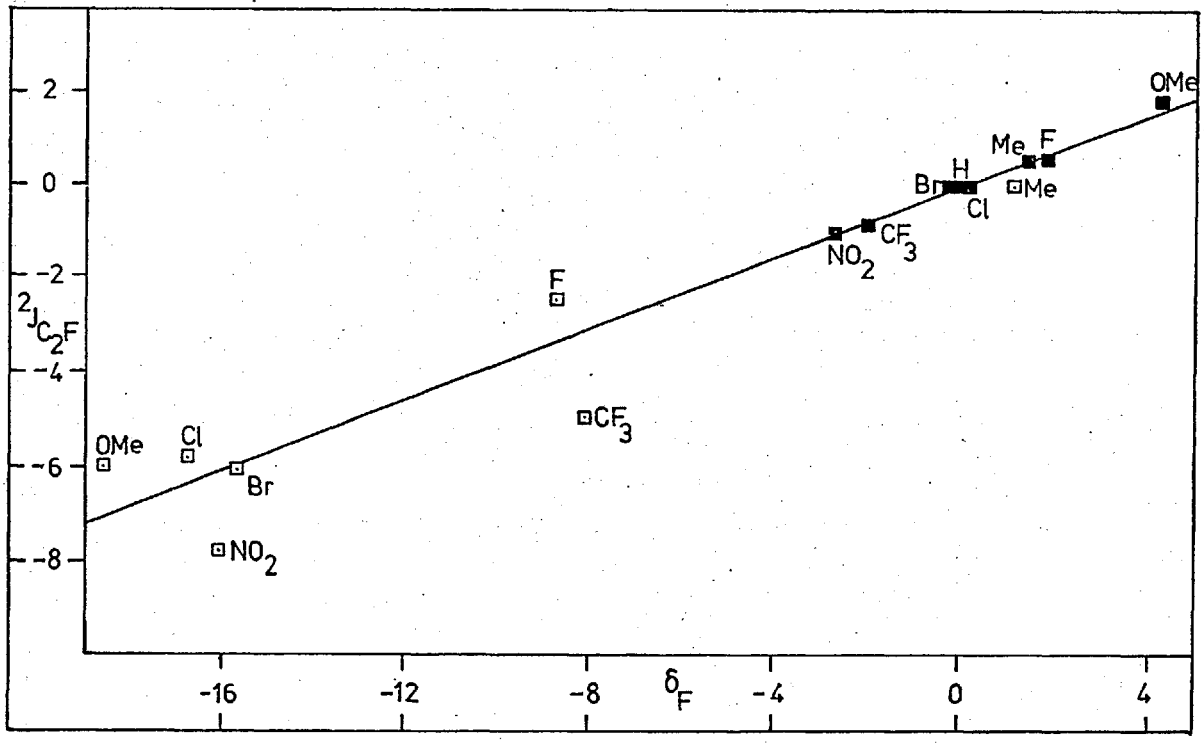


FIG.4-8.27 The Relationship Between $^2J_{C_2F}$ and δ_F in the Type (V) Fluorides

In FIG.4-8.27 the $^2J_{C_2F}$ couplings are plotted against δ_F. This gives a better linear plot than the $^3J_{HF}$ data (see FIG.4-8.4), which is to be expected since the former are far less dependent on dihedral angle terms than the latter. Again this confirms that all fluorine parameters (ie. shifts and couplings) are highly dependent on the electronic environment of the fluorine itself, in agreement with the observations of Muller and Carr[258] (see SECTION 4-8-1).

The $^2J_{C_1,F}$ couplings are illustrated in FIG.4-8.25(b). Compared to the $^2J_{C_2F}$ couplings, they have a very small range (only 3Hz) which makes the uncertainty in the coupling measurement of $\pm$0.5Hz very significant. The couplings appear to fall into three groups separated by 1Hz : (1) oF, Cl, Br, NO_2; (2) All the para derivatives and oOMe; (3) oMe. In the absence of corroborating data these groups cannot be linked to particular structures. However, three geometric arrangements of the C-F bond to the plane of the phenyl ring can readily be proposed, ie. ψ = 0, 60 or 90°; but there is insufficient data to substantiate any further assumptions/conclusions.

4-8-4.3 The $^2J_{C_2H}$ Data

These couplings were observed in the $^{13}C[GD-^1H]$ spectra of the Type (IV) alcohols and as such are subject to high errors. Several of the expected couplings were not observed in the complex splitting patterns, only broadening occurring. These data can be of little help in conformational analysis and are shown only for general interest below. Their average magnitude is in accord

with the value 2.5Hz found in $CH_2Cl\overset{*}{C}HCl_2$.[277]

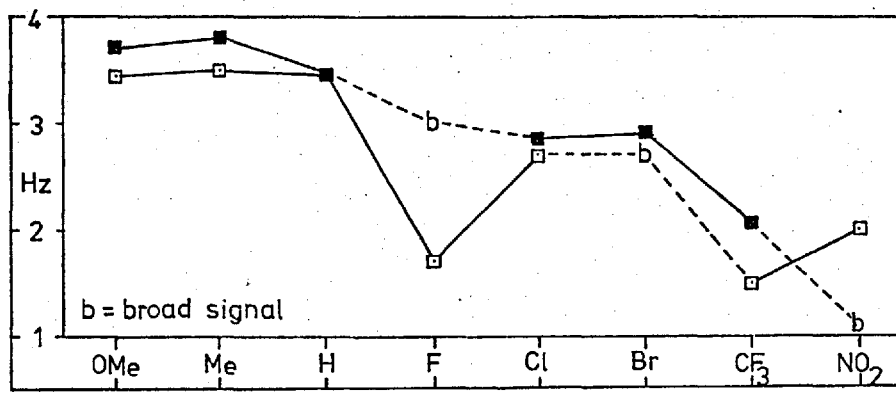


FIG.4-8.28 $^{2}J_{C_2H}$ Couplings from the ^{13}C ^{1}H-Gated Decoupled Spectra of the Type (IV) Alcohols

4-8-5 Conformational Information Contained in the One Bond Coupling Data

Three different one bond couplings were recorded - $^{1}J_{C_1F}$ from the $^{13}C[^{1}H]$ spectra of the Type (V) fluorides and $^{1}J_{C_1H}$ and $^{1}J_{C_2H}$ from the $^{13}C[GD\text{-}^{1}H]$ spectra of the Type (IV) alcohols. These are illustrated in FIG.4-8.29.

Both sets of data from the $^{13}C[GD\text{-}^{1}H]$ spectra are subject to considerable experimental errors ($\sim \pm 1$Hz). This, coupled with their small overall range and seemingly erratic nature, makes them unsuitable for conformational analysis.

The $^{1}J_{C_1F}$ data is little better. Although it has a smaller experimental error (± 0.5Hz) and both ortho and para data show reasonably good dependence on their overall electronic environment (ie. they correlate with Hammett σ_p) the couplings appear to be insensitive towards conformations adopted in the vicinal groups.

4-9 Summary of Conformational Observations

1) Both the chemical shift and coupling constant properties of the Type (IV) and (V) series are very similar, indicating that these series adopt similar conformations. The Type (VI) compounds follow parallel trends, with some evidence of minor conformational differences.

2) The para data in all series tend to be regular, ie. either fairly constant or behaving as predicted by a substituent parameter (eg. σ_p), suggesting that all para derivatives are either in free rotation or in some preferred conformation.

3) In SECTION 4-5-7 it was noted that the couplings in pMe(IV) were unaffected by a lowering of the temperature by 75°C. Again this indicates either full free rotation or a single preferred conformation in the para derivatives.

4) In contrast the ortho data is very erratic, with larger differences in

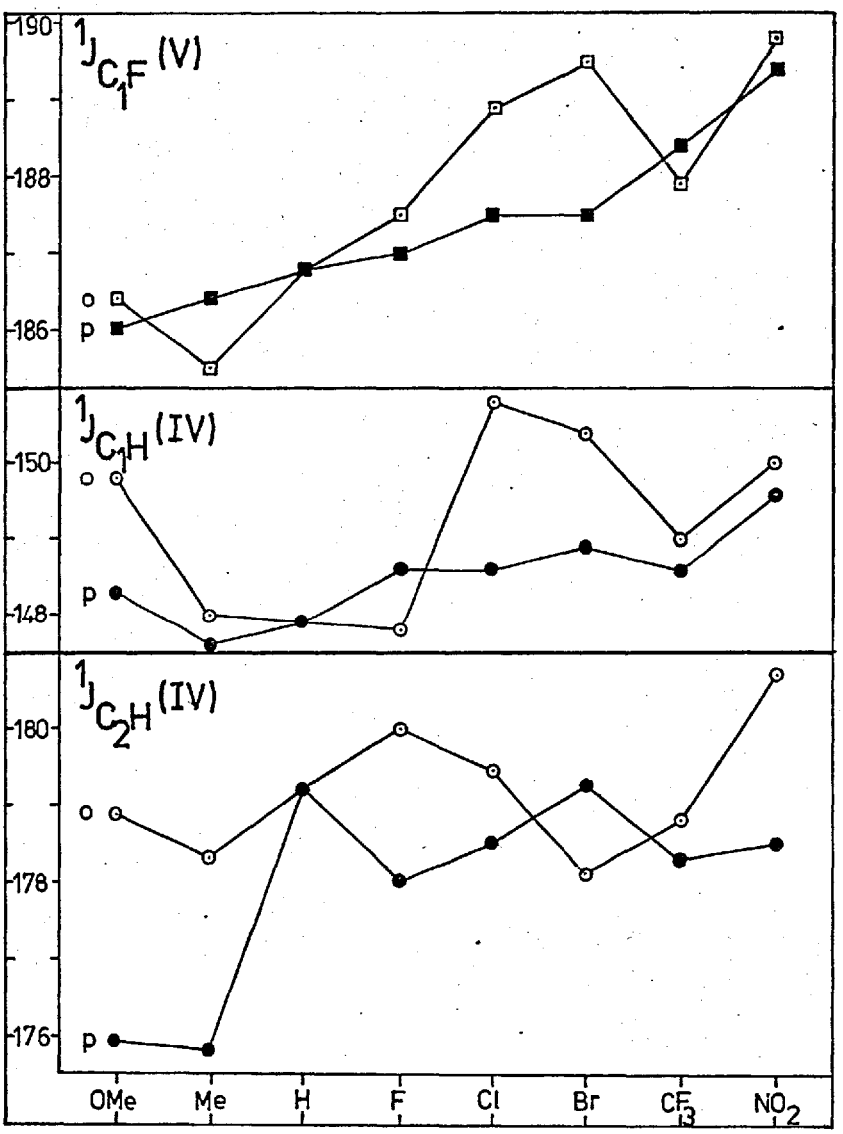


FIG.4-8.29 One Bond Couplings

both shifts and couplings between seemingly similar derivatives, eg. oF and oCl. This indicates steric control of the side-chain by the ortho ring substituents.

5) Comparison of the Type (V) ^{19}F shift data to CXF_2Cabc indicates that resonances from rotamer 3 should occur significantly to higher field (~5.5ppm) than resonances from rotamers 1 or 2. From FIG.4-7.3, therefore, higher rotamer 3 populations are more likely in the following sequence :

oOMe, Cl, Br, NO_2 > oF, CF_3 > oMe and all para derivatives

The observed ortho ^{19}F shift range of ~18ppm is probably not wholly due to rotamer preferences but also contains a large element of through bond substituent effects etc.

6) Differences between the ortho and para ^{13}C-X shifts suggest that in all the ortho methyl groups, and in the oCF_3 group in the Type (IV) alcohol, the side-chain adopts an orientation adjacent to the ring substituent. The reverse appears to hold for the remaining CF_3 groups and the OMe groups.

There is no support for the oMe groups being adjacent to the side-chain in either the ^{1}H shifts or the $^{5}J_{HH}$ coupling data. Long range J_{H_AF} couplings to the Type (VI) oF and oCF_3 groups indicate through space proximity of the side-chain in either rotamers 1 or 3. Similarly a $^{5}J_{FF}$ coupling of 2.6Hz in oCF_3(V) indicates proximity of the side-chain fluorine (rather than the -$CHCl_2$ group) to the ring substituent.

7) By utilising a variety of routes, "best estimates" for the $^{3}J_{HH}$ and $^{3}J_{HF}$ couplings in the individual rotamers of the Type (V) fluorides have been calculated. These values have been used in conjunction with the observed three bond couplings to estimate the rotamer populations present in each of the fifteen Type (V) fluorides. Additional supporting data for the populations obtained comes from the ^{19}F chemical shifts (the rotamer 3 preferences predicted in (5) are observed) and also from the $^{2}J_{C_2F}$ coupling data, which is sensitive enough to be of use in conformational analysis. The estimated rotamer populations are given in TABLES 4-8.8 & 4-8.9.

8) The rotamer preferences, predicted on steric grounds alone, were : rotamer 1 ⋙ rotamer 3 > rotamer 2. The observed ratios (for X = H) were 44.6 : 31.7 : 23.7. This compares favourably with the literature observed[118] populations in $CH\emptyset ClCHCl_2$ of : 53 : 34 : 13, indicating that a purely "steric bulk" approach to the problem of rotamer preferences in inadequate. This can be illustrated by the magnitude of the $^{3}J_{HH}$ couplings in a series of compounds studied by Gutowsky et al[265] (see TABLE 4-9.1). Although one might expect the H-H trans rotamer to be preferred throughout this series, this is clearly not so.

TABLE 4-9.1 $^{3}J_{HH}$ Couplings in a Series of Substituted Ethanes at 295°K[265]

Gauche H-H Preferred	Av $^{3}J_{HH}$		
$CHCl_2CHCl_2$	3.10	$CH_2\emptyset CH_2Cl$	7.48
$CHCl_2CHF_2$	3.47	$CH_2\emptyset CH_2Br$	7.56
$CHCl_2CHFCl$	3.64	$MeCHBrCHBr(CO\emptyset)$	10.48
$CHBr_2CHBr_2$	6.62	$pBr\emptyset CHClCH\emptyset(CO\emptyset)$	10.82
$CH\emptyset_2CH_2(CO\emptyset)$	7.21	$CHBr\emptyset CHBr(CO\emptyset)$	11.31
		Trans H-H Preferred	

4-10 Prediction of Elimination Product Geometries from the Calculated Rotamer Preferences

Four (big) assumptions need to be made before predicting the geometries of the elimination products of the Type (IV) alcohols and Type (V) fluorides from the calculated rotamer populations :

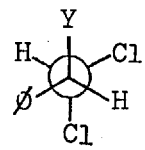
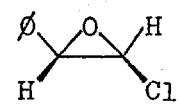
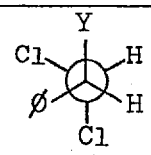
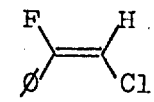
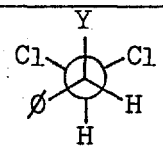
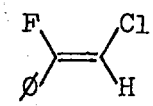
(1) The calculated values are accurate.

(2) The conformational preferences ramain the same under the conditions used for the elimination reactions. (Since different solvents were used this assumption probably does not hold in every case)

(3) That the elimination reactions preserve the geometry of the starting materials, ie. they either proceed via an E2 mechanism or if an ElcB mechanism is involved then the elimination step occurs before bond rotation can take place. This is illustrated in TABLE 4-10.1.

(4) That the elimination rate is identical in the two rotamers in which the leaving groups are trans to each other.

TABLE 4-10.1 Expected Product Geometries from Initial Rotamers

Initial Rotamer	Product Y = OH	Product Y = F
1 	 E	No direct route
2 	 Z	 E
3 	No direct route	 Z

The predicted elimination product geometries are given in TABLE 4-10.2 :

TABLE 4-10.2 Predicted Product Geometries from Elimination of HCl from the Type (IV) Alcohols and the Type (V) Fluorides

DERIV	Predicted Rotamer Pop^n			EPOXIDES		OLEFINES	
X	1	2	3	E	Z	E	Z
para Av	42.3	34.4	23.3	55%	45%	60%	40%
o F	39.9	19.5	40.6	66%	34%	32%	68%
o Cl	18.9	10.6	70.5	64% *	* 36%	13%	87%
o Br	16.4	8.5	75.0	66% *	* 34%	10%	90%
o Me	55.0	21.9	23.1	72%	28%	49% *	* 51%
o OMe	15.0	3.0	83.0	83% *	* 17%	4%	96%
o NO_2	10.3	10.0	79.7	51% *	* 49%	11%	89%
o CF_3	13.1	20.8	66.1	39% *	* 61%	24%	76%

Reactions marked * are likely to be slow as less than 50% of the starting material is in a suitable rotamer for direct elimination (ie. without bond rotation).

CHAPTER 5

5 METHODOLOGY / APPROACH TO CONFORMATIONAL ANALYSIS USING LANTHANIDE INDUCED SHIFTS

Although the McConnell-Robertson Equation (see SECTION 1-6-1) is relatively simple its immediate incorporation into a computer program to calculate the best-fit comformer of a flexible molecule is far from easy. The path chosen for the development of such a program, METFIND VII, is the subject of this short chapter.

The problem has two distinct parts :

(1) Finding the optimum metal position relative to the binding site and its immediate neighbours.

(2) Finding the optimum molecular conformation.

These can normally be treated separately, as in most molecules there are enough "fixed" atoms with LIS adjacent to the binding site, for the best metal position to be located. The rotatable groups further away may then be considered in turn, moving them until the best fit between the observed and calculated LIS is achieved.

This approach was adopted in developing METFIND, where the "rigid case" was completely dealt with before attempting the logistic problems associated with systems containing rotatable species. At all stages the aim has been to write a perfectly general program rather than one tailor-made for the phenyl ethanes under study.

METFIND VII is the final version of a series of programs loosely based on the program METALSEARCH, written by L.O.Ford and modified by D.J.Chadwick, a copy of which was generously given to us. METALSEARCH contained the rudiments of the later METFIND series, but now bears little similarity to the complexity of METFIND VII. The main feature retained was the use of search blocks. METALSEARCH examined 40 search points per run, calculating the "goodness of fit" of the shifts induced by a hypothetical lanthanide at each point, to the observed data. This forms the basis of METFIND although each search block now contains 500 points. The advantage of this method over rapid regression techniques (see SECTION 1-6-4.2) is that it allows fitfactor contour plots to be generated, minimising the chance of finding an isolated secondary maximum.

5-1 Basic Assumptions

The assumptions made were basically those already detailed in SECTION 1-6-4.1. In practice the fourth assumption was checked by monitoring the coupling constants before and after adding the LSR.

5-2 Finding the "Best Metal Position" for a Rigid Substrate

5-2-1 Coordinate Systems

The coordinate systems chosen for the METFIND series are shown in FIG. 5-2.1. Rectangular Cartesian coordinates (X,Y,Z) are used for the substrate arranged so that :

(a) The complexation site is at the origin.

(b) The next atom lies on the +ve X-axis, such that the bulk of the substrate lies within the +ve X-hemisphere, with any major symmetry features in either the XY- or XZ- axial planes.

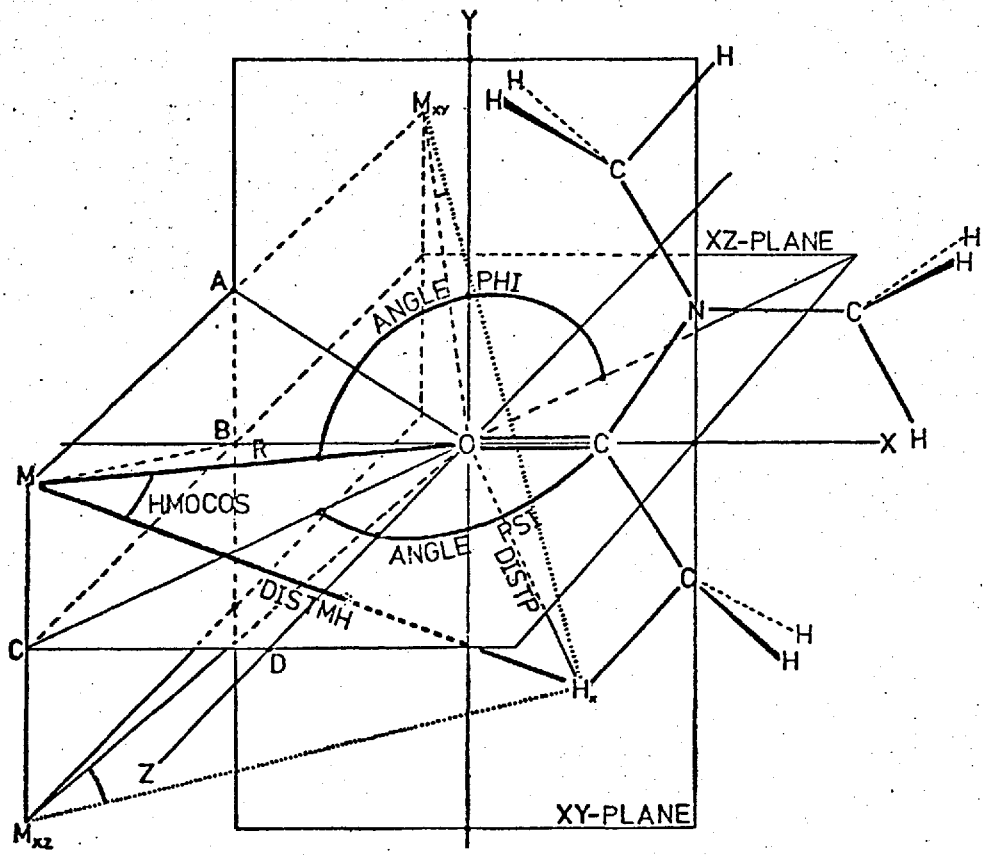


FIG.5-2.1 Definition of the Coordinate Systems Used in METFIND VII

M ... represents the metal position as defined by R, PHI and PSI. Its Cartesian coordinates are calculated as (OA,OB,BC).

M_{XY} and M_{XZ} ... represent the metal positions after reflection in the XY- and XZ- planes.

The metal search position is specified by polar coordinates (R,PHI,PSI) as shown in the diagram. The normal sector of space through which a search is conducted is confined to the -ve X-hemisphere (ie. R(1.5 - 4.5 Å), PHI and PSI (90 - 270°) - typical literature results lie in the range 2.5 - 3.5 Å). Although polar coordinates are convenient because the metal-donor distance is a specifies variable, they have the distinct disadvantage of producing 3-D matrices of results that are difficult to visualize (FIG.5-2.5).

5-2-2 Data Required

The following data is necessary to carry out a block search for a best fit metal position :

(1) The Cartesian coordinates of the substrate (in Å)

(2) The induced shift/broadening data in self consistent units (ie. ppm for mixed ^{1}H, ^{19}F and ^{13}C data).

(3) The metal search parameters (in Å and degrees). R, PHI and PSI each require a minimum, maximum and incremental value in order to define a 5.R x 10.PHI x 10.PSI search block.

(4) The options selected. A large range of these were written into the METFIND series and are discussed later in this chapter and in APPENDIX IV.

5-2-3 Basic Calculations Performed

For each of the 500 search sites in one block :

The metal position is converted to Cartesian coordinates (OB,AB,AC) and the (metal-origin-X-axis) bond angle (180-$\hat{BOM}$), and (metal-origin- XY-plane) dihedral angle ($\hat{ABM}$), are calculated.

Then for each shifted/broadened atom METFIND calculates the expected shift and broadening from the (metal-atom) and (atom-origin) distances (DISTMH and DISTP), and the cosine of the (atom-metal-origin) angle (HMOCOS). The percentage differences of the observed and calculated effects ($SDIFF_i$) are then tested against preset tolerances (see next subsection). If all the tests are passed, an RMS DEVIATION of the observed : calculated data (SFIT) is produced and again tested against a preset tolerance. If this final test is passed a "FITFACTOR" is calculated and printed in the output array.

This illustrates the simplest possible case. Further steps need to be included if the data includes groups to be averaged, or if reflection of the metal position is required (vide infra).

5-2-4 Tolerance Tests and Fitfactors

The fitfactor used in the original program METALSEARCH[155] was based on an average error function :

$$\text{Error} = \frac{\Sigma}{(n-1)}\left[\frac{\Delta_i^{obs} - \Delta_i^{calc}}{\Delta_i^{obs}}\right] \qquad \text{EQN.103}$$

Most authors have preferred an RMS-type parameter such as Hamilton's R-factor (see EQN.30). Since the system used in METFIND treats each nmr signal individually, averaging together the shifts for each atom in a group, a weighting factor (w_i) is not necessary. The agreement factor chosen (SFIT) is a percentage RMS deviation, calculated as follows :

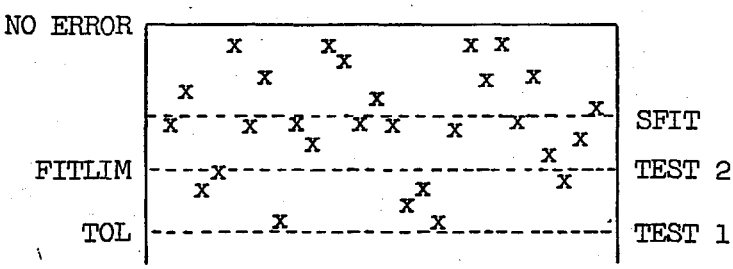
$$SDIFF_i = 100.(\Delta_i^{obs} - \Delta_i^{calc})/\Delta_i^{obs} \qquad \text{EQN.104}$$

$$SFIT = 1.0 - \sqrt{\frac{\Sigma_{i-1}^{n}((\Delta_i^{obs} - \Delta_i^{calc})/\Delta_i^{obs})}{n-1}} \qquad \text{EQN.105}$$

n-1 is used in EQNS.103 and 105 because the calculated shift of the first group is normalised to the observed value.
The larger SFIT the better the agreement (range 0 to 1).

Tests are performed on $SDIFF_i$ and SFIT before producing a "FITFACTOR", to reduce computing time, terminating searches when prohibitively large errors are found. The optional input for METFIND includes an overall error tolerance (FITLIM) outside which all values of SFIT are to be rejected. Values passing this test are scaled so that FITLIM = 0 and 1.0 = 1000 and printed in the output array of FITFACTORS. In addition the individual shift errors ($SDIFF_i$) are tested against a tolerance (TOL) which is weighted by the number of atoms observed (NPROT) to allow for statistical scatter of results (see EQN.106 and FIG. 5-2.2).

$$TOL = (1.25 + 0.0075.NPROT) \times 100(1 - FITLIM) \qquad \text{EQN.106}$$



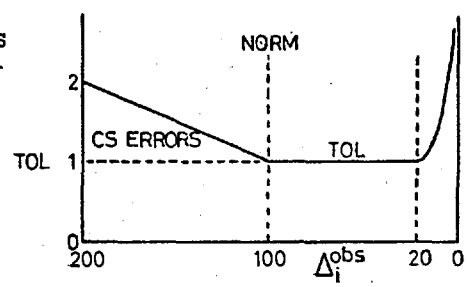
x = $SDIFF_i$ values
This search plot produced shifts within the specified tolerances and a FITFACTOR would be calculated.

FIG.5-2.2 METFIND Tolerance Tests : Any value of $SDIFF_i$ below TOL terminates the calculation for that search point and the FITFACTOR is set to zero.

In the original design of METFIND the group with the largest shift was expected to be used for normalisation. Since this is the most likely shift to have CS contamination, the program was modified so that any shift larger than that used for normalisation is excluded in the calculation of SFIT but is still tested against a modified TOL value. Similarly TOL was adjusted for shifts below 20% of the normalised value to allow higher percentage errors (see FIG. 5-2.3) whilst retaining the shifts in the calculation of SFIT.

FIG.5-2.3 Modification of TOL with Δ_i^{Obs}

TOL is modified to allow for Fermi-contact and shift measurement percentage errors.



5-2-5 Metal Reflection Option

Hofer[142] mentioned the necessity of averaging the calculated LIS of the symmetrically disposed ortho and meta protons in pyridine if the best metal fit was not to be artificially forced into the plane of symmetry (see FIG.5-2.4).

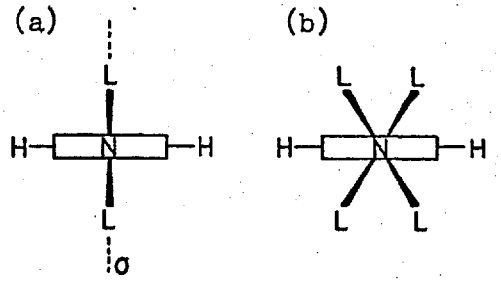


FIG.5-2.4[142] Possible Calculated Lanthanide Positions in Pyridine (a) Without averaging (b) with averaging the symmetrically disposed nuclei.

This approach was taken one step further by Chadwick et al[169(b),278] who argued that if the donor atom has two lone pairs bisected by a local plane of symmetry, then the metal should be expected to occupy both sites equally, and that averaging should be carried out between them. This is a trivial extension in highly symmetrical molecules but may be important in molecules with lower symmetry. For example, in FIG.5-2.1, the oxygen lone pairs would be expected to lie in the XY-plane and so METFIND could carry out metal reflection (and LIS averaging) in the XZ-plane. METFIND VII only caters for equally occupied sites; an extension, to optimise the metal position and weight the calculated LIS accordingly, was considered (see APPENDIX III), but as metal reflection was not heavily used in the study presented here the necessary alterations were not made. (A similar mathematical approach could also be of use in determining the relative metal preferences in molecules with multiple binding sites).

5-2-6 Methyl Group Rotation Option

The necessity for methyl group averaging[157,211] (see SECTION 1-6-5) was highlighted in the initial proving runs on METFIND where calculated ^{1}H shifts for the cis-N-methyl protons in N,N-dimethylamine (see FIG.5-2.1), of -1, 200, 200 were observed! This dramatic variation in the calculated shifts, due to the methyl protons straddling the "magic angle" ($54^{o}44'$), clearly indicates that rotational averaging is essential for methyl groups close to the binding site.

The "100 position" averaging used by Ammon et al[156] is somewhat excessive and the other extremes of only using the mid-point of the three protons[142] is unsatisfactory.[158] A "twelve point averaging" option included in METFIND has been found to be adequate, giving significant improvements in the fit over the unrotated methyl group method.

5-2-7 METFIND Search Methods

METFIND was designed to operate with a unit search block of 500 points, outputting a table of FITFACTORS after each block. Three types of search method were developed :

(a) NON-ITERATIVE MODE - a single block search is performed.

(b) FOCUSING MODE - the initial search uses the input search parameters. The maximum fitfactor in this search is then centered by moving the search

area, and further searches are performed until the maximum FITFACTOR found lies centrally within the search block. The searches are then "focused" by reducing the steps between search points. The maximum FITFACTOR is again centred and a final focusing and centering performed. The three levels of "magnification" are referred to as RUNS; the individual search blocks as ITERATIONS :

RUN 1 ... RSTEP = 0.10Å; PHISTEP = PSISTEP = 5° (or Input values).
RUN 2 ... RSTEP = 0.05Å; PHISTEP = PSISTEP = 2°
RUN 3 ... RSTEP = 0.02Å; PHISTEP = PSISTEP = 1°

(c) MULTISCAN MODE - This enables hemispherical shells to be comprehensively searched by performing a series of 16 block searches in a rectangular pattern.

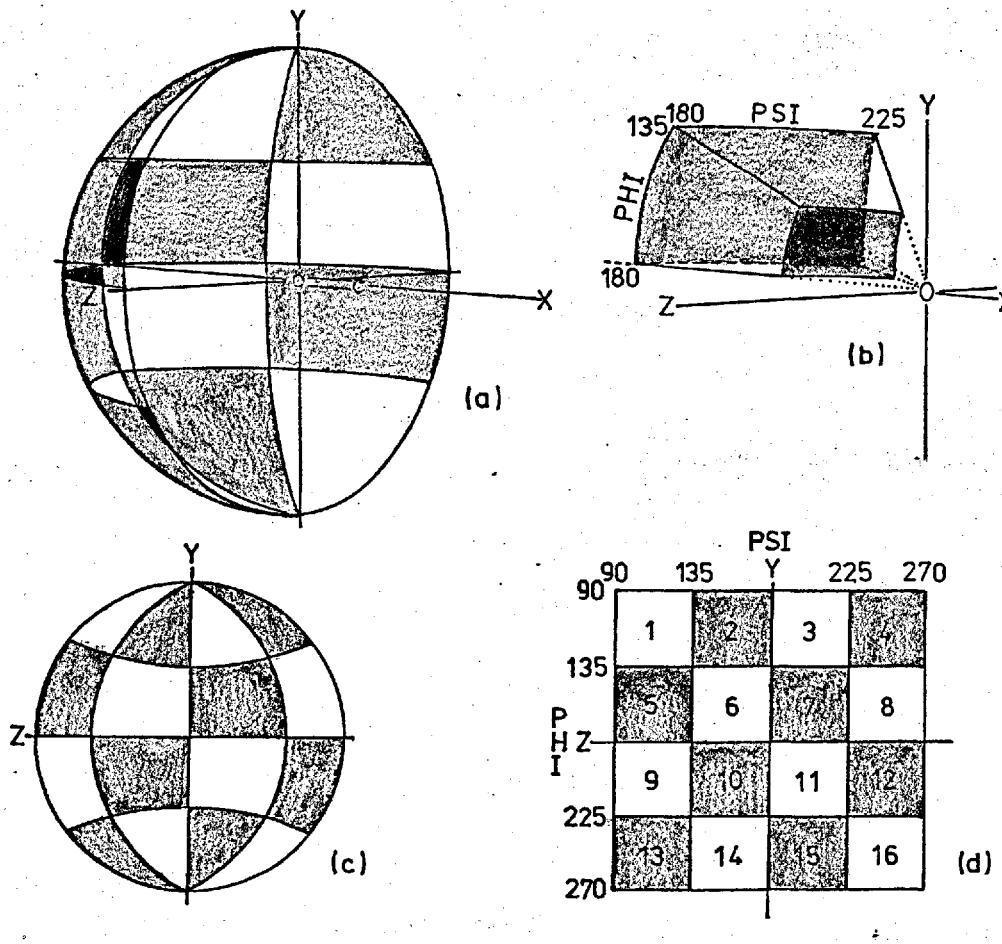


FIG.5-2.5 Search Areas and Multiscan Search Patterns - Their actual shape and diagrammatic appearance from the FITFACTOR Table Output

(a) How the 16 search blocks in a MULTISCAN cover a hemi-spherical shell

(b) A typical search block : R(100-200/20), PHI(135-180/5), PSI(180-225/5)

(c) Actual block appearance - looking along the X-axis

(d) Distorted block appearance - given from the FITFACTOR Tables
Polar coordinate tables distort the spatial shape of the result. As PHI tends to 90 or 270, PSISTEP tends to zero.

The block shading is the same in FIGS. (a), (b) and (c)

(This can be reduced to 8 if planar symmetry and/or metal reflection are present). Within a MULTISCAN the range of R is the same in every block, the only changes in range occurring in the PHI and PSI parameters. On completion of a MULTISCAN, PHI and PSI are reset to 90°, R is incremented and the process repeated until the desired R range has been completely searched. This search technique is obviously extremely useful if a complete picture of the best metal position is to be acquired. The standard search pattern is illustrated in FIG.5-8.5.

This and other METFIND options will be discussed in more detail in APPENDIX IV, together with the program structure and some typical input/output.

5-3 Program Testing - Cholesterol

To test METFIND I, the LIS study of cholesterol by Barry et al[155] (chosen because the shift and coordinate data were given) was repeated. The shift assignments were assumed to be correct, but the peculiar numbering system and search origin chosen were not adopted. The numbering system used in shown in FIG.5-3.1, the orientation of the molecule in FIG.5-3.2, and the induced shifts and transposed coordinates in TABLE 5-3.1.

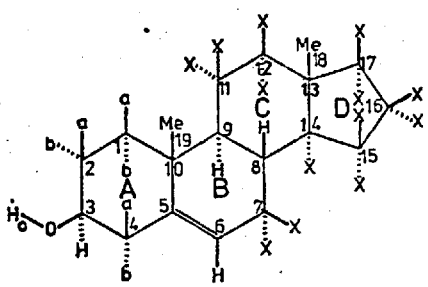


FIG.5-3.1 Numbering System - carbon atoms numbered conventionally; protons numbered as carbons with suffix (a) if above plane, (b) if below (not used if only one proton per carbon). In input, carbons denoted by prefix 6, protons by prefix 1. X signifies no data available. A total of 32 shifted groups were observed. No data was available for the side-chain (C_{20} onwards).

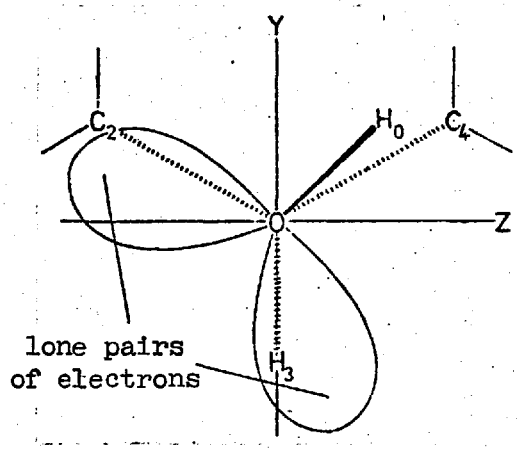


FIG.5-3.2 Orientation Viewed from the -ve X-axis. Ring A positioned symmetrically about the XY-plane as shown. The position of H_0, derived from X-ray data, was used by Barry et al (155). The lone pair syn to H_3 is the least hindered and its occupation is supported by the results obtained(155) : R = 2.69Å MOC = 140°, PHI = 207°, PSI = 155°, (predicted position from figure PHI = 220°, PSI = 170°).

In FIG.5-3.2 the assumption that the -OH group is stationary was made in predicting the metal position. In practice, a variety of groups were used for normalisation in a series of FOCUSING MODE runs and since shifts larger than the normalising value are not used in calculating FITFACTORS the alloted

TABLE 5-3.1 Cholesterol - Induced Shifts and Coordinates (in Å/100)

ATOM NO	X	Y	Z	LIS	NORM RUN	ATOM NO	X	Y	Z	LIS	NORM RUN
100	-25	67	69	1604	(e)	609	553	137	7	57	
601	345	81	-122	132	(b)	109	565	40	-36	49	
101a	378	136	-208	89		610	339	156	5	125	(k)
101b	388	-16	-125	104	(m)	611	615	235	-98	43	
602	193	67	-129	314	(a/d)	612	765	221	-111	0*	
102a	148	164	-137	296	(h/i)	613	840	218	20	25	
102b	165	6	-214	260	(c)	614	773	117	115	25	
603	143	0	0	993	(f)	615	827	108	235	18	
103	178	-101	0	433	(g)	616	1009	124	170	0*	
604	190	71	126	314	(a*/d)	617	987	164	25	18	
104a	147	178	132	296	(h*/i)	618	840	360	82	21	
104b	160	14	212	246	(j)	118	780	427	20		
605	341	85	125	114	(l)	118	801	356	184		
606	437	40	224	85		118	945	398	85		
106	368	-4	304	50		619	356	304	15	100	(n)
607	559	48	229	40		119	251	313	-12		
608	623	143	135	40		119	371	340	120	80	
108	614	240	178	49		119	414	365	-61		

* The zero shifts observed for atoms 612 and 616 were changed to 1 in the METFIND data in order to avoid attempted division by zero.

TABLE 5-3.2 Results of Focusing Metal Searches Using Cholesterol LIS Data

RUN	NORM ATOM	NORM LIS	NO$	BEST METAL POSN R	PHI	PSI	MAX+
(a)	602	314	29	229	217	175	567
(a*)	604	314	29	236	218	174	567
(b)	601	132	23	285	217	169	554
(c)	102b	260	25	290	229	168	474
(d)	602/604	314	28	233	218	175	559
(e)	100	1604	32	205	215	177	536
(f)	603	993	31	140	207	180	444
(g)	103a	433	30	259	224	174	568
(h)	102a	296	27	205	217	177	529
(h*)	104a	296	27	195	219	180	500
(i)	102a/104a	296	26	200	218	178	505
(j)	104b	246	24	328	221	161	556
(k)	610	125	22	157	212	178	436
(l)	605	114	21	377	212	159	509
(m)	101b	104	20	265	218	174	557
(n)	619	100	19	212	217	178	527
Overall range - excluding run (f) and run (l)			MIN	157	212	161	436
			MAX	328	229	180	568

+ FITFACTORS scaled so that 0.75 = 0 and 1 = 1000. ie. a FITFACTOR of 500 = a 12.5% RMS error.

$ indicates the number of groups used in calculating FITFACTORS.

position of H_0 is of no consequence. These are indicated in TABLE 5-3.1 by the letters (a) to (n). In runs (d) and (i) two groups with the same shift were used for normalisation. The results obtained are listed in TABLE 5-3.2. The groups were selected in order to gauge the CS contamination in the observed LIS close to the binding site and the effect on the result obtained of only using part of the LIS data available. All searches were started in the same area, namely : R(220-260/10), PHI(180-225/5), PSI(150-195/5), with METFIND allowed to centre and focus onto the maximum value without constraint. (N.B. Metal search radii will be quoted in $\mathring{A}$/100 when discussing METFIND input/output in order to keep all the search parameters integral).

Several important observations can be made from the results :

(1) They agree with those of Barry et al.[155] The slight differences observed are probably attributable to the different error function used in METALSEARCH.

(2) The choice of normalising group is critical and those likely to have CS contributions, eg. H_0, 603, 605, etc. should be avoided.

(3) The metal-donor radius is much more sensitive to changes than either of the angular terms.

(4) Normalising on H_3(g) gave the best result, (also the closest to Barry et al[155]), indicating little CS. The significantly different results obtained from H_2 and H_4 are possibly due to the omission of all the shifts closer to the binding site, which give the best "fix" on the metal position.

This test work proved that METFIND functioned correctly and provided a useful warning of the precautions required to obtain sensible results.

5-4 Approach to the Rotation Problem

Several major questions had to be answered before molecular rotational optimisation could be undertaken using LIS data :

(1) What operations are required to rotationally optimise complete molecules?

(2) How may the complex instructions required be flexibly incorporated into a general purpose program?

(3) What information/calculations are necessary to rotate a group?

Although (3) is key, the answers to (1) and (2) provided the overall strategy and will therefore be considered first.

5-4-1 Basic Concepts/Logistics of Rotational Optimisation

For maximum flexibility the operation of the program was split into 15 CYCLES, each performing a basic function nominated by a 15-digit input parameter (ROTN). The individual digits (NCYCOP) could then be used to select the sequence of the CYCLE operations, chosen from TABLE 5-4.1.

Option (9) was not incorporated into METFIND due to the prohibitive

computer-time required (up to 600 secs/CYCLE), instead it was envisaged that the max. FITFACTOR for the "fixed atoms" would be determined prior to the ROTATE run.

The constraints imposed by the system within which the NCYCOP options were developed lead to the following features in METFIND VII :

TABLE 5-4.1 METFIND - Rotation CYCLE Options (NCYCOP)

No	NCYCOP OPTION
1	Centre search area onto maxiumum FITFACTOR of fixed atoms (GYRO > 0).
2	Add next group(s) then recentre search area onto maximum FITFACTOR.
3	Observe max. FITFACTOR region - ROTATE group(s) in sequence and optimise.
4	Fix positions of all previously rotated groups (update stored coordinates).
5	ROTATE and optimise indicated group(s) using a smaller increment.
6	Perform complete ROTATION of indicated group (30° STEPS) then optimise.
7	Perform "TWELVE POSITION FREE ROTATIONAL AVERAGING" of indicated group.
8	As 4 then output final atomic coords and results to TAPE9 for punching.
(9)	Perform a full MULTISCAN then centre on max. FITFACTOR.
0	Terminate JOB (STOP 3).

All the molecular manipulation options are able to centre the max FITFACTOR found, passing the working search parameters from one CYCLE to the next. Two sets of coordinate data are used, a stored version and a working version. The unmodified stored version is taken at the beginning of each cycle unless

TABLE 5-4.2 A Typical NCYCOP Sequence for a Type (IV) Alcohol (see FIG.5-4.1)

CYCLE	NCYCOP	OPERATION
1	1	Centre search area onto max. FITFACTOR of "fixed atoms".
2	2	Add side-chain proton - recentre search area.
3	6	Rotate side-chain proton through 360° (in 30°) return to optimum.
4	4	Update stored coordinates
5	2	Add phenyl ring and ortho substituent - recentre search area.
6	6	Rotate ring through 360° (in 30°), return to optimum.
7	4	Update stored coordinates.
8	3	Optimise rotation of side-chain proton and ring in steps of 5°.
9	4	Update stored coordinates.
10	5	Optimise rotation of side-chain proton and ring in steps of 2°.
11	4	Update stored coordinates.
12	5	Optimise rotation of side-chain proton and ring in steps of 1°.
13	8	Update stored coordinates - output results to TAPE9 for punching.
14	7	Perform "FREE ROTATIONAL AVERAGING" of side-chain proton.
15	7	" " " " of phenyl ring.

updated by options (4) or (8). Operations (3) and (5) may be performed on up to four groups, (6) and (7) on only one group per cycle. The increments used in operations (3) and (5) are selected by the user. Option (6) ensures that a secondary maximum is not found while performing rotational optimisation. Option (7) is useful for testing that an optimised orientation gives a significantly better fit than "free rotation", it is however expensive to use.

In addition to the NCYCOP options each atom was given a GYRO option which defined its role within each CYCLE (see SECTION 5-4.2 and APPENDIX IV).

A typical sequence of NCYCOP operations is given in TABLE 5-4.2.

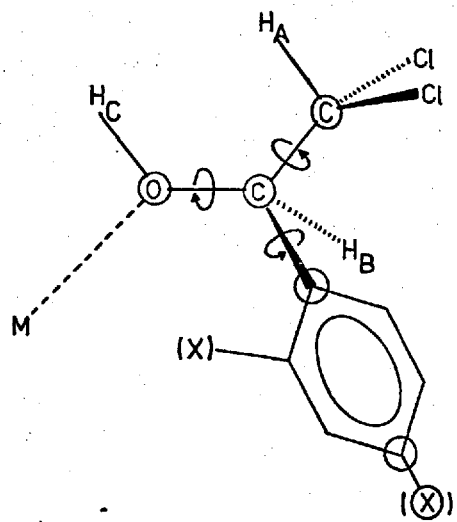


FIG.5-4.1 A Typical Type (IV) Alcohol

showing (a) the "fixed atoms" Ⓒ
(b) the rotatable bonds and the atoms affected.

The ability to manipulate the nmr inactive species was also developed as they were required for a molecule drawing program and also for defining certain rotational operations (vide infra).

5-4-2 Requirements for Group Rotation

These are extremely simple as only the coordinates of the atoms to be rotated and two points on the axis are required. The GYRO system was therefore introduced to define the role of each atom in each CYCLE by using the values :

(0) = Omit ; (1) = Use (fixed) ; (2) (4) (6) (8) Point on axis (fixed) ; (3) (5) (7) (9) Atom to be rotated about axis (2) (4) (6) (8)

METFIND VII can rotate and optimise four groups independently in one CYCLE.

5-4-3 The Calculation of Rotated Coordinates.

X(x,y,z) is to be rotated about the axis defined by A(x,y,z) and B(x,y,z) (see FIG.5-4.2). The following calculations are performed :

(1) Calculate the lengths AB, AX and BX (3-D Pythagoras).

(2) Use cosine rule to calculate cos ϕ.

(3) Calculate ratio AB/AC from AB/(AXcosϕ).

(4) Use difference A(x,y,z) - B(x,y,z) to calculate C(x,y,z).

(5) Use difference C(x,y,z) - A(x,y,z) = $\bar{a}$(x,y,z) ; and
C(x,y,z) - X(x,y,z) = $\bar{b}$(x,y,z) to find values $\bar{a}_x$, $\bar{b}_z$,

etc. The components of the gradient of CY are then given by :

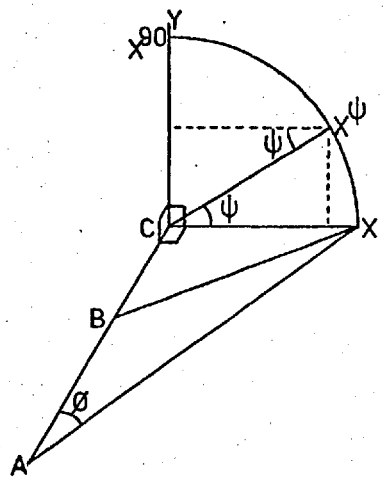


FIG.5-4.2 X to be rotated about axis defined by A and B

$\bar{x}(\bar{a}_y\bar{b}_z - \bar{a}_z\bar{b}_y), \bar{y}(\bar{a}_z\bar{b}_x - \bar{a}_x\bar{b}_z), \bar{z}(\bar{a}_x\bar{b}_y - \bar{a}_y\bar{b}_x)$.

(6) The coordinates of Y are then given by : $(C_x + \bar{x},\ C_y + \bar{y},\ C_z + \bar{z})$.

(7) X^{90^y} is then calculated from the proportions of CX and CY.

(8) Using $\bar{b}(x,y,z)$ calculated in (5) and $\bar{c}(x,y,z)$ from $C(x.y.z) - X^{90}(x,y,z)$, the coordinates of any point X^{ψ} may be calculated from EQN.107 :

$$X = C(x,y,z) - \cos\psi\bar{b}(x,y,z) + \sin\psi\bar{c}(x,y,z) \qquad \text{EQN.107}$$

This process can be repeated for any number of points X_i to find the corresponding C_i, X_i^{90} and X_i^{ψ} for all points. For all atoms whose C_i is on the B side of AB rotation will occur in the same sense (looking along AB from B to A a positive rotation of X_i produces a clockwise movement). If, however, one C_i is on the other side of A, that atom will be rotated in the opposite sense.

In METFIND VII the first axial atom found (even GYRO code) is assigned to A, the second to B. Care, therefore needs to be exercised in the ordering of the atoms in the data deck. For example, if the ortho substituted phenyl ring in FIG.5-4.3 is to be rotated, then the assignment of A and B as shown will only give the correct result if the bond length C-X < 1.4Å(ie.X = H or F).

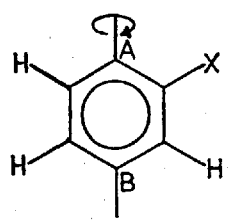


FIG.5-4.3 If C-X > 1.4Å then this assignment of A and B will rotate X in the opposite sense to the rest of the ring.

This chapter covers the main procedures used in METFIND VII and the reasons for their development. Obviously with a highly complex program, many foibles only become apparent with experience, and understanding and adaption only takes place by degrees. By this method many minor improvements have accrued to the METFIND series, making the final version METFIND VII extremely versatile.

A full description of the Input/Output of METFIND VII, together with a program listing and an explanation of the options available, is given in APPENDIX IV.

CHAPTER 6

6 CONFORMATIONAL ANALYSIS OF THE TYPE (IV) ALCOHOLS FROM THEIR LANTHANIDE INDUCED SHIFTS

6-1 Experimental

The recording of the non-shifted spectra is reported in Chapter 4. Shifted spectra were recorded in five 10-mm nmr tubes, kept for this purpose and washed with conc. HNO_3 between samples. The shift reagents, $Eu(fod\text{-}d_9)_3$ and $Yb(fod\text{-}d_9)_3$, were both commercially available and apart from vacuum desiccation no special precautions were taken in their use.

Trial experiments had shown that addition of 100mg of $Eu(fod\text{-}d_9)_3$ or 66mg of $Yb(fod\text{-}d_9)_3$ to 2ml of 0.5M $CDCl_3$ solution of the alcohol substrates induced reasonable shifts in the linear region of an LSR : LIS plot with an acceptable level of line broadening. Incremental additions of LSR to $CDCl_3$ solutions were found to be unsatisfactory, as the weights added (~10mg/aliquot) could not be accurately measured due to solvent evaporation (see FIG.6-1.1).

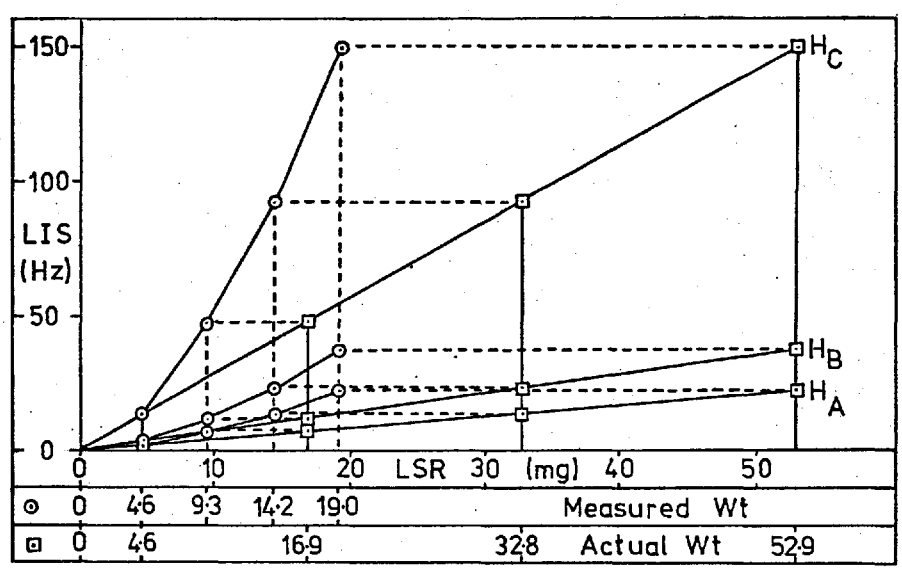


FIG.6-1.1 Cumulative Weighting Errors Due to Solvent Evaporation in the Trial LIS Spectra of H(IV). Actual weights calculated using the correction technique of ApSimon and Beierbeck (196).

The single additions of LSR (100mr or 66mg) to 1mmole of the dry substrate, were therefore made before adding the dried $CDCl_3$ (2ml delivered from a syringe). The tubes were tightly capped and the ^1H, (^{19}F) and ^{13}C shifted spectra recorded within 24 hrs to minimise solvent evaporation.

Little difficulty was found in assigning the shifted spectra. In only one instance, the $Yb(fod\text{-}d_9)_3$ ^1H spectrum of oMe(IV), were incremental additions of LSR necessary, as the $H_{A,B}$ and C lines moved to the edge of the aromatics.

Throughout, the initial and final shifts were measured to the third decimal place in the FT ppm listings to avoid cumulative rounding off errors.

6-2 Choice of LSR

The properties of the various lanthanide metals and chelates were discussed in SECTION 1-6-3. In the current work two LSR's were used :

$Eu(fod\text{-}d_9)_3$ with its extremely low broadening factor proved ideal for checking that substrate conformations do not alter significantly on adding LSR since tha various coupling constants are not destroyed by broadening, as occurs with other lanthanides. The coupling data obtained is discussed in SECTION 6-3-1.

Having established substrate conformational homogeneity between the normal and shifted spectra, $Yb(fod\text{-}d_9)_3$, with its large low-field PCS shifts and negligible CS/CFS contamination, is the best reagent on which to base an LIS conformational study (see TABLE 1-6.1).

6-3 Shifted Spectra of the Type (IV) Alcohols

6-3-1 Coupling Data from the $Eu(fod\text{-}d_9)_3$ Spectra

Comparisons of the normal and shifted $^3J_{H_{AB}}$ and $^nJ_{CF}$ couplings are presented in TABLES 6-3.1 & 6-3.2. Since there is a general trend for all the couplings to decrease by 0.1 to 0.2 Hz on adding the LSR, the effects observed would not appear to be related to changes in conformation but rather due to "chemical exchange spin decoupling"[185-187] (see SECTION 1-6.3).

X	NORM	LIS	Δ	X	NORM	LIS	Δ
H	5.35	5.15	-0.20				
o F	4.50	4.40	-0.10	p F	5.50	5.30	-0.20
o Cl	3.20	3.20	0	p Cl	5.30	5.10	-0.20
o Br	3.00	3.00	0	p Br	5.30	5.10	-0.20
o Me	6.00	5.90	-0.10	p Me	5.50	5.20	-0.30
o OMe	4.10	3.60	-0.50	p OMe	5.50	5.30	-0.20
o NO_2	2.85	2.70	-0.15	p NO_2	4.90	4.80	-0.10
o CF_3	4.00	3.90	-0.10	p CF_3	5.15	4.95	-0.20

TABLE 6-3.1 Changes in $^3J_{H_{AB}}$ Couplings on Adding LSR

NB. 100mg $Eu(fod\text{-}d_9)_3$ gives substrate : LSR ratio of ~ 10 : 1.

The use of LIS data in conformational analysis of the Type (IV) alcohols is therefore justified as there is no evidence of significant conformational changes on adding the LSR.

6-3-2 Shift Data form the Eu and $Yb(fod\text{-}d_9)_3$ Spectra

The LIS values used with METFIND VII were derived by "normalising" the observed shifts such that the LIS of C-1 = 1000. In the case of the $Eu(fod\text{-}d_9)_3$ data no allowances were made for CS and CFS contributions to the shifts, but for the $Yb(fod\text{-}d_9)_3$ data the shift of C-1 was reduced to 4% to eliminate the known CFS contribution.[169] Since Yb(III) chelates give only 5% CS to the

TABLE 6-3.2 Changes in $^{n}J_{CF}$ Couplings on Adding LSR

X	Spectra	C-1'	C-2'	C-3'	C-4'	C-5'	C-6'	C-1	C-2	C-X
oF	NORM	12.8	246.8	21.4	8.7	3.7	3.6	1.8	2.6	
	LIS	12.8	246.8	21.3	8.7	3.6	3.4	1.6	2.5	
	Δ	0	-0.4	-0.1	0	-0.1	-0.2	-0.2	-0.1	
oCF_3	NORM	1.5	30.3	5.8				2.2	1.6	274.0
	LIS	1.5	30.2	5.7				2.1	1.4	273.9
	Δ	0	-0.1	-0.1				-0.1	-0.2	-0.1
pF	NORM	2.4	8.1	21.8	247.6				1.6	
	LIS	3.1	8.2	21.7	247.5				1.5	
	Δ	+0.5	+0.1	-0.1	-0.1				-0.1	
pCF_3	NORM	1.5		3.9						272.2
	LIS	1.2		3.8						272.4
	Δ	-0.3		-0.1						+0.2

α-carbon in amines[145] (compared to 45% for Eu(III)[145]), diminishing to 1% in alcohols,[167,169] and CS effects themselves are short-ranged, no further measures were taken to "correct" the observed shifts.

TABLE 6-3.3 Actual LIS of C-1 Used for Normalisation (in ppm)

DERIV X	H	oF	oCl	oBr	oMe	oOMe	oNO_2	oCF_3
Eu LIS	1.423	1.590	1.232	1.347	0.923	1.699	0.714	0.471
Yb LIS	1.353	1.317	0.964	1.268	0.992	2.113	1.213	0.524
96% Yb	1.299	1.264	0.925	1.217	0.952	2.028	1.164	0.503
DERIV X	H	pF	pCl	pBr	pMe	pOMe	pNO_2	pCF_3
Eu LIS	1.423	0.835	0.830	0.744	1.681	1.880	0.847	0.969
Yb LIS	1.353	0.796	1.217	1.306	2.004	2.170	1.167	1.015
96% Yb	1.299	0.764	1.168	1.254	1.924	2.083	1.120	0.974

The normalised LIS of the Eu and Yb(fod-d_9)$_3$ spectra are listed in TABLES 6-3.4 and 6-3.5. The shifts for H-2 and H-3 were derived from AB approximations to the AA'BB'-system (described in SECTION 4-5-1).

Assuming that the maximum errors in the ^{13}C measurements are ±0.020 ppm and ±0.002 ppm in the ^{1}H and ^{19}F LIS, then the maximum range of errors present in the normalised LIS data may be calculated (see TABLE 6-3.6). Although some of these potential errors are fairly large, most are below 5%. This is not unreasonable when compared to the other sources of error in the LIS calculations (eg. coordinate errors and theoretical approximations).

There are several reasons why additional LSR was not used (eg. to double the LIS and therefore halve the potential measurement errors):

(1) Some difficulty was found in keeping 100mg of either LSR in solution in

TABLE 6-3.4 Observed Shifts on Adding $Eu(fod\text{-}d_9)_3$ to the Type (IV) Alcohols (Normalised on C-1)

X	C-1'	C-2'	C-3'	C-4'	C-5'	C-6'	C-1	C-2	C-X	H_A	H_B	H_C	H_X/F_X	H-2'	H-3'
H	318.3	284.6	137.0	108.9			1000	284.6		315.5	502.5	1924			
oF	343.4	270.4	136.5	106.9	132.7	320.8	1000	279.9		317.0	540.9	2006	205.2		
oCl	467.5	223.2	142.0	106.3	148.5	374.2	1000	258.1		293.0	569.0	2192			
oBr	478.1	188.6	126.9	92.1	150.7	377.1	1000	250.9		239.0	511.5	1990			
oMe	353.2	228.6	176.6	143.0	179.8	374.9	1000	305.5	121.0	308.8	529.8	1844	121.3		
oOMe	343.7	353.1	163.0	75.3	118.9	280.2	1000	294.9	153.6	330.8	473.2	1593	75.4		
oNO_2	525.2		133.1	92.4	162.5	392.2	1000	247.9		331.9	633.1	2521			
oCF_3	675.2		159.2	91.3	159.2	405.5	1000	350.3	256.9	305.7	607.2	2166	32.5		
pF	297.0	285.0	143.7	165.3			1000	273.1		368.9	550.9	2132	67.5	295.2	98.2
pCl	275.9	283.1	143.4	119.3			1000	257.8		404.8	641.0	2663		324.7	84.9
pBr	289.0	303.8	127.7	107.5			1000	276.9		392.5	608.9	2444		377.4	59.1
pMe	258.2	279.0	137.4	113.0			1000	267.1	119.1	385.5	615.7	2379	57.7	313.7	86.4
pOMe	260.1	293.6	143.1	125.5			1000	254.3	50.0	372.9	578.7	2234	38.3	293.4	85.4
pNO_2	328.2	314.0	137.6				1000	297.5		425.0	687.1	2672		347.7	102.1
pCF_3	286.9	290.0	150.7				1000	293.1	58.8	382.9	618.2	2452	0	302.4	76.4
Av o	438.1	258.1	146.8	102.0	150.3	360.7	1000	284.0		305.2	545.9	2029			
Av p	289.2	291.6	144.6	123.3			1000	275.6		381.0	600.4	2365		316.4	84.6

TABLE 6-3.5 Observed Shifts on Adding $Yb(fod\text{-}d_9)_3$ to the Type (IV) Alcohol (Normalised on 96% C-1)

X	C-1'	C-2'	C-3'	C-4'	C-5'	C-6'	C-1	C-2	C-X	H_A	H_B	H_C	H_X/F_X	H-2'	H-3'
H	495.0	311.8	143.2	111.6			1000	505.0		394.1	670.2	1963			
oF	489.7	284.8	141.6	110.0	142.4	337.0	1000	512.7		363.1	623.8	1741	218.4		
oCl	555.7	259.5	144.9	112.4	160.0	406.5	1000	542.7		336.2	649.7	1835			
oBr	489.6	218.6	117.4	98.1	137.5	381.0	1000	514.4		332.0	663.2	1782			
oMe	521.0	302.5	184.9	166.0	217.4	421.2	1000	536.8	164.9	401.8	678.0	1723	173.3		
oOMe	453.1	292.2	139.0	101.1	116.7	282.5	1000	501.2	111.3	367.3	659.0	1779	94.8		
oNO_2	473.4	301.9	134.9	103.1	131.4	380.6	1000	522.3		329.5	667.5	1873			
oCF_3	493.0	292.3	175.0	157.1	188.9	387.7	1000	554.7	161.0	372.8	647.1	1658	125.2		
pF	511.8	331.2	130.9	125.7			1000	520.9		424.7	684.6	2206	38.9	319.8	71.9
pCl	477.7	289.4	155.0	131.8			1000	412.7		335.2	535.5	1614		253.4	66.8
pBr	449.8	304.6	146.7	120.4			1000	518.3		321.8	480.9	1474		244.0	76.2
pMe	477.1	307.7	144.5	116.9			1000	508.2	93.2	337.6	548.4	1500	42.6	275.2	75.4
pOMe	491.6	324.5	161.3	145.5			1000	515.2	70.6	324.8	526.4	1443	54.2	270.8	102.0
pNO_2	433.0	328.5	208.9	164.3			1000	425.0		345.1	604.9	1705		281.3	98.2
pCF_3	416.8	293.6	141.7				1000	518.5	49.3	381.4	637.6	1905	30.5	295.2	100.1
Av o	496.5	264.5	148.2	121.2	156.3	370.9	1000	526.4		357.5	655.5	1802			
Av p	469.1	311.4	154.0	130.9			100	490.5		358.1	586.1	1726		277.1	84.4

2ml of $CDCl_3$ so further additions of LSR would have required weaker samples and consequently longer acquisition times, etc.

(2) The more LSR present, the more likelihood of its affecting the preferred conformations of the substrate.

(3) Increasing the LIS of the ^1H signals would have moved them under the aromatic resonances rendering them useless.

(4) Additional LSR would have increased the line broadening - introducing further measurement errors.

By plotting the Eu-LIS against the adjusted Yb-LIS for each substrate and constructing the best-fit line through the ^1H data a measure of the CS and

TABLE 6-3.6 Potential Measurement Errors in the Yb(fod-d_9)$_3$ LIS Data

X	C-1		SMALLEST ^{13}C LIS		SMALLEST ^{1}H LIS		^{19}F LIS	
	LIS	ERROR	NORM LIS	ERROR	NORM LIS	ERROR	NORM LIS	ERROR
H	1.299	1.5%	111.6	13.8%	392.6	0.4%		
oF	1.264	1.6%	110.0	14.4%	363.1	0.4%	218.4	0.7%
oCl	0.925	2.2%	112.4	19.2%	336.2	0.6%		
oBr	1.244	1.6%	98.1	16.4%	332.0	0.5%		
oMe	0.952	2.1%	166.0	12.7%	173.3	1.2%		
oOMe	2.057	1.0%	101.1	9.6%	94.8	1.0%		
oNO_2	1.164	1.7%	103.1	16.7%	329.5	0.5%		
oCF_3	0.503	4.0%	157.1	25.3%	372.8	1.1%	125.2	3.2%
pF	0.764	2.6%	125.7	20.8%	424.7	0.6%	38.9	6.7%
pCl	1.168	1.7%	131.8	13.0%	335.2	0.5%		
pBr	1.254	1.6%	120.4	13.2%	321.8	0.5%		
pMe	1.924	1.0%	93.2	11.2%	42.6	2.4%		
pOMe	2.083	1.0%	70.6	13.6%	54.2	1.8%		
pNO_2	1.120	1.8%	164.3	10.9%	345.1	0.5%		
pCF_3	0.974	2.0%	49.3	41.6%	381.4	0.5%	30.5	6.7%
	Using 0.020 ppm as the max. error				Using 0.002 ppm as the max. error			

X	1-BOND		2-BONDS		3-BONDS		TYPE
	H_C	C-1	C-2	C-1'	C-2'	C-6'	
H	412	230	-105	-68	45		
oF	495	130	-168	-82	20	30	1
oCl	595	125	-218	-20	0	20	
oBr	640	240	-137	107	24	88	2
oMe	505	220	-115	-52	0	47	1
oOMe	312	280	-62	17	145	72	
oNO_2	692	25	-260	60	/	15	2
oCF_3*	660	95	-150	230	/	55	
	480	0	-155	235		80	
pF*	255	149	-170	-145	0		1
	330	200	-165	-140	-10		
pCl	715	-210	-245	-307	-65		
pBr	580	-265	-280	-378	-80		
pMe	700	-120	-302	-280	-65		
pOMe	1125	-125	-325	-295	-70		3
pNO_2	710	-165	-200	-180	-70		
pCF_3	560	-10	-220	-125	-5		

* Upper line = best fit inc. origin;
Lower line = best fit (^{1}H data only)

TABLE 6-3.7 Estimates of the CS and CFS Contributions to the Eu-LIS Data (Scaled to C-1 = 1000)

CFS contributions to the Eu-LIS may be obtained. Several types of plot emerge (see TABLE 6-3.7), typical examples of which are shown in FIG.6-3.1. The oCF_3(IV) and pF(IV) LIS (FIG.6-3.2) appear to be slightly anomalous.

The alternation of CS shown in the "Type 1" alcohols is in accord with the observations[165,171,174] noted in SECTION 1-6-1.2, whilst the reversal of sign of C-1' present in the "Type 2" alcohols may reflect a difference in the transoidal relationship C-2 and C-1' to the metal (see FIG.1-6.2[158,172,173]).

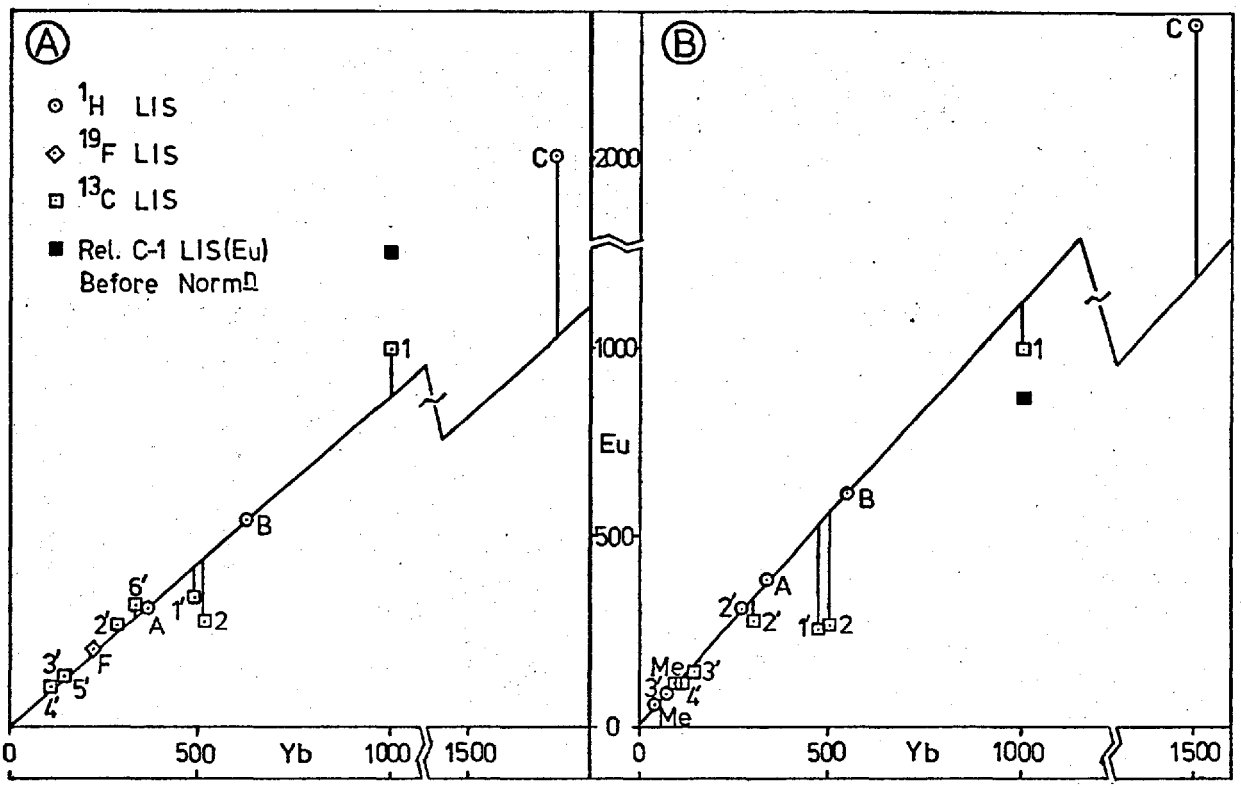


FIG.6-3.1 Plot of Normalised Eu-LIS vs Yb-LIS for (A) oF(IV) - a 'Type 1' Case, and (B) pMe(IV) - a 'Type 3' Case.

The best-fit ^{1}H line is used to measure the CS/CFS contributions in the Eu-^{13}C data (Vertical Bars). In every instance H_C has a large +ve CS whilst C-2 has a large -ve CS. Note that the axes have been compressed for convenience.

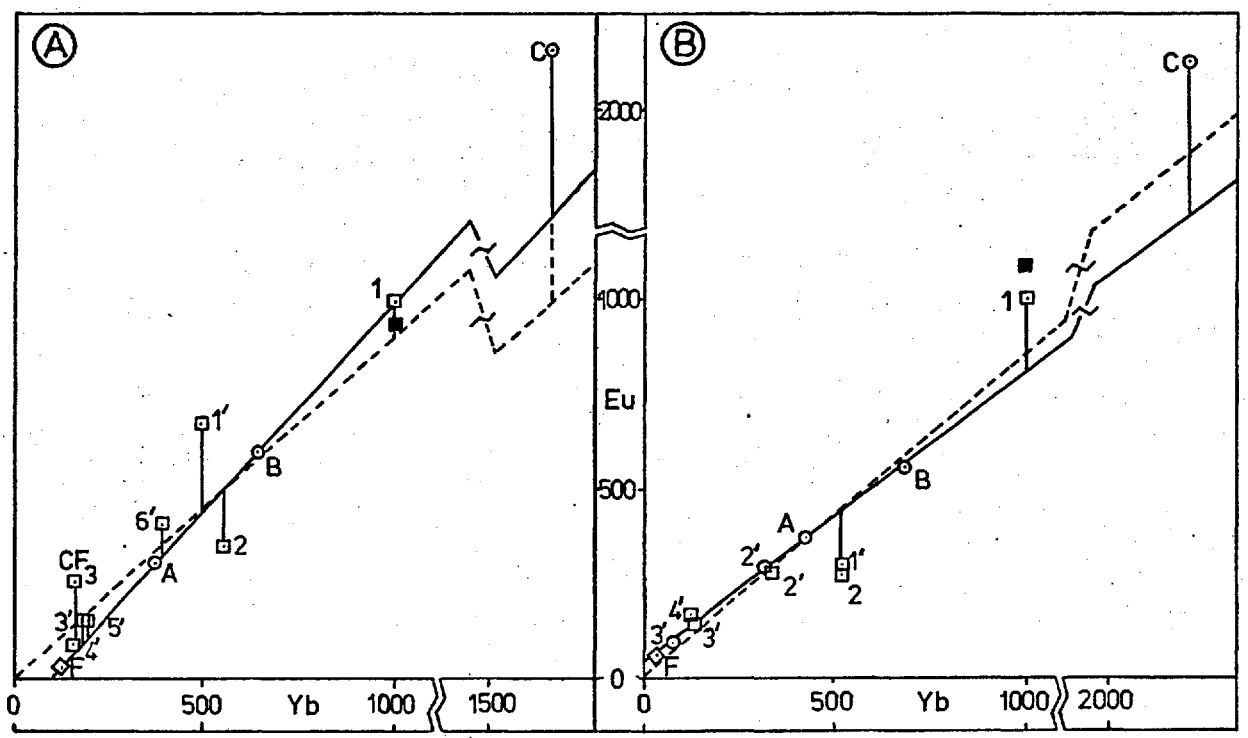


FIG.6-3.2 Plot of Normalised Eu-LIS vs Yb-LIS for (A) oCF_3(IV) - a 'Type 2' Case, and (B) pF(IV) - a 'Type 3' Case.

These plots are anomalous in the 15 Type(IV) alcohols as they are the only cases in which the best-fit ^{1}H line (solid) does not pass through the origin.

The significance of the ^1H best-fit lines for the oCF_3(IV) and pF(IV) alcohols not passing through the origin is elusive but may indicate a conformational change between the Eu and Yb LIS spectra. There is, however, no corroborative coupling evidence that the Eu-substrate structures differ from those in the normal spectra.

The negative CS's for C-1 found in the "Type 3" cases are accompanied by very large positive values for the H_C CS. This effect is obviously linked to the para series but whether it is due to a weakening of the O-Ln "bond", to relief of steric crowding in the vicinity of the binding site or the tendency of the para derivatives to occupy all three side-chain rotamers approximately equally (the ortho derivatives show considerable rotamer selectivity - see FIG. 4-8.14) cannot be satisfactorily determined from the limited data available.

Whatever the causes of the deviations between the Eu-LIS and the Yb-LIS, this brief comparison illustrates the necessity of selecting the $Yb(fod\text{-}d_9)_3$ data, as this is known to contain the highest percentage PCS of all the Lanthanide Shift Reagents (see SECTION 1-6-1.2), and is therefore the best LSR for conformational work.

6-4 Substrate Coordinates

The following assumptions/approximations were made in calculating the coordinate data :

(1) The aromatic ring is planar with all angles equal to 120°.

(2) The two side-chain carbons are fully tetrahedral (bond angles 109.5°) - an approximation as the C-C-Cl angle is known to be 111.5° in C_2H_5Cl and is probably 110.5° in $C_2H_4Cl_2$.[279 280]

(3) The C-O-Me angle = $121.^\circ$[280]

(4) The bond lengths were taken from standard texts[279 280] (see TABLE 6-4.1).

(5) For the initial substrate position a choice of three C-1/C-2 ROTAMERS (ROT1, ROT2, ROT3) and two C-1/C-1' ORIENTATIONS (OR1: C-6' cis to H_B, OR2: C-2' cis to H_B) was available. Normally the preferred rotamer (from FIG.4-8.14) and the orientation which placed the larger LIS of C-2' or C-6' cis to H_B were chosen. Since choice of rotamer/orientation has no bearing on the position of the fixed atoms, and the first operation in the rotational optimisation of the molecule is to rotate all the bonds, selection of the initial substrate conformation is only critical if a very poor fit is obtained in certain orientations.

The atomic naming convention used for the Type (IV) alcohols (see FIG. 6-4.1) was similar to that used for cholesterol in SECTION 5-3. The "Fixed Atoms", ie. those whose positions do not change on rotation of the C-1/C-1' or C-1/C-2 bonds, are also indicated.

The standard program COORD was used to obtain 3-D coordinates from the bond length and bond angle data and this was manipulated using a modified

TABLE 6-4.1 Bond Lengths Used in Calculating the Substrate Coordinates[279,280]

BOND	LENGTH	BOND	LENGTH	BOND	LENGTH
-C—C- (SIDE)	1.54	-C—OH (SIDE)	1.48	=C-O—Me (SUB^n)	1.35
-C=C- (AROM)	1.40	(-C-O—H (SIDE)	0.97)	-C-C—H_3 (SUB^n)	1.11
=C—Me (AROM)	1.52	=C—F (AROM)	1.30	=C—NO_2 (AROM)	1.49
=C—H (AROM)	1.08	=C—Cl (AROM)	1.67	-N—O_2 (SUB^n)	1.22
-C—H (SIDE)	1.09	=C—Br (AROM)	1.86	-C—CF_3 (AROM)	1.52
-C—Cl (SIDE)	1.76	=C—OMe (AROM)	1.36	=C-C—F_3 (SUB^n)	1.33

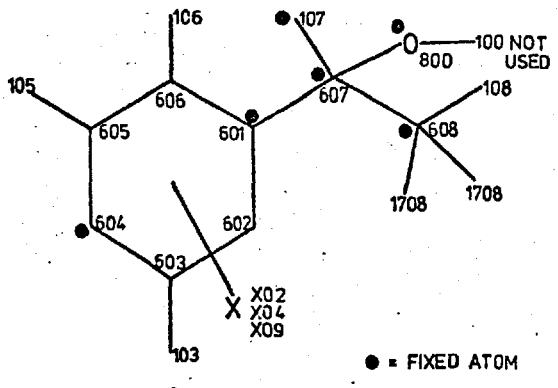


FIG.6-4.1 Atom Naming Convention

Based on four digits...the first two are used for the Atomic Number (ie. C = 6, F = 9 etc.); the second two for the carbon framework number : 1-8(9).

version of S.J.Robert's program XYZFG to obtain coordinates in the desired orientation (ie. with the +X-Y plane passing through C-1, C-1' and C-4').

The calculated coordinates for the various groups of atoms are listed in TABLES 6-4.3 to 6-4.6, the ROTAMER/ORIENTATIONS selected for each of the 15 Type (IV) alcohols being given in TABLE 6-4.2.

TABLE 6-4.2 ROTAMERS/ORIENTATIONS

DERIV	C-1/C-2 ROTAMER	C-1/C-1' ORIENTATION
H+PARA	1	1
o F	1	2
o Cl	3	2
o Br	3	2
o Me	1	2
o OMe	2	1
o NO_2	3	1
o CF_3	2	2

TABLE 6-4.3 Coordinates of Fixed Atoms

ATOM	NAME	X	Y	Z
H_B	107	1.8433333	0.5138310	0.8899812
H-4'*	104	3.2800002	-5.0911688	0.0
C-1	607	1.48	0.0	0.0
C-2	608	1.9933329	0.7259630	-1.2574047
C-1'	601	1.9866667	-1.4330697	0.0
C-4'	604	2.9200001	-4.0729350	0.0
O	800	0.0	0.0	0.0

* In the para series this is replaced by the deriv X.

6-5 Approach to Rotational Optimisation (Rot/Opt) Using LIS and METFIND VII

The method used is outlined in Chapter 5. Two sets of searches/optimisations were made for each set of LIS data : (1) Normalising on C-1 (607), (2) Normalising on H_B (107). The Yb-LIS study of $\overset{\circ}{o}$F(IV) normalising on H_B will be used as an example in this section (supported by APPENDIX IV), the condensed results for all alcohols, from both the Eu- and Yb-LIS, being presented in SECTION 6-6.

TABLE 6-4.4 $-CHCl_2^-$ Rotamer Coordinates

ATOM	NAME	X	Y	Z
		ROTAMER 1		
H_A	108	1.6333332	0.2168460	-2.1392210
Cl	1708	1.4066665	2.3853068	-1.2574047
Cl	1708	3.7533332	0.7259631	-1.2574047
		ROTAMER 2		
H_A	108	1.6333332	1.7441967	-1.2574047
Cl	1708	3.7533332	0.7259631	-1.2574047
Cl	1708	1.4066667	-0.1037092	-2.6944387
		ROTAMER 3		
H_A	108	3.0733333	0.7259631	-1.2574047
Cl	1708	1.4066667	2.3853068	-1.2574047
Cl	1708	1.4066667	-0.1037092	-2.6944387

TABLE 6-4.5 Aromatic Ring Orientation Coords

OR.1		OR.2		X	Y	Z
ATOM	NAME	ATOM	NAME			
C-2'	602	C-6'	606	1.6484524	-2.2951087	-1.05
C-3'	603	C-5'	605	2.1151192	-3.6150413	-1.05
C-5'	605	C-3'	603	3.2582144	-3.2108960	1.05
C-6'	606	C-2'	602	2.7915477	-1.8909634	1.05
H-2'	102	H-6'	106	1.0275443	-1.9418764	-1.86
H-3'	103	H-5'	105	1.8542110	-4.2800428	-1.86
H-5'	105	H-3'	103	3.8791226	-3.5641283	1.86
H-6'	106	H-2'	102	3.0524559	-1.2259620	1.86

TABLE 6-4.6 Ring Substituent Coordinates

SUB^n	ATOM	NAME	OR^n	ORTHO X	ORTHO Y	ORTHO Z	NAME	PARA X	PARA Y	PARA Z
F	F	902	2	3.1056038	-1.0904987	2.0250000	904	3.3533335	-5.2985868	0.0
Cl	Cl	1702	2	3.1949890	-0.8626741	2.3025000	1704	3.4766669	-5.6474261	0.0
Br	Br	3502	2	3.2408895	-0.7456831	2.4450000	3504	3.5400002	-5.8265598	0.0
CH_3	H_1	109	2	3.7969074	-1.4944794	2.9206556	109	3.0566668	-6.0292637	-0.9063112
	H_2	109		2.2337517	-0.6052060	2.6940778	109	3.0566668	-6.0292637	0.9063112
	H_3	109		3.7137157	-0.0819470	1.7877665	109	4.5366669	-5.5060047	0.0
	C	609	2	3.1587518	-0.9550354	2.1900000	609	3.4266668	-5.5060047	0.0
CF_3	F_1	909	2	3.9233887	-1.6013962	3.0654702	909	2.9833335	-6.1329728	-1.0859404
	F_2	909		2.0504184	-0.5358706	2.7939851	909	2.9833335	-6.1329728	-1.0859404
	F_3	909		3.8237518	0.0910975	1.7080446	909	4.7566669	-5.5060046	0.0
OMe	O	802	1	0.8665681	-1.8502977	-2.0699999	804	3.3733335	-5.3551553	0.0
	C	609		0.5404329	-2.6815495	-3.0824999	609	3.0471980	-6.1864071	-1.0125000
	H_1	109		-0.0804753	-2.1566851	-3.7934081	109	3.4941677	-7.1546058	-0.8415918
	H_2	109		1.4404328	-3.0219239	-3.5729540	109	1.9732596	-6.2893670	-1.0620459
	H_3	109		0.0004329	-3.5310409	-2.6911377	109	3.4132595	-5.7802500	-1.9438622
NO_2	N	702	1	0.7918291	-1.0877789	-2.1675000	704	3.4166669	-5.4777205	0.0
	O_1	802		0.3851624	-0.6575520	-2.1674999	804	3.1219373	-6.2289258	-0.9150000
	O_2	802		0.4970995	-2.5589843	-3.0825000	804	4.1180632	-5.8767421	0.9150000

6-5-1 Metal Search Based on Fixed Atoms

The first stage in the rot/opt process is to find the best metal position relative to the "fixed" substrate atoms. In the Type (IV) alcchols these are Atom Nos. 800, 607, 608, 107, 601, 604 and 104 (or pX see FIG.6-4.1). Although this could be done as part of a ROTATE run by using NCYCOP = 1 (in effect a FOCUSING MODE search - see TABLE 5-4.1) it is more thorough to perform a complete MULTISCAN search using the fixed data and then to start the ROTATE run with the known maximum within the initial search area. This saves considerable time in the already lengthy ROTATE runs and ensures that an isolated maximum is not found.

In oF(IV) only five fixed atoms have observable LIS. The data used for the initial MULTISCAN search is shown in APPENDIX IV-1 with part of the output in APPENDIX IV-3. The max FITFACTOR (978) (using FITLIM = 0.500 ie. SFIT = 0.989 or RMS error = 1.1%) was found at (300/155/240).

As H_B (107) was used for normalisation only 4 atoms were used to locate the metal position. Since 3 atoms are the minimum requirement for a unique solution the likelihood of there being several equally plausible maxima is considerable. This is seen for oF(IV) in FIGS.6-5.1 & 6-5.2 where "ridges" in the FITFACTOR tables bifurcate, illustrating how real the possibility of settling on a secondary maximum is when using FOCUSING MODE searches. The occurrence of secondary maxima decreases as the number of atoms with LIS data increase.

6-5-2 Rotational Optimisation

Having established the position of the maximum FITFACTOR a ROTATE run can be considered. The SEARCH PARAMETERS are chosen so that the known max. is within the first search area with the first NCYCOP option = 1 so that this is centred on. Subsequent CYCLES add the side-chain and phenyl ring in turn, initially with crude rot/opt (30° steps), followed by finer adjustments until no further improvement in fit can be obtained. The NCYCOP sequence shown in TABLE 5-4.2 was widely applied although a modified sequence was used for oOMe & pOMe(IV) so that the orientation of the OMe groups could be optimised with respect to the phenyl rings.

The attempts at rot/opt of oF(IV) provide good examples of some of the problems incurred when using METFIND in the ROTATION MODE. These were mainly due to two maxima, present in close proximity, in the early stages of the runs. The problems are best illustrated by "talking through" a complete ROTATE run (see APPENDIX IV, p.278-279) then comparing the results of the two methods used.

A ROTATE run starts with WRITEA output followed by a table of the initial INTER-ATOMIC DISTANCES. Each CYCLE begins with a description of the operation selected and a listing of the atoms to be used. In CYCLE 1 the maximum (and secondary maximum) FITFACTOR of the FIXED ATOMS was centred on (see TABLE 6-5.2). In CYCLE 2, H-108 (in ROT2) was added to the FIXED ATOMS and the search area centred onto the new maximum. Only one rotatable group should be added at a time since the orientation is unlikely to be correct and hence the position of the max. FITFACTOR might move considerably, leaving no results in the search area and terminating the run. In CYCLE 3 a crude rot/opt of H-108 was performed. This involves rotating the group (including any nmr inactive atoms) in steps of 30° through a complete circle. Increments from 30° to 330° were abandoned in favour of a 30 to 180, -30 to -150 pattern as this gave less incidence of the search area "wandering aimlessly" out to R = 600 (at which

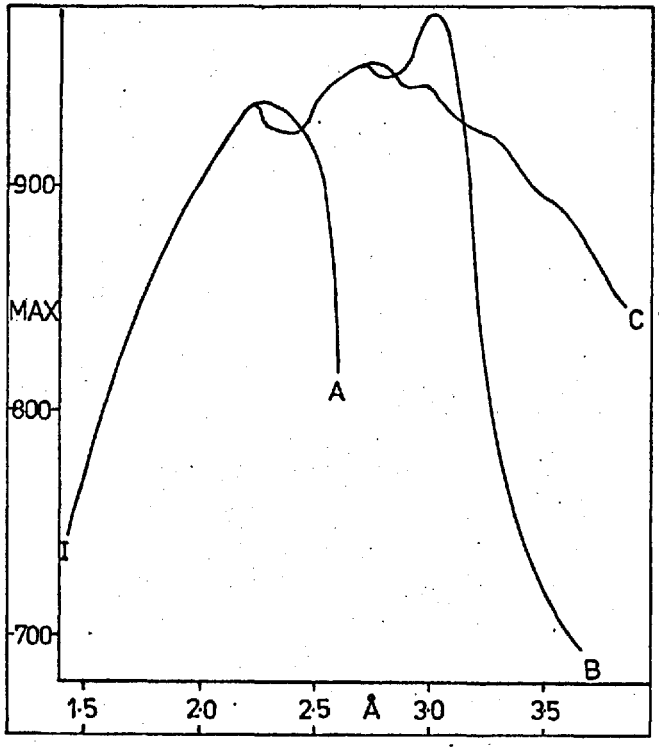


FIG.6-5.1 FITFACTOR MAXIMA vs RADIUS

In both cases where "ridges" in the FITFACTOR tables bifurcate, on increasing the search RADIUS, the higher branches are initially lower than those leading to the secondary maxima and would therefore not be found by a FOCUSING MODE search. This illustrates the necessity for performing full MULTISCAN searches. This type of behaviour is a function of the size of the data set and the tendency for the formation of secondary maxima is considerably reduced by increasing the number of LIS observations used.

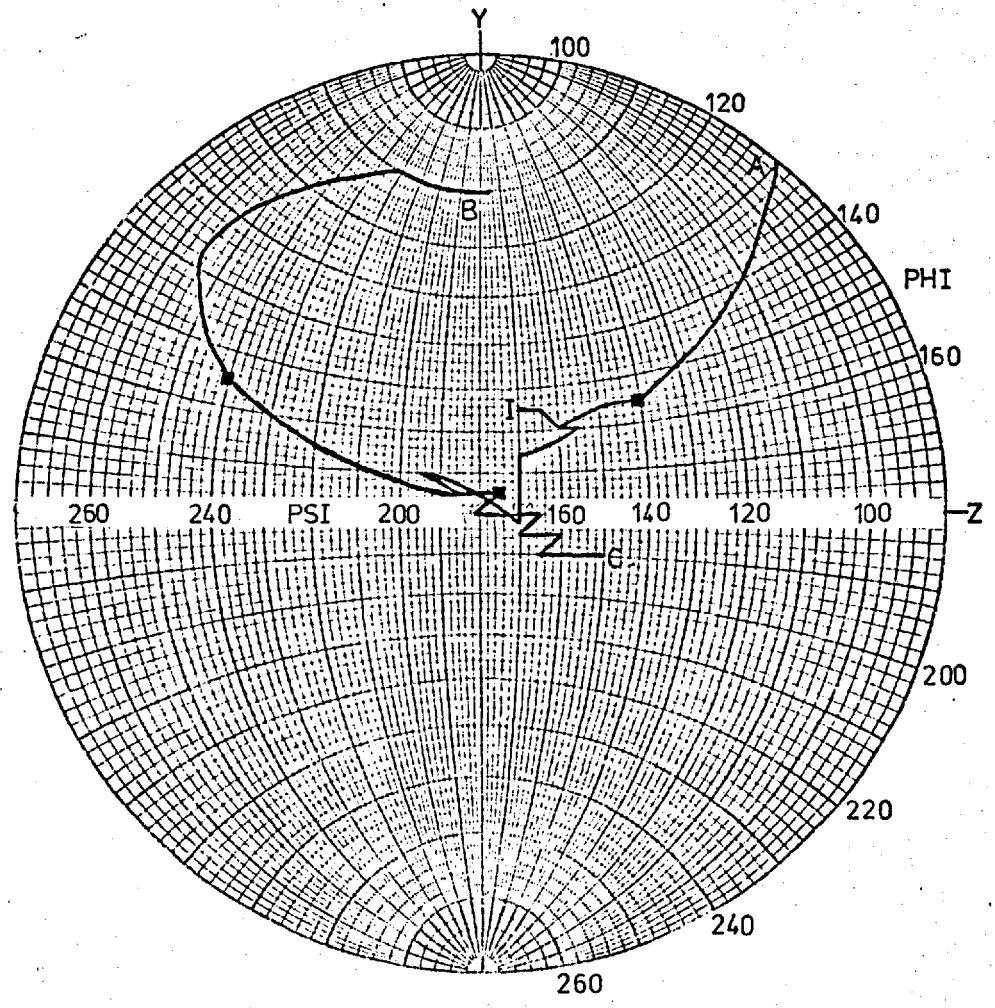


FIG.6-5.2 FITFACTOR MAXIMA : PHI vs PSI At Each Search RADIUS

(■) Indicates maxima in the FITFACTOR "Ridges"
(I) Indicates the position of the max. for the initial search
(A,B,C) Indicate the limits of the FITFACTOR searches

The -X axis is towards the observer (ie. the molecule is behind the page).

point runs are terminated). Even with the improved NCYCOP = 6, ROTATE pattern search areas can become SILLY (see p.277) if the initial direction of rotation is incorrect. This can, however, be overcome by using the NCYCOP = 3, ROTOPT = 6 option (vide infra).

When starting a search, METFIND normally retains the parameters of the last search. This used to be so in ROTATE options when returning to the orientation with the max. FITFACTOR. If, (eg. in NCYCOP = 6 operations) the search area has moved significantly away from the max. FITFACTOR position, the original max. may not be refound. Sometimes a higher, though more frequently a lower "maximum", was found so the program was modified to return to the original max. only. In both the oF(IV) runs, the maxima found at each CYCLE 3 orientation were identical (see TABLE 6-5.1) but the first run found a different "maximum" on returning to the 90° orientation. TABLE 6-5.2 shows this quirk had a dramatic effect on the course of the two rotational optimisation runs.

TABLE 6-5.1 Maximum FITFACTORS Found at Each H-108 Orientation in CYCLE 3

ORIENTN	MAX	R	PHI	PSI	ORIENTN	MAX	R	PHI	PSI
INITIAL	948	270	170	210	-30	963	275	175	182
30	961	290	160	230	-60	916	315	185	177
60	934	290	160	235	-90	864	315	185	182
90	965	310	145	250	-120	844	325	187	179
120	949	270	170	205	-150	862	315	185	179
150	962	275	175	182	+90(1)	750	265	142	129
180	915	315	185	175	+90(2)	965	310	145	250

In CYCLE 4 the stored coordinates were updated with the new H-108 coordinates. CYCLES 5, 6 and 7 repeated the sequence used for H-108 with the ring carbons and ortho fluorine group. In both runs the initial ring orientation was found to be the best.

CYCLE 8, with NCYCOP = 3 (increment = 5°) was the first stage of the finer optimisation of both rotatable groups. NCYCOP = 3 and 5 feature searches which check that new orientations have higher max. FITFACTORS than their predecessors. If the first increment lowers the max. the direction of rotation is changed. Rotation continues until a max. value is passed, the orientation being reset to the average position found at the highest FITFACTOR. Further, up to 4 groups may be rotated in turn, in one CYCLE, provided that the axial and rotating atoms of each are independent. Here, with only two groups to optimise, the process is straightforward, although several repeats are needed in order to overcome interactive effects (rather analogous to shimming a magnet).

Here the two runs differed dramatically, the first rotating H-108 by +60° the second by only +5°. Other differences remained marginal. CYCLE 8

was followed by two further ROTATION CYCLES (10 & 12) with CYCLES 9, 11 & 13 used to update the stored coordinate data. CYCLE 12 was the final stage of the rot/opt process so CYCLE 13 used NCYCOP = 8 to output a copy of the coordinates for card punching.

In the two remaining CYCLES, first the side-chain and then the phenyl ring were subjected to "TWELVE POSITION FREE ROTATIONAL AVERAGING" by using the NCYCOP = 7 option. Although very expensive (taking up to 100 CP secs per ITERATION) this is a very useful test of the significance of the orientation derived by the rot/opt process - if there is no drop in the FITFACTOR max. on "free-rotating" a group then the hypothetical "rigid" orientation has no significance. This judgement should be weighted by the size of the group for if only one atom out of 11 (as occurs here with H-108) is free-rotated then its effect on the FITFACTOR should be expected to be fairly small.

TABLE 6-5.2 Rotational Optimisation of oF(IV) (Normalising on H-107)

CYCLE	NCYCOP	OPERATION	RUN 1					RUN 2				
			ROTN	MAX	R	PHI	PSI	ROTN	MAX	R	PHI	PSI
1	1	FIXED ATOMS		955	270	175	185		978	300	155	240
2	2	ADD H-108	ROT2	948	270	170	210	ROT2	944	280	170	230
3	6	ROTATE H-108	+90°	750	265	142	129	+90°	965	310	145	250
5	2	ADD RING + oF	OR2	897	235	160	192	OR2	893	300	150	235
6	6	ROTATE RING + oF	0°	898	235	162	192	0°	"	"	"	"
8	3	" H-108	+60°	948	271	174	180	+5°	903	305	146	245
	3	" RING + oF	+2.5°	949	272	174	179	-5°	914	305	152	239
10	5	" H-108	0°	950	272	174	179	-4°	916	305	150	241
	5	" RING + oF	0°	"	"	"	"	-1°	"	"	"	"
12	5	" H-108	0°	"	"	"	"	+1.5°	917	304	152	239
	5	" RING + oF	0°	"	"	"	"	-1.5°	917	303	153	238
14	7	FREE ROTN H-108		939	272	175	179		933	263	173	183
15	7	FREE ROTN RING + oF		866	252	135	104		832	178	158	170

Although RUN 2 appears to be better in the first three CYCLES, RUN 1 is clearly better later on. This is borne out by the max. in CYCLE 14 being 11 units lower than in CYCLE 12 for RUN 1 whereas it is 16 units higher in RUN 2! The side-chain orientation is definitely not optimised in RUN 2 but is it optmised in RUN 1? From TABLE 6-5.1 the "TWELVE POSITION AVERAGE" for H-108 with just the 5 FIXED ATOMS is 924 ie. 41 units lower than the max. value 965. Since FITFACTORS are based on an RMS function the expected drop in the max. FITFACTOR on free-rotating H-108 with 11 atoms rather than 6 cannot be directly calculated; here the approximation 6/11 of 41 ie. 22 will suffice. The observed drop (11) is probably less significant than the drop seen in CYCLE 3,

ie. the significance of the side-chain orientation is debatable. On further examination of TABLE 6-5.1 the likelihood of a unique solution to the side-chain orientation can be seen to be very small as maxima (@963±2) exist at -30, +30, +90 and +150.

The drop of 84 and 85 units respectively in max. FITFACTOR on rotating the ring and ortho fluorine appears to be fairly significant but on examining the CYCLE 6 output a secondary maximum of 884 at 185/152/172 is found in both runs, which although at too short a radius to be treated seriously shows the dangers of accepting results at their face value.

6-5-3 Full MULTISCAN Search

Once a ROTATE run has been successfully completed a MULTISCAN MODE search, based on the full data as optimised, is performed to check that a secondary maximum was not used for optimisation. In the case of oF(IV) this was only performed for the RUN 1 final orientation, the maximum found being identical to that found in the ROTATE run ie. 897(FITLIM1 = 0.750) @ 270/175/180.

6-6 Results of Rotational Optimisation Using the Eu- and Yb-LIS

6-6-1 Initial Maxima Found for the FIXED ATOMS

In most cases there were only 5 FIXED ATOMS. In some para derivatives

TABLE 6-6.1 Maxima in Eu-LIS MULTISCAN Searches of the FIXED ATOMS

DERIV X	No. ATOMS	NORM ON C-607				NORM ON H-107				607 2nd	107 2nd
		MAX	R	PHI	PSI	MAX	R	PHI	PSI		
H	5	811	260	105	125	845	280	110	217	/	*
oF	5	897	270	100	190	904	280	105	225	/	*
oCl	5	901	240	155	205	981	200	150	190	/	*
oBr	5	903	170	145	195	943	150	145	190	/	/
oMe	5	743	260	110	195	714	260	115	195	/	*
oOMe	5	905	260	145	110	933	240	155	130	*	*
oNO_2	5	797	210	155	220	907	200	155	220	/	$ *
oCF_3	5	676	225	160	217	966	250	160	130	/	$ *
pF	6	586	270	100	190	541	280	105	225	/	*
pCl	5	635	290	95	270	477	290	90	XXX	/	*
pBr	5	749	290	90	XXX	685	290	95	90	/	*
pMe	9	441	280	100	222	362	290	95	255	/	*
pOMe	5	572	200	95	90	500	290	90	XXX	/	*
pNO_2	4	647	180	210	220	864	200	210	240	/	$
pCF_3	8	105	200	180	220	64	300	170	105	$	$.*

* Secondary maximum at higher radius than max. value (9 of these values occurred at 490/145/115). $ Secondary maximum at shorter radius than max. value. XXX When PHI = 90 all values of PSI are equal.

this number was higher (eg. pF and pMe) whilst with pNO_2 the C-4' LIS signal was not observable, lowering the number to 4. The Eu-LIS results are given in TABLE 6-6.1, the Yb-LIS results in TABLE 6-6.2. Note the Eu-LIS results are generally poorer than the Yb-LIS results, with the radius of the latter usually longer (especially when normalising on C-607). This is probably due to the CS addition to the Eu-LIS of C-607.

TABLE 6-6.2 Maxima in Yb-LIS MULTISCAN Searches of the FIXED ATOMS

DERIV X	No. ATOMS	NORM ON C-607				NORM ON H-107				607 2nd	107 2nd
		MAX	R	PHI	PSI	MAX	R	PHI	PSI		
H	5	976	260	165	150	970	250	155	135	/	/
oF	5	967	290	165	225	978	300	155	240	/	/
oCl	5	966	290	175	205	986	310	185	185	/	/
oBr	5	953	260	170	145	951	310	145	260	/	/
oMe	5	943	300	145	185	985	360	160	170	/	/
oOMe	5	916	260	160	135	924	310	135	265	/	/
oNO_2	5	918	255	170	152	940	310	145	260	/	/
oCF_3	5	951	310	137	207	986	330	150	195	/	/
pF	6	763	320	190	160	769	340	190	155	/	/
pCl	5	898	230	135	165	926	220	125	145	/	/
pBr	5	756	320	140	250	985	220	110	170	/	*
pMe	9	670	300	150	235	661	350	175	205	/	/
pOMe	5	787	300	145	225	782	220	135	125	/	*
pNO_2	5	809	270	125	187	772	305	138	177	/	/
pCF_3	8	793	310	160	245	767	300	175	145	/	/

* Secondary max. = 977 @ 410/180/210 in both cases.

6-6.2 Results of the ROTATION MODE Runs

The results from CYCLE 1 are the same as those given in TABLES 6-6.1 & 6-6.2. In CYCLE 2, H-108 is added and the max. FITFACTOR found. This is used as the 0° reference in the CYCLE 3, NCYCOP = 6 rot/opt of H-108. As illustrated in SECTION 6-5-2 a knowledge of the individual results for the 30° rotation increments is useful in later determining the significance of the optimised geometry. The maxima for CYCLES 2 and 3 are therefore given in TABLES 6-6.3 and 6-6.4, for the Eu- and Yb-LIS data respectively, with the CYCLE 5 and 6 maxima for the phenyl ring optimisation given in TABLES 6-6.5 & 6-6.6. In all cases the upper values are for normalisation on C-607, the lower values for H-107. -S-(an abbreviation for SILLY) indicates the CYCLE and run terminated due to an illegal search area (eg. R greater than 6Å, etc.).

Where Me or CF_3 groups were present these were "free-rotated" using the "TWELVE POSITION AVERAGING" option in addition to any ring rot/opt performed.

TABLE 6-6.3 CYCLES 2 & 3 : H-108 FITFACTOR Maxima for Eu-LIS Data.

DERIV X	Init ROTN	-150	-120	-90	-60	-30	0	30	60	90	120	150	180	NB
H	ROT1	414	534	689	800	818	775	681	579	483	408	362	359	
	ROT1	/	/	/	/	/	763	747	688	657	655	-S-	/	1
oF	ROT2	500	425	384	385	442	562	715	850	873	810	704	597	
	ROT2	658	656	684	745	825	898	925	915	865	807	740	687	2
oCl	ROT3	908	905	883	846	807	785	785	805	840	871	896	906	
	ROT3	847	893	949	923	901	888	904	935	930	871	820	809	3
oBr	ROT3	746	791	779	738	680	630	590	559	530	506	553	767	
	ROT3	663	733	759	740	684	604	535	516	515	525	548	588	
oMe	ROT1	451	542	657	745	759	741	687	609	535	477	440	423	
	ROT1	/	/	/	/	/	717	652	779	753	760	-S-	/	4
oOMe	ROT2	679	641	629	649	709	823	929	892	915	908	825	744	
	ROT2	687	671	687	737	815	909	943	901	931	916	817	724	
oNO_2	ROT3	640	563	543	508	475	452	433	415	395	383	400	625	
	ROT3	314	410	489	516	494	453	401	360	318	280	256	259	5
oCF_3	ROT2	613	601	603	617	637	654	666	675	682	677	661	637	
	ROT2	659	621	618	642	678	715	736	755	777	783	802	795	6
pF	ROT1	256	348	474	565	577	541	483	416	350	293	257	230	
	ROT2	522	527	550	592	641	667	678	666	636	598	561	534	7
pCl	ROT1	/	/	/	-S-	582	511	425	338	255	182	137	138	
	ROT1	/	/	/	/	/	/	/	/	/	/	/	/	8
pBr	ROT1	302	426	583	703	686	608	513	423	341	275	235	240	
	ROT1	/	/	/	/	/	616	556	522	511	-S-	/	/	
pMe	ROT1	160	251	372	445	446	414	366	311	254	194	145	126	
	ROT1	/	/	/	/	/	-S-	/	/	/	/	/	/	9
pOMe	ROT1	158	283	445	560	556	495	412	325	237	156	102	99	
	ROT1	/	/	/	/	/	-S-	/	/	/	/	/	/	9
pNO_2	ROT1	356	418	467	488	471	415	339	274	236	230	253	297	
	ROT2	299	324	384	449	517	590	698	542	133	0	0	0	10
pCF_3	ROT1	103	116	123	120	106	97	82	73	70	72	79	89	
	/	/	/	/	/	/	/	/	/	/	/	/	/	8

Key : (1) Later solved by using ROT2 and NCYCOP = 3

(2) All results at ~R = 500

(3) All results at ~R = 450, Sequence 30 to 330 used

(4) This still occurred with an initial ROT2 position

(5) All at R = 100 to 190 ... too close

(6) Max at R = 80 ... much too close

(7) ROT1 search gave SILLY result in CYCLE 3. With ROT2 all results at R > 500

(8) SILLY result in CYCLE 1

(9) No results found with ROT1 or ROT2

(10) Had to use ROT2 to obtain a result

446 indicates the maximum value; 935 indicates a secondary maximum value.

TABLE 6-6.4 CYCLES 2 & 3 : H-108 FITFACTOR Maxima for Yb-LIS data

DERIV X	Init ROTN	-150	-120	-90	-60	-30	0	30	60	90	120	150	180	NB
H	ROT2	824	805	817	860	928	963	935	919	938	945	956	875	
	ROT2	813	795	813	863	944	968	916	783	823	926	951	867	
oF	ROT2	852	833	844	882	933	944	951	931	951	945	952	901	
	ROT2	862	844	864	916	963	948	961	934	965	949	962	915	1
oCl	ROT3	841	910	943	969	958	950	959	976	942	889	845	830	
	ROT3	913	941	950	969	985	973	987	959	967	934	920	883	
oBr	ROT3	904	926	932	960	927	909	919	947	937	909	880	864	
	ROT3	725	782	904	953	887	903	916	948	950	918	781	647	
oMe	ROT1	924	942	865	808	820	900	944	888	842	826	838	875	
	ROT1	958	824	780	776	803	866	956	931	874	857	878	944	
oOMe	ROT2	817	797	805	842	897	917	826	771	815	893	922	866	
	ROT2	802	783	797	841	898	855	850	847	844	855	914	853	
oNO_2	ROT3	889	899	905	927	903	888	894	919	919	889	872	856	
	ROTX	693	683	702	766	869	923	899	879	885	908	922	910	2
oCF_3	ROT2	848	831	839	870	915	952	876	814	822	901	948	889	
	ROT2	892	874	893	946	990	930	864	813	824	888	972	945	
pF	ROT2	745	736	746	769	783	758	710	694	721	761	783	769	
	ROT2	760	748	757	787	827	834	819	812	822	834	818	788	
pCl	ROT1	751	814	885	907	900	908	875	804	743	706	697	712	
	ROT1	980	902	851	835	851	916	918	808	704	621	566	926	3
pBr	ROT1	714	757	780	755	741	760	689	748	705	676	667	680	
	ROT1	565	715	869	959	959	953	900	807	691	599	529	506	
pMe	ROT1	673	684	692	687	692	688	668	677	662	653	653	662	
	ROT1	480	0	0	0	0	651	688	665	657	675	689	586	
pOMe	ROT1	780	802	802	779	783	808	792	774	748	773	738	755	
	ROT1	603	715	811	766	714	726	793	805	738	650	587	559	
pNO_2	ROT1	719	769	819	826	821	829	803	752	705	675	667	682	
	ROT1	/	/	/	/	/	800	983	/	/	/	/	/	4
pCF_3	ROT1	765	785	768	765	766	745	778	747	716	703	709	731	
	ROT1	766	766	738	728	751	771	765	737	708	698	708	735	

Key : (1) See SECTION 6-5.2 - results given for Run 1 search

(2) Initial Rotamer derived from Max found with Eu-LIS data (at $\emptyset = 123.5^{\circ}$)

(3) Secondary max at R = 225 - Max at R = 455 (Repeat NCYCOP = 3 - Rotated $+17.5^{\circ}$).

(4) NCYCOP = 3 search used as NCYCOP = 6 produced a SILLY result ($R > 6\text{Å}$) Optimised at $+25^{\circ}$ Max @ 500/164/147

TABLE 6-6.5 CYCLES 5 & 6 : Ring FITFACTOR Maxima for Eu-LIS Data.

DERIV X	Init ORN	-150	-120	-90	-60	-30	0	30	60	90	120	150	180	NB
H	OR1 OR1	617 741	588 695	640 700	724 757	749 827	695 816	617 741	588 696	640 701	724 762	749 827	695 816	
oF	OR2 OR2	767 /	716 /	636 /	605 /	623 /	692 799	762 725	685 642	573 435	503 -S-	535 /	616 /	
oCl	OR2 OR2	771 944	833 520	858 521	871 647	878 759	825 817	736 860	638 862	548 890	514 895	567 762	677 626	1
oBr	OR2 OR2	642 629	754 736	809 791	817 798	809 785	761 714	662 596	536 474	432 392	390 358	432 406	531 510	
oMe	OR2 /	655 /	726 /	699 /	686 /	711 /	729 /	675 /	551 /	430 /	334 /	396 /	505 /	
oOMe	OR1 OR1	564 /	571 /	546 /	574 /	586 566	587 560	547 /	483 /	418 /	398 /	445 /	517 /	2
oNO_2	OR1 OR1	568 534	506 514	462 502	447 499	457 507	488 535	559 570	616 595	643 599	643 597	639 592	619 570	
oCF_3	OR2 OR2	470 369	424 106	348 0	350 0	360 0	416 201	420 518	406 594	0 605	0 288	0 554	0 545	3
pF	OR1 OR1	451 /	396 /	474 /	588 /	624 /	574 -S-	440 /	365 /	474 /	588 /	624 /	573 /	
pCl	/ /	/ /	/ /	/ /	/ /	/ /	/ /	/ /	/ /	/ /	/ /	/ /	/ /	
pBr	OR1 /	/ /	/ /	/ /	/ /	/ /	491 /	409 /	-S- /	/ /	/ /	/ /	/ /	
pMe	OR1 /	382 /	312 /	392 /	494 /	522 /	487 /	381 /	315 /	391 /	494 /	522 /	484 /	
pOMe	OR1 /	/ /	/ /	/ /	/ /	/ /	518 /	412 /	292 /	-S- /	/ /	/ /	/ /	
pNO_2	OR1 OR1	/ /	/ /	/ /	/ /	/ /	0 0	/ /	/ /	/ /	/ /	/ /	/ /	
pCF_3	OR1 /	/ /	/ /	/ /	/ /	/ /	0 /	/ /	/ /	/ /	/ /	/ /	/ /	

Note that results are symmetrical for X = H and para X

Key : (1) Actual max observed at R = 420 - returned to max 837 @ 210 Sequence 30-330 used.

(2) NCYCOP = 3, STEP = 5° used as previous NCYCOP = 6 searches had R > 6Å.

(3) All results at ~R = 100!

TABLE 6-6.6 CYCLES 5 & 6 : Ring FITFACTOR Maxima for Yb-LIS Data

DERIV X	Init ORN	-150	-120	-90	-60	-30	0	30	60	90	120	150	180	NB
H	OR1	804	766	816	898	938	891	804	766	816	898	938	891	
	OR1	794	750	807	891	937	885	794	750	807	891	937	885	
oF	OR2	894	934	886	838	879	934	904	838	669	546	621	796	1
	OR2	876	884	815	799	867	897	866	805	729	644	628	817	
oCl	OR2	819	921	957	926	941	905	818	711	599	544	590	702	
	OR2	800	913	932	900	920	898	784	720	598	515	559	676	
oBr	OR2	769	729	872	943	944	894	808	701	578	510	551	657	
	OR2	580	728	925	959	945	890	800	701	580	508	537	641	
oMe	OR2	736	826	857	856	856	825	740	609	411	264	372	574	
	OR2	736	810	832	837	821	763	681	608	539	426	420	609	
oOMe	OR1	739	725	672	618	680	805	900	892	821	759	795	866	
	OR1	726	706	660	589	633	757	882	875	807	747	783	855	
oNO_2	OR1	729	630	504	433	474	582	694	782	867	886	864	808	
	ORX	416	452	561	673	763	877	870	839	786	705	615	485	2
oCF_3	OR2	822	877	845	832	838	841	783	646	0	0	0	620	
	OR2	805	854	824	801	767	759	720	658	548	202	419	615	
pF	OR1	553	475	540	720	815	725	553	475	540	701	815	725	
	OR1	568	497	542	707	806	694	568	497	535	676	758	709	
pCl	OR1	596	520	619	705	734	705	596	520	619	705	734	705	
	OR1	553	523	603	676	743	675	551	520	616	695	686	674	
pBr	OR1	575	494	622	749	776	724	575	494	622	749	776	724	
	OR1	536	500	653	765	678	670	536	505	662	773	684	671	
pMe	OR1	595	517	615	699	718	660	595	517	615	699	718	698	
	OR1	567	520	631	660	697	688	567	518	630	683	666	668	
pOMe	OR1	572	452	573	755	820	754	547	414	553	740	821	777	
	OR1	541	459	528	638	680	658	539	467	532	640	692	675	
pNO_2	OR1	530	426	531	689	747	706	529	426	531	689	747	706	
	OR1	/	/	/	/	737	641	/	/	/	/	7	/	3
pCF_3	OR1	559	491	559	690	759	689	559	491	559	690	759	689	
	OR1	549	496	549	683	769	683	550	497	549	683	769	683	

Key : (1) If two maxima at same value returns to last one found

(2) Initial Ring orient^{n} = result from Eu search ($\omega = 270^{o}$). Runs with OR1 gave lower results.

(3) As with H-108 Rotation NCYCOP = 3 used. Optimised at -35^{o} Max 737 @ 332/165/167.

The NCYCOP sequence was modified for the derivatives containing methoxy groups in order that these could be rotated relative to the phenyl ring. The normal (1) and modified sequences (2) are given below. Initially the OMe groups were set in the plane of the ring pointing away from the side-chain.

(1) 1-2-6-4-2-6-4-3-4-5-4-5-8-7-7

FIXED | H-108 | RING | BOTH | TAPE9 | H-108 | RING

(2) 1-2-6-4-2-6-4-6-4-3-4-3-8-7-7

as (1) | OMe | ALL | OMe | as (1)

TABLE 6-6.7 Rotational Optimisation of the Methoxy Groups (Initial - CYCLE 8 Final CYCLE 12).

DERIV	LSR	-150	-120	-90	-60	-30	0	30	60	90	120	150	180	FINAL OPT°
oOMe	Eu.1	484	556	615	604	602	588	586	603	622	612	579	418	102.5
	Eu.2	0	0	0	637	0	566	571	588	614	588	473	0	-60
	Yb.1	509	713	843	854	885	900	905	868	797	711	639	520	12.5
	Yb.2	535	734	832	838	869	882	887	865	794	691	601	530	17.5
pOMe	Eu.1	Both runs failed before reaching this stage												
	Eu.2													
	Yb.1	820	821	821	821	821	821	820	819	818	818	818	820	-120
	Yb.2	681	684	688	692	693	693	691	688	685	682	680	680	+47.5

Full details of CYCLES 8, 10 and 12 are omitted on grounds of space. The results after full rot/opt (CYCLE 13) and free rotation (CYCLES 14 & 15) are given in TABLES 6-6.8 & 6-6.9. The omitted values in TABLE 6-6.8 are from runs which failed (due to poor LIS data) before completing optimisation, the abbreviations are explained below TABLE 6-6.9.

TABLE 6-6.8 Final Results of the Eu-LIS Rotational Optimisation of the Type (IV) Alcohols

Deriv	N	MAX	R	PHI	PSI	Rot	S	Or	S	Rot(2)	M	Or(2)	M	MAX14	MAX15	V
H	1	753	250	109	153	211	2	216	0	/		/		600	772	1
	1b	837	512	179	125	248	0	190	0	/		/		789	884	0
oF	2	773	251	109	160	209	2	214	0	/		30	=	618	780	1
oCl	3	887	249	152	202	193	1	322	2	/		/		874	752	1
	3b	844	196	145	178	150	1	120	2	0	=	/		821	731	1
oBr	4	819	176	135	178	171	2	298	2	240	=	/		678	630	?
	4b	807	153	142	183	265	2	298	2	145	=	/		655	591	0
oMe	5	732	248	121	189	203	2	353	2	/		/		645	502	1
oOMe	6	626	198	155	162	263	0	180	0	210	=	60	=	610	627	1
oNO_2	7	646	242	111	162	205	2	283	2	/		/		508	569	1
	7b	612	122	150	188	124	2	270	1	/		/		439	570	0
oCF_3	8	479	250	162	213	241	0	157	?	/		30	½	495	/	1
	8b	638	109	147	177	146	?	91	?	/		150	½	/	/	0
pF	9	625	258	111	175	149	2	212	0	/		/		525	665	1
pMe	12	525	277	103	182	220	2	209	0	/		/		425	552	1

The angles specified in the Rot & Rot(2) and Or & Or(2) cloumns of TABLES 6-6.8 & 6-6.9 (Ø and ω respectively - see FIG.1-5.1) were calculated using the following rules :

(1) For ROT1, ROT2 and ROT3, Ø = 180, 300 and 60° respectively.

(2) For OR1 and OR2, ω = 180 and 0° respectively.

(3) METFIND measures side-chain rotations in the opposite sense to Ø.

(4) METFIND measures ring rotation in the opposite sense to ω when X is H

TABLE 6-6.9 Final Results of the Yb-LIS Rotational Optimisation of the Type (IV) Alcohols

Deriv	N	MAX	R	PHI	PSI	Rot	S	Or	S	Rot(2)	M	Or(2)	M	MAX14	MAX15	V
H	1	951	250	171	179	308	1	211	0	150	=	/		945	972	1
	1b	940	230	168	180	295	0	210	0	150	=	/		936	950	1
oF	2	946	243	169	181	155	0	236	2	/		0	=	946	818	1
	2b	950	272	175	179	150	1	3	2	330-150	=	240	=	939	866	1
oCl	3	970	277	176	197	359	2	263	2	120	=	330	=	914	775	1
	3b	967	283	177	197	2	2	262	2	90	=	330	=	914	758	1
oBr	4	959	251	171	149	125	2	323	2	0	=	/		915	722	1
	4b	968	250	156	124	126	2	284	2	330	=	/		927	717	1
oMe	5	863	310	136	193	161	0	270	2	300	=	/		861	472	1
	5b	854	307	141	202	303	0	268	2	150	=	/		851	444	1
oOMe	6	914	227	168	167	163	0	218	2	300	=	/	½	911	759	1
	6b	896	215	170	170	155	0	220	2	330	=	0	½	896	740	1
oNO_2	7	891	262	163	138	129	2	106	2	345	=	/		872	681	1
	7b	886	260	159	130	131	1	282	2	334	=	/		870	672	1
oCF_3	8	884	316	141	219	302	0	242	2	30	=	0	=	885	424	1
	8b	876	316	144	220	303	0	242	2	30	=	/		873	407	1
pF	9	845	293	189	180	331	0	210	1	150	=	/		844	789	1
	9b	838	300	190	179	152	0	209	1	300	=	/		836	779	1
pCl	10	738	213	165	180	168	0	210	0	240	=	/		735	765	1
	10b	746	311	183	179	150	0	210	0	330	L	/		744	737	1
pBr	11	777	213	160	178	285	0	210	0	120	½	/		774	796	1
	11b	785	168	132	162	190	2	234	0	/		/		698	838	?
pMe	12	727	228	163	180	300	0	210	0	210	=	/		727	749	1
	12b	703	303	173	182	25	2	208	1	150	=	/		0	/	1
pOMe	13	832	247	141	174	150	0	215	1	285	=	/		828	814	1
	13b	825	361	169	192	350	1	205	1	120	=	/		802	802	1
pNO_2	14	750	252	141	183	163	0	208	0	240	=	/		745	745	1
	14b	743	324	167	173	135	0	212	1	/		/		735	723	1
pCF_3	15	773	264	178	180	325	0	210	1	150	=	/		770	723	1
	15b	790	293	181	178	148	0	209	1	315	=	/		785	734	1

Notes : N = Normalising group, n = 607, nb = 107.
Rot & Or = Optimised Side-chain and Ring geometries.
Rot(2) & Or(2) = Geometries of secondary maxima found in CYCLES 3 or 6.
S = Significance of Optimised geometry compared to free-rotation maxima
Scale : 0 = No significance; 1 = debatable significance; 2 = significant
L = Larger but at R = 455.
M = Magnitude of Secondary max. compared to max.: (=) = approx. equal, (½) = considerably lower.
MAX14 & 15 : Maxima in CYCLES 14 & 15 - "free rotation" of H-108 and rings respectively.
V = validity of CYCLE 12 maxima - if 2.1 < R < 3.6 results invalid.
Scale . 0 = Invalid; ? = debatable - rather low; 1 = Valid.

or para, and in the same sense when X is ortho.

Points (3) and (4) reflect the choice of the axial atoms A and B (see SECTION 5-4-3) in the ROTATE runs.

The results of the Eu-LIS and Yb-LIS based optimisations (TABLES 6-6.8 and 6-6.9) have little in common. This was expected as the Eu-LIS data contains significant CS distortions in at least three carbon atoms (see FIG.6-3.1) This is reflected in the generally poor FITFACTORS (cf. to the Yb-LIS results) and also in the small number of runs which (a) were completed (15), and (b) produced FITFACTOR maxima in feasible positions (10) - a poor record out of the 30 runs attempted. Also as the same data was used for the two runs with each derivative these should, if no CS/CFS distortions were present, have produced similar maxima and optimised orientations. This is clearly not the case with the Eu-LIS data.

The Eu-LIS results are therefore only reported for comparative purposes and are not intended to be taken as meaningful as there is ample evidence to contradict this. They do, however, serve as a useful warning that apparently sensible rot/opt can be performed using poor LIS data and emphasise the necessity of ensuring that all the LIS data used is based solely on PCS.

6-6-3 Results of the Full MULTISCAN Searches

Having completed a ROTATE run the coord. data output in CYCLE 13 was used in a full MULTISCAN search to check that the results were not based on a secondary max. Where this occurred the data/options were modified and the ROTATE run repeated until a satisfactory result was obtained. All the Yb-LIS rot/opt results fall into this category although several Eu-LIS results do not.

It was intended that the CONTUR output from the full MULTISCAN runs should be used in plotting 3-D contours of the FITFACTORS. A colleague, J.C.Burgess, spent considerable time and effort in tackling the problems associated with handling and converting arrays of up to 50,000 numbers in polar coordinates into sorted cartesian coordinates and then plotting stereoscopic surfaces of the contours produced. Unfortunately this mammoth project could not be finished in the time available and although well advanced had to be shelved. When necessary 3-D contours were plotted on a specially constructed model - see APPENDIX V.

6-7 Interpretation of the Yb-LIS Rot/Opt Results

A major shortcoming of the rot/opt method developed for METFIND VII was the assumption of a unique optimum conformation. This approach may seem very naïve (especially in view of its failure in interpreting three-bond couplings - see SECTION 4-8.2) but the alternative of optimising randomly weighted populations, as well as performing the rot/opt process devised, was discounted for several reasons :

(a) Expense. METFIND VII was already a large complex program whose time and output usage bordered on and sometimes exceeded the maximum available,

ie. 600 CP secs, 5120 lines of output.

(b) Development time. This would have been considerable and the likelihood of successful debugging in the time available was small.

(c) Applicability. The Type (IV) alcohols have only one atom (H-108) on which to base rot/opt of the side-chain. This represents a grave weakness in the results already obtained and would prohibit the use of weighted population averaging such as that described in APPENDIX III.

Point (c) should be borne in mind throughout the discussion in this section.

As the rot/opt method assumed a unique "rigid" conformation care should be exercised in applying the results to the reality of rotating species which possibly possess preferred conformations. If we assume that eclipsed conformations in the side-chain will be disfavoured and that results between two rotamers indicate that both participate, then by a crude "scoring" of the optimised rotations (for both sets of Yb-LIS data including any secondary maxima) it should be possible to obtain guidelines to the preferred conformations of the Type (IV) alcohols. This has been attempted in TABLE 6-7.1 with the inferences "calculated" from the following rules :

(1) Each rotamer has an initial score of 2 - this introduces a rotational factor.

(2) Each maximum is scored according to its significance and whether it is a secondary max. etc. ie.

Significance	Max	$2^{nd}(=)$	$2^{nd}(\frac{1}{2})$	
0	2	2	1	
1	4	3	2	(taken from
2	8	7	5	TABLE 6-6.9)

(3) The score attributed to each rotamer is weighted by the angles between the maxima and the rotamer, ie. 0^{o}factor = 1, 30^{o}factor = $\frac{3}{4}$, 60^{o}factor = $\frac{1}{2}$, 90^{o}factor = $\frac{1}{4}$.

The inferences gained by this method, although very approximate, are substantially in accord with the more reliable rotamer positions calculated from the coupling data. Overall there is a tendency for the inferred results for the ortho Type (IV) alcohols to lie nearer a 33-34-33 distribution with the LIS data than with the coupling data, but where one or two rotamers predominate in the LIS data these normally correspond to the preferred rotamers in the coupling data. For the side-chain, therefore, conformational analysis from the LIS data is severely limited as it is only based on one atom, making the results only useful for corroboration with those obtained from the coupling data. The optimised orientation in the phenyl ring in the para Type (IV) alcohols suffers a different limitation caused by symmetry in the LIS data of the ortho and meta atoms which artificially forces it to be symmetrically disposed to the metal-oxygen vector. This is of little importance as the results for

TABLE 6-7.1 A "Preferred Rotamer" Interpretation of the Yb-LIS H-108 Rot/Opt Results

ROTAMER		ROT1					ROT2						ROT3						TOTAL "SCORE"			INFERENCE			Ch.4 EST POPULATIONS		
FACTOR		1/4 /	1/2 /	3/4 /	1 /	3/4 1/4	1/2 1/2	1/4 3/4	/ 1	1/4 3/4	1/2 1/2	3/4 1/4	1 /	3/4 /	1/2 /	1/4 /			ROTAMER			ROTAMER			ROTAMER		
DERIV	N	90	120	150	180	210	240	270	300	330	0	30	60	90	120	150			1	2	3	1	2	3	1	2	3
H	a			3					4							3			$5\frac{3}{4}$	8	$3\frac{1}{4}$	34	47	19	44	32	24
	b			2					2							2											
oF	a			2						2		2		2		2			7	4	7	39	22	39	40	20	40
	b	2		4												4											
oCl	a		7								8				7				$7\frac{1}{4}$	8	$18\frac{3}{4}$	21	24	55	19	11	70
	b	7									8			7													
oBr	a		8							7	7				8				10	$8\frac{3}{4}$	$15\frac{3}{4}$	29	25	46	16	9	75
	b		8												8												
oMe	a			2					2							2			5	6	3	36	43	21	55	22	23
	b			2					2							2											
oOMe	a			2					2							2			5	$5\frac{1}{2}$	$6\frac{1}{2}$	29	32	39	15	3	82
	b			2						2						2											
oNO_2	a		8							3	4				8				8	$8\frac{1}{2}$	$11\frac{1}{2}$	29	30	41	10	10	80
	b		4							3					4												
oCF_3	a								2			2							2	7	5	14	50	36	13	21	66
	b								2			2															
pF	a			2						2						2			5	$5\frac{1}{2}$	$3\frac{1}{2}$	36	39	25	44	35	21
	b			2					2							2											
pCl	a			1	1		2									1			$7\frac{1}{4}$	$4\frac{1}{2}$	$3\frac{1}{4}$	48	30	22	42	35	23
	b			2						2						2											
pBr	a		1					1	1						1				$9\frac{3}{4}$	$3\frac{3}{4}$	$3\frac{1}{4}$	58	23	19	42	35	23
	b			3	5											3											
pMe	a					2			2										$9\frac{1}{4}$	$6\frac{1}{4}$	10	36	25	39	46	32	22
	b			8								8				8											
pOMe	a			2				1	1							2			5	$5\frac{3}{4}$	6	30	34	36	48	36	16
	b		3								4				3												
pNO_2	a			1	1		2												$5\frac{1}{2}$	3	$2\frac{1}{4}$	51	28	21	34	35	31
	b		1	1												1											
pCF_3	a			2						2						2			5	$5\frac{1}{4}$	5	33	34	33	39	35	36
	b			2					1	1						2											

the para ring optimisations were consistently of low significance, supporting the view that the ring is freely rotating in these derivatives. Fortunately, the ortho ring rot/opt suffers no artificial constraints so the results may be interpreted at face value.

By analogy to the findings of Anderson and Pearson[130] (see FIG.1-5.7) the rotamer with $\omega = 330 \pm 30^{\circ}$ (R1) would be expected to be the most populated, with $\omega = 150 \pm 30^{\circ}$ (R2) as a lesser alternative, at ambient temperatures (see FIG.6-7.1). Ring optimisations at $\omega = 240 \pm 45^{\circ}$ (R3) could indicate interactions between the ortho X and $-CHCl_2$ groups whilst $\omega = 120 \pm 30^{\circ}$ (R4) could

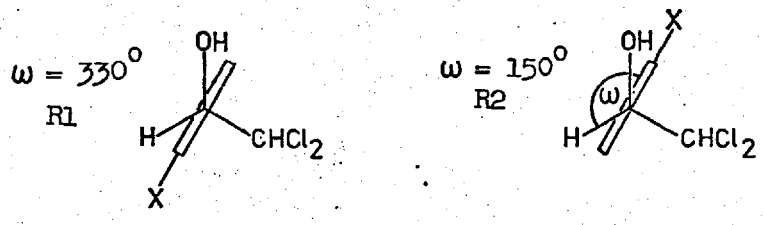


FIG.6-7.1 The two least hindered rotamers for the phenyl ring in the Type (IV) alcohols.

indicate interactions between the bulkier ortho X (eg. Me, OMe, NO_2, CF_3) and the -OH groups.

From TABLE 6-6.9 there is some evidence that oF, Cl and CF_3 occupy R1 about 50% of the time with oOMe lower at ~35%. None of the derivatives have results at $\omega = 150 \pm 30^\circ$ so it seems unlikely that R2 is occupied. Apart from Br and NO_2 all the ortho derivatives have their major optimised orientation within $\omega = 240 \pm 30^\circ$ implying that the ring substituents in these compounds have attractive interactions with the $-CHCl_2$ moiety of the side-chain. Both oBr and oNO_2 have optimised orientations with C-6' and the -OH group approximately eclipsed ($\omega = 283^\circ$) whilst oNO_2 also has the reversed orientation with C-2' and the -OH group approximately eclipsed ($\omega = 106^\circ$). The latter could reflect an interaction between the $-NO_2$ and -OH groups (R4) whilst the former could still indicate an interaction between either -X and the $-CHCl_2$ groups (R3) although this is less certain than with the other ortho derivatives.

Overall, therefore, the rot/opt results for the phenyl ring strongly support the postulate that ortho ring substituents interact with the side-chain $-CHCl_2$ group and thereby control the molecular conformations about both rotatable bonds. The low significance of the para rot/opt results tends to support "free rotation" of the ring with a concommitant absence of direct "control" over the side-chain rotamer preferences by the ring.

Both Yb-LIS runs optimise the ortho methoxy group at ~15° out of the plane of the ring. The FITFACTORS from the complete rotation of this group (see TABLE 6-6.7) show considerable rotamer sensitivity with the optimised geometry highly significant. Although slightly displaced this agrees with the findings of Hofer,[212] ie. methoxy groups prefer the least hindered coplanar orientation to the ring thus enabling maximum overlap of the oxygen lone pairs with the π-system. The orientation of the para methoxy group is less clear, however, with the two runs optimising at -120 and 48°. The reasons for this vast difference are the insensitivity of both runs to the OMe orientation and the search method - METFIND always returns to the last maximum found in an NCYCOP = 6 operation (see TABLE 6-6.7). There is therefore no conclusive evidence about the orientation of the para group but it is assumed that coplanarity prevails.

To conclude this chapter, the FITFACTORS and metal positions of the rot/opt results will be briefly discussed.

The max FITFACTORS found for the FIXED ATOMS are plotted in FIG.6-7.2 This illustrates the generally poorer fit of the Eu-LIS data and also the lowering effect of increasing the number of shifted groups used (as in pF, pMe and pCF_3 and in the Eu(H-107)pNO_2 data based on 3 atoms compared to the Yb(H-107) pNO_2 data based on 4 atoms). This effect also dominates the final rot/opt and "free-rotation" results (see FIG.6-7.3) where the generally poorer fit of the para derivatives reflects the larger number of shifted groups used (NB. The individual ortho and meta protons and carbons were treated as shifted groups rather than averaging them together in pairs).

All of the ortho derivatives show benefits for the rot/opt results over

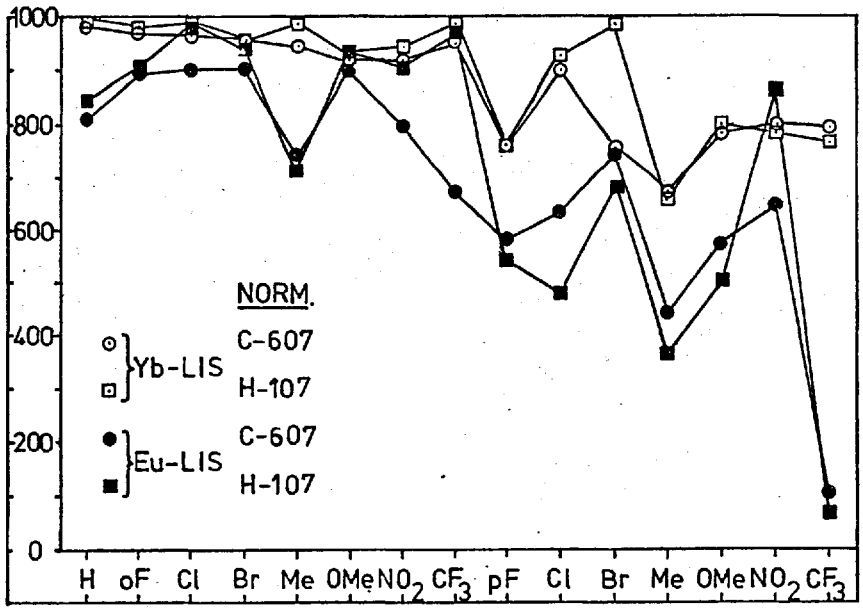


FIG.6-7.2 Maximum FITFACTORS For the Eu- and Yb-LIS FIXED ATOM Searches

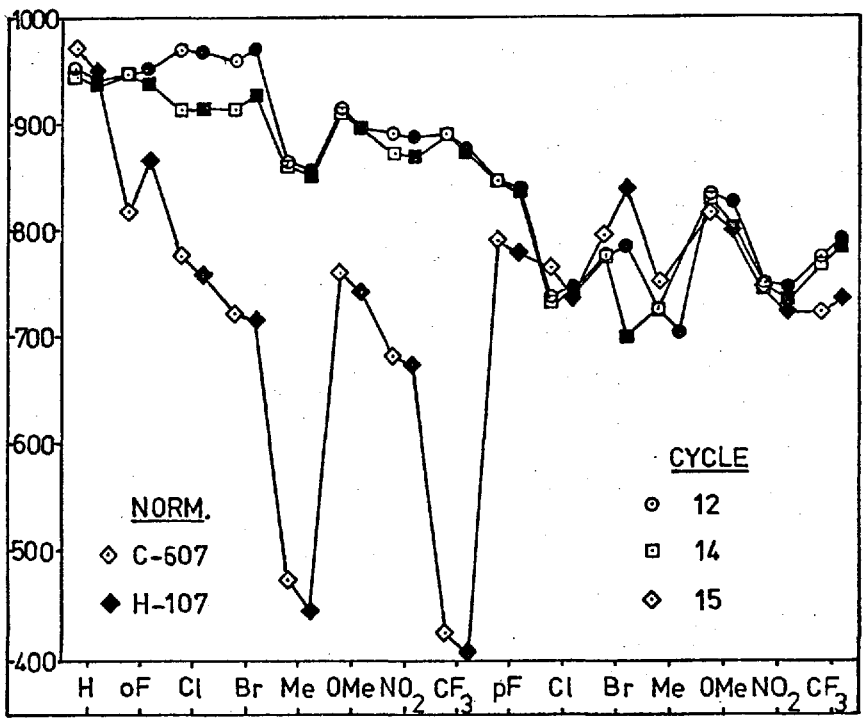


FIG.6-7.3 Maximum FITFACTORS Using Yb-LIS Data for CYCLES 12, 14 and 15

ring "free rotation" with the conspicuous drops in the CYCLE 15 max for oMe and oCF_3 demonstrating the improvements in significance of the rot/opt results when large numbers of shifted groups are available for optimisation. Presumably this is not seen for oOMe because of the rotational freedom of this group.

The overall low significance of the side-chain rot/opt is clear with only oCl, oBr, oNO_2 and pBr(b) standing out. The latter is anomalous for as well as being the only rot/opt result at short radius it is also the only search in which the CYCLE 12 & 14 maxima were in significantly different positions. This defies explanation, especially as the pBr(a) search behaved normally, and can only be attributed to a foible in the search or rot/opt method used. The reader may already have noted several places in which search methods, etc. were modified in order to obtain sensible results. Such decisions were often subjective, based on a detailed knowledge of METFIND's idiosyncrasies, and cannot be readily explained.

Not surprisingly some differences did occur between the positions of tha maxima in CYCLES 12 and 15, but not in the 6 cases where the CYCLE 15 results were better than those in CYCLE 12.

From TABLE 6-6.9 the average metal position is seen to lie at (258/164/177) with the following ranges : R(168-361), PHI(136-190) and PSI(124-220). The distribution of the rot/opt maxima relative to the substrate are illustrated in FIG.6-7.4. Although not as sterically sensitive as expected, there is a definite trend for the maxima to lie in the least hindered zone.

Finally the rot/opt maxima are presented as R-factors for comparison with the literature (best lit. results of ~0.02 are frequently obtained with fewer groups than those used here). There is no linear relationship between the two factors because the R-factor is not a true RMS % Error whereas the FITFACTOR is (see EQNS.30 & 105). This was considered essential as the LIS data used spans two orders of magnitude and optimisation can only be sensibly performed by considering % Errors.

TABLE 6-7.2 Rot/Opt Maxima for the Type (IV) Alcohols Expressed as R-Factors

FACTOR	H	F	Cl	Br	Me	OMe	NO_2	CF_3	SERIES
FIT-	951	946	970	957	863	914	891	883	ORTHO(a)
R-	.0209	.0243	.0126	.0190	.0348	.0380	.0382	.0293	
FIT-	940	950	967	968	854	896	886	875	ORTHO(b)
R-	.0321	.0223	.0175	.0190	.0424	.0583	.0429	.0378	
FIT-	951	845	738	777	727	832	750	791	PARA(a)
R-	.0209	.0470	.0702	.1066	.0695	.0812	.0707	.0846	
FIT-	940	838	746	783	703	825	743	810	PARA(b)
R-	.0321	.0661	.0685	.1729	.0831	.0790	.0908	.1004	

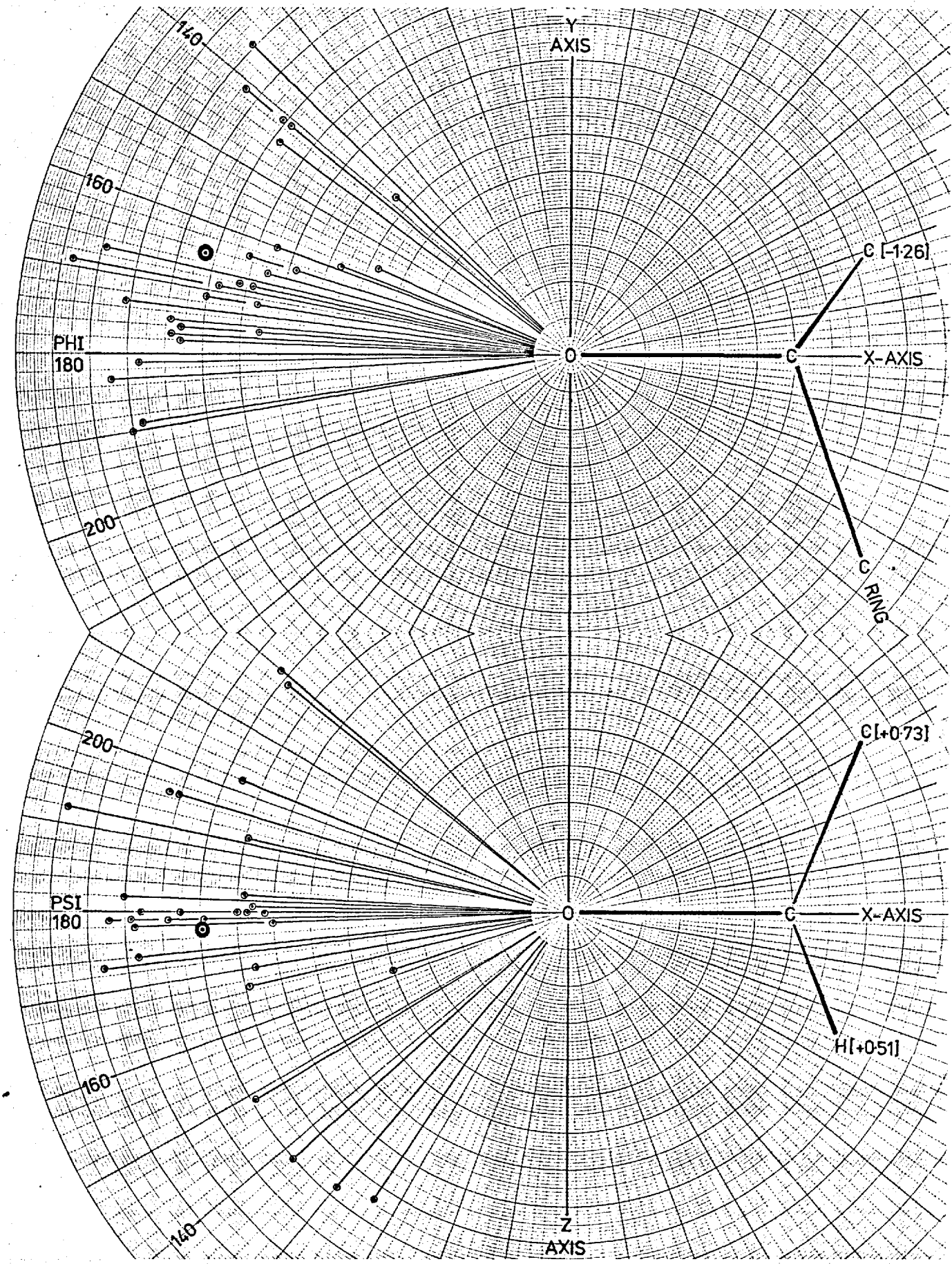


FIG.6-7.4 Distribution of the Rot/Opt Metal Positions for the FITFACTOR Maxima.

The two views are from the +Z axis (PHI) and +Y axis (PSI) respectively, with the radii projected onto the PSI or PHI = 180° plane as appropriate by using R.cosPSI for the PHI view and R.cosPHI for the PSI view.

◎ = Overall Average.

PART 3

ELIMINATION REACTIONS / OVERVIEW

CHAPTER 7

7 ELIMINATION REACTIONS AND CONFORMATIONAL DETERMINATION OF THE PRODUCTS

7-1 Experimental

The details given in SECTION 2-2 apply here.

7-2 The Choice of Base

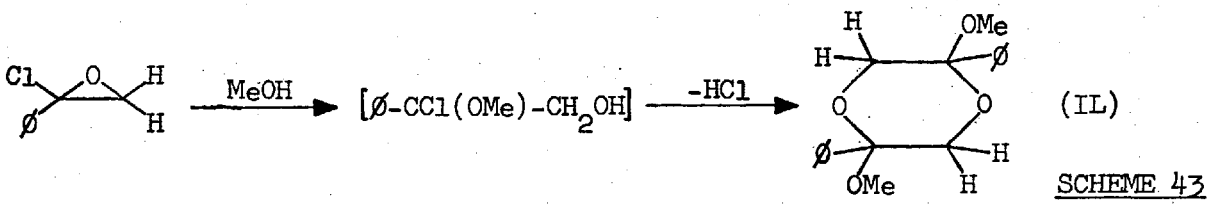
7-2-1 Trial Eliminations of HCl from the Type (IV) Alcohols

The main method reported for preparing α-chloroepoxides from their corresponding dihalogenated alcohols (see SECTION 1-4-3.2[52-3,93-101]) involves reacting the alcohol at ~10°C with an equivalent amount of 10% aqueous potassium or sodium hydroxide, both in the absence, or presence,[93,98] of an organic solvent (eg. methanol).

The only elimination of a Type (IV) alcohol yet reported (X = H) was by Nouri-Bimorghi in 1966.[97] The standard aq. KOH method was used,[96] with the product identified by ^{1}H nmr[53,96] but too unstable to be purified,[97] as it readily rearranged to the aldehyde (see SCHEME 25). The IR (1200, 925, 918, 800 cm^{-1}) and ^{1}H nmr (δ5.28(d,H_A); 4.03(d,H_B)ppm) spectra of the epoxide were reported[53,96] without mention of the coupling constants or geometry. (This has been identified as the cis isomer - see SECTION 7-4).

All attempts at repeating this elimination under a variety of conditions gave absolutely no reaction, with the unchanged alcohol recovered on work-up.

A rapid reaction occurred between H(IV) and potassium ethoxide in ethanol during which the epoxide was probably formed, but the ^{1}H nmr spectrum of the products indicated re-attack by ethoxide to produce an ethoxy analog of the dimer (IL) reported by Kirrmann et al[53,95] (see SCHEME 43).



(IL)

SCHEME 43

It was apparent that elimination required a strong base but a poor nucleophile. Consequently a "phase trensfer reaction" between H(IV) dissolved in CD_2Cl_2 and an equivalent amount of aqueous tetra-n-butyl ammonium hydroxide was attempted : although the organic layer became yellow the nmr showed negligible reaction.

Similarly potassium tertiary butoxide (prepared by the method of Vogel[218] (p290) from freshly cut potassium and purified by double sublimation) gave little reaction with H(IV) in sodium dried ether. It was therefore decided to try absolutely dry THF as the solvent. This was prepared by refluxing "dry" THF over sodium wire until a drop of benzophenone turned the whole solution

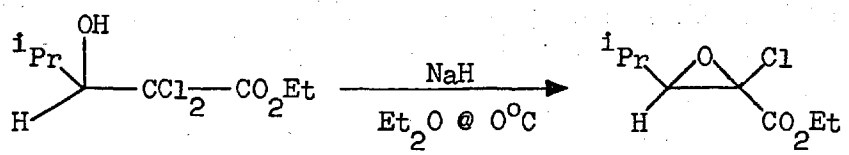
blue. THF was then collected by distillation under dry nitrogen.

Partial elimination (~35%) was achieved with 1 equivalent of potassium butoxide in dry THF at 20°C, but was only marginally increased (to ~40%) by raising the reaction temperature to 45°C. 100% reaction of the starting material was eventually achieved by using two equivalents of butoxide and stirring overnight at 20°C.

The ^{1}H nmr spectrum of the products (see FIG.7-2.1) clearly shows two AB-quartets from the cis- and trans- epoxides.[281]

The 2KOBu^t/THF elimination method was satisfactorily used twice with the full set of Type (IV) alcohols (see SECTION 7-4). It was, however, not as clean as desired so a further method was sought.

Whilst preparing a series of α-chloro-α-ester epoxides from the corresponding dichloroalcohols (see SCHEME 29), Villieras et al[105,106] successfully employed ethereal sodium hydride as the base for one reaction (see SCHEME 44), with the yield of (L) reported as 80%.



(L) SCHEME 44

This reaction was attempted with H(IV), but in dry ether or in DMSO no elimination occurred. With dry THF and 1 equivalent of NaH (in pellet form), however, ~65% elimination was achieved. This was raised to 90% by using 2 equivalents of NaH at 20°C.

Although this reaction was fairly clean, the use of THF had two distinct disadvantages :

(1) Its miscibility with water made the work-up awkward.

(2) It prevented the reaction from being followed by ^{1}H nmr, and because of the low temperatures required in the epoxide work-up, could not be completely removed from the ^{1}H spectra of the products.

To avoid both problems, CCl_4 was investigated as a potential solvent for this reaction. An initial worry was the possible formation of dichlorocarbene under the strong reducing conditions, but a prolonged trial with refluxing CCl_4 showed no visible reaction of the NaH.

Elimination reactions were successful in dry CCl_4, but 3 equivalents of NaH were needed to obtain complete reaction of the Type (IV) alcohols. The bulk of the NaH, however, remained unreacted due to the formation of NaCl on the surface of the pellets, rendering them inert. Optimum efficiency for the elimination was obtained at ~40°C with complete reaction of the alcohols occurring within 1½ hours. Although not completely clean, yields of the epoxide were fairly high, so this reaction was used as the second elimination method

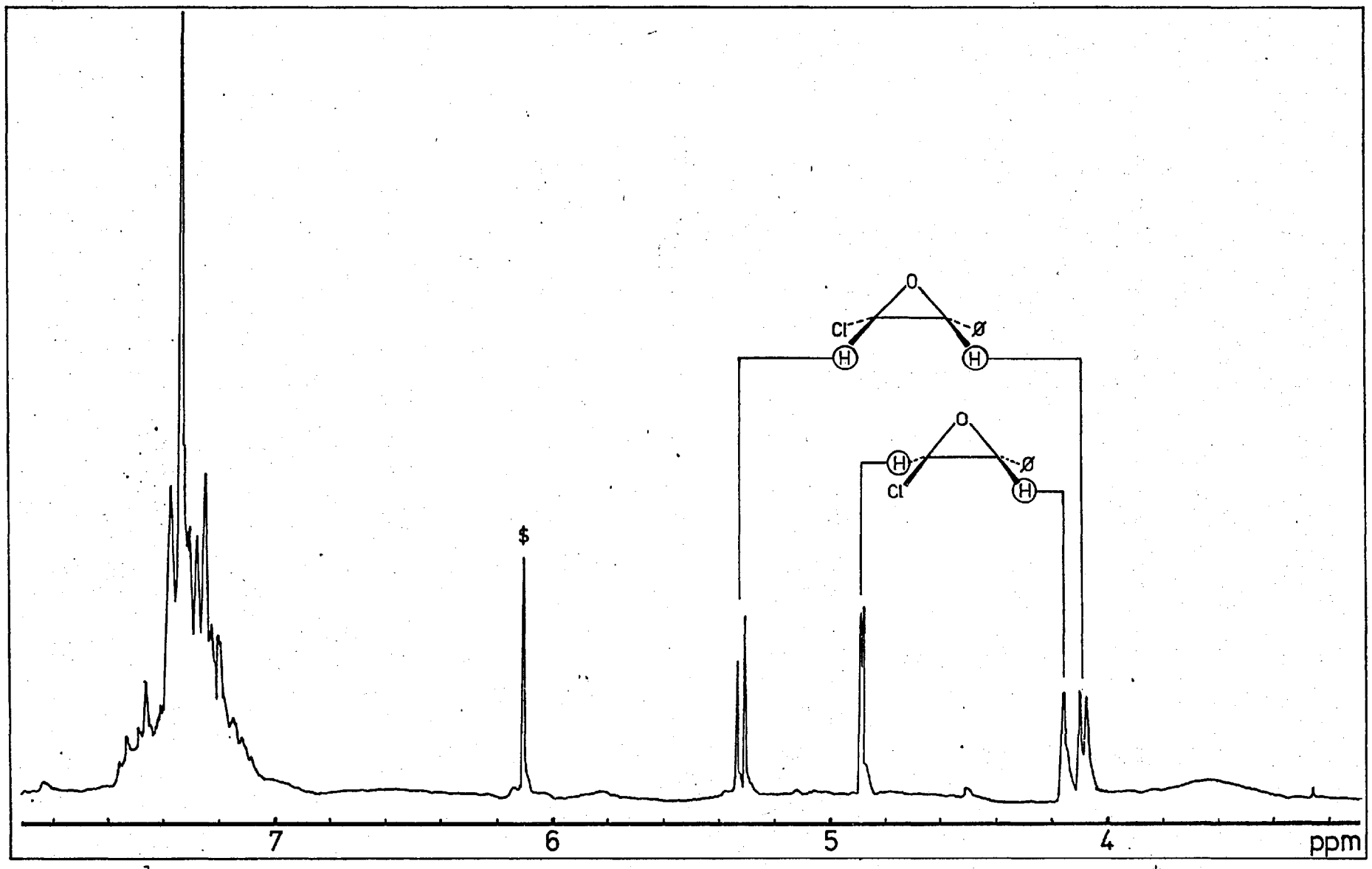


FIG.7-2.1 ^{1}H Spectrum of the Epoxide Products from the Elimination Reaction of H(IV) with 2.KOBu^{t}. Note the broadening of the H_B lines due to long-range coupling into the aromatic ring.

for the Type (IV) alcohol series (see SECTION 7-4)

7-2-2 Trial Eliminations of HCl from the Type (V) Fluorides

Although a dialkyl phosphate analogue (XXV) of the Type (V) fluorides readily underwent elimination of HCl with triethylamine[51] (see SCHEME 20), absolutely no reaction occured with the Type (V) fluorides. It was decided, therefore , to verify that elimination would occur by reacting oCl(V) with 1 eq. of lithium ethoxide (prepared by dissolving freshly cut lithium in Analar ethanol).

Surprisingly, only partial elimination (~25% by ^{1}H nmr) was observed at 25°C; complete reaction requiring 2 eq. and heating at 60°C for 1½ hours. This reaction was reasonably clean and was adopted for general use (see SECTION 7-3).

Sodium hydride was examined as an alternative base, but gave no reaction in CCl_4 after 2½ hours refluxing and showed only 5% elimination after 8 hours stirring in DMSO at 60°C.

The 2KOBu^t/THF method developed for the Type (IV) alcohols gave only partial reaction with the Type (V) fluorides. A modified method was developed in which the Type (V) fluoride, dissolved in the minimum of dry THF, was rapidly run onto 2 eq. of KOBu^t and then heated at 55°C for 2 hours. This reaction was found satisfactory and used for the full series (see SECTION 7-3).

The instability of the epoxides made separation and identification of the Type (IV) alcohol elimination products difficult. The products from the Type (V) fluoride eliminations will therefore be examined first, so that analytical data from this source may be used to supplement the rather sparse data on the alcohol elimination products.

7-3 Products of the Elimination Reactions of the Type (V) Fluorides

7-3-1 The Elimination Reactions

Three series of eliminations were performed on the 1mMolar scale :

METHOD 1 (2.KOBu^t/THF)

The Type (V) fluoride (1mMole) dissolved in dry THF (5ml) was rapidly run onto dry potassium-t-butoxide (2mMole) in a flask heated at 55°C. A yellow colour developed instantly. After stirring under dry nitrogen for 2 hours the mixture was quenched with water. The reaction mixture was ether/water extracted; the two phases requiring "salting out" with sodium chloride. The organic layer was washed with water and then dried over sodium sulphate.

METHOD 2 (2.LiOEt/EtOH)

The Type (V) fluoride (1mMole) was dissolved in Analar ethanol (5ml) and treated with lithium ethoxide (2mMole) in ethanol (5ml) in a 25ml flask. The reaction mixture rapidly became yellow and was stirred for 1½ hrs at 63°C.

METHOD 3 (3.LiOEt/EtOH)

As METHOD 2 except 3 mMoles of lithium ethoxide were used and the reactions were performed at 81°C.

Initial product recovery ratios from the ethoxide reactions were low, but this was remedied by using the following work-up sequence :

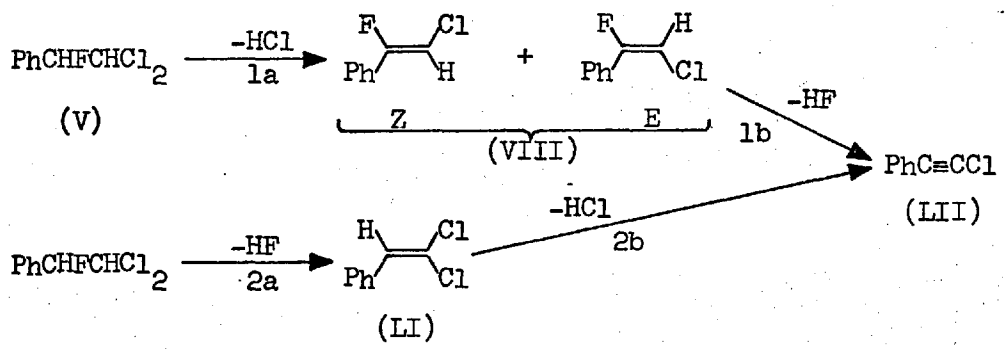
The reaction mixture was transferred to a 100ml separating funnel, and the flask washed alternately with water and chloroform (a total of 30ml each) and finally with acetone (5ml). Dilute hydrochloric acid was added to the aqueous phase until the contents were at pH 7-8. After shaking, the chloroform layer was run off. Ether (30ml) was added and the extraction repeated. The combined ether and chloroform solutions were dried over sodium sulphate prior to removing the solvent under reduced pressure.

The average product recovery (calculated assuming 100% elimination of HCl) was ~85% by all three methods. The product mixtures were examined by ^{1}H and ^{19}F nmr, glc and GC/MS. No attempts were made to isolate individual products as the GC/MS data in combination with the nmr spectra provided sufficient information for identification of all the major reaction products.

7-3-2 GLC Analysis of the Type (V) Fluoride Elimination Products

The components of the three sets of elimination products were examined by glc using the same column and conditions reported in SECTION 2-5-2. Most reactions yielded two major and one or two minor products, the proportions of each varying with the method used. Since the three elimination methods gave essentially the same products (from the retention times in the glc) only those from METHOD 1 (2KOBu^{t}/THF) were examined by GC/MS. (As before both NO_2 derivatives were undetectable by flame ionisation in the glc and by mass spectroscopy).

For simplicity the glc data in TABLE 7-3.1 has been sorted according to compound type. This was done in conjunction with the GC/MS and nmr data, both of which are discussed later in this section. The results indicate that the following reactions occurred :



SCHEME 45 The E and Z isomers of (VIII) were probably not separable under the glc conditions used.

TABLE 7-3.1 The Assignment and Relative Intensities of the Major Peaks in the GLC of the Type (V) Fluoride Elimination Products

DERIV X	STARTING MATERIAL				PEAK 1 - (VIII)				PEAK 2 - (LII)				PEAK 3 - (LI)				VARIOUS			
	RT	INTENSITY			RT	INTENSITY			RT	INTENSITY			RT	INTENSITY			RT	INTENSITY		
		1	2	3		1	2	3		1	2	3		1	2	3		1	2	3
H	100.0	24.3	2.0		38.7	60.5	43.5	55.0	15.7	6.3	6.2	13.6	44.1	8.4	38.3	27.3	35.5		9.9	4.1
o F	61.3				40.0	79.6	75.5	79.1	29.4	14.4	12.3	10.2	52.1	3.7	12.2	8.5				
o Cl	167.6				50.8	80.1	95.3	80.0	30.9	17.7	4.7	20.0								
o Br	287.9				55.9	66.5	76.6	67.1	33.2	25.6	11.1	23.5	57.0		9.7		29.4	5.4	2.5	7.2
o Me	127.2	1.0	1.0	5.1	28.0	56.4	18.9	17.1	15.7	37.1	25.2	28.2	25.2	4.0	55.8	46.7	12.2	2.4		2.8
o OMe	342.2		16.9	22.2	60.4	78.4	78.5	70.3	36.7	16.6	2.9	3.3					32.2	3.9	1.8	4.1
o CF_3	41.0	1.0	11.8	13.6	74.7	51.5	48.4	45.1	35.7	17.9	18.2	13.2	129.0	26.2	17.4	28.1				
p F	110.4				37.7	71.4	41.6	50.8	13.3	23.1	9.5	24.9	44.5		46.8	22.1	26.2	4.0	1.9	2.2
p Cl	368.8				26.2	70.1	64.0	70.1	12.4	25.4	20.2	26.0	44.0		14.5		23.4	1.0	1.0	1.0
p Br	682.6				37.6	60.0	65.1	72.5	12.7	31.7	17.8	20.6	44.0		11.0		23.3	4.6	6.1	6.9
p Me	157.3		13.0		39.8	54.1	33.9	38.1	16.0	45.9	5.4	10.0	48.5		47.7	51.2				
p OMe	637.5				45.4	45.9	18.3	20.5	18.9	54.1	5.0	13.4	56.0		73.1	66.1				
p CF_3	94.5				34.7	54.9	89.4	88.9	10.7	37.0	5.2	3.7					71.0		4.4	3.7
Av	(V)	2.0	3.4	3.1	(VIII)	63.8	57.6	58.0	(LII)	27.1	11.1	16.2	(LI)	3.3	25.1	19.7	(?)	1.6	2.1	2.5

Together the Type (VIII), (LI) and (LII) compounds accounted for ~96.7% of the reaction products. A further 2.1% of the products gave sizeable peaks in the glc (listed under "VARIOUS" above) but none of these gave useful GC/MS or nmr data.

The expected product (VIII) (step 1a in SCHEME 45) was clearly preferred in all three methods with the exception of oMe, pMe and pOMe(V) in METHODS 2 and 3. Significant differences do occur, however, between the proportions of the dichlorostyrene (LI) (step 2a) favoured by METHODS 2 & 3 and the phenylacetylenes (LII) (via either step 1b or 2b) favoured by METHOD 1. From the occurrence of products (LI) and (LII) (eg. in the pMe(V) eliminations), it seems unlikely that step 2b is responsible for the formation of the acetylene. Also, since the hydrogen and fluorine atoms are cis in the E-isomer of (VIII), step 1b is only likely to be significant from the Z-isomer.[282] The routes and mechanisms of the various elimination reactions will be discussed later.

Although the glc traces described above were recorded at constant temperature, temperature programming was used for the GC/MS spectra. A typical example of the results obtained is shown in FIG. 7-3.1 together with the relevant mass spactra.

7-3-3 GC/MS Identification of the Type (V) Fluoride Elimination Products

Only the products of METHOD 1 were examined by GC/MS. The mass spectra of the two major peaks in the glc traces of all the Type (V) elimination products were immediately identifiable as the Type (VIII) and (LII) compounds (see TABLE 7-3.2). Further the Type (LI) styrenes were readily identifiable in the mass spectra of the products from H and oMe(V). The Type (LI) peaks in TABLE 7-3.1 were assigned by reference to the Type (VIII) retention times

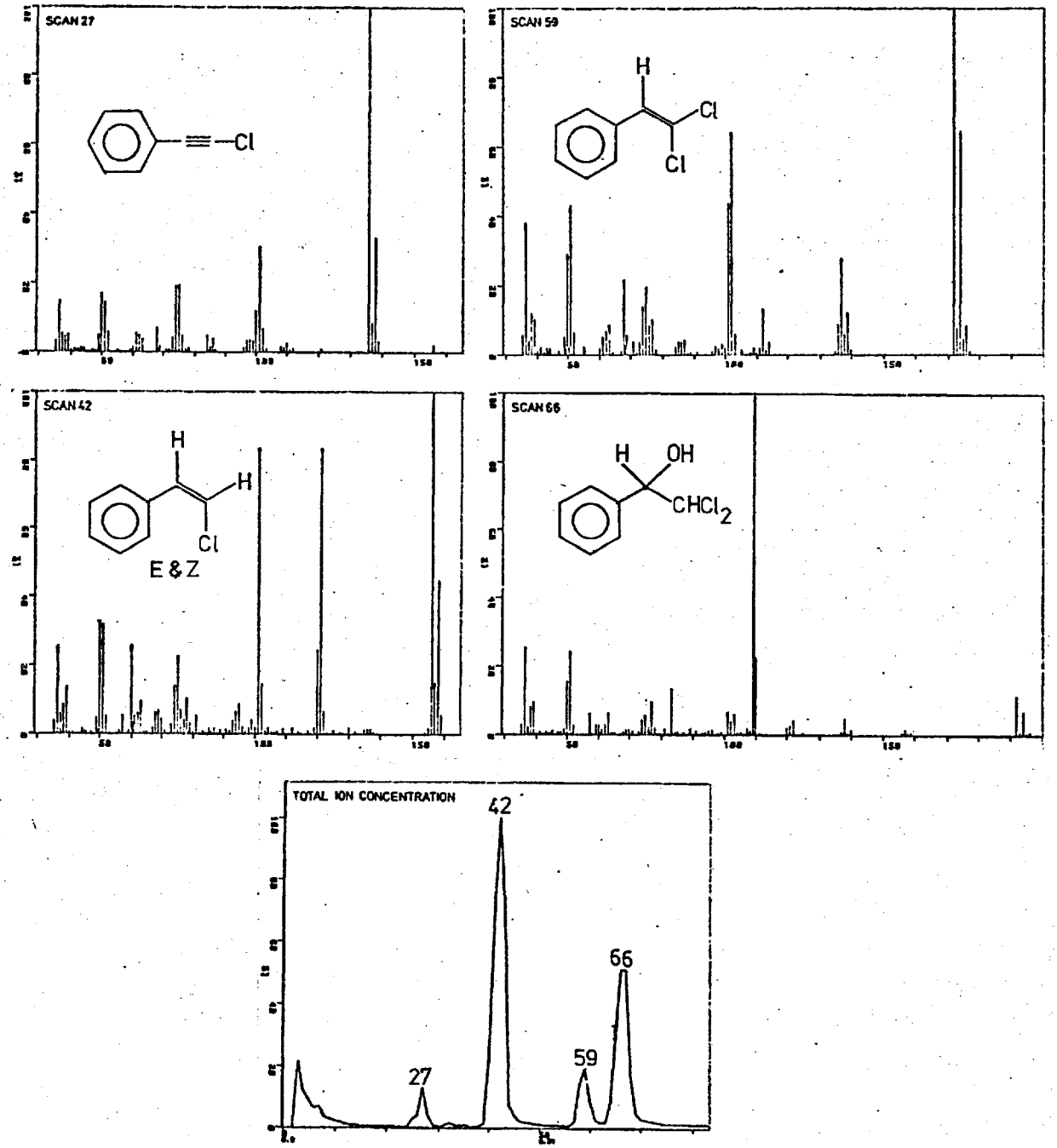


FIG. 7-3.1 The GC/MS of the H(V) Elimination Products (Recorded on an MS-30)

The total ion concentrations of the products emerging from the column (3% OV17 - initial temp 90°C, programmed @ 4°C/min.) are shown in the lower figure. The four mass spectral scans shown above correspond to the peaks in the total ion concentration plot. These clearly identify the sequence : Type (LII) - (VIII) - (LI) - (V) for the main materials present in the glc of the elimination products.

and by the intensity of the olefinic proton in the ^{1}H nmr.

Where present the elimination starting materials (the Type (V) fluorides) gave identical mass spectra to those already reported in TABLE 2-5.3.

TABLE 7-3.2 GC/MS of the Type (V) Elimination Products (by METHOD 1)

Type	Deriv	M+ ION		100%	2nd	3rd	4th	5th	6th
(VIII)	H	156(100)	1Cl	M+	121(68)	101(55)	M+2(30)	120(14)	75(11)
	o F	174(100)	1Cl	M+	139(61)	119(44)	M+2(31)	138(12)	79(11)
	o Cl	190(100)	2Cl	M+	154(88)	120(80)	M+2(66)	156(29)	135(20)
	o Br	*236 (79)	1Cl,1Br	120	M+2(79)	M+(64)	154(48)	198(33)	200(32)
	o Me	170 (64)	1Cl	135	M+(64)	115(61)	113(32)	M+2(20)	134(10)
	o OMe	186(100)	1Cl	M+	109(86)	122(39)	137(36)	143(35)	136(35)
	o CF_3	224 (48)	1Cl	168	M+(48)	169(39)	71(19)	M+2(16)	120(13)
	p F	174(100)	1Cl	M+	139(48)	119(41)	M+2(30)	138(12)	69(11)
	p Cl	190(100)	2Cl	M+	M+2(59)	120(45)	154(44)	156(14)	135(12)
	p Br	*236(100)	1Cl,1Br	M+2	120(81)	M+(75)	M+4(25)	200(13)	198(13)
	p Me	170(100)	1Cl	M+	135(59)	115(36)	133(33)	M+2(32)	57(18)
	p OMe	186(100)	1Cl	M+	171(38)	143(35)	M+2(32)	173(13)	145(11)
	p CF_3	224(100)	1Cl	M+	169(36)	189(33)	M+2(33)	120(21)	/
(LII)	H	136(100)	1Cl	M+	101(53)	M+2(36)	75(21)	121(19)	100(18)
	o F	154(100)	1Cl	M+	M+2(33)	119(25)	99(15)	118(14)	/
	o Cl	170(100)	2Cl	M+	M+2(66)	99(26)	135(23)	75(14)	M+4(12)
	o Br	*216(100)	1Cl,1Br	M+2	M+(78)	135(68)	99(47)	M+4(25)	137(25)
	o Me	150 (56)	1Cl	115	M+(56)	M+2(16)	116(10)	M-1 (9)	89 (9)
	o OMe	166(100)	1Cl	M+	131(70)	123(50)	103(38)	M-1(33)	M+2(32)
	o CF_3	204 (54)	1Cl	169	M+(54)	M+2(16)	170(10)	185 (8)	99 (7)
	p F	154(100)	1Cl	M+	M+2(29)	119(29)	99(15)	139(12)	118(12)
	p Cl	170(100)	2Cl	M+	M+2(67)	99(31)	135(30)	120(20)	155(19)
	p Br	*216(100)	1Cl,1Br	M+2	M+(80)	135(68)	99(50)	120(28)	137(21)
	p Me	150(100)	1Cl	M+	115(99)	M-1(27)	M+2(25)	M+1(15)	114(13)
	p OMe	166(100)	1Cl	M+	151(49)	123(40)	M+2(30)	153(17)	125(15)
	p CF_3	204(100)	1Cl	M+	169(54)	M+2(29)	185(24)	154(21)	189 (6)
(LI)	H	172 (63)	2Cl	156	101(88)	121(78)	M+(63)	158(38)	M+2(37)
	o Me	186 (31)	2Cl	115	M+(31)	135(31)	151(30)	M+2(30)	170(19)

* Indicates M+2 line highest in molecular ion group.

7-3-4 ^1H and ^{19}F Spectra of the Type (V) Fluoride Elimination Products

From the glc and mass spectra four types of compound were expected to occur in the nmr spectra.* Of these the Type (LI) styrenes and the E and Z isomers of the Type (VIII) styrenes were identifiable from their ^1H olefinic singlets and ^1H and ^{19}F olefinic doublets respectively (see FIG.7-3.2). The ^1H and ^{19}F shifts of the ring substituents were also recorded and it was

* Since only mixtures were examined no attempts were made at interpreting the ^1H aromatic region. ^1H spectra were recorded at 100MHz, ^{19}F spectra at 94.1MHz. ^1H shifts are listed in Hz from TMS, ^{19}F shifts are listed in ppm from $CFCl_3$.

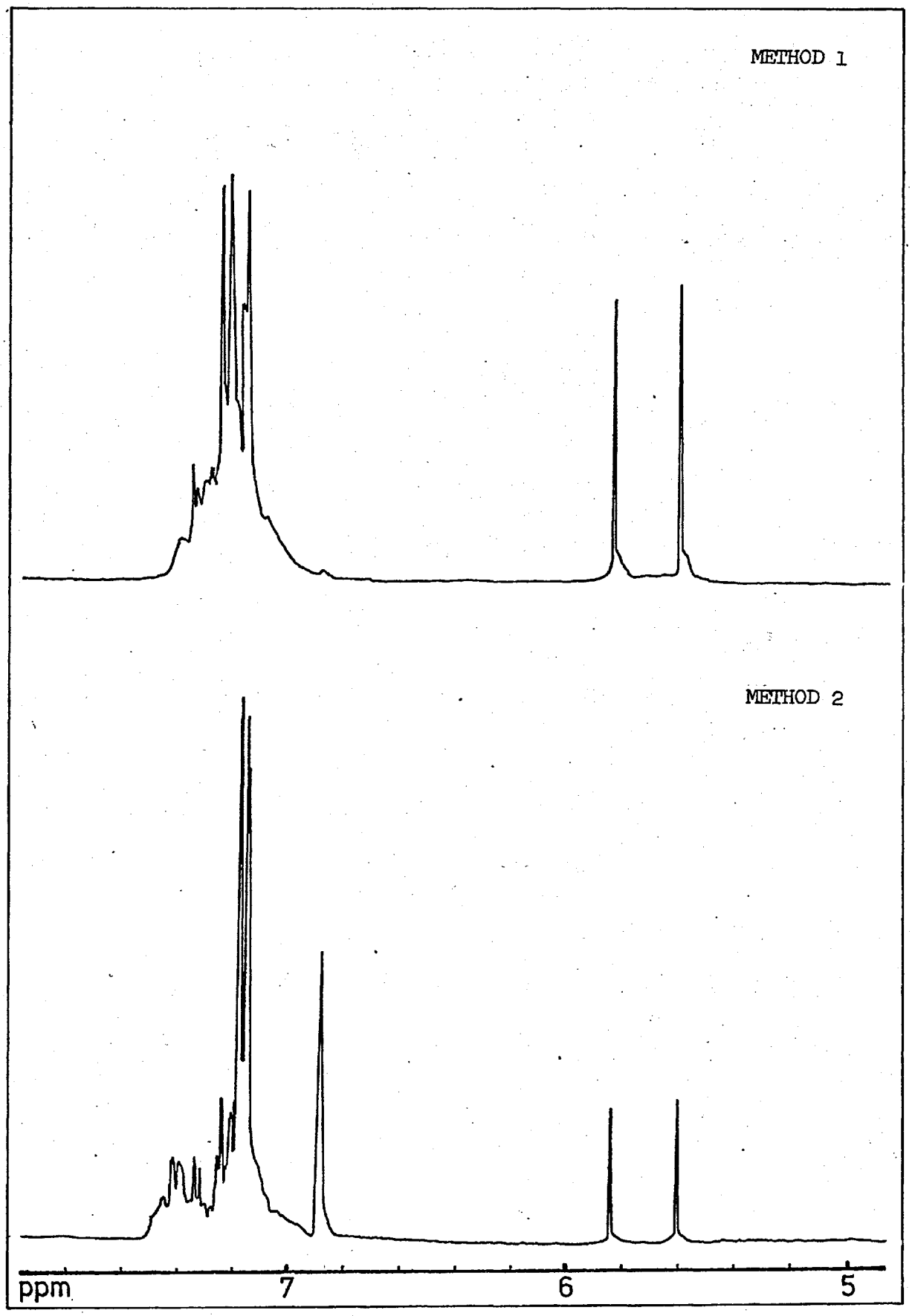


FIG.7-3.2 ^{1}H Spectra of the oMe(V) Elimination Products by METHODS 1 and 2. The 24Hz doublet (δ5.74ppm) is characteristic of the Z-Type (VIII) styrenes, whilst the broad singlet (δ6.85ppm) is characteristic of the Type (LI) styrenes. Note that the aromatics also contain lines from the Type (LII) acetylenes.

from this source that the Type (LII) acetylenes were detected.

All the spectra of the elimination product mixtures contained a prominent olefinic doublet (J = 24.4 ± 2.1Hz) which was immediately assigned to the Type (VIII) styrenes. There was however little trace of a second doublet from the other Type (VIII) isomer. Eventually weak doublets (J = 13.3 ± 0.2Hz) were found in some of the ^{19}F spectra close to the prominent doublets, but it was also noticed that the ^{19}F shifts of the latter were split into two very distinct groups, separated by an average of 14.9ppm (~1,400Hz) with the couplings in the low field group slightly smaller than those in the high field group. The limited ^{1}H and ^{19}F data available on the weak doublets is given in TABLE 7-3.3 with the fuller data on the prominent doublets and their associated ring substituents given in TABLES 7-3.4 to 7-3.6. The identity of the various species present in these spectra will be discussed in the next subsection.

TABLE 7-3.3 The ^{1}H and ^{19}F Chemical Shifts and $^{3}J_{HF}$ Couplings of the Side-Chain Nuclei of the Type (VIII) Styrenes (Weak Peaks)

Deriv	^{19}F Spectra							^{1}H Spectra				
X	O/S	Rel O/S	J	Rel J	1	%$	3	O/S	J	1	%$	3
H	-111.264	0.000	13.50	0.00	/	7	/	not seen		/	/	/
p Cl	-111.489	-0.225	13.20	-0.30	5	8	6	626.1	13.20	3	5	4
p Br	-111.671	-0.407	13.45	-0.05	12	12	5	626.9	13.45	8	8	9
p OMe	-110.600	+0.664	13.40	-0.10	5	14	13	615.7	13.30	5	10	9
p NO_2	-112.323	-1.059	13.50	0.00	22	8	10	642.6	13.40	22	9	7
p CF_3	-112.033	-0.769	13.40	-0.10	25	4	/	635.2	13.30	17	4	/
Av.	-111.563		13.40					629.3	13.35			

$ The % abundance of these isomers was calculated from the FT spectral intensity listings (ie. peak heights not areas) as the % of the total Type (VIII) olefin (ie. 100x[weak]/([weak]+[strong])).

TABLE 7-3.4 ^{1}H and ^{19}F Chemical Shifts of the Ring Substituents of the Type (VIII) Styrenes

^{1}H Spectrum		^{19}F Spectrum	
X	O/S	X	O/S
o Me	239.1	o F	-111.742
o OMe	387.4	o CF_3	-60.571
p Me	238.8	p F	-110.776
p OMe	381.7	p CF_3	-63.501

TABLE 7-3.5 Long Range Couplings Observed in the ^{19}F Spectra of F-1 in the Type (VIII) Styrenes

$n_{J_{FF}}$			$n_{J_{HF}}$			
X	n	J	X	Source	n	J
o F	4	4.7	o F	H-6'	4	1.00d
o CF_3	5	12.8	o Me	Me	5	3.00q
p F	6	0.75	o Me	H-6'	4	0.70d
p CF_3	7	/	o OMe	OMe	6	0.65q
			o NO_2	H-6'	4	0.70d

The shift data for the Type (LI) olefins is given in TABLE 7-3.7 and for

TABLE 7-3.6 The ^{1}H and ^{19}F Chemical Shifts and $^{3}J_{HF}$ Couplings of the Side-Chain Nuclei of the Type (VIII) Styrenes (Prominent Peaks)

Deriv X	^{19}F SPECTRUM						^{1}H SPECTRUM			
	LF LINES		HF LINES		REL	REL		REL		REL
	O/S	J	O/S	J	O/S	J	O/S	O/S	J	J
H	/	/	-113.976	24.40	0	0	609.4	0	24.20	0
o F	/	/	-113.040	25.65	0.936	+1.25	636.3	+26.9	25.60	+1.40
o Cl	-101.855	23.90	/	/	12.121	-0.50	617.0	+7.6	23.80	-0.40
o Br	-99.347	23.30	/	/	14.629	-1.10	603.3	-6.1	23.20	-1.00
o Me	-97.540	23.40	/	/	16.436	-1.00	574.2	-35.2	23.30	-0.90
o OMe	/	/	-111.186	26.5	2.790	+2.10	662.3	+52.9	26.70	+2.50
o NO_2	-99.907	22.35	/	/	14.069	-2.05	593.0	-16.4	22.45	-1.75
o CF_3	-94.992	22.30	/	/	18.984	-2.10	582.3	-27.1	22.30	-1.90
p F	/	/	-112.957	24.10	1.019	-0.30	601.3	-8.1	24.20	0
p Cl	/	/	-114.078	24.00	-0.012	-0.40	607.5	-1.9	24.10	-0.10
p Br	/	/	-114.287	24.10	-0.311	-0.30	609.2	-0.2	24.10	-0.10
p Me	/	/	-113.757	24.20	0.219	-0.20	603.1	-6.3	23.20	0
p OMe	/	/	-112.991	24.40	0.985	0	592.5	-16.8	24.40	+0.20
p NO_2	/	/	-114.941	23.70	-0.965	-0.70	635.2	+25.8	23.75	-0.45
p CF_3	/	/	-114.818	23.95	-0.842	-0.45	662.5	+13.1	24.00	-0.20
Av.	-98.728	23.05	-113.594	24.50	Av Δ : 14.866ppm					

the Type (LII) acetylenes in TABLE 7-3.8. Each figure in TABLES 7-3.3 to 7-3.8 is the average obtained from the three sets of elimination reactions. Spectra were recorded by dissolving the entire elimination products in $CDCl_3$ (2ml) and as recoveries were not 100% the samples were always more dilute than the

TABLE 7-3.7 Chemical Shifts of the Type (LI) Styrenes

Deriv X	H-1		Abundance			Ring	Abundance		
	O/S	Rel O/S	1	2	3	Subnt	1	2	3
H	685.9	0	3	49	23	N/A	N/A	N/A	N/A
o F	Below Aromatics		N/A	N/A	N/A	-115.344	/	9	/
o Br	697.5	+11.6	/	18	/	N/A	N/A	N/A	N/A
o Me	689.7	+3.8	/	133	138	226.8	/	285	194
o CF_3	723.7	+37.8	16	30	19	-63.317	20	11	23
p F	679.7	-6.2	/	79	45	-112.384	/	455	56
p Cl	676.8	-9.1	/	9	/	N/A	N/A	N/A	N/A
p Br	675.4	-10.5	/	9	/	N/A	N/A	N/A	N/A
p Me	683.0	-2.9	/	92	89	237.2	/	150	567
p OMe	677.1	-8.8	/	194	163	380.2	/	1150	567

TABLE 7-3.8 Chemical Shifts of the Type (LII) Acetylenes

Deriv X	^1H / ^{19}F O/S	Abundance 1	2	3
o F	-110.748	20	12	16
o Me	244.5	54	133	113
o OMe	386.1	37	5	5
o CF_3	-62.959	27	16	22
p F	-110.680	32	11	41
p Me	235.9	108	/	/
p OMe	378.3	113	/	50
p CF_3	-63.481	69	/	/

nominal 0.5M. Concentration effects on shifts, between samples, were however fairly small, ie. normally within ± 2Hz.

The Abundance data in TABLES 7-3.7 & 7-3.8 was again calculated from peak heights but for these compounds the results are relative to the amount of Type (VIII) present, not a % of the whole product ie :

$$\text{Abundance} = \frac{[LI]}{[VIII]} \times 100$$

The relative abundance of the Type (VIII), (LI) and (LII) compounds from the FT peak intensities shows reasonable agreement with the glc data (which is far more accurate).

The H-1 singlets of the Type (LI) dichlorostyrenes all showed line broadening due to long range couplings into the phenyl ring. The ^1H shifts of H(LI) agree with the lit. spectrum of β,β-dichlorostyrene - δ7.25(5H,m), 6.72(1H,s).[283]

7-3-5 ^1H and ^{19}F NMR Identification of the Geometry of the Type (VIII) Fluorostyrenes

Some typical literature values for the differences in the ^{19}F shifts[255] and $^3J_{HF}$ couplings[284] between the cis and trans* fluoro olefins are given in TABLES 7-3.9 & 7-3.10. These show that $^3J_{HF}$ is always significantly different in the cis and trans isomers of fluoro-olefins whilst the shift difference between the ^{19}F signals is not always large.

TABLE 7-3.9 Chemical Shifts in Fluoro-Olefins

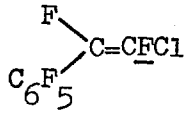
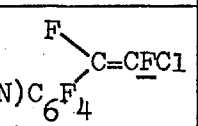
Fluoro-Olefin	CIS	TRANS	Δ
1. FMeC=CHCl	-89.66	-87.18	+2.48
2. 	-126.9	-142.5	-15.6
3. 	-124.8	-140.4	-15.6

TABLE 7-3.10 $^3J_{HF}$ Coupling in Fluoro-Olefins

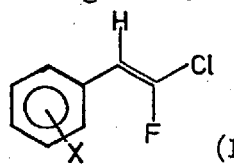
Fluoro-Olefin	CIS	TRANS	Δ
1. $FHC=CH_2$	20	52.55	32.55
2. FHC=CHF	2.8	19.63	16.83
3. $FClC=CH_2$	8	40	32
4. FClC=CHCl	4.05	18.10	14.05
5. FMeC=CHCl	10.8	24.2	13.4
6. FØC=CHMe	22	37	15
7. FØC=CHØ	21	67	46

* As this section is specifically about F/H interactions the cis/trans nomenclature will be used to describe the relationship between the fluorine and proton rather than E/Z which is less specific.

The only conclusion that can be drawn from this is that all the 24.4 ± 2.1Hz doublets in TABLE 7-3.6 belong to the trans (Z) Type (VIII) fluorostyrenes whilst the 13.35 ± 0.15Hz doublets in TABLE 7-3.3 are from the cis (E) isomers.

The separation of the Z-isomers into two distinct groups gave cause for concern. The possibility that one of these groups was due to a rearranged product (eg. LIII) was considered, but discounted on several grounds :

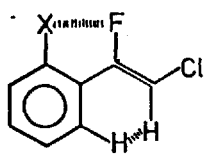
(1) The coupling data in TABLE 7-3.6 all indicate that the fluorine is attached to C-1.
(2) The lack of broadening of the ^{1}H doublets.
(3) The similar break-down patterns in the mass spectra of the two groups.



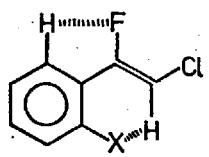
(LIII)

Although the separation of the two Z-isomer groups is fairly large (~ 14.9ppm) the range of the Type (V) fluoride shifts (23.3ppm), which were discussed in terms of preferred side-chain orientations in SECTION 4-7, is even larger. There is, however, no sensible correlation between the ortho ^{19}F shifts in the Type (V) and (VIII) series, although the para derivatives do lie on a straight line (see FIG.7-3.3).

The two obvious conformations for the Type (VIII) styrenes are shown in FIG.7-3.4. The large couplings seen between the oMe and oCF_3 groups and the side-chain fluorine suggest that the low field group of ^{19}F signals arise from conformer (a) whilst the high field group are in conformer (b).



(a)



(b)

FIG.7-3.4 Preferred Conformers of the Z-Isomer of the Type (VIII) Styrenes (⋯⋯ = steric interaction)

Although a planar relationship between the phenyl ring and the side-chain would be preferred for maximum conjugation, steric repulsions, especially in conformer (b), are likely to force non-planarity. For the oF and oOMe derivatives, however, attractive hydrogen bonding interactions are possible in conformer (b) which would facilitate molecular planarity (see FIG.7-3.5) giving rise to the maximum obtainable $^{3}J_{HF}$ olefinic couplings. For the bulkier ortho substituents conformer (a) clearly offers less steric hindrance than (b), but repulsions between the substituents and the olefinic fluorine would probably inhibit complete planarity with a concomitant lowering of the $^{3}J_{HF}$ coupling. (The $^{3}J_{HF}$ couplings do increase inversely to the substituent's size, but this could also include a considerable through-bond electronic component).

For the para substituents the small drop in $^{H}J_{HF}$ relative to oF and oOMe

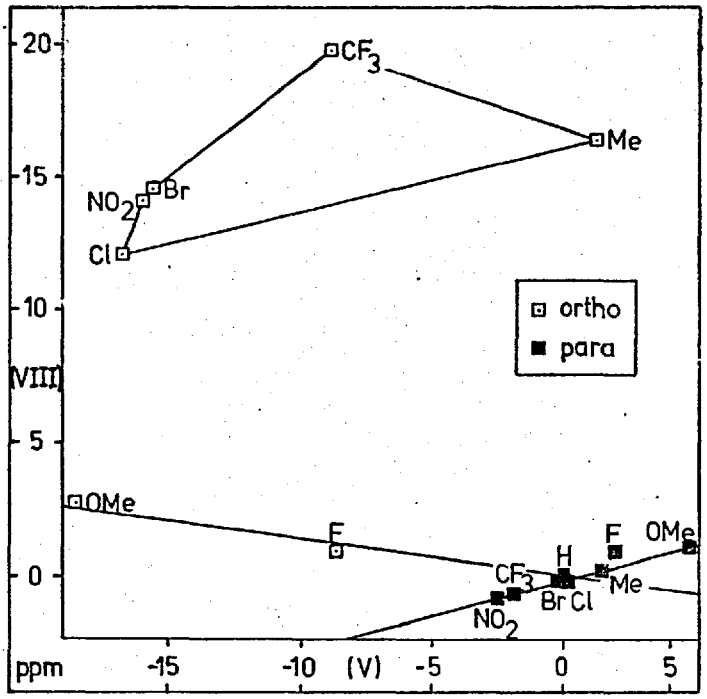
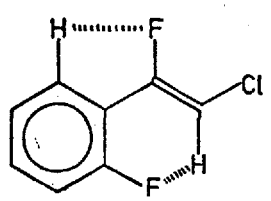


FIG.7-3.3 ^{19}F Chemical Shifts : Type (V) Fluorides v Type (VIII) Olefins

is not surprising as a repulsive H-H interaction rather than the attractive H-X interaction will occur in (b) causing a small degree of non-planarity (The small fluctuations in the couplings observed are in accord with the expected Hammett σ_p-type effects).

The shifts of the olefinic fluorine and proton in both the E & Z isomers of (VIII) gave reasonable straight line plots against σ_p (see FIGS. 7-3.6 & 7-3.7). No sensible trends appeared with the ortho data.



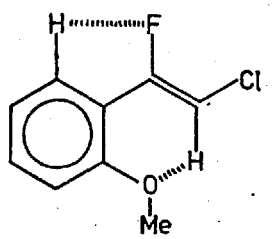


FIG.7-3.5 Possible attractive interaction in conformer (b) of the Z-isomer Type (VIII) styrene

The ^1H olefinic shifts of the para Type (LI) styrenes showed little correlation to σ_p and the limited ortho data showed even less.

7-3-6 Possible Elimination Mechanisms

In Chapter 4 the variations in the chemical shifts and coupling constants of the Type (IV) alcohols and Type (V) fluorides were interpreted as arising from different rotamer preferences in the ortho derivatives. This view was generally supported by the LIS rotational optimisation of the Type (IV) alcohols (see TABLE 6-7.1). Since in both series the direct anti-elimination of HCl is possible in two of the three side-chain rotamers, leading to two isomeric products, it was argued that preferred rotamers would lead to preferred elimination routes and hence characteristic E:Z isomer product ratios (see SECTION 4-10). The expected elimination product geometries were predicted (see TABLE 4-10.2) by making tha qualified assumption that elimination would proceed from the two appropriate rotamers in proportion to their relative populations. The predicted and observed E:Z ratio for the Type (VIII) fluorostyrenes are given in TABLE 7-3.10.

Although the three elimination methods produced different ratios of

TABLE 7-3.10 Predicted and Observed Elimination Products from the Type (V) Fluorides

DERIV X	PREDICTED		OBSERVED														
	TYPE (VIII)		METHOD 1					METHOD 2					METHOD 3				
			TYPE (VIII)			TYPE (LI)	TYPE (LII)	TYPE (VIII)			TYPE (LI)	TYPE (LII)	TYPE (VIII)			TYPE (LI)	TYPE (LII)
	E	Z	%	E	Z			%	E	Z			%	E	Z		
H	60	40	81	/	100	11	8	49	7	93	44	7	57	/	100	29	14
o F	32	68	81	/	100	4	15	76	/	100	12	12	81	/	100	9	10
o Cl	13	87	82	/	100	/	18	95	/	100	/	5	80	/	100	/	20
o Br	10	90	72	/	100	/	28	79	/	100	10	11	74	/	100	/	26
o Me	49	51	58	/	100	4	38	19	/	100	56	25	19	/	100	30	51
o OMe	4	96	83	/	100	/	17	96	/	100	/	4	94	/	100	/	4
o NO_2	11	89	*	/	100	/	*	*	/	100	/	*	*	/	100	/	*
o CF_3	24	76	54	/	100	27	19	58	/	100	20	22	52	/	100	33	15
p F	60	40	76	/	100	/	24	42	/	100	48	10	52	/	100	23	25
p Cl	60	40	73	5	95	/	27	65	8	92	15	20	73	4	96	/	27
p Br	60	40	65	12	88	/	35	69	12	88	11	20	78	5	95	/	22
p Me	60	40	54	/	100	/	46	39	/	100	55	6	38	/	100	52	10
p OMe	60	40	46	5	95	/	54	19	14	86	76	5	21	13	87	66	13
p NO_2	60	40	*	22	78	/	*	*	8	92	/	*	*	10	90	/	*
p CF_3	60	40	60	25	75	/	40	94	4	96	/	6	96	/	100	/	4

* The oNO_2 and pNO_2 products were not detectable by glc. The ^1H nmr spectra showed no olefinic singlets from (LI) and contained insufficient information to calculate the abundance of the Type (LII) aceltylenes.

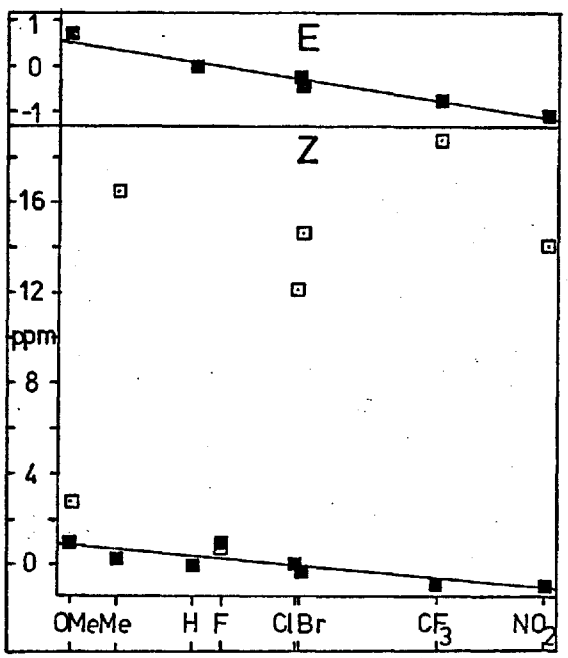


FIG. 7-3.6 Plot of Type (VIII) E & Z $\delta^{19}F$ vs Hammett σ_p

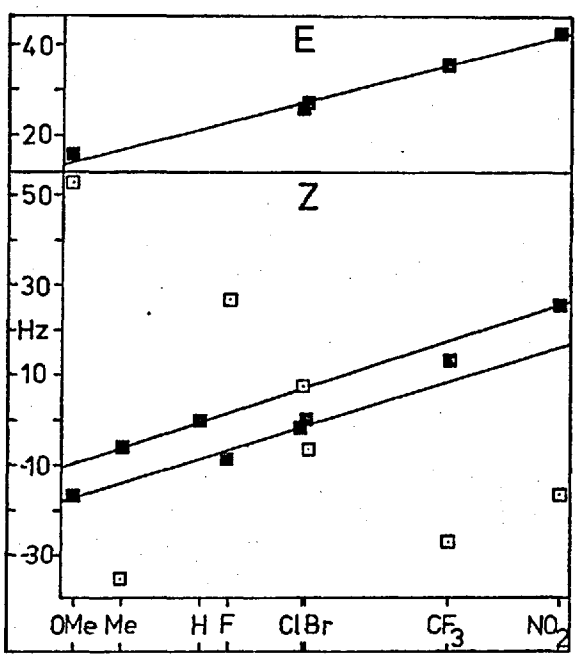


FIG. 7-3.7 Plot of Type (VIII) E & Z δH-2 vs Hammett σ_p

(VIII) : (LI) : (LII) the E:Z ratios for each fluorostyrene were similar. With the exception of oMe(V), in which the unreactive rotamer 1 population was calculated as 55% (see TABLE 4-10.2), the Z-isomer was predicted to dominate the ortho products. In fact all the ortho eliminations proceeded stereospecifically to the Z-isomer!

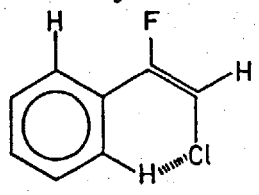


FIG.7-3.8 The E-isomer of the Type (VIII) product

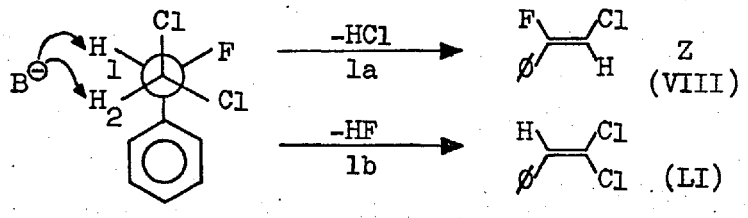
In the para derivatives an E:Z ratio of 60 : 40 was expected but the average obtained was 6.4 : 93.6. The clue to this unexpected behaviour is the increased steric hindrance in the E-styrene (see FIG.7-3.8) which has the phenyl ring and chlorine cis.

If elimination proceeded via an E2 mechanism, then unless the two routes had very different reaction rates the E:Z product ratio would equal the Rotamer 2 : Rotamer 3 ratio. That this does not occur strongly suggests an ElcB or ElcB-like mechanism with a product-like transition state (see SECTION 1-4-1.4). A C-1 carbanion would be well stabilised by the three electron withdrawing groups (F, Ø and $CHCl_2$) and this would allow either (a) rotation of the side-chain to produce the least hindered product or (b) if the product is hindered a reverse reaction to the starting material (k_{-1} in SCHEME 16). Thus the favoured product (Z) could be formed exclusively.

There appears to be no pattern to the stereoselectivity of the elimination reactions of the para derivatives, with both electron donating and withdrawing groups allowing moderate levels of E-isomer formation (cf. pOMe & pNO_2).

Although the elimination of HF from $ØCHFCH_2Cl$ has been reported to proceed via an El mechanism[285] this is unlikely here as strong basic conditions were necessary to form the Type (LI) styrenes from the Type (V) fluorides. Apart from the oCF_3 derivative, little formation of the Type (LI) styrenes occurred in the $2KOBu^t$/THF (METHOD 1) eliminations. Elimination of HF was, however, very significant in the 2LiOEt/EtOH/63°C (METHOD 2) elimination, but with more base and a higher temperature (3LiOEt/EtOH/81°C - METHOD 3) the formation of (LI), with the exception of the oCF_3 and pMe derivatives, showed a marked decrease.

The direct anti-elimination of HF can only occur from Rotamer 3 (see SCHEME 46) which also produces the Z-isomer of (VIII) by elimination of HCl.



SCHEME 46 The Possible Eliminations from Rotamer 3

Two factors favour the elimination of HCl over HF from Rotamer 3 :

(1) Chlorine is easier to displace than fluorine.

(2) The base approach to H-1 is likely to be less hindered by the phenyl

ring than the approach to H-2 (which is also adjacent to the two bulky chlorine atoms).

Point (2) probably accounts for the lack of significant (LI) formation with $KOBu^t$. LiOEt is a sufficiently strong base to overcome point (1) and its small size decreases the problems of steric hindrance. The difference in product ratios between METHODS 2 and 3 probably represents a shift from kinetic to thermodynamic control, the Z-isomers of (VIII) being preferred to (LI) as there is less steric interaction between H-2 and the phenyl ring in (VIII) than with the corresponding chlorine in (LI). The oF and oCF_3 elimination may be rationalised in terms of an interaction between H-1 and the ring fluorines hindering the elimination of HCl whilst the oMe group might aid elimination of HF by interacting with the fluorine and encouraging a high degree of C-F bond polarisation (see FIG.7-3.9(a)). This could also account for the powerful activation by those para groups capable of stabilising carbonium ion character at C-1 (see FIG.7-3.9(b)) and is supported by the sequence OMe > Me (hyperconjugation) > F ≈ H > Cl > Br for the % formation of (LI).

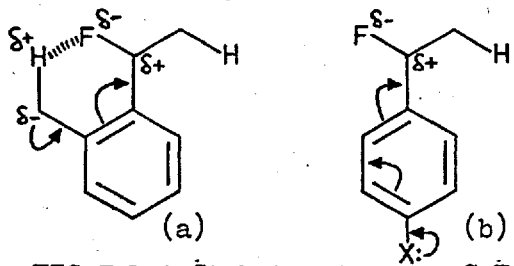


FIG.7-3.9 Stabilisation of C-F Bond Polarisation

In SECTION 7-3.2 it was suggested that step 1b, the elimination of HF from Z(VIII), rather than step 2b, the elimination of HCl from (LI) (see SCHEME 45) was the most probable route to the Type (LII) acetylenes. This is certainly supported by the data in TABLE 7-3.10 where the levels of (LI) and (LII) produced by METHODS 1 and 2 indicate that (LI) resists further elimination.

As stated above, butoxide (METHOD 1) forms little (LI) because of steric hindrance, it therefore initially forms a high level of (VIII) (predominantly in the Z-isomer) which can then be re-attacked to produce the acetylene. This limitation does not apply to ethoxide (METHOD 2) which can form significant amounts of (LI), but on going from METHOD 2 to 3 there is a clear trend for the level of (LI) to fall whilst the levels of (LII) and sometimes (VIII) rise. The lower yield of (LI) represents a change to thermodynamic control which favours (VIII) and since more base is available in METHOD 3 a higher level of second stage elimination would be expected. The overall effect, therefore, is the observed shift from the formation of (LI) to the formation of (LII).

As with the E:Z isomer ratios of (VIII), there is no descernable pattern in the (LII) : (VIII) product ratios, and as the observed effects could not have been caused by varying reaction conditions (all derivatives were reacted simultaneously, starting and finishing at 5 minute intervals, in the same thermostated oil bath) no explanation can be offered.

7-4 Products of the Elimination Reactions of the Type (IV) Alcohols

7-4-1 The Elimination Reactions

Three series of elimination reactions were performed on the 1mM scale using two methods, the first being used twice :

METHOD 1 ($2.KOBu^t/THF$)

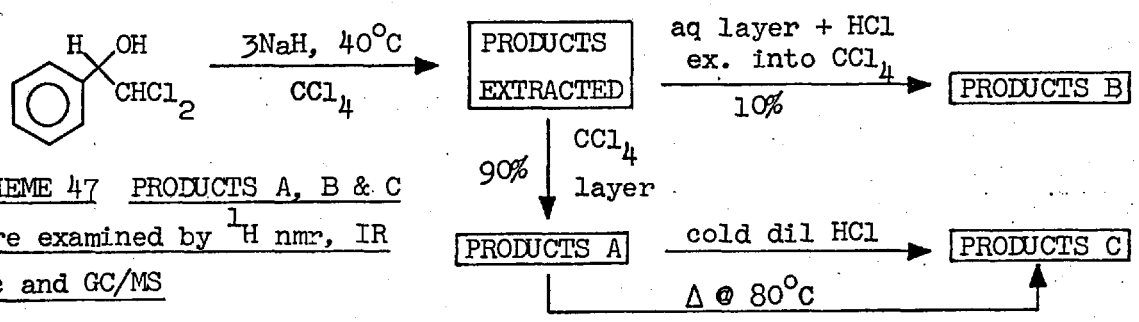
The Type (IV) alcohol (1mMole) was dissolved in dry THF (12ml) and added dropwise to a solution of potassium-t-butoxide (2mMole) in dry THF (20ml) at 20°C. A yellow colour rapidly developed. Stirring was continued overnight under dry nitrogen before quenching with water. The products were ether/water extracted as described for METHOD 1 in SECTION 7-3.1. The yellow colour passed into the aqueous phase but was later taken into ether by acidification with dil. HCl. This normally accounted for 5-15% of the products.

METHOD 2 ($3.NaH/CCl_4$)

The Type (IV) alcohol (1mMole) was dissolved in dry CCl_4 (20ml) and stirred under dry nitrogen in a thermostated oil bath at 41°C. Sodium hydride pellets (3mMole) were added and the solution became yellow. After overnight stirring at 41°C the sodium hydride was removed by filtration, the filter being thoroughly rinsed with CCl_4. On extraction with water the yellow colour passed into the aqueous phase and was recovered lated by acidification as in METHOD 1. The organic phase was dried over sodium sulphate prior to removing the solvent under reduced pressure.

7-4-2 Identification of the Type (IV) Alcohol Elimination Products by METHOD 1

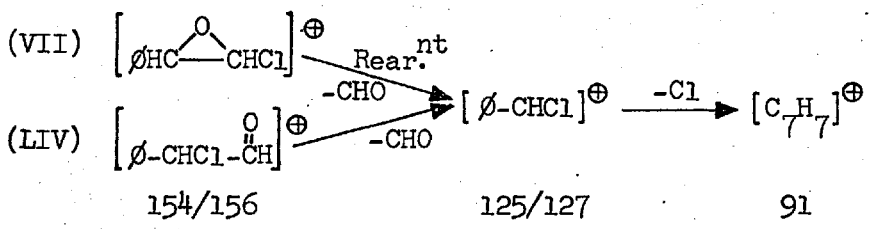
As mentioned earlier, no suitable method was found for separating the Type (IV) elimination products without the epoxides rearranging to the aldehyde. This reaction readily proceeded as was discovered in a detailed study of the elimination reactions of H(IV) by METHOD 2 :



SCHEME 47 PRODUCTS A, B & C were examined by ^1H nmr, IR glc and GC/MS

Analysis of the data obtained on the products, especially A, proved difficult as several contradictory observations were made. The IR spectrum contained three bands in the carbonyl region (1670m, 1690m, 1730w, cm^{-1}) as well as the epoxide bands reported by Nouri-Bimorghi[53,96] (918s, 925s, 1200m cm^{-1}) The ^1H nmr, however, showed no peaks corresponding to either the expected

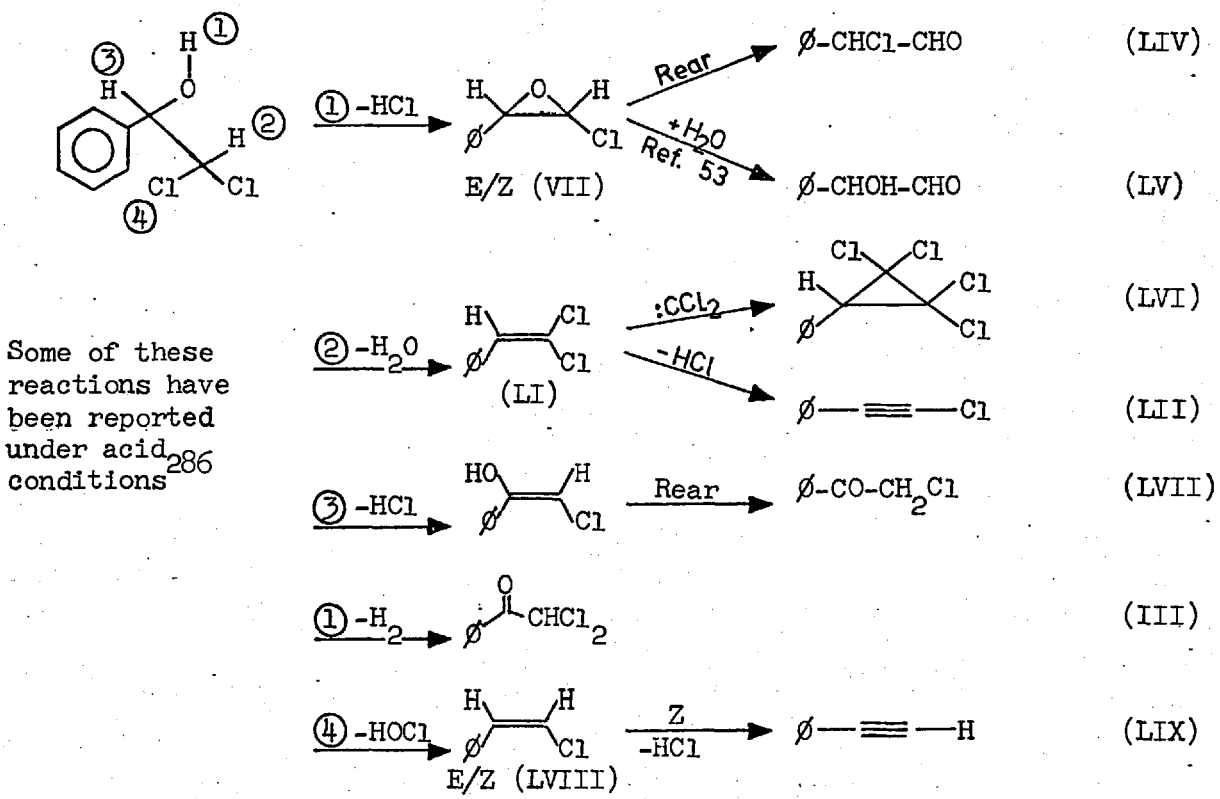
aldehyde (ØCHClCHO) or ketone ($ØCOCH_2Cl$). Glc (column ; 3% OV-17 on Chromosorb G, $\frac{1}{8}$" x 1m; Temp Oven 100°C, Inj 250°C) showed two major products (rf.86 & 100) which by GC/MS were virtually identical (M+ 154(156), main fragmentation to 125(127) then 91), ie. the epoxide and aldehyde :



SCHEME 48 The similar mass spectral fragmentations of the Type (VIII) epoxides and Type (LIV) aldehydes.

The ratios of (VII) and (LIV) in the glc traces of PRODUCTS A varied with the column conditions indicating that the aldehyde was being formed by decomposition of the epoxide on the column. The only product identifiable from the GC/MS arising from the original reaction was therefore the epoxide. Unfortunately this was not fully supported by the ^1H nmr : δ7.397(~9.5H,s,aromatics); 5.365(1H,d,J=2.8Hz,H-2 in cis (VII)), 4.133(1H,d, J=2.8Hz,H-1 in cis (VII)) ppm.

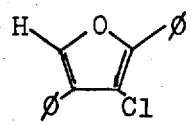
This reaction was repeated several times and apart from a weak singlet at δ0.17ppm in some of the spectra no other lines occurred. The major product was clearly the cis-Type (VII) epoxide from both its ^1H nmr and IR spectra[53,96] but the identity of the compound(s) enhancing the aromatic signal is uncertain. SCHEME 49 shows some of the possible elimination reactions of H(IV) with NaH. The probability of $H^{\ominus}$ attack at the four sites indicated should follow the sequence : ①≫②>③≫④.



Some of these reactions have been reported under acid conditions[286]

SCHEME 49 Possible Elimination Reactions of the Type (IV) Alcohols

Although (LI), the most likely secondary product, was not present both (LII) and (LVI) fit the observed ^{1}H nmr. The presence of the cyclo-propyl derivative (LVI) was supported by the mass spectrum of PRODUCTS A (without glc separation) which contained a weak line at 254 and 256 and also by the very high-field signals in some of the ^{1}H nmr spectra. All of the alternative products given in SCHEME 49 do not fit the observed ^{1}H nmr spectra because of the occurrence of non-aromatic signals (none of which correspond to the singlets marked $ in FIG.7-2.1 observed in the METHOD 1 eliminations).

(LX) 

The GC/MS of PRODUCTS A also suggest the presence of isomers of (LX) and (LXI) but again these may be the results of reaction on the glc column.

Ph.CO.CH-CCl.Ph
(LXI)

The major material in PRODUCTS C, the Type (LV) aldehyde, was readily identified by its GC/MS, IR (1730s cm^{-1}) and ^{1}H nmr (δ9.383 (1H,d,J=2.65Hz),5.033(1h,d,J=2.65Hz)ppm) Again the aromatics appeared as a sharp singlet (δ7.167 (~10.25H)ppm) with a sharp high-field line (δ0.20(~0.77H)ppm). This suggests that in the reaction studied the elimination proceeded to ~55% of the Z-isomer of (VII) with ~35% of the Type (LVI) cyclopropane and ~10% of the Type (LII) acetylene : On treatment with dil. acid or heat the Type (VII) epoxide suffers complete rearrangement to the aldehyde.

Identification of PRODUCTS B was far from straightforward. The ^{1}H nmr spectrum contained the following : δ8.3-7.7(1Hm,aromatics), 7.6-6.8(4Hm,aromatics), 4.8-3.2(0.42Hm, olefinics), 0.2(0.33Hs, cyclopropyl)ppm. The aromatic region was reminiscent of benzoic acid and this was supported by a sizeable peak in the GC/MS of M+122. This would appear to be one of the major products after treatment of the aqueous layer with dil. HCl. The GC/MS also contained a host of other products with parent ions as high as 250 and 310 without any chlorine substitution patterns. How many of these were formed by reaction on the column was not determined but these probably account for the various signals in the ^{1}H olefinic region. Significant peaks corresponding to the Type (LVI) cyclopropane were not seen in the GC/MS. The route from the Type (IV) alcohol to the benzoic acid is unknown but a similar reaction was found to occur by METHOD 1 (ie. 5-10% of final product was a benzoic acid).

Finally FIG.4-7.1 shows a series of ^{1}H nmr spectra following the first stages of the reaction of H(IV) with NaH in CCl_4, recorded using a T-1 program on an XL100. The first 10 spectra were recorded at 100 second intervals, the second 10 at 15 minute intervals. The poor resolution was due to precipitation of NaCl during the reaction.

The spectra clearly show the disappearance of the H_C signal as the alkoxide (LXII) (indicated by the high field shift of the H_A, H_B and H_ϕ signals

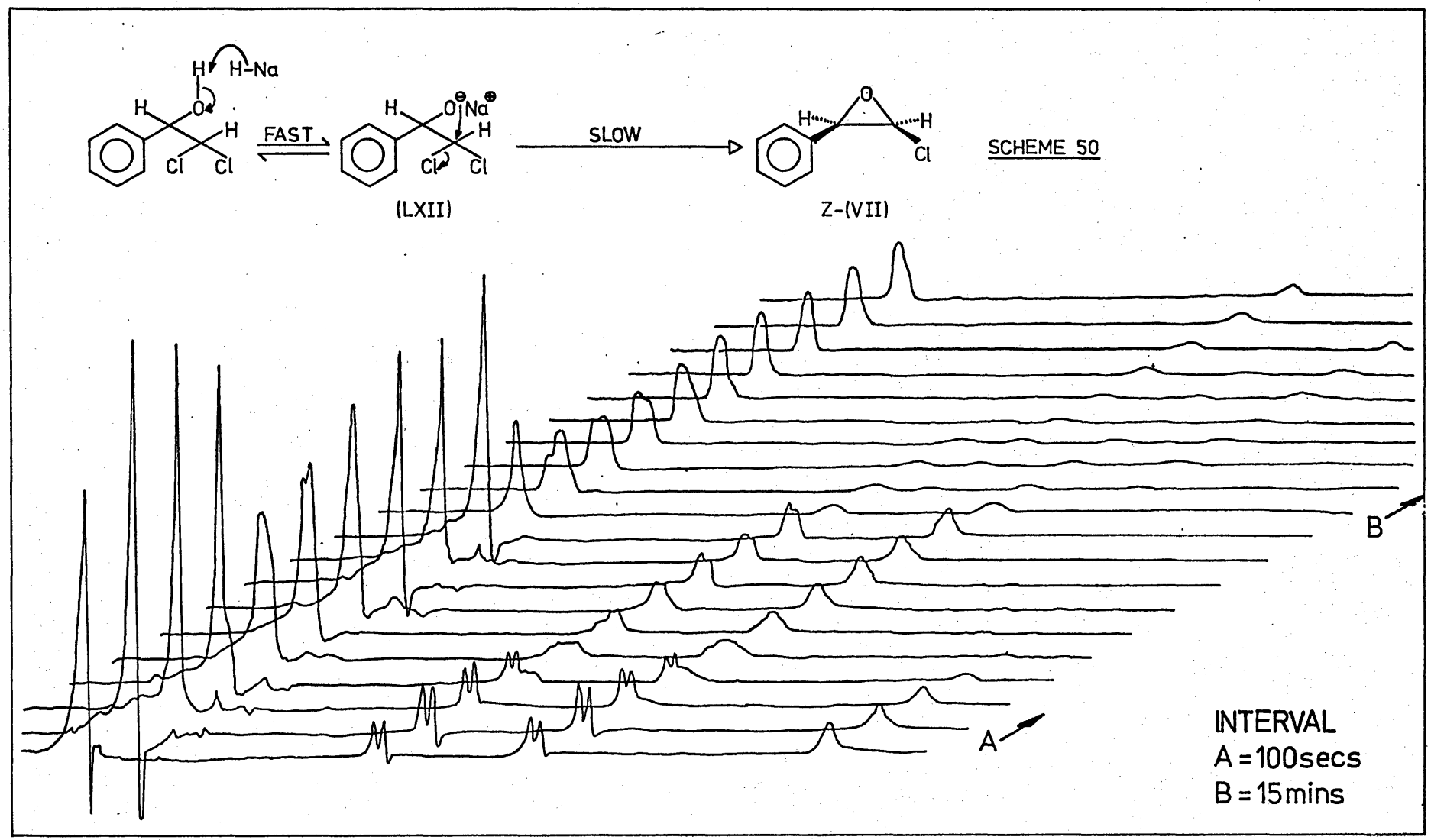


FIG.7-4.1 Single Pulse FT "Kinetic" Spectra of the Reaction between H(IV) and NaH in CCl_4. Note the high field shift (spectra 4-7) as the alkoxide is formed and the subsequent slow emergence of the epoxide signals (spectrum 12 onwards). The structures shown in SCHEME 50 are drawn directly over the aromatic signals to which they relate.

in the presence of the $-O^{\ominus}Na^{\oplus}$ moiety) is formed. This then undergoes a slow elimination reaction to the Z-epoxide (see SCHEME 50).

7-4-3 The Epoxide Product Isomer Ratios Produced by METHODS 1 and 2

So far we have only examined the products of METHOD 2 which comprised 50-70% (depending on the ring substituent) of the epoxide (Z-isomer only). Overall epoxide yields were similar by METHOD 1, but here both epoxides and also an additional product, giving rise to a singlet at $\delta 6.0 \pm 0.3$ppm (see FIG.7-2.1), were formed. The structure of the latter remains a mystery as its ^1H nmr does not correspond to any of the likely products in SCHEME 49.

The identity of the cis-(Z) epoxides formed by METHOD 2 was comfirmed by its ^1H nmr and IR spectra.[53,96] The trans-(E)-Type (VII) epoxides have not been reported but the assignment shown in FIG.7-2.1 is supported by ^1H data on analogous epoxides.[281,287,291] The observed couplings (2.8 ± 0.15Hz assigned as cis $^3J_{HH}$ and 0.65 ± 0.15Hz assigned as trans $^3J_{HH}$) agree well with the classic study of Lehn and Riehl[281] in which the cis $^3J_{HH}$ in $\phi\overset{O}{\overbrace{CH-CH}}X$ was shown to vary from 4.1 to 2.5 Hz and trans $^3J_{HH}$ from 2.5 to 0.5Hz depending on the electronegativity of X. This was explained by the geometry of epoxides - the cis bonds are co-planar whilst the trans bonds have a dihedral angle of ~147° giving a $\cos^2\phi$ factor of 0.7 in the Karplus equation (see EQN.9).

TABLE 7-4.1 ^1H NMR Spectra of the E and Z Type (VII) Epoxides

DERIV X*	CIS (Z) EPOXIDE							TRANS (E) EPOXIDE						
	^1H NMR				RATIO			^1H NMR				RATIO		
	ν_A	ν_B	δ_{AB}	J_{AB}	1	1	2	ν_A	ν_B	δ_{AB}	J_{AB}	1	1	2
H	536.5	413.3	123.2	2.80	19	47	100	492.7	419.8	72.9	0.80	81	53	
o F	539.2	433.7	105.5	2.75	27	25	100	494.2	443.7	50.5	0.60	73	75	
o Cl	541.8	433.4	108.4	2.80	16	9	100	472.7	449.4	23.3	0.50	84	91	
o Br	541.7	427.5	114.2	2.85	58	2	100	470.9	445.2	25.7	0.65	42	98	
o Me	542.5	417.4	125.1	2.85	55	72	100	473.4	426.8	46.6	0.80	45	28	
o CF_3	539.9	441.9	98.0	2.95			90	465.1	446.6	18.5	0.70	100	100	10
p F	534.0	410.0	124.0	2.85	38	54		487.9	415.9	72.0	0.75	62	46	
p Cl	534.0	408.8	125.2	2.75	59	50	100	486.9	413.9	73.0	0.60	41	50	
p Br	533.4	407.8	125.6	2.65	40	32	100	485.6	412.0	73.6	0.50	60	68	
p Me	535.5	410.6	124.8	2.80	24	47		494.7	419.6	75.1	0.75	76	53	
p CF_3	537.6	416.9	120.7	2.80	39	72	100	492.0	424.0	68.0	0.60	61	28	

* The oOMe, oNO_2 pOMe and pNO_2 derivatives either did not react with any of the bases tried or where reaction did occur failed to produce any epoxide. Both pF(IV) and pMe(IV) failed to form epoxides with NaH (pF(IV) yielded the aldehyde - $\delta 9.491$(1H,d,J=2.65Hz); 5.173(1H,d,J=2.65Hz)ppm in all three attempted reactions whilst pMe(IV) appeared to polymerise - the ^1H nmr signals were extremely broad and almost entirely in the aromatic region).

The E:Z isomer ratios for the three sets of elimination reactions, calculated from the 100MHz ^{1}H nmr spectral intensities, are given in TABLE 7-4.1.

The large variation in ν_A on going from the cis to the trans epoxide is probably due to the influence of the benzene ring current on the H_A proton when cis to the ring, ie. in the trans-epoxide. Several authors have attempted to calculate the preferred rotamer in styrene oxide and results of $\phi = 125^{\circ}$,[289] 55° [290] and 30° [291] have been reported (see FIG.7-4.2) with barriers to rotation quoted as approximately 3.5kcal/mole.[289,291]

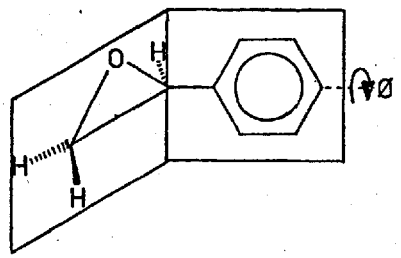
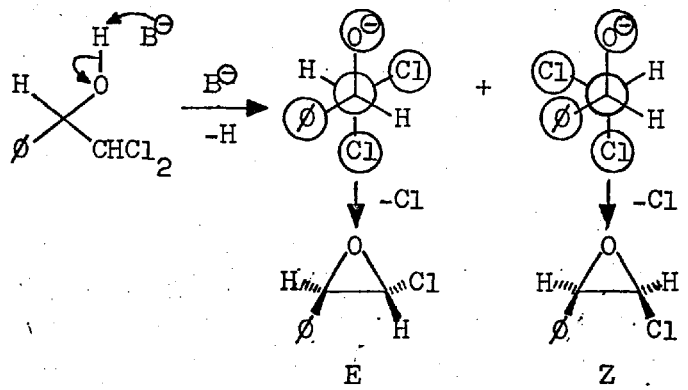


FIG.4-7.2 Definition of the angle ϕ

Turning to the epoxide isomer ratios - the stereospecificity of the NaH eliminations is surprising, especially when it is realised that the Z-isomer is the least sterically favoured. The expected elimination route is shown in SCHEME 51.



SCHEME 51 Elimination Routes to the E/Z Epoxides

Note that the Z product is least favoured on steric grounds in the starting material, product and transition state.

Since METHOD 1 was duplicated (both sets of eliminations were performed under identical conditions) the two sets of results should be averaged. Differences between the two sets indicate considerable sensitivity in the E:Z isomer ratio to reaction conditions and ideally further replicates should have been performed to more accurately fix the isomer ratios. In TABLE 7-4.2 the averaged results obtained by the two methods are compared to those predicted in Chapter 4 from the coupling data.

With the exception of oMe and oCF_3 the E:Z isomer ratio predicted from the coupling data was realised by METHOD 1. This included several derivatives in which Rotamer 3 (which allows no direct elimination route) was present in large amounts (40-75%).

TABLE 7-4.2 Predicted and Observed Type (VII) Epoxide Isomer Ratios

DERIV X	PREDICTED			METHOD 1		METHOD 2	
	ROT3	E	Z	E	Z	E	Z
H	23.3	55	45	67	33	/	100
o F	40.6	66	34	74	28	/	100
o Cl	70.5	64	36	87	13	/	100
o Br	75.0	66	34	70	30	/	100
o Me	22.1	72	28	37	63	/	100
o CF_3	66.1	39	61	100	/	10	90
p F	23.3	55	45	54	46	/	/
p Cl	23.3	55	45	46	54	/	100
p Br	23.3	55	45	64	36	/	100
p Me	23.3	55	45	64	36	/	/
p CF_3	23.3	55	45	45	55	/	100

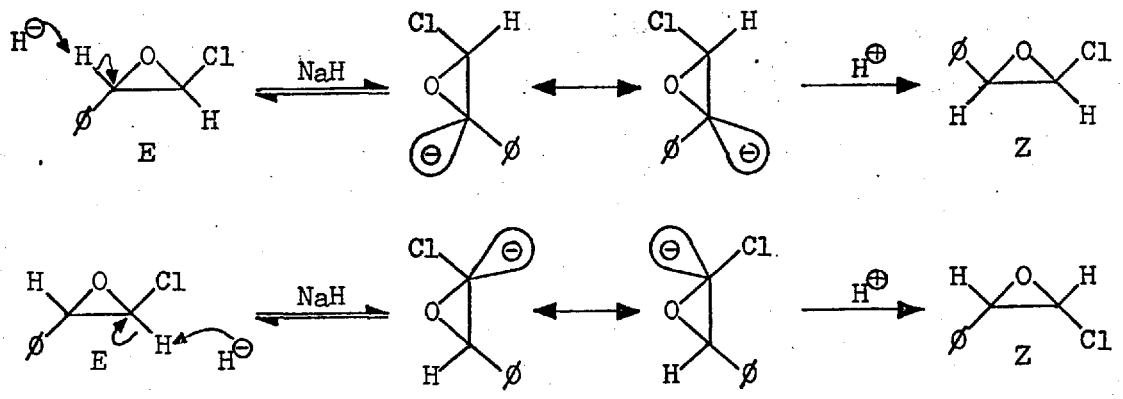
7-4-4 Possible Elimination Mechanisms for Epoxide Formation

The formation of epoxides from β-chloroalcohols has been shown to proceed via a γ-ElcB mechanism[81-83] (see SECTION 1-4-2). Because of the stability of the carbanion intermediate in β-ElcB mechanisms the stereochemical outcome is normally unpredictable. In γ-eliminations, however, the presence of the stabilised $-O^{\ominus}$ species need not necessarily upset the rotamer preferences of the ground state alcohol so elimination may proceed to the expected products. This appears to be the case for the bulk of the eliminations performed with butoxide (METHOD 1) with only the oMe(IV) and oCF_3(IV) derivatives going substantially to the unexpected epoxide. This appears to be a function of the size of the ortho substituent.

In SECTION 6-7 interpretation of the rot/opt LIS results indicated that the Type (IV) alcohols all adopted conformations in which the ortho ring substituent was orientated towards the $-CHCl_2$ group, thus "controlling" the C-1/C-2 bond rotation. On ionising the alcohol function this orientation may be destabilised for the bulky oMe and oCF_3 groups, the former being attracted towards the oxide ion, the latter being repelled. Having altered this controlling influence the side-chain would be free to change its conformational preferences and hence produce unexpected product ratios.

There is strong evidence (FIG.7-4.1) that the NaH eliminations (METHOD 2) also proceeded, initially at least, by an ElcB mechanism. The stereospecificity* for the least favoured Z-isomer is, however, puzzling as a mixture of E:Z isomers was expected.

Let us assume that, in the first instance, elimination occured to the expected E:Z products (see SCHEME 51). NaH is a very powerful base which could then abstract either of the epoxide protons (see SCHEME 52). The carbanions produced would undergo rapid inversions between the two pyramidal forms with addition of a proton (from either another alcohol molecule or from the



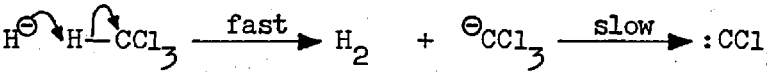
SCHEME 52 Possible Formation of the Z-Epoxide by Base-Induced Rearrangement.

* With the exception of oCF_3 in which the 10% E-isomer probably reflects the stereospecificity of METHOD 1 for the E-isomer.

aqueous work-up) occuring predominantly in the most stable carbanion. This would have the charged orbital away from the electron rich -Cl or -Ø groups and would therefore favour the Z-epoxide.

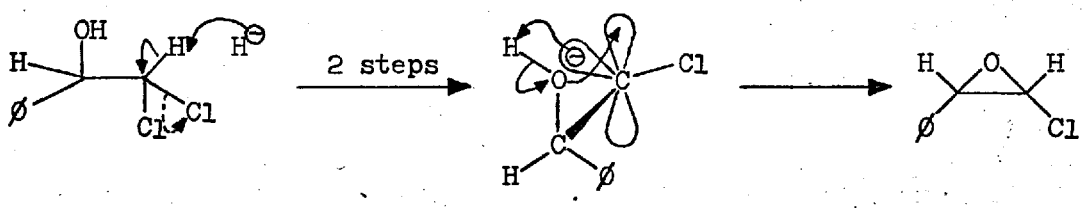
The thermodynamic control of SCHEME 52 is the most plausible route to the exclusive formation of the Z-epoxide. An alternative reaction involving an α-elimination of HCl could also participate :

The formation of dichlorocarbene from treating chloroform with NaH is well known :



SCHEME 53

A similar 2-step reaction could occur with the Type (IV) alcohols giving rise to the highly reactive intermediate (LXIII). Again the carbanion would prefer to lie away from the phenyl ring allowing an intramolecular rearrangement to form the Z-epoxide. The presence of $:CCl_2$ and species such as (LXIII) in the NaH eliminations may account for some of the high MW species seen in the GC/MS (see SECTION 7-4-2).



(LXIII)

SCHEME 54

CHAPTER 8

8 OVERVIEW

8-1 Stereoselectivity Towards Diastereotopic Leaving Groups - Was this observed ?

The simple answer is yes, as under some conditions stereospecificity was found in the eliminations from both the Type (IV) alcohols and the Type (V) fluorides (see TABLES 7-4.2 and 7-3.10 respectively). The results provide a clear demonstration of the expected non-equivalence of paired groups on a prochiral centre which is adjacent to a chiral centre (see SECTION 1-1).

Taking the question deeper - "Was the expected stereoselectivity observed ?" - a simple answer cannot be given.

Throughout this work the strategy has been to find the conformation(s) preferred in the ground state and from these to predict the expected stereochemical outcome of elimination reactions. Even assuming that accurate calculation of the preferred orientations was achieved (see Chapters 4 & 6) several major assumptions were still needed in order to predict product isomer ratios (see SECTION 4-10).

Bearing this in mind, the epoxide product ratios produced by the reaction of butoxide with the Type (IV) alcohols (METHOD 1) were, with the exception of the oMe and oCF_3 derivatives, in extremely good agreement with those predicted (eg. average para E:Z ratio predicted = 55:45; observed = 56.7:43.3 - see TABLE 7-4.2). This appears to indicate that the rotamer populations calculated in $CDCl_3$ solution were similar to those present under the reaction conditions (THF solution) and that elimination proceeded towards the prochiral leaving groups in direct proportion to the appropriate rotamer populations.

All previous work has indicated that the epoxide forming γ-eliminations follow ElcB kinetics (see SECTION 1-4). As such, preservation of stereochemistry would not normally be expected. In SECTION 7-4-4, however, it was pointed out that the $-O^{\ominus}$ carbanion is one bond removed from the stereochemically important C-C bond (ie. there can be no loss of stereoselectivity by the usual method - pyramidal inversion at the carbanion) so except by through-space steric repulsions, interference with the preferred ground state conformations prior to elimination need not occur. In addition, the butoxide-induced eliminations from the Type (IV) alcohols failed to produce the expected product ratios only when the extremely bulky oMe and oCF_3 ring substituents were present (see SECTION 7-4-4).

Clearly, in the sodium hydride induced elimination from the Type (IV) alcohols (METHOD 2), stereospecific formation of the Z-epoxide was not anticipated (see SECTION 7-4). There is very strong evidence (FIG.7-4.1), however, that the reaction initially followed the expected mechanism (ElcB),

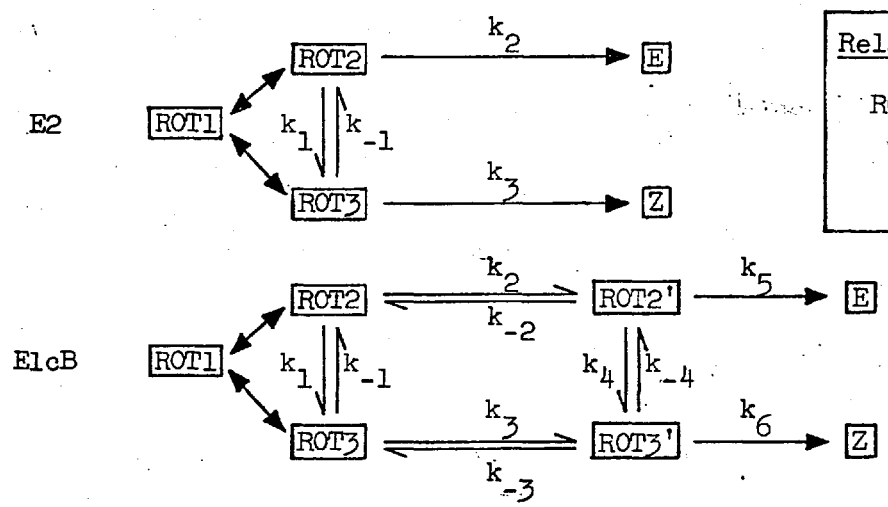
but it seems unlikely that the sterically unfavoured route to the Z-epoxide (SCHEME 51) would have been followed exclusively. Rather, the E/Z epoxides were probably formed in the expected ratio, and on re-attack by $H^{\ominus}$ (SCHEME 52) suffered rearrangement to the Z-epoxide (see SECTION 7-4-4).

Turning to the Type (V) fluoride eliminations; although the proportions of the Type (VIII) fluorostyrenes formed varied with the base, the E:Z ratio was similar in all three methods. Summarising TABLE 7-3.10 :

ortho derivatives - expected E:Z ratio = 20 : 80; observed = 0 : 100

para derivatives - expected E:Z ratio = 60 : 40; observed = 6.4 : 93.6

In predicting the E:Z isomer ratios the eliminations from rotamers 2 and 3 (see TABLES 4-10.1 & 4-10.2) were assumed to proceed at identical rates without loss of configuration (ie. via the E2 mechanism). In the event, stereospecificity was observed throughout the ortho derivatives, including oMe(V) which was expected to give an E:Z ratio of 49:51; indicating that, if the calculated rotamer populations in the Type (V) fluorides were approximately correct, then the rates of elimination from rotamers 2 and 3 were markedly different (ie. by several orders of magnitude). This was interpreted in SECTION 7-3-6 as strongly suggesting an ElcB or ElcB-like mechanism and is best appreciated by examining the possible reaction pathways (see SCHEME 55).



Relative Steric Hindrance
ROT1 < ROT3 < ROT2
ROT3' < ROT2'
Z < E

SCHEME 55 Elimination Reaction Pathways for Converting Type (V) to Type (VIII)

Using oMe(V) as an extreme case (ROT2:ROT3 ≒ 1:1 but E:Z = 0:2): to form the Z-isomer exclusively by the E2 mechanism the reaction rates must have the relative magnitudes - $k_1(k_{-1}) \gg k_3 \gg k_2$

Rapid interchange is expected between rotamers (k_1/k_{-1}), but substantial differences between rates k_2 and k_3 seem unlikely (rotamers 2 and 3 have fairly similar steric hindrance) unless the transition states are very "product-like" (see SECTION 1-4-1.4). The ElcB (or ElcB-like) mechanism does, however, leave more room for stereospecificity, for not only are all the first

stages of the elimination reaction (k_2 and k_3) reversible, but the stabilised intermediates (ROT2' and ROT3' - the carbanions of SCHEME 16) may also interconvert. As both ROT2' and E are more hindered than ROT3' and Z the sequences $k_4 \gg k_{-4}$, $k_{-2} > k_{-3}$ and $k_6 > k_5$ would be expected. Also the interconversion rates $k_1(k_{-1})$ and $k_4(k_{-4})$ would be expected to be fast relative to the reaction rates k_2 to k_6. A situation could easily arise, therefore, in which rates k_4 and k_{-2} could dominate the fate of ROT2' preventing elimination via k_5 to the E-isomer, ie $k_4 + k_{-2} > k_2 + k_{-4} \gg k_5$. Provided that $k_6 \ll k_{-3} + k_{-4}$ reactions would proceed stereospecifically to the Z-isomer.

The prediction of such stereospecific reactions was not possible from the data available without a prior knowledge of the elimination mechanism preferred.

8-2 Relationship of the Type (IV) and (V) Eliminations to the 'Abnormal' Michaelis-Becker Reaction

This work was prompted by the suggestion of P.A.Worthington[18] that the Type (IV) alcohols might be good models for the study of postulated ortho interactions in the α-hydroxy phosphonate intermediates of the 'abnormal' Michaelis-Becker reaction (see SECTION 1-3). Variations in the stereoselectivity of this reaction, especially on modifying the ortho phenyl substituent (see TABLE 1-3.3), were attributed to changes in the preferences for particular side-chain rotamers (see SCHEME 9 and FIG.1-3.3). These preferences were thought to be controlled by interactions between the ortho ring substituent and the $-O^{\ominus}$ moiety. This was supported by previous observations[47] but could not be directly verified due to the reactivity of the intermediates.

FIG.8-2.1 compares the structure of the Type (IV) and (V) compounds and their elimination reactions to those of the α-hydroxy phosphonates. Whilst the Type (IV) alcohols are structurally closer to the α-hydroxy phosphonates than the Type (V) fluorides, the latter do have the advantage of performing elimination reactions from the same rotamers and to the same olefin isomers as the α-hydroxy phosphonates. Neither of the model systems however, mimicked the unique cyclisation-elimination process performed by the α-hydroxy phosphonates (see SCHEME 8).

As we have seen the Type (V) fluorides underwent more or less stereospecific elimination to the Z-fluorostyrenes despite predictions to the contrary. This was probably due to the formation and stabilisation of a carbanion intermediate (ie. an ElcB mechanism) which allowed complete thermodynamic control of the product geometry. These results are therefore of no help in verifying the postulated structures of the α-hydroxy phosphonates[18] the reactions of which were substantially under kinetic control (see TABLE 1-3.5).

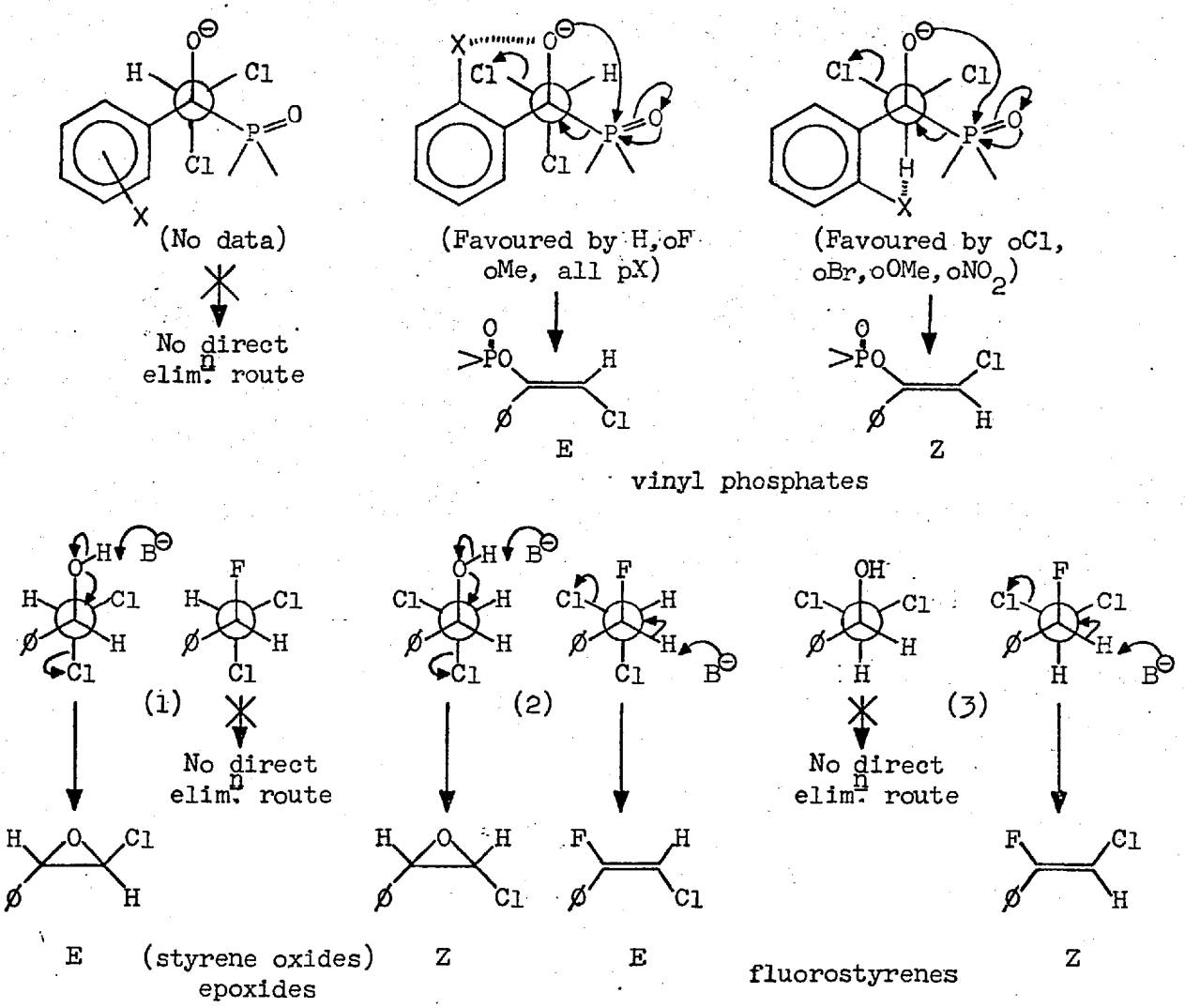


FIG.8-2.1 Comparison of Type (IV) & (V) Compounds to the α-hydroxyphosphonates

Similarly, although the Type (IV) alcohol eliminations showed stereoselectivity, this was in effect monitoring the rotamer 1 : rotamer 2 ratio and not the rotamer 2 : rotamer 3 ratio (see FIG.8-2.1), and is therefore not directly applicable to the α-hydroxy phosphonates.

Solace is found in the rotamer population predictions for the Type (IV) and (V) series derived from the coupling data in Chapter 4 (see TABLE 8-2.1 - compiled from TABLES 1-3.3 & 4-10.2). If the E:Z vinyl phosphate ratios are compared directly to the rotamer 2 : rotamer 3 ratios there appears to be little correlation, but plots of %E vs. ROT2 and %Z vs. ROT3 show surprisingly good correlation when the sources of the sets of data are considered (see FIGS.8-2.2 & 8-2.3). In fact, excepting the oNO_2(V) rotamer 3 population, the calculated rotamer populations for the Type (IV) & (V) series successfully predict the rank of the E/Z isomer formation in the 'abnormal' Michaelis-Becker reaction.

Further support for the concept of elimination from preferred rotamers controlling the vinyl phosphate isomer ratio comes from the side-chain ^{19}F

TABLE 8-2.1 Comparison of E:Z Vinyl Phosphate Ratios to the Type (IV) & (V) Series Rotamer Populations

DERIV	Vinyl Phosphate Product Ratios.		Type (V) & (V) Rotamer Population Predictions		
X	E	Z	1	2	3
H	95	5	42.3	34.4	23.3
o F	60	40	39.9	19.5	40.6
o Cl	17	83	18.9	10.6	70.5
o Br	9	91	16.4	8.5	75.0
o Me	77	23	55.0	21.9	22.0
o OMe	5	95	15.0	3.0	83.0
o NO_2	37.5	62.5	10.3	10.0	79.7
p X	95	5	42.3	34.4	23.3

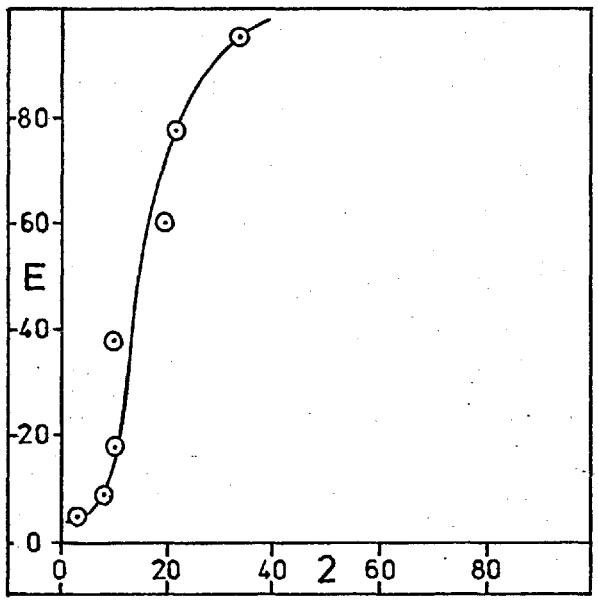


FIG.8-2.2 Rotamer 2 vs. E-Isomer

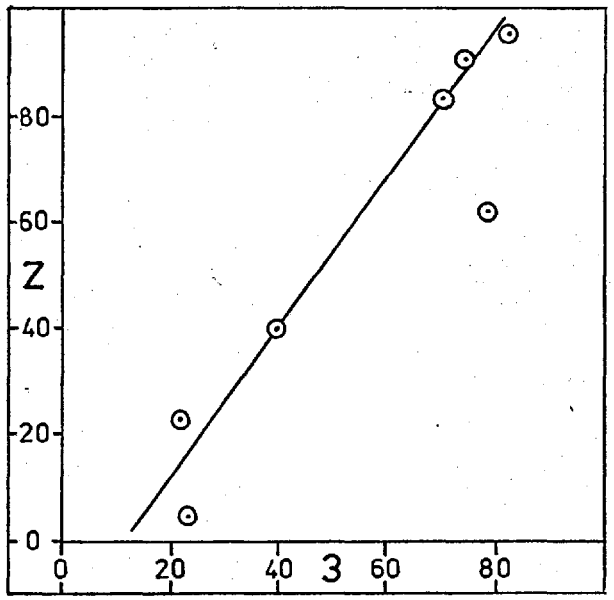


FIG.8-2.3 Rotamer 3 vs. Z-Isomer

Plots of the predicted rotamer populations of the Type (IV) & (V) series vs. the observed product isomer ratios of the 'abnormal' Michaelis-Becker Reaction

shifts in the Type (V) fluorides (see SECTION 4-9, point (5)). These suggest the sequence : oOMe, Cl, Br, NO_2 > oF, oCF_3 > oMe, all pX for the rotamer 3 populations, which agrees with the observed incidence of the Z-vinyl phosphate isomer in the α-hydroxy phosphonate cyclisation/eliminations.

No evidence was found, from either the conventional nmr shifts and couplings or the LIS data, to support the suggested ring substituent interactions with the side-chain hydroxy group.[18] Instead the LIS data, almost unanimously, indicated that the major ring orientation throughout the Type (IV) series was such that the X substituent and $-CHCl_2$ group were adjacent, ie. the ideal orientation for the "control" of the side-chain rotamer

preferences by the ring substituent (see SECTION 6-7).

Overall, therefore, data from the Type (IV) & (V) series is useful in increasing our understanding of the structures of the α-hydroxy phosphonate intermediates, but the elimination reactions so far observed, especially for the Type (V) fluorides, possessed too much thermodynamic control for sensible correlation to the 'abnormal' Michaelis-Becker reaction which was primarily kinetically controlled. This last problem may be insurmountable if the Type (V) fluorides always eliminate via an ElcB mechanism.

8-3 Success/Validity of the Approaches to Conformational Analysis Based on the Conventional NMR Spectra (Chapter 4) and the LIS Data (Chapters 5 & 6)

With the exception of the METHOD 1 Type (IV) elimination results (see TABLE 7-4.2), which were subject to an unknown degree of bond rotation during the reaction, there is no independent corroboratory measure of the success or accuracy of the side-chain rotamer predictions for the Type (IV) & (V) series made in SECTIONS 4-8-2.1 & 6-7. For the most part, however, the results from the LIS data and the $^{3}J_{HH}/^{3}J_{HF}$ data (together with those from the $^{2}J_{CF}$ and δ_{F} data) are mutually supporting.

Whilst X-ray crystallography appears attractive as the only absolute method of verifying the preferred overall geometry it has two major limitations:

(1) The molecule is examined in the solid state and not in solution where it performs its reactions.

(2) Only one internal orientation of the molecule will be seen, which will probably correspond to the structure most occupied in solution but will give no data on conformational preferences between the various rotamers.

A stereoselective reaction such as those already attempted with the Type (IV) & (V) series, is the only true method of confirming the rotamer populations, but, as we have seen, unless conditions can be found under which the product isomer ratio reflects the starting material rotamer ratio (which the Type (V) results clearly do not), the results will be of little value.

The validity of both approaches to the conformational determination of the Type (IV) & (V) series should be questioned.

In Chapter 4 the conventional nmr parameters of chemical shift and coupling constant were used to obtain indications of conformational preferences. In this context the availability of a series or several series of compounds, within which to make comparisons, is essential as observations are largely relative and not absolute.

Studies concentrated on the C-1/C-2 conformation, since this was important in directing the course of the elimination reactions and also contained the mainstay of the conformational data : the $^{3}J_{HH}$ and $^{3}J_{HF}$ couplings. The

complexity of the structural and substituent dependence of the $^{3}J_{HF}$ coupling was demonstrated with a series of deoxyfluoro pyranoses in SECTION 4-8-2.2. This indicated that a simple empirical approach (eg. EQN.86) would not satisfactorily predict both the trans and gauche $^{3}J_{HF}$ (or $^{3}J_{HH}$) coupling constants in a multisubstituted species (eg. a Type (V) fluoride). It was therefore decided to use a model approach to estimate the coupling constants for the individual side-chain rotamers in the Type (V) fluorides (see SECTION 4-8-2.3). Considerable care was taken, both in the choice of the model couplings and in their conversion to the estimates of the couplings in the Type (V) fluorides, every effort being made to justify and correct any approximations. The rotamer populations were then calculated from the observed "time averaged" $^{3}J_{HH}$ & $^{3}J_{HF}$ couplings, and the estimated couplings of the individual rotamers. The determinant method used (EQNS.92-95,99-101) is perfectly sound provided that the assumption - that only the three staggered rotamers are occupied for any length of time - is valid.

As the C-1/C-2 conformational analyses were quantitative, the results, unlike those from the remaining qualitative observations, are liable to close scrutiny. By the nature of the determinant method, however, it is difficult to judge the likely errors in the final rotamer figures, especially after the "para adjustment" made to the ortho derivatives (see TABLE 4-8.9). The observed couplings should be accurate to $\pm$0.05Hz whilst the errors in the calculated couplings should be within $\pm$1.0Hz. Overall the expected errors in the rotamer predictions should be within $\pm$10% with the proviso that if significant errors are present the relative rotamer differences between the various derivatives should not change unduly.

In Chapter 5 the rotational optimisation approach to conformational analysis by LIS was introduced and developed. In Chapter 6 this method was applied to the analysis of the LIS data of the Type (IV) alcohols using the program METFIND VII.

Two LSR's were used : firstly Eu(fod-d_9)$_3$, to establish conformational homogeneity in the substrate during addition of the LSR (the low broadening of Eu(III) allowed successful monitoring of the various coupling constants) - secondly Yb(fod-d_9)$_3$, as this has very low CS/CFS contamination and is therefor the ideal shift reagent for conformational studies.

The general rot/opt method is subject to several limitations :

(1) the accuracy of the molecular coordinate and LIS data. For the simple molecules studied, standard bond lengths and angles should generate coordinates accurate to within $\pm$0.03Å relative to the binding site (ie. errors in Ln-X radii within 3%). Potential measurement errors in the LIS data were, however, more serious (see TABLE 6-3.6). Although some ^{13}C LIS were

potentially subject to large errors (due to digitisation rate and solubility limitations on LSR concentration - see SECTION 6-3-2), 76% of the data had max. errors $<\pm 5\%$ with the average max. error of the remainder rising to ~15%.

(2) the size of the data set. The accuracy of the general method is good with large data sets but progressively diminishes as the data set decreases. (NB. With very small data sets, eg. 3-4 atoms, excellent but generally meaningless fits are obtained!). In particular the accuracy of a rot/opt step is very dependent on the number of shifted groups being optimised. This limitation was particularly felt in this study as only one atom (H-108) was available for rot/opt of the C-1/C-2 bond.

(3) the ease with which a search or rot/opt may concentrate on a false or secondary maximum metal position. This is well illustrated in FIGS.6-5.1 & 6-5.2 and demonstrates that the utmost care is required to ensure that a rot/opt search produces sensible results. The problem of secondary maxima is mainly a function of the small FIXED ATOM data set available for the Type (IV) alcohols.

(4) interpretation of the result obtained. The method is analogous to X-ray crystallography in that the final result only indicates one molecular conformation. The METFIND rot/opt technique differs, however, in the ability to compare the maximum rot/opt position obtained with all the other orientations examined, to (a) determine the significance of the "max" result over free-rotation and (b) to evaluate contributions of other rotamers to the overall state in solution. As was seen in SECTION 6-7 the interpretation of these results is rather intuitive which unfortunately reduces their usefulness and reliability.

In summary, the METFIND VII rot/opt method is basically sound as the only assumptions it requires are now accepted throughout the literature (eg. the alignment of the lanthanide's principal symmetry axis, etc.), or demonstrable before performing an optimisation (eg. substrate conformational homogeneity before and after adding LSR) (see SECTIONS 1-6-4.1 & 5-1). The method is, however, not completely straightforward to apply, as the rot/opt process is both complex and fraught with potential pitfalls, with considerable care essential in the interpretation of the results.

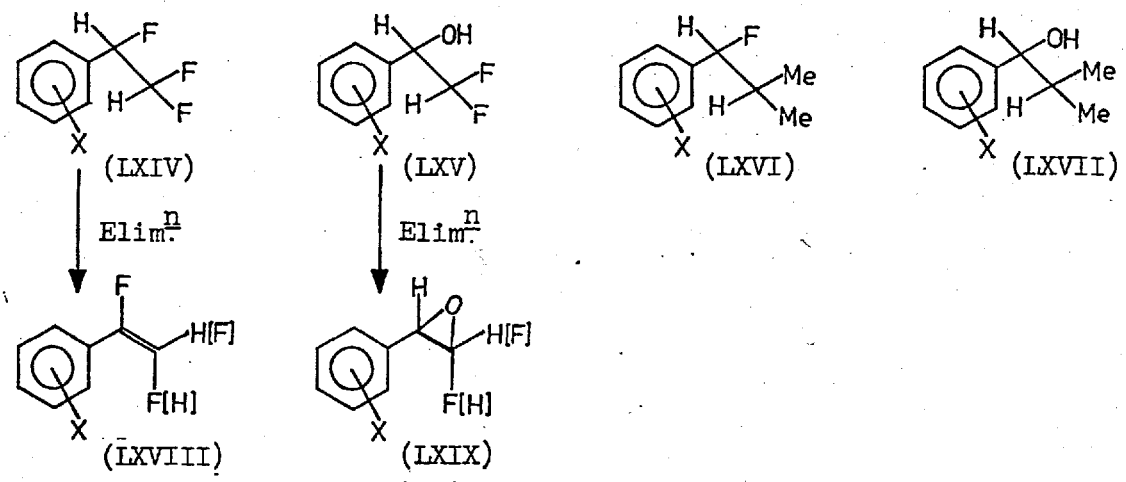
The system studied (the Type (IV) alcohols) was not ideally suited to the rot/opt process, due to (a) the overall number of shifted atoms in the molecules and (b) the presence of only one nmr active atom in the key rotating species. Nevertheless useful results were obtained which both supported the conventional conformational analyses of Chapter 4 and supplied additional information on the orientation of the phenyl ring substituents to the side-chain (see SECTION 6-7).

8-4 Areas for Further Work

Several areas should be considered for further work :

The conformational predictions made for the Type (IV) & (V) series remain substantially unconfirmed in the absence of appropriate reaction conditions for the proportionate conversion of the starting material rotamers to the product isomers. Further work may well establish suitable conditions (ie. favouring an E2 mechanism) at least for the Type (V) fluoride, and possibly for the Type (IV) alcohol eliminations.

Further studies on conformational analysis in related systems, using both the conventional nmr and LIS techniques would also be interesting. The main limitation of the Type (IV) & (V) series (ie. only one nmr-active species on C-2) could be overcome by examining compounds of the general type (LXIV-LXVII).



Compounds (LXIV) & (LXV) would be of interest from both their nmr and chemical properties. These compounds would all be useful in demonstrating the the diastereotopic nature of the paired groups on the prochiral centre and should all possess ortho derivative dependent side chain conformations.

The steric control of side-chain reactions, exercised by ortho ring substituents, could be exploitable in stereoselective/stereospecific organic syntheses, where selection of the appropriate ring substituent could be used to predetermine the isomer ratio of a reaction intermediate.

APPENDICES

APPENDIX I : GRAPHICAL METHODS FOR SPECTRAL ANALYSIS

During the course of the theoretical work on the ABX-spin system, graphical aids were found to be essential tools for understanding the movements of the spectral lines under various conditions; the most illustrative of these have been reproduced in Chapter 3 (see FIGS.3-2.5 to 3-2.12). A natural extension to this work included attempts to perform spectral analysis graphically. Applying Abraham's method of sub-spectral analysis[242] to the AB-region of ABX spectra involves the individual treatment of the two apparent AB-quartets to obtain δ^*_{AB} values (see EQNS 32 & 54), and so FIG.I-1 which is a plot of δ_{AB} against $Sep^n(A_{HF} - B_{LF})$ was produced. (Throughout the graphs in this section and in Chapter 3 δ_{AB}, J_{AX}, J_{BX} L and N are scaled in units of J_{AB} as this removes one spectral variable and makes the plots universally useful instead of applying in only one instance).

Using FIG.3-1.1, if we define $\delta = A_{HF} - B_{LF}$; then $\delta_{AB} = \sqrt{\delta(\delta + 2)}$. FIG.I-1 is therefore a plot of δ_{AB} against δ with the 1st order approximation $\delta_{AB} = \delta + 1$ also plotted for comparison.

When drawing the 24 AB-regions in FIGS.3-2.5 & 3-2.6 it was necessary to solve a total of 20 AB-spectra in reverse, ie. given δ_{AB}, to calculate the line separations and intensities. Again a graphical route was chosen to calculate intensities (see EQN.33). From TABLE 3-2.3 the total intensity of any pair of AB-region lines, ie. $A_\alpha(8\text{-}6)$ or $B_\beta(3\text{-}1)$, is 2 (the $\sin\phi_+$ terms cancel). This was taken as "UNIT INTENSITY" and the heights of the "inner" and "outer" quartet lines were calculated as fractions of this from the following relationship :

From EQN.33 $\quad [\text{outer}] \,/\, [\text{inner}] = \delta/(\delta + 2)$

$$[\text{outer}] + [\text{inner}] = 1$$

$$\therefore\ [\text{outer}] = 1 - \frac{1}{(\delta/(\delta + 2)) + 1}$$

$$= 1 - \frac{1}{(2\delta + 2)/(\delta + 2)}$$

$$\underline{[\text{outer}] = \frac{\delta}{(2\delta + 2)}} \quad \text{and} \quad \underline{[\text{inner}] = \frac{(\delta + 2)}{(2\delta + 2)}}$$

In FIG.I-2 [outer] is plotted against δ_{AB}. Note that [outer] has still not attained the true 1st order value of 0.5 even at $\delta_{AB} = 20J_{AB}$, so in the minimum AX case of $\delta_{AB} = 10J_{AB}$ there is still a 10% distortion of the quartet in intensity terms (ie. [45] : [55]), but the actual distortion of the midpoints of the doublets is less, at approximately 5% (J_{AB}).

Using FIGS.I-1 & I-2 any AB-spectrum (or sub-spectrum) may be rapidly analysed, and conversely, given δ_{AB}, the appearance of an AB-region can be rapidly predicted.

When referring to the distortion of an AB-quartet, an analogy that is often made is that the true positions of A and B (ν_A and ν_B) are at the "centres of gravity" of the doublets from A and B. This is only approximately true (see FIG.I-2). Using this argument, if the ratio of the peak intensities is A : B (where A+B = 1) then the centre of gravity of the pair of lines will be distance A from the foot of peak B. Therefore the plot of [outer] against δ_{AB} (FIG.I-2) shows the movement of the "centre of gravity" of the quartet. The true offset of ν_A from A_{HF} (the more intense line) may be found from FIG.I-1 using : Offset = $\frac{1}{2}(\delta_{AB} - \delta)$. This produces the lower plot shown in FIG.I-2 which has a significantly different course from the "centre of gravity" line. The "error" between the two lines is plotted on the left and reaches a maximum value of $0.15J_{AB}$ when $\delta_{AB} = 0.75J_{AB}$.

Unfortunately, ABX spectra have too many variables for their complete analysis to be attempted in one or two graphs; for even after removing the influence of J_{AB} one is still left with δ_{AB}, L and N which would have to be plotted simultaneously (ie. in families of curves, etc.) to obtain line positions, intensities or assignments. However, once the basic mechanism of formation of an ABX spectrum has been visualised (see FIGS.3-2.5; 3-2.6; 3-2.8) the line assignment process becomes fairly straightforward and further "aids" to assignment would probably be more complicated to decipher than the spectrum itself. Also, once one assignment has been chosen as correct, its subsequent analysis is relatively straightforward, and if Abraham's sub-spectral method is used[242] the AB-analyses may be performed graphically (see above).

The key area, therefore, in which graphical methods are useful, is in determining which assignment is correct. The only difficulty - that for each assignment there were two possible solutions for [14,15] (see FIGS.3-2.9 to 3-2.11) - was eventually resolved empirically and this enabled a graphical route to the calculation of [14,15] to be developed (see FIG.3-2.13 and the relevant text in SECTION 3-2-4.1). FIG.I-3 is a more accurate version of FIG.3-2.13 and should be used in conjunction with the method given in SECTION 3-2-4.1 to calculate [14,15] from the basic parameters $|J_{AB}/2D_{\pm}|$ via $\Delta_{\pm}$.

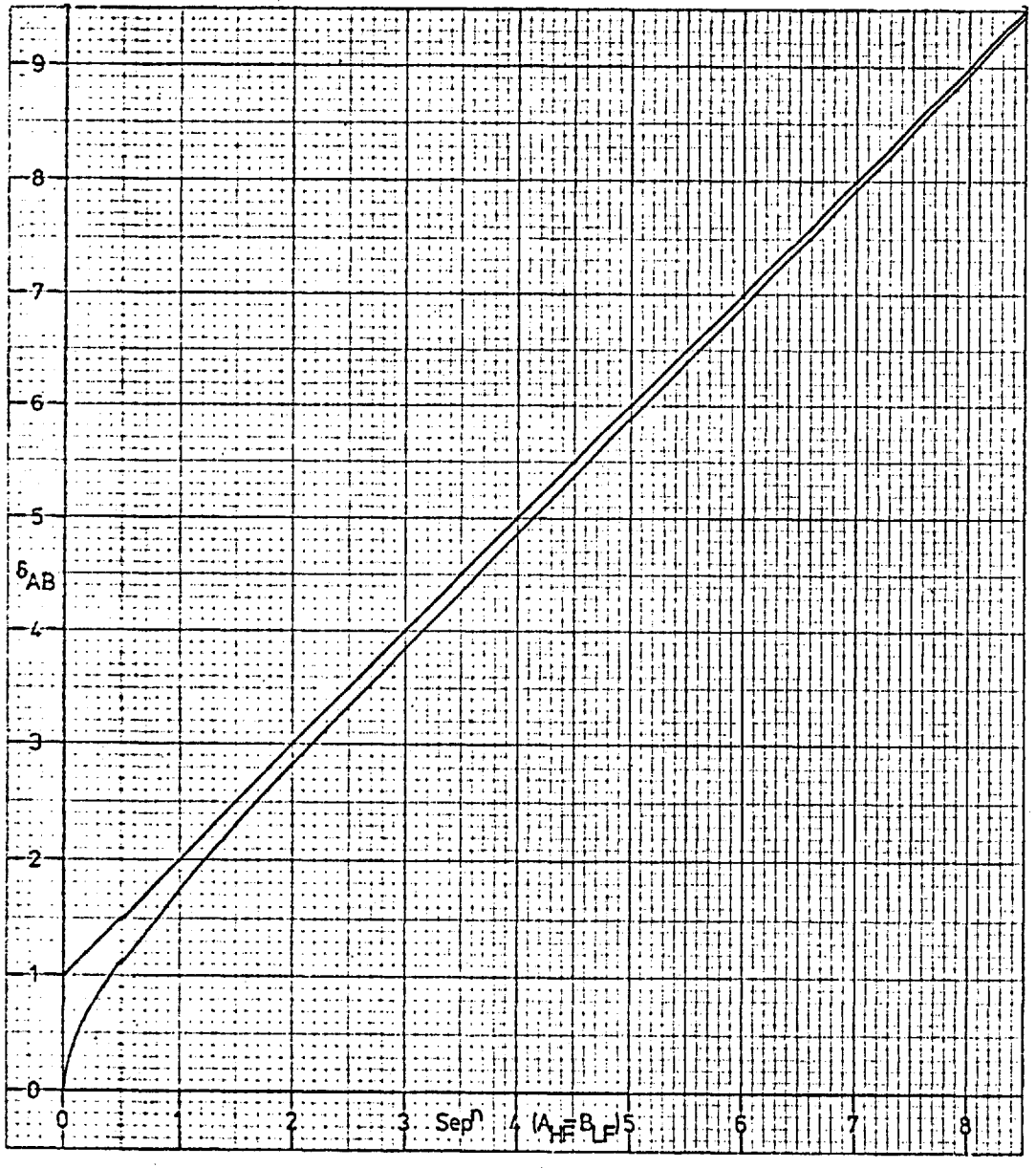


FIG.I-1 Plot of δ_{AB} vs δ (A_{HF} - B_{LF})

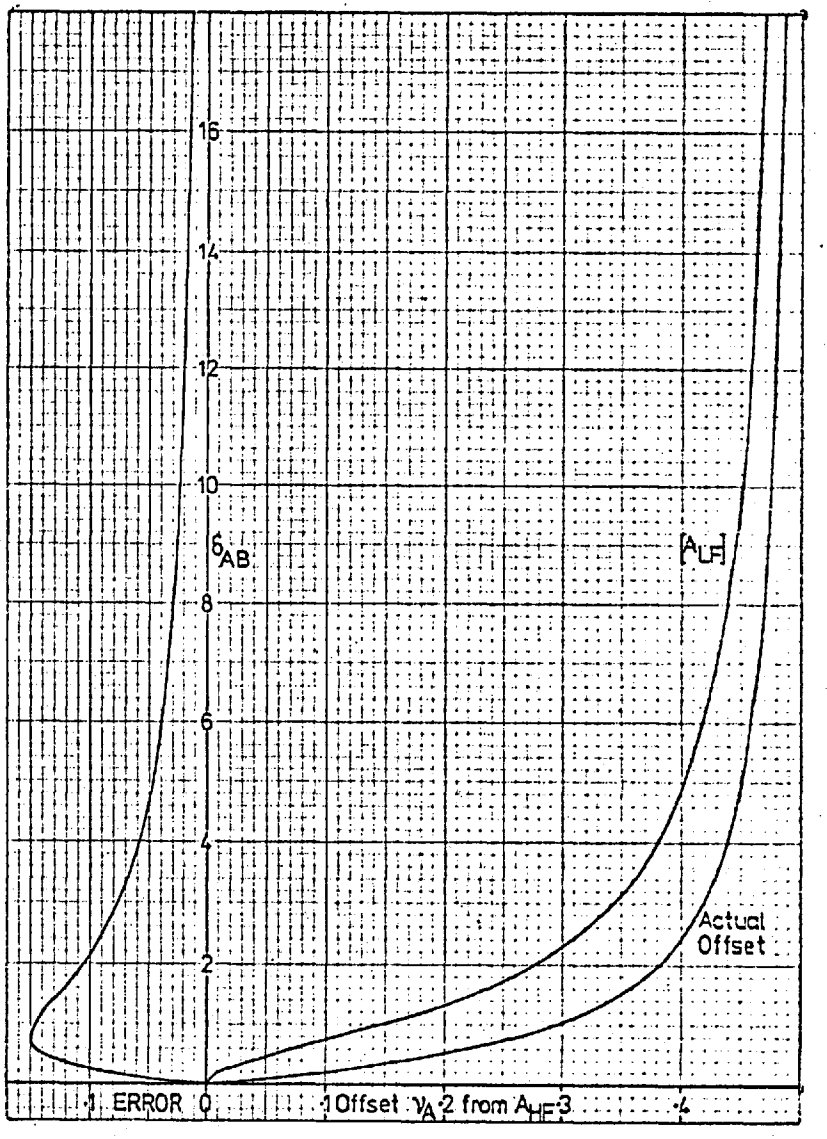


FIG.I-2 A Comparison of the Distortions seen in AB-Quartets in the Chemical Shifts and Intensities of the signals showing that these are not directly related.

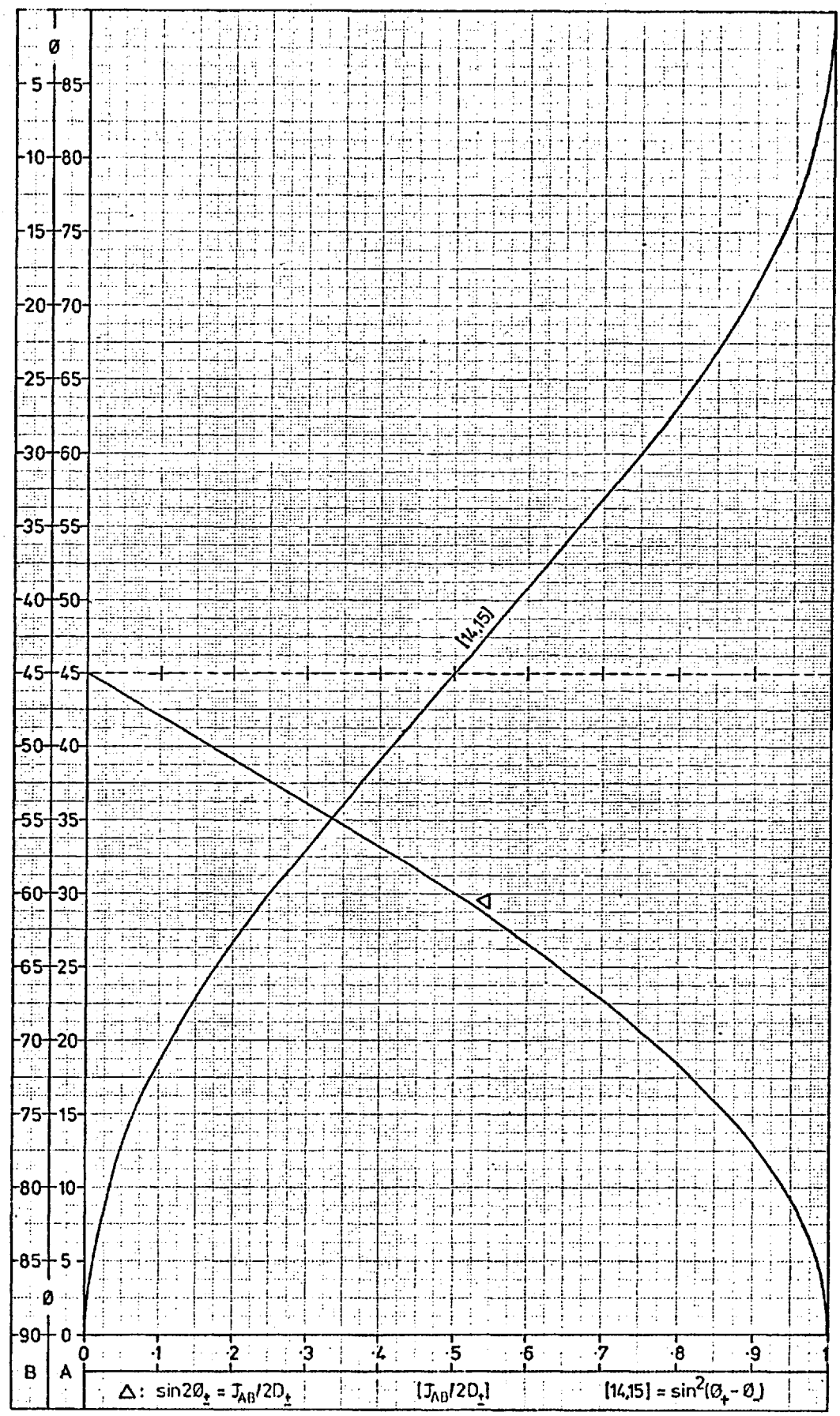


FIG.I-3 A Ready Reckoner for Calculating [14,15]. For details of method of use see SECTION 3-2-4.1

APPENDIX II : ABX ANALYSIS - CONDITIONS UNDER WHICH [14,15] > [10,11]

From FIG.3-2.11 it can be seen that for $\delta_{AB} > L$, $[14,15] < [10,11]$. For part of the range $\delta_{AB} < L$, $[14,15] > [10,11]$, but the lower limit of this condition requires quantifying.

From TABLE 3-2.3 : $[14,15] = \sin^2(\phi_+ - \phi_-)$

$[10,11] = \cos^2(\phi_+ - \phi_-)$

Since : $\sin^2 A + \cos^2 A = 1$; this occurs when $\sin^2(\phi_+ - \phi_-) > 0.5$.

ϕ_+ and ϕ_- are defined in EQNS.35-37 : $D_{\pm}\cos 2\phi_{\pm} = \frac{1}{2}\delta_{AB} \pm \frac{1}{2}L$ (1)

$D_{\pm}\sin 2\phi_{\pm} = \frac{1}{2}J_{AB}$ (2)

Dividing (2) by (1) we obtain : $\tan 2\phi_+ = J_{AB}/(\delta_{AB} + L)$ (3)

$\tan 2\phi_- = J_{AB}/(\delta_{AB} - L)$ (4)

Applying the standard relation : $\tan(A - B) = (\tan A - \tan B)/(1 + \tan A.\tan B)$

we obtain : $\tan 2(\phi_+ - \phi_-) = (2L.J_{AB})/(L^2 - \delta_{AB}^2 - J_{AB}^2)$ (5)

Let $\delta_{AB} = \sqrt{(n-1)}.J_{AB}$ ie. $n = (\delta_{AB}/J_{AB})^2 + 1$ (6)

then (5) reduces to : $\tan 2(\phi_+ - \phi_-) = (2L.J_{AB})/(L^2 - nJ_{AB}^2)$ (7)

Substituting for tanA as sinA/cosA and squaring, we obtain :

$\sin^2 2(\phi_+ - \phi_-)/\cos^2 2(\phi_+ - \phi_-) = (4L^2.J_{AB}^2)/(L^2 - nJ_{AB}^2)^2$ (8)

but $\sin^2 A = 1 - \cos^2 A$; substituting in (8) and expanding, we obtain :

$\cos^2 2(\phi_+ - \phi_-).((L^2 - nJ_{AB}^2)^2 + 4L^2.J_{AB}^2) = (L^2 - nJ_{AB}^2)^2$ (9)

$\therefore \cos 2(\phi_+ - \phi_-) = (L^2 - nJ_{AB}^2)/((L^2 - nJ_{AB}^2)^2 + 4L^2.J_{AB}^2)^{\frac{1}{2}}$ (10)

but $\cos 2A = 1 - 2\sin^2 A$; $\cos 2(\phi_+ - \phi_-) = 1 - 2\sin^2(\phi_+ - \phi_-)$.

Since we want to know when $\sin^2(\phi_+ - \phi_-) > 0.5$ we may find this by evaluating the conditions under which $\cos 2(\phi_+ - \phi_-) < 0.0$.

This occurs when $L^2 - nJ_{AB}^2 < 0$; ie. when $nJ_{AB}^2 > L^2$

$\therefore$ Lines 14 and 15 are more intense than lines 10 and 11 when $J_{AB} > L/\sqrt{n}$

Substituting (6) for n, this occurs when $(\delta_{AB}^2 + J_{AB}^2) > L^2$

With the lower limit of the intensity relation quantified we may now write the full relation as :

$[14,15] > [10,11]$ when $L > \delta_{AB} > \sqrt{(L^2 - J_{AB}^2)}$

APPENDIX III : Optimisation of Metal Reflection

For the two metal positions M and M_R, the individual calculated shifts/broadenings for each group have percentage differences D and D_R from the observed data. To calculate the optimum proportions of M and M_R it is necessary to find the minimum RMS error of a linear combination of M and M_R given by : $(x.M + (1 - x).M_R)$

$\therefore$ Wish to find the minimum value of : $\Sigma(x.D + (1 - x).D_R)^2$

Expanding $= \Sigma(x^2D^2 + D_R^2 + x^2D_R^2 + 2x.DD_R - 2x^2DD_R - 2x.D_R^2)$

$= x^2.\Sigma(D^2 + D_R^2 - 2DD_R) + x.\Sigma(2DD_R - 2D_R^2) - \Sigma D_R^2$

For a minimum value $\frac{d}{dx} = 0$ and $\frac{d^2}{dx^2} = +ve$.

$\therefore$ a minimum occurs when $x.\Sigma(D^2 + D_R^2 - 2DD_R) + \Sigma(DD_R - D_R^2) = 0$

ie. when $\underline{x = \Sigma((D_R^2 - DD_R)/(D^2 + D_R^2 - 2DD_R))}$

AND $\underline{\Sigma(D^2 + D_R^2 - 2DD_R) > 0}$

Threrfore, in order to find the optimum value of x, only the cumulative values of ΣD^2, ΣD_R^2 and ΣDD_R need to be stored (ie. 3 extra variables). Unfortunately, if the individual errors between the weighted calculated shifts/broadenings and the observed data are required, the individual values of D and D_R also need to be stored (ie. 2 x NGROUP variables).

The following series of operations would be required to optimise the distribution between the two metal positions :

(1) Check that : $\Sigma(D^2 + D_R^2 - 2DD_R) > 0$.

If this is the case then proceed to (2). If no, then a minimum value cannot arise from a linear combination of M and M_R and the optimum position will therefore be the one with the lower overall error (ΣD or ΣD_R).

(2) Calculate x from the equation deduced above

(3) Check that $0 < x < 1$. If this is not the case proceed as in (1). If this test is passed, then the overall RMS error is given by :

$$\sqrt{\frac{\Sigma(x.D + (1 - x).D_R)^2}{n - 1}}$$

This is comparable with the standard equation : $\sqrt{\frac{\Sigma D^2}{n-1}}$

This process may be equally well applied in determining the relative metal site preferences with two (or more) binding sites.

APPENDIX IV : METFIND VII (MET7IND)

IV-1 Input Data Decks

An example of a typical data deck is given below. This was used for the initial "FIXED ATOM" MULTISCAN search of the Yb-LIS data of oF(IV). The supplementary decks show how the first deck was modified for (a) normalisation on C-1 (607), and (b) a full ROTATE run :

```
TITLE(          *X = ORTHO F   TYPE(IV) ALCOHOL  ROT2/OR2*          ) ORTHO F
NATOM(05/13),NCENTR(11),SBOPT(1),NSIGN(3),NORM(1),ROTN(0            )ORTHO F
ITER(7),REFLEC(3),LIM(2),TEST(0),BONGLE(000),CONTUR(1),OMITA(0),OMITC(0)ORTHO F
FITLIM1(0.500),FITLIM2(0.500),FITLIM3(0.500),TYPLIM(0.500)          ORTHO F
 107/1/01  1.8433333 0.5138310 0.8899812 02/  /  /      111111111111111 ORTHO F
 607/1/02  1.48      0.0       0.0       01/03/05/16   112211122222221 ORTHO F
 608/1/03  1.9933329 0.7259630-1.2574047 02/06/17/18   112211122222221 ORTHO F
 604/1/04  2.9200001-4.0729350 0.0       08/09/13/     111112244444412 ORTHO F
 601/1/03  1.9866667-1.4330697 0.0       02/07/10/     111112244444412 ORTHO F
 108/1/06  1.6333333 1.7441967-1.2574047 03/  /  /      13311133333331 ORTHO F
 602/1/07  2.7915477-1.8909534 1.05      05/08/11/        13355555513 ORTHO F
 603/1/08  3.2582144-3.2108960 1.05      04/07/12/        13355555513 ORTHO F
 605/1/09  2.1151192-3.6150413 1.05      04/10/14/        13355555513 ORTHO F
 606/1/10  1.6484524-2.2951087-1.05      05/09/15/        13355555513 ORTHO F
 902/1/11  3.1056038-1.0904987 2.025     07/  /  /        13355555513 ORTHO F
 103/1/12  3.8791226-3.5641283 1.86      08/  /  /        13355555513 ORTHO F
 104/1/13  3.2800002-5.0911688 0.0       04/  /  /        13355555513 ORTHO F
 105/1/13  1.8542110-4.2800428-1.86      09/  /  /        13355555513 ORTHO F
 106/1/15  1.0275443-1.9418764-1.86      10/  /  /        13355555513 ORTHO F
 800/1/16  0.0       0.0       0.0       02/  /  /           111111111 ORTHO F
1708/1/17  1.4066667-0.1037092-2.6944387 03/  /  /      13311133333331 ORTHO F
1708/1/18  3.7533332 0.7259631-1.2574047 03/  /  /      13311133333331 ORTHO F
NGROUP( 1),SHIFT( 623.8)                                               ORTHO F
NGROUP( 2),SHIFT(1000.0)                                               ORTHO F
NGROUP( 3),SHIFT( 512.7)                                               ORTHO F
NGROUP( 4),SHIFT( 110.0)                                               ORTHO F
NGROUP( 5),SHIFT( 589.7)                                               ORTHO F
NGROUP( 6),SHIFT( 363.1)                                               ORTHO F
NGROUP( 7),SHIFT( 284.8)                                               ORTHO F
NGROUP( 8),SHIFT( 141.6)                                               ORTHO F
NGROUP( 9),SHIFT( 142.4)                                               ORTHO F
NGROUP(10),SHIFT( 337.0)                                               ORTHO F
NGROUP(11),SHIFT( 218.4)                                               ORTHO F
SEARCH RADIUS FROM (150) to (190) IN STEPS OF (10)                     ORTHO F
SEARCH ANGLE PHI FROM (-90) TO (135) IN STEPS OF ( 5) DEGREES          ORTHO F
SEARCH ANGLE PSI FROM ( 90) TO (135) IN STEPS OF ( 5) DEGREES          ORTHO F

(a)
 607/1/01  1.48      0.0       0.0       02/03/05/16   112211122222221 ORTHO F
 107/1/02  1.8433333 0.5138310 0.8899812 01/  /  /      111111111111111 ORTHO F
[608/1/03  1.9933329 0.7259630-1.2574047 01/06/17/18   112211122222221 ORTHO F
 601/1/05  1.9866667-1.4330697 0.0       01/07/10/     111112244444412 ORTHO F
 800/1/16  0.0       0.0       0.0       01/  /  /        111111111111 ORTHO F]
NGROUP( 1),SHIFT(1000.0)                                               ORTHO F
NGROUP( 2),SHIFT( 623.8)                                               ORTHO F
```

Changing the cards in parentheses is optional (see next section)

(b)

```
NATOM(11/07),NCENTR(11),SBOPT(1);NSIGN(3),NORM(1),ROTN(31264264344545877)ORTHO F
SEARCH RADIUS FROM (250) TO (290) IN STEPS OF (10)                      ORTHO F
SEARCH ANGLE PHI FROM (135) TO (180) IN STEPS OF ( 5) DEGREES           ORTHO F
SEARCH ANGLE PSI FROM (180) TO (225) IN STEPS OF ( 5) DEGREES           ORTHO F
```

The input formats to METFIND VII are annotated, where possible, as this allows easy interpretation of punched decks and ensures correct formatting. Example (b) illustrates the ease with which the type of run can be modified without changing the basic COORD and SHIFT data cards.

IV-2 Card Formats and Brief Descriptions of the Various Parameters and Options

METFIND VII has ten different data cards :

CARDS 1, 2, 3, 4, 7, 8 and 9 only appear once in any data deck.

CARDS 5 and 6 are repeated and form the COORD and SHIFT DATA BLOCKS.

CARD 10 is optional and may be repeated. The full 80 characters are used.

All entries must be numerical apart from the TITLE on CARD 1 and the IDENTIFICATION NAME marked 'nnaa' on CARD 5.

CARD 1 ... REFERENCE INFORMATION

```
TITLE(          *                                        *          ) DATA 001
```

This may contain any alphanumeric name up to 64 characters.

CARD 2 ... OBLIGATORY DATA

```
NATOM(  /  ),NCENTR(  ),SBOPT( ),NSIGN( ),NORM( ),ROTN(                )DATA 002
```

NATOM = The two numbers indicate the total number of SHIFTED/BROADENED ATOMS and NMR INACTIVE ATOMS for which data is given in the COORD DATA BLOCK. As this contains ONE CARD PER ATOM the sum of these numbers must equal the number of cards in the BLOCK (maximum value = 100).

NCENTR = The total number of SHIFTED/BROADENED GROUPS with an entry in the SHIFT DATA BLOCK. The same constraints apply as with NATOM.

SBOPT = SHIFT/BROADENING OPTION. This informs the program what data is to be read from the SHIFT DATA BLOCK. SBOPT can have only three values: (1) = shift data only; (2) = shift and broadening data; (3) broadening data only

NSIGN = The sign of the SHIFT of the normalising (first) GROUP. Again this can have three values : (1) negative; (2) unknown; (3) positive. This is used to check that the sign of the first shift calculated is correct, and can obviously save considerable wasted computer time.

NORM = The number of SHIFTED/BROADENED ATOMS in the first GROUP.

ROTN = ROTATION OPTION. The first digit (ROTOPT) determines whether rotation is required and at which rotational increment (see TABLE IV-2.1) The remaining 15 digits are the NCYCOP parameters for each of the 15 CYCLES (see TABLE 5-4.1). Each time NCYCOP = 5 is used the

rotational increment is decreased together with the R, PHI and PSI increments to effect a degree of FOCUSING.

TABLE IV-2.1 Rotational Increments for NCYCOP = 3/5 as Determined by ROTOPT

ROTOPT	NCYCOP			ROTOPT	NCYCOP		
	3	(1st) 5	(2nd)		3	(1st) 5	(2nd)
1	1	1	1	6*	20	10	5
2	2	1	1	7	30	15	5
3*	5	2	1	8	45	20	10
4*	10	5	2	9	60	30	15
5*	15	5	2	0	ROTATION OPTION NOT SELECTED		

* Indicates the normal range of ROTOPT.

CARD 3 ... OPTION SELECTION INFORMATION

ITER( ),REFLEC( ),LIM( ),TEST( ),BONGLE( ),CONTUR( ),OMITA( ),OMITC( ),DATA 003

ITER = ITERATION OPTION. This may have ten values (see SECTION 5-2-7) :

When = 0 ... NON-ITERATIVE MODE. Searches one block using the input SEARCH DATA.

When = 1 ... FOCUSING MODE. Performs an iterative search.

When = 2-9 ... MULTISCAN MODE. Performs (ITER - 1) MULTISCANS (see FIG.5-2.5)

REFLEC = REFLECTION/ROTATION/SYMMETRY OPTION. This may have ten values and informs the program whether XY- or XZ- plane METAL REFLECTION and/or METHYL GROUP ROTATION are required (see SECTIONS 5-2-5 & 5-2-6) and also whether SYMMETRY will be present in the FITFACTOR TABLES (this can arise from either molecular symmetry or the use of METAL REFLECTION). If SYMMETRY is present, half of the search blocks normally performed in the MULTISCAN MODE are suppressed. There is NO EFFECT on the output of the NON-ITERATIVE or FOCUSING MODES. For XZ-SYMMETRY blocks 9-16 are omitted, for XY-SYMMETRY blocks 3,4,7,8 11,12,15 and 16 are omitted (see FIG.5-2.5d - NB. XY-SYMMETRY corresponds to PSI = 180, XZ-SYMMETRY to PHI = 180).

TABLE IV-2.2 REFLEC OPTION

REFLEC	REFN	ROTN	SYMM	REFLEC	REFN	ROTN	SYMM
0	none	none	none	5	XZ	ROTN	XZ
1	XY	none	XZ	6	none	none	XY
2	XZ	none	XZ	7	none	none	XZ
3	none	ROTN	none	8	none	ROTN	XY
4	XY	ROTN	XY	9	none	ROTN	XZ

LIM = LIMIT OPTION. This is used to control the TOLERANCE TESTS in METFIND (see SECTION 5-2.4) and may have three values :

When = 0 ... Preset values for FITLIM(1,2,3) and TYPLIM of 0.9, 0.97, 0.985 and 0.994 are selected. CARD 4 is not read but must be present.

When = 1 or 2 ... The values of FITLIM(1,2,3) and TYPLIM are read from CARD 4.

When = 0 or 1 ... After completing the last FITFACTOR TABLE (when ITER = 0 or 1) a detailed listing of the SOLUTIONS whose FITFACTORS exceed TYPLIM will be given (WRITEB output).

When = 2 ... Only the SOLUTION to the MAXIMUM FITFACTOR will be given, REGARDLESS OF WHETHER IT EXCEEDS TYPLIM. If there are several identical maxima the SOLUTION to the average position will be given.

TEST = TEST OPTION. This is mainly used for diagnosis of input data errors and may have six values :

When = 0 ... NO TESTING is performed. This is the normal running condition.

When = 1 ... The input COORD data is TESTED by (a) calculating every interatomic distance, and (b) calculating bond angles specified by the BONGLE OPTION. This test is routinely performed when NCYCOP = 4 in ROTATION MODE runs.

When = 2 or 3 ... These options are intended for use when the input data gives absolutely no results or when line assignments require checking.

When = 2 ... This cancels all TOLERANCE TESTS and automatically gives WRITEB output for each search point. Output is usually stopped by line- or time-limits so the values of RMIN, PHIMIN and PSIMIN should be set to the most likely metal position. The aim is to find which ATOMS/GROUPS have SHIFTS/BROADS which consistently fail TOL TESTS.

When = 3 ... This is a desperation measure only used if TESTS 1 & 2 are insufficient. It produces a listing of every calculation performed in each search and shows at which point a test was failed. Details of the DIAGNOSTICS given by TESTS 1, 3 & 4 are given in the next section.

When = 4 or 5 ... These are designed for use when <u>only</u> SHIFT(TEST = 4) or BROAD(TEST = 5) data is submitted and it is desired to know the other. This only affects WRITEB output (if present).

BONGLE = BOND ANGLE TEST OPTION. For use with TEST = 1 or in the ROTATION MODE.

When = n (max value 50) ... The 'n' bond angles described in the CARD 10 BLOCK are calculated. To find the angle between AB and BC the SEQUENCE NUMBERS of the three ATOMS A, B and C are listed on CARD 10.

CONTUR = CONTOURING OPTION. When set to 1 the initial INPUT DATA and all the FITFACTOR DATA from a full MULTISCAN search are written onto a file (TAPE9) for subsequent handling by a contour plotting package.

OMITA = OMIT WRITEA OPTION. When = 1 WRITEA output is suppressed.

OMITC = OMIT WRITEC OPTION. This works in a similar manner to OMITA :

When = 0 ... All WRITEC output (FITFACTOR TABLES) will be printed.

When = 1-8 ... The first 1-8 ITERATIONS of WRITEC output will be suppressed provided that the max. FITFACTOR of an ITER=1,RUN=3 search is not within the edge of the search (ie. FOCUSING has been completed) or that an ITER=0 search is being performed. This ensures that the last WRITEC table will always be printed before any WRITEB output.

When = 9 ... All WRITEC output will be suppressed with the exception of any message informing the user that the table would have been suppressed anyway due to nil or duplicated results. This option is designed for use with the CONTUR option.

CARD 4 ... OPTIONAL INFORMATION (LIM)

FITLIM1(.),FITLIM2(.),FITLIM3(.),TYPLIM(.) DATA 004

This card is only read if LIM = 1 or 2, but should always be present.

FITLIM(1,2,3) = FITFACTOR LIMITS for RUNS (1,2,3)(see SECTION 5-2.4). When ITER ≠ 1, METFIND always operates under RUN = 1 (FITLIM1) conditions.

TYPLIM = TYPE (WRITEB) LIMIT. Only used when LIM = 1 whereupon WRITEB output will only be produced for those SOLUTIONS whose FITFACTOR > TYPLIM.

CARD 5 ... COORD DATA BLOCK

nnaa/c/dd xx.xxxxxxyy.yyyyyyyzz.zzzzzzz b1/b2/b3/b4 gggggggggggggg DATA 005

This card has no pre-punched structure as it may be supplied as output from either of the programs COORD or XYZFG whereupon 'nn' will contain the atom's ATOMIC NUMBER and 'xyz its COORDINATES. There will be ONE CARD PER ATOM. The ordering of these cards is crucial, as are the numbers 'c' and 'dd'.

nnaa = ATOM IDENTIFICATION NAME. This may consist of any alphanumeric string.

c = NUMAV. The number of ATOMS in the same GROUP as this ATOM. All of the ATOMS in a GROUP MUST APPEAR TOGETHER in the data block although their sequence is unimportant.

dd = GROUP IDENTIFICATION NUMBER. These numbers must appear sequentially within the data block, starting from dd = 1. All ATOMS in the same GROUP MUST HAVE THE SAME dd NUMBER.

xyz = The ATOM'S COORDINATE DATA.

b(1-4) = The SEQUENCE NUMBERS of the ATOMS to which this atom is BONDED.

g = The GYROCODE NUMBER for the 15 ROTATION MODE CYCLES.

Both b(1-4) and g are only used in the ROTATION MODE. Incorrect values of b(1-4) will not affect the running of METFIND as they are included only for molecular structure drawing in the contouring package, and for bond labelling (*) in the INTER-ATOMIS DISTANCE Tables.

CARD 6... SHIFT/BROADENING DATA BLOCK

NGROUP( ),SHIFT(.),BROAD(.) DATA 006

This block contained ONE CARD PER SHIFTED/BROADENED GROUP (NB. Single ATOMS class as GROUPS for this purpose).

NGROUP = GROUP IDENTIFICATION NUMBER. This should correspond to 'dd' in the COORD DATA BLOCK (Other numbers, such as 'aa' may be placed here if convenient. If the value of NGROUP differs from 'dd' the warning "QUERY" is printed in the WRITEA output).

SHIFT = The OBSERVED SHIFT of the GROUP on adding LSR.

BROAD = The OBSERVED BROADENING of the GROUP on adding LSR.

SHIFT and BROAD may be presented in any convenient self-consistent units.

CARDS 7, 8 and 9 ... SEARCH PARAMETERS

SEARCH RADIUS FROM ( ) TO ( ) IN STEPS OF ( ) DATA 007

SEARCH ANGLE PHI FROM ( ) TO ( ) IN STEPS OF ( ) DEGREES DATA 008

SEARCH ANGLE PSI FROM ( ) TO ( ) IN STEPS OF ( ) DEGREES DATA 009

These cards are self-explanatory. All entries should be integers, the RADIUS parameters being divided by 100 in the program (ie. 372 = 3.72Å). The angles PHI and PSI should lie between 90 and 270°.

CARD 10 ... OPTIONAL DATA TESTING INFORMATION (BONGLE)

/ / , / / , / / , / / , / / , / / , / / , / / , / /

This card has been treated under the heading BONGLE = n.

IV-3 Output

METFIND VII has four WRITE routines which serve the following functions :

WRITEA : This outputs all the input data in an ordered fashion so that identification of the run and checking of data/options can be performed. Typical WRITEA printout is shown on p.276 (for the data given on p.270. Also illustrated are messages given when (1) the ROTATION MODE and (2) the CONTUR option are selected.

WRITEB : This outputs the detailed SOLUTIONS to individual search points, examples of which can be seen on p.279 & 280.

WRITEC : This produces the FITFACTOR TABLES and associated messages - see p.277

WRITED : This is only used in the ROTATION MODE and is responsible for most of the output reproduced on p.278-9. This is discussed in SECTION 6-5-2.

Additional output is produced by subroutine DATEST (the INTER-ATOMIC DISTANCE and BOND ANGLE TABLES - see p.278 & 280) and by the TEST = 3 option in subroutine DONEST - see p.280.

```
NOMETFINOMETFINOMETFINOMETFINOMETFINOMETFINOMETFINOMETFINOMETFINOMETFINOMETFINOMET
OMETFINOMETFINOMETFINOMETFINOMETFINOMETFINOMETFINOMETFINOMETFINOMETFINOMETFINOMETF
ME  INO   TF     TF     FI     FI     TF   OME   IN     INOMETFI   MET   NO    IN    FI
ET   O    FI   METFINO  TFIN  ETFINO  TFI   ET   NO   TF  OMETFIN  ETF  OME  INOM  FIN
TF        IN     FINOM  FINO   FINOM  FIN    F   OM  FIN  ETFINO  TFI  MET  NOME  INO
FI        NO     INOME  INOM   INOME  INO   T    ME  INO   TFINOME  I  METF  OMET  NOM
IN   ETF  OM  FINOMET  NOME  INOMET  NOM   FI   ET  NO  TFINOMETF  METFI  METF  OME
NO   TFI  ME     METF  OMET   NOMET   ME  INO  TF     TFINOMETFIN METFI    TF   ET
OMETFINOMETFINOMETFINOMETFINOMETFINOMETFINOMETFINOMETFINOMETFINOMETFINOMETFINOMETF
METFINOMETFINOMETFINOMETFINOMETFINOMETFINOMETFINOMETFINOMETFINOMETFINOMETFINOMETFI
```

X = ORTHO F   TYPE(I/) ALCOHOL   RCT2/OR2

DATA INPUT : SD OPTION = -1 I.E. ONLY SHIFT DATA HAS BEEN GIVEN

TOTAL NUMBER OF SHIFTED ATOMS = 5 , TOTAL NUMBER OF NMR INACTIVE ATOMS = 13 , TOTAL NUMBER OF SHIFTED CENTRES = 11

ATOM NUMBER	REFERENCE NUMBERS	X-CO-ORD	Y-CO-ORD	Z-CO-ORD	NGROUP	OBSERVED SHIFT	OBSERVED BROAD	BONDED TO ATOM NUMBER	GYRO-CODE
1	107/1/ 1	1.3433333	.5139340	.9930812	1	623.8	I	02/ / /	111111111111111
2	607/1/ 2	1.4333330	0	0	2	1000.0	I	01/03/05/16	112211122222221
3	603/1/ 3	1.3933339	.7253639	-1.2574047	3	512.7	I	01/06/17/18	112211122222221
4	604/1/ 4	2.3201331	-4.0723350	0	4	110.0	I	08/09/13/	111112244444412
5	601/1/ 5	1.3366667	-1.4330637	0	5	489.7	I	01/07/10/	111112244444412
6	103	1.6333333	1.7441967	-1.2374047				03/ / /	133111333333331
7	602	2.7315477	-1.3303634	1.0500000				05/08/11/	13355555513
8	603	3.2537144	-3.2133060	1.0500000				04/07/12/	13355555513
9	605	2.1151102	-3.5150413	-1.0500000				04/10/14/	13355555513
10	506	1.6434524	-2.2351097	-1.0500000				05/09/15/	13355555513
11	902	3.1153339	-1.3994387	2.0259100				07/ / /	13355555513
12	103	3.3791226	-3.5541253	1.8000000				08/ / /	13355555513
13	104	3.2303002	-5.3911689	0				04/ / /	13355555513
14	105	1.9542110	-4.2503429	-1.8500000				09/ / /	13355555513
15	106	1.3275443	-1.3419704	-1.8600000				10/ / /	13355555513
16	800	0	0	0				01/ / /	11111111111
17	1709	1.4066667	-.1037333	-2.6344337				03/ / /	133111333333331
18	1708	3.7533332	.7259631	-1.2574047				03/ / /	133111333333331

FIRST ATOM LISTED USED FOR NORMALISATION

SIGN OF SHIFT OF NORMALISING ATOM/GROUP ASSUMED TO BE POSITIVE

PARAMETERS GIVEN FOR THE INITIAL METAL SEARCH WERE ...

RADIUS OF SEARCH FROM 150 TO 190 IN STEPS OF 10 NANO-METRES FROM THE ORIGIN

DIRECTION OF SEARCH FROM 90 TO 135 IN STEPS OF 5 DEGREES FROM THE XZ-PLANE THROUGH THE Y-AXIS

AND FROM 90 TO 135 IN STEPS OF 5 DEGREES FROM THE X-AXIS IN THE XZ-PLANE

.... OPTIONS SELECTED ....

ITERATION OPTION = 7 I.E. MULTISCAN MODE . PERFORMS 6 BLOCK SEARCH PATTERNS

THE ROTATE OPTION HAS NOT BEEN SELECTED

REFLEC OPTION = 3 I.E. REFLECTION OF THE METAL POSITION HAS NOT BEEN REQUESTED
TWELVE POINT ROTATIONAL AVERAGING OF METHYL GROUPS HAS BEEN REQUESTED
SYMMETRY OF MULTISCAN OUTPUT HAS NOT BEEN ASSUMED

THE ALLOWABLE TOLERANCES FOR THE SHIFT AND BROADENING DATA HAVE BEEN SET AS FOLLOWS ...
TOLERANCE FOR RUN(1) = 50.0   TOLERANCE FOR RUN(2) = 50.0   TOLERANCE FOR RUN(3) = 50.0
DATA WHICH FALLS OUTSIDE THESE LIMITS , WILL BE GIVEN A FITFACTOR OF ZERO IN THE TABLES
LIM OPTION = 2 I.E. ONLY THE SOLUTION TO THE MAXIMUM FITFACTOR WILL BE PRINTED

TEST OPTION = 0 I.E. TESTING OF THE PROGRAM/DATA NOT REQUESTED

CONTUR OPTION = 0 I.E. GRAPHICAL OUTPUT HAS NOT BEEN REQUESTED

(1)

.... OPTIONS SELECTED ....

ITERATION OPTION = 1 I.E. FOCUSING MODE . SEARCHES FOR MAXIMUM FITFACTOR

. THE ROTATE OPTION HAS BEEN SELECTED AND HAS BEEN GIVEN THE VALUE - 126+26434545877
THE MAGNITUDE OF THE FIRST DIGIT HAS SELECTED AN INITIAL ROTATIONAL STEP OF 5.- DEGREES
THE SUBSEQUENT DIGITS (ONE PER CYCLE) INDICATE THE REQUIRED OPERATION FOR EACH CYCLE . THESE PARAMETERS ARE
USED IN CONJUNCTION WITH THE ATOMIC GYROCODE TO CONTROL THE ROTATIONAL OPTIMISATION PROCESS - SEE PROGRAM GUIDE

(2)

CONTUR OPTION = 1 I.E. GRAPHICAL OUTPUT HAS BEEN REQUESTED

********** A METDATA TAPE WILL BE CREATED **********

PRINTING OF THE TABLE FOR ITERATION 12 , MULT 2 , SUPPRESSED AS ALL RESULTS DUPLICATED ON THE FOLLOWING TABLE(S)

9 RESULTS IN THE FINAL PHI ROW OF ITERATION 8
6 RESULTS IN THE FINAL PSI COL OF ITERATION 11

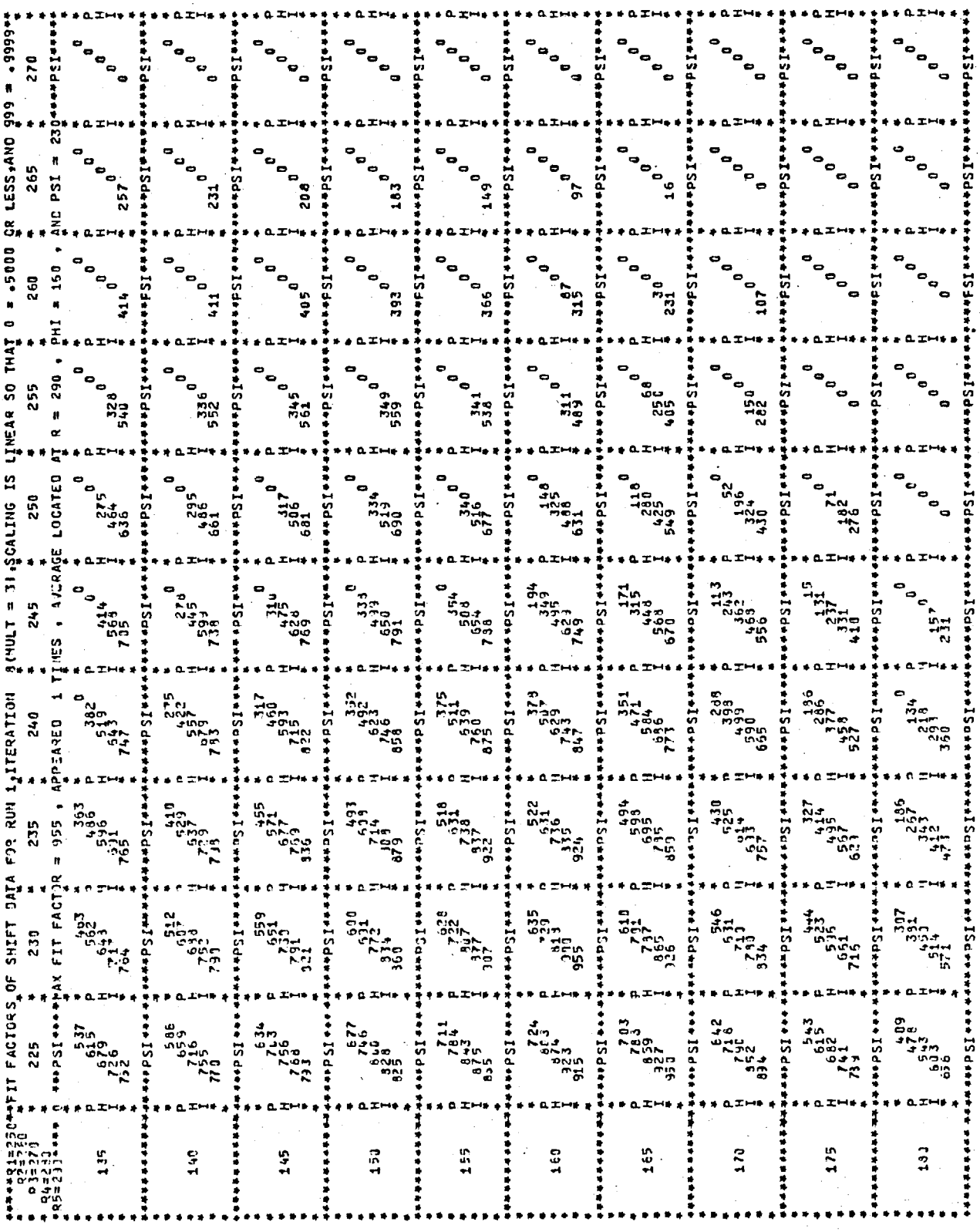
NO RESULTS FOR ITERATION 13 , MULT 2 , SEARCH AREA R(200-240/10) , PHI(225-270/ 5) , PSI(90-135/ 5)

NO RESULTS FOR ITERATION 14 , MULT 2 , SEARCH AREA R(200-240/10) , PHI(225-270/ 5) , PSI(135-180/ 5)

NO RESULTS FOR ITERATION 15 , MULT 2 , SEARCH AREA R(200-240/10) , PHI(225-270/ 5) , PSI(180-225/ 5)

NO RESULTS FOR ITERATION 16 , MULT 2 , SEARCH AREA R(200-240/10) , PHI(225-270/ 5) , PSI(225-270/ 5)

SEARCH AREA BECOMING SILLY THEREFORE PROGRAM STOPPED
THE ATTEMPTED SEARCH AREA WAS : R(- /) , PHI(- /) , PSI(- /)



INTER-ATOMIC DISTANCE TABLE . BONDS MARKED (*) . FROM INITIAL CO-ORD DATA BEFORE COMMENCING ROTATIONAL OPTIMISATION

	1	2	3	4	5	6	7	8	9	10	11	12	13	14	15	16
0	2.1104	1.4800	2.4661	5.0115	2.4496	2.7002	3.5314	4.6934	4.3180	3.0145	3.8845	5.5366	6.0563	5.0216	2.8785	0
18	2.8817	2.6974	1.7600*	5.0304	3.0600	2.3519	3.6190	4.5900	4.6445	3.6879	3.8070	5.3046	5.9703	5.3879	3.8614	4.0244
17	3.6633	2.6974	1.7600*	5.0304	3.0600	2.3519	4.3741	5.2061	3.9415	2.7504	5.1121	6.2314	5.9703	4.2823	2.0540	3.0413
16	2.1104	1.4800*	2.4661	5.0115	2.4496	2.7002	3.5314	4.6934	4.3180	3.0145	3.8645	5.5366	6.0563	5.0216	2.8786	
15	3.7760	2.7268	2.9006	3.4033	2.1537	3.7838	3.4033	3.8800	2.1537	1.0800*	4.4874	4.9600	4.2955	2.4800		
14	5.5266	4.6817	5.0441	2.1537	3.4033	6.0583	3.8800	3.4033	1.0800*	2.1537	5.1800	4.2955	2.4800			
13	5.8542	5.4000	6.0890	1.0800*	3.8800	7.1425	3.4033	2.1537	2.1537	3.4033	4.4874	2.4800				
12	4.6599	4.6817	5.6284	2.1537	3.4033	6.5529	2.1537	1.0800*	3.4033	3.8800	2.5970					
11	2.3357	2.8165	3.9129	3.6097	2.3388	4.5801	1.3000*	2.3388	4.1000	3.6097						
10	3.4193	2.5295	3.0478	2.4249	1.4000*	4.0447	2.4249	2.8000	1.4000*							
9	4.5700	3.8176	4.3477	1.4000*	2.4249	5.3848	2.8000	2.4249								
8	3.9876	3.8176	4.7353	1.4000*	2.4249	5.7024	1.4000*									
7	2.5899	2.5295	3.5790	2.4249	1.4000*	4.4587										
6	2.4838	2.1556	1.0800*	6.0890	3.4352											
5	2.1455	1.5200*	2.4985	2.8000												
4	4.7948	4.3200	5.0467													
3	2.1630	1.5400*														
2	1.0900*															

	17	18
0	3.0413	4.0244
18	2.8741	

CYCLE NUMBER 1 , OPERATION 1 SELECTED I.E. CENTRE SEARCH AREA ONTO MAX FITFACTOR OF CURRENT ATOMS (GYRO .GT. 0)
THE ATOMS TO BE USED IN THIS CYCLE ARE -

ATOM NUMBER	REFERENCE NUMBERS	X-CO-ORD	Y-CO-ORD	Z-CO-ORD	OBSERVED SHIFT	GYRO CODE
1	107/1/ 1	1.8433333	.5138310	.8899812	623.8	1
2	607/1/ 2	1.4800000	0	0	1000.0	1
3	608/1/ 3	1.9933329	.7259630	-1.2574047	512.7	1
4	604/1/ 4	2.9200001	-4.0729350	0	110.0	1
5	601/1/ 5	1.9866667	-1.4330697	0	489.7	1

CYCLE 1 ITERATION 1 . MAX FITFACTOR = 978 APPEARED 1 TIMES , AVERAGE LOCATED AT R = 300 , PHI = 155 , PSI = 240

******* FITFACTOR Table omitted here

CYCLE NUMBER 2 , OPERATION 2 SELECTED I.E. ADD NEXT GROUP(S) THEN RE-CENTRE SEARCH AREA ONTO MAXIMUM FITFACTOR
THE ATOMS TO BE USED IN THIS CYCLE ARE -

******* Table as above with one extra line :

6	108/1/ 6	1.6333333	1.7441967	-1.2574047	363.1	1

CYCLE 2 ITERATION 3 . MAX FITFACTOR = 944 APPEARED 1 TIMES , AVERAGE LOCATED AT R = 280 , PHI = 170 , PSI = 230

******* FITFACTOR Table omitted here

CYCLE NUMBER 3 , OPERATION 6 SELECTED I.E. PERFORM COMPLETE ROTATION OF INDICATED GROUP (30' STEP) THEN OPTIMISE
THE ATOMS TO BE USED IN THIS CYCLE ARE -

******* Table as above with atoms 6,17 and 18 added. GYRO-CODE of atoms 2 & 3 = 2 ; 6, 17 & 18 = 3

GYROCODE NUMBER OF ATOMS A AND B IS 2 AND OF ROTATED ATOMS IS 3 . THE ROTATED ATOMS HAVE BEEN MOVED + 30.0 DEGREES

CYCLE 3 ITERATION 5 . MAX FITFACTOR = 961 APPEARED 1 TIMES , AVERAGE LOCATED AT R = 290 , PHI = 160 , PSI = 230

CYCLE 6 ITERATION 6 . MAX FITFACTOR = 961 APPEARED 1 TIMES , AVERAGE LOCATED AT R = 290 , PHI = 160 , PSI = 230

GYROCODE NUMBER OF ATOMS A AND B IS 2 AND OF ROTATED ATOMS IS 3 . THE ROTATED ATOMS HAVE BEEN MOVED + 60.0 DEGREES

CYCLE 3 ITERATION 7 . MAX FITFACTOR = 934 APPEARED 1 TIMES , AVERAGE LOCATED AT R = 290 , PHI = 160 , PSI = 235

GYROCODE NUMBER OF ATOMS A AND B IS 2 AND OF ROTATED ATOMS IS 3 . THE ROTATED ATOMS HAVE BEEN MOVED + 90.0 DEGREES

CYCLE 3 ITERATION 8 . MAX FITFACTOR = 965 APPEARED 1 TIMES , AVERAGE LOCATED AT R = 310 , PHI = 145 , PSI = 250

******* This continues through 120,150 180,-30,-60,-90,-120 to -150°:

GYROCODE NUMBER OF ATOMS A AND B IS 2 AND OF ROTATED ATOMS IS 3 . THE ROTATED ATOMS HAVE BEEN MOVED -150.0 DEGREES

CYCLE 3 ITERATION 26 . MAX FITFACTOR = 852 APPEARED 2 TIMES , AVERAGE LOCATED AT R = 315 , PHI = 185 , PSI = 179

THE ROTATION OF ATOMS OF GYROCODE 3 HAS BEEN OPTIMISED AT + 90.0 DEGREES . THE CO-ORDS OF THE CURRENT ATOMS ARE NOW

ATOM NUMBER	REFERENCE NUMBERS	X-CO-ORD	Y-CO-ORD	Z-CO-ORD	OBSERVED SHIFT	GYRO CODE
1	107/1/ 1	1.8433333	.5138310	.8899812	623.8	1
2	607/1/ 2	1.4800000	.0	0	1000.0	2
3	608/1/ 3	1.9933329	.7259630	-1.2574047	512.7	2
4	604/1/ 4	2.9200001	-4.0729350	0	110.0	1
5	601/1/ 5	1.9866667	-1.4330697	0	489.7	1
6	108/1/ 6	1.2819485	.6017304	-2.0604601	363.1	3
17	1708/*/**	3.5437373	.0444984	-1.7364163	0	3
18	1708/*/**	2.1888883	2.4395545	-.9067436	0	3

CYCLE NUMBER 4 , OPERATION 4 SELECTED I.E. FIX POSITION OF ALL PREVIOUSLY ROTATED GROUPS (REPLACE CO-ORDINATES)
THE NEW CO-ORD DATA OF THE ATOMS SUPPLIED IS :

******* CO-ORD & INTER-ATOMIC DISTANCE Tables omitted here

CYCLES 5, 6 and 7 are repeats of CYCLES 2, 3 and 4 using the rotating ring atoms instead of the side-chain atoms

CYCLE NUMBER 8 , OPERATION 3 SELECTED I.E. OBSERVE MAX FITFACTOR REGION - ROTATE GROUPS IN SEQUENCE AND OPTIMISE
THE ATOMS TO BE USED IN THIS CYCLE ARE -

******* CO-ORD Table omitted here ... Full set of atoms (1 - 18) with GYROCODES of atoms 2 & 3 = 2; 3 & 4 = 4; 6, 17 & 18 = 3; and 7 to 15 = 5. This allows the side-chain and ring to be rotated/optimised separately.

GYROCODE NUMBER OF ATOMS A AND B IS 2 AND OF ROTATED ATOMS IS 3 . THE ROTATED ATOMS HAVE BEEN MOVED + 5.0 DEGREES

CYCLE 8 ITERATION 64 . MAX FITFACTOR = 903 APPEARED 1 TIMES , AVERAGE LOCATED AT R = 305 , PHI = 150 , PSI = 239

GYROCODE NUMBER OF ATOMS A AND B IS 2 AND OF ROTATED ATOMS IS 3 . THE ROTATED ATOMS HAVE BEEN MOVED + 10.0 DEGREES

CYCLE 8 ITERATION 65 . MAX FITFACTOR = 901 APPEARED 2 TIMES , AVERAGE LOCATED AT R = 310 , PHI = 149 , PSI = 241

CYCLE 8 ITERATION 66 . MAX FITFACTOR = 902 APPEARED 1 TIMES , AVERAGE LOCATED AT R = 310 , PHI = 149 , PSI = 241

THE ROTATION OF ATOMS OF GYROCODE 3 HAS BEEN OPTIMISED AT + 5.0 DEGREES . THE CO-ORDS OF THE CURRENT ATOMS ARE NOW

******* CO-ORD & FITFACTOR Table omitted here

GYROCODE NUMBER OF ATOMS A AND B IS 4 AND OF ROTATED ATOMS IS 5 . THE ROTATED ATOMS HAVE BEEN MOVED + 5.0 DEGREES

CYCLE 8 ITERATION 68 . MAX FITFACTOR = 889 APPEARED 1 TIMES , AVERAGE LOCATED AT R = 310 , PHI = 143 , PSI = 245

GYROCODE NUMBER OF ATOMS A AND B IS 4 AND OF ROTATED ATOMS IS 5 . THE ROTATED ATOMS HAVE BEEN MOVED - 5.0 DEGREES

CYCLE 8 ITERATION 69 . MAX FITFACTOR = 914 APPEARED 2 TIMES , AVERAGE LOCATED AT R = 305 , PHI = 152 , PSI = 239

GYROCODE NUMBER OF ATOMS A AND B IS 4 AND OF ROTATED ATOMS IS 5 . THE ROTATED ATOMS HAVE BEEN MOVED - 10.0 DEGREES

CYCLE 8 ITERATION 70 . MAX FITFACTOR = 913 APPEARED 1 TIMES , AVERAGE LOCATED AT R = 305 , PHI = 153 , PSI = 239

THE ROTATION OF ATOMS OF GYROCODE 5 HAS BEEN OPTIMISED AT - 5.0 DEGREES . THE CO-ORDS OF THE CURRENT ATOMS ARE NOW

******* CO-ORD & FITFACTOR Table omitted here

CYCLES 9,10,11 and most of 12 are omitted as they are finer repeats of CYCLES 7 and 8 . CYCLE 12 ends with a WRITEB :

THIS CYCLE STOPPED IN ROTATE SUB-CYCLE 3 AS NO FURTHER ATOMS TO ROTATE

SOLUTION NUMBER = 2 , TYPLIM NOT SELECTED - SOLUTION TO MAX FITFACTOR ONLY , SCAN NUMBER = 1
FITFACTOR OF SHIFT DATA FOR THIS SOLUTION = 917 , AS TOLERANCE = .5000 , GOODNESS OF FIT = .9585
SEARCH PARAMETERS FOR THIS SOLUTION WERE ..... RADIUS = 3.03 , ANGLE PHI = 153 , ANGLE PSI = 238
M-O-C BOND ANGLE = 118.175 DEGREES ..... M-O-C-(XY-PLANE) DIHEDRAL ANGLE = 59.002 DEGREES
METAL CO-ORDINATES IN ANGSTROMS FROM THE BONDING SITE : X = -1.4306 , Y = 1.3756 , Z = -2.2895
NORMALISING ATOM/GROUP : ACTUAL CALCULATED SHIFT = 161.6088 , CALCULATED BROADENING = 99.6325

NGROUP	SHIFTS : OBSERVED	CALCULATED	DIFFERENCE	STAND.DEV.	DISTMH	EMOCOS
1	623.800	623.800	0	0	4.644	.93436
2	1000.000	1047.338	4.734	0	3.950	.94389
3	512.700	518.502	1.132	0	3.635	.74050
4	110.000	115.372	4.884	0	7.339	.85271
5	489.700	493.420	.760	0	4.981	.92728
6	363.100	360.421	-.738	0	2.860	.63731
7	284.800	258.569	-9.210	0	6.313	.94606
8	141.600	148.745	5.046	0	7.374	.92106
9	142.400	137.098	-3.724	0	6.230	.78718
10	337.000	341.917	1.459	0	4.929	.82877
11	218.4	218.776	.172	0	6.757	.95719

TEST=1, BONGLE=11

```
BOND ANGLE  1 BETWEEN ATOMS (12-10- 4. ) =  76.038 DEGREES
BOND ANGLE  2 BETWEEN ATOMS ( 3-11- 5) =  45.599 DEGREES
BOND ANGLE  3 BETWEEN ATOMS ( 1- 2- 3) =  51.437 DEGREES
BOND ANGLE  4 BETWEEN ATOMS ( 5- 6- 7) =  59.695 DEGREES
BOND ANGLE  5 BETWEEN ATOMS ( 9-11-12) =  30.061 DEGREES
BOND ANGLE  6 BETWEEN ATOMS ( 3- 8- 6) =  35.993 DEGREES
BOND ANGLE  7 BETWEEN ATOMS ( 1- 6- 9) =  18.653 DEGREES
BOND ANGLE  8 BETWEEN ATOMS ( 5- 2- 7) =  22.256 DEGREES
BOND ANGLE  9 BETWEEN ATOMS ( 5- 8-10) =  47.713 DEGREES
BOND ANGLE 10 BETWEEN ATOMS ( 5- 2- 9) = 101.897 DEGREES
BOND ANGLE 11 BETWEEN ATOMS ( 3-12- 6) =  44.323 DEGREES
```

TEST=3...output for a carbon atom & 3 methyl protons in DMA, ie. $\frac{1}{3}$ of the TEST=3 output for 1 search point.

```
NSCAN =  4 , R = 300 , PHI = 180 , PSI = 150 , X/Y/ZMETAL =  -2.5981       0  1.5000

NPROT =  1 , NUMAV = 1 , ITOT = -9 , NTOT =  0 , PROTX/Y/Z =    2.0208  1.2975      0
DISTX/Y/Z =  -4.6189 -1.2975  1.5000 , SHIFTA = ( 132.186,7633.100) , BROADA = (  61.990, 100.000)
DISTX/Y/Z =  -4.6189 -1.2975  1.5000 , SHIFTB = ( 132.186,7633.100,7633.100) , BROADB = (  61.990, 100.000, 100.000)
SHIFT OBS = 7633.100 , CALC = 7633.100 , PC DIFF =       0 , TESTOL =  67.000
NPROT =  2 , NUMAV = 3 , ITOT =  3 , NTOT = 12 , PROTX/Y/Z =    3.7637  -.5001  -.8899
DISTX/Y/Z =  -6.3618   .5001  2.3899 , SHIFTA = (  60.177,3474.918) , BROADA = (   9.988,  16.113)
DISTX/Y/Z =  -6.3618   .5001  -.6101 , SHIFTB = (  55.729,3218.074,3346.496) , BROADB = (  14.409,  23.245,  19.679)
NPROT =  3 , NUMAV = 3 , ITOT =  2 , NTOT = 11 , PROTX/Y/Z =    3.7637   .5001   .8899
DISTX/Y/Z =  -6.3618   .5001   .6101 , SHIFTA = (  55.729,3218.074) , BROADA = (  14.409,  23.245)
DISTX/Y/Z =  -6.3618  -.5001 -2.3899 , SHIFTB = (  60.177,3474.918,3346.496) , BROADB = (   9.998,  16.113,  19.679)
NPROT =  4 , NUMAV = 3 , ITOT =  1 , NTOT = 10 , PROTX/Y/Z =    3.8712  2.0378      0
DISTX/Y/Z =  -6.4693 -2.0378  1.5000 , SHIFTA = (  45.015,2599.403) , BROADA = (   8.900,  14.357)
DISTX/Y/Z =  -6.4693 -2.0378 -1.5000 , SHIFTB = (  45.015,2599.403,2599.403) , BROADB = (   8.900,  14.357,  14.357)
NPROT =  4 , NUMAV = 3 , ITOT =  0 , NTOT =  9 , PROTX/Y/Z =    3.7375  -.7860  -.5138
DISTX/Y/Z =  -6.3355   .7860  2.0138 , SHIFTA = (  60.768,3509.061) , BROADA = (  11.112,  17.926)
DISTX/Y/Z =  -6.3355   .7860  -.9862 , SHIFTB = (  58.269,3364.767,3436.914) , BROADB = (  13.762,  22.200,  20.063)
NPROT =  4 , NUMAV = 3 , ITOT = -1 , NTOT =  8 , PROTX/Y/Z =    3.7375  -.2085   .5138
DISTX/Y/Z =  -6.3355   .2086   .9862 , SHIFTA = (  60.852,3513.898) , BROADA = (  14.436,  23.142)
DISTX/Y/Z =  -6.3355   .2086 -2.0138 , SHIFTB = (  63.201,3549.533,3581.715) , BROADB = (  11.551,  18.633,  20.888)
NPROT =  4 , NUMAV = 3 , ITOT = -2 , NTOT =  7 , PROTX/Y/Z =    3.7995   .1018 -1.0276
DISTX/Y/Z =  -6.3976  -.1018  2.5276 , SHIFTA = (  59.420,3431.203) , BROADA = (   9.433,  15.217)
DISTX/Y/Z =  -6.3976  -.1018  -.4724 , SHIFTB = (  54.226,3131.260,3281.231) , BROADB = (  14.338,  23.129,  19.173)
NPROT =  4 , NUMAV = 3 , ITOT = -3 , NTOT =  6 , PROTX/Y/Z =    3.7995  1.2567  1.0276
DISTX/Y/Z =  -6.3976 -1.2567   .4724 , SHIFTA = (  48.070,2775.800) , BROADA = (  12.816,  20.674)
DISTX/Y/Z =  -6.3976 -1.2567 -2.5276 , SHIFTB = (  53.829,3108.356,2942.078) , BROADB = (   8.554,  13.798,  17.236)
NPROT =  4 , NUMAV = 3 , ITOT = -4 , NTOT =  5 , PROTX/Y/Z =    3.8616  1.5671  -.5138
DISTX/Y/Z =  -6.4597 -1.5671  2.0138 , SHIFTA = (  51.039,2947.244) , BROADA = (   8.909,  14.371)
DISTX/Y/Z =  -6.4597 -1.5671  -.9862 , SHIFTB = (  48.177,2781.993,2864.618) , BRAODB = (  10.861,  17.520,  15.946)
NPROT =  4 , NUMAV = 3 , ITOT = -5 , NTOT =  4 , PROTX/Y/Z =    3.8616  2.1445   .5138
DISTX/Y/Z =  -6.4597 -2.1445   .9862 , SHIFTA = (  41.511,2397.032) , BROADA = (   9.450,  15.245)
DISTX/Y/Z =  -6.4597 -2.1445 -2.0138 , SHIFTB = (  44.593,2575.063,2486.034) , BROADB = (   7.820,  12.614,  13.930)
NPROT =  4 , NUMAV = 3 , ITOT = -6 , NTOT =  3 , PROTX/Y/Z =    3.7279  -.6793      0
DISTX/Y/Z =  -6.3260   .6793  1.5000 , SHIFTA = (  61.711,3563.526) , BROADA = (  12.818,  20.677)
DISTX/Y/Z =  -6.3260   .6793 -1.5000 , SHIFTB = (  61.711,3563.526,3563.526) , BROADB = (  12.818,  20.677,  20.677)
NPROT =  4 , NUMAV = 3 , ITOT = -7 , NTOT =  2 , PROTX/Y/Z =    3.8354   .8584  -.8899
DISTX/Y/Z =  -6.4335  -.8584  2.3899 , SHIFTA = (  56.556,3266.810) , BROADA = (   9.134,  14.735)
DISTX/Y/Z =  -6.4335  -.8684  -.6101 , SHIFTB = (  51.806,2996.730,3131.270) , BROADB = (  13.028,  21.016,  17.876)
NPROT =  4 , NUMAV = 3 , ITOT = -8 , NTOT =  1 , PROTX/Y/Z =    3.8354  1.8586   .8899
DISTX/Y/Z =  -6.4335 -1.8586   .6101 , SHIFTA = (  42.469,2452.398) , BROADA = (  10.817,  17.450)
DISTX/Y/Z =  -6.4335 -1.8586 -2.3899 , SHIFTB = (  47.764,2758.109,2605.253) , BROADB = (   7.739,  12.484,  14.967)
SHIFT OBS = 3548.000 , CALC = 3098.753 , PC DIFF = -12.662 , TESTOL =  67.000
```

TEST=4

```
SOLUTION NUMBER =  1 , TYPLIM NOT SELECTED - SOLUTION TO MAX FITFACTOR ONLY , SCAN NUMBER =  1
FITFACTOR OF SHIFT DATA FOR THIS SOLUTION = 675 , AS TOLERANCE = .5000 , GOODNESS OF FIT = .8375
SEARCH PARAMETERS FOR THIS SOLUTION WERE ..... RADIUS = 3.40 , ANGLE PHI = 225 , ANGLE PSI = 135
M-O-C BOND ANGLE = 120.000 DEGREES .....  M-O-C-(XY-PLANE) DIHEDRAL ANGLE =  35.264 DEGREES
METAL CO-ORDINATES IN ANGSTROMS FROM THE BONDING SITE :  X = -1.7000 , Y = -2.4042 , Z =  1.7000
NORMALISING ATOM/GROUP : ACTUAL CALCULATED SHIFT =  107.0710 , CALCULATED BROADENING =  35.4660
```

NGROUP	SHIFTS : OBSERVED	CALCULATED	DIFFERENCE	STAND.DEV.	BROADS : OBSERVED	CALCULATED	DIFFERENCE	STAND.DEV.	DISTMH	HMOCOS
1	7633.100	7633.100	0	0	100.000	100.000	0	0	5.517	.96573
2	3548.000	3076.972	-13.276	2.366	100.000	36.481	-63.519	4.614	6.635	.86816
3	7553.000	5403.331	-28.461	23.505	100.000	59.026	-40.974	12.803	6.236	.95562
4	5516.000	5808.403	5.301	0	100.000	1434.076	1334.076	0	3.539	.67362
5	3089.600	3626.800	17.387	0	100.000	92.819	-7.181	0	5.585	.79303
6	6399.000	6478.859	1.248	33.125	100.000	652.707	552.707	215.004	4.424	.75922

IV-4 Program Structure and Listing

METFIND VII consists of 11 subroutines, which, in order of listing, are : MAIN, READ, DATEST, WRITEA, WHICH, ROTATE, DONEST, WRITEB, WRITEC, WRITED, NEWLIM. The functions of WRITEA/B/C and D have already been mentioned. Briefly the remaining subroutines perform the following operations :

MAIN (METFIND) : Controls most of the inter-subprogram communication (see BLOCK DIAGRAM 1) and is split into two distinct parts. The first deals with the NON-ITERATIVE, FOCUSING and MULTISCAN MODES, the second with the ROTATE MODE. With the exception of the NON-ITERATIVE MODE, METFIND always operates in a cyclic manner. After the initial READ and WRITEA calls, both the FOCUSING and MULTI-SCAN MODES perform ITERATIONS based on a (DONEST-WRITEC-LEWLIM) cycle; WRITEB normally only being called once at the end of a FOCUSING (or NON-ITERATIVE) run. ROTATE CYCLES vary considerably with the NCYCOP option, but are generally based on a (WHICH-ROTATE-DONEST-WRITED) sequence; WRITEC only being called once at the end of each CYCLE and NEWLIM only when necessary. The basic "primary" CYCLE sequence is further complicated by many "secondary" subroutine calls (see BLOCK DIAGRAM 1).

READ : Merely reads the input data deck.

DATEST : Calculates and outputs the INTER-ATOMIC DISTANCE & BOND ANGLE Tables.

WHICH : Only used in the ROTATE MODE. WHICH selects the ATOMS/GROUPS to be used in each CYCLE from the GYRO and NCYCOP options and transfers coordinate data between the working and stored files.

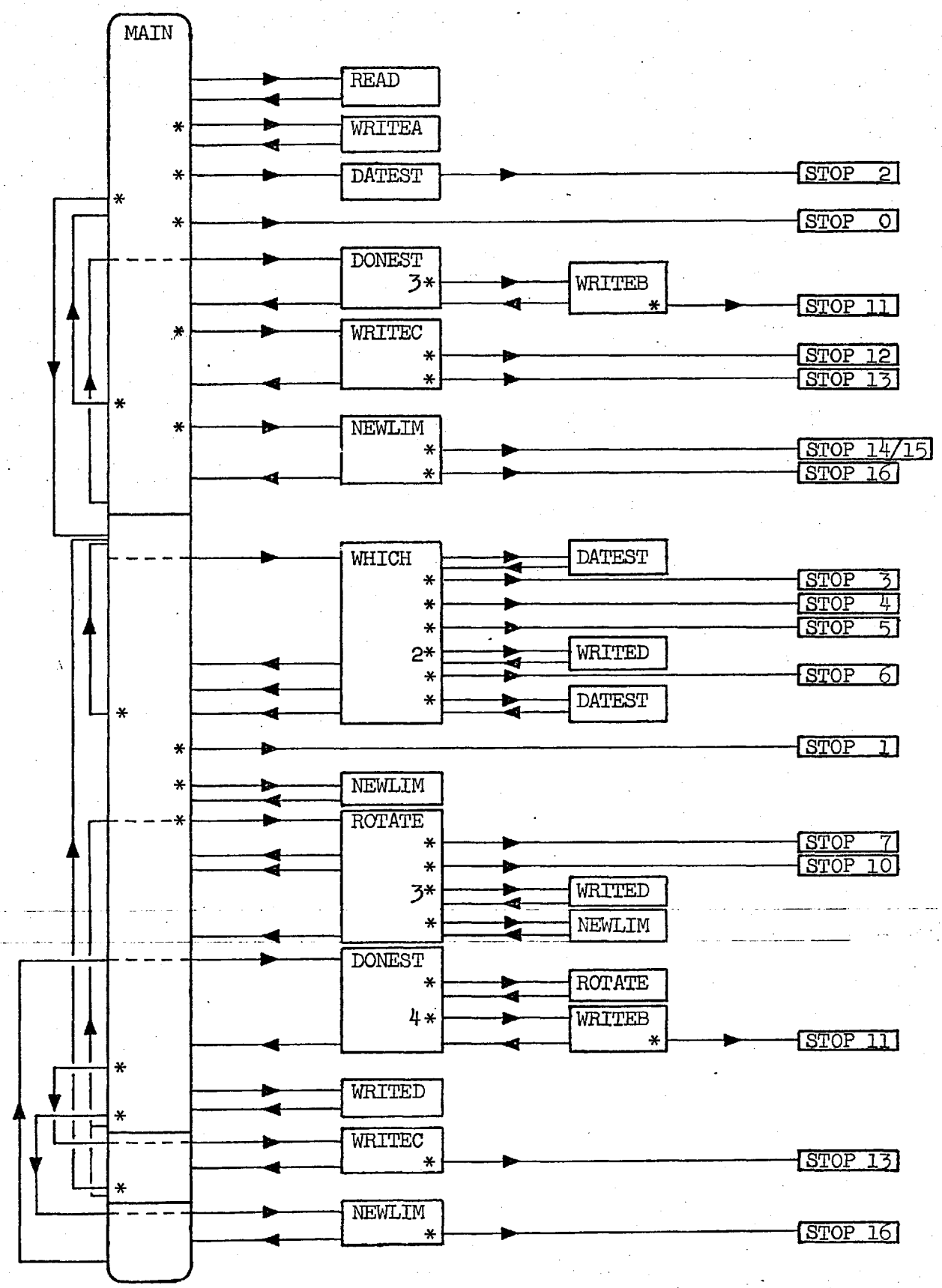
ROTATE : Only used in the ROTATE MODE. ROTATE performs incremental ROTATIONS on the ATOMS specified by the GYRO-CODES. Note that TWELVE POSITION AVERAGING of methyl group protons in done by DONEST.

DONEST : The operating centre of the program responsible for calculating the SHIFT and BROADENING data, group averaging, methyl group rotation, metal reflection, testing tolerances and producing the FITFACTORS for each of the 500 search points in each search block. This involves using 4 nested DO loops, 3 of which select the coordinates of the search point, the fourth controlling the ATOM/GROUP manipulations.

NEWLIM : Calculates the limits of R, PHI and PSI for the next ITERATION.

It was originally intended to include detailed flowcharts and documentation for METFIND VII, but the 20-30 pages required to do this thoroughly is prohibitive and the alternative of producing a diluted version would be inadequate for the interested reader. A complete GUIDE TO METFIND VII will therefore be produced as a separate publication. A program listing is attached for reference.

BLOCK DIAGRAM 1 : POSSIBLE SUBPROGRAM COMMUNICATION WITHIN METFIND VII



(*) Is used to indicate a conditional transfer of control

(n*) Indicates that 'n' conditional transfers occur close together

```
      PROGRAM METZIND(INPUT=2018,OUTPUT=2018,TAPE5=INPUT,TAPE4=OUTPUT,
     +TAPE6=TAPE4=1018,TAPE9=10216)
      COMMON IRMIN,IPMAX,IPSTEP,IPHIMN,IPHIMX,IPHIST,IPSIMN,IPSIMX,IPSIS
     +T,ITER,NITER,LIM,ROTEMP(7,100),LOCATE(100),BOND(200)
      COMMON          /DATA/NCENTR,NGROUP(100),SOBS(100),BOBS(100),NPROT
     +,NSIGN,NORM,NAME(100),NUMAV(100),PROTX(100),PROTY(100),PROTZ(100),
     +JGROUP(100),TITLE(8)/FITLIM/FITLIM(3),TYPLIM,FIT(3),TOL(3)/WRITEC/
     +SCALC(100),BCALC(100),SDIFF(100),BDIFF(100),SSTDEV(100),BSTDEV(100
     +),NSCAN,NSOLN,PANGLE,OANGLE,XMETAL,YMETAL,ZMETAL,SHIFTN,BGROAON,KI
     +,J,K,N2,NPHI,NPSI/MXFIT/MAXR,MAXPHI,MAXPSI,MFLAG(16),LAF(16,4),NSM
     +AX,MXSFIT,MXSF,MXSPHI,MXSPSI,NSMAX,MX3FIT,MXPR,MXBPHI,MXBPSI/TABLE
     +S/ISFIT(6,10,10),IBFIT(6,10,10)/JUMP/JUMP,PI,MULT,MPHI,MPSI
      DIMENSION MAG(10)
      INTEGER/NAME/REFLEC,SBOPT,RUN,TEST,BONGLE,OMITA,OMITC,CONTUR,ATOM/
     +ROTN/CYCLE,GYRO(100),ROTN,ROTWAY,ROTOPT
      DATA MAG/0.1,2.5,10.15.20.30.45.60/
C
C     SELECT 8 LINES-TO-THE-INCH
      WRITE(6,1)
    1 FORMAT(1H1)
      CALL SECOND(T1)
C     SET CONSTANTS AND FLAGS , PRESET TOLERANCES
      RUN = MULT = MPHI = MPSI = NCYCOP = ROTWAY = 1
      NSCAN=ITER=NSOLN=NITER=JUMP=NSIGN=REFLEC=LIM=TEST=0
      SBOPT = -1
      NCALL = LAST = CYCLE = 0
      FITLIM(1) = 0.90
      FITLIM(2) = 0.9750
      FITLIM(3) = 0.9850
      TYPLIM = 0.994
      PI = 3.1415926E395 / 180.0
C
      CALL READ
C
C     CALCULATE P.C. TOLERANCES (FIT) AND INDIVIDUAL TOL (TOL)
      DO 2 N = 1,3
      FIT(N) = 100.0 - 100.0 * FITLIM(N)
    2 TOL(N) = (1.25 + 0.0075 * NPROT) * FIT(N)
C
      IF(ROTOPT .EQ. 0) GO TO 3
      ROTOPT = ROTOPT + 1
      ROTINC = FLOAT(MAG(ROTOPT))
      CONTUR = MAXROT = 0
      ITER = NCALL = 1
      RUN = 3
    3 IF(OMITA .EQ. 1)  WRITE(6,4)
    4 FORMAT(1H1/22X,*THE LISTING OF INPUT DATA AND PARAMETERS HAS BEEN
     +SUPPRESSED TO OVERCOME LINE-LIMIT RESTRICTIONS*/)
      IF(OMITA .EQ. 0 .OR. CONTUR .EQ. 1)  CALL WRITEA(ROTINC)
C
      IF(TEST .EQ. 1)  CALL DATEST(PROTX,PROTY,PROTZ,NPROT,ATOM,BOND,
     +  BONGLE,PI,NCALL)
C
      IF(OMITC .GT. 0) WRITE(6,5) OMITC
    5 FORMAT(/13XI*THE FIRST *,I1,* TABLES OF FITFACTORS WILL NOT BE LIS
     +TED , UNLESS RUN=3 AND JUMP=1 , TO OVERCOME LINE-LIMIT RESTRICTION
     +S*////)
C
      IF(SBOPT .EQ. 0) GO TO 7
      DO 6 N = 1,NCENTR
      IF(SBOPT .LT. 0) BOBS(N) = 100.0
      IF(SBOPT .GT. 0) SOBS(N) = 100.0
    6 CONTINUE
      IF(ROTOPT .GT. 0) GO TO 8
      IF(JUMP.EQ.2 .AND. LIM.LT.2 .AND. MXSFIT.LT.TYPLIM .AND. MX3FIT.
     +LT.TYPLIM) STOP0
C
    7 CALL DONEST(MAXROT,ROTWAY,ROTOPT,NCYCOP,GYRO,T1)
      IF(NITER.GT.OMITC .OR. JUMP.GE 1 .OR  OMITC.EQ.9)  CALL WRITEC
C
      IF(ITER .EQ. 0) GO TO 6
      CALL NEWLIM
      GO TO 7
C
    8 CYCLE = CYCLE + 1
      CALL SECOND(T)
      WRITE(4,2222) CYCLE,T-T1
 2222 FORMAT(/10X,*START OF CYCLE *,I2,* , TIME USED = *,F8.3,* SECONDS*
     +)
      K = 2
      ROTWAY = 1
      CALL WHICH(NCYCOP,NROT,ATOM,PI,BONGLE,NCALL)
      IF(NCYCOP .EQ. 4) GO TO 8
      IF(NCYCOP .EQ. 8) GO TO 10
      IF(NCYCOP .EQ. 2) MAXROT = 0
      IF(NCYCOP .LT. 3) GO TO 10
      IF(NCYCOP .EQ. 5 .AND. ROTOPT .GE. 3) ROTOPT = ROTOPT - 1
      IF(NCYCOP .EQ. 5 .AND. ROTOPT .GE. 6) ROTOPT = ROTOPT - 2
      IF(MAXROT .EQ. 0) STOP1
      IRSTEP = 5
      IPHIST = IPSTST = 2
      IF(ROTOPT .EQ. 2) RUN = 2
      IF(NCYCOP .LT. 6) GO TO 13
      RUN = 3
      IPSTEP = 10
      IPHIST = IPSTST = 5
   13 CALL NEWLIM
      ROTINC = FLOAT(MAG(ROTOPT)) * PI
      LAST = JUMP = 0
    9 IF(NROT .GE. 0) CALL ROTATE(ROTINC,GYRO,ROTWAY,LAST,MAXROT,M,PI,
     +NROT,NCYCOP,MXSFIT,1)
C
      IF(LAST .EQ. 2 .AND. NCYCOP .NE. 5) GO TO 8
      IF(LAST .EQ. 2) JUMP = 2
C
   10 CALL DONEST(MAXROT,ROTWAY,ROTOPT,NCYCOP,GYRO,T1)
      IF(JUMP .EQ. 2 .OR. NCYCOP .EQ. 8) GO TO 8
      IF((LAST.EQ.1.AND.ROTWAY.EQ.0).OR.(NCYCOP.LE.2.AND.JUMP.EQ.1)) GO
     + TO 11
      IF(NCYCOP .EQ. 7 .AND. ROTWAY .NE. -2) GO TO 11
      CALL WRITEO(4,NITER,MXSFIT,NSMAX,MAXR,FLOAT(MAXPHI),FLOAT(MAXPSI))
      IF(ROTWAY .EQ. -2 .OR. JUMP .EQ. 0 .AND. NCYCOP .LE. 2) GO TO 12
      GO TO 9
   11 JUMP = 0
      CALL WRITEC
      IF(NCYCOP .LE. 2 .OR. NCYCOP .EQ. 7) GO TO 8
      GO TO 9
   12 CALL NEWLIM
      GO TO 10
C
      END
      SUBROUTINE READ
      COMMON IRMIN,IPMAX,IPSTEP,IPHIMN,IPHIMX,IPHIST,IPSIMN,IPSIMX,IPSIS
     +T,ITER,NITER,LIM,ROTEMP(7,100),LOCATE(100),BOND(200)
      COMMON          /DATA/NCENTR,NGROUP(100),SOBS(100),BOBS(100),NPROT
     +,NSIGN,NORM,NAME(100),NUMAV(100),PROTX(100),PROTY(100),PROTZ(100),
     +JGROUP(100),TITLE(8)/FITLIM/FITLIM(3),TYPLIM,TOL(3),FIT(3)
      INTEGER/NAME/REFLEC,SBOPT,RUN,TEST,BONGLE,OMITA,OMITC,CONTUR,ATOM/
     +ROTN/CYCLE,GYRO(100),ROTN,ROTWAY,ROTOPT
C
C     READ BLOCK ... DATA FOR SHIFTED CENTRES AND SEARCH PARAMETERS
C
      READ(5,10) (TITLE(I),I=1,8)
   10 FORMAT(8A4,8A4)
C     OBLIGATORY INFORMATION
      READ(5,11) NPROT,ATOM,NCENTR,SEOPT,NSIGN,NORM,ROTOPT,ROTN
   11 FORMAT(6X,I2,1X,I2,9X,I2,2(8X,I1),7X,I1,7X,I1,I15)
      SBOPT = SBOPT - 2
C     OPTIONS REQUIRED
      READ(5,12) ITER,REFLEC,LIM,TEST,BONGLE,CONTUR,OMITA,OMITC
   12 FORMAT(5X,I1,9X,I1,6X,I1,7X,I1,9X,I3,9X,I1,2(8X,I1))
C     TOLERANCES FOR FITFACTORS
      IF(LIM .GE. 1) READ(5,13) (FITLIM(I),I=1,3),TYPLIM
   13 FORMAT(8X,F5.3,10X,F5.3,10X,F5.3,9X,F5.3)
      IF(LIM .EQ. 0) READ(5,14) DUMMY
   14 FORMAT(A1)
C     NAME/COORDINATE DATA
      READ(5,15) (NAME(I),NUMAV(I),NGROUP(I),PROTX(I),PROTY(I),PROTZ(I),
     +BOND(2*I-1),BOND(2*I),GYRO(I),I = 1,NPROT)
   15 FORMAT(A4,1X,I1,1X,I2,1X,3F10.7,2A6,4X,I15)
      IF(ATOM .EQ. 0) GO TO 160
      READ(5,16) (NAME(I),PROTX(I),PROTY(I),PROTZ(I),BOND(2*I-1),BOND(2*
     + I),GYRO(I),I = NPROT+1 , NPROT+ATOM)
   16 FORMAT(A4,6X,3F10.7,2A6,4X,I15)
C     SHIFT/BROAD DATA
  160 IF(SBOPT) 17,19,21
   17 READ(5,18) (JGROUP(J),SOBS(J), J = 1,NCENTR)
   18 FORMAT(7X,I2,8X,F6.1)
      GO TO 23
   19 READ(5,20) (JGROUP(J),SOSS(J),BOBS(J), J = 1,NCENTR)
   20 FORMAT((7X,I2,2(8X,F6.1)))
      GO TO 23
   21 READ(5,22) (JGROUP(J),BOBS(J), J = 1,NCENTR)
   22 FORMAT(7X,I2,22X,F6.1)
C     INITIAL SEARCH AREA
   23 READ(5,24) IRMIN,IPMAX,IPSTEP
   24 FORMAT(2(3X,I3,6X,I3,15X,I2))
      READ(5,25) IPHIMN,IPHIMX,IPHIST
      READ(5,25) IPSIMN,IPSIMX,IPSIST
   25 FORMAT(2(3X,I3,6X,I3,15X,I2))
C
```

```
      END
      SUBROUTINE DATEST(X,Y,Z,NPROT,ATOM,BOND,BONGLE,PI,NCALL)
      DIMENSION D(50,50),NHEAD(50),X(100),Y(100),Z(100),BOND(200),STAR(2
     +),WORD(16),M(4)
      DATA STAR/'*','*'/
      INTEGER A(50),B(50),C(50),BONGLE,ATOM
C     SET FLAGS AND MARKERS . ENTER COORDS OF ORIGIN AS NPROT+1
      NCALL = NCALL + 1
      JFLAG = 0
      NSTART = NTABLE = 1
      NPRINT = NPROT + ATOM
      X(NPRINT+1) = Y(NPRINT+1) = Z(NPRINT+1) = 0.0
      IF(NCALL .EQ. 1) WRITE(6,899)
  899 FORMAT(1H1/32X,'INTER-ATOMIC DISTANCE TABLE . BONDS MARKED (*) . G
     +ENERATED BY TEST OPTION = 1')
C     FILL D AND NHEAD ARRAYS ... I=HORIZONTAL : J,K=VERTICAL AXES
      DO 900 I = 1,NPRINT+1
      NHEAD(I) = I
      DO 900 J = 1,NPRINT+1
  900 D(I,J) = SQRT((X(I)-X(J))**2 + (Y(I)-Y(J))**2 + (Z(I)-Z(J))**2)
C     COUNTS TABLES ... DETECTS LAST TABLE
      TABLES = FLOAT(NPRINT)/16.0
  901 IF(TABLES - NTABLE .LE. 0.0) JFLAG = 1
      NFIN = NSTART + 15
      IF(JFLAG .EQ. 1) NFIN = NPRINT
C     WRITE HEADINGS
      WRITE(6,902)(NHEAD(I), I = NSTART, NFIN)
  902 FORMAT(1HO//2X,16I4)
C     WRITE DISTANCES FROM ORIGIN
      WRITE(6,903)(D(I,NPRINT+1),I =  NSTART,NFIN)
  903 FORMAT(/2X,'0 ',16F8.4)
C     WRITE HALF-DIAGONAL SUPPRESSED DISTANCE TABLE
      DO 910 K = 2 , NPRINT
      J = NPRINT + 2 - K
      NSTOP = J - 1
      IF(J .GT. NFIN) NSTOP = NFIN
      IF(NSTOP-NSTART+1 .EQ. 0) GO TO 911
      REWIND 8
      WRITE(8,905) BOND(2*J-1),BOND(2*J)
  905 FORMAT(2A6)
      REWIND 8
      READ(8,906) (M(I),I = 1,4)
  906 FORMAT(4(1X,I2))
      DO 907 KI = 1,16
  907 WORD(KI) = STAR(1)
      DO 908 KJ = 1,4
      N = M(KJ)
      IF(N.GT.0.AND.N.GE.NSTART.AND.N.LE.NSTOP) WORD(N-NSTART+1)=STAR(2)
  908 CONTINUE
      WRITE(6,909) K,(D(I,J),WORD(I-NSTART+1) , I = NSTART,NSTOP)
  909 FORMAT(/1X,I2,2X,16(F7.4,A1))
  910 CONTINUE
C     CHECK IF LAST TABLE ... IF NOT RESET MARKERS
  911 IF(JFLAG .EQ. 1) GO TO 912
      NTABLE = NTABLE + 1
      NSTART = NSTART + 16
      GO TO 901
C     NOW CALCULATES REQUESTED BOND ANGLES
  912 IF(BONGLE .EQ. 0) GO TO 917
      IF(NCALL .GT. 2) GO TO 915
      READ(5,913) (A(I),B(I),C(I),I = 1,BONGLE)
  913 FORMAT(100(I2,2(1X,I2)/))
      WRITE(6,914)
  914 FORMAT(1H1/55X,'TABLE OF SPECIFIED BOND ANGLES'//)
  915 DO 917 N = 1,BONGLE
      SA = D(B(N),C(N))
      SB = D(A(N),C(N))
      SC = D(A(N),B(N))
      ANGABC = ACOS((SC**2 + SA**2 - SB**2)/(2.0 * SC * SA)) / PI
      IF(A(N) .EQ. NPROT+1) A(N) = 0
      IF(B(N) .EQ. NPROT+1) B(N) = 0
      IF(C(N) .EQ. NPROT+1) C(N) = 0
      WRITE(6,916) N,A(N),B(N),C(N),ANGABC
  916 FORMAT(/30X,'BOND ANGLE ',I2,' BETWEEN ATOMS (',I2,'-',I2,'-',I2,'
     +) = ',F7.3,' DEGREES')
  917 CONTINUE
      IF(NCALL .GE. 2) RETURN
      STOP
      END
      SUBROUTINE WRITE4(ROTINC)
      COMMON IRMIN,IRMAX,IRSTEP,IPHIMN,IPHIMX,IPHIST,IPSIMN,IPSIMX,IPSIS
     +T,ITER,NITER,LIM,ROTEMP(7,100),LOCATE(100),BOND(200)
      COMMON          /DATA/NOENTR,NGROUP(100),SOBS(100),BOBS(100),NPROT
     +,NSIGN,NORM,NAME(100),NUMAV(100),PROTX(100),PROTY(100),PROTZ(1 (),
     *JGROUP(100),TITLE(8)/FITLIM/FITLIM(3),TYPLIM,FIT(3),TOL(3)
      INTEGER/NAME/REFLEC,SBOPT,RUN,TEST,BONGLE,OMITA,OMITC,CONTUR,ATOM/,
     +ROTN/CYCLE,GYRO(100),ROTN,ROTMAT,ROTOPT
      DIMENSION WORDS(6),WORDS(11),QUERY(2)
      DATA QUERY/'  ',' QUERY'/
      DATA WORDS/'SHIFT',' ','BROAD','NEGATIVE','UNKNOWN','POSITIVE'/
      DATA WORDS/'XY','XZ',' ','XY','XZ','XY','XZ','XY','XZ','S','H'/
C
C     WRITE BLOCK 1 ... OUTPUTS INPUT DATA
C
      IF(OMITA .EQ. 0) GO TO 499
      IF(CONTUR .GT. 0 .AND. OMITA .EQ  1) GO TO 544
      RETURN
  499 WRITE(6,500) (TITLE(I), I=1,8)
  500 FORMAT(1H1/29X,'OMETFINDMETFINDMETFINDMETFINDMETFINDMETFINDMETFIN
     +DMETFINDMETFINDMETFINDMETFINDMETFINDMETFINDMETFINDMETFINDMETFINDMETFI
     +NDMETFINDMETFINDMETFINDMETFINDMETFINDMETFINDMETFINDMETFINDMETFINDMETF'/29X,'ME
     +TND  TF   TE    ET   FI   FI    TF   OME  IN      INDMETFI   MET  ND
     +    IN    ET'/29X,'ET   D   FI  METFIND  TFIN  ETFIND  TFI   ET  N
     +D  TF  OMETFIN  ETF   DME  INDM  FIN'/29X,'TF       IN     FINDM  FI
     +ND   FINDM  FIN    F   DM  FIN  ETFIND  TFI  MEI  NDME  IND'/29X,'F
     +I  N T   ND      INDME  INDM   INDME  IND T   ME  IND  TFINDME   I
     +METF  OMET  NDME'/29X,'IN  ETF  DM  FINDMEI  NDME  INDMET  NDM  FI
     +   ET   ND   TFINDMETF    METFI   METF  DME'/29X,'ND   TFI   ME      METF
     + DMET   NDMFI     ME   IND   IF      TFINDMETFIN METFI     TF     EI'/29X
     +,'DMETFINDMETFINDMETFINDMETFINDMETFINDMETFINDMETFINDMETFINDMETFINDMETFIND
     +METFINDMETFINDMETF'/29X,'METFINDMETFINDMETFINDMETFINDMETFINDMETFINDMETFIN
     +DMETFINDMETFINDMETFINDMETFINDMETFINDMETFI'//38X,8A8)
C
      IF(SBOPT) 501,503,501
  501 WRITE(6,502) SBOPT,WORDS(SBOPT+2)
  502 FORMAT(//37X,'DATA INPUT : SB OPTION = ',I2,'  I.E.  ONLY ',A5,' O
     +ATA HAS BEEN GIVEN')
      GO TO 505
  503 WRITE(6,504) SBOPT
  504 FORMAT(//32X,'DATA INPUT : SB OPTION = ',I2,'  I.E.  BOTH SHIFT AN
     +D BROAD DATA HAVE BEEN GIVEN')
  505 WRITE(6,506) NPROT,ATOM,NCENTR
  506 FORMAT(/12X,'TOTAL NUMBER OF SHIFTED ATOMS = ',I2,' , TOTAL NUMBER
     + OF NMR INACTIVE ATOMS = ',I2,' , TOTAL NUMBER OF SHIFTED CENTRES
     += ',I2)
C
      WRITE(6,507)
  507 FORMAT(//5X,'ATOM    REFERENCE     X-CO-ORD       Y-CO-ORD       Z-CO
     +-ORD      NGROUP  OBSERVED  OBSERVED       BONDED TO          GYRO-C
     +ODE'/4X,'NUMBER    NUMBERS',5X,'SHIFT      BROAD          ATOM NUMBER'
     +/)
C
C     LOOP FOR ONLY PRINTING SHIFT AND BROAD DATA ONCE PER GROUP
C
      I = J = 1
      GO TO 509
  508 I = I + 1
      IF(I .EQ. NPROT+1) GO TO 546
      IF(NGROUP(I) .EQ. NGROUP(I-1)) GO TO 511
      J = J + 1
  509 N = 1
      IF(NGROUP(I) .NE. JGROUP(J)) N = 2
      WRITE(6,510) I,NAME(I),NUMAV(I),NGROUP(I),PROTX(I),PROTY(I),PROTZ(
     +I),QUERY(N),JGROUP(J),SOBS(J),BOBS(J),QUERY(N),BOND(2*I-1),BOND(2*
     +I),GYRO(I)
  510 FORMAT(6X,I2,4X,A4,'/',I1,'/',I2,3(4X,F10.7),A6,I3,1X,2(4X,F6.1),
     +3A6,4X,I15)
      GO TO 508
  511 WRITE(6,512) I,NAME(I),NUMAV(I),NGROUP(I),PROTX(I),PROTY(I),PROTZ(
     +I),BOND(2*I-1),BOND(2*I),GYRO(I)
  512 FORMAT(6X,I2,4X,A4,'/',I1,'/',I2,3(4X,F10.7),36X,2A6,4X,I15)
      GO TO 508
  546 IF(ATOM .EQ. 0) GO TO 513
      WRITE(6,547)(I,NAME(I),PROTX(I),PROTY(I),PROTZ(I),BOND(2*I-1),BOND
     +(2*I),GYRO(I),I = NPROT+1 , NPROT+ATOM)
  547 FORMAT((6X,I2,4X,A4,9X,3(F10.7,4X),32X,2A6,4X,I15))
C
  513 IF(NORM .EQ. 1) WRITE(6,514)
  514 FORMAT(1HO/50X,'FIRST ATOM LISTED USED FOR NORMALISATION')
      IF(NORM .GT. 1) WRITE(6,515) NORM
  515 FORMAT(1HO/47X,'FIRST GROUP OF ',I1,' ATOMS USED FOR NORMALISATION
     +')
      IF(SBOPT .LE. 0) WRITE(6,516) WORDS(NSIGN+3)
  516 FORMAT(1HO,38X,'SIGN OF SHIFT OF NORMALISING ATOM/GROUP ASSUMED TO
     + BE ',A8)
C
      WRITE(6,517) IRMIN,IRMAX,IRSTEP,IPHIMN,IPHIMX,IPHIST,IPSIMN,IPSIMX
     +, IPSIST
  517 FORMAT(1HO/43X,'PARAMETERS GIVEN FOR THE INITIAL METAL SEARCH WERE
     + ...'//28X,'RADIUS OF SEARCH FROM ',I3,' TO ',I3,' IN STEPS OF ',I
     +2,' NANO-METRES FROM THE ORIGIN'//25X,'DIRECTION OF SEARCH FROM ',
```

```
     +I3,* TO *,I3,* IN STEPS OF *,I2,* DEGREES FROM THE XZ-PLANE THROUG
     +H THE Y-AXIS*//41X,*AND FROM *,I3,* TO *,I3,* IN STEPS OF *,I2,* D
     +EGREES FROM THE X-AXIS IN THE XZ-PLANE*)
C
      WRITE(6,518) ITER
  518 FORMAT(1H0//57X,*... OPTIONS SELECTED ....*//32X,*ITERATION OPTION
     + = *,I1,*  I.E.*)
      IF(ITER .EQ. 0) WRITE(6,519)
  519 FORMAT(1H+,59X,*NON-ITERATIVE MODE . ONLY ONE SEARCH PERFORMED*)
      IF(ITER .EQ. 1) WRITE(6,520)
  520 FORMAT(1H+,59X,*FOCUSING MODE . SEARCHES FOR MAXIMUM FITFACTOR*)
      IF(ITER .GT. 1) WRITE(6,521) ITER-1
  521 FORMAT(1H+,59X,*MULTISCAN MODE . PERFORMS *,I1,* BLOCK SEARCH PATT
     +ERNS*)
C
      IF(ROTOPT .EQ. 0) WRITE(6,548)
  548 FORMAT(1H0/60X,*THE ROTATE OPTION HAS NOT BEEN SELECTED*)
      IF(ROTOPT .GE.1) WRITE(6,549) ROTN,ROTINC
  549 FORMAT(1H0/28X,*THE ROTATE OPTION HAS BEEN SELECTED AND HAS BEEN G
     +IVEN THE VALUE = *,I15/1H0,24X,*THE MAGNITUDE OF THE FIRST DIGIT H
     +AS SELECTED AN INITIAL ROTATIONAL STEP OF *,F4.1,* DEGREES*/1H0,14X
     +,*THE SUBSEQUENT DIGITS (ONE PER CYCLE) INDICATE THE REQUIRED OPERA
     +TION FOR EACH CYCLE . THESE PARAMETERS ARE*/1H ,12X,*USED IN CONJU
     +NCTION WITH THE ATOMIC CYPOCODE TO CONTROL THE ROTATIONAL OPTIMISA
     +TION PROCESS - SEE PROGRAM GUIDE*)
C
      GO TO (522,524,524,522,524,524,522,522,522,522) , (REFLEC+1)
  522 WRITE(6,523) REFLEC
  523 FORMAT(1H0/25X,*REFLEC OPTION = *,I1,*  I.E.  REFLECTION OF THE ME
     +TAL POSITION HAS NOT BEEN REQUESTED*)
      GO TO 526
  524 WRITE(6,525) REFLEC,NWORD(REFLEC)
  525 FORMAT(1H0/25X,*REFLEC OPTION = *,I1,*  I.E.  REFLECTION OF THE ME
     +TAL POSITION IN THE *,A2,*-PLANE HAS BEEN REQUESTED*)
C
  526 GO TO (527,527,527,529,529,529,527,527,529,529) , (REFLEC+1)
  527 WRITE(6,528)
  528 FORMAT(/60X,*ROTATIONAL AVERAGING OF METHYL GROUPS HAS NOT BEEN RE
     +QUESTED*)
      GO TO 531
  529 WRITE(6,530)
  530 FORMAT(/60X,*TWELVE POINT ROTATIONAL AVERAGING OF METHYL GROUPS HA
     +S BEEN REQUESTED*)
C
  531 GO TO (537,537,532,532,532,532,532,532,532,532) , (ITER+1)
  532 GO TO (533,535,535,533,535,535,535,535,535,535) , (REFLEC+1)
  533 WRITE(6,534)
  534 FORMAT(/60X,*SYMMETRY OF MULTISCAN OUTPUT HAS NOT BEEN ASSUMED*)
      GO TO 537
  535 NWORD = 10
      IF(REFLEC.EQ.2.OR.REFLEC.EQ.5.OR.REFLEC.EQ.7.OR.REFLEC.EQ.9)
     + NWORD = 11
      WRITE(6,536) NWORD(NWORD),NWORD(REFLEC)
  536 FORMAT(/60X,*SYMMETRY OF MULTISCAN OUTPUT ABOUT P*,A1,*I=180 HAS B
     +EEN ASSUMED (MOLECULAR *,A2,*-SYMMETRY)*)
C
  537 WRITE(6,538) (FIT(I),I = 1,3)
  538 FORMAT(1H0/26X,*THE ALLOWABLE TOLERANCES FOR THE SHIFT AND BROADEN
     +ING DATA HAVE BEEN SET AS FOLLOWS ...*//26X,*TOLERANCE FOR RUN(1)
     += *,F4.1,*   TOLERANCE FOR RUN(2) = *,F4.1,*   TOLERANCE FOR RUN(3
     +) = *,F4.1//26X,*DATA WHICH FALLS OUTSIDE THESE LIMITS , WILL BE G
     +IVEN A FITFACTOR OF ZERO IN THE TABLES*)
      IF(LIM .EQ. 2) WRITE(6,539)
  539 FORMAT(/29X,*LIM OPTION = 2  I.E.  ONLY THE SOLUTION TO THE MAXIMU
     +M FITFACTOR WILL BE PRINTED*)
      IF(LIM .LT. 2) WRITE(6,540) LIM,TYPLIM
  540 FORMAT(/29X,*LIM OPTION = *,I1,*  I.E.  ONLY SOLUTIONS WHOSE FITFA
     +CTORS EXCEED *,FF.4,* WILL BE PRINTED*)
C
      IF(TEST .EQ. 0) WRITE(6,541)
  541 FORMAT(1H0/38X,*TEST OPTION = 0  I.E.  TESTING OF THE PROGRAM/DATA
     + NOT REQUESTED*)
      IF(TEST .NE. 0) WRITE(6,542) TEST
  542 FORMAT(1H0/38X,*TEST OPTION = *,I1,*  I.E.  TESTING REQUESTED  .
     +SEE PROGRAM GUIDE*)
C
      IF(CONTUR .GT. 0) GO TO 544
      WRITE(6,543)
  543 FORMAT(1H0/38X,*CONTUR OPTION = 0  I.E.  GRAPHICAL OUTPUT HAS NOT
     +BEEN REQUESTED*////)
      RETURN
  544 WRITE(6,545) CONTUR
  545 FORMAT(1H0/38X,*CONTUR OPTION = *,I1,*  I.E.  GRAPHICAL OUTPUT HAS
     + BEEN REQUESTED*//38X,**********  A METDATA TAPE WILL BE CREAT
     +ED  ***********////)
C
```

```
C     WRITES CONTOUR INFORMATION ONTO TAPE9 FOR METDATA AND METPLOT
      CALL ATTACH(5HTAPE9,7HMETDATA,0,0,5HWRITE)
C     WRITE BLOCK 1 ONTO TAPE9
      WRITE(9,700)(TITLE(I),I=1,8),IRMIN,IRSTEP,NPROT+ATOM,ITER-1,REFLEC
  700 FORMAT(8A8/2(I3,2X),I2,2(2X,I1))
C     WRITE BLOCK 2 ONTO TAPE9
      WRITE(9,701) (NAME(I),PROTX(I),PROTY(I),PROTZ(I),BOND(2*I-1),BOND(
     +2*I),I = 1,NPROT+ATOM)
  701 FORMAT((A4,3(10X,F10.7),10X,2A6))
C
      RETURN
      END
      SUBROUTINE WHICH(NCYCOP,NROT,ATOM,PI,BONGLE,NCALL)
      INTEGER TEMP,ATOM/ROTN/CYCLE,GYRO(100),ROTN
      COMMON IRMIN,IRMAX,IRSTEP,IPHIMN,IPHIMX,IPHIST,IPSIMN,IPSIMX,IPSIS
     +T,ITER,NITER,LIM,ROTEMP(7,100),LOCATE(100),BOND(200)
      COMMON/DATA/NCENTR,NGROUP(100),SOBS(100),SOBS(100),NPROT,NSIGN,NOR
     +M,NAME(100),NUMAV(100),PROTX(100),PROTY(100),PROTZ(100)
C
      IF(CYCLE .GT. 1) GO TO 301
      L = NPROT
      J = NCENTR
      WRITE(6,299)
  299 FORMAT(1H1/13X,*INTER-ATOMIC DISTANCE TABLE . BONDS MARKED (*) . F
     +ROM INITIAL CO-ORD DATA BEFORE COMMENCING ROTATIONAL OPTIMISATION*
     +)
      CALL DATEST(PROTX,PROTY,PROTZ,NPROT,ATOM,BOND,BONGLE,PI,NCALL)
      DO 300 I = 1,NPROT+ATOM
      ROTEMP(1,I) = NUMAV(I)
      ROTEMP(2,I) = NGROUP(I)
      ROTEMP(3,I) = PROTX(I)
      ROTEMP(4,I) = PROTY(I)
      ROTEMP(5,I) = PROTZ(I)
      ROTEMP(6,I) = GYRO(I)
  300 ROTEMP(7,I) = SOBS(I)
C
  301 K = M = II = 0
      N = 15 - CYCLE
      N = 10**N
      NCYCOP = ROTN / N
      ROTN = ROTN - NCYCOP * N
      IF(NCYCOP .EQ. 0) STOP3
      IF(NCYCOP .NE. 4 .AND. NCYCOP .NE. 8) NROT = 0
C
      DO 303 I = 1,L+ATOM
      GYRO(I) = ROTEMP(6,I) / N
      ROTEMP(6,I) = ROTEMP(6,I) - GYRO(I) * N
      IF(NCYCOP .EQ. 4 .OR. NCYCOP .EQ. 8) GO TO 303
      NUMAV(I)=NGROUP(I)=PROTX(I)=PROTY(I)=PROTZ(I)=SOBS(I) = 0
      IF(GYRO(I).EQ.0.OR.I.GT.L.AND.GYRO(I).LT.2) GO TO 303
      IF(GYRO(I) .EQ. 0) GO TO 303
      IF(GYRO(I) .GT. 2 .AND. NROT .EQ  0) NROT = 1
      M = M + 1
      NUMAV(M) = ROTEMP(1,I)
      NGROUP(M) = ROTEMP(2,I)
      PROTX(M) = ROTEMP(3,I)
      PROTY(M) = ROTEMP(4,I)
      PROTZ(M) = ROTEMP(5,I)
      GYRO(M) = GYRO(I)
      LOCATE(M) = I
      IF(I .GT. L) GO TO 302
      IF(M .GT. 1) II = 1
      IF(NGROUP(M).EQ.NGROUP(M-II).AND.GYRO(M).NE.GYRO(M-II)) STOP4
      IF(M.GT.1.AND.NGROUP(M).EQ.NGROUP(M-II)) GO TO 303
      K = K + 1
      TEMP = NGROUP(M)
      SOBS(K) = ROTEMP(7,TEMP)
      GO TO 303
  302 NROT = NROT + 1
  303 CONTINUE
      IF(NCYCOP .EQ. 4 .OR. NCYCOP .EQ. 8) GO TO 304
C
      IF(M .LT. 3) STOP5
      SOBS(1) = ROTEMP(7,1)
      NCENTR = K
      NROT = NROT - 1
      NPROT = M - NROT
      IF(NPROT .EQ. -1) NPROT = M
      CALL WRITED(1,NCYCOP,CYCLE,L,NROT,M,ROTN)
      RETURN
C
  304 DO 305 M = 1,NPROT+NROT
      TEMP = LOCATE(M)
      ROTEMP(3,TEMP) = PROTX(M)
      ROTEMP(4,TEMP) = PROTY(M)
      ROTEMP(5,TEMP) = PROTZ(M)
```

```
      IF(ROTEMP(1,TEMP) .NE. NUMAV(M)) STOP6
  305 CONTINUE
C
      CALL WRITED(1,NCYCOP,ATOM,L,K,M,ROTN)
      IF(NCYCOP .EQ. 8) RETURN
      WRITE(6,306)
  306 FORMAT(1H1/15X,*INTER-ATOMIC DISTANCE TABLE . BONDS MARKED (*) . F
     *ROM NEW CO-ORD DATA GENERATED BY THE PREVIOUS ROTATION CYCLE*)
      DO 307 I = 1,L+ATOM
      PROTX(I) = ROTEMP(4,I)
      PROTY(I) = ROTEMP(5,I)
  307 PROTZ(I) = ROTEMP(6,I)
      CALL DATEST(PROTX,PROTY,PROTZ,L,ATOM,BOND,BONGLE,PI,NCALL)
      RETURN
      END
      SUBROUTINE ROTATE(ROTINC,GYRO,ROTWAY,LAST,MAXROT,N,PI,NROT,NCYCOP,
     *MXSFIT,MARKX)
      COMMON/MXFIT/MAXR,MAXPHI,MAXPSI
      COMMON/DATA/NCENTR,NGROUP(100),SOBS(100),BOBS(100),NPROT,NSIGN,NOR
     *M,NAME(100),NUMAV(100),PROTX(100),PROTY(100),PROTZ(100)
      DIMENSION A(3),B(3),C(20,3),X(20,3),CX(20,3),CY(20,3)
      INTEGER GYRO(100),ROTWAY
C
      IF(NCYCOP .EQ. 7 .AND. LAST .EQ. 9) GO TO 326
      IF(ROTWAY .NE. 1 .AND. LAST .LE. 0) GO TO 315
      IF(LAST .EQ. 0) GO TO 310
      N = N + 2
      ROTWAY = 1
  310 IF(ROTWAY .EQ. 1) IC=JC=KC=LC=NC=NC=MANGLE=LAST = 0
C
      IWAY = 1
      DO 313 I = 1,NPROT+NROT
      IF(GYRO(I) .NE. N) GO TO 312
      JC = JC + 1
      IF(JC .GT. 2) STOP7
      IF(JC .EQ. 2) GO TO 311
      A(1) = PROTX(I)
      A(2) = PROTY(I)
      A(3) = PROTZ(I)
      GO TO 313
C
  311 B(1) = PROTX(I)
      B(2) = PROTY(I)
      B(3) = PROTZ(I)
      GO TO 313
C
  312 IF(GYRO(I) .NE. N+1) GO TO 313
C
      KC = KC + 1
      X(KC,1) = PROTX(I)
      X(KC,2) = PROTY(I)
      X(KC,3) = PROTZ(I)
  313 CONTINUE
C
      IF(KC .EQ. 0 .OR. JC .LT. 2) GO TO 324
C
      BA1 = B(1) - A(1)
      BA2 = B(2) - A(2)
      BA3 = B(3) - A(3)
      AB = SQRT(BA1**2 + BA2**2 + BA3**2)
C
      DO 314 I = 1,KC
      AX2 = ((A(1)-X(I,1))**2+(A(2)-X(I,2))**2+(A(3)-X(I,3))**2)
      BX2 = ((B(1)-X(I,1))**2+(B(2)-X(I,2))**2+(B(3)-X(I,3))**2)
      AC = (AB**2 + AX2 - BX2) / (2 * AB)
      AC = AC / AB
C
      CA1 = AC * BA1
      CA2 = AC * BA2
      CA3 = AC * BA3
      C(I,1) = A(1) + CA1
      C(I,2) = A(2) + CA2
      C(I,3) = A(3) + CA3
      CX(I,1) = X(I,1) - C(I,1)
      CX(I,2) = X(I,2) - C(I,2)
      CX(I,3) = X(I,3) - C(I,3)
      CY1 = CA2 * CX(I,3) - CA3 * CX(I,2)
      CY2 = CA3 * CX(I,1) - CA1 * CX(I,3)
      CY3 = CA1 * CX(I,2) - CA2 * CX(I,1)
      YC2 = CY1**2 + CY2**2 + CY3**2
      YC = SQRT(CX(I,1)**2 + CX(I,2)**2 + CX(I,3)**2 / YC2)
      CY(I,1) = - CY1 * YC
      CY(I,2) = - CY2 * YC
      CY(I,3) = - CY3 * YC
  314 CONTINUE
      IF(NCYCOP .EQ. 7) RETURN
C
  315 IC = IC + 1
      LC = MARK = 0
      IF(NCYCOP .EQ. 6) GO TO 325
      IF(IC .GT. 1) GO TO 316
      TOTROT = ROTINC
      GO TO 319
  316 IF(IC .EQ. 2 .AND. ROTWAY .EQ. -1) IWAY = -1
      IF(IC .EQ. 2 .AND. ROTWAY .EQ. 0) IWAY = LAST = -1
      IF(IC.EQ.3.AND.LAST.EQ.-1.AND.ROTWAY.LT.0)IWAY=LAST=ROTWAY=0
      IF(IC.EQ.3.AND.LAST.EQ.-1.AND.ROTWAY.EQ.0) GO TO 316
      IF(ROTWAY .NE. 0 .AND. ROTWAY .NE. 2) GO TO 317
      IF(LAST .EQ. -1 .AND. ROTWAY .EQ. 0) GO TO 319
      MC = MC + 1
      TOTROT = TOTROT + ROTINC
      IF(ROTWAY .EQ. 2) MC = LAST = 0
  317 IF(IC.GE.2.AND.ROTWAY.NE.-1.OR.IC.EQ.2.AND.ROTWAY.EQ.-1) GO TO 319
      IF(MC .GT. 0) TOTROT = TOTROT - 0.5*(FLOAT(MC)+2.0)*ROTINC
  318 IF(MC .EQ. 0) TOTROT = TOTROT - ROTINC
      LAST = 1
  319 COSR = COS(TOTROT)
      SINR = SIN(TOTROT)
      IF(ABS(COSR) .LT. 1E-7) COSR = 1E-7
      IF(ABS(SINR) .LT. 1E-7) SINR = 1E-7
C
      IF(NCYCOP .EQ. 7 .AND. LAST .EQ. 9) GO TO 3191
      I1 = 1
      I2 = NPROT + NROT
      GO TO 3192
 3191 I1 = I2 = MARKX
      IF(MARKX .GT. MARK) LC = LC + 1
C
 3192 DO 322 I = I1, I2
      IF(GYRO(I) .NE. N+1) GO TO 322
      IF(NCYCOP .NE. 7) LC = LC + 1
      IF(IWAY) 321,320,320
  320 PROTX(I) = C(LC,1) + CY(LC,1)*COSR + CY(LC,1)*SINR
      PROTY(I) = C(LC,2) + CX(LC,2)*COSR + CY(LC,2)*SINR
      PROTZ(I) = C(LC,3) + CY(LC,3)*COSR + CY(LC,3)*SINR
      GO TO 322
  321 PROTX(I) = C(LC,1) + CX(LC,1)*COSR - CY(LC,1)*SINR
      PROTY(I) = C(LC,2) + CX(LC,2)*COSR - CY(LC,2)*SINR
      PROTZ(I) = C(LC,3) + CX(LC,3)*COSR - CY(LC,3)*SINR
  322 CONTINUE
      IF(NCYCOP .EQ. 7 .AND. LAST .EQ. 9) RETURN
      IF(KC .NE. LC) STOP10
      IF(LAST .EQ. 1) GO TO 323
C
      TOTROT = TOTROT / PI
      CALL WRITED(2,N,N+1,KC,IWAY,TOTROT,ROTINC)
      TOTROT = TOTROT * PI
      RETURN
  323 TOTROT = TOTROT / PI
      CALL WRITED(3,NROT,N+1,KC,IWAY,TOTROT,ROTINC)
      TOTROT = TOTROT * PI
      IF(N .EQ. 8) GO TO 324
      RETURN
C
  324 LAST = 2
      CALL WRITED(5,N,N+1,KC,IWAY,TOTROT,ROTINC)
      RETURN
C
  325 IF(MXSFIT .LT. MAXROT) GO TO 326
      MANGLE = NC
      MXTR = MAXR
      MXTPSI = MAXPSI
      MXTPHI = MAXPHI
  326 NC = NC + 1
      NNC = NC
      IF(MARKX .LT. MARK) LC = 1
      IF(NCYCOP .EQ. 7 .AND. NROT .EQ. 2) MARK = MARKX
      IF(NCYCOP .EQ. 7) NNC = NROT
      IF(NC .GE. 12 .AND. NCYCOP .NE. 7) GO TO 327
      IF(NC .GT. 6 .AND. NCYCOP .NE. 7) IWAY = -1
      IF(IWAY .EQ. -1) NNC = NC - 6
      TOTROT = FLOAT(NNC) * 30.0 * PI
      GO TO 319
  327 NCYCOP = 3
      MAXR = MXTR
      MAXPHI = MXTPHI
      MAXPSI = MXTPSI
      CALL NEWLIM
      LAST = IWAY = 1
      IF(MANGLE .GT. 6) IWAY = -1
      IF(IWAY .EQ. -1) MANGLE = MANGLE - 6
      TOTROT = FLOAT(MANGLE) * 30.0 * PI
```

```
      GO TO 319
      END
      SUBROUTINE DONEST(MAXROT,ROTWAY,ROTOPT,NCYCOP,GYRO,T1)
      COMMON IRMIN,IRMAX,IRSTEP,IPHIMN,IPHIMX,IPHIST,IPSIMN,IPSIMX,IPSIS
     +T,ITER,NITER,LIM/DATA/NRENTR,NGROUP(100),SOBS(100),BOBS(100),NPROT
     +,NSIGN,NORM,NAME(100),NUMAV(100),PROTX(100),PROTY(100),PROTZ(100),
     +JGROUP(100),TITLE(8)/FITLIM/FITLIM(3),TYPLIM,FIT(3),TOL(3)/WRITER/
     +SCALC(100),SCALC(100),SDIFF(100),BDIFF(100),SSTDEV(100),BSTDEV(100
     +),NSCAN,NSOLN,RANGLE,DANGLE,XMETAL,YMETAL,ZMETAL,SHIFTN,BROADN,R,I
     +,J,K,NR,NPHI,NPSI/MXFIT/MAXR,MAXPHI,MAXPSI,MFLAG(16),LAP(16,4),NSM
     +AX,MXSFIT,MXSR,MXSPHI,MXSPSI,NSMAX,MXBFIT,MXBR,MXBPHI,MXBPSI/TABLE
     +S/ISFIT(5,10,10),IBFIT(5,10,10)/JUMP/JUMP,PI,MULT,MPHI,MPSI
      INTEGER/NAME/REFLEC,SHOPT,RUN,TEST,BONGLE,OMITA,OMITC
      INTEGER ROTWAY,ROTOPT,GYRO(100)
      DIMENSION DIST(100),COSHMO(100),X(12),Y(12),Z(12),WORDS(2)
      DATA WORDS/'SHIFT','BROAD'/
C
C     BEGINNING OF DO NEST FOR METAL SCANNING
C
      IF(NCYCOP .NE. 8) GO TO 38
      LIM = JUMP = 2
   38 NITER = NITER + 1
      CALL SECOND(T)
      WRITE(4,2223) NITER,T-T1
 2223 FORMAT(10X,'START OF ITERATION ',I3,' , TIME USED = ',F8.3,' SECON
     +DS')
      NR = NSCAN = MFLAG(NITER) = ITOT = NTOT = MXSFIT = MXBFIT = 0
      LAP(NITER,1) = LAP(NITER,2) = LAP(NITER,3) = LAP(NITER,4) = 0
      SFIT = BFIT = 0.0
C
      DO 100 I = IRMIN,IRMAX,IRSTEP
      NR = NR + 1
      R = FLOAT(I) * 0.01
      NPHI = 0
C
      IF(NCYCOP .NE. 7) GO TO 39
      CALL SECOND(T)
      WRITE(4,2223) NITER,T-T1
   39 IF(JUMP .LT. 2 .OR. LIM .NE. 2) GO TO 40
      IF(ABS(FLOAT(I-MAXR)) .LE. FLOAT(IRSTEP)/2.0) GO TO 40
      GO TO 100
C
   40 DO 100 J = IPHIMN,IPHIMX,IPHISI
      NPHI = NPHI + 1
      PHI = FLOAT(180 - J) * PI
      NPSI = 0
C
      IF(JUMP .LT. 3 .OR. LIM .NE. 2) GO TO 41
      IF(ABS(FLOAT(J-MAXPHI)) .LE. FLOAT(IPHIST)/2.0) GO TO 41
      GO TO 100
C
   41 DO 100 K = IPSIMN,IPSIMX,IPSIST
      NPSI = NPSI + 1
      PSI = FLOAT(180 - K) * PI
C
      IF(JUMP .LT. 2 .OR. LIM .NE. 2) GO TO 42
      IF(ABS(FLOAT(K-MAXPSI)) .LE. FLOAT(IPSIST)/2.0) GO TO 42
      GO TO 100
C
   42 NSCAN = NSCAN + 1
      IGROUP = ISFIT(NR,NPHI,NPSI) = IBFIT(NR,NPHI,NPSI) = JFLAG = 0
      NSTOL = NBTOL = -1
      SSMDIF = BSMDIF = 0.00000000001
C
C     CALCULATES THE X,Y,Z COORDINATES OF THE METAL
      RXZPLN = R * COS(ABS(PHI))
      XMETAL = - RXZPLN * COS(ABS(PSI))
      YMETAL = R * SIN(PHI)
      ZMETAL = RXZPLN * SIN(PSI)
C
      IF(TEST .NE. 3) GO TO 43
      WRITE(6,920) NSCAN,I,J,K,XMETAL,YMETAL,ZMETAL
  920 FORMAT(/10X,'NSCAN = ',I3,' , R = ',I3,' , PHI = ',I3,' , PSI = ',
     +I3,' , X/Y/ZMETAL = ',3F9.4/)
C
C     CALCULATES BOND AND DIHEDRAL ANGLES
   43 IF(JUMP .NE. 2 .AND. TEST .NE. 2) GO TO 45
      RANGLE = 180.0 - ATAN(ABS(SQRT(YMETAL**2 + ZMETAL**2) / XMETAL))
     + / PI
      IF(YMETAL .NE. 0.0) GO TO 44
      DANGLE = 0.0
      GO TO 45
   44 DANGLE = ATAN(ABS(ZMETAL / YMETAL)) / PI
C
C     NOW CALCULATES PC SHIFT AND BROAD FOR EACH SHIFTED CENTRE
C
   45 DO 74 L = 1,NPROT
      SSTDV = BSTDV = 0.0
C
C     TESTS FOR WHETHER SINGLE SHIFTED CENTRE OR GROUP FOR AVERAGING
      IF(NUMAV(L) .EQ. 1 .AND. NCYCOP .NE. 7) GO TO 46
      IF(NUMAV(L) .EQ. 1) IFLAG = 6
      IF(IFLAG .EQ. NUMAV(L)) GO TO 46
      SSUM = BSUM = SSUM2 = BSUM2 = SMDIST = SUMCOS = 0.0
      ITOT = NTOT = NUMAV(L)
      IF(REFLEC.GT.2.AND.REFLEC.NE.6.AND.REFLEC.NE.7.AND.NUMAV(L).EQ.3)
     +  NTOT = 12
C
C     CALCULATES DISTANCE OF ATOM FROM METAL , ANGLE , SHIFT AND BROAD
   46 DISTX = XMETAL - PROTX(L)
      DISTY = YMETAL - PROTY(L)
      DISTZ = ZMETAL - PROTZ(L)
      DISMH2 = DISTX*DISTX + DISTY*DISTY + DISTZ*DISTZ
      DISTMH = SQRT(DISMH2)
      DISTP2=PROTX(L)*PROTX(L)+PROTY(L)*PROTY(L)+PROTZ(L)*PROTZ(L)
      HMOCOS= (DISMH2 + R**R - DISTP2) / (2.0 * DISTMH * R)
      SHIFTA = 10000.0 * (3.0 * HMOCOS**2 - 1.0)/(DISTMH*DISMH2)
      BROADA = 1.0E+06 / (DISTMH * DISMH2)**2
C
      IF(TEST .NE. 3) GO TO 47
      WRITE(6,921) L,NUMAV(L),ITOT,NTOT,PROTX(L),PROTY(L),PROTZ(L)
  921 FORMAT(10X,'NPROT = ',I2,' , NUMAV = ',I1,' , ITOT = ',I2,' , NTOT
     + = ',I2,' , PROTX/Y/Z = ',3F9.4)
      IF(L .GT. NORM) GO TO 922
      SHIFTN = SHIFTA
      BROADN = BROADA
  922 SHNORM = SHIFTA * SOBS(1) / SHIFTN
      BRNORM = BROADA * BOBS(1) / BROADN
      WRITE(6,923) DISTX,DISTY,DISTZ,SHIFTA,SHNORM,BROADA,BRNORM
  923 FORMAT(10X,'DISTX/Y/Z = ',3F9.4,' , SHIFTA = (',F8.3,',',F8.3,') ,
     + BROADA = (',F8.3,',',F8.3,')')
C
   47 IF(REFLEC.EQ.1.OR.REFLEC.EQ.2.OR.REFLEC.EQ.4.OR.REFLEC.EQ.5)GOTO48
      SHIFT = SHIFTA
      BROAD = BROADA
      GO TO 49
C
C     REFLECTS METAL IN XY OR XZ PLANE AND RECALCULATES DATA
   48 IF(REFLEC.EQ.1.OR.REFLEC.EQ.4) DISTZ = -ZMETAL - PROTZ(L)
      IF(REFLEC.EQ.2.OR.REFLEC.EQ.5) DISTY = -YMETAL - PROTY(L)
      DISMH2 = DISTX*DISTX + DISTY*DISTY + DISTZ*DISTZ
      DISTMH = SQRT(DISMH2)
      HMOCOS= (DISMH2 + R**R - DISTP2) / (2.0 * DISTMH * R)
      SHIFTB = 10000.0 * (3.0 * HMOCOS**2 - 1.0)/(DISTMH*DISMH2)
      SHIFT = (SHIFTA + SHIFTB) / 2.0
      BROADB = 1.0E+06 / (DISTMH * DISMH2)**2
      BROAD = (BROADA + BROADB) / 2.0
C
      IF(TEST .NE. 3) GO TO 49
      IF(L .GT. NORM) GO TO 924
      SHIFTN = SHIFT
      BROADN = BROAD
  924 SHNORM = SHIFTB * SOBS(1) / SHIFTN
      BRNORM = BROADB * BOBS(1) / BROADN
      SHNAV  = SHIFT  * SOBS(1) / SHIFTN
      BRNAV  = BROAD  * BOBS(1) / BROADN
      WRITE(6,925) DISTX,DISTY,DISTZ,SHIFTB,SHNORM,SHNAV,BROADB,BRNORM,
     + BRNAV
  925 FORMAT(10X,'DISTX/Y/Z = ',3F9.4,' , SHIFTB = (',F8.3,',',F8.3,',',
     +F8.3,') , BROADB = (',F8.3,',',F8.3,',',F8.3,',',F8.3,')')
C
C     NOW APPLIES TEST TO SEE IF PART OF A GROUP TO BE AVERAGED
   49 IF(NUMAV(L).EQ.1.AND.GYRO(L).NE.3.OR.NUMAV(L).EQ.1.AND.GYRO(L).EQ.
     +3.AND.NCYCOP.NE.7) GO TO 62
      SMDIST = SMDIST + DISTMH
      SUMCOS = SUMCOS + HMOCOS
      SSUM = SSUM + SHIFT
      BSUM = BSUM + BROAD
      SSUM2 = SSUM2 + SHIFT**2
      BSUM2 = BSUM2 + BROAD**2
      IF(NCYCOP .NE. 7 .OR. GYRO(L) .NE. 3) GO TO 491
      JFLAG = JFLAG + 1
      CALL ROTATE(0.5,GYRO,ROTWAY,9,MAXROT,2,PI,JFLAG,7,MXSFIT,L)
      IF(JFLAG .EQ. 12) GO TO 491
      GO TO 46
C     COUNTS NUMBER OF PROTONS IN GROUP , IF LAST ONE AVERAGES RESULT
  491 IFLAG = NUMAV(L)
      ITOT = ITOT - 1
      X(NTOT) = PROTX(L)
      Y(NTOT) = PROTY(L)
      Z(NTOT) = PROTZ(L)
```

```
      NTOT = NTOT - 1
      JFLAG = 0
      IF(ITOT .GT. 0) GO TO 74
      IF(NUMAV(L) .EQ. 2 .OR. NCYCOP .EQ. 7) GO TO 61
      IF(ITOT .LT.0)  GO TO 50
      XTEMP = PROTX(L)
      YTEMP = PROTY(L)
      ZTEMP = PROTZ(L)
   50 IF(NTOT.EQ.0)  GO TO 60
      GO TO (51,52,53,54,55,56,57,58,59) , NTOT
   51 PROTX(L) =  + 0.66667*X(10)  + 0.66667*X(11)  - 0.33333*X(12)
      PROTY(L) =  + 0.66667*Y(10)  + 0.66667*Y(11)  - 0.33333*Y(12)
      PROTZ(L) =  + 0.66667*Z(10)  + 0.66667*Z(11)  - 0.33333*Z(12)
      GO TO 46
   52 PROTX(L) =  + 0.66667*X(10)  - 0.33333*X(11)  + 0.66667*X(12)
      PROTY(L) =  + 0.66667*Y(10)  - 0.33333*Y(11)  + 0.66667*Y(12)
      PROTZ(L) =  + 0.66667*Z(10)  - 0.33333*Z(11)  + 0.66667*Z(12)
      GO TO 46
   53 PROTX(L) =  - 0.33333*X(10)  + 0.66667*X(11)  + 0.66667*X(12)
      PROTY(L) =  - 0.33333*Y(10)  + 0.66667*Y(11)  + 0.66667*Y(12)
      PROTZ(L) =  - 0.33333*Z(10)  + 0.66667*Z(11)  + 0.66667*Z(12)
      GO TO 46
   54 PROTX(L) =  + 0.91068*X(10)  + 0.33333*X(11)  - 0.24401*X(12)
      PROTY(L) =  + 0.91068*Y(10)  + 0.33333*Y(11)  - 0.24401*Y(12)
      PROTZ(L) =  + 0.91068*Z(10)  + 0.33333*Z(11)  - 0.24401*Z(12)
      GO TO 46
   55 PROTX(L) =  + 0.91068*X(10)  - 0.24401*X(11)  + 0.33333*X(12)
      PROTY(L) =  + 0.91068*Y(10)  - 0.24401*Y(11)  + 0.33333*Y(12)
      PROTZ(L) =  + 0.91068*Z(10)  - 0.24401*Z(11)  + 0.33333*Z(12)
      GO TO 46
   56 PROTX(L) =  + 0.33333*X(10)  + 0.91068*X(11)  - 0.24401*X(12)
      PROTY(L) =  + 0.33333*Y(10)  + 0.91068*Y(11)  - 0.24401*Y(12)
      PROTZ(L) =  + 0.33333*Z(10)  + 0.91068*Z(11)  - 0.24401*Z(12)
      GO TO 46
   57 PROTX(L) =  + 0.33333*X(10)  - 0.24401*X(11)  + 0.91068*X(12)
      PROTY(L) =  + 0.33333*Y(10)  - 0.24401*Y(11)  + 0.91068*Y(12)
      PROTZ(L) =  + 0.33333*Z(10)  - 0.24401*Z(11)  + 0.91068*Z(12)
      GO TO 46
   58 PROTX(L) =  - 0.24401*X(10)  + 0.91068*X(11)  + 0.33333*X(12)
      PROTY(L) =  - 0.24401*Y(10)  + 0.91068*Y(11)  + 0.33333*Y(12)
      PROTZ(L) =  - 0.24401*Z(10)  + 0.91068*Z(11)  + 0.33333*Z(12)
      GO TO 46
   59 PROTX(L) =  - 0.24401*X(10)  + 0.33333*X(11)  + 0.91068*X(12)
      PROTY(L) =  - 0.24401*Y(10)  + 0.33333*Y(11)  + 0.91068*Y(12)
      PROTZ(L) =  - 0.24401*Z(10)  + 0.33333*Z(11)  + 0.91068*Z(12)
      GO TO 46
   60 PROTX(L) = XTEMP
      PROTY(L) = YTEMP
      PROTZ(L) = ZTEMP
   61 IF((REFLEC.EQ.3.OR.REFLEC.EQ.4.OR.REFLEC.EQ.5.OR.REFLEC.EQ.6.OR.RE
     +FLEC.EQ.9).AND.NUMAV(L).EQ.3)  NUMAV(L) = 12
      IF(NCYCOP .EQ. 7 .AND. NUMAV(L) .EQ. 12) NUMAV(L) = 3
      IF(NCYCOP .EQ. 7 .AND. GYRO(L) .EQ. 3) NUMAV(L) = NUMAV(L) * 12
C
C     AVERAGES GROUP RESULTS
      IFLAG = 1
      DISTMH = SMDIST / FLOAT(NUMAV(L))
      HMOCOS = SUMCOS / FLOAT(NUMAV(L))
      SHIFT = SSUM / FLOAT(NUMAV(L))
      AVSH2 = SSUM2 /FLOAT(NUMAV(L))
      BROAD = BSUM / FLOAT(NUMAV(L))
      AVB2 = BSUM2 / FLOAT(NUMAV(L))
      SSTDV = SQRT(ABS(AVSH2 - SHIFT**2))
      BSTDV = SQRT(ABS(AVB2 - BROAD**2))
      IF(NCYCOP .EQ. 7 .AND. GYRO(L) .EQ. 3) NUMAV(L) = NUMAV(L) / 12
      IF(NUMAV(L) .EQ. 12)  NUMAV(L) = 3
C
C     SET NORMALISING SHIFT AND BROAD
   62 IF(L .NE. NORM) GO TO 69
      SHIFTN = SHIFT
      BROADN = BROAD
      IF(SBOPT .GT. 0) GO TO 68
C     TESTS IF NORMALISING GROUP HAS CORRECT SIGN OF SHIFT
      GO TO (63,64) , NSIGN
   63 IF(SHIFTN .GT. 0) GO TO 100
      GO TO 68
   64 IF(SHIFTN .LT. 0) GO TO 100
C
C     CALC PC SHIFTS AND BROADS .. TESTS IF WITHIN TOLERANCES
   69 IGROUP = IGROUP + 1
      JGROUP(IGROUP) = NGROUP(L)
      DIST(IGROUP) = DISTMH
      COSHMO(IGROUP) = HMOCOS
      IF(TEST .EQ. 5 .AND. JUMP .EQ. 2) GO TO 69
C
      IF(SBOPT) 69,69,71
   69 SCALC(IGROUP) = SOBS(1) * SHIFT / SHIFTN
      SDIFF(IGROUP) = (SCALC(IGROUP)-SOBS(IGROUP))*100.0/SOBS(IGROUP)
      ABDIFF = ABS(SDIFF(IGROUP))
      SSTDV(IGROUP) = SSTDV
      IF(TEST .EQ. 2)  GO TO 70
      TESTOL = TOL(RUN)
      IF(SOBS(IGROUP) .LT. 0.2*SOBS(1)) TESTOL = TOL(RUN) *0.2 * SOBS(1)
     +  / SOBS(IGROUP)
      IF(SOBS(IGROUP).GT.SOBS(1)) TESTOL=TOL(RUN)*SOBS(IGROUP)/SOBS(1)
      IF(TEST .EQ. 3) WRITE(6,926) WORDS(1),SOBS(IGROUP),SCALC(IGROUP),
     + SDIFF(IGROUP),TESTOL
  926 FORMAT(10X,A5,* OBS = *,F8.3,* , CALC = *,F8.3,* , PC DIFF = *,F8.
     +3,* , TESTOL = *,F8.3)
      IF(TEST .EQ. 5 .AND. SBOPT .EQ. 1) GO TO 71
      IF(ABDIFF.GT.TESTOL)  GO TO 100
      IF(SOBS(IGROUP) .GT. SOBS(1))  GO TO 71
   70 SSMDIF = SSMDIF + SDIFF(IGROUP)**2
      NSTOL = NSTOL + 1
C
   71 IF(TEST .EQ. 4 .AND. JUMP .EQ. 2) GO TO 72
      IF(SBOPT) 74,72,72
   72 BCALC(IGROUP) = BOBS(1) * BROADN / BROADN
      BDIFF(IGROUP) = (BCALC(IGROUP)-BOBS(IGROUP))*100.0/BOBS(IGROUP)
      ABDIFF = ABS(BDIFF(IGROUP))
      BSTDV(IGROUP) = BSTDV
      IF(TEST .EQ. 2) GO TO 73
      TESTOL = TOL(RUN)
      IF(BOBS(IGROUP) .LT. 0.2*BOBS(1)) TESTOL = TOL(RUN) *0.2 * BOBS(1)
     +  / BOBS(IGROUP)
      IF(BOBS(IGROUP).GT.BOBS(1)) TESTOL=TOL(RUN)*BOBS(IGROUP)/BOBS(1)
      IF(TEST .EQ. 3) WRITE(6,926) WORDS(2),BOBS(IGROUP),BCALC(IGROUP),
     + BDIFF(IGROUP),TESTOL
      IF(TEST .EQ. 4 .AND. SBOPT .EQ. -1) GO TO 74
      IF(ABDIFF .GT. TESTOL)  GO TO 100
      IF(BOBS(IGROUP) .GT. BOBS(1)) GO TO 74
   73 BSMDIF = BSMDIF + BDIFF(IGROUP)**2
      NBTOL = NBTOL + 1
   74 CONTINUE
C
C     IF GET HERE THEN ALL TESTS OK
C
C     CALCULATES GOODNESS OF FIT FACTORS
      IF(SBOPT) 75,75,77
   75 IF(NSTOL .EQ. 0) GO TO 76
      SFIT = 1.0 - SQRT(SSMDIF / FLOAT(NSTOL)) / 100.0
      IF(SFIT .GT. FITLIM(RUN)) ISFIT(NR,NPHI,NPSI) = IFIX((SFIT -FITLIM
     +(RUN)) * 1000.0 / (1.0 - FITLIM(RUN)))
C
   76 IF(SBOPT) 78,77,77
   77 IF(NBTOL .EQ. 0) GO TO 78
      BFIT = 1.0 - SQRT(BSMDIF / FLOAT(NBTOL)) / 100.0
      IF(BFIT .GT. FITLIM(RUN)) IBFIT(NR,NPHI,NPSI) = IFIX((BFIT -FITLIM
     +(RUN)) * 1000.0 / (1.0 - FITLIM(RUN)))
C
C     TESTS FOR CALLING WRITEB
   78 IF(TEST .EQ. 2)  CALL WRITEB(DIST,COSHMO,LIM,FITLIM,TYPLIM,ROTOPT)
      IF(NCYCOP .EQ. 8)  CALL WRITEB(DIST,COSHMO,NCYCOP,FITLIM,TYPLIM,ROT
     +OPT)
      IF(NCYCOP .EQ. 8) RETURN
      IF(JUMP.LT.2)  GO TO 79
      IF(LIM .EQ. 2) CALL WRITEB(DIST,COSHMO,LIM,FITLIM,TYPLIM,ROTOPT)
      IF(ROTOPT .GT. 0 .AND. JUMP .EQ. 2 .OR. NCYCOP .EQ. 8) RETURN
      IF(((SBOPT.EQ.-1 .OR. SBOPT.EQ.0).AND. SFIT.GT.TYPLIM) .OR. ((SBOP
     +T.EQ.0 .OR. SBOPT.EQ.1).AND. BFIT.GT.TYPLIM))  CALL WRITEB(DIST,CO
     +SHMO,LIM,FITLIM,TYPLIM,ROTOPT)
C
C     FINDS MXFIT TO CENTRE SEARCH
C
   79 IF(SBOPT) 80,80,83
   80 IF(ISFIT(NR,NPHI,NPSI) .LT. MXSFIT) GO TO 86
      IF(ISFIT(NR,NPHI,NPSI) .GT. MXSFIT) GO TO 81
      NSMAX = NSMAX + 1
      MXSR = MXSR + I
      MXSPHI = MXSPHI + J
      MXSPSI = MXSPSI + K
      GO TO 82
   81 MXSFIT = ISFIT(NR,NPHI,NPSI)
      NSMAX = 1
      MXSR = I
      MXSPHI = J
      MXSPSI = K
C
   82 IF(SBOPT) 86,83,83
   83 IF(IBFIT(NR,NPHI,NPSI) .LT. MXBFIT) GO TO 86
      IF(IBFIT(NR,NPHI,NPSI) .GT. MXBFIT) GO TO 84
      NBMAX = NBMAX + 1
```

```
      MXBR = MXBR + I
      MXBPHI = MXBPHI + J
      MXBPSI = MXBPSI + K
      GO TO 86
   84 MXBFIT = IBFIT(NR,NPHI,NPSI)
      NBMAX = 1
      MXBR = I
      MXBPHI = J
      MXBPSI = K
C
C     CHECKS IF ONLY RESULTS ON EDGE OF TABLE
   85 IF(SBOPT .GT. 0) GO TO 100
      IF(MFLAG(NITER).EQ.1.OR.ISFIT(NR,NPHI,NPSI).EQ.0.OR.ITER.LT.2)
     + GO TO 100
      GO TO (87,88,89,87,88,89,88,89,88,89) , (REFLEC+1)
   87 IF(J.EQ.135.OR.J.EQ.180.OR.J.EQ.225.OR.K.EQ.135.OR.K.EQ.180.OR.K.
     + EQ.225)  GO TO 91
      GO TO 90
   88 IF(J.EQ.135.OR.J.EQ.180.OR.J.EQ.225.OR.K.EQ.135) GO TO 91
      GO TO 90
   89 IF(J.EQ.135.OR.K.EQ.135.OR.K.EQ.180.OR.K.EQ.225) GO TO 91
   90 MFLAG(NITER) = 1
      GO TO 100
   91 IF(NPSI .EQ. 1) LAP(NITER,1) = LAP(NITER,1) + 1
      IF(NPSI .EQ. 10) LAP(NITER,2) = LAP(NITER,2) + 1
      IF(NPHI .EQ. 1) LAP(NITER,3) = LAP(NITER,3) + 1
      IF(NPHI .EQ. 10) LAP(NITER,4) = LAP(NITER,4) + 1
C
  100 CONTINUE
C
C     PRODUCES REFERENCE COORDINATES FOR CENTERING SEARCH
C
      IF(SBOPT .LT. 0) GO TO 101
      MAXR = MXBR = MXBR / NBMAX
      MAXPHI = MXBPHI = MXBPHI / NBMAX
      MAXPSI = MXBPSI = MXBPSI / NBMAX
C
      IF(SBOPT .GT. 0) GO TO 102
  101 MAXR = MXSR = MXSR / NSMAX
      MAXPHI = MXSPHI = MXSPHI / NSMAX
      MAXPSI = MXSPSI = MXSPSI / NSMAX
C
  102 IF(ROTOPT .GT. 0) GO TO 106
      IF(MFLAG(NITER) .EQ. 1 .OR. SBOPT .GT. 0 .OR. ITER .LT. 2) RETURN
      IF(LAP(NITER-1) .EQ. 0) GO TO 103
      IF(MFLAG(NITER-1) .EQ. 0) MFLAG(NITER) = 1
  103 IF(LAP(NITER-3) .EQ. 0) RETURN
      GO TO (104,105,104,104,104,105,104,105,104,105,104) , (REFLEC+1)
  104 IF(MFLAG(NITER-4) .EQ. 0) MFLAG(NITER) = 1
      RETURN
  105 IF(MFLAG(NITER-2) .EQ. 0) MFLAG(NITER) = 1
      RETURN
C
  106 IF(MAXR.EQ.IRMIN.OR.MAXR.EQ.IRMAX.OR.MAXPHI.EQ.IPHIMN.OR.MAXPHI.EQ
     +.IPHIMX.OR.MAXPSI.EQ.IPSIMN.OR.MAXPSI.EQ.IPSIMX) GO TO 110
      IF(MXSFIT - MAXROT) 107,108,109
  107 ROTWAY = -1
      RETURN
  108 ROTWAY = 0
      RETURN
  109 ROTWAY = 2
      MAXROT = MXSFIT
      RETURN
  110 ROTWAY = -2
      RETURN
C
      END
      SUBROUTINE WRITE8(DIST,COSHMO,LIM,FITLIM,TYPLIM,ROTOPT)
      COMMON/DATA/NCENTR,NGROUP(100),SOBS(100),BOBS(100),NPROT,NS,NO,NAM
     +E(100),NUMAV(100),PROTX(100),PROTY(100),PROTZ(100),JGROUP(100)/TAB
     +LES/ISFIT(5,10,10),IBFIT(5,10,10)/WRITE8/SCALC(100),BCALC(100),SDI
     +FF(100),BDIFF(100),SSTDEV(100),BSTDEV(100),NSCAN,NSOLN,BANGLE,DANG
     +LE,XMETAL,YMETAL,ZMETAL,SHIFTN,BROADN,R,I,J,K,NR,NPHI,NPSI
      INTEGER/NAME/REFLEC,SBOPT,RUN,TEST
      DIMENSION DIST(100),COSHMO(100),WORDS(2),FITLIM(3)
      DATA WORDS/'SHIFT','BROADN'/
C
C     WRITE BLOCK NUMBER 2 ... OUTPUTS SOLUTIONS TO INDIVIDUAL SEARCHES
C
      NSOLN = NSOLN + 1
      IF(LIM .EQ. 8) GO TO 624
      WRITE(6,600) NSOLN,NSCAN
  600 FORMAT(1H0/19X,*SOLUTION NUMBER = *,I3,* ,*,54X,*, SCAN NUMBER = *
     +,I7)
      IF(TEST .EQ. 2) GO TO 603
      IF(LIM .EQ. 2) WRITE(6,601)
  601 FORMAT(1H+,42X,*TYPLIM NOT SELECTED - SOLUTION TO MAX FITFACTOR ON
     +LY*)
      IF(LIM .LT. 2) WRITE(6,602) TYPLIM
  602 FORMAT(1H+,42X,*TYPLIM HAS BEEN SELECTED ... IF FIT LT *,F5.4,* IG
     +NORED*)
      GO TO 605
  603 WRITE(6,604)
  604 FORMAT(1H+,42X,*TYPLIM NOT SELECTED - SOLUTIONS TO ALL SEARCH POIN
     +TS*)
C
  605 IF(SBOPT) 606,606,607
  606 FACTOR=(1.-FITLIM(RUN))*(FLOAT(ISFIT(NR,NPHI,NPSI))/1000.0)
     + + FITLIM(RUN)
      N = 1
      WRITE(6,608) WORDS(N),ISFIT(NR,NPHI,NPSI),FITLIM(RUN),FACTOR
      IF(SBOPT) 609,607,607
  607 FACTOR=(1.-FITLIM(RUN))*(FLOAT(IBFIT(NR,NPHI,NPSI))/1000.0)
     + + FITLIM(RUN)
      N = 2
      WRITE(6,608) WORDS(N),IBFIT(NR,NPHI,NPSI),FITLIM(RUN),FACTOR
  608 FORMAT(/19X,*FITFACTOR OF *,A5,* DATA FOR THIS SOLUTION = *,I3,* ,
     + AS TOLERANCE = *,F5.4,* , GOODNESS OF FIT = *,F5.4)
C
  609 WRITE(6,610) R,J,K
  610 FORMAT(/19X,*SEARCH PARAMETERS FOR THIS SOLUTION WERE ... .  RADIUS
     + = *,F4.2,* , ANGLE PHI = *,I3,* , ANGLE PSI = *,I3)
C
      WRITE(6,611) BANGLE,DANGLE
  611 FORMAT(/19X,*M-O-C BOND ANGLE = *,F7.3,* DEGREES     .....    M-O-C
     +-(XY-PLANE) DIHEDRAL ANGLE = *,F7.3,* DEGREES*)
C
      WRITE(6,612) XMETAL,YMETAL,ZMETAL
  612 FORMAT(/19X,*METAL CO-ORDINATES IN ANGSTROMS FROM THE BONDING SIT
     + E  X = *,F7.4,* , Y = *,F7.4,* , Z = *,F7.4)
C
      WRITE(6,613) SHIFTN,BROADN
  613 FORMAT(/19X,*NORMALISING ATOM/GROUP : ACTUAL CALCULATED SHIFT = *,
     +F9.4,* , CALCULATED BROADENING = *,F9.4)
C
      IF(TEST .EQ. 4 .OR. TEST .EQ. 5) GO TO 616
      IF(SBOPT) 614,616,614
  614 WRITE(6,615) WORDS(N)
  615 FORMAT(/28X,*NGROUP    *,A5,*S : OBSERVED  CALCULATED DIFFERENC  ST
     +AND.DEV.   DISTMH    HMOCOS*/)
      GO TO 618
  616 WRITE(6,617)
  617 FORMAT(/2X,*NGROUP    SHIFTS : OBSERVED  CALCULATED DIFFERENCE STAN
     +D.DEV.    BROADS : OBSERVED  CALCULATED DIFFERENCE STAND.DEV.   DIST
     +MH    HMOCOS*/)
C
      IF(TEST .EQ. 4 .OR. TEST .EQ. 5) GO TO 620
      IF(SBOPT) 618,620,622
  618 WRITE(6,619)(JGROUP(I),SOBS(I),SCALC(I),SDIFF(I),SSTDEV(I),DIST(I)
     + ,COSHMO(I) , I = 1,NCENTR)
  619 FORMAT((30X,I2,14X,4(F8.3,3X),F6.3,3X,F6.5))
      GO TO 623
  620 WRITE(6,621)(JGROUP(I),SOBS(I),SCALC(I),SDIFF(I),SSTDEV(I),BOBS(I)
     + ,BCALC(I),BDIFF(I),BSTDEV(I),DIST(I),COSHMO(I) , I = 1,NCENTR)
  621 FORMAT((3XI2,1X,2(1X,F8.3,3XF8.3,3XF8.3,3XF8.3,3XF8.3)3XF6.3,3XF6.5))
      GO TO 623
  622 WRITE(6,619)(JGROUP(I),BOBS(I),BCALC(I),BDIFF(I),BSTDEV(I),DIST(I)
     + ,COSHMO(I) , I = 1,NCENTR)
C
  623 IF(LIM .EQ. 2 .AND. TEST .NE. 2 .AND. ROTOPT .EQ. 0) STOP11
      RETURN
C
  624 WRITE(9,625) FITLIM(RUN),ISFIT(NR,NPHI,NPSI),R,J,K,XMETAL,YMETAL,
     +ZMETAL
  625 FORMAT(F5.3,3X,I3,3X,F4.2,2(3X,I3),3(3X,F10.7))
      WRITE(9,626)(JGROUP(I),SOBS(I),SCALC(I),SDIFF(I),SSTDEV(I),DIST(I)
     +,COSHMO(I) , I = 1,NCENTR)
  626 FORMAT((I2,4(3X,F8.3),3X,F6.3,3X,F6.5))
      RETURN
      END
      SUBROUTINE WRITEC
      COMMON IRMIN,IRMAX,IRSTEP,IPHIMN,IPHIMX,IPHIST,IPSIMN,IPSIMX,IPSIS
     +T,ITER,NITER,LIM/MXFIT/MAXR,MAXPHI,MAXPSI,MFLAG(16),LAP(16,4),NSMA
     +X,MXSFIT,MXSR,MXSPHI,MXSPSI,NBMAX,MXBFIT,MXBR,MXBPHI,MXBPSI/TABLES
     +/ISFIT(5,10,10),IBFIT(5,10,10)/JUMP/JUMP,PI,MULT,MPHI,MPSI/FITLIM/
     +FITLIM(3)
      INTEGER/NAME/REFLEC,SBOPT,RUN,TEST,BONGLE,OMITA,OMITC,CONTUR,ATOM/
     +ROTN/CYCLE,GYRO(100),ROTN,ROTWAY,ROTOPT
      DIMENSION WORDZ(10),IPSI(10)
      DATA WORDZ/'FIRST','FINAL','PHI','PSI','ROW','COL','+','1','SHIFT'
     + ,'BROAD'/
```

```
C
C     WRITE BLOCK NUMBER 3 ... GOODNESS OF FIT 3-D TABLES
C
      IF(JUMP .EQ. 2) STOP12
      IF(ROTOPT .GT. 0) LEAP = 1
C     TABLE SUPPRESSION BLOCK ... BECAUSE OF LACK OF RESULTS
      IF(SBOPT .EQ. 1) GO TO 813
C     WRITE BLOCK 3 ONTO TAPE9
      IF(CONTUP .GT. 0) WRITE(9,702) MPSI,MPHI,MULT,MXSFIT,MXSPSI,MXSPHI
     *,MXSR
  702 FORMAT(3(I2,2X),4(I3,2X))
C
      IF(MXSFIT .EQ. 0) GO TO 800
      GO TO 802
  800 WRITE(6,801) NITER,MULT,IRMIN,IRMAX,IRSTEP,IPHIMN,IPHIMX,IPHIST,
     * IPSIMN,IPSIMX,IPSIST
  801 FORMAT(1H0/20X,*NO RESULTS FOR ITERATION *,I2,* , MULT *,I1,* : SE
     +ARCH AREA R(*,I3,*-*,I3,*/*,I2,*) , PHI(*,I3,*-*,I3,*/*,I2,*) : PS
     +I(*,I3,*-*,I3,*/*,I2,*)*)
      IF(ITER .LE. 1) STOP13
      LEAP = 1
      RETURN
C     TABLE SUPPRESSED ... ONLY CONTAINS RESULTS DUPLICATED ELSEWHERE
C     WRITE BLOCK 4 ONTO TAPE9
  802 IF(CONTUP .GT. 0) WRITE(9,703) ISFIT
  703 FORMAT(25I3)
      IF(OMITC .EQ. 9) RETURN
      IF(FLAG(NITER).EQ.1.OR.SBOPT.GT.0.OR.ITER.LT.2) GO TO 813
      WRITE(6,803) NITER,MULT
  803 FORMAT(1H0/1X,*PRINTING OF THE TABLE FOR ITERATION *,I2,* , MULT
     +*,I1,* , SUPPRESSED AS ALL RESULTS DUPLICATED ON THE FOLLOWING TAB
     +LE(S) : */)
C     LISTS DETAILS OF OVERLAPPING EDGES
      IF(LAP(NITER,3) .EQ. 0) GO TO 806
      GO TO (804,805,804,804,805,804,805,804,805,804) , (REFLEC+1)
  804 WRITE(6,811) LAP(NITER,3),WORDZ(2),WORDZ(3),WORDZ(5),NITER-4
      GO TO 806
  805 WRITE(6,811) LAP(NITER,3),WORDZ(2),WORDZ(3),WORDZ(5),NITER-2
  806 IF(LAP(NITER,1) .EQ. 0) GO TO 807
      WRITE(6,811) LAP(NITER,1),WORDZ(2),WORDZ(4),WORDZ(6),NITER-1
  807 IF(LAP(NITER,4) .EQ. 0) GO TO 810
      GO TO (808,809,808,808,809,808,809,808,809,808) , (REFLEC+1)
  808 WRITE(6,811) LAP(NITER,4),WORDZ(1),WORDZ(3),WORDZ(5),NITER+4
      GO TO 810
  809 WRITE(6,811) LAP(NITER,4),WORDZ(1),WORDZ(3),WORDZ(5),NITER+2
  810 IF(LAP(NITER,2) .EQ. 0) GO TO 812
      WRITE(6,811) LAP(NITER,2),WORDZ(1),WORDZ(4),WORDZ(6),NITER+1
  811 FORMAT(43X,I2,* RESULTS IN THE *,A6,1XA3,1XA3,* OF ITERATION *,I2)
     +
  812 LEAP = 1
      RETURN
C
C     NOW WRITES OUT FITFACTOR TABLES
  813 IF(ITER .EQ. 0) JUMP = 2
      DO 814  I = 1,10
  814 IPSI(I) = IPSIMN + I * IPSIST - IPSIST
      IR2 = IRMIN + IRSTEP
      IR3 = IRMIN + 2 * IRSTEP
      IR4 = IRMAX - IRSTEP
      IF(NITER .EQ. OMITC+1 .AND. MULT .EQ. 1) LEAP = 1
      N = LEAP + 7
      IF(SBOPT)815,815,817
  815 WRITE(6,820)WORDZ(N),IRMIN,WORDZ(9),RUN,NITER,MULT,FITLIM(RUN)
     +,IR2
      WRITE(6,821) IR3,(IPSI(I),I = 1,10)
      WRITE(6,822) IR4,IRMAX,JUMP,MXSFIT,NSMAX,MXSR,MXSPHI,MXSPSI
      DO 816 I = 1 ,10
      K = IPHIMN + IPHIST * I - IPHIST
      WRITE(6,823) (ISFIT(1,I,J),J = 1,10)
      WRITE(6,824) (ISFIT(2,I,J),J = 1,10)
      WRITE(6,825) K,(ISFIT(3,I,J),J = 1,10)
      WRITE(6,826) (ISFIT(4,I,J),J = 1,10)
      WRITE(6,827) (ISFIT(5,I,J),J = 1,10)
  816 WRITE(6,828)
      WRITE(6,829)
      N = 7
      IF(SBOPT)819,817,817
  817 WRITE(6,820)WORDZ(N),IRMIN,WORDZ(10),RUN,NITER,MULT,FITLIM(RUN)
     +,IR2
      WRITE(6,821) IR3,(IPSI(I),I = 1,10)
      WRITE(6,822) IR4,IRMAX,JUMP,MXBFIT,NBMAX,MXBR,MXBPHI,MXBPSI
      DO 818 I = 1 ,10
      K = IPHIMN + IPHIST * I - IPHIST
      WRITE(6,823) (IBFIT(1,I,J),J = 1,10)
      WRITE(6,824) (IBFIT(2,I,J),J = 1,10)
      WRITE(6,825) K,(IBFIT(3,I,J),J = 1,10)
      WRITE(6,826) (IBFIT(4,I,J),J = 1,10)
      WRITE(6,827) (IBFIT(5,I,J),J = 1,10)
  818 WRITE(6,828)
      WRITE(6,829)
  819 LEAP = 0
      RETURN
  820 FORMAT(A1,*****R1=*,I3,***FIT FACTORS OF *,A5,* DATA FOR RUN *,I1
     +,*,ITERATION *,I2,*(MULT = *,I1,*),SCALING IS LINEAR SO THAT 0 = *
     +,F5.4,* OR LESS,AND 999 = .9999***/1X,**   R2=*,I3,*  **,10(11X,**
     +**))
  821 FORMAT(1X,**  R3=*,I3,*    **,(10(4X,I3,4X,**)))
  822 FORMAT(1X,** R4=*,I3,*    **,1(11X,**)/1X,**P=*,I3,***** *,11,*
     + ***PSI****MAX FIT FACTOR = *,I3,* , APPEARED *,I2,* TIMES , AVERA
     +GE LOCATED AT R = *,I3,* , PHI = *,I2,* , AND PSI = *,I3,*****PSI*
     +******)
  823 FORMAT((1X,**,11(11X,**)/1X,**,11X,**,10(6X,I3,*  **)))
  824 FORMAT((1X,**,11X,*R*,10(5X,I3,*    R*)))
  825 FORMAT(1X,**,4X,I3,*    H*,10(4X,I3,*    H*)))
  826 FORMAT((1X,**,11X,*I*,10(3X,I3,5X,*I*)))
  827 FORMAT((1X,**,11X,**,10(2X,I3,6X,**)))
  828 FORMAT(1Y,**,11(11X,**)/1X,11(**),10(*****PSI******))
  829 FORMAT(1X)
      RETURN
      END
      SUBROUTINE WRITTEN(I1,I2,I3,I4,I5,A6,A7)
      COMMON IRMIN,IRMAX,ISTEP,IPHIMN,IPHIMX,IPHIST,IPSIMN,IPSIMX,IPSIS
     +T,ITER,NITER,LIM,ROTEMP(7,100),LOCATE(100),BOND(200)
      COMMON/DATA/NCENTR,NGROUP(100),OBS(100),NPROT,NSIGN,NOR
     +M,NAME(100),NUMAV(100),PROTX(100),PROTY(100),PROTZ(100),JGROUP(100
     +),TITLE(8)
      INTEGER TEMP/ROTN/CYCLE,GYRO(100)
      DIMENSION SIGN(2)
      DATA SIGN/'+','-'/
      GO TO (400,421,423,425,427) , I1
  400 WRITE(6,401) CYCLE,I2
  401 FORMAT(1H1,13X,*CYCLE NUMBER *,I2,* , OPERATION *,I1,* SELECTED  I
     +,E,*)
      GO TO (402,404,406,408,410,429,431,433) , I2
  402 WRITE(6,403)
  403 FORMAT(1H+,58X,*CENTRE SEARCH AREA ONTO MAX FITFACTOR OF CURRENT A
     +TOMS (GYRO .GT. 0)*)
      GO TO 412
  404 WRITE(6,405)
  405 FORMAT(1H+,58X,*ADD NEXT GROUP(S) THEN RE-CENTRE SEARCH AREA ONTO
     +MAXIMUM FITFACTOR*)
      GO TO 412
  406 WRITE(6,407)
  407 FORMAT(1H+,58X,*OBSERVE MAX FITFACTOR REGION - ROTATE GROUPS IN SE
     +QUENCE AND OPTIMISE*)
      GO TO 412
  408 WRITE(6,409)
  409 FORMAT(1H+,58X,*FIX POSITIONS OF ALL PREVIOUSLY ROTATED GROUPS (RE
     +PLACE CO-ORDINATES)*)
      GO TO 412
  410 WRITE(6,411)
  411 FORMAT(1H+,58X,*START ROTATING INDICATED GROUP(S) ALREADY CURRENT
     +(SMALLER INCREMENT)*)
      GO TO 412
  429 WRITE(6,430)
  430 FORMAT(1H+,58X,*PERFORM COMPLETE ROTATION OF INDICATED GROUP (30*
     +STEP) THEN OPTIMISE*)
      GO TO 412
  431 WRITE(6,432)
  432 FORMAT(1H+,58X,*PERFORM TWELVE POSITION 'FREE-ROTATION' AVERAGING
     +OF INDICATED GROUP*)
      GO TO 412
  433 WRITE(6,434)
  434 FORMAT(1H+,58X,*FINAL ATOMIC COORDINATES AND RESULTS TO BE OUTPUT
     +TO TAPE9 FOR PUNCHING*)
      GO TO 435
C
  412 WRITE(6,413)
  413 FORMAT(1H0,50X,*THE ATOMS TO BE USED IN THIS CYCLE ARE -*)
  414 WRITE(6,415)
  415 FORMAT(1H0/20X,*ATOM       REFERENCE          X-CO-ORD          Y-C
     +O-ORD          Z-CO-ORD       OBSERVED       GYRO*/19X,*NUMBER
     +    NUMBERS*,64X,*SHIFT       CODE*/)
C
      M = J = 0
      IF(IS .EQ. -1) IS = 0
      DO 417 I = 1,NPROT+IS
      M = M + 1
      IF(I .GT. 1) J = 1
      IF(NGROUP(I).EQ.NGROUP(I-J)) M = M - J
      TEMP = LOCATE(I)
      WRITE(6,416) LOCATE(I),NAME(TEMP),NUMAV(I),NGROUP(I),PROTX(I),PROT
```

```
     *Y(I),PROTZ(I),SOBS(M),GYRO(I)
 416 FORMAT(1H0,20X,I2,8X,A4,*/*,I1,*/*,I2,3(8X,F10.7),8X,F6.1,8X,I1)
 417 CONTINUE
     WRITE(6,438)
 438 FORMAT(1H0/)
     RETURN
C
 418 WRITE(6,419)
 419 FORMAT(1H0,47X,*THE NEW CO-ORD DATA OF THE ATOMS SUPPLIED IS *)
     WRITE(6,415)
C
     M = J = 0
     DO 420 I = 1,I4+I3
     M = M + 1
     NUMAV(I) = ROTEMP(1,I)
     NGROUP(I) = ROTEMP(2,I)
     IF(I .GT. 1) J = 1
     IF(NGROUP(I).EQ.NGROUP(I-J)) M = M - J
 420 WRITE(6,416) I,NAME(I),NUMAV(I),NGROUP(I),ROTEMP(3,I),ROTEMP(
    *4,I),ROTEMP(5,I),ROTEMP(7,M),GYRO(I)
     RETURN
C
 421 I = 1
     IF(I5 .LT. 0) I = 2
     WRITE(6,422) I2,I3,SIGN(I),A6
 422 FORMAT(1H0,//13X,*GYROCODE NUMBER OF ATOMS A AND B IS *,I1,* AND OF
    *ROTATED ATOMS IS *,I1,* . THE ROTATED ATOMS HAVE BEEN MOVED *,A1,
    *F5.1,* DEGREES*)
     RETURN
C
 423 I = 1
     IF(I5 .LT. 0) I = 2
     WRITE(6,424) I3,SIGN(I),A6
 424 FORMAT(1H1,13X,*THE ROTATION OF ATOMS OF GYROCODE *,I1,* HAS BEEN
    *OPTIMISED AT *,A1,F5.1,* DEGREES . THE CO-ORDS OF THE CURRENT ATOM
    *S ARE NOW*)
     I5 = I2
     GO TO 414
C
 425 I6 = IFIX(A6)
     I7 = IFIX(A7)
     WRITE(6,426) CYCLE,I2,I3,I4,I5,I6,I7
 426 FORMAT(1H0/13X,*CYCLE *,I2,* ITERATION *,I3,* . MAX FITFACTOR = *,
    *I*,* APPEARED *,I2,* TIMES . AVERAGE LOCATED AT R = *,I3,* , PHI =
    * *,I3,* , PSI = *,I3)
     RETURN
C
 427 WRITE(6,428) (I2 / 2)
 428 FORMAT(1H0/35X,*THIS CYCLE STOPPED IN ROTATE SUB-CYCLE *,I1,* AS N
    *O FURTHER ATOMS TO ROTATE*)
     RETURN
C
 435 WRITE(9,436) TITLE
 436 FORMAT(6X,8A8)
     WRITE(9,437) (NAME(I),NUMAV(I),NGROUP(I),ROTEMP(3,I),ROTEMP(4,I),
    *ROTEMP(5,I),BOND(2*I-1),BOND(2*I),I , I = 1,I3+I4)
 437 FORMAT((A4,*/*,I1,*/*,I2,1X,3F10.7,2A6,1X,I2))
     RETURN
     END
     SUBROUTINE NEWLIM
     COMMON IRMIN,IRMAX,IRSTEP,IPHIMN,IPHIMX,IPHIST,IPSIMN,IPSIMX,IPSIS
    *T,ITER,NITER,LIM/MXFIT/MAXR,MAXPHI,MAXPSI/JUMP/JUMP,PI,MULT,MPHI,M
    *PSI
     INTEGER/NAME/REFLEC,SBOPT,RUN,TEST,BONGLE,OMITA,OMITC,CONTJR
C
C    SELECTS FOCUSING OR MULTISCAN MODE
     IF(ITER .GT. 1)  GO TO 204
C
C    FOCUSING MODE ... CHECK IF MXFIT ON EDGE OF SEARCH
     IF(MAXR.EQ.IRMIN.OR.MAXR.EQ.IRMAX.OR.MAXPHI.EQ.IPHIMN.OR.MAXPHI
    *.EQ.IPHIMX.OR.MAXPSI.EQ.IPSIMN.OR.MAXPSI.EQ.IPSIMX) GO TO 202
     IF(RUN .LT. 3) GO TO 200
     JUMP = JUMP + 1
     GO TO 203
C    FOCUS SEARCH AREA
 200 RUN = RUN + 1
     IF(RUN .EQ. 3) GO TO 201
C    SET SEARCH STEPS FOR RUN = 2
     IRSTEP = 5
     IPHIST = IPSIST = 2
     GO TO 203
C    SET SEARCH STEPS FOR RUN = 3
 201 IRSTEP = 2
     IPHIST = IPSIST = 1
     GO TO 203
C    SHIFT SEARCH AREA TO CENTRE MXFIT
 202 JUMP = 0
 203 IRMIN = MAXR - 2 * IRSTEP
     IRMAX = MAXR + 2 * IRSTEP
     IPHIMN = MAXPHI - 5 * IPHIST
     IPHIMX = MAXPHI + 4 * IPHIST
     IPSIMN = MAXPSI - 5 * IPSIST
     IPSIMX = MAXPSI + 4 * IPSIST
     IF(IRMIN.LT.*.OR.IRMAX.GT.600.OR.IPHIMN.LT.30.OR.IPSIMN.LT.30.OR.I
    *PHIMX.GT.330.OR.IPSIMX.GT.330) GO TO 212
     RETURN
C
C    MULTISCAN MODE ... SELECT TYPE OF BLOCK SEARCH REQUIRED
 204 GO TO (207,205,206,207,205,206,205,206,207,206),(REFLEC+1)
C    CHOOSE NEXT SEARCH BLOCK
 205 GO TO (208,209,208,209,208,209,208,210) , NITER
 206 GO TO (208,208,208,209,208,208,208,210) , NITER
 207 GO TO (208,208,208,209,208,208,209,208,208,208,208,209,208,208,208
    *,210) , NITER
C    INCREMENT ALONG PSI AXIS
 208 IPSIMX = IPSIMX + 45
     IPSIMN = IPSIMN + 45
     MPSI = MPSI + 1
     RETURN
C    INCREMENT ALONG PHI AXIS
 209 IPSIMN = 90
     IPSIMX = 135
     IPHIMN = IPHIMN + 45
     IPHIMX = IPHIMX + 45
     MPHI = MPHI + 1
     MPSI = 1
     RETURN
C    START NEW MULTISCAN BLOCK ... INCREMENT ALONG R AXIS
 210 IF(MULT .EQ. ITER+1) GO TO 211
     IRMIN = IRMIN + 50
     IRMAX = IRMAX + 50
     IPHIMN = IPSIMN = 90
     IPHIMX = IPSIMX = 135
     MULT = MULT + 1
     MPSI = MPHI = 1
     NITER = 0
     RETURN
 211 IF(CONTUR .EQ. 0) STOP14
     REWIND 9
     CALL RETURN(5HTAPE9)
     STOP15
C
 212 WRITE(6,213) IRMIN,IRMAX,IRSTEP,IPHIMN,IPHIMX,IPHIST,IPSIMN,IPSIMX
    *,IPSIST
 213 FORMAT(1H1/10X,*SEARCH AREA BECOMING SILLY THEREFORE PROGRAM STOPP
    *ED*/10X,*THE ATTEMPTED SEARCH AREA WAS : R(*,I3,*-*,I3,*/*,I2,*) ,
    * PHI(*,I3,*-*,I3,*/*,I2,*) , PSI(*,I3,*-*,I3,*/*,I2,*)*//)
     STOP16
     END
```

APPENDIX V : MODEL FOR PLOTTING 3D-FITFACTOR CONTOURS

This perspex model was specially constructed in the Chemistry Department Workshop and consists of a base and back-plate as shown, at half scale, in FIGS. V-1 and V-2. The base-plate carries grooves at 5° intervals which locate a total of 35 PSI sheets, a template for which is given in FIG.V-3. FITFACTOR contours were plotted on these sheets with water soluble crayons (eg. Stabilo) using the data output by METFIND in the MULTISCAN MODE.

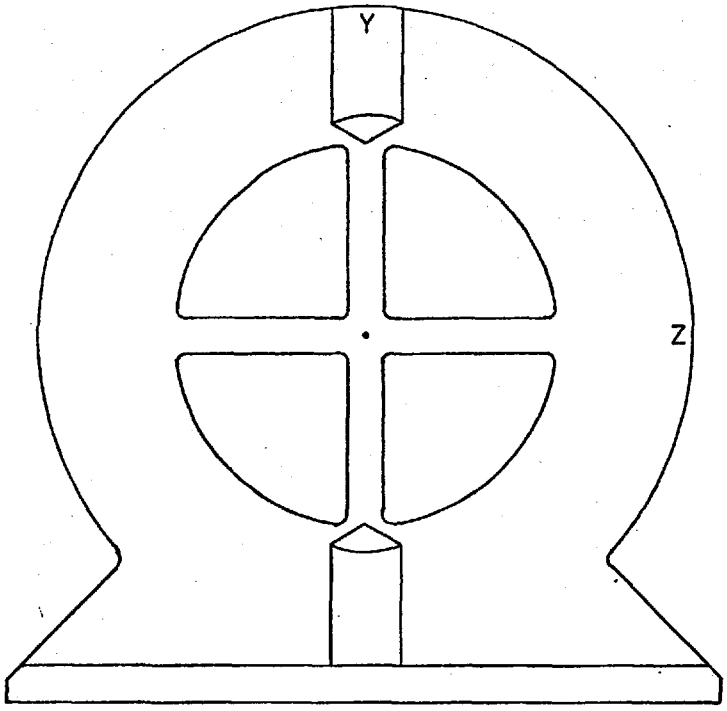


FIG.V-1. Front Elevation and Plan of the Back Plate

A small hole, designed to support a Drieding model, is drilled in the centre of the back-plate. This enables the FITFACTOR contours to be "fitted" to the proposed molecular geometry.

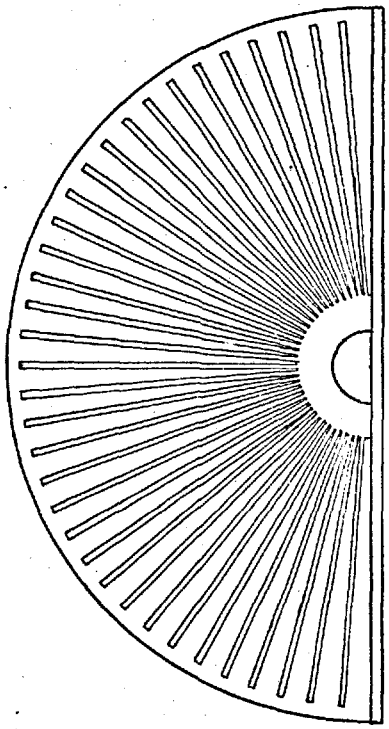


FIG.V-2. Plan and Side Elevation of the Base

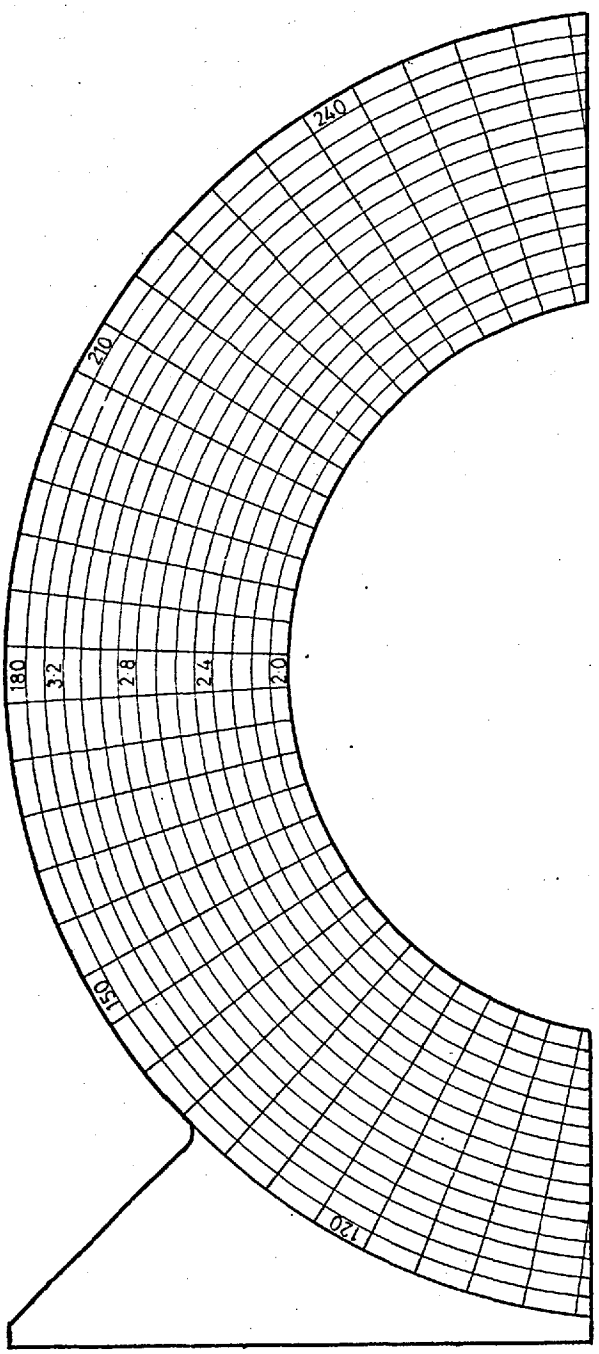
No top guide is necessary for the 35 PSI sheets as they are chamferred to pack tightly around the central spine of the back-plate.

Reference to FIG.5-2.5 explains the need for a model such as this for examining polar coordinate results, for even with considerable practice it is difficult to visualize relationships between arrays of numbers in the FITFACTOR Tables and the shape and orientation of the actual data to the substrate.

3-D MODEL FOR DISPLAYING POLAR COORDINATE RESULTS FROM PROGRAM METFIND

FIG.V-3. TEMPLATE FOR MARKING OUT 'PSI' SHEETS WITH FITFACTOR DATA

Each sheet covers the area : R(2.0-3.4/0.1) , PHI(100-260/5)



There are a total of 35 'PSI' sheets to cover the range : PSI(95-265/5)

LITERATURE CITED

1. K.R.Hanson, JACS., 88, 2731, (1966)
2. R.S.Cahn, C.Ingold, V.Prelog, Angew.Chem.Int.Ed., 5, 385 & 511, (1966)
3. R.S.Cahn, J.Chem.Ed., 41, 116, (1964)
4. H.Hirschmann, K.R.Hanson, Eur.J.Biochem., 22, 301, (1971)
5. K.Mislow, M.Raban, Topics in Stereochemistry, 1, 1, (1966)
6. H.Hirschmann, Comprehensive Biochemistry, 12, (Ed.Florkin, Stotz), Elsevier, p236, (1964)
7. J.A.Pople, Mol.Phys., 1, 1, (1958)
8. H.S.Gutowsky, J.Chem.Phy., 37, 2196, (1962)
9. I.Dabrowsky, E.Ejchart, Org.Mag.Res., 4, 131, (1972)
10. W.B.Jennings, "Chemical Shift Non-Equivalence in Prochiral Groups", Chem.Rev., 75, 307, (1975)
11. M.M.Moloney, "Non-Equivalence of Diastereotopic Groups", Dissertation - Imperial College Chem.Dept., (Ref.402), (1974)
12. R.D.Norris, G.Binsch, JACS, 95, 182, (1973)
13. J.E.Anderson, Tet., 32, 2789, (1976)
14. Soon Ng, J.Mag.Res., 17, 244, (1975)
15. W.Klyne, V.Prelog, Exp., 16, 521, (1960)
16. R.S.Cahn, Introduction To Chemical Nomeclature, 4th Ed, Butterworths, London, (1974)
17. J.E.Blackwood, G.L.Gladys, K.L.Loening, A.E.Petrarca, J.E.Rush, JACS., 90, 509, (1968)
18. P.A.Worthington, Ph.D. Thesis, Univ.London, (1974)
19. A.Michaelis, T.H.Becker, Ber., 30, 1003, (1897)
20. A.Michaelis, T.H.Becker, Ber., 87, 1048, (1898)
21. W.F.Barthel, P.A.Giang, S.A.Hall, JACS., 76, 4186, (1954)
22. W.Lorenz, A.Henglein, G.Schrader, JACS., 77, 2554, (1955)
23. W.F.Barthel, B.H.Alexander, P.A.Giang, S.A.Hall, JACS., 77, 2424, (1955)
24. T.Agawe, T.Kubo, Y.Ohshiro, Synthesis, (1971), 27
25. N.Kreutzkamp, H.Kayser, Chem.Ber., 89, 1614, (1956)
26. B.A.Arbuzov, V.S.Vinogradova, Izvest.Akad.Nauk SSSR Ser.Khim., (1963), 1380 . (CA., 59, 15306f, (1963))
27. B.A.Arbuzov, V.S.Vinogradova, N.A.Poleshaeva, Doklady Akad.Nauk SSSR., 111, 107, (1956)
28. B.A.Arbuzov, M.E.Movsesyam, Otdel.Khim.Nauk., (1959), 267
29. B.A.Arbuzov, V.S.Vinogradova, N.A.Poleshaeva, Otdel.Khim.Nauk SSSR., (1959), 41 . (CA., 53, 15035e, (1959))

30. B.A.Arbuzov,V.S.Vinogradova,N.A.Poleshaeva,Otdel.Khim.Nauk SSSR., (1960),832 . (CA.,54,24454f,(1960))
31. B.A.Arbuzov,Chem.Soc.Spec.Pub.,8,47,(1959)
32. G.Wittig,U.Schollkopf,Ber.Deut.Chem.Ges.,87,1318,(1954)
33. F.Cramer,Angew.Chem.,72,236,(1960)
34. W.Perkow,Ber.Deut.Chem.Ges.,87,755,(1954)
35. D.E.Poel,N.Fekkes,Shell Group Research Report,AMGR.0206.70
36. I.S.Bengledorf,M.S.Kharasch,J.Org.Chem.,20,1356,(1955)
37. I.S.Bengledorf,J.Org.Chem.,21,475,(1956)
38. V.S.Abramov,A.S.Kapustina,Zhur.Obs.Khim.,27,1012,(1957) . (CA.,52, 3666,(1958))
39. N.D.Dawson,A.Burger,JACS.,74,5312,(1952)
40. A.N.Pudovik,R.D.Gareev,J.Gen.Chem.USSR.,42,1845,(1972) . (CA.,78, 43590v,(1973))
41. B.A.Arbuzov,V.S.Vinogradova,N.A.Poleshaeva,A.K.Shamsutchinova,Izvest. Akad.Nauk SSSR.Ser.Khim.,8,1380,(1963)
42. E.M.Gaydon,J.R.Llinas,Org.Mag.Res.,6,23,(1974)
43. C.Pascuel,J.Meier,W.Simon,Helv.Chim.Acta.,49,164,(1966)
44. S.W.Tobey,J.Org.Chem.,34,1281,(1969)
45. D.J.Cram,A.Elhafez,JACS.,74,5828,(1952)
46. J.W.Cornforth,R.H.Cornforth,K.K.Mathews,JCS.,(1959),112
47. M.G.Belsham,A.R.Muir,M.Kinns,L.Phillips,Li-Ming Twanmoh,JCS.P.II., (1974),119
48. M.Karplus,J.Chem.Phy.,30,11,(1959)
49. M.Karplus,JACS.,85,2870,(1963)
50. T.Sato,K.Goto,Chem.Comm.,(1973),494
51. C.B.C.Boyce,S.B.Webb,L.Phillips,I.R.Ager,JCS.P.I.,(1974),1644
52. R.Nouri-Bimorghi,Bull.Soc.Chim.Fr.,11,3178,(1965)
53. A.Kirrmann,R.Nouri-Bimorghi,Bull.Soc.Chim.Fr.,14,3213,(1968)
54. W.H.Saunders,A.F.Cockerill,Mechanisms of Elimination Reactions,Wiley, N.Y.,(1973)
55. W.Hanhart,C.K.Ingold,JCS.,(1927),997
56. E.D.Hughes,C.K.Ingold,JCS.,(1933),523
57. E.D.Hughes,JACS.,57,708,(1935)
58. E.D.Hughes,C.K.Ingold,C.S.Patel,JCS.,(1933),526
59. F.G.Bordwell,A.C.Knipe,K.C.Yee,JACS.,92.5945,(1970)
60. Z.Rappoport,E.Shohamy,JCS.B.,(1971),2060
61. D.J.Cram,F.D.Green,C.H.DePuy,JACS.,78,790,(1956)
62. J.F.Bunnett,Angew.Chem.Int.Ed.,1,225,(1962)

63. J.F.Bunnett, "Olefin Forming Reactions", Survey Prog.Chem., 5, 33, (1969)
64. J.Závada, J.Krupička, J.Sicher, Coll.Czech.Chem.Comm., 33, 1393, (1968)
65. P.B.D.de la Mare, C.A.Vernon, JCS., (1956), 41
66. E.L.Eliel, R.S.Ro, JACS., 79, 5995, (1957)
67. S.Winstein, D.Darwish, N.J.Holness, JACS., 78, 2915, (1956)
68. D.J.McLennan, Tet.(Report), 31, 2999, (1975)
69. A.J.Parker, M.Ruane, G.Biale, S.Winstein, Tet.Let., (1968), 2113
70. G.Biale, A.J.Parker, S.G.Smith, I.D.R.Stevens, S.Winstein, JACS., 92, 115, (1970)
71. W.T.Ford, Acc.Chem.Res., 6, 410, (1973)
72. S.J.Cristol, N.L.Hause, J.S.Meek, JACS., 73, 674, (1951)
73. W.Hückel, W.Tappe, G.Legutke, Ann.Chem., 543, 191, (1940)
74. C.K.Ingold, Proc.Chem.Soc., (1962), 265
75. J.Sicher, J.Závada, Coll.Czech.Chem.Comm., 33, 1278, (1968)
76. D.J.McLennan, Quart.Rev., 21, 490, (1967)
77. M.P.Cooke, J.L.Coke, JACS., 90, 5556, (1968)
78. S.J.Cristol, N.L.Hause, JACS., 74, 2193, (1952)
79. V.Fiandanese, C.V.Maffeo, G.Marchese, F.Naso, JCS.P.II., (1975), 221 (et seq)
80. M.Charton, JACS., 97, 6159, (1975)
81. C.G.Swain, A.D.Kettey, R.F.W.Bader, JACS., 81, 2353, (1959)
82. R.D.Bartlett, JACS., 57, 224, (1935)
83. S.Winstein, H.J.Lucas, JACS., 61, 1576, (1939)
84. A.W.Hofmann, Ann.Chem., 78, 253, (1851)
85. A.Saytzeff, Ann.Chem., 179, 296, (1875)
86. D.J.McLennan, R.J.Wong, JCS.P.II., (1974), 526 & 1373
87. A.B.N.Gray, D.J.McLennan, JCS.P.II., (1974), 1377 & 1818
88. S.Alunni, E.Baciocci, JCS.P.II., (1976), 877 (et seq)
89. Z.Rappoport, JCS.B., (1971), 171
90. V.Fiandanese, G.Marchese, F.Naso, Chem.Comm., (1972), 251
91. G.Berti, "Stereochemistry of Epoxide Synthesis", Topics in Stereochemistry, 7, 187-218, (1974) (and refs. therein)
92. G.Berti, F.Battari, P.L.Ferrarini, B.Machia, J.Org.Chem., 30, 4091, (1965)
93. E.Elkik, M.Le Blanc, Bull.Soc.Chim.Fr., (1971), 870
94. M.ATlanti, J.Leroy, C.R.Acad.Sci.Paris, C, 269, 349, (1969)
95. A.Kirrmann, P.Duhamel, R.Nouri-Bimorghi, Bull.Soc.Chim.Fr., (1964), 3264
96. A.Kirrmann, P.Duhamel, R.Nouri-Bimorghi, Liebigs Ann.Chem., 691, 33, (1965)
97. R.Nouri-Bimorghi, C.R.Acad.Sci.Paris, C, 262, 759, (1966)
98. L.Duhamel, J.Gralak, Bull.Soc.Chim.Fr., (1974), 2124
99. B.Delmond, J.C.Pommier, J.Valade, C.R.Acad.Sci.Paris, C, 275, 1037, (1972)
100. P.Duhamel, L.Duhamel, J.Gralak, C.R.Acad.Sci.Paris, C, 269, 1658, (1969)

101. P.Duhamel,L.Duhamel,J.Gralak,Bull.Soc.Chim.Fr.,(1970),3641

102. V.F.Martinov,M.I.Titov,Zhur.Obs.Khim.,32,319,(1962) . (CA.,56,12373c, (1962))

103. G.Darz . s,G.Levy,C.R.Acad.Sci.Paris,24,272,(1937)

104. R.M.McDonald,P.A.Schwab,J.Org.Chem.,29,2459,(1964)

105. B.Castro,J.Villieras,N.Ferracutti,C.R.Acad.Sci.Paris,C,267,1502,(1968)

106. J.Villieras,B.Castro,N.Ferracutti,Bull.Soc.Chim.Fr.,(1970),1450

107. G.Köbrich,J.Grosser,W.Werner,Chem.Ber.,106, 2610 & 2620,(1973)

108. F.de Reinach-Hirtzback,T.Durst,Tet.Let.,(1976),3677

109. A.Fougerousse,J.J.Riehl,Tet.Let.,(1973),3593

110. R.E.Glick,A.A.Bothner-By,J.Chem.Phy.,25,362,(1956)

111. R.J.Abraham,K.G.R.Pachler,Mol.Phy.,6,165,(1963)

112. N.S.Bhacca,D.H.Williams,Applications of NMR Spectroscopy in Organic Chemistry,Holden Day,N.Y.,(1964)

113. H.Booth,Tet.Let.,(1965),41

114. L.M.Jackman,S.Sternhell,Applications of NMR Spectroscopy in Organic Chemistry,(2^{nd}Edn.),Org.Chem.Mono.,Vol.5,Pergamon Press,(1969)

115. R.J.Abraham,G.Gatti,JCS.B.,(1969),961

116. L.Phillips,V.Wray,JCS.P.II.,(1972),536

117. W.F.Reynolds,D.J.Wood,Can.J.Chem.,49,1209,(1971)

118. W.F.Reynolds,D.J.Wood,Can.J.Chem.,51,2659,(1973)

119. R.J.Abraham,J.Phy.Chem.,73,1192,(1969)

120. L.Phillips,Spectroscopy,Vol.1,Chapter 2,(Ed.B.P.Straughan,S.Walker), Chapman & Hall,London,(1976)

121. J.Kowalewski,"Calculations of Nuclear Spin-Spin Coupling Constants", Prog.In NMR.,11,1,(1977)

122. R.Wasylishen,T.Schaefer,Can.J.Chem.,50,2710,(1972)

123. G.Govil,Mol.Phy.,21,953,(1971)

124. R.Wasylishen,T.Schaefer,Can.J.Chem.,51,961,(1973)

125. K.L.Williamson,Y.F.Li Hon,F.H.Hall,S.Swager,M.S.Coulder,JACS.,90,6717, (1968)

126. L.Phillips,V.Wray,JCS.B.,(1971),1618

127. J.B.Grutzner,M.Jautelat,J.B.Dence,R.A.Smith,J.D.Roberts,JACS.,92, 7107,(1970)

128. J.B.Stothers,Carbon-13 NMR Spectroscopy,Acad.Press,N.Y.,(1972)

129. C.E.Johnson,F.A.Bovey,J.Chem.Phy.,29,1012,(1958)

130. J.E.Anderson,H.Pearson,JCS.P.II.,(1977),699

131. C.C.Hinkley,JACS.,91,5160,(1969)

132. J.K.M.Sanders,D.H.Williams,Chem.Comm.,(1970),422

133. W.DeW.Horrocks,J.P.Sipe,JACS.,93,6800,(1971)
134. T.H.Siddall,Chem.Comm.,(1971),452
135. W.DeW.Horrocks,Inorg.Chem.,9,690,(1970)
136. H.M.McConnell,R.E.Robertson,J.Chem.Phy.,29,1361,(1958)
137. an early example : J.Briggs,F.A.Hart,G.P.Moss,Chem.Comm.,(1970),1506
138. J.Reuben,Prog.in NMR.,9,1,(1973)
139. B.C.Mayo,Chem.Soc.Review,2,49,(1973)
140. A.F.Cockerill,G.L.O.Davies,R.C.Harden,D.M.Rackman,Chem.Rev.,73,553,(1973)
141. M.I.Foreman,"Medium Effects",Chem.Soc.Spec.Per.Rep.NMR.,Vol.3-5,(1974-6)
142. O.Hofer,Topics in Stereochem.,9,111,(1976)
143. M.Mednejad,Ph.D.Thesis,Univ.London,(1977)
144. E.R.Birnbaum,T.Moeller,JACS.,91,7274,(1969)
145. K.Ajisaka,M.Kainosho,JACS.,97,330,(1975)
146. B.F.G.Johnson,J.Lewis,P.McArdle,J.R.Norton,JCS.Dalton,(1974),1253
147. W.DeW.Horrocks,E.S.Greenberg,Inorg.Chem.,10,2190,(1971)
148. R.E.Cramer,R.Dubois,K.Seff,JACS.,96,4125,(1974)
149. R.E.Cramer,K.Seff,Chem.Comm.,(1972),400
150. J.J.Uebel,R.M.Wing,JACS.,94,8910,(1972)
151. D.S.Dyer,J.A.Cunningham,J.J.Brooks,R.E.Sievers,R.E.Rondeau,NMR Shift Reagents,(Ed.Sievers),Acad.Press,NY,p21,(1973)
152. W.DeW.Horrocks,JACS.,96,3022,(1974)
153. G.E.Hawkes,D.Leibfritz,D.W.Roberts,J.D.Roberts,JACS.,95,1659,(1973)
154. G.E.Hawkes,C.Marzin,D.Leibfritz,S.R.Johns,K.Herwig,R.A.Cooper,D.W. Roberts,J.D.Roberts,NMR Shift Reagents,(Ed.Sievers),Acad.Press, NY,p129,(1973)
155. C.D.Barry,C.M.Dobson,D.A.Sweigart,L.E.Ford,R.J.P.Williams, ibid ,p193
156. H.L.Ammon,P.H.Mazzocchi,W.J.Kopecky,H.J.Tamburin,P.H.Watts,JACS.,95, 1968,(1973)
157. R.M.Wing,J.J.Uebel,K.K.Anderson,JACS.,95,6046,(1973)
158. J.D.Roberts,G.E.Hawkes,J.Husar,A.W.Roberts,D.W.Roberts,Tet.,30,1833, (1974)
159. D.J.Chadwick,Tet.Let.,(1974),1375
160. J.Reuben,D.Fiat,Inorg.Chem.,8,1821,(1969)
161. J.Reuben,D.Fiat,J.Chem.Phy.,51,4909,(1969)
162. A.A.Chalmers,K.G.R.Pachler,JCS.P.II.,(1974),749
163. F.A.Cotton,G.Wilkinson,"Advanced Inorganic Chemistry",(2nd Ed),Wiley, Chap.31,(1966)
164. J.Reuben,J.Mag.Res.,11,103,(1973)
165. J.W.ApSimon,H.Beierbeck,J.K.Sanders,Can.J.Chem.,51,3874,(1973)

166. K.L.Williamson,D.R.Clutter,R.Emch,M.Alexander,A.E.Burroughs,C.Chua, M.E.Bozel,JACS.,96,1471,(1974)
167. H.J.Sneider,E.F.Weigand,Tet.,31,2125,(1975)
168. B.F.G.Johnson,J.Lewis,P.McArdle,J.R.Norton,Chem.Comm.,(1972),535
169. D.J.Chadwick,D.H.Williams,JCS.P.II.,(1974),1202 & 1903
170. H.E.Francis,W.F.Wagner,Org.Mag.Res.,4,189,(1972)
171. R.E.Davies,M.R.Willcott,NMR Shift Reagents,(Ed.Sievers),Acad.Press, NY,p143,(1973)
172. I.Morishima,K.Okada,T.Yonezawa,K.Goto,JACS.,95,1662,(1973)
173. S.J.Angyal,Tet.,30,1695,(1974)
174. G.E.Hawkes,C.Marzin,S.R.Johns,J.D.Roberts,JACS.,95,1662,(1973)
175. B.Bleaney,C.M.Dobson,B.A.Levine,R.B.Martin,R.J.P.Williams,A.V.Xavier, Chem.Comm.,(1972),791
176. K.Tori,Y.Yoshimura,Tet.Let.,(1973),3127
177. J.J.Uebel,C.Pacheco,R.M.Wing,Tet.Let.,(1973),4383
178. C.D.Barry,A.C.T.North,J.A.Glasel,R.J.P.Williams,A.V.Xavier,Nature, 232,236,(1971)
179. L.R.Morss,Chem.Rev.,76,827,(1976) (and refs therein)
180. D.H.Templeton,C.H.Dauben,JACS.,76,5237,(1954)
181. C.S.Springer,A.H.Bruder,S.R.Tanny,M.Pickering,H.A.Rockefeller,NMR Shift Reagents,(Ed.Sievers),Acad.Press,NY,p283,(1973)
182. D.R.Crump,J.K.M.Sanders,D.H.Williams,Tet.Let.,(1970),4419
183. D.A.Gansow,P.A.Loeffler,R.E.Davies,M.R.Willcott,R.E.Lenkinski,JACS., 95,3389,(1973)
184. G.H.Frost,F.A.Hart,Chem.Comm.,(1970),749
185. J.K.M.Sanders,D.H.Williams,JACS.,93,641,(1971)
186. J.Reuben,J.S.Leigh,JACS.,94,2789,(1972)
187. J.W.Faller,G.N.La Mar,Tet.Let.,(1973),1381
188. B.Birdsall,N.J.Birdsall,J.Feeney,J.Thornton,JACS.,97,2845,(1975)
189. I.M.Armitage,L.D.Hall,A.G.Marshall,L.G.Werbelow,JACS.,95,1437,(1973)
190. M.R.Willcott,R.E.Lenkinski,R.E.Davies,JACS.,94,1742 & 1744,(1972)
191. J.W.ApSimon,H.Beierbeck,Tet.Let.,(1973),581
192. A.J.Rafalski,J.Barciszewski,M.Karonski,J.Mol.Struct.,19,223,(1973)
193. M.D.Johnston,D.J.Raker,N.K.DeGennaro,A.D'Angelo,J.W.Perry,JACS.,98, 6042,(1976)
194. W.C.Hamilton,Acta.Cryst.,18,502,(1965)
195. P.V.Demerco,B.J.Cerimele,R.W.Crane,A.L.Thakkar,Tet.Let.,(1972),3539
196. J.W.ApSimon,H.Beierbeck,Chem.comm.,(1972),172
197. C.C.Hinkley,W.C.Brumley,JACS.,98,1331,(1976)

198. C.C.Hinkley, W.C.Brumley, J.Mag.Res., 24, 239, (1976)
199. W.E.Gore, I.M.Armitage, J.Org.Chem., 41, 1926, (1976)
200. G.Montaudo, V.Librando, S.Caccamese, P.Maravigna, JACS., 95, 6365, (1973)
201. R.E.Cramer, C.K.Faruike, D.Dubois, J.Mag.Res., 19, 382, (1975)
202. T.Heigl, G.K.Mucklow, Tet.Let., (1973), 649
203. S.Farid, A.Ateya, M.Maggio, Chem.Comm., (1971), 1285
204. A.Recce, P.Finocchiaro, Tet.Let., (1974), 4185
205. H.L.Goering, A.C.Backus, C.S.Chang, D.Masilamann, J.Org.Chem., 40, 1533, (1975)
206. P.Camps, J.Font, J.M.Marques, Tet., 31, 2581, (1975)
207. R.E.Craig, A.C.Craig, G.D.Smith, Tet.Let., (1975), 1189
208. N.S.Angerman, S.S.Danyluk, T.A.Victor, JACS., 94, 7137, (1972)
209. M.Celotti, G.V.Fazakerley, JCS.P.II., (1977), 1319
210. I.Gulkis, G.W.Everett, Tet., 32, 913, (1976)
211. R.E.Lenkinski, J.Reuben, JACS., 98, 4065, (1976)
212. O.Hofer, Tet.Let., (1975), 3415
213. G.Montaudo, S.Caccamese, V.Librando, P.Maravigna, Tet., 29, 3915, (1973)
214. H.Falk, K.Grubmayr, U.Herzig, O.Hofer, Tet.Let., (1975), 559
215. G.R.Sullivan, JACS., 98, 7162, (1976)
216. D.K.Lavellee, A.H.Zeltmann, JACS., 96, 5552, (1974)
217. J.Klein, E.D.Bergmann, J.Org.Chem., 22, 1019, (1957)
218. A.I.Vogel, Practical Organic Chemistry, Longmans, London, p881, (1957)
219. N.N.Yarovenka, M.A.Racka, Zh.Obs.Khim., 29, 2159, (1959)
220. L.H.Knox, E.Velarde, S.Berger, D.Cuadreillo, A.D.Cross, J.Org.Chem., 29, 2187, (1964)
221. R.L.Pruet, J.T.Barr, K.E.Rapp, C.T.Bahner, J.D.Gibson, R.H.Lafferty, JACS., 72, 3646, (1950)
222. Organic Reactions in Steroid Chemistry, (Ed.Fried & Edwards), Van Nostrand, p436, (1960)
223. W.J.Middleton, J.Org.Chem., 40, 574, (1975)
224. T.Bergkvist, Svensk.Kem.Tid., 59, 24, (1947) . (CA., 41, 5119i, (1947))
225. I.A.Lapkin, E.V.Dormidontara, Uch.Zap.Perm.Gos.Univ., 159, 276, (1966) (CA., 68, 114672e, (1968))
226. F.Bergmann, A.Kalmus, E.Breuer, JACS., 80, 4540, (1958)
227. J.Villieras, Bull.Soc.Chim.Fr., (1967), 1520
228. H.L.Haller et (11) al., JACS., 67, 1591, (1945)
229. D.Woodcock, JCS., (1949), 203
230. A.Allais, P.Girault, French Patent, 1,550,129 . (CA., 72, 111004k, (1970))
231. B.L.Jenson, R.E.Connell, J.Org.Chem., 38, 835, (1973)
232. Ya.G.Bal'on, M.D.Shulman, Khim-Farm.Zh., 9, 36, (1975) . (CA., 82, 170240p, (1975))

233. Y.Shimiza,R.Y.Hsu,Chem.Pharm.Bull.,23,2179,(1975)
234. R.Guedj,R.Nabet,T.Wade,Tet.Let.,12,907,(1973)
235. M.Voronkov et al.,Latv.PSR.Zinad.Akad.Vestis.Kim.Ser.,(1968),565 (CA.,70,46978y,(1969))
236. A.V.Kalakina et al.,Izvest.Sibir.Otdel.Akad.Nauk.SSR.,(1958),9 (CA.,53,17033g,(1959))
237. UK.Patent, 1,229,992 (1971)
238. B.L.Jenson.S.E.Burke,S.E.Thomas,W.H.Klausmeier,Tet.Let.,(1977),2639
239. J.A.Pople,W.G.Schneider,H.J.Bernstein,"High Resolution NMR",McGraw-Hill Inc.,NY,p103-138,(1959)
240. C.N.Banwell,"NMR For Organic Chemists",(Ed.D.W.Mathieson),Acad.Press, London,Chapter 6,p85-108,(1967)
241. A.J.Kerslake,L.Phillips, publication pending
242. R.J.Abraham,"Analysis of High Resolution NMR Spectra",Elsevier, Amsterdam,p58-83,(1971)
243. T.J.Batterham,C.J.Bigum,Org.Mag.Res.,4,67,(1972)
244. R.Freeman,N.S.Bhacca,J.Chem.Phy.,45,3795,(1966)
245. R.J.Abraham,H.J.Bernstein,Can.J.Chem.,39,216,(1961)
246. F.J.Weigert,J.D.Roberts,JACS.,91,4940,(1969)
247. G.C.Levy,G.L.Nelson,"Carbon-13 NMR For Organic Chemists",Wiley,NY, TABLE 4.1,p81,(1972)
248. L.P.Hammett,"Physical Organic Chemistry",2nd Ed,McGraw-Hill,NY,(1970)
249. A.J.Gordon,R.A.Ford,"The Chemist's Companion",Wiley,p144-155,(1972)
250. R.W.Taft,JACS.,79,1045,(1957)
251. J.Niwa,M.Yamazaki,Chem.Let.,4,765,(1974)
252. N.Inamoto,S.Masuda,K.Tori,Y.Yoshimura,Tet.Let.,(1977),737
253. L.Phillips,V.Wray,JCS.P.II.,(1972),214
254. L.Phillips,V.Wray,JCS.P.II.,(1972),224
255. J.W.Emsley,L.Phillips,Prog.In NMR.,(Ed.Emsley,Feeney,Sutcliff),Vol.9 TABLE A2,(1971)
256. J.M.Gascoyne - unpublished results
257. D.Doddrell,D.Jordan,N.V.Riggs,Chem.Comm.,(1972),1158
258. N.Muller,D.T.Carr,J.Phy.Chem.,67,112,(1963)
259. F.J.Weigert,J.D.Roberts,JACS.,93,2361,(1971)
260. F.A.Bovey,E.W.Anderson,F.P.Hood,R.L.Kornegay,J.Chem.Phy.,40,3099,(1964)
261. R.J.Abraham,L.Cavalli,Mol.Phy.,9,67,(1965)
262. A.M.Ihrig,S.L.Smith,JACS.,92,759,(1970)
263. L.D.Hall,D.L.Jones,Can.J.Chem.,51,2925,(1973)
264. L.D.Hall,J.F.Manville,Carbohydrate Res.,4,512,(1967) et seq.(L.D.H)

265. H.S.Gutowsky, G.G.Belford, P.E.McMahon, J.Chem.Phy., 36, 3353, (1967)
266. G.Govil, H.Bernstein, J.Chem.Phy., 47, 2818, (1967)
267. T.D.Alger, H.S.Gutowsky, R.L.Vold, J.Chem.Phy., 47, 3130, (1967)
268. R.R.Dean, J.Lea, Trans.Faraday Soc., 64, 1409, (1968)
269. F.J.Weigert, J.D.Roberts, JACS., 93, 2361, (1971)
270. P.J.Mitchell - unpublished results
271. L.Ernst, D.N.Lincoln, V.Wray, J.Mag.Res., 21, 115, (1976)
272. S.L.Mannatt, M.A.Cooper, JACS., 99, 4561, (1977)
273. D.Doddrell, M.Barfield, W.Adcock, M.Awangzeb, D.Jordan, JCS.P.II., (1976), 402
274. W.Adcock, B.D.Gupta, T.C.Khor, D.Doddrell, D.Jordan, W.Kitching, JACS., 96, 1595, (1974)
275. M.H.Pendlebury, L.Phillips, V.Wray, JCS.P.II., (1974), 787
276. L.Phillips, V.Wray, JCS.P.II., (1974), 928
277. G.Miyaziwa, Y.Utsumi, K.Takahashi, J.Phy.Chem., 73, 1370, (1969)
278. D.J.Chadwick, Tet.Let., (1974), 1375
279. CRC Handbook of Chemistry and Physics, 58th Edn. (CRC Press), F215-218, (1977)
280. Interatomic Distances, Chem.Soc.Spec.Pub.No.11., (1958)
281. J-M.Lehn, J-J.Riehl, Mol.Phy., 7, 33, (1964)
282. P.Sykes, "A Guidebook to Mechanism in Organic Chemistry", (3rd Edn.), Longman, p217, (1970)
283. E.Kiehlmann, R.J.Bianchi, W.Reeve, Can.J.Chem., 47, 1521, (1969)
284. J.W.Emsley, L.Phillips, V.Wray, Prog.in NMR., (Ed.Emsley, Feeney, Sutcliffe), Vol.10, (1976)
285. G.Gambaretto, M.Napoli, Atti.Ist.Veneto Sci.Let.Arti.Cl.Sci.Mat.Nat., 131, 525, (1972)
286. B.L.Jenson, S.E.Burke, S.E.Thomas, W.H.Klausmeier, Tet.Let., (1977), 2639
287. C.C.Tung, A.J.Speziale, H.W.Frazier, J.Org.Chem., 28, 1514, (1963)
288. L.Villa, L.Schenetti, F.Taddei, Org.Mag.Res., 5, 593, (1973)
289. F.Lazzeretti, I.Moretti, F.Taddei, G.Torre, Org.Mag.Res., 5, 385 & 391, (1973)
290. G.Aranda, H.de Luze, Bull.Soc.Chim.Fr., (1968), 2169
291. S.Sorriso, F.Stefani, E.Semprini, A.Flanini, JCS.P.II., (1976), 374